



# Load and Resistance Factor Design (LRFD) Pile Driving Project – Phase II Study

Minnesota  
Department of  
Transportation

**RESEARCH  
SERVICES  
&  
LIBRARY**

**Office of  
Transportation  
System  
Management**

Aaron S. Budge, Principal Investigator  
Department of Mechanical and Civil Engineering  
Minnesota State University, Mankato

**April 2014**

Research Project  
Final Report 2014-16



To request this document in an alternative format call [651-366-4718](tel:651-366-4718) or [1-800-657-3774](tel:1-800-657-3774) (Greater Minnesota) or email your request to [ADArequest.dot@state.mn.us](mailto:ADArequest.dot@state.mn.us). Please request at least one week in advance.

## Technical Report Documentation Page

1. Report No. MN/RC 2014-16		2.		3. Recipients Accession No.	
4. Title and Subtitle  Load and Resistance Factor Design (LRFD) Pile Driving Project – Phase II Study				5. Report Date April 2014	
				6.	
7. Author(s) Samuel G. Paikowsky, Mary Canniff, Seth Robertson, and Aaron S. Budge				8. Performing Organization Report No.	
9. Performing Organization Name and Address Minnesota State University, Mankato Dept. of Mechanical and Civil Engineering 205 Trafton Science Center East Mankato, MN 56001				10. Project/Task/Work Unit No.	
				11. Contract (C) or Grant (G) No.  (C) 96272	
12. Sponsoring Organization Name and Address Minnesota Department of Transportation Research Services & Library 395 John Ireland Boulevard, MS 330 St. Paul, MN 55155				13. Type of Report and Period Covered Final Report	
				14. Sponsoring Agency Code	
15. Supplementary Notes <a href="http://www.lrrb.org/pdf/201416.pdf">http://www.lrrb.org/pdf/201416.pdf</a>					
16. Abstract (Limit: 250 words)  Driven piles are the most common foundation solution used in bridge construction (Paikowsky et al., 2004). Their safe use requires to reliable verification of their capacity and integrity. Dynamic analyses of driven piles are methods attempting to obtain the static capacity of a pile, utilizing its behavior during driving. Dynamic equations (aka pile driving formulas) are the earliest and simplest forms of dynamic analyses. The development and the examination of such equation tailored for MnDOT demands is presented. In phase I of the study reported by Paikowsky et al. (2009, databases were utilized to investigate previous MnDOT (and other) dynamic formulas and use object oriented programming for linear regression to develop a new formula that was then calibrated for LRFD methodology and evaluated for its performance. This report presents the findings of phase II of the study in which a comprehensive investigation of the Phase I findings were conducted. The studies lead to the development of dynamic formulae suitable for MnDOT foundation practices, its calibrated resistance factors and its application to concrete and timber piles. Phase II of the study also expanded on related issues associated with Wave Equation analyses and static load tests, assisting the MnDOT in establishing requirements and specifications.					
17. Document Analysis/Descriptors Piles, Dynamics, LRFD, Resistance (mechanics), Bridge foundations				18. Availability Statement No restrictions. Document available from: National Technical Information Services, Alexandria, VA 22312	
19. Security Class (this report) Unclassified		20. Security Class (this page) Unclassified		21. No. of Pages 514	
				22. Price	

# **Load and Resistance Factor Design (LRFD) Pile Driving Project – Phase II Study**

## **Final Report**

*Prepared by:*

Aaron S. Budge

Department of Mechanical and Civil Engineering  
Minnesota State University, Mankato

Samuel G. Paikowsky  
Mary Canniff  
Seth Robertson

Geotechnical Engineering Research Lab  
University of Massachusetts Lowell

**April 2014**

*Published by:*

Minnesota Department of Transportation  
Research Services & Library  
395 John Ireland Boulevard, MS 330  
St. Paul, Minnesota 55155

This report documents the results of research conducted by the authors and does not necessarily represent the views or policies of the Minnesota Department of Transportation or Minnesota State University, Mankato. This report does not contain a standard or specified technique.

The authors, the Minnesota Department of Transportation, and Minnesota State University, Mankato do not endorse products or manufacturers. Trade or manufacturers' names appear herein solely because they are considered essential to this report.



## **Acknowledgments**

The presented research was supported by Minnesota Department of Transportation (MnDOT) via a grant to Minnesota State University, Mankato. The Technical Advisory Panel (TAP) is acknowledged for its support, interest, and comments. In particular we would like to mention Richard Lamb, Gary Person, Dan Mattison and Derrick Dasenbrock of the Foundations Unit, Paul Rowekamp (Technical Liaison), Paul Pilarsky, Dustin Thomas, Dave Dahlberg, Kevin Western, Bruce Iwen, and Paul Kivisto of the Bridge Office and Nelson Cruz of the Research Services office.

The research presented in this manuscript makes use of a large database specifically developed for MnDOT purposes. This database makes use of data originally developed for a Federal Highway Administration (FHWA) study by Paikowsky et al. (1994) followed by an updated database denoted as PD/LT 2000 presented by Paikowsky and Stenersen (2000), which was also used for the LRFD development for deep foundations (presented in NCHRP Report 507 by Paikowsky et al., 2004). The contributors for those databases are acknowledged for their support as detailed in the referenced publications. Carl Ealy and Albert DiMillio of the FHWA were constructive in support of the original research studies and facilitated data gathering via FHWA sources. Significant additional data were added to those databases, most of which were provided by six states: Illinois, Iowa, Tennessee, Connecticut, West Virginia, and Missouri. The data obtained from Leo Fontaine of the Connecticut DOT was extremely valuable to enlarge the MnDOT databases to the robust level presented in this study. In addition, the data provided by Betty Bennet of the Ontario ministry of Transportation were invaluable for developing the timber piles database.

Previous students of the Geotechnical Engineering Research Laboratory at the University of Massachusetts Lowell are acknowledged for their contribution to the aforementioned databases and various studies, namely: John J. McDonell, John E. Regan, Kirk Stenersen, Colin O'Hearn and Jorge Fuentes. Dr. Shailendra Amatya, a post-doctoral fellow at the Geotechnical Engineering Research Laboratory, is acknowledged for his assistance in employing object oriented programming in the code SPlus for the development of the newly proposed MnDOT dynamic equation as presented in Phase I of the study. Christopher Jones of GeoDynamica, Inc. is acknowledged for his assistance in developing the timber piles database and conducting the WEAP simulations.

## Table of Contents

1	BACKGROUND.....	1
1.1	Resistance Factor for MnDOT’s Pile Driving Formula – Phase I Study.....	1
1.2	Research Objectives.....	3
1.2.1	Overview.....	3
1.2.2	Concise Objectives.....	4
1.2.3	Specific Tasks .....	4
1.3	Manuscript Outline .....	6
2	REVIEW ALTERNATE FORMULAS AND CONSTRUCTION PILE PRACTICES IN MIDWEST STATES.....	7
2.1	Overview.....	7
2.2	Illinois Department of Transportation – Long and Maniaci (2000) .....	7
2.2.1	Overview.....	7
2.2.2	Databases Summary.....	10
2.2.3	Olson and Flaate, 1967 .....	13
2.2.4	Conclusions.....	23
2.3	Illinois Department of Transportation – Long et al. (2009a).....	24
2.3.1	Overview.....	24
2.3.2	International Database .....	24
2.3.3	Comprehensive Database.....	26
2.3.4	Illinois Database.....	31
2.3.5	Development of Correction Factors.....	36
2.3.6	Resistance Factors and Reliability.....	41
2.3.7	Summary and Comparison of Results to Phase I of the Mn Study (Paikowsky et al., 2009).....	44
2.4	Report Submitted to the State of Wisconsin Department of Transportation – Long et al., 2009b.....	47
2.4.1	Overview.....	47
2.4.2	Databases .....	47
2.4.3	Summary of Findings.....	47
2.4.4	Conclusions and Comment .....	49
2.5	Gates Formulae .....	50
2.5.1	Gates (1957).....	50
2.5.2	Evaluation of Gates (1957) Equation.....	53
2.5.3	Modified Gates Equation (Olson and Flaate, 1967) .....	53
2.5.4	FHWA-Modified Gates Equation (USDOT, 1988).....	55
2.5.5	Evaluation of FHWA Modified Gates Equation.....	55
3	EVALUATION OF MNDOT BRIDGE OFFICE DATA.....	57
3.1	Overview.....	57
3.2	Data Review .....	57

3.3	Data Match.....	58
3.4	Summary of Data .....	60
3.5	Observations Regarding MnDOT Dynamic Measurements Database .....	62
3.6	Preliminary Evaluation of the Capacity Predictions .....	63
3.7	Conclusions Derived from the Initial Evaluation .....	76
3.7.1	General .....	76
3.7.2	Analysis.....	77
3.8	Final Evaluation of the Capacity Predictions.....	77
3.8.1	Overview.....	77
3.8.2	Performed Analyses .....	77
3.8.3	Presentation of Results.....	78
3.8.4	Conclusions.....	78
4	RE-ASSESSMENT OF FORMAT AND LRFD RESISTANCE FACTORS FOR THE NEW MNDOT PILE DRIVING FORMULA (MPF12).....	84
4.1	Overview .....	84
4.2	Examination of the Extreme Over-Prediction Cases in the Database.....	84
4.2.1	Rationale and Method of Approach .....	84
4.2.2	Examination of the H Pile Cases .....	87
4.2.3	Examination of the Pipe-Pile Cases .....	89
4.2.4	MnDOT Research Panel Evaluation.....	92
4.3	Re-Evaluation of Dynamic Equations Considering Outliers .....	92
4.3.1	Initial Analysis .....	92
4.3.2	Evaluation of Outliers .....	98
4.3.3	MnDOT Research Panel Evaluation.....	99
4.4	Re-Evaluation of the New MnDOT Dynamic Equation for EOD and BOR Low and High Blow Count .....	99
4.4.1	Summary Tables .....	99
4.4.2	Intermediate Conclusions.....	99
4.5	Evaluation of MPF12 and Resistance Factors Development.....	108
4.5.1	Graphical Presentation .....	108
4.5.2	Summary Tables .....	118
4.5.3	Driving Resistance Bearing Graphs.....	119
4.5.4	Calculated Resistance Factors.....	119
4.6	MPF12 Final Format and Recommended Resistance Factors .....	120
5	EVALUATION OF MPF12 FOR PRECAST PRESTRESSED CONCRETE PILES .....	122
5.1	Overview .....	122
5.2	PSC Database Summary .....	122
5.3	Statistical Analysis.....	124
5.4	Broader Examination of the MPF12 Equation.....	131
5.5	Resistance Factors.....	134

5.6	Recommendations.....	134
6	EVALUATION OF MPF12 FOR TIMBER PILES.....	135
6.1	Overview.....	135
6.2	Timber Pile Database.....	135
6.2.1	Summary.....	135
6.2.2	Pile Capacity Evaluation.....	136
6.2.3	Extrapolated Non-Failed Load Tests.....	137
6.3	Statistical Analysis.....	140
6.3.1	Equation Modification.....	140
6.3.2	Performance and Graphical Presentation.....	140
6.3.3	Control Cases.....	143
6.4	Resistance Factors.....	143
6.5	Recommendations.....	143
7	MINNESOTA LOAD TESTING PROGRAM.....	144
7.1	Overview.....	144
7.2	TP1 Load Test at Victoria, MN.....	145
7.2.1	General.....	145
7.2.2	Static Capacity Evaluation.....	145
7.2.3	Load and Resistance.....	146
7.2.4	Dynamic Observations, Predictions, and Static Load Test Results.....	147
7.3	TP2 Load Test at Arden Hills (Old Snelling).....	150
7.3.1	General.....	150
7.3.2	Static Load Test.....	150
7.3.3	Dynamic Observations and Predictions.....	154
7.4	Comparisons Between Statically Measured and Dynamically Predicted Capacity...156	
7.4.1	Nominal Resistance.....	156
7.4.2	Factored Resistance.....	156
8	WEAP ANALYSIS (WAVE EQUATION ANALYSIS PROGRAM).....	159
8.1	Overview.....	159
8.2	Design and Construction Process of Deep Foundations.....	160
8.3	The Accuracy of WEAP for Capacity Evaluation.....	160
8.4	WEAP Analyses for Typical MnDOT Pile Driving Conditions.....	164
8.4.1	Overview.....	164
8.4.2	Typical WEAP Analyses for MnDOT Conditions.....	165
8.4.3	Driving Resistance Charts.....	165
8.5	WEAP Adjustment Following Dynamic Measurements.....	177
8.5.1	Overview – Victoria Load Test.....	177
8.5.2	Subsurface Conditions.....	177
8.5.3	Design stage WEAP Analysis.....	181
8.5.4	Construction Stage WEAP Analysis.....	187

8.5.5	GeoDynamica Modified WEAP for the Construction Stage .....	187
8.5.6	Instructions for WEAP Modifications Following Dynamic Measurements .....	193
8.6	WEAP – Wave Equation Analysis of Piles – Submittal .....	194
8.6.1	Description .....	194
8.6.2	Submittals .....	195
8.7	MnDOT Specifications .....	197
9	STATIC LOAD TEST – PROCEDURES, INTERPRETATIONS AND SPECIFICATIONS .....	199
9.1	Background .....	199
9.1.1	Overview .....	199
9.1.2	Principles .....	200
9.1.3	Pile Testing in Light of Pulse Duration and Relative Wavelength .....	201
9.2	Review of Static Pile Load Testing Methods .....	203
9.2.1	ASTM Procedures .....	203
9.2.2	Massachusetts Department of Transportation (MassDOT) Procedures .....	206
9.2.3	Static-Cyclic (Express) Load Test .....	208
9.3	Static Pile Load Test Interpretation Procedures .....	209
9.3.1	Overview .....	209
9.3.2	Consistent Presentation of Load-Settlement Relationship .....	209
9.3.3	Davisson’s Criterion .....	210
9.3.4	Shape of Curve .....	212
9.3.5	Limited Total Settlement Methods .....	212
9.3.6	DeBeer’s Log-Log Method .....	212
9.3.7	Representative Static Capacity .....	213
9.4	Full Scale Pile Testing Examining Testing Methods and Driven Piles Capacity Evaluation .....	214
9.4.1	Overview .....	214
9.4.2	Static Load Test Set-Up .....	214
9.4.3	Static Load Testing Procedures and Records .....	217
9.4.4	Test Pile #1 .....	217
9.4.5	Test Pile #2 .....	223
9.4.6	Test Pile #3 .....	230
9.4.7	Conclusions .....	237
9.5	Deep Foundations Nominal Strength for Reliability Based Design .....	237
9.5.1	Overview .....	237
9.5.2	The Uncertainty of the Various Failure Criteria .....	237
9.5.3	Evaluation of a Modification for Davisson’s Criterion .....	239
9.5.4	Load Test Procedure for Statically Loaded Driven Piles .....	242
9.6	Extrapolation of Non—Failed Static Load Test .....	244

9.6.1	Background .....	244
9.6.2	Paikowsky and Tolosko (1999) Extrapolation Method .....	244
9.6.3	Evaluation of the Extrapolation Method .....	247
9.6.4	Extrapolation Implementation in MnDOT Load Test Database and Program .....	250
9.7	Recommended Load Test Procedures and Submittals for the MnDOT .....	250
9.7.1	Recommended Load Test Procedures and Interpretation .....	250
9.7.2	Pre Load-Test Submittal Requirements .....	251
9.7.3	Load Test Reporting .....	252
9.7.4	Database/Data Requirements for MnDOT Load Testing Program .....	253
10	SUMMARY CONCLUSIONS AND RECOMMENDATIONS .....	255
10.1	Summary .....	255
10.2	Conclusions .....	259
10.3	Recommendations .....	262
	REFERENCES .....	263

APPENDIX A	Summary Tables
APPENDIX B	Hammer Specifications
APPENDIX C	Load Testing Report – TP1 in Victoria, MN, July 2012, Minnowa Construction, Inc.
APPENDIX D	Load Testing Report – TP2 in Aren Hills, MN, January 2013, American Engineering Testing, Inc., Prepared for Lunda Construction Company

## List of Figures

Figure 1. Graphic representation of predicted vs measured capacity .....	11
Figure 2. Predicted versus measured capacity from Flaate 1964.....	12
Figure 3. Predicted versus measured capacity from Frigaszy 1988, 1989.....	14
Figure 4. Predicted versus measured capacity from Paikowsky et al., 1994 .....	15
Figure 5. Predicted versus measured capacity for Florida DOT.....	16
Figure 6. Predicted versus measured capacity from Eslami, 1996 .....	17
Figure 7. Predicted versus measured capacity for FHWA database using EOD data) .....	21
Figure 8. Predicted versus measured capacity for FHWA database using BOR data .....	22
Figure 9. International database selected predictions of dynamic equations vs. SLT dynamic. ..	26
Figure 10. Comprehensive database selected dynamic and static methods vs. SLT. ....	28
Figure 11. FHWA-Gates vs. static methods .....	29
Figure 12. Dynamic vs. static capacities for the Illinois database .....	32
Figure 13. Cumulative distribution of FHWA-Gates/IDOT static data, Illinois database.....	35
Figure 14. Dynamic vs. corrected static capacities for the Corrected Illinois database .....	37
Figure 15. Dynamic vs. corrected static capacities for the comprehensive database .....	39
Figure 16. Resistance factors vs. reliability index for different predictive methods using FOSM. .....	43
Figure 17. Resistance factors vs. reliability index for different predictive methods using FORM .....	44
Figure 18. Graphic solutions of formula.....	52
Figure 19. Probability distribution and cumulative distribution function for energy transfer when driving Pipe-Piles with diesel hammers in the MnDOT dynamic measurements database. ....	59
Figure 20. CAPWAP vs. Energy Approach prediction method all CIP piles.....	67
Figure 21. CAPWAP vs. Energy Approach prediction 16" x 5/16" CIP piles .....	67
Figure 22. CAPWAP vs. Energy Approach prediction 16" x 1/4" CIP piles .....	67
Figure 23. CAPWAP vs. Energy Approach prediction 12.75" x 1/4" CIP piles .....	67
Figure 24. CAPWAP vs. Energy Approach prediction 12" x 1/4" CIP piles .....	67
Figure 25. CAPWAP vs. Energy Approach prediction 12.75" x 5/16" CIP piles .....	67
Figure 26. CAPWAP vs. Energy Approach prediction 12" x 5/16" CIP piles .....	68
Figure 27. CAPWAP vs. Gates formula all CIP piles .....	68
Figure 28. CAPWAP vs. Gates formula 16" x 5/16" CIP piles.....	68
Figure 29. CAPWAP vs. Gates formula 16" x 1/4" CIP piles.....	68
Figure 30. CAPWAP vs. Gates formula 12.75" x 1/4" CIP piles.....	68
Figure 31. CAPWAP vs. Gates formula 12" x 1/4" CIP piles.....	68
Figure 32. CAPWAP vs. Gates formula 12.75" x 5/16" CIP piles.....	69
Figure 33. CAPWAP vs. Gates formula 12" x 5/16" CIP piles.....	69
Figure 34. CAPWAP vs. Gates formula all CIP piles .....	69
Figure 35. CAPWAP vs. Gates formula 16" x 5/16" CIP piles.....	69
Figure 36. CAPWAP vs. Gates formula 16" x 1/4" CIP piles.....	69

Figure 37. CAPWAP vs. Gates formula 12.75" x 1/4" CIP piles.....	69
Figure 38. CAPWAP vs. Gates formula 12" x 1/4" CIP piles.....	70
Figure 39. CAPWAP vs. Gates formula 12.75" x 5/16" CIP piles.....	70
Figure 40. CAPWAP vs. Gates formula 12" x 5/16" CIP piles.....	70
Figure 41. CAPWAP vs. Gates formula all CIP piles .....	70
Figure 42. CAPWAP vs. Gates formula 16" x 5/16" CIP piles.....	70
Figure 43. CAPWAP vs. Gates formula 16" x 1/4" CIP piles.....	70
Figure 44. CAPWAP vs. Gates formula 12.75" x 1/4" CIP ples.....	71
Figure 45. CAPWAP vs. Gates formula 12" x 1/4" CIP piles.....	71
Figure 46. CAPWAP vs. Gates formula 12.75" x 5/16" CIP piles.....	71
Figure 47. CAPWAP vs. Gates formula 12" x 5/16" CIP piles.....	71
Figure 48. CAPWAP vs. WSDOT formula all CIP piles .....	71
Figure 49. CAPWAP vs. WSDOT formula 16" x 5/16" CIP piles .....	71
Figure 50. CAPWAP vs. WSDOT formula 16" x 1/4" CIP piles .....	72
Figure 51. CAPWAP vs. WSDOT formula 12.75" x 1/4" CIP piles .....	72
Figure 52. CAPWAP vs. WSDOT formula 12" x 1/4" CIP piles .....	72
Figure 53. CAPWAP vs. WSDOT formula 12.75" x 5/16" CIP piles .....	72
Figure 54. CAPWAP vs. WSDOT formula 12" x 5/16" CIP piles .....	72
Figure 55. CAPWAP vs. current MnDOT formula all CIP piles .....	72
Figure 56. CAPWAP vs. current MnDOT formula 16" x 5/16" CIP piles.....	73
Figure 57. CAPWAP vs. current MnDOT formula 16" x 1/4" CIP piles.....	73
Figure 58. CAPWAP vs. current MnDOT formula 12.75" x 1/4" CIP piles.....	73
Figure 59. CAPWAP vs. current MnDOT formula 12" x 1/4" CIP piles.....	73
Figure 60. CAPWAP vs. current MnDOT formula 12.75" x 5/16" CIP piles.....	73
Figure 61. CAPWAP vs. current MnDOT formula 12" x 5/16" CIP piles.....	73
Figure 62. CAPWAP vs. New MnDOT formula (35) All CIP piles .....	74
Figure 63. CAPWAP vs. New MnDOT formula (35) 16" x 5/16" CIP piles.....	74
Figure 64. CAPWAP vs. New MnDOT formula (35) 16" x 1/4" CIP piles.....	74
Figure 65. CAPWAP vs. New MnDOT formula (35) 12.75" x 1/4" CIP piles.....	74
Figure 66. CAPWAP vs. New MnDOT formula (35) 12" x 1/4" CIP piles.....	74
Figure 67. CAPWAP vs. New MnDOT formula (35) 12.75" x 5/16" CIP piles.....	74
Figure 68. CAPWAP vs. New MnDOT formula (35) 12" x 5/16" CIP piles.....	75
Figure 69. CAPWAP vs. New MnDOT formula (30) All CIP piles .....	75
Figure 70. CAPWAP vs. New MnDOT formula (30) 16" x 5/16" CIP piles.....	75
Figure 71. CAPWAP vs. New MnDOT formula (30) 16" x 1/4" CIP piles.....	75
Figure 72. CAPWAP vs. New MnDOT formula (30) 12.75" x 1/4" CIP piles.....	75
Figure 73. CAPWAP vs. New MnDOT formula (30) 12" x 1/4" CIP piles.....	75
Figure 74. CAPWAP vs. New MnDOT formula (30) 12.75" x 5/16" CIP piles.....	76
Figure 75. CAPWAP vs. New MnDOT formula (30) 12" x 5/16" CIP piles.....	76
Figure 76. CAPWAP vs. Energy Approach prediction method all CIP piles.....	82



Figure 77. CAPWAP vs. Modified Gates formula ( $W \cdot H$ ) all CIP piles .....	82
Figure 78. CAPWAP vs. Modified Gates formula ( $75\% \cdot E_n$ ) all CIP piles .....	82
Figure 79. CAPWAP vs. Modified Gates formula ( $E_n$ ) all CIP piles .....	82
Figure 80. CAPWAP vs. WSDOT formula ( $E = W_r \cdot h$ ) all CIP piles .....	82
Figure 81. CAPWAP vs. current MnDOT all CIP piles .....	82
Figure 82. CAPWAP vs. New MnDOT formula (35) ( $E = E_n$ ) all CIP piles .....	83
Figure 83. CAPWAP vs. New MnDOT formula (35) ( $E = W_r \cdot h$ ) all CIP piles .....	83
Figure 84. CAPWAP vs. New MnDOT formula (30) ( $E = E_n$ ) all CIP piles .....	83
Figure 85. CAPWAP vs. New MnDOT formula (30) ( $E = W_r \cdot h$ ) all CIP piles .....	83
Figure 86. Bias vs. blow count for Pipe Pile EOD cases only (low and high outliers removed) for the New MnDOT Equation (coefficient 40, 75% energy); (a) linear scale, and (b) log scale....	109
Figure 87. Bias vs. blow count for Pipe Pile EOD cases only (low and high outliers removed) for the New MnDOT Equation (coefficient 40, 75% energy) where the blow count is limited to 15bpi maximum; (a) linear scale, and (b) average and standard deviation per 2bpi segments. .	110
Figure 88. Bias vs. blow count for Pipe Pile BOR cases only.....	111
Figure 89. Bias vs. blow count for Pipe Pile BOR cases only.....	112
Figure 90. Bias vs. blow count for H Pile EOD cases only.....	113
Figure 91. Bias vs. blow count for H Pile EOD cases only.....	114
Figure 92. Bias vs. blow count for H Pile BOR cases only.....	115
Figure 93. Bias vs. blow count for H Pile BOR cases only . .....	116
Figure 94. Average and standard deviation of the bias vs. blow count for H Pile cases .....	117
Figure 95. New MnDOT equation vs. blow count for set energy values. ....	120
Figure 96. Measured static capacity vs. New MnDOT dynamic equation prediction for 38 EOD cases. ....	126
Figure 97. Measured static capacity vs. New MnDOT dynamic equation prediction for 31 EOD cases ( $B.C. \geq 2$ bpi).....	126
Figure 98. Measured static capacity vs. New MnDOT dynamic equation prediction for 99 BOR cases. ....	127
Figure 99. Measured static capacity vs. New MnDOT dynamic equation prediction for 96 BOR cases ( $B.C. \geq 2$ bpi).....	127
Figure 100. Bias vs. blow count for PSC EOD cases for the New MnDOT Equation.....	128
Figure 101. Bias vs. blow count for PSC BOR cases for the New MnDOT Equation.....	129
Figure 102. Bias versus PSC pile size (in) for (a) EOD cases and (b) BOR cases.....	130
Figure 103. Davisson's criteria predicted static capacity versus CAPWAP prediction for 35 EOD cases. ....	132
Figure 104. Davisson's criteria predicted static capacity versus CAPWAP prediction for 99 BOR cases. ....	132
Figure 105. CAPWAP predicted static capacity versus New MnDOT dynamic equation prediction for 38 EOD cases. ....	133

Figure 106. CAPWAP predicted static capacity versus New MnDOT dynamic equation prediction for 106 BOR cases.....	133
Figure 107. Shape of Curve versus Davisson's Criteria for determining the static capacity of 28 timber piles.....	137
Figure 108. Extrapolated load-displacement curve for TS #13 Pile #1.....	138
Figure 109. Extrapolated load-displacement curve for TS #13 Pile #2.....	138
Figure 110. Extrapolated load-displacement curve for TS #13 Pile #12.....	139
Figure 111. Extrapolated load-displacement curve for TS #13 Pile #14.....	139
Figure 112. Measured static capacity vs. New MnDOT dynamic equation prediction for 28 timber pile cases.....	141
Figure 113. Bias vs. blow count for timber pile cases for the (0.50)*MPF12 (75% energy).....	142
Figure 114. 500 ton MnDOT load frame being used at Bridge 10003 in Victoria, Minnesota..	145
Figure 115. Static pile capacity predictions for Bridge 10003 in Victoria, Minnesota .....	146
Figure 116. Additional load vs. displacement of pile top – static load test results for Bridge 10003 in Victoria, Minnesota .....	148
Figure 117. Load versus pile head movement for each of the pile's top LVDT sensors of Test Pile 2 (per Report No. 22-01025 submitted to MnDOT by American Engineering Testing, Inc.) .....	151
Figure 118. Load-displacement relations for TP2 based on top displacement of LVDT 1-4 and tip displacement based on LVDT 6.....	152
Figure 119. Load-displacement relations for TP2 based on top displacement of LVDT 1-2 and tip displacement based on LVDT 6.....	152
Figure 120. Measured and extrapolated load-displacement relations for TP2 based on LVDT's 1 – 4.....	153
Figure 121. Measured and extrapolated load-displacement relations for TP2 based on LVDT's 1 – 2.....	153
Figure 122. Nominal resistance static capacity ( $R_s$ ) vs. predicted dynamic capacity ( $R_u$ ): (a) EOD and (b) restrikes .....	157
Figure 123. Factored resistance of the nominal static capacity ( $R_s$ ) vs. the factored predicted dynamic capacity ( $R_u$ ): (a) EOD and (b) restrikes .....	158
Figure 124. Design and construction process for deep foundations (Paikowsky et al., 2004) ...	161
Figure 125. WEAP utilization in the design and construction process of driven piles .....	162
Figure 126. WEAP analysis results presenting static capacity vs. driving resistances for HP 12x53 piles driven by a D-12 hammer.....	170
Figure 127. WEAP analysis results presenting static capacity vs. driving resistances for HP 12x53 piles driven by a D-19 hammer .....	171
Figure 128. WEAP analysis results presenting static capacity vs. driving resistances for HP 12x53 piles driven by a D-19 hammer.....	172
Figure 129. WEAP analysis results presenting static capacity vs. driving resistances for CEP 12in x 0.25in piles driven by a D-12 hammer .....	173

Figure 130. WEAP analysis results presenting static capacity vs. driving resistances for CEP 12in x 0.25in piles driven by a D-19 hammer .....	174
Figure 131. WEAP analysis results presenting static capacity vs. driving resistances for CEP 12in x 0.25in piles driven by a D-25 hammer .....	175
Figure 132. WEAP analysis results presenting static capacity vs. driving resistances for CEP 16in x 0.3125in piles driven by a D-30 hammer .....	176
Figure 133. Victoria, Minnesota Bridge 10003 longitudinal cross-section of subsurface conditions based on drilled SPT boring (T05).....	178
Figure 134. Victoria, Minnesota Bridge 10003 longitudinal cross-section of subsurface conditions based on drilled CPT boring (T05) .....	179
Figure 135. Boring T05.....	180
Figure 136. Resistance distribution input file – Victoria L.T. design stage .....	182
Figure 137. Input file for drivability analysis and resistance distribution along the pile based on the input table presented in Figure 136.....	183
Figure 138. Drivability analysis results .....	184
Figure 139. Driving log of TP1 Victoria static load test.....	185
Figure 140. Abutment W input file.....	188
Figure 141. Abutment W driving resistance graph.....	189
Figure 142. Input file for GeoDynamica modified WEAP analysis using CAPWAP EOD results .....	191
Figure 143. GeoDynamica modified WEAP driving resistance graph.....	192
Figure 144. Driving resistance summary of Geodynamica modified WEAP, MPF12 and the static load test results.....	193
Figure 145. Sample pile driving equipment data form .....	196
Figure 146. Typical load testing values for Pile A acceleration vs. (a) relative wavelength, and (b) force duration .....	200
Figure 147. Typical loading durations for various tests performed on Test Pile #3 by the Geotechnical Engineering Research Laboratory of the University of Massachusetts Lowell, at the Newbury test site.....	203
Figure 148. Static pile load testing procedures according to ASTM.....	204
Figure 149. Static pile load testing procedures according to MassDOT .....	207
Figure 150. Load-settlement curve with (a) a non-specific scale for Pile Case No. 5, and (b) with the elastic compression line inclined at 20 degrees .....	210
Figure 151. Load-settlement curve for Pile Case No. 5 of the PD/LT data set with the elastic compression line inclined at 20 degrees and different ultimate capacity interpretation methods .....	211
Figure 152. Load-settlement data plotted on a logarithmic scale for Pile Case No. 5 to determine the failure load according to DeBeer’s method .....	213
Figure 153. General soil profile and planned test pile layouts .....	215
Figure 154. Plan view of test pile layout and reaction piles .....	216

Figure 155. Static load test frame used for test pile cluster in Newbuty, MA .....	216
Figure 156. Short duration test plots: (a) load vs. time, (b) displacement vs. time, and (c) load vs. displacement (Paikowsky and Hajduk, 1999).....	218
Figure 157. Osterberg static-cyclic test plots: (a) load vs. time, (b) displacement vs. time, and (c) load vs. displacement .....	219
Figure 158. Test Pile #1 load vs. displacement for static cyclic test .....	219
Figure 159. Incremental static-cyclic test plots: (a) load vs. time, (b) displacement vs. time, and (c) load vs. displacement.....	220
Figure 160. Details of the load vs. displacement relationship for Test Pile #1 .....	221
Figure 161. Applied load vs. permanent displacement of incremental static cyclic test .....	221
Figure 162. Static-cyclic test plots: (a) load vs. time, (b) displacement vs. time, and (c) load vs. displacement .....	221
Figure 163. Test Pile #1 load vs. displacement for static cyclic test .....	222
Figure 164. Short duration test plots: (a) load vs. time, (b) displacement vs. time, and (c) load vs. displacement .....	222
Figure 165. Slow maintained test plots: (a) load vs. time, (b) displacement vs. time, and (c) load vs. displacement.....	224
Figure 166. Short duration test plots: (a) load vs. time, (b) displacement vs. time, and (c) load vs. displacement .....	225
Figure 167. Static-cyclic test plots: (a) load vs. time, (b) displacement vs. time, and (c) load vs. displacement .....	225
Figure 168. Test Pile #2 load vs. displacement for static cyclic test .....	226
Figure 169. Comparison of load vs. displacement for various tests on TP#2 .....	226
Figure 170. Test Pile #2 short duration test load distribution.....	227
Figure 171. Test Pile #2 slow maintained test load distribution.....	229
Figure 172. Test Pile #2 static cyclic test load distribution .....	229
Figure 173. Test Pile #2 short duration & static cyclic comparison of load distributions.....	229
Figure 174. Test Pile #2 slow maintained & static cyclic comparison of load distributions.....	229
Figure 175. Slow maintained test plots: (a) load vs. time, (b) displacement vs. time, and (c) load vs. displacement.....	231
Figure 176. Short duration test plots: (a) load vs. time, (b) displacement vs. time, and (c) load vs. displacement .....	232
Figure 177. Static-cyclic test plots: (a) load vs. time, (b) displacement vs. time, and (c) load vs. displacement .....	232
Figure 178. Test Pile #3 load vs. displacement for static cyclic test .....	233
Figure 179. Comparison of load vs. displacement for various tests on TP#3 .....	233
Figure 180. Test Pile #3 slow maintained test load distributions .....	234
Figure 181. Test Pile #3 short duration test load distributions .....	236
Figure 182. Test Pile #3 static cyclic test load distribution .....	236
Figure 183. Test Pile #3 slow maintained test & static cyclic comparison of load distributions.....	236

Figure 184. Test Pile #3 short duration test & static cyclic comparison of load distributions ...	236
Figure 185. Histogram and frequency distributions of $K_{SD}$ for 186 PD/LT2000 pile cases in all types of soils .....	238
Figure 186. Histogram and frequency distributions of $K_{SD}$ and $K_{SLD}$ for 30 and 20 PD/LT2000 pile-cases, respectively, in all types of soils .....	241
Figure 187. $K_{SLD}$ values vs. pile diameter for all large diameter PD/LT2000 pile-cases, all types of soils.....	242
Figure 188. Comparison between pile capacity based on davisson's criterion for slow maintained load tests and static cyclic load test capacity for 75 piles.....	243
Figure 189. Displacement over load versus displacement for Pile Case No. 5 according to chin's failure determination method.....	245
Figure 190. Actual and extrapolated load-settlement relations for the re-analysis of Pile Case No. 14 using ranges of available data .....	248
Figure 191 actual and extrapolated load-settlement relations for the analysis of Pile Case No. 14 using ranges of the designated static capacity .....	248

## List of Tables

Table 1. Construction pile evaluation practices Midwest states (May 2010 with updates).....	8
Table 2. Statistical parameters for $Q_p/Q_m$ values for all load test data from Flaate 1964.....	12
Table 3. Statistical parameters for $Q_p/Q_m$ values for all load test data from Frigaszy 1988, 1989. .....	14
Table 4. Statistical parameters for $Q_p/Q_m$ values for all load test data from Paikowsky et al., 1994.....	15
Table 5. Statistical parameters for $Q_p/Q_m$ values for all load test data from Davidson and Townsend, 1996. (Long and Maniaci, 2000).....	17
Table 6. Statistical parameters for $Q_p/Q_m$ values for data from Eslami, 1996. (Long and Maniaci, 2000).....	18
Table 7. Statistical parameters for $Q_p/Q_m$ for FHWA database (Long and Maniaci, 2000).....	19
Table 8. International database selected dynamic/SLT statistics for all piles (Long et al., 2009a) .....	25
Table 9. Comprehensive database dynamic and static methods vs. SLT statistics (Long et al., 2009a).....	28
Table 10. Dynamic vs. static method statistics (Long et al., 2009a).....	30
Table 11. Capacity ratio statistics for all piles in the Illinois database.....	33
Table 12. Capacity ratio statistics for H-Piles in the Illinois database.....	33
Table 13. Capacity ratio statistics for Pipe-Piles in the Illinois database.....	33
Table 14. Capacity ratio statistics for piles in sand in the Illinois database.....	33
Table 15. Capacity ratio statistics for piles in clay in the Illinois database.....	34
Table 16. Capacity ratio statistics for H-Piles in the Illinois database.....	34
Table 17. Capacity ratio statistics for H-Piles in clay in the Illinois database.....	34
Table 18. Capacity ratio statistics for H-Piles in the Illinois database.....	34
Table 19. Capacity ratio statistics for Pipe Piles in clay in the Illinois database.....	35
Table 20. Correction factors.....	36
Table 21. Statistics for dynamic vs. corrected static methods, corrected Illinois database (Long et al., 2009a).....	38
Table 22. Statistics for dynamic vs. corrected static methods, comprehensive database (Long et al., 2009a).....	39
Table 23. Databases best agreement methods summary.....	40
Table 24. Parameter $F_{eff}$ to be used in Equation 9 for hammer and pile type combinations.....	40
Table 25. Correction factors for Equation 10.....	41
Table 26. Statistical parameters and resistance factors for the predictive methods based on $Q_M/Q_P$ values using FOSM and FORM (Long et al. 2009).....	42
Table 27. Long et al. (2009a) vs. Paikowsky et al. (2009) statistical results.....	46
Table 28. Long et al. (2009a), vs. Paikowsky et al. (2009) statistical results regarding the bias definition and extreme cases excluded.....	46
Table 29. Statistical parameters developed by Long et al., 2009b. ....	48

Table 30. Summary of resistance factors developed using FORM and at a target reliability ( $\beta_T = 2.33$ ) (Long et al., 2009b).	49
Table 31. Summary of resistance factors using FORM and $\beta_T = 2.33$ , based on distributions matching the extreme cases (Long et al., 2009b).	49
Table 32. Gates 1957 dynamic equation prediction for H and Pipe Piles (summary of results from Paikowsky et al., 2009).	53
Table 33. FHWA (1988) Modified Gates dynamic equation prediction for H and Pipe Piles (summary of results from Paikowsky et al., 2009).	56
Table 34. Hammers with different rated energy	57
Table 35. Summary of driving data statistics for MnDOT database	58
Table 36. Summary of total pile length	61
Table 37. Summary of pile cases categorized based on soil conditions	61
Table 38. Summary of driving criteria – pile performance	61
Table 39. Equipment summary	61
Table 40. Investigated equations.	64
Table 41. Summary of available cases for CAPWAP and Energy Approach based on dynamic measurements.	64
Table 42. Summary of statistical analysis and best fit line correlation (page 1/2)	65
Table 43. Updated investigated equations	79
Table 44. Summary of statistical analysis and best fit line correlation	80
Table 45. Summary of statistical analysis and best fit line correlation	81
Table 46. Summary of the extreme data cases related to MnDOT study	86
Table 47. Dynamic equation predictions for H-Piles EOD condition only	93
Table 48. Dynamic equation predictions for Pipe Piles EOD condition only	94
Table 49. Summary of selective outlier references for H Piles	95
Table 50. Summary of selective outliers references for Pipe Piles.	96
Table 51. Details of additional low end outliers encountered in the analyses of the Pipe Piles database.	97
Table 52. Dynamic equation predictions for Pipe Piles EOD condition only	100
Table 53. Dynamic equation predictions for Pipe Piles EOD condition only blow count limited to max 15BPI (20 cases)	101
Table 54. Dynamic equation predictions for Pipe Piles BOR condition only	102
Table 55. Dynamic equation predictions for Pipe Piles BOR condition only blow count limited to max 15 BPI (17 cases)	103
Table 56. Dynamic equation predictions for H-Piles EOD condition only	104
Table 57. Dynamic equation predictions for H-Piles EOD condition only blow count limited to max 15 BPI (50 cases)	105
Table 58. Dynamic equation predictions for H-Piles BOR condition only	106
Table 59. Dynamic equation predictions for H-Piles BOR condition only blow count limited to max 15 BPI (16 cases)	107

Table 60. Statistical summary based on blow count of Pipe Pile EOD cases (low and high outliers removed) for the New MnDOT Equation (coefficient 40, 75% energy) .....	118
Table 61. Statistical summary based on blow count of Pipe Pile BOR cases (low and high outliers removed) for the New MnDOT Equation (coefficient 40, 75% energy) .....	118
Table 62. Statistical summary based on blow count of H Pile EOD cases (low and high outliers removed) for the New MnDOT Equation (coefficient 40, 75% energy) .....	119
Table 63. Statistical summary based on blow count of H Pile BOR cases (low and high outliers removed) for the New MnDOT Equation (coefficient 40, 75% energy) .....	119
Table 64. Summary of PSC data set attributes .....	123
Table 65. PSC cases categorized by pile shape/size, time of driving and driving resistance .....	123
Table 66. Summary of statistics and resistance factors for PSC piles categorized by pile shape/size, time of driving and driving resistance .....	125
Table 67. Summary of timber pile data set attributes .....	135
Table 68. Range of timber pile dimensions .....	136
Table 69. Summary of statistics and resistance factors for timber piles .....	140
Table 70. Summary of timber pile control cases .....	143
Table 71. Computed pile load and required nominal pile bearing resistances for Bridge 10003 in Victoria, Minnesota (per project plans) .....	147
Table 72. Nominal resistances from dynamic analyses of the test pile TP1 .....	149
Table 73. Nominal and factored resistances of the various testing methods .....	149
Table 74. Nominal resistances from dynamic analyses of the test pile TP2 .....	155
Table 75. Nominal and factored resistances of the various testing methods .....	155
Table 76. The performance of the dynamic methods: statistical summary and resistance factors compared to MPF12 performance .....	164
Table 77. WEAP plan of study for MnDOT prevailing driving conditions .....	166
Table 78. Summary of typical pile, hammer and soil conditions for MnDOT pile driving to be used in WEAP analysis .....	168
Table 79. Drivability analysis results table .....	184
Table 80. Summary of WEAP predicted and measured during pile driving .....	186
Table 81. Abutment W driving resistance table .....	189
Table 82. Summary table for WEAP parameters prior and post construction along with CAPWAP parameters .....	190
Table 83. GeoDynamica modified WEAP driving resistance table .....	192
Table 84. Typical Key Attributes of Different Types of Pile Tests .....	202
Table 85. Summary of static load test procedures .....	204
Table 86. Summary of static load tests conducted on Newbury test pile cluster .....	217
Table 87. Summary of pile capacity interpretation for Test Pile #2 .....	224
Table 88. Relations between tip and applied loads for test pile #2 distribution analysis .....	228
Table 89. Summary of pile capacity interpretation for Test Pile #3 .....	231
Table 90. Relations between tip and applied loads for test pile #3 distribution analysis .....	235



Table 91. Summary of the interpretation methods applied to the static load test curves in PD/LT2000 .....	239
Table 92. Mean and standard deviation of the ratio between the extrapolated capacity based on the extrapolation method and the actual capacity .....	249
Table 93. Mean and standard deviation of the ratio between the extrapolated capacity based on the extrapolation method and the actual capacity .....	249
Table 94. Summary of the final formulation known as MPF12 (Minnesota Pile Formula 2012) adopted for use .....	261

## EXECUTIVE SUMMARY

Driven piles are the most common foundation solution used in bridge construction across the U.S. (Paikowsky et al., 2004). The major problem associated with the use of deep foundations is the ability to reliably verify the capacity and the integrity of the installed element in the ground. Dynamic analyses of driven piles are methods attempting to obtain the static capacity of a pile, utilizing its behavior during driving. The dynamic analyses are based on the premise that under each hammer blow, as the pile penetrates into the ground, a quick pile load test is being carried out. Dynamic equations (aka pile driving formulas) are the earliest and simplest forms of dynamic analyses. MnDOT used its own pile driving formula; however, its validity and accuracy has never been thoroughly evaluated. With the implementation of Load Resistance Factor Design (LRFD) in Minnesota in 2005, and its mandated use by the Federal Highway Administration (FHWA) in 2007, the resistance factor associated with the use of the MnDOT driving formula needed to be calibrated and established.

Systematic probabilistic-based evaluation of a resistance factor requires quantifying the uncertainty of the investigated method. As the investigated analysis method (the model) contains large uncertainty itself (in addition to the parameters used for the calculation), doing so requires:

- (i) Knowledge of the conditions in which the method is being applied, and
- (ii) A database of case histories allowing comparison between the calculated value to one measured.

The first phase of the research addressed these needs via:

- (i) Establishing the MnDOT state of practice in pile design and construction, and
- (ii) Compilation of a database of driven pile case histories (including field measurements and static load tests to failure) relevant to Minnesota design and construction practices.

The first phase of the study was presented in a research report by Paikowsky et al. (2009). Phase I concentrated on establishing MnDOT practices, developing databases related to these practices and examining different dynamic equations as well as developing new equations. The proposed resistance factors developed in Phase I for the driving of pipe piles were assessed to be conservative in light of the MnDOT traditional design and construction practices, and hence, Phase II of the research was initiated.

Phase II of the study was established to:

1. Re-evaluate resistance factors for the Load Resistance Factor Design (LRFD) implementation as obtained in the Phase I study,
2. Examine other dynamic pile driving formulae and other Midwest states practices,
3. Recommend to MnDOT an appropriate formula (and associated resistance factors) for implementation,

4. Examine the recommended formula in use with timber and prestressed precast concrete piles,
5. Examine WEAP analyses procedures for MN conditions and recommend procedures to be implemented, and
6. Examine load test procedures, interpretations and submittals.

The operative findings in Phase II relevant to the dynamic pile formula to be used by the MnDOT are the following:

1. The final formulation known as MPF12 (Minnesota Pile Formula 2012) that was adopted for use:

$$R_n = 20 \sqrt{\frac{W \times H}{1,000}} \times \log\left(\frac{10}{s}\right)$$

where  $R_n$  = nominal resistance (tons),  $H$  = stroke (height of fall) (ft),  $W$  = weight of ram (lbs),  $s$  = set (pile permanent displacement per blow) (inch). The value of the energy ( $W \cdot H$ ) used in the dynamic formula shall not exceed 85% of the manufacturer's maximum rated energy for the hammer used considering the settings used during driving.

2. The MPF12 is to be used with the following resistance factors (RF) in order to obtain the factored resistance:

$$R_r = \phi \times R_n$$

For pipe and concrete piles,  $\phi = 0.50$ ,  $2 < BC \leq 15BPI$

For H piles,  $\phi = 0.60$ ,  $2 < BC \leq 15BPI$

3. The MPF12 recommended for timber piles is:

$$R_n = 10 \sqrt{\frac{W \times H}{1,000}} \times \log\left(\frac{10}{s}\right)$$

Where  $\phi = 0.60$

4. Although the equations were developed for hammers with  $E_h \leq 165$  kip-ft, its use should be applicable for hammers with higher energies but this was not verified directly in the study.

The independent examination of the developed equations against an independent data, dynamic measurements in MN and load tests conducted by the MnDOT, affirmed the effectiveness and accuracy of the proposed equations. Further monitoring and calibration is recommended by following the outcome of piles installed during construction, utilizing dynamic measurements and conducting static load tests for MnDOT typical design practices.

# **1 BACKGROUND**

## **1.1 Resistance Factor for MnDOT's Pile Driving Formula – Phase I Study**

Driven piles are the most common foundation solution used in bridge construction across the U.S. (Paikowsky et al., 2004). The major problem associated with the use of deep foundations is the ability to reliably verify the capacity and the integrity of the installed element in the ground. Dynamic analyses of driven piles are methods attempting to obtain the static capacity of a pile, utilizing its behavior during driving. The dynamic analyses are based on the premise that under each hammer blow, as the pile penetrates into the ground; a quick pile load test is being carried out. Dynamic equations (aka pile driving formulas) are the earliest and simplest forms of dynamic analyses. MnDOT uses its own pile driving formula; however, its validity and accuracy has never been thoroughly evaluated. With the implementation of Load Resistance Factor Design (LRFD) in Minnesota in 2005, and its mandated use by the Federal Highway Administration (FHWA) in 2007, the resistance factor associated with the use of the MnDOT driving formula needed to be calibrated and established.

Systematic probabilistic-based evaluation of a resistance factor requires quantifying the uncertainty of the investigated method. As the investigated analysis method contains large uncertainty itself (in addition to the parameters used for the calculation), doing so requires: (i) Knowledge of the conditions in which the method is being applied, and (ii) A database of case histories allowing comparison between calculated and measured values.

Phase I of the research addressed these needs via: (i) Establishing the MnDOT state of practice in pile design and construction, and (ii) Compilation of a database of driven pile case histories (including field measurements and static load tests to failure) relevant to Minnesota design and construction practices.

Establishing the MnDOT state of practice in pile design and construction was achieved by conducting: review of previously completed questionnaires, review of the MnDOT bridge construction manual, compilation and analysis of construction records of 28 bridges, and interviews with contractors, designers, and DOT personnel.

Compilation of a database of driven pile case histories included field measurements and static load tests to failure relevant to Minnesota design and construction practices. Based on the analyzed bridges, the majority of the Minnesota recently constructed bridge foundations comprised of Closed-Ended Pipe (CEP) and H piles. The most common CEP piles are 12"  $\times$  0.25 and 16"  $\times$  0.3125, installed as 40% and 25% of the total number of CEP compiled in the dataset. The most common H pile is 12  $\times$  53 used in 57% of the total number of H piles compiled in the dataset. The typical CEP is 12"  $\times$  0.25, average length is 70 ft long and carries 155 kips (average factored load). The typical H pile is 12  $\times$  53, 40 ft long and carries 157 kips. The piles are driven

by diesel hammers ranging in energy from 42 to 75 kip/ft. with 90% of the piles driven to or beyond 4 Blows Per Inch (BPI) and 50% of the piles driven to or beyond 8 BPI. Updated data statistics developed in Phase II of the study (presented in Chapter 3) refers to projects around Minneapolis where the most common piles were CEP 16"  $\times$  0.3125 and 16"  $\times$  0.25 installed at 34% and 21% of the total number of CEP piles compiled in that database. These values are somehow different from the statistics presented in Phase I report, which is more applicable to the entire state.

Large data sets were assembled, answering to the above practices. As no data of static load tests were available from MnDOT, the databases were obtained from the following: (i) Relevant case histories from the dataset PD/LT 2000 used for the American Association of State Highway and Transportation Officials (AASHTO) specification LRFD calibration (Paikowsky and Stenersen, 2000, Paikowsky et al., 2004) (ii) Collection of new relevant case histories from DOTs and other sources.

In total, 166 H pile and 104 pipe pile case histories were assembled in the MnDOT LT 2008 database. All cases contain static load test results as well as driving system and, driving resistance details. Fifty three percent (53%) of the H piles and 60% of the pipe piles in dataset MnDOT LT 2008 were driven by diesel hammers.

The static capacity of the piles was determined by Davisson's failure criterion, established as the measured resistance. The calculated capacities were obtained using different dynamic equations, namely, *Engineers News Record* (ENR), Gates, Modified Gates, WSDOT, and MnDOT. The statistical performance of each method was evaluated via the bias of each case, expressed as the ratio of the measured capacity over the calculated capacity. The mean, standard deviation, and coefficient of variation of the bias established the distribution of each method's resistance.

The distribution of the resistance along with the distribution of the load and established target reliability (by Paikowsky et al. 2004 for the calibration of the AASHTO specifications) was utilized to calculate the resistance factor associated with the calibration method under the given condition. Two methods of calibration were used: MCS (Monte Carlo Simulation), using iterative numerical process, and FOSM (First Order Second Moment), using a closed form solution.

The MnDOT equation generally tends to over-predict the measured capacity with a large scatter. The performance of the equation was examined by detailed subset databases for each pile type: H and pipe. The datasets started from the generic cases of all piles under all driving conditions (258 pile cases) and ended with the more restrictive set of piles driven with diesel hammers within the energy range commonly used by MnDOT practice and driving resistance of 4 or more BPI. The 52 data sub-categorizations (26 for all driving conditions and 26 for EOD alone) were presented in the form of a flow chart along all statistical data and resulting resistance factors. Further detailed investigations were conducted on specific subsets along with examination of the

obtained resistance distribution using numerical method (Goodness of Fit tests) and graphical comparisons of the data vs. the theoretical distributions.

Due to the MnDOT dynamic equation over-prediction and large scatter, the obtained resistance factors were consistently low and a resistance factor of  $\phi = 0.25$  was recommended to be used with the original equation, for both H and pipe piles. The reduction in the resistance factor from  $\phi = 0.40$  currently in use, to  $\phi = 0.25$ , reflects a significant economic loss for a gain in a consistent level of reliability. Alternatively, one can explore the use of other pile field capacity evaluation methods that perform better than the currently used MnDOT dynamic equation, hence allowing for higher efficiency and cost reduction.

Two approaches for remediation were presented. In one, a subset containing dynamic measurements during driving was analyzed, demonstrating the increase in reliability when using dynamic measurements along with a simplified field method known as the Energy Approach. Such a method requires field measurements that can be accomplished in several ways.

An additional approach was taken by developing independently a dynamic equation to match MnDOT practices. A linear regression analysis of the data was performed using a commercial software product featuring object oriented programming. The simple obtained equation (in its structure) was calibrated and examined. A separate control dataset was used to examine both equations, demonstrating the capabilities of the proposed new MnDOT equation. In addition, the database containing dynamic measurements was used for detailed statistical evaluations of existing and proposed MnDOT dynamic equations, allowing comparison on the same basis of the field measurement-based methods and the dynamic equations.

Finally, an example was constructed based on typical piles and hammers used by MnDOT. The example demonstrated that the use of the proposed new equation may result at times with savings and at others with additional cost, when compared to the existing resistance factor currently used by the MnDOT. The proposed new equation resulted in consistent savings when compared to the MnDOT current equation used with the recommended resistance factor developed in this study for its use ( $\phi = 0.25$ ).

## **1.2 Research Objectives**

### ***1.2.1 Overview***

The first phase of the study concentrated on establishing MnDOT practices, developing databases related to these practices and examining different dynamic equations as well as developing new equations. The proposed resistance factors developed in Phase I for the driving of pipe piles were assessed to be conservative relevant to the traditional design practices, and

hence, Phase II was initiated in order to examine other practices, review MN related data and re-examine target reliabilities and associated resistance factors.

### ***1.2.2 Concise Objectives***

Phase II of the study was established to:

1. Re-evaluate resistance factors for the Load Resistance Factor Design (LRFD) implementation as obtained in the Phase I study,
2. Examine other dynamic pile driving formulae and other Midwest states practices,
3. Recommend to MnDOT an appropriate formula (and associated resistance factors) for implementation,
4. Examine the recommended formula in use with timber and prestressed precast concrete piles,
5. Examine pile hammer qualification and WEAP analyses procedures for MN conditions and recommend procedures to be implemented, and
6. Examine load test procedures and interpretations.

### ***1.2.3 Specific Tasks***

The following task numbering follows by and large the awarded research contract with the exception of renumbering for chronological clarity.

Task 1: Review Alternate Formulas and Construction Pile Practices in Midwest States

1. Summarize the practices, developments and major findings of the pile driving formulae developed by Wisconsin DOT, Illinois DOT, Iowa DOT, Gates (1957) and FHWA Modified Gates (1982).
2. Evaluate data related to other DOT's including data used by Long et al. (1007, 2009), Iowa (charts and current research), Flaate (1964), Olson and Flaate (1967), databases, and other available data sources. Examine the performance of the above equations using MnDOT/LT2008 databases. This examination includes statistical analysis breakdown according to pile type, hammer type, energy level and driving resistances, presented in the form of tables and flow charts.

Task 2: Evaluation of Bridge Office Field Data

1. Evaluate along with MnDOT personnel, the databases used in the development of the above equations in comparison with MnDOT practice as established by Phase I study (Paikowsky et al., 2009) emphasizing data for which energy is available.
2. Analyze construction data (gathered in MnDOT bridge projects) utilizing the various aforementioned methods along with their calibrated resistance factors and those recommended in Phase I of the study (Paikowsky et al., 2009).

### Task 3: Back Analysis

Analyses of the information gathered in Tasks 1 and 2 in order to identify resistance factors and risk associated with maintaining the current MnDOT practice (i.e. MnDOT driving equation and  $R.F. = 0.4$ ) implemented with the methods investigated in Tasks 1 and 2.

### Task 4: Recommend Appropriate Hammer Qualification

1. Establish effective and nominal hammer qualifications based on the statistics presented in Tasks 1 and 2.
2. Perform Wave Equation (WEAP) analyses examining the typical pile sizes, loads and hammers used on MnDOT bridge projects.
3. Compare the data obtained from dynamic measurements or MnDOT projects to the information above.
4. Establish hammer qualification specifications based on the information gathered in steps 1 to 3.

### Task 5: Field Testing

Load test data interpretation, analysis and implementation as requested by the Load Testing Program Development project conducted by MnDOT. The extent of involvement will be determined by the MnDOT liaison for this project.

### Task 6: Examine the recommended MnDOT Dynamic Equation (MPF12) for Timber and PPC Piles

1. Search, identification and analysis of data to build a dataset of timber piles driven and static load tested.
2. Search, identification and analysis of data to build a dataset of PPC piles driven and static load tested.
3. Analyze the databases and recommend the MPF12 implementation and associated resistance factors for Timber and PPC piles.

### Task 7: Static Pile Load Test – Procedures, Interpretation and Specifications

1. Examine methods to conduct and interpret axial static pile load tests on driven piles.
2. Outline detailed procedures (chose selected procedures from ASTM, DOTs and researchers own developments).
3. Detail interpretation procedures.

### Task 8: WEAP – Outline Details of Requirements for Submittal and Procedures for Modifications Once Dynamic Measurements are Available.

1. Run WEAP analyses for a set of typical hammer/piles/soil combinations for MN conditions.



2. Detail what kind of analyses needs to be performed as required submittal for DOT authorization. This includes the study of the subsurface, evaluation of possible ranges of pile lengths and soil parameters. Determine what type of tables should be built to cover possible results. Provide a detailed example showing what ‘typically’ is submitted, what we specify and the consequences for the difference so contractors also understand the importance of the requirement for their advantage.
3. Ways to get information from signal matching and update the WEAP based on field observations of energy, blow count, etc.

Task 9: Final Report – This task includes the development and submittal of the draft final report. The project team will incorporate the technical and editorial review comments from the review process into the report, as appropriate. The report will then be submitted to the MnDOT for publication.

### **1.3 Manuscript Outline**

Background information dealing with the project, research objectives and research execution are presented in Chapter 1. Chapter 2 establishes alternate formulas and the MnDOT state of practice, being in line with Task 1. The developed databases and their investigation for their relevance to MnDOT practices are presented in Chapter 3 being in line with Task 2. The first and second stage analysis of the databases presented in Chapter 3 relate to Tasks 3 and 4 as the analyses presented followed by LRFD calibrations. Chapter 3 also compares different methods’ performance including those based on dynamic measurements. Chapter 4 presents the development of an independent MnDOT dynamic equation, its evaluation and re-evaluation. The application of the new MnDOT dynamic equation to precast concrete piles is presented in Chapter 5. Chapter 6 presents the application of the new MnDOT dynamic equation to timber piles. Both Chapters 5 and 6 address Task 6. The Minnesota load testing program established to answer Task 5 is presented in Chapter 7. WEAP analysis and dynamic measurements as compared to the new MnDOT dynamic equation is presented in Chapter 8, addressing Task 8. Chapter 9 establishes the static load test procedures and specifications as pertain to the MnDOT, answering Task 7. Chapter 10 summarizes the findings, conclusions and presents the recommendations of this research study.

## **2 REVIEW ALTERNATE FORMULAS AND CONSTRUCTION PILE PRACTICES IN MIDWEST STATES**

### **2.1 Overview**

The first task of the research was achieved by a review summarizing the practices, developments and major findings of the pile driving formulae in the Midwest states. Development by Illinois DOT (Long et al., 2009a), Wisconsin DOT (Long et al., 2009b), Iowa DOT (charts and ongoing research at Iowa State University), Washington DOT (Allen, 2005), Gates (1957) and Modified Gates (1982) were conducted. The summary in Table 1 outlines findings and sources of research material used in the review. The following sections present the summaries with critical review.

### **2.2 Illinois Department of Transportation – Long and Maniaci (2000)**

#### **2.2.1 Overview**

Long and Maniaci (2000) presented a report to IDOT for the design of friction bearing piles in which a large database was collected and investigated. The databases included those developed originally by Flaate (1964), Olson and Flaate (1967), Frigaszy et al. (1988), Paikowsky et al. (1994), Davidson and Townsend (1996), and by the Federal Highway Administration (FHWA Rausche et al., 1996). An additional database reporting cone penetration tests (Eslami, 1996) was also investigated. The report focused on six methods that used driving resistance to predict pile capacity: the Engineering News (EN) formula, the Gates formula, the Wave Equation Analysis Program (WEAP), The Pile Driving Analyzer (PDA), the Measured Energy Method, and the Case Pile Wave Analysis Program (CAPWAP).

The first three methods estimate pile capacity based on field observations of driving resistance (i.e. blow count), hammer stroke, pile type and soil type, applying this information to a relationship developed between capacity and driving resistance. The last three methods (PDA, Measured Energy Method, CAPWAP), require measurements of the variation of force and velocity with respect to time during driving (under each blow) and their interpretation. The methods reviewed by Long and Maniaci (2000) make use of the pile behavior, at the end of driving (EOD) or beginning of restrike (BOR). When it is possible and practical, re-striking the pile is a prudent procedure since time effects can influence significantly the final pile capacity. Typically, due to a tight construction schedule, it is common to restrike the pile after 24 hours only; however, a longer time may be required for fine-grained soils to allow development of full set-up conditions (FHWA, 1995).

**Table 1. Construction pile evaluation practices Midwest states (May 2010 with updates)**

State	Contact Person	Material	Findings	Comments
Illinois	Bill Kramer 217-782-1224 <a href="mailto:William.Kramer@illinois.gov">William.Kramer@illinois.gov</a>	1. Report R27-24 “Evaluation/Modification of IDOT Foundation Piling Design and Construction Policy”, Long, Hendrix and Baratta, Jan 2007 to March 2009, 204pp. 2. Bridge Manual directions. 3. Proposal for new research 4. Various inspection and relations for evaluation.	1. H pile (~60%), Pipe pile (~38%) 2. ENR until 2006 3. Mod. Gates with $\phi=0.50$ (arbitrary) 2007-2009 4. Long study tried to develop independent equation but it was not working well (B.K. believes the budget was limited). They therefore decided to use WS-DOT but just started to check its performance with the new study (see comments) with purchasing a PDA.	1. Original study budget \$150,000 2. New research “Improving IDOT Pile Design Procedure through Dynamic and Static Test Data Analysis”, using mainly PDA, is currently under way \$300,000 budget. 3. Third phase to start at the present time (update by B.K., Aug. 2011)
	Robert Stanley 515-239-1026 <a href="mailto:Robert.Stanley@dot.iowa.gov">Robert.Stanley@dot.iowa.gov</a>  Ahamad Abu-Hawash 515-239-1393 <a href="mailto:Ahmad.Abu-Hawash@dot.iowa.gov">Ahmad.Abu-Hawash@dot.iowa.gov</a>	1. Design Charts based on load test interpretations (300 carried out over 20 years ago). 2. Possible data from Iowa state research that is planned to be completed by year end. 3. Bridge Manual.	1. H pile (80-90%), All others including drilled shafts 10-20%, do not use Pipe piles. Drive with diesel hammers. 2. Did not start to implement LRFD yet. 3. Pile design is based on the charts. Construction runs WEAP on every hammer submittal using that WEAP in the field. 4. PDA used by construction (own one) whenever needed but not routinely.	1. Engaged with Iowa State University in a research project to examine the design charts, LRFD application and conduct load tests. 2. Research includes 10 static L.T. mostly as part of construction with a load frame available from a previous work. Total budget \$700,000 3. Update from Prof. M. Sulliman and S. Sriharan on Feb. 20, 2011 that database is accessible.
Wisconsin	Robert Andorfer 608-243-5993 <a href="mailto:Robert.Andorfer@dot.state.wi.us">Robert.Andorfer@dot.state.wi.us</a>	1. “Comparison of Five Different Methods for Determining Pile Bearing Capacities”, report by Long, Hendrix and Jaromin, February 2009, 160pp. 2. Collaboration in checking the equations developed for MN.	1. H piles (75%) 10×42, 12×53; Pipe piles – closed ended (25%) 10¾ – 12¾ 2. D – 12 to D – 30 3. Mod. Gates with $\phi=0.50$ without distinction between H to Pipe.	1. The research was an “experience”, aware of the differences between H and Pipe piles (budget was \$30,000 as an offshoot of Illinois’ research). 2. Listened to Sam’s lecture in the February meeting in Minneapolis and plans to check the equation developed for MN.

To estimate the ultimate capacity,  $Q_u$ , of a pile under axial load, the sum of the pile tip capacity,  $Q_p$ , and the shaft capacity,  $Q_s$ , was used by Long and Maniaci in the format traditionally being presented:

$$Q_u = Q_p + Q_s \quad (1)$$

Equation (1) can be further broken down as follow:

$$Q_u = (q_p * A_p - W) + \sum_{i=1}^n f_{si} C_i l_i \quad (2)$$

Where  $q_p$  = bearing capacity at the pile's tip,  $A_p$  = area of pile tip,  $W$  = weight of pile,  $f_{si}$ =ultimate skin resistance per unit area of pile shaft segment  $i$ ,  $C_i$  = perimeter of pile segment  $i$ ,  $l_i$ = length of pile segment  $i$ , and  $n$  number of pile segments

In order to evaluate the ultimate pile capacity, the magnitude  $f_s$  for each pile segment and the pile tip resistance  $q_p$  must be estimated. Most of this information is based on empirical methods, derived from correlations of measured pile capacity with soil data.

The dynamic formulae are an energy balance equations which relate the energy delivered by the pile hammer to the work produced during pile penetration. The dynamic formulae are expressed in equations of the following form:

$$eWH = Rs \quad (3)$$

Where  $e$ = efficiency of hammer system,  $W$ = ram weight,  $H$ = ram stroke,  $R$ = pile resistance, and  $s$ = pile set (pile displacement per hammer blow). The pile resistance,  $R$ , is assumed to be related directly to the ultimate capacity,  $Q_u$ .

Dynamic formulae provide a simple method to estimate pile capacity; however, there are several shortcomings associated with their simplified approach (FHWA, 1995):

- Dynamic formulae focus only on the kinetic energy of driving, not on the driving system,
- Dynamic formulae assume constant soil resistance rather than a velocity dependent resistance, and
- The length and axial stiffness of the pile are ignored.

Two techniques were used to identify how well predicted pile capacity agreed with measured pile capacity. The first is a graphic representation of predicted capacity versus the measured capacity both on a logarithmic scale. Such scatter grams allow visualizing and determining trends for the predictive method like over or under predicted capacity, also the scatter exhibited by the plot indicates the reliability of the method to predict capacity. For this purpose, a table of fictitious load test results was created and those results plotted using two different methods of prediction (Figure 1). The use of a logarithmic scale by Long and Maniaci (2000) creates a visual

distortion of the match between measured to calculated values and the viewer needs to be aware of that when examining such presentation.

The second technique uses statistical methods to quantify the degree of agreement between predicted and measured capacity for a specific method. The statistical analysis used by Long and Maniaci was done with the relationship between predicted values versus measured values ( $Q_p/Q_m$ ). Bias and precision, were used as two simple statistical parameters for defining a method's ability to predict capacity. Bias is the systematic error between the average ratio of  $Q_p/Q_m$  and the ideal ratio of  $Q_p/Q_m$  (which is unity). Statistically, the bias can be estimated with a sample mean. Precision is the scatter or "variability of a large group of individual test results obtained under similar conditions" (ASTM C670-90a, 1990). Statistically variability can be estimated with a sample standard deviation. The distribution  $Q_p/Q_m$  is log-normal (Cornell, 1969). A log-normal distribution means that the values of  $\ln(Q_p/Q_m)$  are normally distributed. Accordingly Long and Maniaci (2000) estimated the mean and standard deviation for the  $\ln(Q_p/Q_m)$  for the predictive measures as a method to assess the bias and precision.

It should be noted that Long and Maniaci (2000) presented the bias ratio as that of predicted value over measured value, opposite to the common way, and hence, required at the end of their report to re-evaluate the reversed ratio (correct bias) to be used in their calculations. As will be detailed at a later stage (section 2.3.7), this reversed ratio affected our ability to compare the data used for analyzing Mn DOT Phase I study to that presented by Long and Maniaci (2000) and Long et al. 2009a,b.

The analyses of the load test databases were investigated separately and together to identify the effects of using EOD data versus BOR data to estimate capacity. The results from cone penetration methods were compared with those obtained using driving data. The Gates equation was investigated further and modifications to improve the equation were provided.

## **2.2.2 Databases Summary**

### **2.2.2.1 Flaate, 1964**

The pile load test data used by Flaate represents pile types and installation methods related to the period of time that pre-dates 1964. The Flaate (1964) database includes, pile types and installation methods that are no longer common in today's practice, hence, these data bias the result of the general database (Long and Maniaci, 2000). For example, several of the pile load tests in the Flaate database were conducted on timber piles. Timber piles are not used in current bridge construction in Minnesota or elsewhere. Furthermore, over half of the piles (62) in the Flaate database were driven with gravity hammers, while the remaining piles (54) were driven with diesel or steam hammers. Gravity hammers are rarely used in driving piles mostly for small projects or restrrike, but not for typical bridge foundations. The database was analyzed by Long and Maniaci (2000) accordingly and the relationships between predicted and measured pile capacities are presented in Table 2 and plotted in Figure 2.

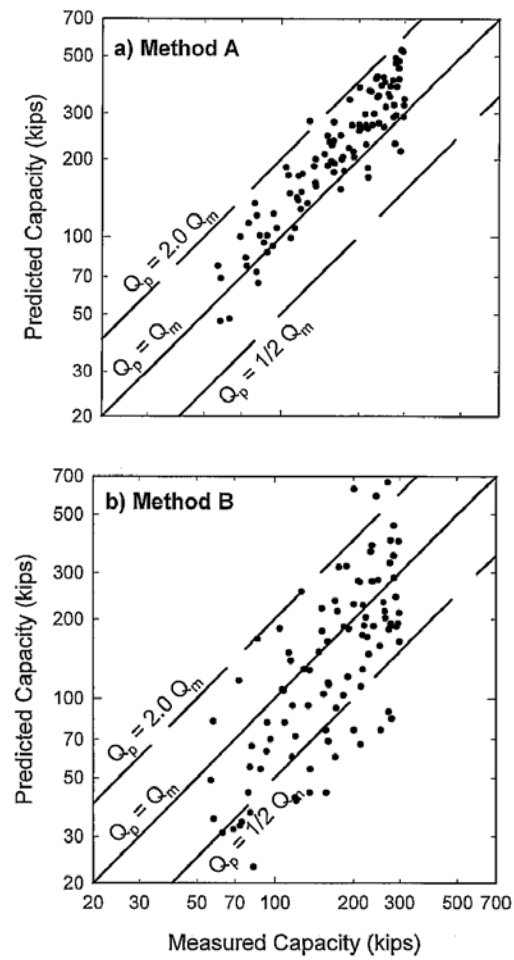


**Figure 1. Graphic representation of predicted vs measured capacity (Long and Maniaci, 2000)**

**Table 2. Statistical parameters for  $Q_p/Q_m$  values for all load test data from Flaate 1964. (Long and Maniaci, 2000)**

Method	Hammer Type	n	$\mu$	$\sigma_{\ln}$
EN	All hammer types	116	1.23	0.790
Hiley		116	0.82	0.499
Janbu		116	1.03	0.307
Gates		116	0.78	0.429
EN	All hammer types except gravity	54	2.45	0.523
Hiley		54	0.74	0.614
Janbu		54	1.08	0.397
Gates		54	0.85	0.459
EN	Gravity hammer only	62	0.68	0.393
Hiley		62	0.91	0.346
Janbu		62	0.98	0.192
Gates		62	0.73	0.391

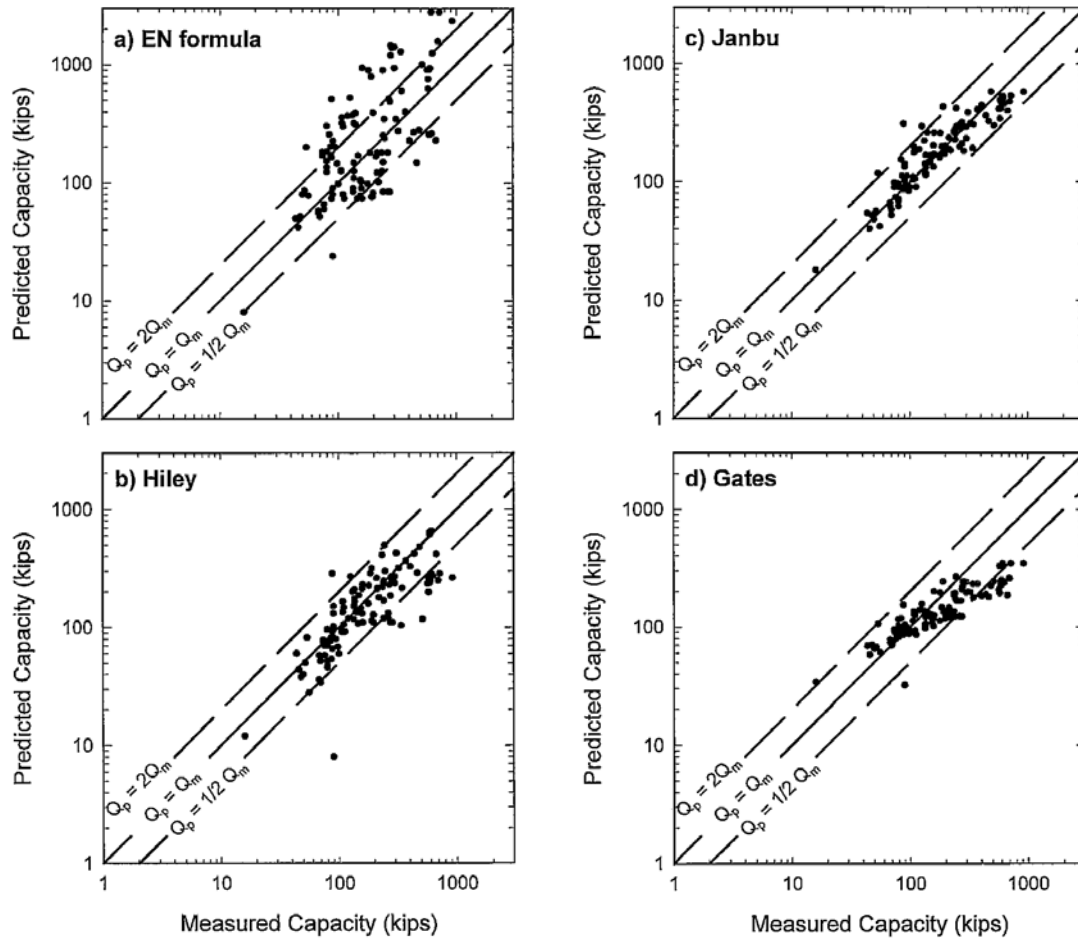


**Figure 2. Predicted versus measured capacity from Flaate 1964 (Long and Maniaci, 2000)**

### 2.2.3 Olson and Flaate, 1967

The database used by Olson and Flaate (1967) is nearly identical to the database used by Flaate (1964). The predicted versus measured relationships, and the statistical parameters presented by Olson and Flaate (1967) are similar to those determined by Flaate (1964). The Olson and Flaate database also includes piles driven by gravity hammers and other types of hammers and no separation of data based on hammer types took place. Olson and Flaate suggested that Gates equation could be modified to provide a better statistical fit between predicted and measured pile capacities. The modifications to the Gates formula were provided based on piles driven with all hammer types other than gravity hammers:

$$R_u = 1.11\sqrt{e * E_r} \log(10N) - 34; \text{ Timber Piles} \quad (4)$$

$$R_u = 1.39\sqrt{e * E_r} \log(10N) - 54; \text{ Concrete Piles} \quad (5)$$

$$R_u = 2.01\sqrt{e * E_r} \log(10N) - 166; \text{ Steel Piles} \quad (6)$$

$$R_u = 1.55\sqrt{e * E_r} \log(10N) - 96; \text{ All Piles} \quad (7)$$

Where units of  $R_u$  are in kips,  $N$  is in blows per inch and  $E_r$  is in units of ft-lb.

#### 2.2.3.1 Fragaszy et al., 1988, 1989

The statistical results of the predicted over the measured capacities reported by Fragaszy et al., are presented in Table 3 and are plotted in Figure 3.

A comparison of the four methods, EN, Hiley, Janbu, and Gates can be made using the statistical parameters presented in Table 3. The EN formula overpredicts capacity by a factor of 2.58, while the Hiley and Janbu methods are fairly neutral. The Gates method underpredicts capacity by a factor of 0.63 indicating that recalibration of the original Gates equation is necessary. The scatter quantified by the magnitude of standard deviation, shows that the Gates method possesses the least scatter with a standard deviation of 0.307.

As presented in the previous section, the Gates method was modified to develop a better fit between measured and predicted capacity, so identical procedures were repeated to develop a modified Gates equation from Fragaszy's data, leading to the following relations for all piles except timber:

$$R_u = 1.46\sqrt{eE_r} \log(10N_b) + 26 \quad (8)$$

Where  $R_u$  is in kips and  $E_r$  is in ft-lb.



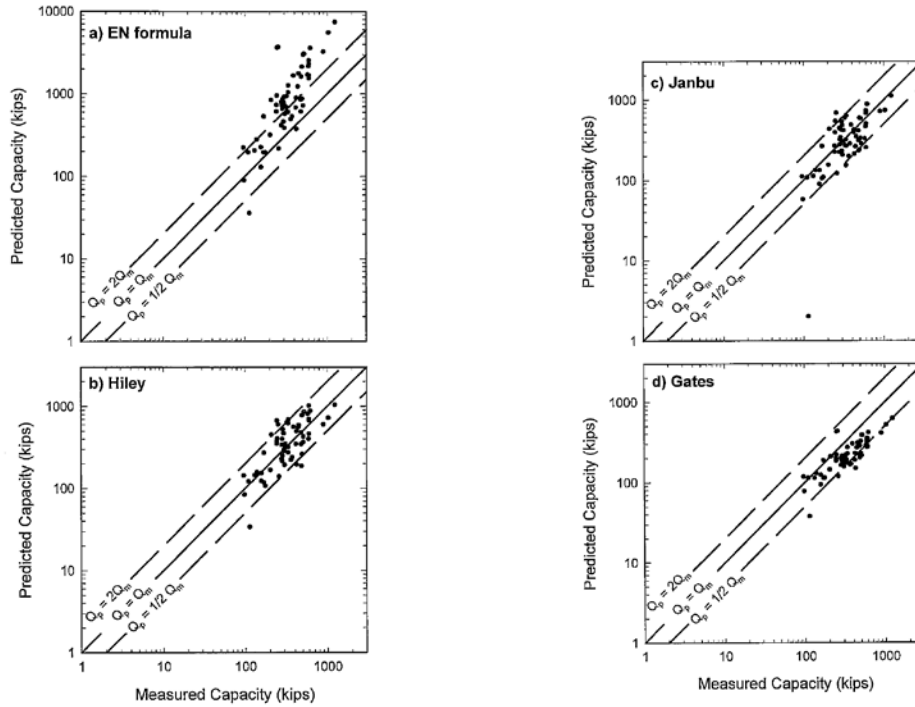


**Figure 3. Predicted versus measured capacity from Fragaszy 1988, 1989 (Long and Maniaci, 2000)**

**Table 3. Statistical parameters for  $Q_p/Q_m$  values for all load test data from Fragaszy 1988, 1989 (Long and Maniaci, 2000)**

Method	$\mu_{ln}$	$\mu$	$\sigma_{ln}$
EN	0.950	2.58	0.610
Hiley	0.045	1.05	0.438
Janbu	-0.060	0.94	0.437
Gates	-0.459	0.63	0.307

#### 2.2.3.2 Paikowsky et al., 1994

Two large datasets were collected and interpreted in this study. One set (labeled PD/LT) had 208 dynamic measurements on 120 piles tested statically to failure. The other set (labeled PD) contained 403 piles monitored during driving without static load tests. The measured and predicted capacities reported by Paikowsky et al., 1994, are plotted in Figure 4. The Measured Energy (ME) method (termed so by Long and Maniaci, 2000) is what described as the Energy Approach by Paikowsky (1982), Paikowsky et al. (1994), Paikowsky and Stenerson (2000) and Paikowsky et al. (2004). Measured maximum displacement and energy from dynamic measurements are employed along with driving resistance (set) in energy equilibrium equation to provide highly accurate long term pile capacity during driving. The pile capacity predictions utilizing the Energy Approach results are plotted in Figure 4, for predictions made with driving

behavior recorded at the end of driving (EOD) and the predictions made by allowing the pile to set for several days and then recording the driving behavior at the beginning of restrike (BOR). The ME approach using EOD data appear to predict capacity well and a very small degree of scatter. Statistics for the ME approach and the other methods are presented in Table 4 for both EOD and BOR conditions.

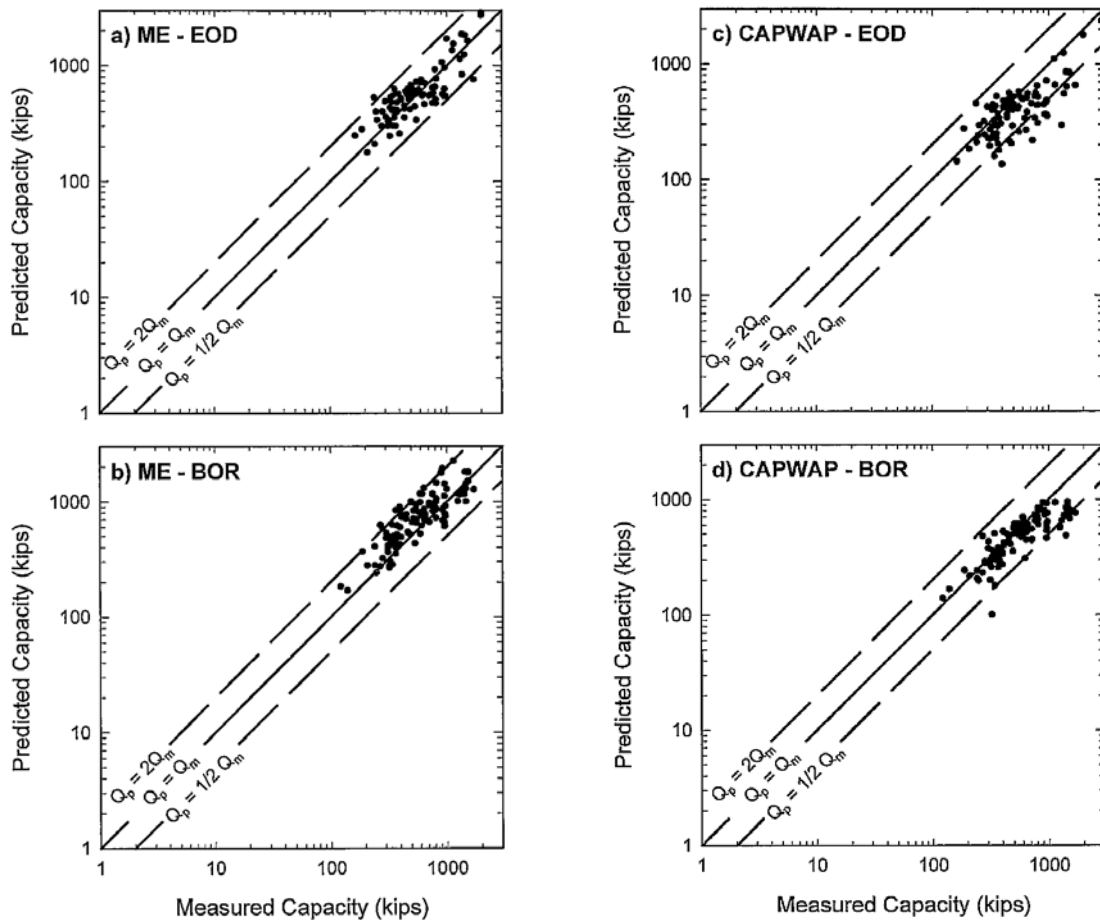


**Figure 4. Predicted versus measured capacity from Paikowsky et al., 1994 (Long and Maniaci, 2000)**

**Table 4. Statistical parameters for  $Q_p/Q_m$  values for all load test data from Paikowsky et al., 1994. (Long and Maniaci, 2000)**

Method	$\mu_{ln}$	$\mu$	$\sigma_{ln}$
ME-EOD	0.04	1.03	0.309
ME-BOR	0.22	1.25	0.303
CAPWAP-EOD	-0.31	0.73	0.398
CAPWAP-BOR	-0.18	0.83	0.304

This dataset provides insight into possible errors associated with the dynamic formulas investigated previously. For example, a very similar formula to the EN formula was used for the ME approach, but the correlations are improved. A possible reason for improved accuracy may be because pile dynamic monitoring results in more reliable estimates for energy delivered to the pile and the quake developed by the pile as compared to the rough estimates of hammer energy. (Long and Maniaci, 2000). A detailed analysis and explanations are provided by Paikowsky et al. (1994) and the aforementioned references (not detailed by Long and Maniaci, 2000).

### 2.2.3.3 Davidson and Townsend, 1996

The measured and predicted capacities reported by Davidson and Townsend, 1996, are plotted in Figure 5, and statistical results are presented in Table 5. All the data presented are related to concrete piles driven in Florida. The predicted capacities were obtained using PDA data and analysis, CAPWAP analyses, and static method evaluation using SPT94. There are two estimates of capacity using the PDA (the Case Method) and CAPWAP under both driving conditions, EOD and BOR.

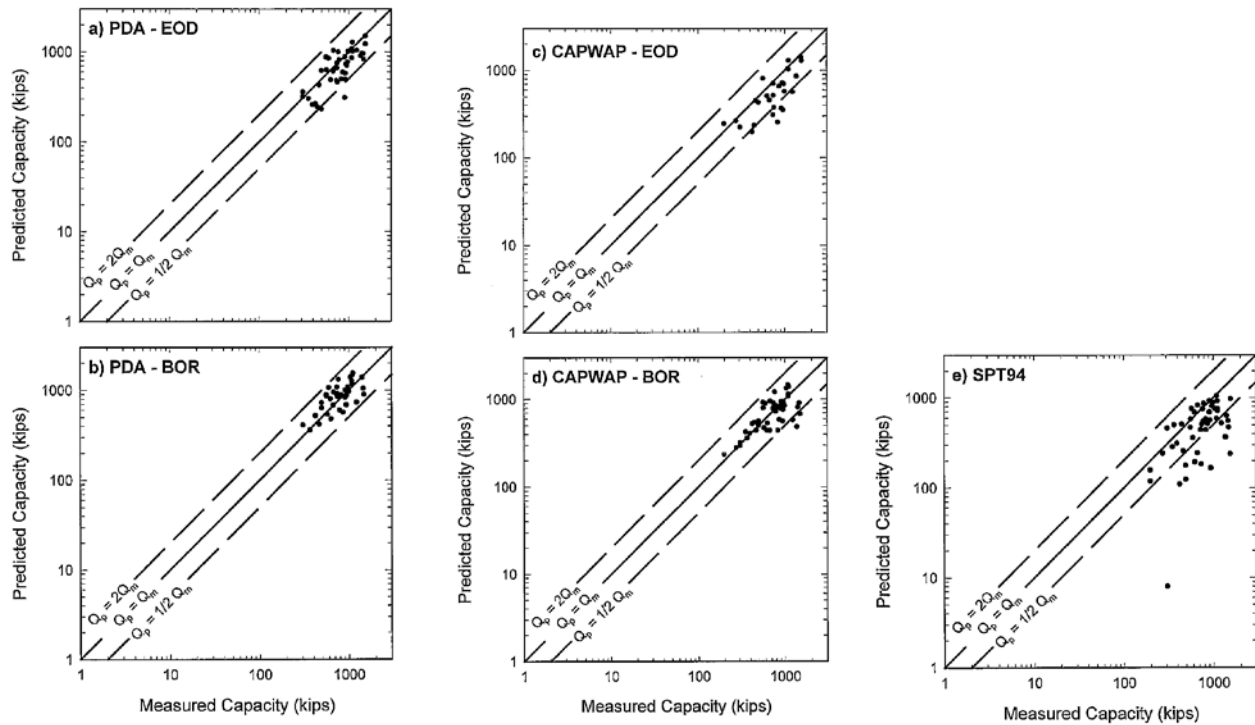


**Figure 5. Predicted versus measured capacity for Florida DOT from Davidson and Townsend, 1996 (Long and Maniaci, 2000)**

**Table 5. Statistical parameters for  $Q_p/Q_m$  values for all load test data from Davidson and Townsend, 1996 (Long and Maniaci, 2000)**

Method	$\mu_{ln}$	$\mu$	$\sigma_{ln}$
PDA-EOD	-0.171	0.84	0.298
PDA-BOR	0.070	1.07	0.266
CAPWAP-EOD	-0.356	0.70	0.375
CAPWAP-BOR	-0.052	0.95	0.317
SPT94	-0.626	0.53	0.734

#### 2.2.3.4 Eslami, 1996

Eslami only considered methods that use results of cone penetration test to predict the static capacity of piles. He investigated six methods and the graphical presentation of the predicted versus measured capacities are provided in Figure 6. The statistical parameters for  $Q_p/Q_m$  values are presented in Table 6. All methods provide a very narrow range and relatively small scatter considering the static capacity prediction methods are very different from one method to another. The predictions and the statistical parameters identify much better agreement between predicted and measured capacity using cone methods than using other static methods such as the SPT94 method reported by Davidson et al. (1994).

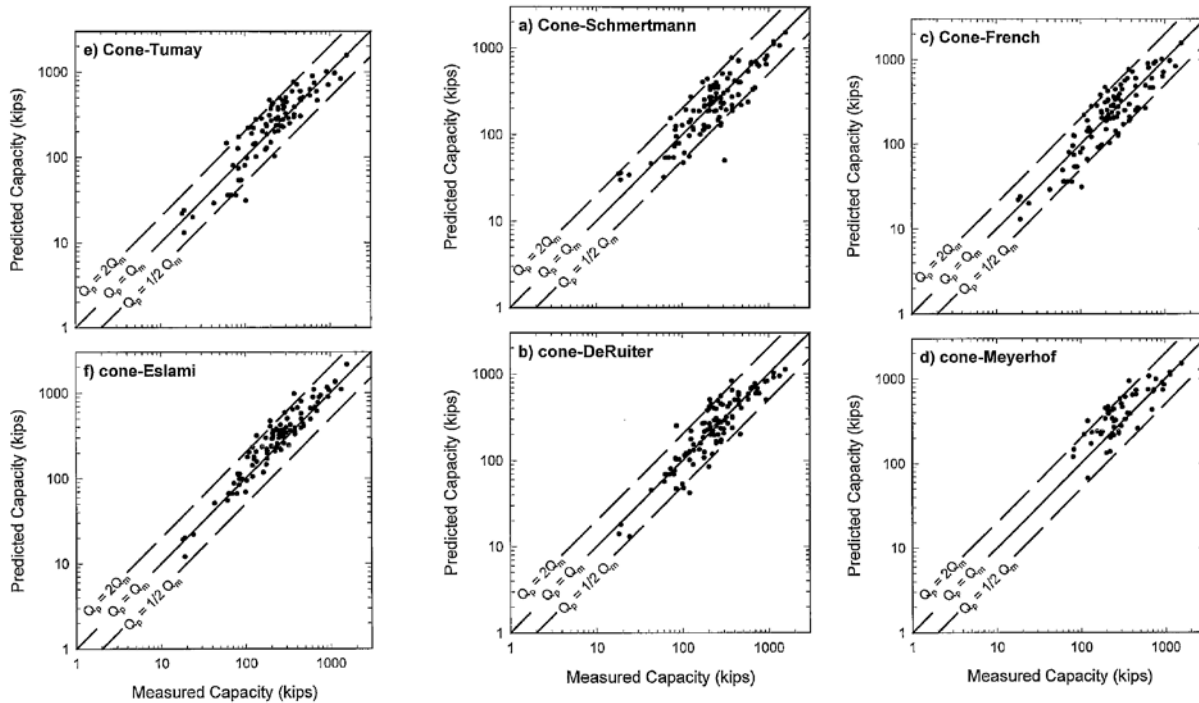


**Figure 6. Predicted versus measured capacity from Eslami, 1996 (Long and Maniaci, 2000)**

**Table 6. Statistical parameters for  $Q_p/Q_m$  values for data from Eslami, 1996 (Long and Maniaci, 2000)**

Cone Method	$\mu_{ln}$	$\mu$	$\sigma_{ln}$
Schmertmann	-0.058	0.944	0.443
DeRuiter	0.002	1.002	0.390
French	-0.063	0.939	0.447
Meyerhof	0.230	1.258	0.391
Tumay	0.142	1.153	0.374
Elsami	0.180	1.197	0.276

#### 2.2.3.5 FHWA Database

The Federal Highway Administration (FHWA) made available their database described by Rausche et al. (1996). Out of 200 pile cases, only 123 presented enough information for Long's study (Long and Maniaci, 2000). It needs to be noted that there is a major overlap between the 120 cases presented by Paikowsky et al. (1994) (see section 3.1.2.4) and this database, not identified or commented by Long and Maniaci (2000), who used the database presented by Paikowsky et al. (1994).

The so-called FHWA database was used to compare capacity predictions using BOR results with predictions using EOD results. Only load tests were included in which pile capacities could be predicted for both EOD and BOR. For each method, the mean ( $\mu$ ) and standard deviation ( $\sigma_{ln}$ ) for the ratio  $Q_p/Q_m$  (predicted capacity to measured capacity) along with the number of load tests used to assess the statistics are presented in Table 7. It is observed that the mean ( $\mu$ ) for BOR conditions is greater than the mean ( $\mu$ ) for EOD for all predictive methods. This result is due to the increase in pile resistance with time. A greater pile resistance for BOR conditions results in a prediction of a greater capacity than that at EOD condition. The standard deviation ( $\sigma_{ln}$ ) for all methods decrease for BOR conditions as expected, since  $Q_p/Q_m$  based on BOR conditions are more representative of pile resistance at some time after driving and closer to the time in which the static load test was conducted. The results show that the most empirical method (Gates) exhibits the least change in  $\sigma_{ln}$  while the most rigorous method (CAPWAP) exhibits the greatest change in  $\sigma_{ln}$ .

**Table 7. Statistical parameters for  $Q_p/Q_m$  for FHWA database (Long and Maniaci, 2000)**

Method		n	$\mu$	$\sigma_m$
End of Driving (EOD)	EN	123	2.60	6.75
	Gates	123	0.53	0.410
	WEAP	88	0.64	0.501
	ME	73	0.93	0.462
	PDA	77	0.71	0.454
	CAPWAP	75	0.58	0.591
Beginning of Restrike (BOR)	EN	116	4.62	0.514
	Gates	116	0.72	0.392
	WEAP	114	1.11	0.385
	ME	92	1.41	0.363
	PDA	85	0.91	0.319
	CAPWAP	112	0.86	0.269
Static Formula		112	1.15	0.556

\*Note: All load tests are included in which a method could be used to compute capacity.

The conclusions obtained by Long and Maniaci (2000) from the study are presented based on the prediction method analyzed (See Figures 7 and 8 for the performance of the various methods).

- EN Formula. This method appears to over-predict capacity and exhibits poor precision. The method requires calibration to address the issue of over-prediction. The precision of the EN method is poor and is slightly improved when BOR conditions are used; however, the improvement is not enough to make this a precise method for predicting dynamic pile capacity.
- Gates Formula. The Gates formula under-predicts capacity and exhibits good precision. The method requires calibration to address the issue of under-prediction. The precision for the Gates method is good – to – fair and the use of data from BOR conditions did not improve the precision of the method.
- WEAP. WEAP under-predicts capacity for EOD conditions and slightly over-predicts capacity when using BOR. Precision was good when using BOR conditions, but only fair when using EOD information. It appears that WEAP predictions benefits significantly from using BOR data.
- Measured Energy (ME) Method (Energy Approach). The ME approach predicts capacity well for EOD conditions and over-predicts capacity when using data from BOR conditions. Precision is good when using EOD and BOR information. It appears that EOD results are preferred with the ME approach for predicting capacity
- PDA Method. The PDA method (the Case Method) predicts capacity very well for BOR conditions and with less precision for EOD conditions. There is a tendency to under-predict capacity by 20-30 percent with EOD conditions. Precision is very good to good when using BOR information and good to fair when using EOD results.

- f. CAPWAP. The CAPWAP method predicts capacity very well for BOR conditions and with less precision for EOD conditions. There is a tendency to under-predict capacity by 20 – 30 percent with EOD results. Precision is very good to good when using BOR information and good to poor when using EOD results.
- g. Static Method. The static methods based on Cone Penetration Test results (CPT) exhibit better accuracy and precision than the other pile static analyses methods. The CPT analysis method proposed by Eslami, predicts capacity with very good precision, but most of the other cone methods predict capacity with good to fair precision. The static methods exhibit overall poor to very poor precision.

The investigation identified the modified Gates formula as a most efficient and economical method to predict axial capacity of piles using EOD measurements. The CAPWAP method was found to provide on the average more accurate results for predicting pile capacity using BOR measurements.

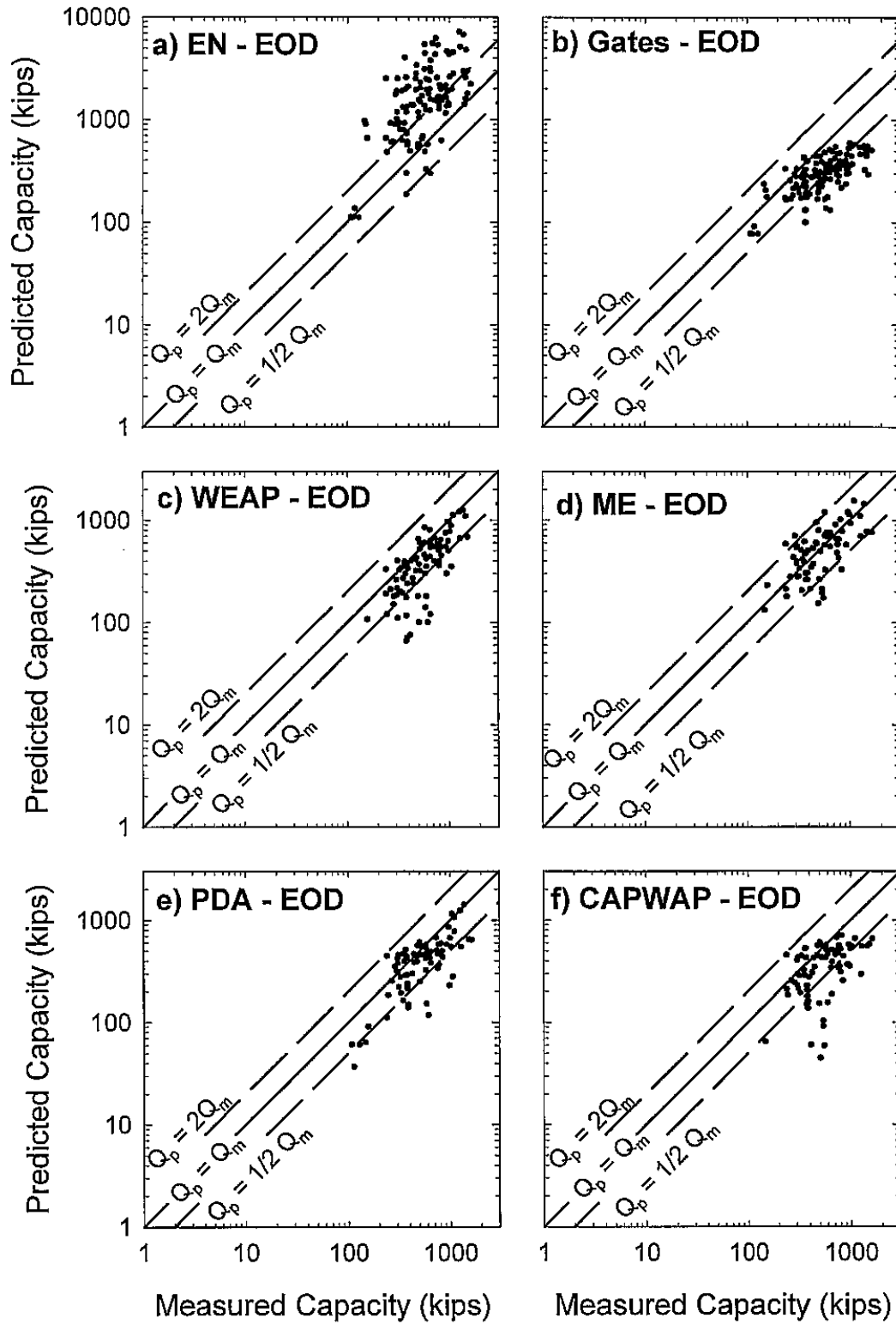
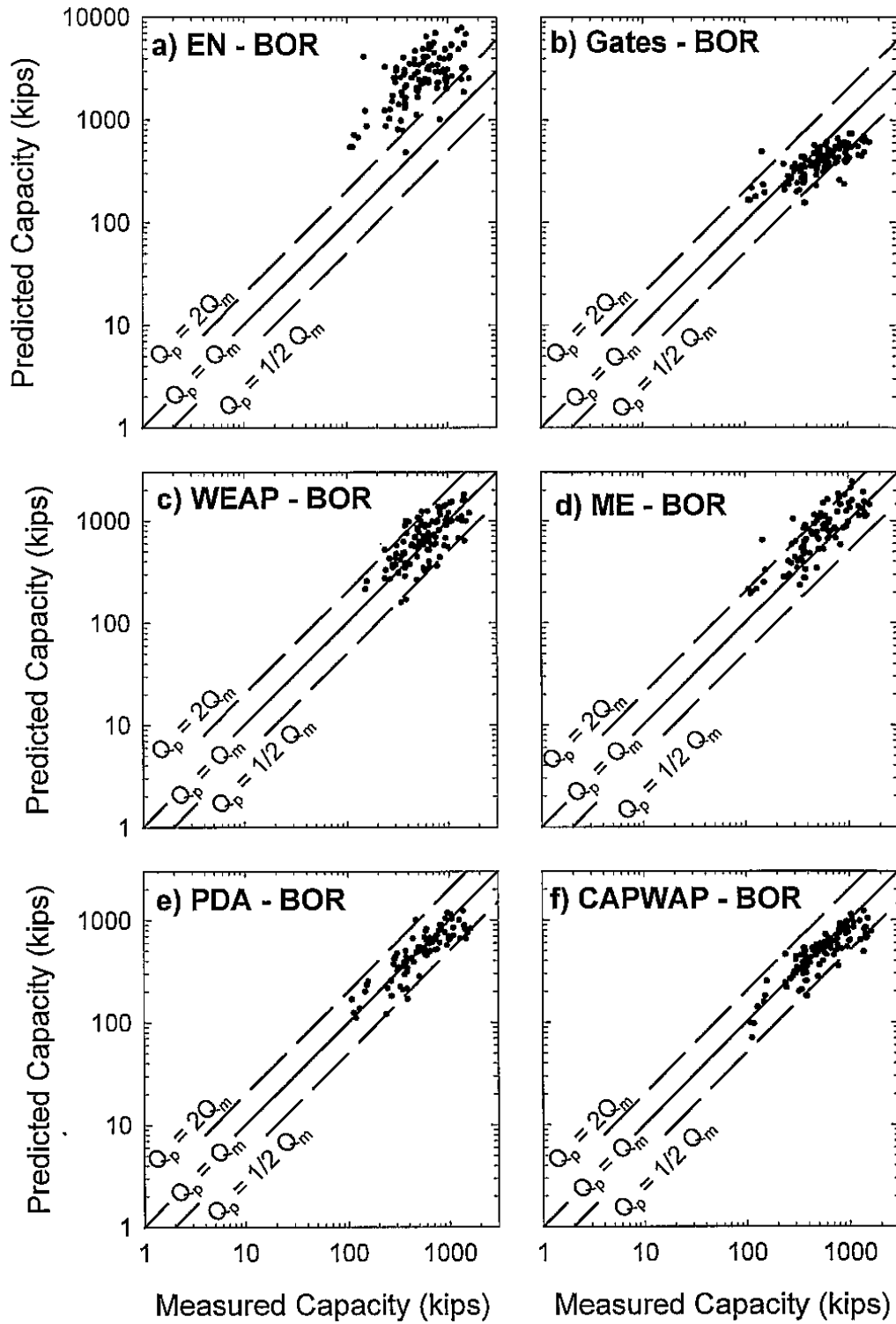


Figure 7. Predicted versus measured capacity for FHWA database using EOD data (Long and Maniaci, 2000)





**Figure 8. Predicted versus measured capacity for FHWA database using BOR data (Long and Maniaci, 2000)**

#### 2.2.4 Conclusions

1. The purpose of the report prepared by Long and Maniaci (2000) was to evaluate the effectiveness of the current practices of IDOT when predicting driven pile capacity. At the time Long and Maniaci report was written, LRFD was being developed in different States but was not yet adopted for practice by IDOT.
2. Long and Maniaci used different databases from the literature that did not match well the pile types, soil characteristics, and driving conditions of the current practice in the State of Illinois. These conditions are, by and large, similar to those found in Minnesota in the way of driven steel piles though most piles driven in Illinois are H piles and not pipe piles.
3. Several dynamic methods were analyzed to estimate their accuracy and validity, EN, Gates, WEAP, PDA, EM, and CAPWAP. The first three methods estimate pile capacity based on field observations of driving resistance, like hammer energy based on stroke, pile type, soil type, and with this information develop a relationship between capacity and driving resistance. The last three methods, required dynamic measurements of the variation of force and velocity with respect to time during driving. The methods studied by Long and Maniaci, utilized pile behavior at the end of driving (EOD) or beginning of restrike (BOR).
4. Each of the databases utilized by Long and Maniaci used pile capacity (failure) based on a different static load test interpretation method, which presents just a variation in the pile capacity (typically 3.5 - 5%, see Paikowsky et al., 2004). The database presented by Flaate (1964), and the one presented by Paikowsky et al. (1994), used Davisson's failure criteria to evaluate the pile's capacity. Frigaszy (1988, 1989) used Q-D over 30 method and Olson tangent intersection method.
5. The statistical analyses was conducted based on the relationship between predicted values versus measured values ( $Q_p/Q_m$ ), which are the inverse of the bias definition in reliability and the one used by Paikowsky et al. (2004) to develop the LRFD parameters. This approach indicates that for mean values above unity, the method is over-predicting capacity and if it is under unity, the method under-predicts pile capacity. The distribution was found to be log-normal.
6. Long and Maniaci (2000) analyzed the databases separately and together to identify the effects using EOD versus BOR data for estimated capacity. The results are presented graphically and statistically. No relationships were investigated regarding soil conditions and restrike effects.
7. Long and Maniaci (2000) report suggests that the Gates formula is an efficient and economical method to predict axial capacity of piles using EOD measurements in comparison to the EN formula, and the CAPWAP method provides on the average more accurate results for predicting pile capacity using BOR measurements. The ME (Energy

Approach) was found most effective in providing pile capacity in the field based on dynamic measurements during driving.

## **2.3 Illinois Department of Transportation – Long et al. (2009a)**

### **2.3.1 Overview**

The research objective was the improvement of the design and construction practices for deep foundations in the state of Illinois.

The specific research goals were:

1. Improve the relationship between the design pile capacity and the one obtained in the field based on driving behavior.
2. Improve the agreement between estimated pile lengths and driven pile lengths.
3. Improve the selection method to determine pile capacity based on the soil properties behavior.
4. Select a combination of dynamic and static pile driving formulae In order to obtain the most efficient pile design.

Several static and dynamic methods were investigated during this research:

- a. Static Methods: IDOT-Static, Olson's Method, DRIVEN (FHWA), ICP, K-IDOT
- b. Dynamic Methods: EN-IDOT, FHWA-Gates, WSDOT, WEAP, UI-FHWA

No single database was found to be sufficient to satisfy all aforementioned four goals; therefore three databases were compiled to conduct the study. The International Database, the Comprehensive Database, and the Illinois Database.

The following sections summarize each of the databases analyzed by Long et al. (2009a), and presents tables summarizing the statistical results and the best agreement between dynamic and static methods.

### **2.3.2 International Database**

The International database comprised of the following information:

- 132 pile load tests
- static load tests included
- EOD conditions
- Enough information to allow the prediction of pile capacity using a simple dynamic formula.

The information obtained with this database was sufficient to allow the development of the resistance factors for dynamic formulae, also for the development of an optimized method to improve the agreement between design and field values.

This database compiles the data from several smaller load test databases. The databases include those developed by Flaate (1964), Olson and Flaate (1967), Frigaszy et al. (1988), FHWA (Rausche et al., 1996), Allen (2007), and Paikowsky et al. (2004). A total of 132 load tests were collected for this database. Sufficient information is available for each pile so that the pile capacity based on any of the dynamic formulae evaluated can be determined. Sufficient information is not available so that the pile capacity can be estimated based on static methods. The results of a static load test are available for each pile.

Based on the piles in the International Database, the FHWA-UI formula predicts capacity with the most accuracy and precision. This formula is followed by the WSDOT, then FHWA-Gates formulae in degree of accuracy and precision, see Figure 9 and Table 8 presenting and summarizing the obtained results. Based on the analysis of the data, Long et al. (2009a), group the FHWA-Gates, FHWA-UI, and WSDOT formulae into one category of prediction that performs fairly well and group WEAP and the EN-IDOT formula into a category of capacity prediction that does not perform as well.

**Table 8. International database selected dynamic/SLT statistics for all piles (Long et al., 2009a)**

		WSDOT	FHWA-Gates	FHWA-UI
<b>vs. SLT</b>	Mean	1.14	1.22	1.02
	Std. Dev.	0.51	0.59	0.41
	COV	0.45	0.49	0.41
	$r^2$	0.35	0.31	0.42
	n	132	132	132

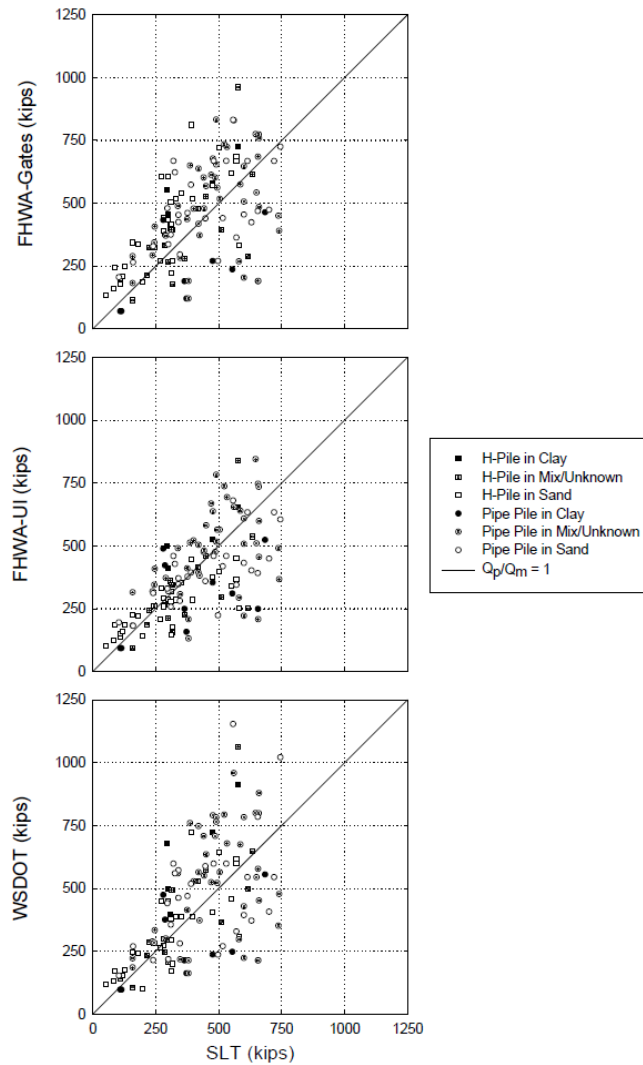


**Figure 9. International database selected predictions of dynamic equations vs. SLT dynamic (Long et al. 2009a)**

### 2.3.3 Comprehensive Database

#### 2.3.3.1 Extent and Data

The Comprehensive database comprised of the following information:

- 26 piles
- EOD conditions

The Comprehensive Database is comprised of 26 piles gathered to include sufficient information for pile capacity estimations using all of the dynamic formulae and static capacity methods evaluated in the study as well as the results of a static load test conducted to failure. This

database allowed the prediction of pile capacity using both static and dynamic formulae based on EOD conditions. This was the only database that allowed the determination of resistance factors for static methods.

The resistance factors developed with this database can only be considered as tentative, or as an independent source to confirm or reject conclusions obtained with the other two databases.

#### *2.3.3.2 Analysis of dynamic Formulae*

Each of the dynamic formulae presented by Long et al. (2009a) was analyzed and compared to the SLT capacity data as shown in Figure 10. A clear trend does not appear for the ratio of Dynamic over SLT capacities. Three of the methods seem to over-predict capacity for most piles.

An empirical correction was suggested to be applied to a group of dynamic formulae, so that the average capacity ratio (Table 9) becomes one. It is much more difficult to reduce the COV of a group of capacity predictions. Based on the COV of the average capacity ratios, the formulae can be grouped into three sets. The first set includes the FHWA-Gates and the WSDOT formulae. Their COV are very similar and the lowest of the dynamic formulae studied (about 0.3). The second set is the FHWA-UI formulae and WEAP. The third set is the EN-IDOT formula with the largest COV of all the methods analyzed (Table 9).

#### *2.3.3.3 Analysis of the Static methods*

One trend appears for all static methods. The average capacity ratio in sand tends to be larger than the average capacity ratio in clay, while sometimes the difference is small. The K-IDOT method displays a larger difference between the average capacity ratio in sand and clay. This is to be expected, based on the K-IDOT assumptions. The K-IDOT method was developed with the goal of improving agreement between methods, knowing that empirical corrections were required to bring predicted and measured capacity into agreement.

The static methods analyzed using the Comprehensive Database fall into three groups based on the COV. The first is the ICP method, presenting the lowest COV from all the methods. The second group consists of the IDOT Static method, the Kinematic IDOT method, and Olson's method, showing a moderate amount of scatter. The third group consists of Driven, with a much larger COV.

Based on the agreement between static methods and static load test results, the ICP, the IDOT Static, the K-IDOT methods showed the most accurate value to predict capacity (Figure 10).

**Table 9. Comprehensive database dynamic and static methods vs. SLT statistics (Long et al., 2009a)**

	WSDOT/SLT	FHWA-Gates/SLT	FHWA-UI/SLT	IDOT-S/SLT	K-IDOT/SLT	ICP/SLT
Mean	1.02	1.02	0.97	1.30	2.00	1.85
Std. Dev.	0.29	0.31	0.42	0.88	1.37	0.94
COV	0.29	0.31	0.43	0.67	0.68	0.51
$r^2$	0.52	0.73	0.52	0.36	0.42	0.55
n	26	23	23	26	26	26

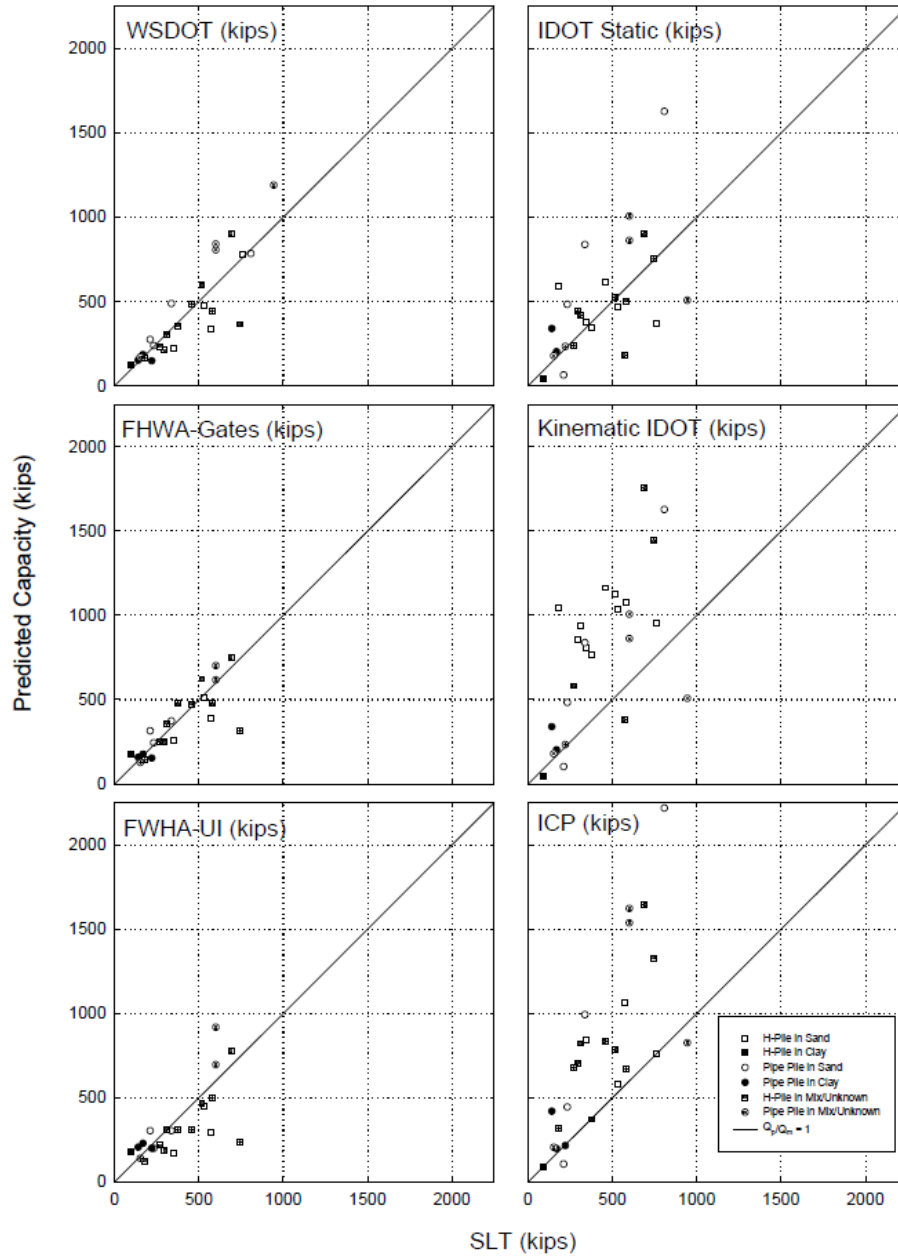


**Figure 10. Comprehensive database selected dynamic and static methods vs. SLT (Long et al 2009)**

#### 2.3.3.4 Agreement between static methods and dynamic formulae

Some general trends appear when comparing the Dynamic vs. Static capacity predictions. For piles in clay the general trend is for the dynamic formula to predict higher capacity than the static method, with the exception of the WSDOT/ICP data (Figure 11). In sand, the K-IDOT and ICP methods predict higher capacities than the dynamic formulae. The IDOT static method does the opposite, predicting a smaller capacity in sand than dynamic formulae. In pipe piles, the dynamic formula will generally predict a higher capacity than the IDOT-S and K-IDOT methods. The opposite occurs with the ICP method, it predicts a higher capacity than the dynamic formulae. In H piles, the K-IDOT and ICP methods tend to predict higher capacity than the dynamic formulae. The dynamic formulae tend to predict higher capacities overall when compared to the static analyses. The dynamic formulae tend to predict higher capacities in H-piles than the IDOT-S method.

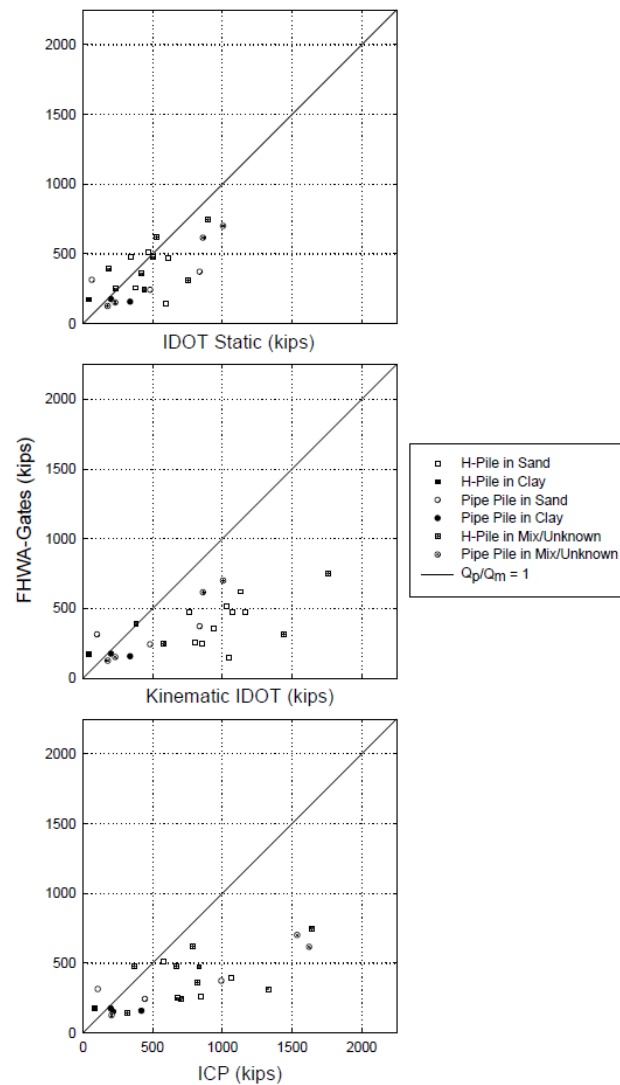


Figure 11. FHWA-Gates vs. static methods (Long et al., 2009a)



The dynamic/static analyses provide information only for the agreement between a dynamic and static method; they do not indicate how accurately either method predicts the actual pile capacity. A considerable amount of scatter can be seen in all the Dynamic/Static analyses. This indicates it would not be uncommon for any single pile to produce capacity ratios appreciably different than the average capacity ratios (Long et al. 2009a).

Based on the comprehensive database, the WSDOT and the FHWA-Gates formulae were found to be the most precise dynamic formulae, while the EN-IDOT formula is the least precise. WEAP and the FHWA-UI formulae have intermediate precisions between the two above categories.

Table 10 presents the statistical analysis for the relationship between a dynamic method and a static method. Note that the good agreement between any two methods does not indicate that either of the methods accurately predicts the capacity of a pile, but rather indicates that the compared methods agree well with each other.

The ICP method appears to offer the best agreement with dynamic formulae (Table 10). The WSDOT, FHWA-Gates, and FHWA-UI/Static average capacity ratios display the lowest COV with the ICP method, followed by the IDOT Static method, and then the K-IDOT method. The lowest COV was displayed by the WSDOT formulae, combined with the IDOT, K-IDOT, and ICP methods.

Based on the comprehensive database, the WSDOT and the FHWA-Gates formulae were found to be the most precise dynamic formulae, while the EN-IDOT formula is the least precise. WEAP and the FHWA-UI formulae have intermediate precisions between the two above categories.

**Table 10. Dynamic vs. static method statistics (Long et al., 2009a)**

		<b>WSDOT</b>	<b>FHWA-Gates</b>	<b>FHWA-UI</b>
<b>vs. IDOT Static</b>	Mean	1.16	1.11	1.12
	Std. Dev.	0.86	0.88	0.97
	COV	0.74	0.80	0.87
	$r^2$	0.37	0.29	0.29
	n	26	23	23
<b>vs. Kinematic IDOT</b>	Mean	0.79	0.74	0.77
	Std. Dev.	0.66	0.64	0.81
	COV	0.84	0.87	1.05
	$r^2$	0.27	0.30	0.18
	n	26	23	23
<b>vs. ICP</b>	Mean	0.72	0.69	0.75
	Std. Dev.	0.46	0.47	0.58
	COV	0.63	0.67	0.81
	$r^2$	0.47	0.41	0.38
	n	26	23	23

The ICP method is the most precise static method, while Driven is the least precise static method. The IDOT, K-IDOT, and Olson's Methods have intermediate precisions between the two presented above. For the Dynamic/Static data, the ICP method and the WSDOT formula offer the best agreement. The Comprehensive Database is considered an important check on the results of the other two databases as it is the only database for which capacity predictions can be made using every prediction method considered in Long et al. (2009a) study and these predictions could be compared to static load test results.

### **2.3.4 Illinois Database**

#### **2.3.4.1 Extent and Data**

- 92 pile cases
- No static load test were performed on these pile cases

This database provided sufficient information to predict capacity using both, dynamic and static formulae. It was used to quantify relations between predictions of capacity using static and dynamic formulae, as well as to develop methods of improving the agreement between the two prediction methods. This database was broken into the following categories (refer to the sub-categorization in Figure 12):

- H piles in sand
- H piles in clay
- Pipe piles in sand
- Pipe piles in clay

The Illinois Database consists of pile information provided by IDOT. Ninety-two (92) piles are included in the database and the number of cases split fairly evenly between the different categories, namely; H-piles in sand, H-piles in clay, pipe piles in sand, and pipe piles in clay. Sufficient information is available to predict the capacity of a pile based on all static and dynamic methods considered. Static load tests were not conducted on any of the piles.

#### **2.3.4.2 Statistical Analysis**

Statistical analyses were performed on each of the database subcategories. Ratios of the capacity of each method were calculated by  $Q_{p1}/Q_{p2}$ , where  $Q_{p1}$  and  $Q_{p2}$  are the predicted capacities for a given pile using two different methods. The mean, standard deviation, coefficient of variation and correlation coefficient were calculated for each set of ratios and are summarized in Table 11 to 19.

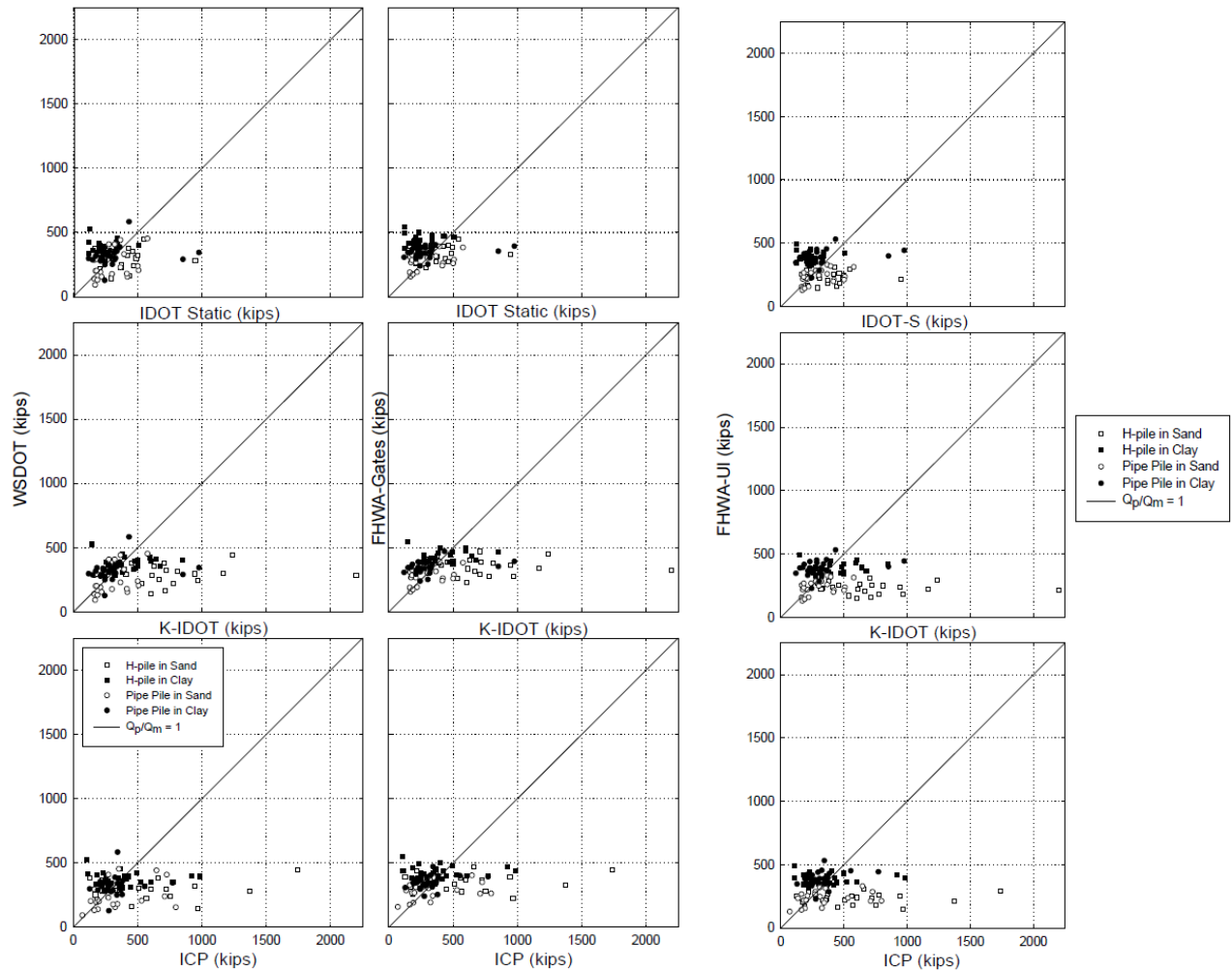


**Figure 12. Dynamic vs. static capacities for the Illinois Database (Long et al., 2009a)**

The Illinois database offered information that was very useful as it consists of data gathered only from the state of Illinois; however static load tests were not performed on any of the piles. As such, no firm conclusions can be drawn about the accuracy of any given method. Instead, conclusions can be drawn about how well a given dynamic formula agrees with a given static method. This information is useful, as a low COV between Dynamic/Static data indicates that the length of pile estimated to be necessary using a static method will be similar to the length driven using the correlated dynamic formula.

Based on this database, the IDOT static method, used in combination with either the FHWA-Gates or WSDOT formula, will tend to offer the best agreement, for all the pile-driving conditions presented above.

**Table 11. Capacity ratio statistics for all piles in the Illinois database**

		WSDOT	FHWA-Gates	FHWA-UI
vs. IDOT Static	Mean:	1.20	1.40	1.28
	Std. Dev:	0.60	0.70	0.74
	COV:	0.50	0.50	0.58
	$r^2$ :	0.00	0.00	0.00
	n:	92	92	92
vs. Kinematic IDOT	Mean:	0.94	1.08	1.02
	Std. Dev:	0.59	0.63	0.75
	COV:	0.63	0.57	0.74
	$r^2$ :	0.01	0.03	0.03
	n:	92	92	92
vs. ICP	Mean:	1.07	1.21	1.13
	Std. Dev:	0.75	0.76	0.85
	COV:	0.70	0.63	0.75
	$r^2$ :	0.01	0.02	0.01
	n:	92	92	92

**Table 12. Capacity ratio statistics for H-Piles in the Illinois database**

		WSDOT	FHWA-Gates	FHWA-UI
vs. IDOT Static	Mean:	1.4	1.6	1.33
	Std. Dev:	0.8	0.8	0.86
	COV:	0.5	0.5	0.65
	$r^2$ :	0.05	0.06	0.15
	n:	46	46	46
vs. Kinematic IDOT	Mean:	0.80	0.91	0.76
	Std. Dev:	0.55	0.58	0.57
	COV:	0.68	0.63	0.75
	$r^2$ :	0.05	0.07	0.16
	n:	46	46	46
vs. ICP	Mean:	1.09	1.24	1.04
	Std. Dev:	0.91	0.97	0.93
	COV:	0.84	0.78	0.90
	$r^2$ :	0.01	0.01	0.07
	n:	46	46	46

**Table 13. Capacity ratio statistics for Pipe-Piles in the Illinois database**

		WSDOT	FHWA-Gates	FHWA-UI
vs. IDOT Static	Mean:	1.1	1.2	1.25
	Std. Dev:	0.5	0.5	0.67
	COV:	0.4	0.4	0.53
	$r^2$ :	0.06	0.10	0.05
	n:	46	46	46
vs. Kinematic IDOT	Mean:	1.09	1.23	1.25
	Std. Dev:	0.57	0.54	0.67
	COV:	0.52	0.44	0.53
	$r^2$ :	0.06	0.10	0.05
	n:	46	46	46
vs. ICP	Mean:	1.05	1.19	1.20
	Std. Dev:	0.56	0.56	0.65
	COV:	0.53	0.47	0.55
	$r^2$ :	0.05	0.06	0.01
	n:	46	46	46

**Table 14. Capacity ratio statistics for piles in sand in the Illinois database**

		WSDOT	FHWA-Gates	FHWA-UI
vs. IDOT Static	Mean:	0.9	1.1	1.62
	Std. Dev:	0.4	0.5	0.73
	COV:	0.5	0.4	0.45
	$r^2$ :	0.06	0.07	0.06
	n:	50	50	50
vs. Kinematic IDOT	Mean:	0.72	0.86	0.71
	Std. Dev:	0.49	0.53	0.52
	COV:	0.67	0.62	0.74
	$r^2$ :	0.05	0.08	0.00
	n:	50	50	50
vs. ICP	Mean:	0.85	1.01	0.82
	Std. Dev:	0.64	0.72	0.64
	COV:	0.75	0.71	0.78
	$r^2$ :	0.02	0.11	0.0
	n:	50	50	50

Adapted from Long et al., 2009a

**Table 15. Capacity ratio statistics for piles in clay in the Illinois database**

		WSDOT	FHWA-Gates	FHWA-UI
vs. IDOT Static	Mean:	1.5	1.7	1.62
	Std. Dev:	0.7	0.7	0.73
	COV:	0.5	0.4	0.45
	$r^2$ :	0.00	0.00	0.06
	n:	50	50	50
vs. Kinematic IDOT	Mean:	1.11	1.24	1.26
	Std. Dev:	0.51	0.55	0.66
	COV:	0.46	0.44	0.52
	$r^2$ :	0.07	0.14	0.05
	n:	50	50	50
vs. ICP	Mean:	1.24	1.36	1.35
	Std. Dev:	0.66	0.68	0.70
	COV:	0.53	0.50	0.52
	$r^2$ :	0.01	0.05	0.02
	n:	50	50	50

**Table 16. Capacity ratio statistics for H-Piles in the Illinois database**

		WSDOT	FHWA-Gates	FHWA-UI
vs. IDOT Static	Mean:	0.9	1.1	0.82
	Std. Dev:	0.5	0.5	0.45
	COV:	0.5	0.5	0.55
	$r^2$ :	0.00	0.00	0.00
	n:	21	21	21
vs. Kinematic IDOT	Mean:	0.51	0.62	0.45
	Std. Dev:	0.32	0.37	0.30
	COV:	0.62	0.59	0.66
	$r^2$ :	0.00	0.01	0.01
	n:	21	21	21
vs. ICP	Mean:	0.75	0.90	0.64
	Std. Dev:	0.63	0.72	0.54
	COV:	0.84	0.80	0.84
	$r^2$ :	0.05	0.02	0.02
	n:	21	21	21

**Table 17. Capacity ratio statistics for H-Piles in clay in the Illinois database**

		WSDOT	FHWA-Gates	FHWA-UI
vs. IDOT Static	Mean:	1.7	2.0	1.72
	Std. Dev:	0.8	0.8	0.64
	COV:	0.4	0.4	0.37
	$r^2$ :	0.00	0.00	0.00
	n:	25	25	25
vs. Kinematic IDOT	Mean:	1.00	1.13	0.99
	Std. Dev:	0.43	0.46	0.43
	COV:	0.43	0.41	0.43
	$r^2$ :	0.00	0.02	0.02
	n:	25	25	25
vs. ICP	Mean:	1.36	1.53	1.33
	Std. Dev:	0.87	0.95	0.84
	COV:	0.65	0.62	0.63
	$r^2$ :	0.00	0.00	0.00
	n:	25	25	25

**Table 18. Capacity ratio statistics for H-Piles in the Illinois database**

		WSDOT	FHWA-Gates	FHWA-UI
vs. IDOT Static	Mean:	0.9	1.1	0.94
	Std. Dev:	0.4	0.4	0.39
	COV:	0.5	0.4	0.42
	$r^2$ :	0.14	0.18	0.18
	n:	21	21	21
vs. Kinematic IDOT	Mean:	0.91	1.09	0.94
	Std. Dev:	0.45	0.43	0.39
	COV:	0.50	0.39	0.42
	$r^2$ :	0.14	0.18	0.18
	n:	21	21	21
vs. ICP	Mean:	0.93	1.13	0.99
	Std. Dev:	0.58	0.67	0.60
	COV:	0.62	0.59	0.61
	$r^2$ :	0.11	0.10	0.10
	n:	21	21	21

Adapted from Long et al., 2009a

**Table 19. Capacity ratio statistics for Pipe Piles in clay in the Illinois database**

		WSDOT	FHWA-Gates	FHWA-UI
vs. IDOT Static	Mean:	1.2	1.3	1.52
	Std. Dev:	0.5	0.5	0.79
	COV:	0.4	0.4	0.52
	$r^2$ :	0.04	0.10	0.10
	n:	25	25	25
vs. Kinematic IDOT	Mean:	1.23	1.35	1.52
	Std. Dev:	0.61	0.61	0.79
	COV:	0.50	0.45	0.52
	$r^2$ :	0.04	0.10	0.10
	n:	25	25	25
vs. ICP	Mean:	1.13	1.23	1.37
	Std. Dev:	0.48	0.43	0.56
	COV:	0.43	0.35	0.41
	$r^2$ :	0.02	0.11	0.10
	n:	25	25	25

The cumulative distribution of the FHWA-Gates/IDOT Static data is plotted in Figure 13. The y-axis of the figure indicates the probability that the FHWA-Gates/IDOT Static capacity ratio will be less than or equal to the capacity ratio on the x-axis. The solid line represents the theoretical distribution for a log normal distribution data.

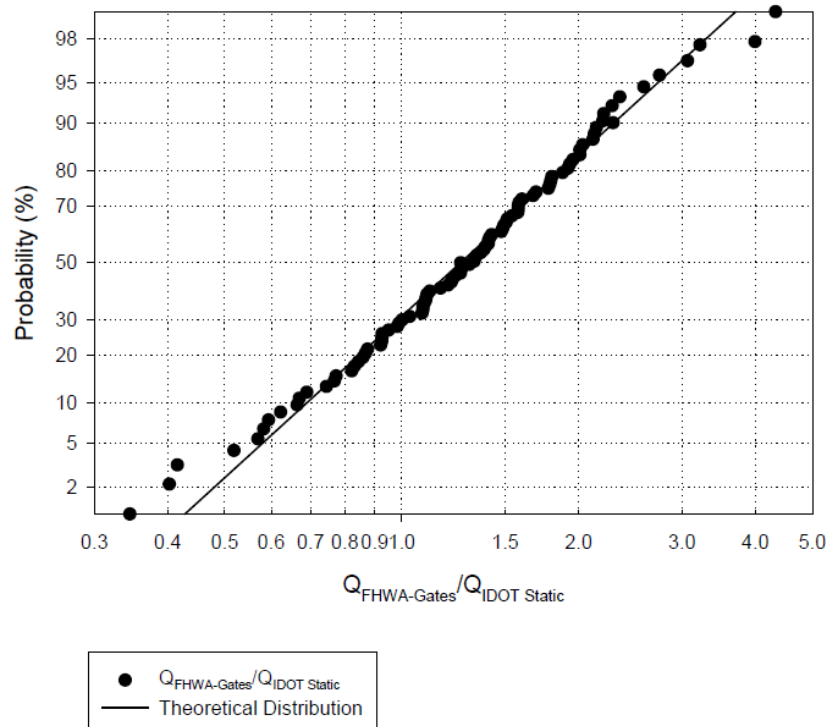


**Figure 13. Cumulative distribution of FHWA-Gates/IDOT static data, Illinois database (Long et al., 2009a)**

### 2.3.5 Development of Correction Factors

#### 2.3.5.1 Overview

Based upon the results of the analyses carried out on the above reviewed three databases, methods were defined as most useful utilizing terms of actual accuracy and precision, and in the agreement between static and dynamic methods. The IDOT Static, K-IDOT, and ICP methods were found to be the most promising static methods, while the FHWA-Gates, FHWA-UI, and WSDOT formulae were found to be the most promising dynamic methods. To further refine these results, correction factors were applied to each static method. These correction factors are based on pile type and soil type, and are unique to each method. Table 20 presents the proposed correction factors for each Dynamic/Static combination. Based on these correction factors, corrected statistics were determined for the Dynamic/Static data for both; the Illinois and the Comprehensive Databases. The International Database was not analyzed due to insufficient information to determine the pile capacity using static methods.

**Table 20. Correction factors**

	Pipe, Clay	Pipe, Sand	H, Clay	H, Sand
<b>WSDOT/ICP</b>	1.067	0.730	1.277	0.353
<b>FHWA-Gates/ICP</b>	1.178	0.924	1.438	0.461
<b>FHWA-UI/ICP</b>	1.355	0.677	1.226	0.300
<b>WSDOT/IDOT-S</b>	1.174	0.758	1.500	0.724
<b>FHWA-Gates/IDOT-S</b>	1.284	0.955	1.500	1.073
<b>FHWA-UI/IDOT-S</b>	1.500	0.711	1.500	0.500
<b>WSDOT/K-IDOT</b>	1.174	0.758	1.500	0.300
<b>FHWA-Gates/K-IDOT</b>	1.284	0.955	1.500	0.387
<b>FHWA-UI/K-IDOT</b>	1.500	0.711	1.353	0.300

#### 2.3.5.2 Corrected Illinois Database

Figure 14 and Table 21 present the corrected analyses for Illinois database using the above correction factors with the range in average (for each group) between 1.09 to 1.22, indicating that the correction factors brought the average capacity ratios to a value close to unity. For the corrected Illinois database, the K-IDOT method appears to be the static method that best agrees with the dynamic formulae, both with respect to the COV. All the dynamic formulae performed well when analyzed using the K-IDOT method, the range in Dynamic/K-IDOT COV's is only 0.06, while the range in value of the average capacity ratios is 0.02. Based on the presented sub-categories, the H-piles in clay tend to over-predict capacity; generally the pipe piles show better agreement between the dynamic and the static methods. The range in value of the average capacity ratio for pipe piles in sand is closer to unity than that for pipe piles in clay.

In reviewing Figure 14 and Table 21, and the observations made by Long et al., 2009a, one must emphasize the fact that the use of a correction factor alone in order to obtain a better bias is very

misleading. For example, all the graphs presented in Figure 14 show very large scatter (besides being presented on an unreasonably large scale) that is associated with a coefficient of determination  $r^2$  of a very low value (see Table 21). This coefficient suggests practically no correlation between the two values. Paikowsky et al. (1994) defined ranges of a coefficient of determination for geotechnical data to be  $r^2 < 0.60$  poor,  $0.60 \leq r^2 < 0.80$  moderate, and  $r^2 \geq 0.80$  having a good correlation. The ‘corrected’ data presented in Table 21 shows  $r^2 < 0.15$  in spite of average means smaller than 1.22, hence of very poor value. One should also note that the COV of the averages reported in Table 21 is in the range of 0.43 to 0.53, again suggesting large scatter as observed in Figure 14.

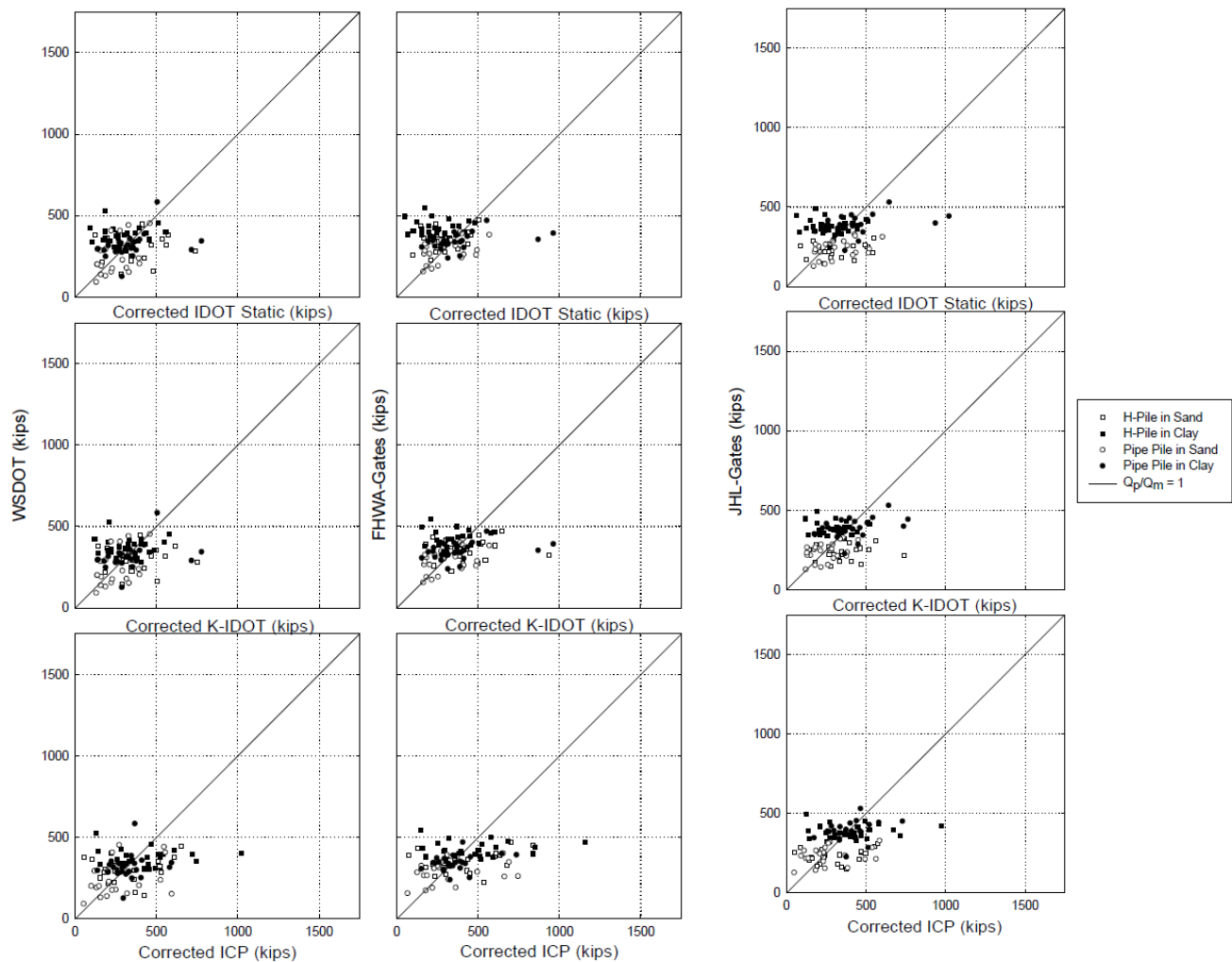


**Figure 14. Dynamic vs. corrected static capacities for the Corrected Illinois database (Long et al., 2009a)**



**Table 21. Statistics for dynamic vs. corrected static methods, corrected Illinois database (Long et al., 2009a)**

		WSDOT	FHWA-Gates	FHWA-UI
<b>vs. Corrected IDOT Static</b>	Mean	1.19	1.16	1.22
	Std. Dev.	0.62	0.54	0.67
	COV	0.52	0.46	0.55
	$r^2$	0.05	0.01	0.08
	n	92	92	92
<b>vs. Corrected Kinematic IDOT</b>	Mean	1.11	1.12	1.10
	Std. Dev.	0.54	0.48	0.53
	COV	0.49	0.43	0.49
	$r^2$	0.07	0.05	0.08
	n	92	92	92
<b>vs. Corrected ICP</b>	Mean	1.16	1.14	1.13
	Std. Dev.	0.67	0.62	0.63
	COV	0.58	0.55	0.56
	$r^2$	0.09	0.11	0.15
	n	92	92	92

### 2.3.5.3 Corrected Comprehensive Database

Predicted static capacities in the Comprehensive Database were corrected using the correction factors determined for the Illinois database (Table 20). The statistical results for the Comprehensive database are summarized in Table 22, and presented graphically in Figure 15.

The corrected K-IDOT method best agrees with the WSDOT and FHWA-Gates formulae. For the sub-categories of the WSDOT/Corrected K-IDOT data, there appears to be little bias between pipe piles and H-piles; however, there is a stronger tendency to over-predict capacity for pipe piles. The degree of scatter is smaller for H-piles than Pipe-piles.

The sub-categories of the FHWA-Gates/Corrected K-IDOT data suggested that there is a tendency to under-predict capacity for both H-piles and pipe-piles. There is a tendency to over-predict capacity in clay with a higher degree of scatter.

For the statistical evaluation of these results, refer to the commentary provided in the previous section, noting that the COV values in Table 22 range between 0.56 to 0.78 (!) and  $r^2$  for all cases is smaller than 0.37.

**Table 22. Statistics for dynamic vs. corrected static methods, comprehensive database (Long et al., 2009a)**

		WSDOT	FHWA-Gates	FHWA-UI
<b>vs. Corrected IDOT Static</b>	Mean	1.20	0.94	1.17
	Std. Dev.	0.86	0.72	0.91
	COV	0.71	0.77	0.78
	$r^2$	0.37	0.29	-
	n	26	23	23
<b>vs. Corrected Kinematic IDOT</b>	Mean	1.09	0.90	0.96
	Std. Dev.	0.63	0.56	0.62
	COV	0.58	0.62	0.65
	$r^2$	0.27	0.30	-
	n	26	23	23
<b>vs. Corrected ICP</b>	Mean	0.94	0.78	0.84
	Std. Dev.	0.60	0.53	0.56
	COV	0.64	0.67	0.66
	$r^2$	0.00	0.00	-
	n	26	23	23

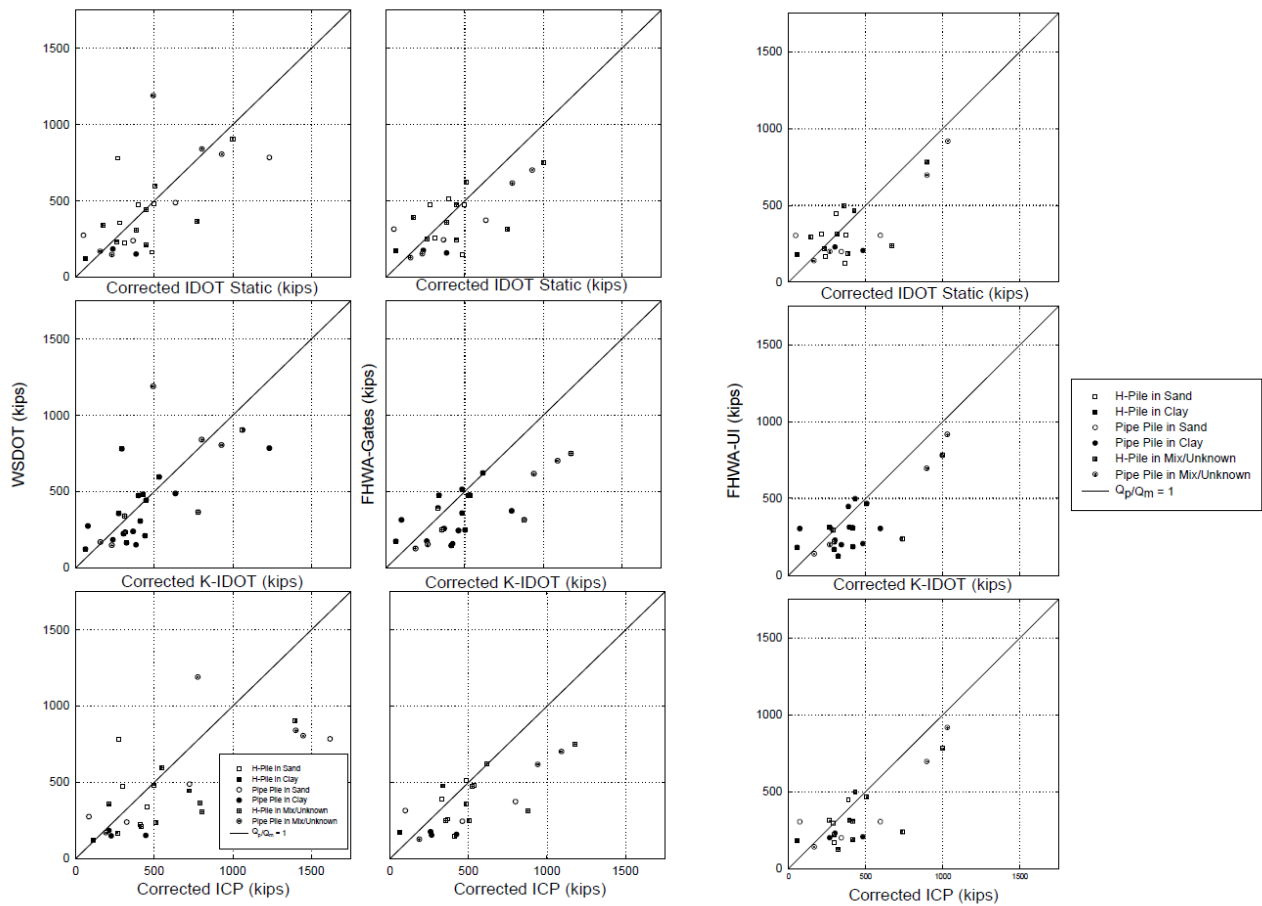


**Figure 15. Dynamic vs. corrected static capacities for the comprehensive database (Long et al., 2009a)**

#### 2.3.5.4 Recommended Methods

Table 23 summarizes the best agreement between the different methods of pile capacity analysis and the databases utilized. Based on their research, Long et al. (2009a) proposed that the WSDOT formula replaces the FHWA Gates formula as the standard method of design, construction and verification for pile capacity, and the Modified IDOT static method shall be used to develop the Structure Geotechnical Report (SGR) pile design tables. The equation to be used, therefore, is:

$$R_n = 6.6F_{eff}WH\ln(10N) \quad (9)$$

Where  $F_{eff}$  is provided in Table 24.

**Table 23. Databases best agreement methods summary**

	<b>DYNAMIC METHOD</b>	<b>STATIC METHOD</b>
<b>International Database</b>	UI-FHWA,WSDOT,FHWA-GATES	K-IDOT
<b>Comprehensive Database</b>	WSDOT,FHWA-GATES,UI-FHWA	*K-IDOT
<b>Illinois Database</b>	H-PILES IN SAND: • FHWA-GATES H-PILES IN CLAY: • UI-FHWA ALL H-PILES: • FHWA-GATES PP IN SAND: • FHWA-GATES PP IN CLAY: • FHWA-GATES ALL PP: • WSDOT ALL PILES IN SAND: • FHWA-GATES ALL PILES IN CLAY: • FHWA-GATES ALL PILES: • FHWA-GATES	H-PILES IN SAND: • IDOT H-PILES IN CLAY: • IDOT ALL H-PILES: • IDOT PP IN SAND: • IDOT PP IN CLAY: • Driven ALL PP: • Driven ALL PILES IN SAND: • IDOT ALL PILES IN CLAY: • K-IDOT ALL PILES: • IDOT

\*The corrected K-IDOT provided the best agreement with the prediction of capacity from dynamic formula and static load tests.

**Table 24. Parameter  $F_{eff}$  to be used in Equation 9 for hammer and pile type combinations**

$F_{eff}$	<b>STEEL</b>	<b>TIMBER</b>	<b>CONCRETE</b>	<b>REDUNDANT</b>
<b>Air/Steam</b>	0.55	0.55	0.55	0.55
<b>Open-ended Diesel</b>	0.47	0.37	0.37	0.55
<b>Close-ended Diesel</b>	0.35	0.35	0.35	0.55

The use of the corrected K-IDOT (Equation 10), method is recommended for a static analysis with the correction factors presented in Table 25:

$$Q_{total} = Q_{sand} * Factor(pile\ type) + Q_{clay} * Factor(pile\ type) \quad (10)$$

**Table 25. Correction factors for Equation 10**

PILE TYPE	SAND	CLAY
H-PILE	0.30	1.5
PIPE-PILE	0.758	1.174

The corrected K-IDOT method requires two calculations of static pile capacity, one capacity is calculated as if the soil/pile failure occurs at the contact between the soil and the pile, and end bearing is developed only for the steel area. A second capacity is calculated as if failure occurs along an enclosed box around the pile perimeter, and end bearing is developed for the whole enclosed area. The smaller of the two capacities is used.

### 2.3.6 Resistance Factors and Reliability

Load and Resistance Factor Design became the required design methodology for bridge foundations. Two procedures for determining resistance factors follow those outlined by Paikowsky et al. (2004) in NCHRP Research Report 507 and are identified as; a) the first order second moment method (FOSM), and b) the first order reliability method (FORM).

#### a. First Order Second Moment (FOSM)

The FOSM can be used to determine the resistance factor using the following expression proposed by Barker et al. (1991):

$$\phi = \frac{\lambda_R \left( \frac{\gamma_D Q_D}{Q_L} + \gamma_L \right) \sqrt{\left[ \frac{(1 + COV_{Q_D}^2 + COV_{Q_L}^2)}{(1 + COV_R^2)} \right]}}{\left( \frac{\lambda_{Q_D} Q_D}{Q_L} + \lambda_{Q_L} \right) \exp \left\{ \beta_T \sqrt{\ln \left[ (1 + COV_R^2)(1 + COV_{Q_D}^2 + COV_{Q_L}^2) \right]} \right\}} \quad (11)$$

$\lambda_R$  = resistance bias factor

$COV_{Q_L}$  = COV of the live load

$\beta_T$  = target reliability index

$Q_D/Q_L$  = dead to live load ratio factors

$COV_R$  = COV of the resistance

$COV_{Q_D}$  = COV of the dead load

$\gamma_D, \gamma_L$  = dead and live load factors

$\lambda_{Q_D}, \lambda_{Q_L}$  = dead & live load bias factors

Using values adopted by AASHTO based on NCHRP Research Report 507, the following values were used from parameters in Equation 11:

$$\begin{aligned}\lambda_R &= \text{mean value of } Q_P/Q_M \text{ as determined from database study} \\ \text{COV}_{QD} &= 0.1 \\ \text{COV}_{QL} &= 0.2 \\ \text{COV}_R &= \text{COV as determined from database study} \\ \beta_T &= \text{target reliability index (generally between 2 and 3.2)} \\ \gamma_D &= 1.25 \\ \gamma_L &= 1.75 \\ Q_D/Q_L &= 2.0 \\ \lambda_{QD} &= 1.05 \\ \lambda_{QL} &= 1.15\end{aligned}$$

The values for bias and the coefficient of variation for the resistance factors used in Equation 11 are based on  $Q_M/Q_P$ ; however, all the statistics determined in Long et al. (2009a) report were presented for  $Q_P/Q_M$ . Long et al. (2009a) presented the converted bias and COV values for  $Q_M/Q_P$  (as detailed in Table 26).

Using Equation 11 with the statistical parameters presented in Table 26, the resistance factor was determined for several values of the Target Reliability Index ( $\beta_T$ ). The results are shown in Figure 16.

NCHRP 507 recommends using a Target Reliability Index of 2.33 for driven piling when used in groups of 5 or more piles. A Reliability Index of 3.0 is recommended for single piles and groups containing 4 or less piles. Table 26 provides resistance factors for target reliability values of 2.33 and 3.0 for each of the predictive methods.

**Table 26. Statistical parameters and resistance factors for the predictive methods based on  $Q_M/Q_P$  values using FOSM and FORM (Long et al. 2009)**

Predictive Method	Bias, $\lambda$	COV	Resistance Factor, $\phi$ Using FOSM		Resistance Factor, $\phi$ Using FORM	
			$\beta_T = 2.33$	$\beta_T = 3.00$	$\beta_T = 2.33$	$\beta_T = 3.00$
FHWA	1.02	0.485	0.37	0.27	0.40	0.30
FHWA-UI	1.15	0.405	0.50	0.37	0.55	0.42
WSDOT	1.05	0.451	0.42	0.30	0.45	0.34
S-IDOT	1.11	0.666	0.28	0.18	0.29	0.19
Corrected S-IDOT	0.97	0.650	0.25	0.16	0.26	0.18
Corrected K-IDOT	1.09	0.525	0.37	0.26	0.40	0.28

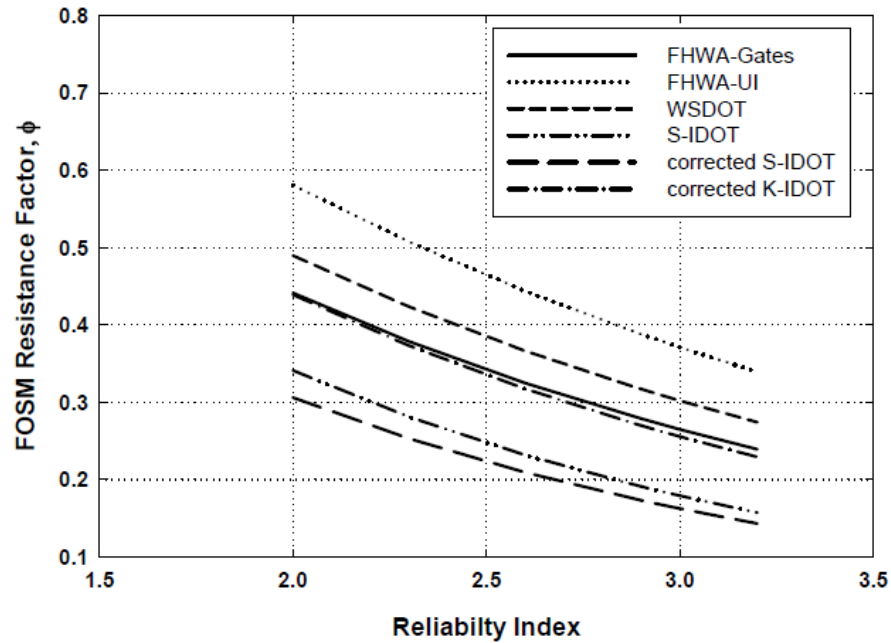


**Figure 16. Resistance factors vs. reliability index for different predictive methods using FOSM (Long et al., 2009a)**

b. First Order Reliability Method (FORM)

The resistance factors evaluation via FORM provide a more accurate estimate when multiple variables are included, and the variables are not normally distributed, which is the case for the load and resistance values for pile design. Long et al. (2009a) presented the same information regarding the FORM as it is presented in the NCHRP 507 Report (Paikowsky et al., 2004). The resistance factors obtained using FORM are also presented in Table 26. Figure 17 provides a graphical representation of the results.

In that regard, it should be commented that while Long et al. (2009a) use the FORM procedures presented by Paikowsky et al. (2004), all current developments of resistance factors is performed based on Monte Carlo (MC) simulations and FORM is very rarely used. Current analyses (e.g. Paikowsky et al., 2010) or Phase I of the MnDOT study, all utilized the MC simulation for accurate evaluation of the resistance factors.

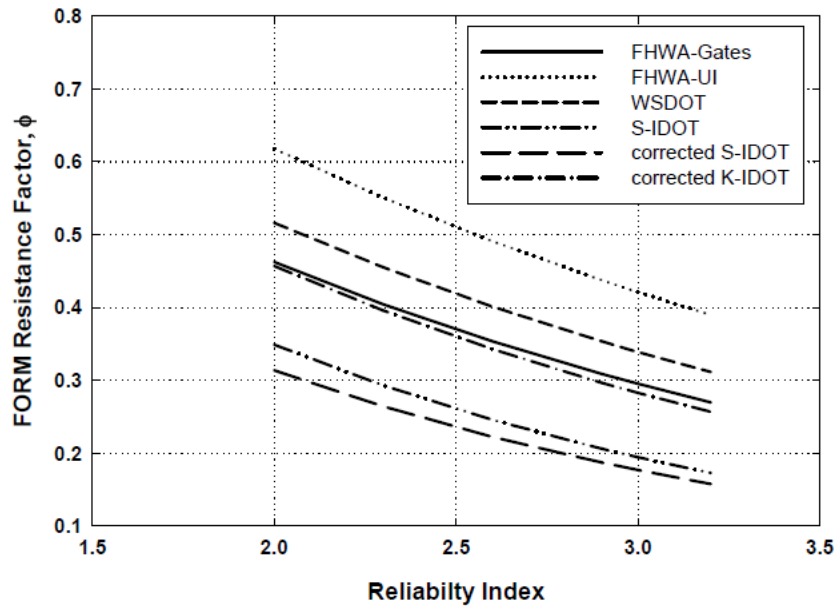


**Figure 17. Resistance factors vs. reliability index for different predictive methods using FORM (Long et al., 2009a)**

### **2.3.7 Summary and Comparison of Results to Phase I of the Mn Study (Paikowsky et al., 2009)**

The report presented by Long et al. (2009a), follows the same statistical approach presented by Long and Maniaci, 2000. In these statistical analyses and correlation developments, the bias was defined as the ratio of calculated to measured value opposite to its traditional definition of the measured value over the calculated value (i.e. capacity). As such, a comparison for all the statistical details is difficult (note the reverse of the mean of the bias used by Long et al. is not the true mean's bias, neither are the other statistical parameters). Long et al. (2009a) presented only a summary table of the reversed (correct) bias ratio (see Table 26) and the cases, therefore, cannot be examined one for one. Long et al. (2009a) study includes the data developed by Paikowsky et al. (2004), which only partially addresses the Mn needs as discussed in Phase I of the study. More so, most of Long and Maniaci (2000) and Long et al., 2009a,b, publications do not include in the presentation of the results (either in the graphs or the tables) the exact number of cases associated with each analysis.

The statistical analysis and results For the International Database and the Comprehensive Database categorized by pile type and presented by Long et al. (2009a) and Paikowsky et al. (2009) are presented in Table 27.

Analyzing the data presented by Long et al. (2009a) allowed to identify several cases that were excluded by Long et al. (2009a). The reason for this exclusion of the extreme unsafe cases is not

clear and some possible investigation follows. Excluding these cases decreases the mean bias significantly, and therefore the resistant factors changed accordingly.

In order to allow for valid comparison, the data of Paikowsky et al. (2009) was reversed to present the bias ratio used by Long et al. (2009a). Table 28 shows the statistical analysis presented by Long et al. (2009a) and the statistical analysis presented by Paikowsky et al. (2009). The results were found to be very different to the ones presented in the report by Long et al., however, the observed trend follows that presented by Long et al., the pipe-piles data show a larger mean, standard deviation, and COV.

Detailed evaluation of the extreme cases was conducted and details are presented in Chapter 5. Following the exclusions of the cases presented in Chapter 5, from Paikowsky et al. database, the mean, standard deviation, and COV, values are very close to the ones presented by Long et al. (2009a), (Table 28), for the H piles and still show larger bias (though similar COV) for the pipe piles. In order to allow for valid comparison, the data of Paikowsky et al. (2009) was reversed to present the ratio used by Long et al. (2009a).

The analysis results presented in Table 28 explains that omitting the extreme dangerous cases (over-prediction) by Long et al. (2009a) changed the bias of the prediction. It should be noted that as Long et al. had used a reversed ratio (calculated over measured), a ratio greater than 1.0 is over-prediction and is on the unsafe side (opposite to the traditional ratio smaller than 1.0). The elimination of those cases is most dangerous when developing resistance factors for LRFD analysis as the calculated resistance factors are matched to a distribution, which is not based on the existence of those cases, hence its COV and mean bias are smaller and as a result the calculated RF is higher. These cases need further evaluation of case by case and any elimination of such cases must be factually and rationally justified (if possible).



**Table 27. Long et al. (2009a) vs. Paikowsky et al. (2009) statistical results**

		PILE TYPE															
		H-PILES								PIPE-PILES							
		Long et., al.				Paikowsky at., al.				Long et., al.				Paikowsky at., al.			
Method	Database	n	Mean $\lambda$	S.D. $\lambda$	COV $\lambda$	n	Mean $\lambda$	S.D. $\lambda$	COV $\lambda$	n	Mean $\lambda$	S.D. $\lambda$	COV $\lambda$	n	Mean $\lambda$	S.D. $\lambda$	COV $\lambda$
FHWA-GATES	International	52	1.390		0.390	125	0.8129	0.3232	0.3976	80	1.090		0.500	99	0.878	0.549	0.6255
	Comprehensive	14	0.990		0.350					9	1.070		0.220				
	Illinois	NO SLT AVAILABLE								NO SLT AVAILABLE							
WSDOT	International	52	1.210		0.380	125	0.8738	0.329	0.3765	80	1.120		0.500	99	0.816	0.4925	0.6038
	Comprehensive	15	0.910		0.290					11	1.160	0.260	0.220				
	Illinois	NO SLT AVAILABLE								NO SLT AVAILABLE							

**Table 28. Long et al. (2009a), vs. Paikowsky et al. (2009) statistical results regarding the bias definition and extreme cases excluded**

		PILE TYPE															
		H-PILES								PIPE-PILES							
		Long et., al.				Paikowsky at., al.				Long et., al.				Paikowsky at., al.			
Method	Database	n	Mean $\lambda$	S.D. $\lambda$	COV $\lambda$	n	Mean $\lambda$	S.D. $\lambda$	COV $\lambda$	n	Mean $\lambda$	S.D. $\lambda$	COV $\lambda$	n	Mean $\lambda$	S.D. $\lambda$	COV $\lambda$
FHWA-GATES	International	52	1.390	0.550	0.390	122	1.3575	0.4230	0.3116	80	1.090	0.540	0.500	95	1.3860	0.6210	0.4480
	Comprehensive	14	0.990	0.350	0.350					9	1.070	0.240	0.220				
	Illinois	NO SLT AVAILABLE								NO SLT AVAILABLE							
WSDOT	International	52	1.210	0.460	0.380	122	1.2615	0.4180	0.3314	80	1.120	0.560	0.500	95	1.4570	0.5740	0.3940
	Comprehensive	15	0.910	0.260	0.290					11	1.160	0.260	0.220				
	Illinois	NO SLT AVAILABLE								NO SLT AVAILABLE							

## **2.4 Report Submitted to the State of Wisconsin Department of Transportation – Long et al., 2009b**

### **2.4.1 Overview**

The Wisconsin Department of Transportation (WisDOT) evaluated driven pile capacity in the field using the Engineering News Record (ENR or ENR) equation. The study by Long et al. (2009b) was conducted to assess the accuracy and precision with which four methods can predict axial pile capacity and also to evaluate the impact of the transition into LRFD. Overall, it was a sub-study to that conducted for the Illinois Department of Transportation and utilizing the same databases as previously described in section 3.2, related to Long et al. (2009a).

The methods studied under this investigation were the Engineering News formula, the FHWA-Gates formula, the Pile Driving Analyzer, and the method developed by Washington State DOT (Allen, 2005). Additional analysis was conducted in order to improve the performance of the FHWA-Gates equation. The application of the equation was restricted to piles with axial capacity less than 750 kips, and to adjustment factors based on the pile type, the hammer, and the soil conditions.

### **2.4.2 Databases**

Two databases were put together in order to conduct this investigation, the data included static and dynamic load tests.

The first database included those developed by Flaate (1964), Olson and Flaate (1967), Frigaszy et al. (1988), by the FHWA (Rausche et al., 1996), by Allen (2007) (which utilized the data of Paikowsky et al., 1994), and Paikowsky et al. (2004). A total of 156 load tests were collected for this database. Only steel H-piles, pipe piles, and metal shell piles were used in this database.

The second database contains records for 316 piles driven only in Wisconsin. Only a few cases contained static load tests and several cases included CAPWAP analyses conducted on re-strikes. The limited number of static load tests and CAPWAP analyses for piles with axial capacities less than 750 kips were not enough to develop correction factors for the corrected-FHWA Gates. However, predicted and measured capacities for these cases were in good agreement with the results from the first database.

### **2.4.3 Summary of Findings**

The ratio of predicted capacity ( $Q_p$ ) to measured capacity ( $Q_m$ ) was used as the measure for quantifying how well or poorly a predictive method performs. Statistics for each of the predictive methods were used to quantify the accuracy and precision for several pile driving formulas. In addition to assessing the accuracy of existing methods, modifications were developed for the FHWA-Gates method to improve its predictions.

The results of the investigation recommended that a “corrected” FHWA-Gates or the WSDOT formulas should be used to predict axial pile capacity.

The FHWA-Gates method tended to over-predict at low capacities and under-predict at capacities greater than 750 kips. Additionally, the performance was also investigated for assessing the effect of different pile types, pile hammers, and soil types.

All these factors were combined to develop a “corrected” FHWA Gates method. The corrected FHWA Gates applies adjustment factors to the FHWA-Gates method as follows:

$$\text{Corrected Gates Pile Capacity} = (\text{FHWA-Gates Capacity}) * F_0 * F_H * F_S * F_P \quad (12)$$

Where:

- 1)  $F_0$  – an overall correction factor, = 0.94
- 2)  $F_H$  - a correction factor to account for the hammer used to drive the pile,  
 $F_H = 1.00$  Open-ended diesel (OED)  
 $F_H = 0.84$  Closed- end diesel (CED)  
 $F_H = 1.16$  Air/Steam - single acting  
 $F_H = 1.01$  Air/Steam - double acting  
 $F_H = 1.00$  Hydraulic (truly unknown)
- 3)  $F_S$  - a correction factor to account for the soil surrounding the pile,  
 $F_S = 1.00$  Mixed soil profile  
 $F_S = 0.87$  Sand soil profile  
 $F_S = 1.20$  Clay soil profile
- 4)  $F_P$  - a correction factor to account for the type of pile being driven.  
 $F_P = 1.00$  Closed-end pipe (CEP)  
 $F_P = 1.02$  Open-end pipe (OEP)  
 $F_P = 0.80$  H-pile (HP)

A summary of the statistics (for  $Q_p/Q_m$ ) associated with each of the methods is provided in Table 29.

**Table 29. Statistical parameters developed by Long et al., 2009b**

Method	Mean	COV
Wisc-EN	0.43	0.47
WSDOT	1.11	0.39
FHWA-Gates	1.13	0.42
PDA	0.73	0.40
FHWA-Gates for all piles <750 kips	1.20	0.40
“corrected” FHWA-Gates for piles <750 kips	1.02	0.36

The corrected FHWA-Gates method predicts axial pile capacity with the greatest degree of precision; however, the method is restricted for piles with axial capacity less than 750 kips. The

method results in a mean value of 1.02 and a COV equal to 0.36 which is the smallest COV for all the methods investigated.

The WSDOT method exhibited a slight tendency to over-predict capacity and exhibited the greatest precision (lowest COV) for all the method except the corrected FHWA-Gates.

Resistance factors were determined for each of the methods for reliability index values ( $\beta_T$ ) equal to 2.33 and 3.0 (given in Tables 6.1 and 6.2 in the report) for the First Order Second Moment (FOSM) method and for the First Order Reliability Method (FORM), respectively. Using a target reliability index of 2.33 and FORM result in the following values for resistance factors for the different methods:

**Table 30. Summary of resistance factors developed using FORM and at a target reliability ( $\beta_T = 2.33$ ) (Long et al., 2009b)**

Method	Resistance Factor
EN-Wisc	0.90
FHWA-Gates	0.42
PDA	0.64
WSDOT	0.46
Corrected FHWA-Gates	0.54

A more detailed investigation was carried out on the better performing three methods (UI-Gates, WSDOT, and FHWA-Gates). The cumulative distribution for the ratio  $Q_p/Q_m$  was found to be approximately log-normal; however, a fit to the extremal data resulted in a more accurate representation for portion of the distribution that affects the determination of the resistance factor fitting to the extremal data results in greater resistance factors. Employing FORM at a target reliability index of 2.33 results in the resistance factors detailed in Table 31.

**Table 31. Summary of resistance factors using FORM and  $\beta_T = 2.33$ , based on distributions matching the extreme cases (Long et al., 2009b)**

Method	Resistance Factor
FHWA-Gates	0.47
WSDOT	0.55
Corrected FHWA-Gates	0.61

#### **2.4.4 Conclusions and Comment**

Long et al. (2009b) commented that following the completion of their investigation, the impact of moving from current foundation design into LRFD, will increase the required capacity by about 50 percent; however if the “corrected” FHWA-Gates method or the WSDOT method were to be adopted by the WisDOT, the increment of the required foundation capacity would increase by less than 15%.

It should be noted that the procedures used by Long et al. (2009b) arriving to the above conclusions, suffer from the major drawbacks detailed below and should not be relied on without a further evaluation.

- a) The corrected FHWA Gates equation is a correction of a correction, and hence, raises the question of independent development to answer the deficiencies rather than to correct a correction.
- b) The database for which the “new” corrected equation was applied to is the same database for which the methods were examined to begin with; hence, there is a need for a control (independent) database to examine the results.
- c) The manipulation in which the distribution is matched to the extreme cases is a procedure “adapted” by Allen (2005) and is discouraged. This method in which the “tail wags the dog”, i.e. the distribution that matches all the cases is adjusted by the extreme tail of the data. A procedure that should not be implemented easily if at all.

## **2.5 Gates Formulae**

### **2.5.1 Gates (1957)**

Gates (1957) presents the development of an empirical formula that aimed at predicting the bearing capacity of driven piles. Gates’ publication presents only the developed equation and does not provide the details of the data used for the development. Gates states that 100 pile load-test results were analyzed for the correlation, including the following hammer types:

- 15 drop hammers,
- 7 single acting hammers,
- 5 double-acting hammers.

The gross hammer energies varied from 4,550 to 52,000 ft-lb. The pile set ranged from 0.000 in to 4.4 in. The distribution of pile types was as follows:

- Steel, 73;
- Timber, 38;
- Precast concrete, 11;
- Thin-shell cast in place, 4;
- Pipe, 3;
- Composite 1.

All the pile load-test results utilized were collected from existing literature and were not detailed in Gates’ publication. The development of the empirical formula presented by Gates was based on the Redtenbacher’s formula (no reference provided), which assumes that temporary compression is a function of the resistance to penetration  $R$ , the first relationship established was:

$$R \sim \sqrt{E} \quad (13)$$

Where:  $E$  = net hammer energy.

The failure loads at failure for all piles driven with certain hammer were then plotted against the logarithm of the set,  $s$ . The resulting curve was nearly a straight line; hence:

$$R \sim \log s \quad (14)$$

Combining equations 12 and 13 and introducing a constant of equality,  $a$ , yields,

$$R = a\sqrt{E} \log s \quad (15)$$

Since the range of pile driving involves negative as well as positive values of  $\log s$ , a second constant,  $b$ , was introduced so that positive values of  $R$  will be obtained when  $s$  is equal to or less than unity.

$$\frac{R}{\sqrt{E}} = a \log s + b \quad (16)$$

Gates then applied statistical methods and curve-fitting analysis, and found the relationship between  $a$  and  $b$ . When introducing a theoretical factor of safety of 3, the final result was as:

$$B = \frac{1}{7}\sqrt{E}(1 - \log s) \quad (17)$$

Where  $B$  = Safe load-carrying capacity of pile, in tons

$E$  = Gross energy of pile-driving hammer, in ft-lb, times 75 percent for drop hammers and 85 percent for all other hammers unless otherwise stated by manufacturer.

$s$  = Set per blow, in inches

In order to facilitate the usage of Gates Formula, a unit conversion development is presented as follow:

$$B \left( \text{tons} * \frac{2 \text{ kips}}{\text{tons}} \right) = 2 * \frac{1}{7} \sqrt{E(\text{lb} - \text{ft})} (1 - \log s(\text{in}))$$

$$\frac{B(\text{kips})}{\sqrt{1000}} = \frac{2}{7} \sqrt{E(\text{lb} - \text{ft}) * \frac{(1\text{kip} - \text{ft})}{1000(\text{lb} - \text{ft})}} (1 - \log s(\text{in}))$$

$$B(\text{kips}) = \frac{2\sqrt{1000}}{7} \sqrt{E(\text{kip} - \text{ft})} (1 - \log s(\text{in}))$$

Excluding the Factor of Safety:

$$B(kips) = \frac{6\sqrt{1000}}{7} \sqrt{E(kip - ft)(1 - \log s(in))}$$

$$R_u = 27.11 \sqrt{E_n * e_h(1 - \log s)} \quad (18)$$

Where  $R_u$  = Ultimate pile capacity, in kips

$E_n$  = Rated energy of hammer per blow, in kips-foot

$e_h$  = Hammer efficiency (0.75 for drop hammers, 0.85 for all others)

$s$  = Final pile set per blow, in inches

After a probability analysis was conducted, Gates indicated that the proposed formula will yield more consistently accurate determination of bearing capacity than even the most complex “complete” rational type equation. Figure 18 presents the graphical solution provided by Gates (1957) with the formula applied to nine popular pile-driving hammers of the time. The General solution was also plotted, showing straight-line relation between  $s$ , permanent set per blow, and  $\frac{R}{\sqrt{E}}$  given a factor of safety of 3, based on 130 load tests (note: both 100 and 130 tests are referred to in Gates, 1957). Ordinates in this graph are not related but abscissa is common to both.

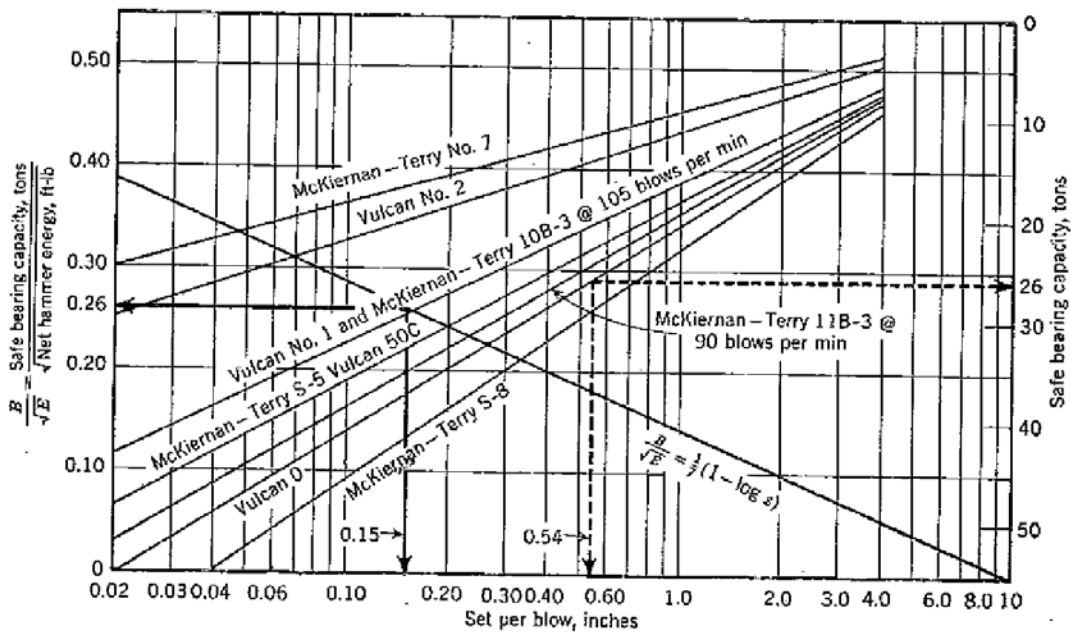


Figure 18. Graphic solutions of formula (Gates, 1957)

Gates concluded that as long as the pile is capable of transmitting the applied load to the supporting soil, it is of no significance of what material the pile is constructed. However, other

aspects must be considered before specifying a pile type, that is, ability to withstand driving conditions without damage, resistance to the elements , and of course economy.

Gates research was based on an analysis limited to correlating the load at failure to the net energy of the pile-driving hammer and set per blow. Gates believed that even considering the formula presented to be the most accurate offered at the time, it could be improved with additional data and would be able to predict capacity within a maximum deviation of 20 percent, regardless of driving conditions.

### 2.5.2 Evaluation of Gates (1957) Equation

Earlier large scale evaluations were presented by Paikowsky and Stenersen (2000) and Paikowsky et al., (2004). Paikowsky et al., (2009) investigated the accuracy of the Gates 1957 equation as part of Phase I of this research. The analysis was broken down into four different subset categories; predictions for all H-piles with 135 cases, predictions for H-Piles EOD condition only with 125 cases, predictions for all Pipe-Piles with 128 cases, and predictions for Pipe-Piles EOD conditions only with 102 cases. Table 32 presents a summary for the analyses conducted by Paikowsky et al. (2009) as provided in Equation 18, noting that no factor of safety is included in the analyzed equation.

The findings presented in Table 32 suggest that the original Gates (1957) formulation, under predicts significantly the piles' capacity when applied to more modern (and larger size) hammers.

**Table 32. Gates 1957 dynamic equation prediction for H and Pipe Piles (summary of results from Paikowsky et al., 2009)**

Pile Type/ Conditions	No. of Cases (n)	Mean Bias Meas./ Calc. ( $m_b$ )	Stan. Dev. ( $\sigma_b$ )	Coef. Of Var. ( $COV_b$ )	Best Fit Line Equation (least sq)	Coef. Of Determination ( $r^2$ )	Resistance Factor $\phi$ $\beta=2.33$ , $p_r=1\%$ , Redundant			$\phi/\lambda$ Efficiency Factor (%)
							FOSM	MC <sup>3</sup>	Recom	
H-Piles	135	1.447	0.521	0.360	$R_u=0.612*R_s$	0.88	0.697	0.781 0.771	0.75	51.8
H-Piles EOD	125	1.430	0.506	0.354	$R_u=0.625*R_s$	0.90	0.698	0.782	0.75	52.5
Pipe Piles	128	1.495	0.772	0.516	$R_u=0.387*R_s$	0.91	0.514	0.558	0.55	36.8
Pipe Piles EOD	102	1.575	0.831	0.528	$R_u=0.570*R_s$	0.85	0.527	0.572	0.55	34.9

### 2.5.3 Modified Gates Equation (Olson and Flaate, 1967)

The original Gates Formula was modified in 1967 by Olson and Flaate, the modification offered was developed based on the pile type, and statistical fit through the predicted versus measured data. The data used by Olson and Flaate, was a collection from 116 load tests on timber, precast



concrete, and steel piles driven into sandy soils previously reported by Flaate (1964). For review, see sections 2.2.2.1 and 2.2.2.2 of this manuscript.

Attempts to apply dynamic pile-driving formulas to the piles used in these tests involved a number of uncertainties, including the following:

- The efficiencies of the various pile hammers were not reported. The values tabulated by Chellis, (Pile Foundations, 2<sup>nd</sup> ed., McGraw-Hill Book Co., Inc., New York, N.Y., 1961, pp. 28-33), were used in the study. The actual field values of  $e_h$  depend greatly on the condition of the hammer at the time of driving and may differ significantly from the values used in the analysis.
- The cushion materials used on top of the piles were not usually specified. The cushion exerts great influence on the shape of the load pulse applied to the pile and thus influence the energy actually delivered to the pile.
- Only about ten piles were driven entirely through cohesion-less soils. At many of the sites the piles were driven through soft cohesive soils into underlying sands. In other cases the sand was interstratified with clay, silt, and sometimes organic soil, or was described as silty sand or clayey sand.
- The capacities of most of the piles were reported without presenting the actual load-settlement diagrams. It is believed that a scatter of perhaps 15% has resulted from use of different failure criteria.
- Based on recent field studies (Davidson and Townsend, 1996), it is believed that many of the measured pile capacities are in error by 10% or more because of friction in hydraulic loading jacks, and improper calibration of equipment.

Attempts to account for the various sources of error by adjusting the field data were not considered possible because:

- The adjustment procedures would be too complex for normal field use
- Data were not available for making most of the corrections
- Arbitrary choices involved in making such adjustments would introduce bias.

Olson and Flaate (1967) modifications are as follows:

$$R_u = 1.11\sqrt{e * E_r} \log(10N) - 34; \text{ Timber Piles} \quad (19)$$

$$R_u = 1.39\sqrt{e * E_r} \log(10N) - 54; \text{ Concrete Piles} \quad (20)$$

$$R_u = 2.01\sqrt{e * E_r} \log(10N) - 166; \text{ Steel Piles} \quad (21)$$

$$R_u = 1.55\sqrt{e * E_r} \log(10N) - 96; \text{ All Piles} \quad (22)$$

Where:  $R_u$  = The ultimate pile capacity in kips

$E_r$  = Rated or observed energy in ft-lbs

$N$  = Number of hammer blows per inch at final penetration in b/in.

To conclude, the study Olson and Flaate recommended that the modified equation must be used to obtain more accurate predictions; however, it was suggested that more data is needed to establish the formula parameters.

#### **2.5.4 FHWA-Modified Gates Equation (USDOT, 1988)**

The Federal Highway Administration (FHWA) modification refers to FHWA (1982). The FHWA (1988) provided a generic driven pile specification manual, which contained state-of-the-art procedures for proper construction control of piles and details the use of the recommended equation.

For the dynamic pile capacity prediction it stated as follow, “the ultimate pile capacity will only be determined by dynamic formula if either the contract documents contain a provision that dynamic formula shall be used or the Engineer approves dynamic formula use. In such case piles shall be driven to a length necessary to obtain the ultimate pile capacity according to the following formula:”

$$R_u = 1.75\sqrt{E}\log(10N) - 100 \quad (23)$$

Where:  $R_u$  = the ultimate pile capacity in kips

$E$  = The manufacturers rated hammer energy (ft-lbs)

$N$  = number of hammer blows per inch at final penetration in b/in.

The commentary of the same publication (p. 21 of 37) explains that “the dynamic formula shown in this specification (referring to equation 23) is the Gates formula which has been revised to reflect ultimate pile capacity. The formula shown in this specification already includes the 80 percent efficiency factor on the rated energy, E recommended by Gates“ (underline added). A similar equation can be obtained by observing the equations for steel and concrete piles proposed by Olson and Flaate as reviewed in section 2.2.2.2.

The publication explains that the formula was selected for its relative accuracy, consistency and simplicity of use. However, the top priority for highway agencies should be to introduce a change from dynamic formula to wave equation analysis.

#### **2.5.5 Evaluation of FHWA Modified Gates Equation**

Earlier large scale evaluations were presented by Paikowsky and Stenersen (2000) and Paikowsky et al., (2004). Paikowsky et al., (2009) investigated the accuracy of the FHWA Modified Gates equation as part of Phase I of this research. The analysis was broken down into four different subset categories; predictions for all H-piles with 135 cases, predictions for H-Piles

EOD condition only with 125 cases, predictions for all Pipe-Piles with 128 cases, and predictions for Pipe-Piles EOD conditions only with 102 cases. Table 34 presents a summary for the analyses conducted by Paikowsky et al. (2009) as provided in Equation 23, noting that no factor of safety is included in the analyzed equation and the energy inserted is the nominal energy of the hammer. Table 33 summarizes the results obtained by Paikowsky et al. (2009) for the FHWA Modified Gates, similarly to the summary presented in Table 32 for the original Gates (1957) equation.

The findings presented in Table 33 suggest that the FHWA modified Gates formulation, over predicts the piles' capacity when applied to the MnDOT database but at the same time provides very reasonable coefficient of variation (COV) and excellent coefficient of determination ( $r^2$ ).

**Table 33. FHWA (1988) Modified Gates dynamic equation prediction for H and Pipe Piles (summary of results from Paikowsky et al., 2009)**

Pile Type/ Conditions	No. of Cases (n)	Mean Bias Meas./ Calc. ( $m_\lambda$ )	Stan. Dev. ( $\sigma_\lambda$ )	Coef. Of Var. ( $COV_\lambda$ )	Best Fit Line Equation (least sq)	Coef. Of Determination ( $r^2$ )	Resistance Factor $\phi$ $\beta=2.33$ , $p_r=1\%$ , Redundant			$\phi/\lambda$ Efficiency Factor (%)
							FOSM	MC <sup>3</sup>	Recom	
H-Piles	135	0.818	0.324	0.396	$R_u=1.168R_s$	0.88	0.365	0.408 0.400	0.40	48.9
H-Piles EOD	125	0.813	0.323	0.397	$R_u=1.118R_s$	0.89	0.362	0.404	0.40	49.2
Pipe Piles	128	0.838	0.503	0.600	$R_u=1.132R_s$	0.85	0.240	0.256	0.25	29.8
Pipe Piles EOD	102	0.891	0.545	0.612	$R_u=1.078R_s$	0.84	0.248	0.256	0.25	28.0

### 3 EVALUATION OF MNDOT BRIDGE OFFICE DATA

#### 3.1 Overview

A database containing dynamic measurements and signal matching analyses was provided by MnDOT. The database was compiled and provided by Messrs. Ben Borree and Derrick Dasenbrock of the MnDOT Foundations unit. The database consists of accumulated PDA data from various projects with supplemented DOT data (stroke, blow count, etc.), and was entered into formatted spreadsheets provided by UML. The compiled database contains 126 pipe-pile cases including hammer type and rated energies that match for the most part the MnDOT practice as previously established. A copy of the database is presented in Appendix A. The dataset did not include any static load test information and 50% of it was assessed to relate to bridges within one square mile area of Minneapolis/St. Paul (Rowekamp, 2011). The evaluation of the data was aimed at:

- a) Examine typical energy transfer values as well as hammer performance regarding observed strokes and ram weight.
- b) Compare the performance of the signal matching analyses to various dynamic equations including the newly developed MnDOT equation.

Following a review of the dataset and resolving of mismatch in some denoted hammer energies, a set of equations for comparison was chosen and evaluations of the dynamic formulas predictions vs. the signal matching analyses were carried out. This evaluation examines the provided data and the associated dynamic predictions, leading to relevant observations, and conclusions.

#### 3.2 Data Review

Initial review suggested that some of the hammers rated energy listed in the provided database does not match the manufacturers' rated energy. The cases in question are presented in Table 34. Appendix B presents the manufacturer's specifications for the various relevant hammers.

**Table 34. Hammers with different rated energy**

Hammer Type	Rated Energy Provided (lb-ft)	GRL WEAP Database 08/28/09	Rated Energy from Manufacturer* (lb-ft)
APE D30-42	91088	74,420	74,750
APE D19-42	42820	47,130	47,335
APE Holland D25-32	57880	62,010	58,248

\*values used in modified analysis

### 3.3 Data Match

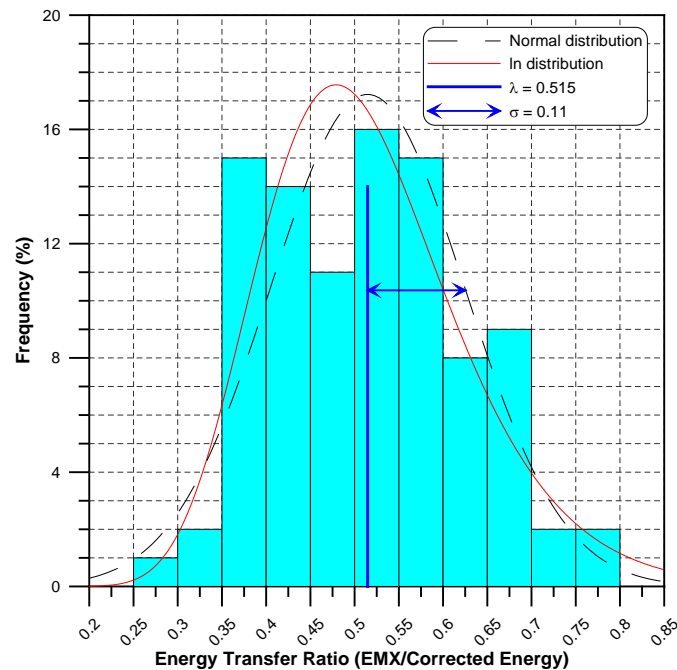
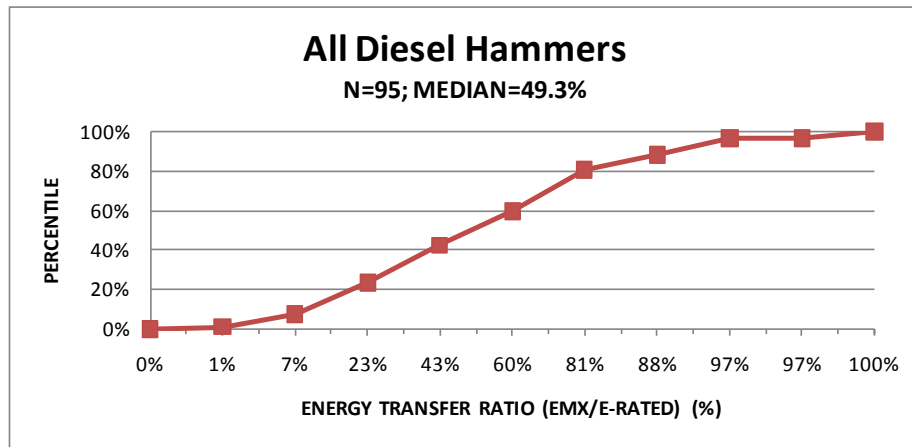
From the 126 cases listed, 95 include dynamic measurements that enable to calculate the rates of energy transferred. Two sets of data are presented in Table 35, the first one named “Rated Energy”, relates to the original hammer rated energy provided by MnDOT, and the second one named “Modified Rated energy” includes the replacement of the energy provided with the manufacturer’s nominal one listed in Table 34.

Table 35 shows that the mean energy transfer for diesel hammers on Pipe Piles in the database for the Rated and the corrected were 49.8% and 51.5% respectively, compared to 39.8% for the 56 cases of diesel hammer on pipe piles, and 38.4% of GRL database for all diesel hammers on steel piles as presented in Tables 3.17 and Figure 3.5, respectively, of our Phase I report (Paikowsky et al., 2009). The standard deviations of the current MnDOT database are 10.1% and 10.9% compared to 13.6% and 9.8% of our original and GRL’s databases. The energy transfer present a noticeable difference that suggests that the data presented in the MnDOT dynamic measurements database for diesel hammer impact on pipe piles has about 10% higher rate of transferred energy compared to the national database (GRL) and the load test database used for the calibrations of Phase I research. This is a sizeable difference of about 25% higher energy transfer performance. The source for such a difference is not clear, other than the observation that most of the data relates to a small number of projects and possibly small number of actual hammers used in all projects. This aspect requires further investigation in the future when more data are available.

**Table 35. Summary of driving data statistics for MnDOT database**

Pile Type	Driving System Efficiency (PDA)						Stroke Measurements					
	Rated Energy			Modified Rated Energy			Rated Energy			Modified Rated Energy		
	n	Mean%	S.D.%	n	Mean%	S.D.%	n	Mean%	S.D.%	n	Mean%	S.D.%
Pipe	95	49.76	10.11	95	51.47	11.06	126	76.35	10.94	126	78.11	10.91

A graphical representation of the driving system efficiency is presented in Figure 19 in the form of cumulative distribution of the energy transfer ratio to the rated energy and a probability distribution function for the ratio of measured over rated energy.



**Figure 19. Probability distribution and cumulative distribution function for energy transfer when driving Pipe-Piles with diesel hammers in the MnDOT dynamic measurements database (rated energy corrected)**

The database included 126 stroke measurements, allowing the evaluation of the hammer efficiency, i.e. the ratio between energy provided according to the hammer's stroke to the nominal energy according to the hammer's manufacturer (again as reported by MnDOT and as listed in Table 34). Energy manufactured by the hammer depends upon the setting of the fuel pump as well as the driving resistance. Only full (highest) setting and high blow count would allow the hammer to produce nominal energy (neglecting hammer internal losses and problematic operation like early ignition).

The efficiency related to stroke measurements allows examining the ratio between the calculated potential energy (based on stroke times ram weight) relative to the nominal (maximum) energy. These values can serve as a rough indication for the hammer's efficiency and can be compared to the MnDOT practice when hammer measured stroke is not available.

The analysis of the above stroke measurements presented in Table 35 suggests that typically the diesel hammers' stroke for the rated energy and the corrected energy are 76.4% and 78.1%, respectively. These values compare well with the assumed hammer efficiency formerly recommended by the MnDOT (i.e. 75 % of nominal energy) when stroke information is not recorded.

### **3.4 Summary of Data**

Data summary are presented in Appendix A. Table A-1 providing details of bridge names, locations, bridge type, number of spans, total length and width of the bridge, type of construction, and the year the bridge was completed. The 41 projects were submitted by the MnDOT personnel and represent the most recent design and practices over the past years. Table A-2 provides the bridge construction classification based on Paikowsky et al (2005) used for the categorization of Table A-1.

Table A-3 provides the soil conditions and pile type with pile size details of the selected representative bridges.

Table A-4 provides a summary of the side and tip soil strata for each of the different pile types for each bridge, final energy of the pile driving hammer, final set of the pile, and evaluation of capacity using Energy Approach, WSDOT formula, MnDOT formula, new MnDOT formula, it also provides CAPWAP capacity evaluation when available.

Tables 36 to 39 present a summary and statistical analysis of the 41 selected bridge projects. Table 36 summarizes the range of pile length, the average pile length and percentage of pile usage out of all piles categorized according to pile type. For example, the data of Table 36 suggests that the most commonly used pile (34.3%) was CIP 16" x 0.3125" with an average length of 82 ft, and overall 16" O.D. piles were used in 71% of the pile's installation whereas 12" O.D. pipe piles were used in 29% of the pile's installations based on driven pile length. Note: as discussed in section 1.1, these values are representative of the selected bridges whereas the piles most commonly used across the state are 12" x 0.25 piles as detailed in Phase I of the study.

Table 37 summarizes the soil condition along the skin and the pile's tip. For example, out of 109 piles (17 piles did not have strata information), 2 were driven to rock, 77 to sand or sand and gravel, meaning that in 72% of the cases (79 out of 109) the piles were driven to a competent bearing layer.

**Table 36. Summary of total pile length**

Pile Type	# of Piles	Total Length	% of Total Use	Range of lengths (ft)
CEP 12" × 0.25"	18	1449	13.8	50 – 109
CEP 12" × 0.3125"	5	430	4.1	45 – 120
CEP 12" × 0.375"	2	186	1.8	86 – 100
CEP 12.75" × 0.25"	24	2122	20.1	53 – 128
CEP 12.75" × 0.3125"	6	436	4.1	50 – 91
CEP 16" × 0.25"	26	2183	20.7	50 – 110
CEP 16" × 0.3125"	44	3614	34.3	50 – 136
CEP 20" × 0.375"	1	115	1.1	115
<b>Totals</b>	<b>126</b>	<b>10,535</b>	<b>100</b>	<b>N/A</b>

**Table 37. Summary of pile cases categorized based on soil conditions**

Soil Condition Pile Location	Rock	Sand & Gravel	Sand	Silt	Clay	Organics
Tip	1	6	71	9	21	0
Side	0	18	58	4	20	2

**Table 38. Summary of driving criteria – pile performance**

Driving Resistance (BPI)	0 – 4	4 – 8	> 8
Number of Piles	25	47	54
% of Cases	19.8	37.3	42.9

**Table 39. Equipment summary**

Hammer Type	Maximum Energy (kip-ft)*	Ram Weight (lb)	No. of Projects used	Total Pile Length Driven (ft)	% of Total Use
<b>APE D19-32</b>	42440	4000	5	1028.5	9.8
<b>APE D25-32</b>	66340	5513	3	568	5.4
<b>APE D30-42</b>	91088	6615	6	1969.4	18.7
<b>DELMAG 30-02</b>	66200	6600	1	186	1.8
<b>DELMAG D19-32</b>	42440	4000	6	832.4	7.9
<b>DELMAG D19-42</b>	66340	5513	8	1203.1	11.4
<b>DELMAG D25-32</b>	66340	5513	12	2456.7	23.3
<b>DELMAG D30-32</b>	75440	6600	4	1090.1	10.3
<b>DELMAG D36-31</b>	90560	7930	1	124.5	1.2
<b>DELMAG D36-32</b>	90560	7930	3	581.5	5.5
<b>ICE I-30V2</b>	90824	6615	1	179	1.7
<b>MKT DE-40</b>	32000	4000	1	175.5	1.7
<b>MKT DE-42/35</b>	42000	4200	1	90	0.9
<b>MVE M-19</b>	49380	4015	1	50	0.5
<b>Totals</b>				<b>10534.7</b>	<b>100</b>

\*as listed by MnDOT, refer to Table 34



The data are further examined by summarizing the driving resistance at the end of driving as presented in Table 38. In 43% of the cases (54 out 126) the piles were driven to a blow count of or exceeding 8 bpi. Additional 37% were driven to a resistance between 4 to 8 bpi which is the range beyond “easy driving”. The data matches quite well with that of Table 37 suggesting 80% of the piles being driven to resistance in a competent layer. The data differs, however, from the large database examining the MnDOT state of practice in Phase I. Table 2.7 of Phase I report indicated that only 8.8% of the 34 piles examined had blow count lower than 4 bpi.

Table 39 provides a summary of driving equipment used for the 126 piles. All hammers are diesel hammers ranging in nominal energy from 32 to 95 kips-ft, with the most common hammer per project (12 out of 53 projects) and the most length driven (23.3% of all pile length driven) being the Delmag D25-32. About 74% of the piles were driven with hammers having nominal energy of 78 kip-ft (ranging from 66.2 to 90.8 kip-ft) and a ram weight of about 6,500 lbs (ranging from 5,500 to 7,930 lbs).

### **3.5 Observations Regarding MnDOT Dynamic Measurements Database**

The developed summary tables provide quantitative information that can be compared to the data related to MnDOT state of practice and load test databases established in Phase I of our study:

- (i) CEP piles are the dominant pile type to be used. In the dynamic measurements database, the piles ranged in diameter from 12" to 20"
- (ii) While most piles to be used across the state are 12" CEP, most common CEP piles used in the dynamic measurements database are 16"  $\times$  0.3125" and 16"  $\times$  0.25", installed as 34.3% and 20.7% of the total foundation length, respectively (based on 53 projects).
- (iii) Typical (average) driven pile length is 84 feet. More specific categorization is provided in Table 36, e.g. Average CIP 16"  $\times$  0.3125" pile length is 82 ft.
- (iv) Diesel hammers are the only hammer type used for driving the piles. The hammers ranged in sizes from MKT DE 40 (32 kip-ft) to ICE I-30V2 (90.8 kip-ft).
- (v) Around 80% of the piles are driven beyond the easy driving resistance zone of 4 bpi, hence allowing more accurate capacity evaluation when utilizing the dynamic methods. Forty-three percent (43%) of the piles were driven to a final penetration of 8 or more bpi.
- (vi) Energy transfer differs from the typical one established by a national database or the one used for examining and developing dynamic equations in Phase I of the study.
- (vii) Stroke measurements assured the current practice of assuming 75% of hammer performance when stroke measurements are not available, to be a reasonable and reliable assumption.

### **3.6 Preliminary Evaluation of the Capacity Predictions**

Dynamic analyses of the MnDOT Dynamic Measurements Database have been conducted using the following Dynamic equations: Washington State DOT formula, MnDOT equation, proposed new MnDOT equation developed in Phase I of the study with coefficients 30 and 35 and the Gates formula. Table 40 lists the dynamic equations and their different formulations used in the capacity evaluation.

The dynamic capacities based on the dynamic measurements, i.e., CAPWAP and the Energy Approach methods, are used as a reference in the evaluation of the prediction methods due to the fact that static load test had not been carried out for these case histories. The MnDOT dynamic measurements database contained 95 cases for which a CAPWAP analysis had been carried out, of which 89 cases included sufficient data to obtain Energy Approach (EA) predictions. Table 41 summarizes those cases broken down by pile type.

The various relations between the CAPWAP, the EA and the various dynamic equation results broken down by the relations and pile type are summarized in Table 42. The relationships summarized in Table 42 are presented visually in Figures 20 through 75 in the same order as they appear in the table.

Two lines had been added to each of the scatter graphs; a best fit line equation presented as a dashed line and CAPWAP measurements equal to the other predictions as a continuous blue line. The scatter of the data allows the evaluation of the prediction. For example, all data above the solid line means that the calculated capacity using the examined prediction method. is higher than the CAPWAP predications based on dynamic measurements, however since SLT data is not available one is unable to categorize the data into safe or unsafe in a reliable way.

**Table 40. Investigated equations**

No.	Equation	Comment	Reference
1	$R_u = \frac{EMX * 12}{s + \frac{DMX - s}{2}}$	Requires Dynamic Measurements	Energy Approach Prediction Method Paikowsky (1982), Paikowsky et al. (1994)
2	$R_u = 1.75\sqrt{E} * \log(10 * N) - 100$	Using E=W*H	Modified Gates FHWA (1988)
3	$R_u = 1.75\sqrt{E} * \log(10 * N) - 100$	Using E=75%En	Modified Gates FHWA (1988)
4	$R_u = 1.75\sqrt{E} * \log(10 * N) - 100$	Using E=En	Modified Gates FHWA (1988)
5	$R_u = 6.6 * F_{eff} * E * \ln(10N)$		Washington State DOT (Allen, 2005)
6	$R_u = \frac{10.5 * E}{S + 0.2} * \frac{W + (0.1 * M)}{W + M}$		Minnesota DOT (2006)
7	$R_u = 35\sqrt{E_n} * \log(10N)$	General all hammers, all energies, all conditions	First Stage Proposed New MnDOT Equation Paikowsky et al. (2009)
8	$R_u = 30\sqrt{E_n} * \log(10N)$	EOD, BC > 4 BPI Diesel Hammers	First Stage Proposed New MnDOT Equation Paikowsky et al. (2009)

Notes:  $R_u$ = ultimate capacity of pile, in kips (lbs for eq. 6)  
 EMX= maximum measured energy in kips-ft  
 DMX= maximum calculated top pile displacement based on acceleration measurement  
 W= mass of the striking part of the hammer (ram) in kips  
 M= total mass of pile plus mass of the driving cap in kips  
 Ln= the natural logarithm, in base “e”  
 E= developed energy, equal to W times H, in foot-kips (eq. 1, 2, 4)  
 E= energy per blow for each full stroke in foot-pounds (eq. 5 and 6)  
 $e_h$ = efficiency  
 $F_{eff}$ = hammer efficiency factor  
 S= final set of pile, in inches  
 $E_n$ = rated energy of hammer per blow, in kips-foot  
 N= blows per inch (BPI)  
 Q= Quake = Dmax-set

**Table 41. Summary of available cases for CAPWAP and Energy Approach based on dynamic measurements**

Pile Type	Number of Cases	
	CAPWAP	Energy Approach (EA)
16 × 0.3125	40	40
16 × 0.25	19	16
12 ¾ × 0.3125	4	4
12 ¾ × 0.25	15	13
12 × 0.3125	3	3
12 × 0.25	14	13
<b>Total</b>	<b>95</b>	<b>89</b>

**Table 42. Summary of statistical analysis and best fit line correlation (page 1/2)**

Relations	Category	No. of Cases n	Statistics			Best Fit Line	Coefficient of Determination (r <sup>2</sup> )
			mean	S.D.	COV		
<b>CAPWAP/ E.A.</b>	All Piles	89	0.6479	0.1825	0.2817	$R_u=1.620*R_c$	0.940
	CIP 16" X 5/16"	40	0.6366	0.1852	0.2910	$R_u=1.695*R_c$	0.944
	CIP 16" X 1/4"	16	0.6083	0.1342	0.2206	$R_u=1.633*R_c$	0.963
	CIP 12.75" X 1/4"	13	0.6956	0.2712	0.3899	$R_u=1.385*R_c$	0.895
	CIP 12" X 1/4"	13	0.7271	0.1306	0.1796	$R_u=1.343*R_c$	0.965
	CIP 12" X 5/16"	4	0.6032	0.0885	0.1468	$R_u=1.788*R_c$	0.982
	CIP 12.75" X 5/16"	3	0.5411	0.0941	0.1738	$R_u=1.689*R_c$	0.989
<b>CAPWAP/ WSDOT</b>	All Piles	95	0.6482	0.1109	0.1711	$R_u=1.592*R_c$	0.974
	CIP 16" X 5/16"	40	0.6158	0.0913	0.1483	$R_u=1.656*R_c$	0.978
	CIP 16" X 1/4"	19	0.6066	0.0793	0.1307	$R_u=1.647*R_c$	0.985
	CIP 12.75" X 1/4"	15	0.7025	0.1228	0.1748	$R_u=1.454*R_c$	0.97
	CIP 12" X 1/4"	14	0.7579	0.0950	0.1254	$R_u=1.314*R_c$	0.987
	CIP 12" X 5/16"	4	0.6217	0.0336	0.0540	$R_u=1.599*R_c$	0.932
	CIP 12.75" X 5/16"	3	0.6030	0.1727	0.2865	$R_u=1.610*R_c$	0.998
<b>CAPWAP/ Modified Gates (W*h)</b>	All Piles	95	0.6905	0.1210	0.1752	$R_u=1.442*R_c$	0.973
	CIP 16" X 5/16"	40	0.7279	0.1197	0.1645	$R_u=1.404*R_c$	0.976
	CIP 16" X 1/4"	19	0.6603	0.1115	0.1688	$R_u=1.498*R_c$	0.974
	CIP 12.75" X 1/4"	15	0.6510	0.1242	0.1909	$R_u=1.489*R_c$	0.966
	CIP 12" X 1/4"	14	0.6920	0.1138	0.1644	$R_u=1.441*R_c$	0.976
	CIP 12" X 5/16"	4	0.7071	0.0319	0.0451	$R_u=1.647*R_c$	0.951
	CIP 12.75" X 5/16"	3	0.5894	0.1506	0.2555	$R_u=1.403*R_c$	0.999
<b>CAPWAP/ Modified Gates (0.75*En)</b>	All Piles	95	0.6927	0.1338	0.1931	$R_u=1.425*R_c$	0.965
	CIP 16" X 5/16"	40	0.7318	0.1238	0.1691	$R_u=1.381*R_c$	0.973
	CIP 16" X 1/4"	19	0.6571	0.1253	0.1907	$R_u=1.493*R_c$	0.965
	CIP 12.75" X 1/4"	15	0.6299	0.1419	0.2253	$R_u=1.508*R_c$	0.954
	CIP 12" X 1/4"	14	0.7013	0.1252	0.1785	$R_u=1.423*R_c$	0.969
	CIP 12" X 5/16"	4	0.8034	0.0820	0.1020	$R_u=1.638*R_c$	0.938
	CIP 12.75" X 5/16"	3	0.5933	0.1647	0.2776	$R_u=1.209*R_c$	0.993
<b>CAPWAP/ Modified Gates (En)</b>	All Piles	95	0.5866	0.1126	0.1919	$R_u=1.680*R_c$	0.966
	CIP 16" X 5/16"	40	0.6207	0.1033	0.1665	$R_u=1.626*R_c$	0.974
	CIP 16" X 1/4"	19	0.5580	0.1059	0.1898	$R_u=1.758*R_c$	0.965
	CIP 12.75" X 1/4"	15	0.5322	0.1207	0.2267	$R_u=1.780*R_c$	0.954
	CIP 12" X 1/4"	14	0.5917	0.1041	0.1759	$R_u=1.683*R_c$	0.97
	CIP 12" X 5/16"	4	0.6752	0.0722	0.1069	$R_u=1.944*R_c$	0.938
	CIP 12.75" X 5/16"	3	0.4996	0.1377	0.2757	$R_u=1.437*R_c$	0.992

Notes:  $R_u$  is the calculated capacity using each of the dynamic formulae

$R_c$  is the measured Capacity determined by CAPWAP

**Table 42. Summary of statistical analysis and best fit line correlation (cont. page 2/2)**

Relations	Category	No. of Cases n	Statistics			Best Fit Line	Coefficient of Determination (r <sup>2</sup> )
			mean	S.D.	COV		
<b>CAPWAP/ Mn. DOT (2006)</b>	All Piles	95	0.4232	0.1194	0.2821	$R_u=2.498*R_c$	0.944
	CIP 16" X 5/16"	40	0.4495	0.1347	0.2996	$R_u=2.419*R_c$	0.948
	CIP 16" X 1/4"	19	0.3622	0.0854	0.2358	$R_u=2.767*R_c$	0.958
	CIP 12.75" X 1/4"	15	0.3985	0.0950	0.2383	$R_u=2.615*R_c$	0.935
	CIP 12" X 1/4"	14	0.4343	0.1060	0.2440	$R_u=2.371*R_c$	0.953
	CIP 12" X 5/16"	4	0.5692	0.0108	0.0190	$R_u=2.501*R_c$	0.899
	CIP 12.75" X 5/16"	3	0.3946	0.1319	0.3343	$R_u=1.769*R_c$	1.000
<b>CAPWAP/ Proposed MnDOT (35)</b>	All Piles	95	0.8260	0.1632	0.1976	$R_u=1.178*R_c$	0.964
	CIP 16" X 5/16"	40	0.9058	0.1326	0.1464	$R_u=1.108*R_c$	0.978
	CIP 16" X 1/4"	19	0.7987	0.1621	0.2030	$R_u=1.229*R_c$	0.962
	CIP 12.75" X 1/4"	15	0.7210	0.1717	0.2381	$R_u=1.290*R_c$	0.953
	CIP 12" X 1/4"	14	0.7827	0.1316	0.1681	$R_u=1.260*R_c$	0.972
	CIP 12" X 5/16"	4	0.8933	0.1185	0.1327	$R_u=1.488*R_c$	0.949
	CIP 12.75" X 5/16"	3	0.6522	0.1686	0.2586	$R_u=1.080*R_c$	0.988
<b>CAPWAP/ Proposed MnDOT (30)</b>	All Piles	95	0.9637	0.1904	0.1976	$R_u=1.009*R_c$	0.964
	CIP 16" X 5/16"	40	1.0568	0.1547	0.1464	$R_u=0.950*R_c$	0.978
	CIP 16" X 1/4"	19	0.9318	0.1891	0.2030	$R_u=1.054*R_c$	0.962
	CIP 12.75" X 1/4"	15	0.8412	0.2003	0.2381	$R_u=1.106*R_c$	0.953
	CIP 12" X 1/4"	14	0.9131	0.1535	0.1681	$R_u=1.080*R_c$	0.972
	CIP 12" X 5/16"	4	1.0422	0.1383	0.1327	$R_u=1.276*R_c$	0.949
	CIP 12.75" X 5/16"	3	0.7609	0.1968	0.2586	$R_u=0.926*R_c$	0.988

Notes:  $R_u$  is the calculated capacity using each of the dynamic formulae  
 $R_c$  is the measured Capacity determined by CAPWAP

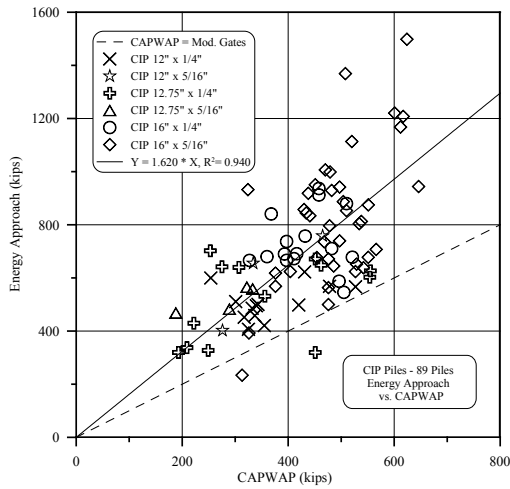


**Figure 20. CAPWAP vs. Energy Approach prediction method all CIP piles**

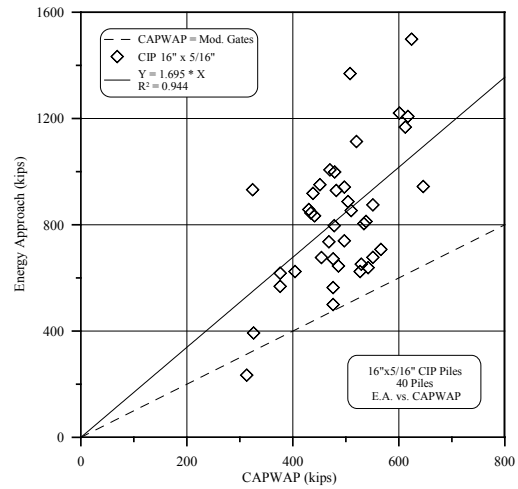


**Figure 21. CAPWAP vs. Energy Approach prediction 16" x 5/16" CIP piles**

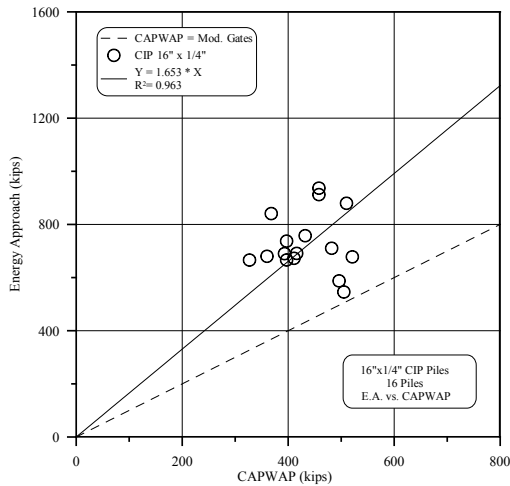


**Figure 22. CAPWAP vs. Energy Approach prediction 16" x 1/4" CIP piles**

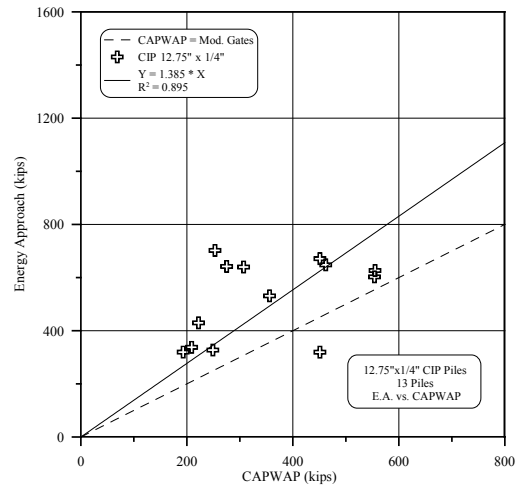


**Figure 23. CAPWAP vs. Energy Approach prediction 12.75" x 1/4" CIP piles**

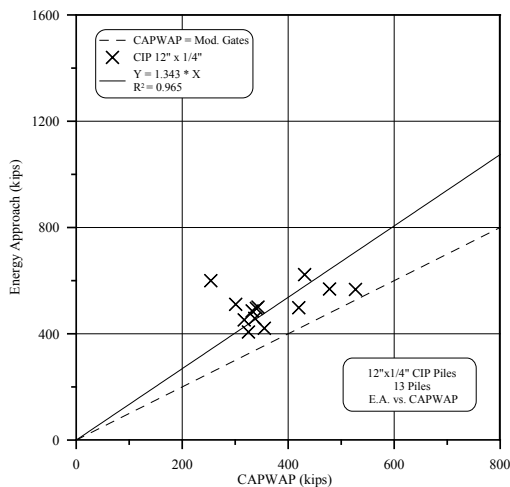


**Figure 24. CAPWAP vs. Energy Approach prediction 12" x 1/4" CIP piles**

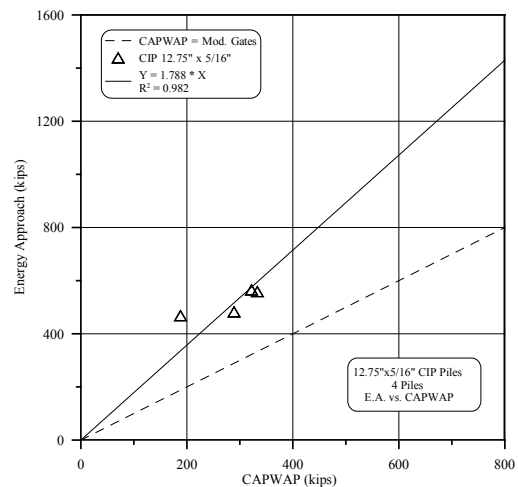


**Figure 25. CAPWAP vs. Energy Approach prediction 12.75" x 5/16" CIP piles**

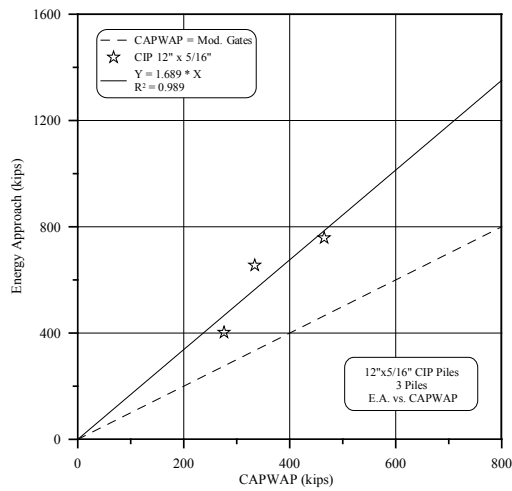


**Figure 26. CAPWAP vs. Energy Approach prediction 12" x 5/16" CIP piles**

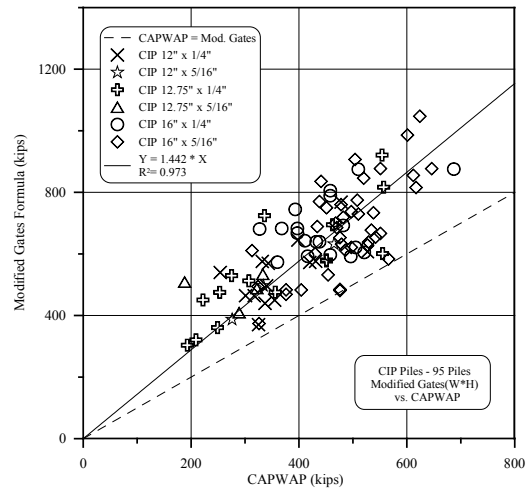


**Figure 27. CAPWAP vs. Gates formula all CIP piles**

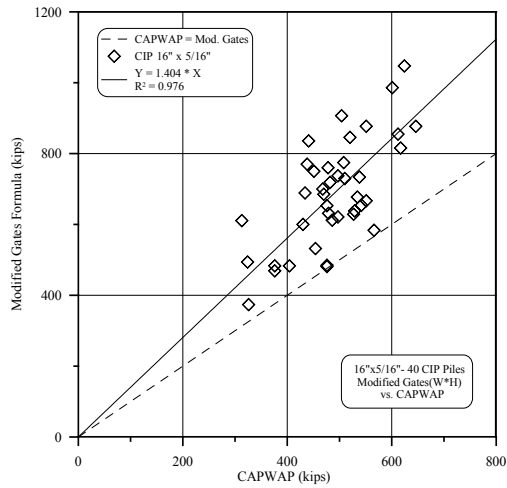


**Figure 28. CAPWAP vs. Gates formula 16" x 5/16" CIP piles**

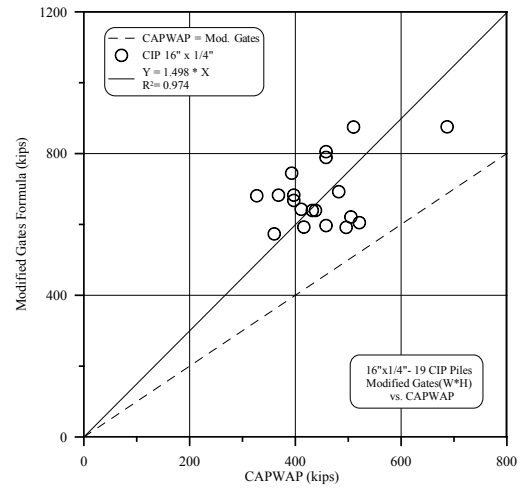


**Figure 29. CAPWAP vs. Gates formula 16" x 1/4" CIP piles**

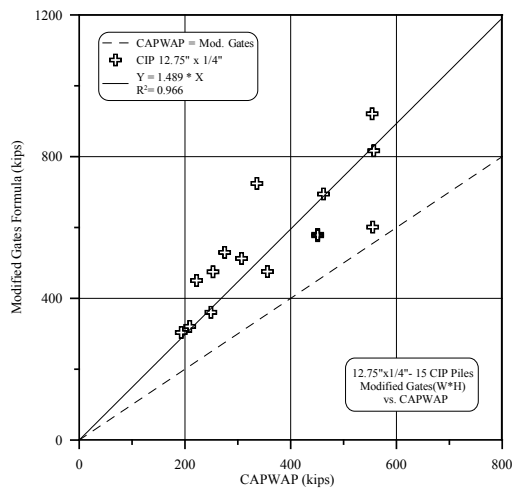


**Figure 30. CAPWAP vs. Gates formula 12.75" x 1/4" CIP piles**

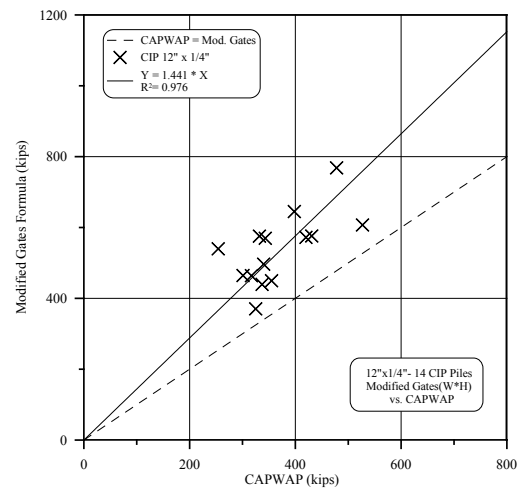


**Figure 31. CAPWAP vs. Gates formula 12" x 1/4" CIP piles**

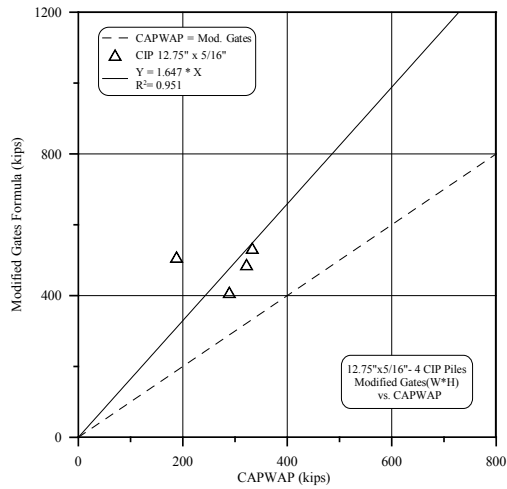


**Figure 32. CAPWAP vs. Gates formula  
12.75" x 5/16" CIP piles**

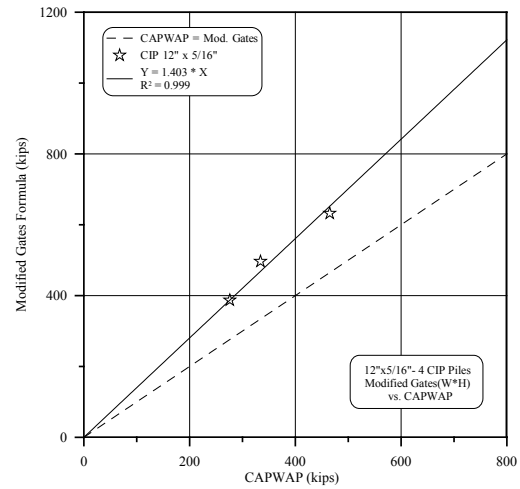


**Figure 33. CAPWAP vs. Gates formula  
12" x 5/16" CIP piles**

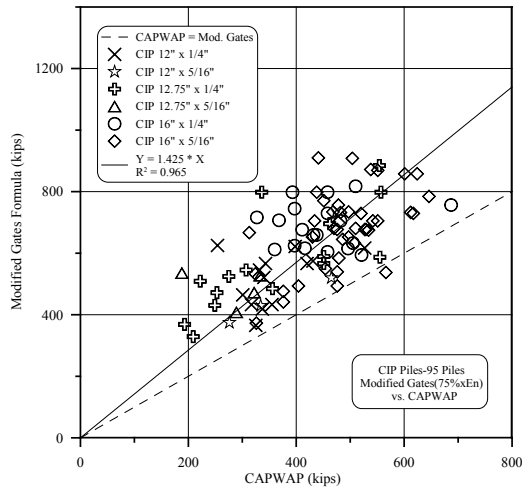


**Figure 34. CAPWAP vs. Gates formula  
all CIP piles**

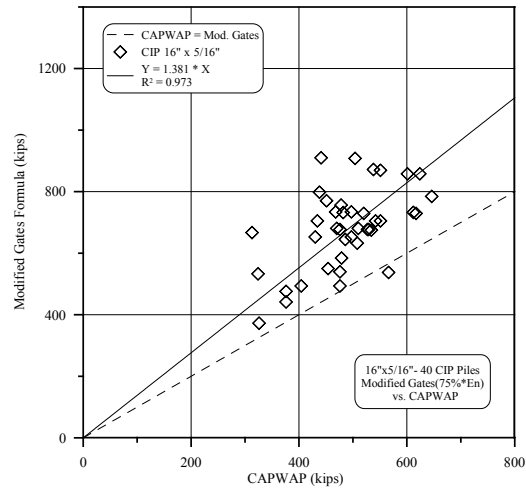


**Figure 35. CAPWAP vs. Gates formula  
16" x 5/16" CIP piles**

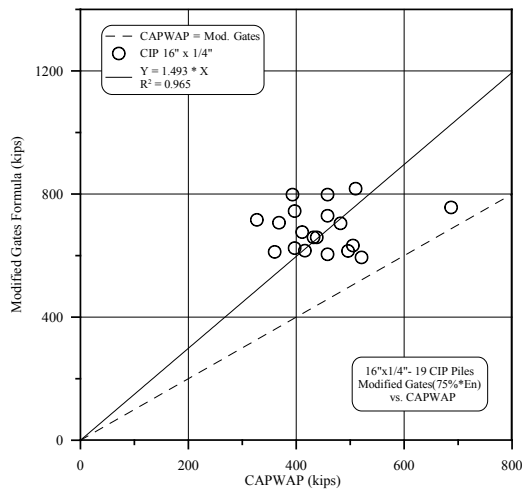


**Figure 36. CAPWAP vs. Gates formula  
16" x 1/4" CIP piles**

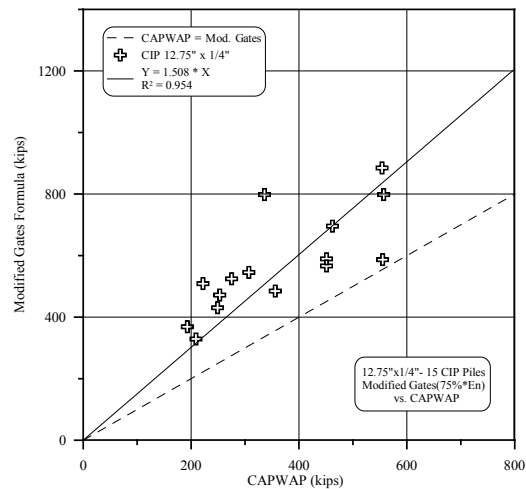


**Figure 37. CAPWAP vs. Gates formula  
12.75" x 1/4" CIP piles**



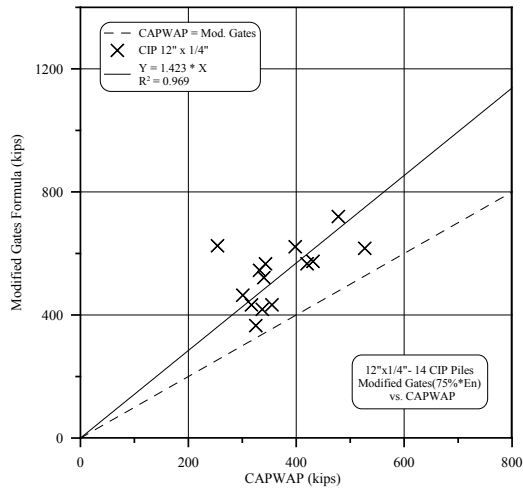


**Figure 38. CAPWAP vs. Gates formula  
12" x 1/4" CIP piles**

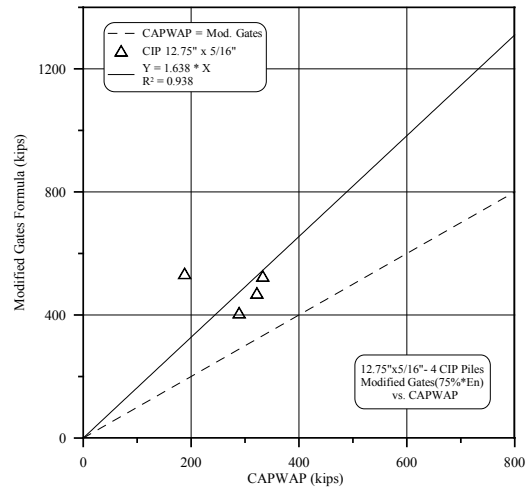


**Figure 39. CAPWAP vs. Gates formula  
12.75" x 5/16" CIP piles**

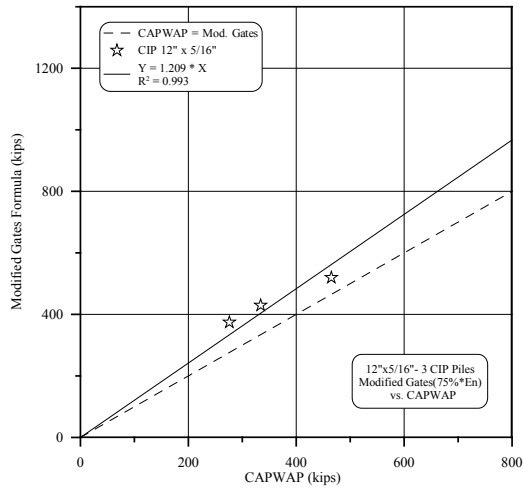


**Figure 40. CAPWAP vs. Gates formula  
12" x 5/16" CIP piles**

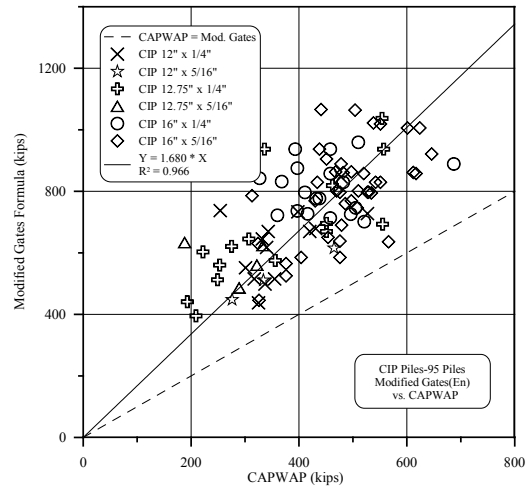


**Figure 41. CAPWAP vs. Gates formula  
all CIP piles**

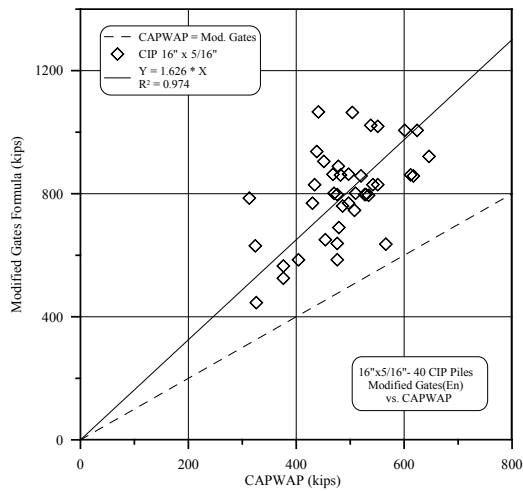


**Figure 42. CAPWAP vs. Gates formula  
16" x 5/16" CIP piles**

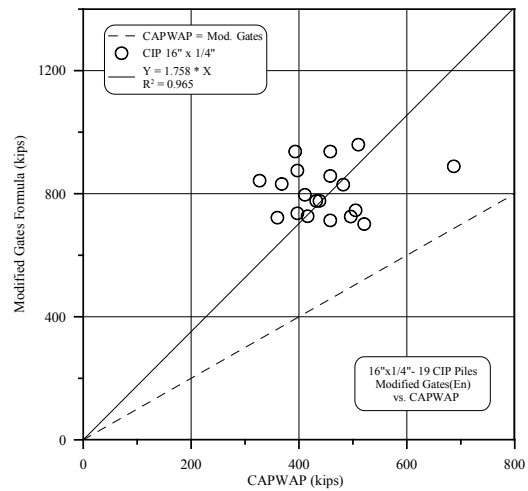


**Figure 43. CAPWAP vs. Gates formula  
16" x 1/4" CIP piles**

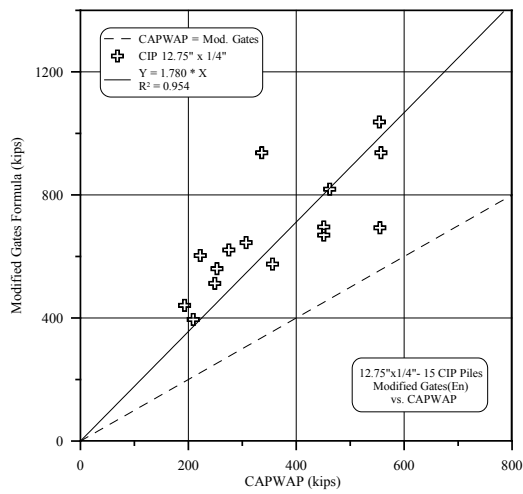


**Figure 44. CAPWAP vs. Gates formula  
12.75" x 1/4" CIP piles**

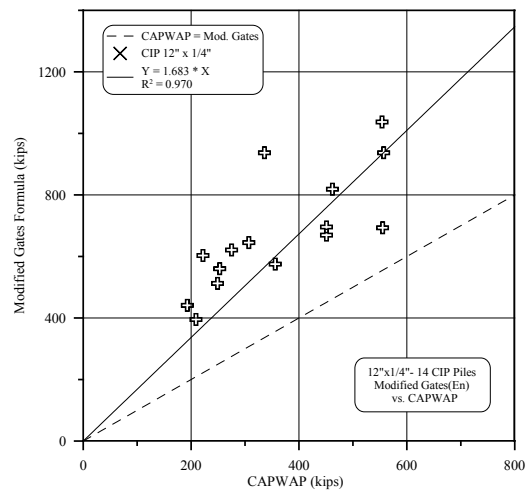


**Figure 45. CAPWAP vs. Gates formula  
12" x 1/4" CIP piles**

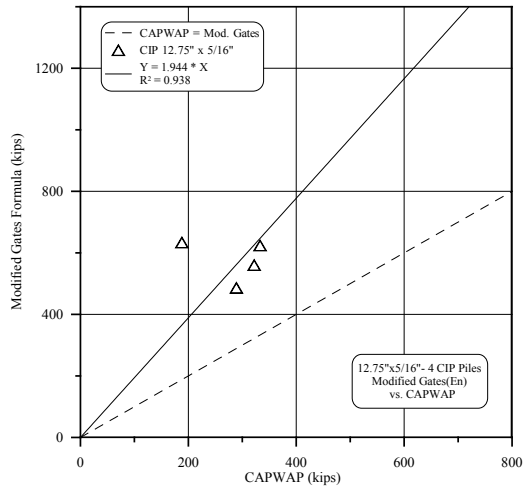


**Figure 46. CAPWAP vs. Gates formula  
12.75" x 5/16" CIP piles**

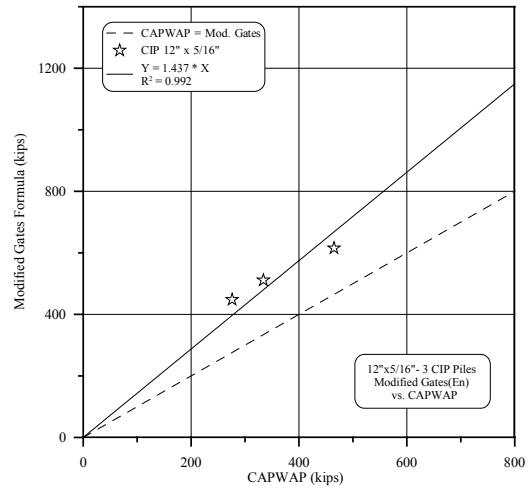


**Figure 47. CAPWAP vs. Gates formula  
12" x 5/16" CIP piles**

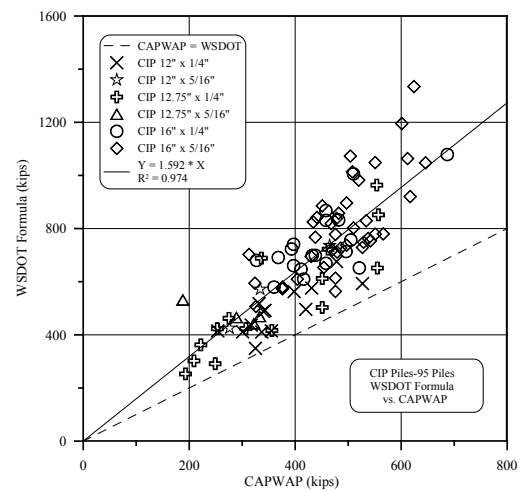


**Figure 48. CAPWAP vs. WSDOT formula  
all CIP piles**

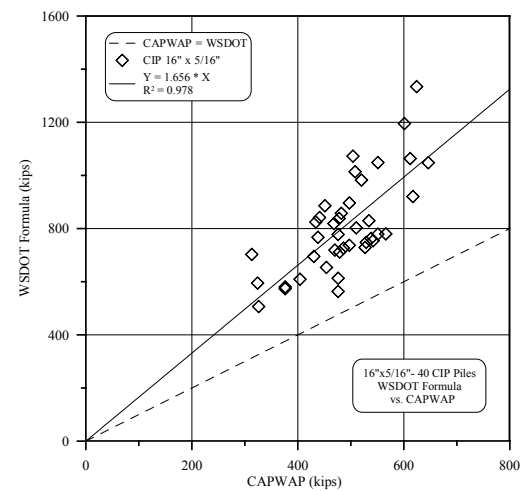


**Figure 49. CAPWAP vs. WSDOT formula  
16" x 5/16" CIP piles**

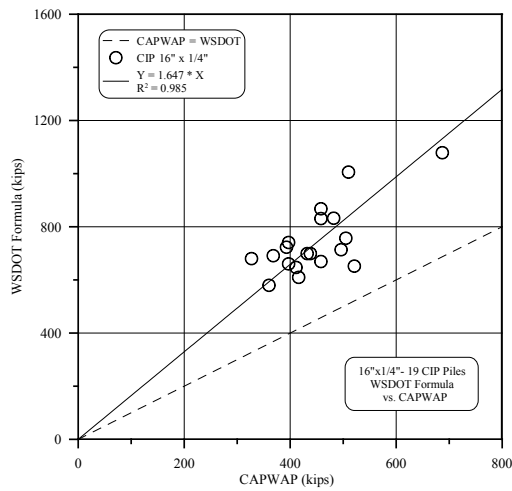


**Figure 50. CAPWAP vs. WSDOT formula  
16" x 1/4" CIP piles**

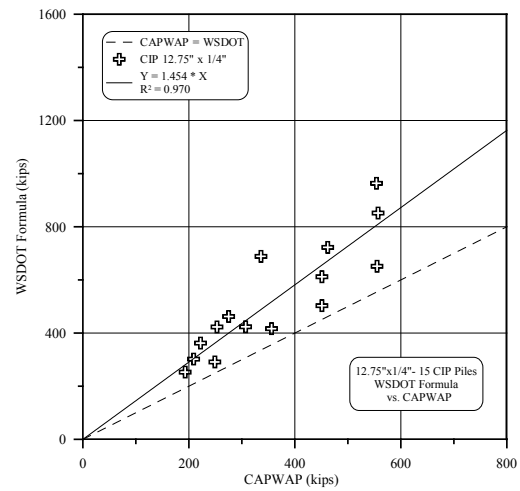


**Figure 51. CAPWAP vs. WSDOT formula  
12.75" x 1/4" CIP piles**

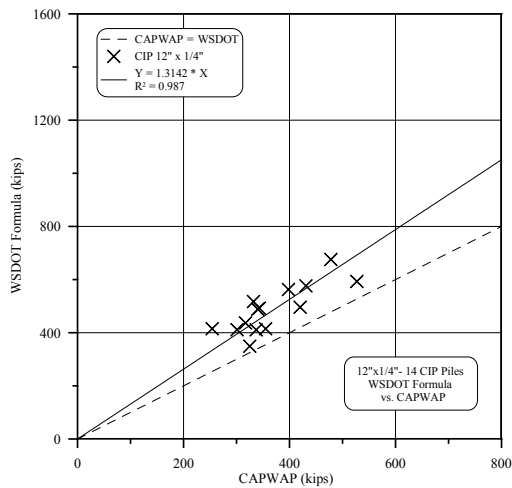


**Figure 52. CAPWAP vs. WSDOT formula  
12" x 1/4" CIP piles**

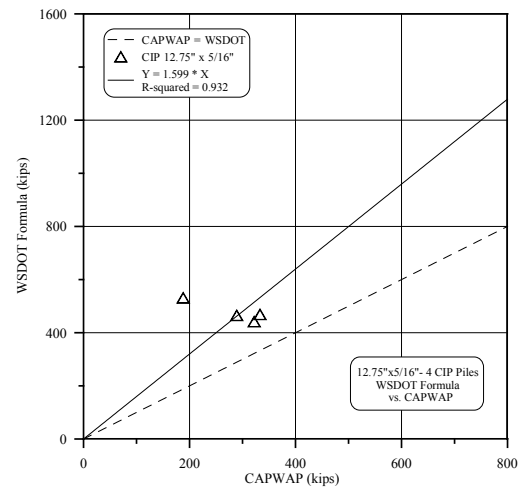


**Figure 53. CAPWAP vs. WSDOT formula  
12.75" x 5/16" CIP piles**

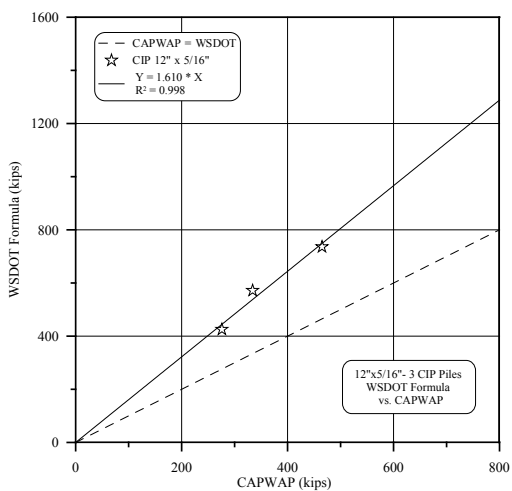


**Figure 54. CAPWAP vs. WSDOT formula  
12" x 5/16" CIP piles**

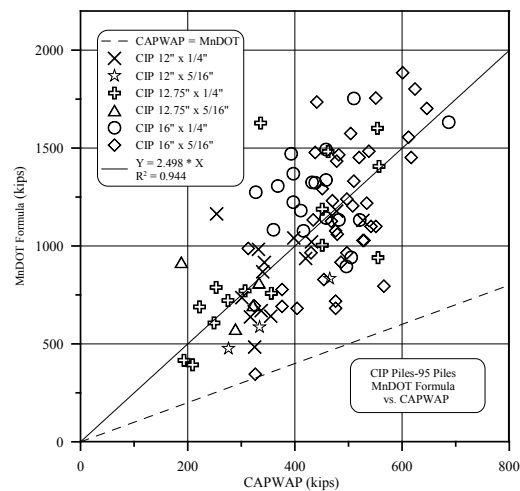


**Figure 55. CAPWAP vs. current MnDOT  
formula all CIP piles**

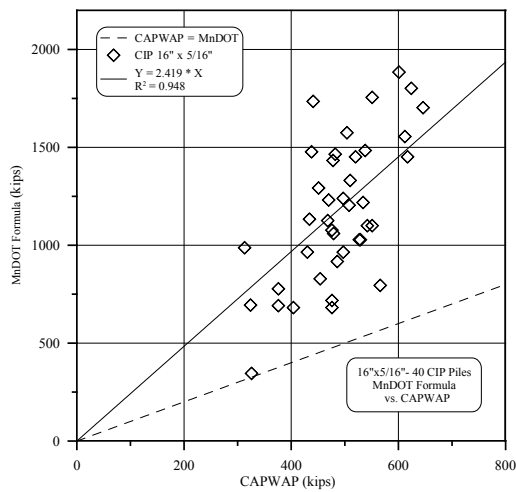


**Figure 56. CAPWAP vs. current MnDOT formula 16" x 5/16" CIP piles**

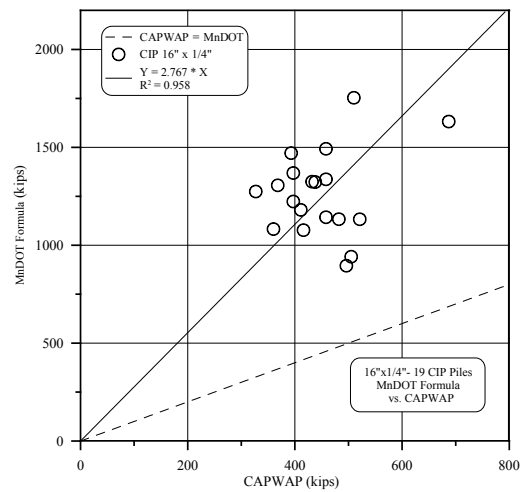


**Figure 57. CAPWAP vs. current MnDOT formula 16" x 1/4" CIP piles**

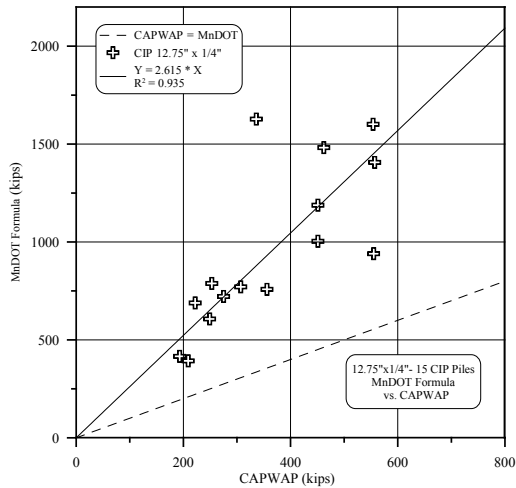


**Figure 58. CAPWAP vs. current MnDOT formula 12.75" x 1/4" CIP piles**

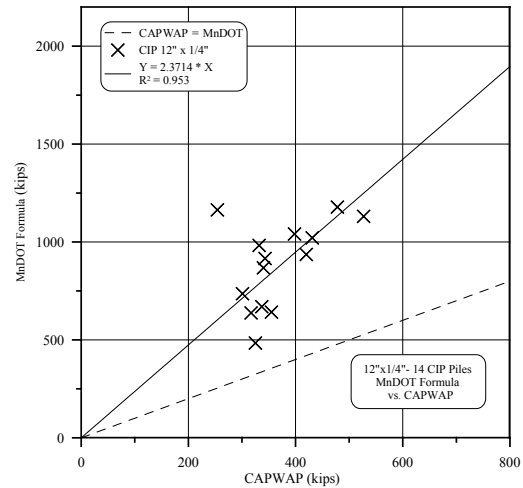


**Figure 59. CAPWAP vs. current MnDOT formula 12" x 1/4" CIP piles**

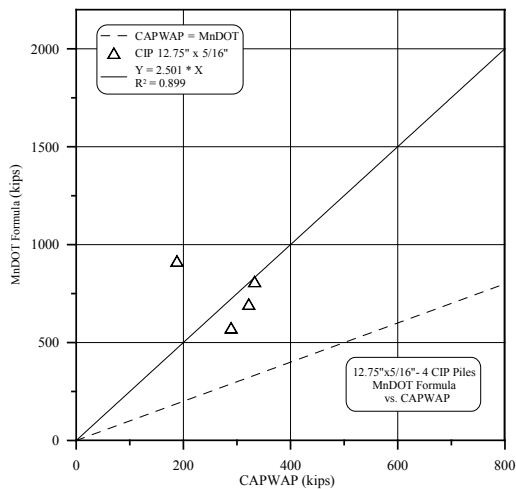


**Figure 60. CAPWAP vs. current MnDOT formula 12.75" x 5/16" CIP piles**

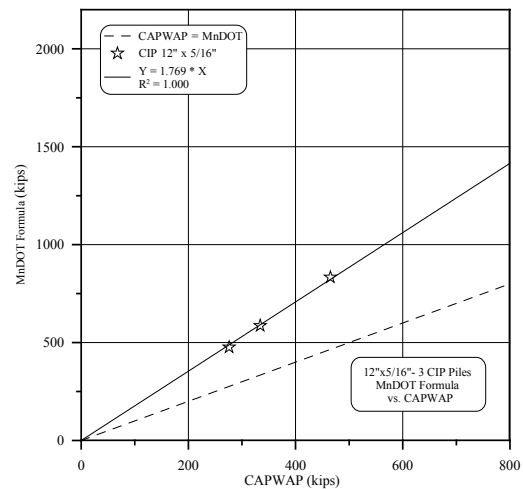


**Figure 61. CAPWAP vs. current MnDOT formula 12" x 5/16" CIP piles**

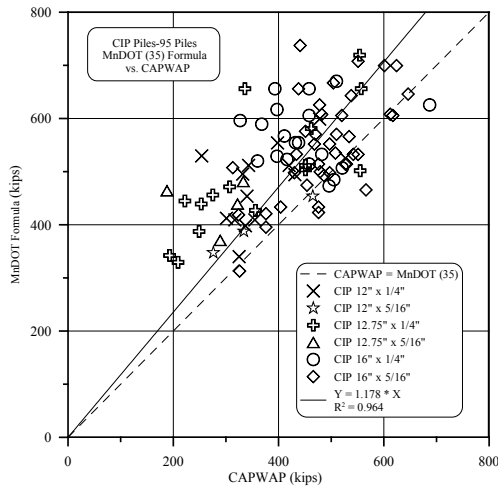


**Figure 62. CAPWAP vs. New MnDOT formula (35) All CIP piles**

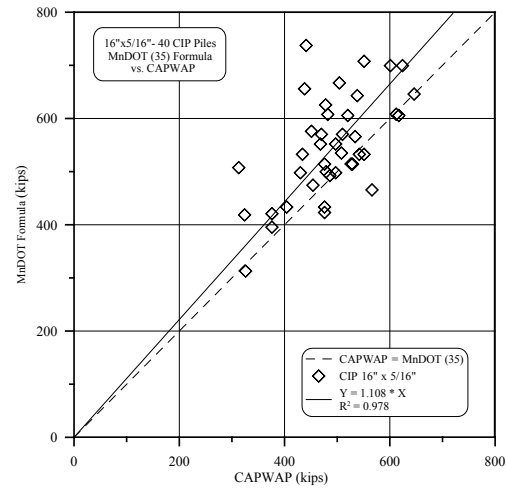


**Figure 63. CAPWAP vs. New MnDOT formula (35) 16" x 5/16" CIP piles**

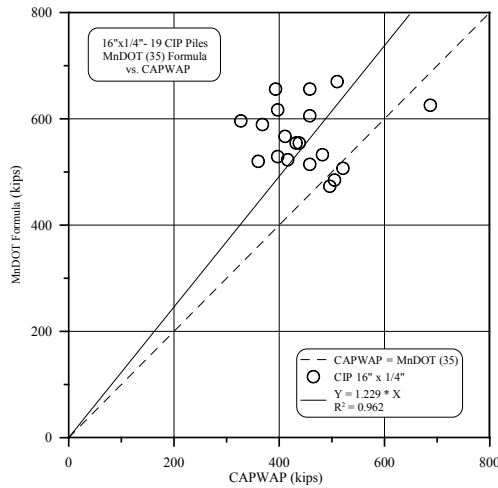


**Figure 64. CAPWAP vs. New MnDOT formula (35) 16" x 1/4" CIP piles**

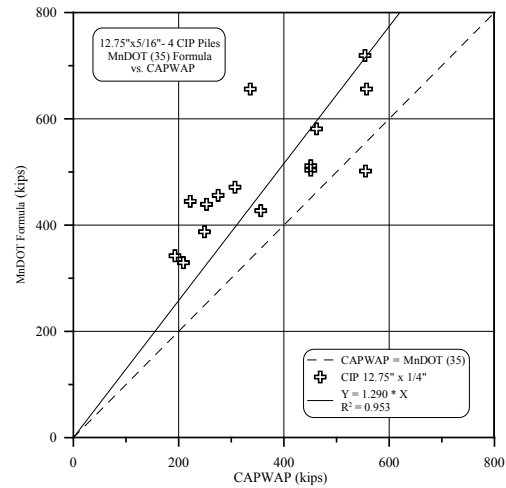


**Figure 65. CAPWAP vs. New MnDOT formula (35) 12.75" x 1/4" CIP piles**

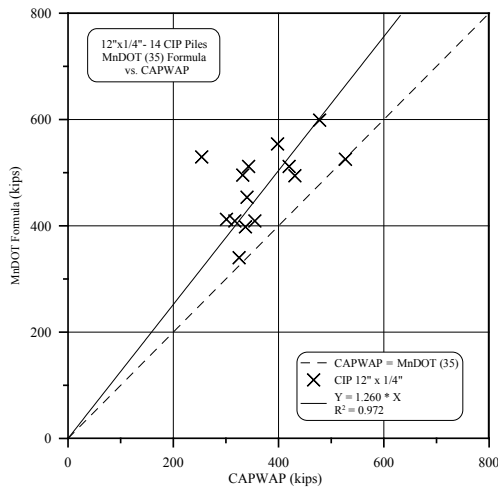


**Figure 66. CAPWAP vs. New MnDOT formula (35) 12" x 1/4" CIP piles**

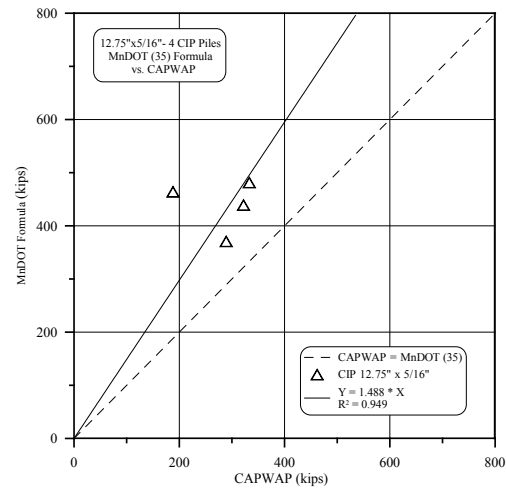


**Figure 67. CAPWAP vs. New MnDOT formula (35) 12.75" x 5/16" CIP piles**

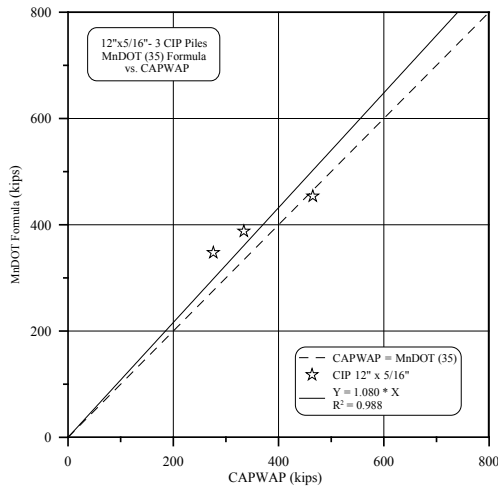


**Figure 68. CAPWAP vs. New MnDOT formula (35) 12" x 5/16" CIP piles**

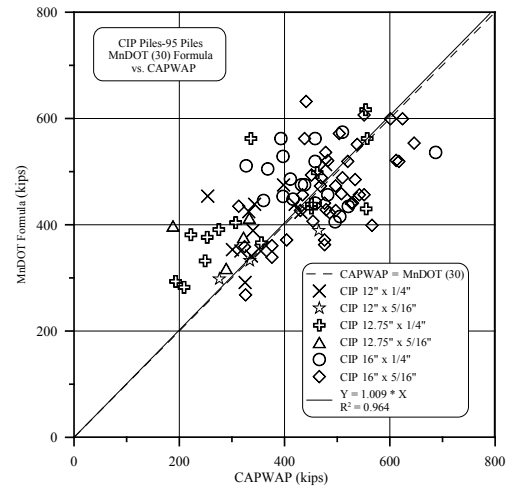


**Figure 69. CAPWAP vs. New MnDOT formula (30) All CIP piles**

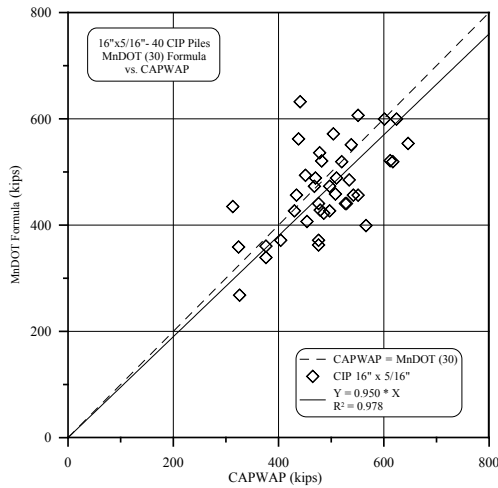


**Figure 70. CAPWAP vs. New MnDOT formula (30) 16" x 5/16" CIP piles**

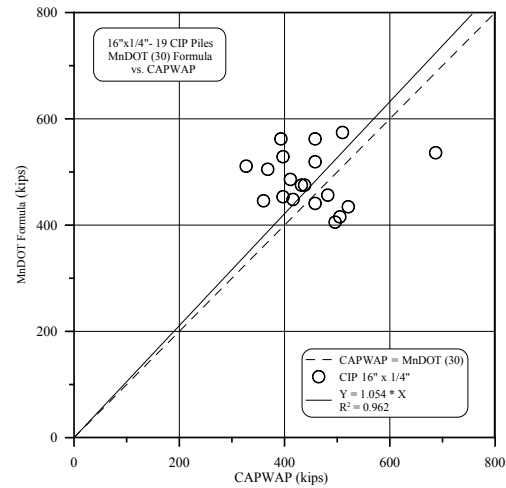


**Figure 71. CAPWAP vs. New MnDOT formula (30) 16" x 1/4" CIP piles**

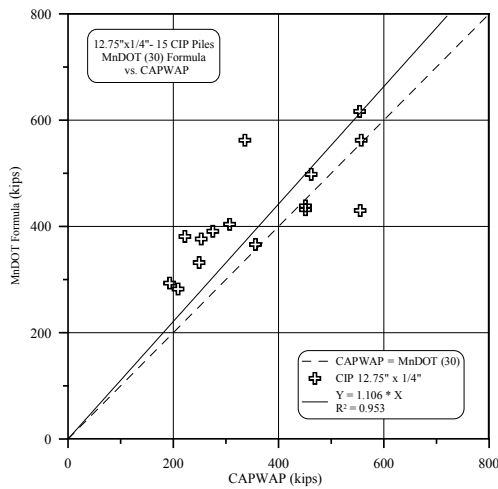


**Figure 72. CAPWAP vs. New MnDOT formula (30) 12.75" x 1/4" CIP piles**

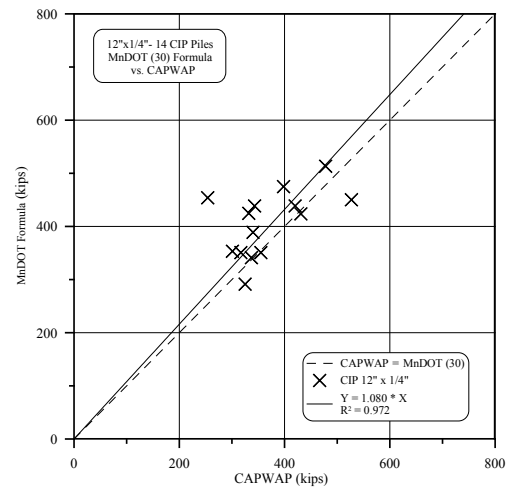


**Figure 73. CAPWAP vs. New MnDOT formula (30) 12" x 1/4" CIP piles**

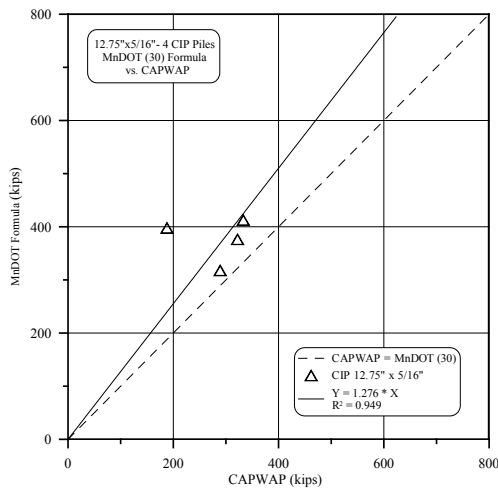


**Figure 74. CAPWAP vs. New MnDOT formula (30) 12.75" x 5/16" CIP piles**

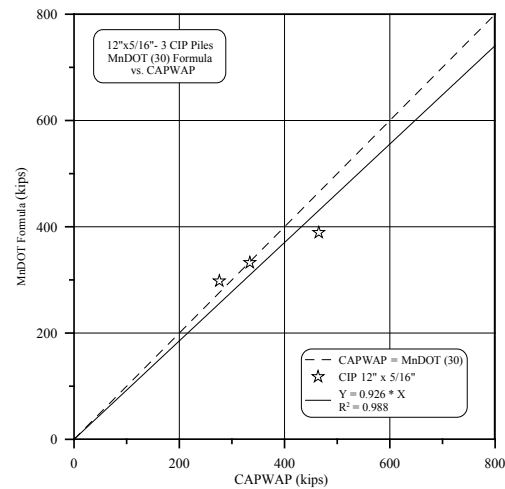


**Figure 75. CAPWAP vs. New MnDOT formula (30) 12" x 5/16" CIP piles**

### 3.7 Conclusions Derived from the Initial Evaluation

#### 3.7.1 General

The stroke measurements presented on the new database by MnDOT personnel; suggest that typically, the diesel hammers' stroke for the rated energy and the corrected energy are 76.35% and 78.31% respectively. These values compared quite well with the assumed stroke formerly recommended by the MnDOT (i.e. 75 % of nominal energy), when stroke information is not recorded.

The developed summary tables provide quantitative information matching previous data and reports provided by the MnDOT personnel.

- (i) CIP piles range in diameter from 12" to 20"
- (ii) Most common CIP piles used in the dynamic database are 16" x 0.3125" and 16" x 0.25", installed as 34.3% and 20.7% of the total foundation length, respectively (based on 53 projects).
- (iii) Typical (average) driven pile length is 84 feet. More specific categorization is provided in Phase I report, Table 2.4, e.g. Average CIP 16" x 0.3125" pile length is 82 feet.
- (iv) Diesel hammers are most commonly used for driving piles ranging in sizes from DE 40 (32 kip-ft) to I-30V2 (90.8 kip-ft).
- (v) Around 80% of the piles are driven beyond the easy driving resistance zone of 4 bpi, hence allowing more accurate capacity evaluation when utilizing the dynamic methods. Forty-three percent (43%) of the piles were driven to a final penetration of 8 or more bpi.

### **3.7.2 Analysis**

Noting that all analyses are not compared to a benchmark (i.e. SLT) capacity, the analyses presented in Figures 20 through 75 and summarized in Table 42 lead to the following observations and conclusions:

1. The ratio of CAPWAP to EA of approximately 0.65 (or the reverse of 1.54) most likely represents a typical conservatism of CAPWAP at EOD and a marginal possible over prediction by the EA. Previous analyses of static load test over CAPWAP (377 cases of EOD and BOR) resulted with a ratio of 1.368 while static load test over the EA (371 cases) resulted with the ratio of 0.894 and for EOD only (128 cases) with the ratio of 1.084, (Paikowsky et. al, 2004). Though the result of the current analyses fall into that range, further evaluation is required, separating the easy driving ( $BC < 4$  BPI) from the other and investigating the methods.
2. The WSDOT equation performed well compared to the EA method and Gates FHWA modified equation, all showing similar over prediction compared to CAPWAP.
3. MnDOT traditional equation performed the worst when compared to CAPWAP, producing a very large scatter and typical capacity of 2.36 times that of CAPWAP.
4. The proposed new MnDOT equation designated for Diesel hammers, EOD and  $BC > 4$  bpi (coeff = 30) performed the best with a mean ratio of 1.0 compared to CAPWAP. This will be further investigated separating the cases for  $BC \geq 4$  bpi and  $BC < 4$  bpi.
5. The general proposed new MnDOT equation designed for all hammers, all piles, all cases (coeff = 35) provided the second best ratio compared to CAPWAP. A bit on the unsafe side but probably considering CAPWAP conservatism, very close to what one could expect in a SLT.

## **3.8 Final Evaluation of the Capacity Predictions**

### **3.8.1 Overview**

The major conclusion of the preliminary analysis regarding the MnDOT dynamic measurements database was that the equations developed in Phase I of the study were found to predict best the pile capacity for an independent dataset from MN. As such, the final evaluation of the data was conducted using various approaches to the application of the equation and concentrated on limited number of comparisons.

### **3.8.2 Performed Analyses**

Table 43 provides an updated list of investigated equations and represents a modification of Table 40 in the following ways:



- a) The Energy Approach and the equations originally developed in Phase I of the study for the rated hammer energy ( $E_n$ ) were also investigated when  $E_{max}$  and  $E_n$  were replaced by the observed developed energy, i.e.  $E = W_r \cdot h$ .
- b) Selected comparisons of equations and figures were developed using a uniform scale for all analyses and statistical analyses for “all piles” category.

### **3.8.3 Presentation of Results**

Table 44 presents a summary of the statistical analyses and best fit line correlation for the equations presented in Table 43 for “all piles” category. Table 45 provides expanded details for the same equations each subdivided into four categories, namely (i) All Piles, (ii) EOID, (iii) BOR, and (iv) EOID & BC > 4BPI. Tables 44 and 45 also list the figure numbers for the graphs presenting the relevant relationship. Figures 76 to 85 present the above investigated equations for all piles under a uniform scale in all figures. The graphs very clearly illustrate the differences of the methods’ performance in bias and scatter, and Figure 69 presents a match that outperforms them all by far. This presentation was done for two reasons: a) the uniform scale allows better judgment and b) the ramifications of the final analyses are made clear.

### **3.8.4 Conclusions**

The statistical and correlation values presented in Tables 44 and 45, and Figures 76 to 85, show unequivocally that the equations developed in Phase I of the study specifically for the MnDOT outperform all other equations either when using the nominal energy or the one observed in the field. Figure 85 shows the best performance when using the stroke and ram weight along with the proposed equation with a coefficient of 35 (Equation 1.7a of Table 43). The relations between equation 1.7a and CAPWAP resulted with a mean of 0.970 and a COV of 0.158 for EOID conditions checked on 40 cases.

**Table 43. Updated investigated equations**

No.	Equation	Description	Figure No.	Reference
1.1	$R_u = \frac{E * 12}{s + \frac{Q}{2}}$	E=W <sub>r</sub> *h	20, 76	Energy Approach Prediction Method (1982)
1.2	$R_U = 1.75\sqrt{E} * \log(10 * N) - 100$	E=W <sub>r</sub> *h	27, 77	Modified Gates FHWA(1988)
1.3	$R_U = 1.75\sqrt{E} * \log(10 * N) - 100$	E=75%En	34, 78	Modified Gates FHWA(1988)
1.4	$R_U = 1.75\sqrt{E} * \log(10 * N) - 100$	E=En	41, 79	Modified Gates FHWA(1988)
1.5	$R_u = 6.6 * F_{eff} * E * \ln(10N)$	F <sub>eff</sub> = 0.47 OED	48, 80	Washington State DOT (Allen, 2005)
1.6	$R_u = \frac{10.5 * E}{S + 0.2} * \frac{W + (0.1 * M)}{W + M}$	E=W <sub>r</sub> *h	55, 81	Minnesota DOT (2006)
1.7	$R_u = 35\sqrt{E_n} * \log(10N)$	All piles, All Conditions	62, 82	First Stage Proposed New MnDOT Equation (2009)
1.7a	$R_u = 35\sqrt{E} * \log(10N)$	E=W <sub>r</sub> *h All piles, All Conditions	83	Modified First Stage Proposed New MnDOT Equation (2009)
1.8	$R_u = 30\sqrt{E_n} * \log(10N)$	EOD, BC ≥4BPI	69, 84	First Stage Proposed New MnDOT Equation (2009)
1.8a	$R_u = 30\sqrt{E} * \log(10N)$	E=W <sub>r</sub> *h EOD, BC ≥4BPI	85	Modified First Stage Proposed New MnDOT Equation (2009)

Notes: R<sub>u</sub>= ultimate carrying capacity of pile, in kips (lbs for eq. 1.6)  
W<sub>r</sub>= mass of the striking part of the hammer, in kips  
M= total mass of pile plus mass of the driving cap, in kips  
W<sub>r</sub>= weight of falling mass, in kips  
Ln= the natural logarithm, in base “e”  
E= developed energy, equal to W<sub>r</sub> times h, in kips-foot (Eq. No: 1.1, 1.2)  
E= energy per blow for each full stroke in foot-pounds (eq. 5 and 6)  
F<sub>eff</sub>= hammer efficiency factor  
s= Set, permanent displacement of the pile at the end of the analyzed blow, in inches  
E<sub>n</sub>= rated energy of hammer per blow, in kips-foot (Eq. No: 1.4, 1.7, 1.8)  
N= blows per inch (BPI)  
Q= Quake = D<sub>max</sub>-set  
D<sub>max</sub>= measured maximum pile top displacement, in inches  
OED= Open ended diesel hammers

**Table 44. Summary of statistical analysis and best fit line correlation**

Relations	Figure No	Category	No. of Cases n	Statistics			Best Fit Line	Coefficient of Determination ( $r^2$ )
				mean	S.D.	COV		
CAPWAP/ E.A.	20, 76	All Piles	89	0.6479	0.1825	0.2817	$R_u=1.620*R_c$	0.940
CAPWAP/ Modified Gates ( $W_r*h$ )	27, 77	All Piles	95	0.6905	0.1210	0.1752	$R_u=1.442*R_c$	0.973
CAPWAP/ Modified Gates ( $0.75*E_n$ )	34, 78	All Piles	95	0.6927	0.1338	0.1931	$R_u=1.425*R_c$	0.965
CAPWAP/ Modified Gates ( $E_n$ )	41, 79	All Piles	95	0.5866	0.1126	0.1919	$R_u=1.680*R_c$	0.966
CAPWAP/ WSDOT	48, 80	All Piles	95	0.6482	0.1109	0.1711	$R_u=1.592*R_c$	0.974
CAPWAP/ MnDOT (2006)	55, 81	All Piles	95	0.5467	0.1505	0.2753	$R_u=2.011*R_c$	0.942
CAPWAP/ Proposed MnDOT (35) $E_n$	62, 82	All Piles	95	0.8260	0.1632	0.1976	$R_u=1.178*R_c$	0.964
CAPWAP/ Proposed MnDOT (35) $W_r*h$	83	All Piles	95	0.9339	0.1586	0.1698	$R_u=1.051*R_c$	0.975
CAPWAP/ Proposed MnDOT (30) $E_n$	69, 84	All Piles	95	0.9637	0.1904	0.1976	$R_u=1.009*R_c$	0.964
CAPWAP/ Proposed MnDOT (30) $W_r*h$	85	All Piles	95	1.0896	0.1850	0.1698	$R_u=0.901*R_c$	0.975

Notes:  $R_u$  is the calculated capacity using each of the dynamic formulae  
 $R_c$  is the Capacity determined by CAPWAP

**Table 45. Summary of statistical analysis and best fit line correlation**

Relations	Figure No	Category	No. of Cases n	Statistics			Best Fit Line	Coefficient of Determination ( $r^2$ )
				mean	S.D.	COV		
CAPWAP/ E.A.	20, 76	All Piles	89	0.6479	0.1825	0.2817	$R_u=1.620*R_c$	0.940
		EOID	38	0.6877	0.1841	0.2677	---	---
		BOR	51	0.6183	0.1773	0.2868	---	---
		EOID&BC $\geq$ 4BPI	31	0.6918	0.1852	0.2677	---	---
CAPWAP/ Modified Gates ( $W_r*h$ )	27, 77	All Piles	95	0.6905	0.1210	0.1752	$R_u=1.442*R_c$	0.973
		EOID	40	0.7194	0.1131	0.1573	---	---
		BOR	55	0.6695	0.1231	0.1839	---	---
		EOID&BC $\geq$ 4BPI	33	0.7037	0.1068	0.1548	---	---
CAPWAP/ Modified Gates ( $0.75*E_n$ )	34, 78	All Piles	95	0.6927	0.1338	0.1931	$R_u=1.425*R_c$	0.965
		EOID	40	0.6924	0.1184	0.1711	---	---
		BOR	55	0.6929	0.1450	0.2092	---	---
		EOID&BC $\geq$ 4BPI	33	0.6790	0.1124	0.1655	---	---
CAPWAP/ Modified Gates ( $E_n$ )	41, 79	All Piles	95	0.5866	0.1126	0.1919	$R_u=1.680*R_c$	0.966
		EOID	40	0.5865	0.1000	0.1705	---	---
		BOR	55	0.5866	0.1218	0.2077	---	---
		EOID&BC $\geq$ 4BPI	33	0.5758	0.0950	0.1649	---	---
CAPWAP/ WSDOT	48, 80	All Piles	95	0.6482	0.1109	0.1711	$R_u=1.592*R_c$	0.974
		EOID	40	0.6727	0.1012	0.1504	---	---
		BOR	55	0.6304	0.1151	0.1826	---	---
		EOID&BC $\geq$ 4BPI	33	0.6685	0.1035	0.1548	---	---
CAPWAP/ MnDOT (2006)	55, 81	All Piles	95	0.5467	0.1505	0.2753	$R_u=2.011*R_c$	0.942
		EOID	40	0.5652	0.1206	0.2133	---	---
		BOR	55	0.5333	0.1687	0.3164	---	---
		EOID&BC $\geq$ 4BPI	33	0.5336	0.0970	0.1818	---	---
CAPWAP/ Proposed MnDOT (35) $E_n$	62, 82	All Piles	95	0.8260	0.1632	0.1976	$R_u=1.178*R_c$	0.964
		EOID	40	0.8438	0.1591	0.1886	---	---
		BOR	55	0.8131	0.1664	0.2047	---	---
		EOID&BC $\geq$ 4BPI	33	0.8314	0.1533	0.1843	---	---
CAPWAP/ Proposed MnDOT (35) $W_r*H$	83	All Piles	95	0.9339	0.1586	0.1698	$R_u=1.051*R_c$	0.975
		EOID	40	0.9698	0.1529	0.1576	---	---
		BOR	55	0.9078	0.1589	0.1750	---	---
		EOID&BC $\geq$ 4BPI	33	0.9559	0.1457	0.1524	---	---
CAPWAP/ Proposed MnDOT (30) $E_n$	69, 84	All Piles	95	0.9637	0.1904	0.1976	$R_u=1.009*R_c$	0.964
		EOID	40	0.9844	0.1857	0.1886	---	---
		BOR	55	0.9486	0.1941	0.2047	---	---
		EOID&BC $\geq$ 4BPI	33	0.9700	0.1788	0.1843	---	---
CAPWAP/ Proposed MnDOT (30) $W_r*H$	85	All Piles	95	1.0896	0.1850	0.1698	$R_u=0.901*R_c$	0.975
		EOID	40	1.1315	0.1783	0.1576	---	---
		BOR	55	1.0591	0.1854	0.1750	---	---
		EOID&BC $\geq$ 4BPI	33	1.1153	0.1700	0.1524	---	---

Notes:  $R_u$  is the calculated capacity using each of the dynamic formulae  
 $R_c$  is the Capacity determined by CAPWAP

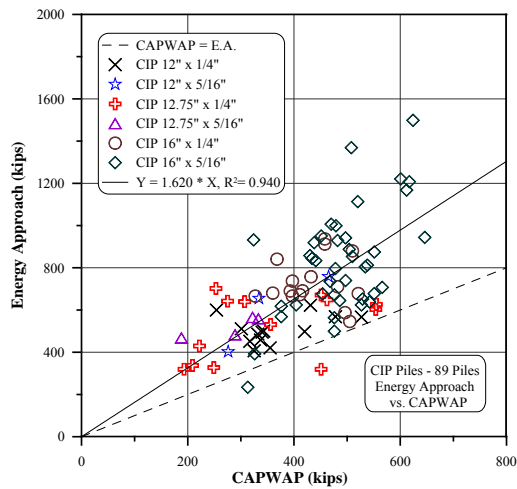


**Figure 76. CAPWAP vs. Energy Approach prediction method all CIP piles**

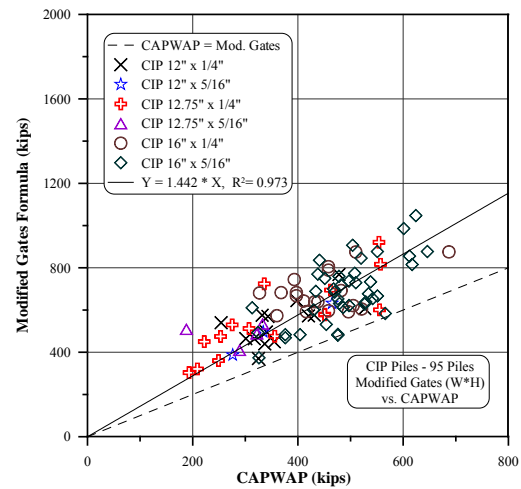


**Figure 77. CAPWAP vs. Modified Gates formula (W\*H) all CIP piles**

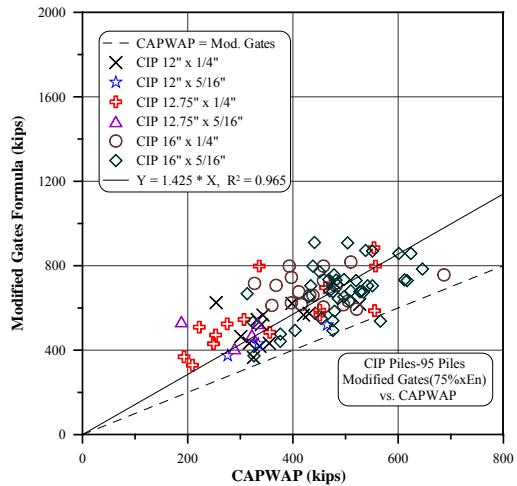


**Figure 78. CAPWAP vs. Modified Gates formula (75%\*En) all CIP piles**

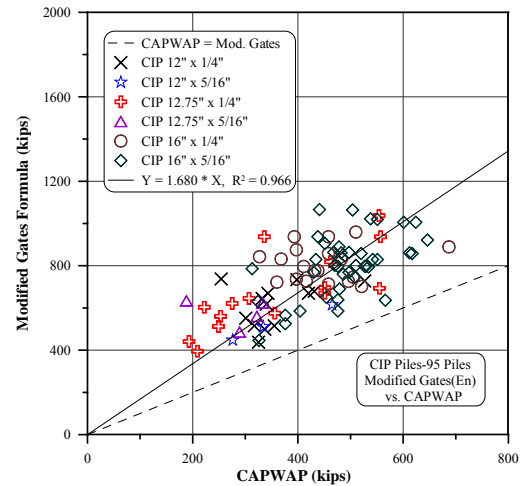


**Figure 79. CAPWAP vs. Modified Gates formula (En) all CIP piles**

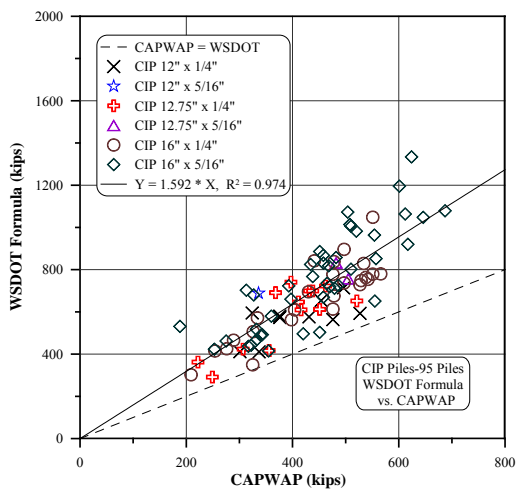


**Figure 80. CAPWAP vs. WSDOT formula ( $E=W_r \cdot h$ ) all CIP piles**

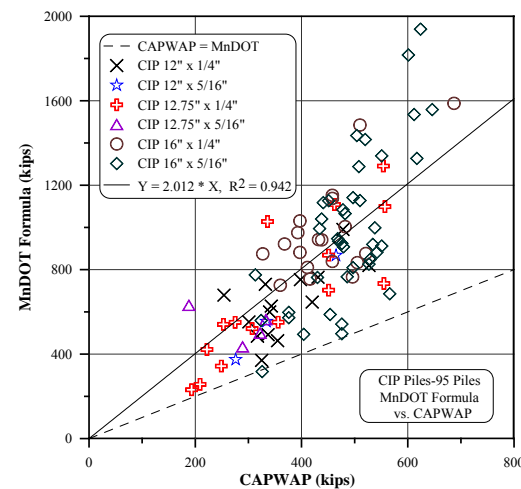


**Figure 81. CAPWAP vs. current MnDOT all CIP piles**

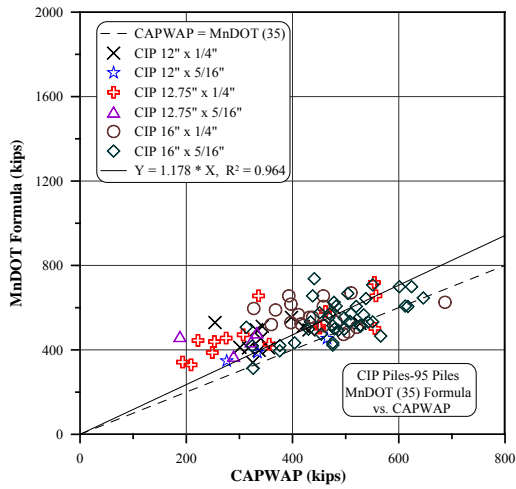


**Figure 82. CAPWAP vs. New MnDOT formula (35) ( $E=E_n$ ) all CIP piles**

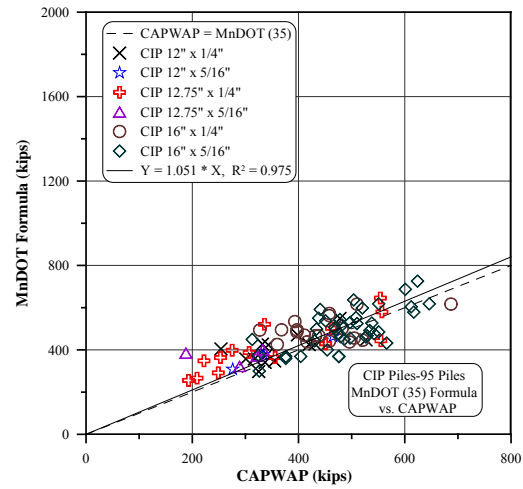


**Figure 83. CAPWAP vs. New MnDOT formula (35) ( $E=W_r * h$ ) all CIP piles**

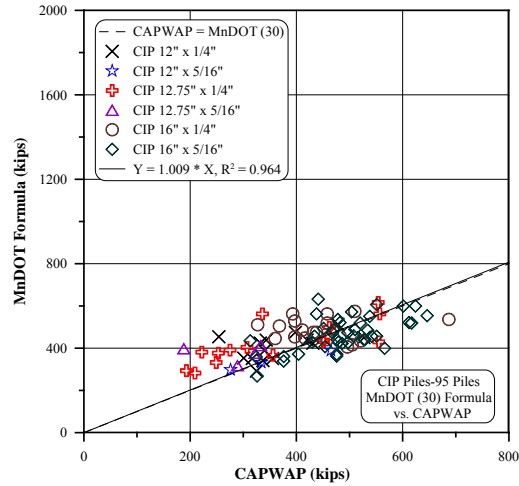


**Figure 84. CAPWAP vs. New MnDOT formula (30) ( $E=E_n$ ) all CIP piles**

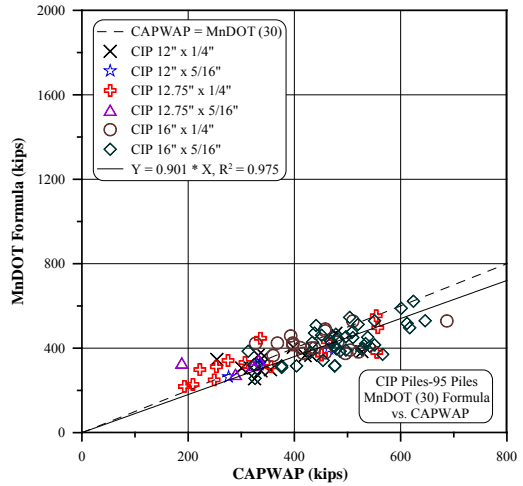


**Figure 85. CAPWAP vs. New MnDOT formula (30) ( $E=W_r * h$ ) all CIP piles**

## **4 RE-ASSESSMENT OF FORMAT AND LRFD RESISTANCE FACTORS FOR THE NEW MNDOT PILE DRIVING FORMULA (MPF12)**

### **4.1 Overview**

Phase II of the study initially focused on the review of other practices and a comparison of equations (Chapter 2) and the evaluation of various dynamic equations and the equation developed in Phase I of the study via dynamic measurements and signal matching (CAPWAP) analyses on piles in MN (Chapter 3). The evaluation presented in Chapter 3 also included the modification of the equation developed in Phase I, to reflect stroke measurements and ram weight instead of nominal hammer energy. When both investigations confirmed the soundness of the developed equation, Phase II of the study concentrated on the specific cases of the database and re-evaluation of the proposed equation in a manner better suited to MnDOT field practices.

### **4.2 Examination of the Extreme Over-Prediction Cases in the Database**

#### ***4.2.1 Rationale and Method of Approach***

The preceding review of Chapter 2 revealed that beyond the difficulties associated with data source, consistency of interpretation, systematic approach and analyses, the extreme cases of unsafe over-predictions were not included in the studies presented by Long and Maniaci (2000) and Long et al. (2009a,b). Section 2.3.7 addresses the issue and the present section provides an in-depth examination of these case histories.

The databases used in Phase I of the MnDOT research (Paikowsky et al., 2009) were re-analyzed by reversing the bias to represent the calculated over measured values such that comparison can be held with the analyses reviewed in Chapter 2. The outlier cases were defined as those outside the range of the mean  $\pm 2$  standard deviation typically recognized as the extreme zone.

Approximately 95 percent of the data falls within the two standard deviations around the mean of a normal distribution. Seven cases outside of this zone were identified and are presented in Table 46. The sources of these case histories were reviewed and analyzed. Davisson (1972) failure criterion was reapplied to the static load test load-displacement curve. No errors found in any of the cases compared to the original interpretations. When examining the outliers in comparison to other case histories of similar conditions, no major reasons could have been identified as contributors to the unsafe over-prediction in these cases. Thirty-five (35) H pile cases were identified to have similar pile size, soil type, hammer type and maximum applied load to those identified as extreme cases. Thirty (30) pipe pile cases were identified as having the same pile type out of which ten cases had similar soil conditions and hammer types. All the cases identified in Table 46 fall into the criteria used by Long and Maniaci (2000), or Long et al. (2009a,b) to analyze the data presented to IDOT. No clear explanation exists as to why the cases were excluded beyond the speculations presented in section 2.3.7. The ratios of the predicted over

measured capacities varied from 2.3 to 5.1 for the H piles and 3.4 to 7.7 for the pipe piles (referring to FHWA modified Gates and WSDOT equations combined). These extreme unsafe cases should have been taken into consideration since they are those in which “failure” or exceedance of the criteria takes place.

Two sources were identified for the cases in Table 46. The first, “Pile Load and Extraction Tests 1954 – 1992”, Ontario, Ministry of Transportation, Report EM- 48 (rev. 93), and one additional H-pile case obtained from the Connecticut DOT Results of Static Load Tests from 13 Projects.

The piles tested and included in our database are steel H piles and concrete filled steel tube piles. All analyzed piles were driven, soil conditions vary considerably across the 41 sites and include many of the various soil deposits found in the province of Ontario, Canada, such as organic soils, alluvial deposits, lacustrine clays, and glacial and glacio-fluvial deposits. Piles driven to bedrock are founded on either shale or limestone.

All the examined cases relate to vertical piles statically loaded in procedure either identical or similar to ASTM standards and a period of 10 days was generally allowed between pile driving and load testing. This interval permitted thixotropic regain and cementation effects to take place in the soil surrounding the pile.



**Table 46. Summary of the extreme data cases related to MnDOT study**

Pile Type	Case Number	Loc.	Pile Type	Length (ft)	Soil Type	Hammer Type	Rated Energy (kips-ft)	BPI	Static Capacity by Davisson's (kips)						
H-PILE	23-3	CAN.	12 × 74	15	MC, Clay	OED Delmag D-12	22.61	5.42	100						
	91-118-1	CONN	12 × 53	68	F,C,S	Hydraulic Junttan HHK 4a	34.72	1	56						
	37-6	CAN.	12 × 53	50	Sand	CED LB 640	51.63	2	160						
PIPE PILE	14-2	CAN.	CEP 12.75"	63	Silty Clay	OED Delmag D-12	22.61	6	54						
	22-3	CAN.	CEP 12.75"	92	Clayey Silt	OED Delmag D-12	22.61	5	50						
	22-5	CAN.	CEP 12.75"	83	Clayey Silt	OED Delmag D-12	22.61	7	50						
	25-1	CAN.	CEP 12.75"	31	Silty Clay	OED Delmag D-12	22.61	3	72						

Notes: Cases analyzed in this table are outside of the mean + 2 Std. deviations ranges, Mean + 2 Std. Deviation for **H-piles, Mod-Gates: 2.467, WSDOT: 2.444** Mean + 2 Std. Deviation for **Pipe-piles, Mod-Gates: 3.972, WSDOT: 3.418**

#### 4.2.2 Examination of the H Pile Cases

##### 4.2.2.1 Case Number 23-3, Site No. 23, Pile No. 3 (PDLT2000 No. MH 61)

- Location Hwy. 401 and Country Road 14 Iona Station (St. Thomas),
- Pile type HP 310 × 110 (metric), 12 × 74, the embedded length is 3.05(m), 10 ft, Total Length: 4.57(m), 15.00 ft
- The Soil around the shaft was Hard to Very Stiff - Silty clay, The Soil under the tip, was Hard - Silty Clay
- The hammer type used to drive the pile was a Diesel Delmag D-12 with a max. Rated energy 30510 J/ Blow, 22.61 k-ft/Blow
- Final Set: 64 Blows/0.3m, 5.42 Blows/in
- Based on the information provided, the driving logs and the load test results (applying Davisson's failure criterion), the static capacity was determined to be: 100 Kips

Modified Gates:

$$R_u = 1.75\sqrt{E_n} * \log(10 * N) - 100$$

$$\begin{aligned} R_u &= 1.75\sqrt{22.61 * 1000} * \log(10 * 5.42) - 100 \\ &= 356.28 \text{ kips} \end{aligned}$$

WSDOT:

$$R_u = 6.6 * F_{eff} * E * \ln(10N)$$

$$\begin{aligned} R_u &= 6.6 * 1.6 * WH * \ln(10 * 5.42) \\ &= 288.88 \text{ kips} \end{aligned}$$

##### 4.2.2.2 Case Number 37-6, Site No. 37, Pile No. 6 (PDLT2000 No. MH 38)

- Case under the pdlt2000 was registered as a 12 X 53 H pile
- Location Q.E.W. and Burlington Skyway, Hamilton
- Pile type HP 310 × 110 (metric), 12 × 74 (English Units), the embedded length is 14.48(m), 47 ft 6 in, Total Length 15.24(m), 50 ft
- The Soil around the shaft was Sand to Silty Sand Compacted to Very Dense, The Soil under the tip, was Silty Sand to Sandy Silt Compacted to Very Dense
- The hammer type used to drive the pile was a Diesel LB 640 with a max. Rated energy 54200 J/ Blow, 51.6 k-ft/Blow
- Final Set: 2 Blows/25mm, 2 Blows/in

- Based on the information provided, the driving logs and the load test results (applying Davisson's failure criterion), the static capacity was determined to be: 160 Kips

Modified Gates:

$$R_u = 1.75\sqrt{E_n} * \log(10 * N) - 100$$

$$R_u = 1.75\sqrt{51.6 * 1000} * \log(10 * 2) - 100$$

$$= 417.34 \text{ kips}$$

WSDOT:

$$R_u = 6.6 * F_{eff} * E * \ln(10N)$$

$$R_u = 6.6 * 1.6 * WH * \ln(10 * 2)$$

$$= 371.21 \text{ kips}$$

#### 4.2.2.3 Case Number 91-118-1 (PDLT2000 No. MH49)

- Location West Haven Connecticut
- Pile type HP 12 X 53, Total length 68 ft,
- The Soil around the shaft was F, C, S, The Soil around the tip, was not specified in the database
- The hammer type used to drive the pile was a Hydraulic hammer Junttan HHK 4a with a rated energy of 34.72 k-ft / Blow
- Final Set: 1 BPI
- The static pile capacity applying Davisson's failure criterion was 56 kips.
- Note: Allowing a net settlement of 0.25 inches and projecting the pile's rebound produces the exceedance of the criteria intercept @ 28-30 Tons. Top 30 ft of the pile was isolated by casing. 68 ft-30 ft = 38 ft of pile supports 28 tons, allowing 3 Tons for end bearing. Overall skin friction = 25 Tons/38 ft = 0.65 Tons/lft, Using S.F.=2 working skin friction = 0.33Tons/lft

Modified Gates:

$$R_u = 1.75\sqrt{E_n} * \log(10 * N) - 100$$

$$R_u = 1.75\sqrt{34.72 * 1000} * \log(10 * 1) - 100$$

$$= 226.08 \text{ kips}$$

WSDOT:

$$R_u = 6.6 * F_{eff} * E * \ln(10N)$$

$$\begin{aligned} R_u &= 6.6 * 1.8 * WH * \ln(10 * 1) \\ &= 287.80 \text{ kips} \end{aligned}$$

#### **4.2.3 Examination of the Pipe-Pile Cases**

##### **4.2.3.1 Case Number 14-2, Site No. 14, Pile No. 2 (PDLT2000 No. 64)**

- Location Q.E.W. and Niagara Street, St Catherine's
- Pile type Steel Tube 324 O.D. x 5.0 wall (metric), 12.75" x 0.20", the embedded length is 18.29(m), 60.ft total length 19.2(m), 63 ft.
- The Soil around the shaft was Silty Clay – Firm to Very Stiff, The Soil under the tip, Silty Clay - Stiff
- The hammer type used to drive the pile was a Diesel Delmag D-12 with a max. Rated energy 30506 J/ Blow, 22.61 k-ft/Blow
- Final Set: 6 Blows/25mm, 6 Blows/in
- Based on the information provided, the driving logs and the load test results (applying Davisson's failure criterion), the static pile capacity was determined to be: 54 kips

Modified Gates:

$$R_u = 1.75\sqrt{E_n} * \log(10 * N) - 100$$

$$\begin{aligned} R_u &= 1.75\sqrt{22.61 * 1000} * \log(10 * 6) - 100 \\ &= 367.90 \text{ kips} \end{aligned}$$

WSDOT:

$$R_u = 6.6 * F_{eff} * E * \ln(10N)$$

$$\begin{aligned} R_u &= 6.6 * 1.6 * WH * \ln(10 * 6) \\ &= 296.23 \text{ kips} \end{aligned}$$

#### 4.2.3.2 Case Number 22-3, Site No. 22, Pile No. 3 (PDLT2000 No. MP18)

- Location Hwy. 401 and Leslie Street, Toronto
- Pile type Steel Tube 324 O.D. x 5.0 wall (metric), 12.75" x 0.20", the embedded length is 15.30 (m), 50.200 ft, total length 28.04(m), 91.99 ft.
- The Soil around the shaft was Clayey Silt – Firm to Very Stiff, The Soil under the tip, Clayey Silt - Stiff
- The hammer type used to drive the pile was a Diesel Delmag D-12 with a max. Rated energy 30506 J/ Blow, 22.61 k-ft/Blow
- Final Set: 5 Blows/25mm, 5 Blows/in
- Based on the information provided, the driving logs and the load test results (applying Davisson's failure criterion), the static pile capacity was determined to be: 50 kips

Modified Gates:

$$R_u = 1.75\sqrt{E_n} * \log(10 * N) - 100$$

$$\begin{aligned} R_u &= 1.75\sqrt{22.61 * 1000} * \log(10 * 5) - 100 \\ &= 347.07 \text{ kips} \end{aligned}$$

WSDOT:

$$R_u = 6.6 * F_{eff} * E * \ln(10N)$$

$$\begin{aligned} R_u &= 6.6 * 1.6 * WH * \ln(10 * 5) \\ &= 283.04 \text{ kips} \end{aligned}$$

#### 4.2.3.3 Case Number 22-5, Site No. 22, Pile No. 5 (PDLT2000 No. MP23)

- Location Q.E.W. and Niagara Street, St Catherine's
- Pile type Steel Tube 324 O.D. x 5.0 wall (metric), 12.75" x 0.20", the embedded length is 15.28(m), 50.130 ft total length 25.30(m), 83 ft.
- The Soil around the shaft was Silty Clay – Firm to Very Stiff, The Soil under the tip, Silty Clay - Stiff
- The hammer type used to drive the pile was a Diesel Delmag D-12 with a max. Rated energy 30506 J/ Blow, 22.61 k-ft/Blow
- Final Set: 7 Blows/25mm, 7 Blows/in
- Based on the information provided, the driving logs and the load test results (applying Davisson's failure criterion), the static pile capacity was determined to be: 50 kips

Modified Gates:

$$R_u = 1.75\sqrt{E_n} * \log(10 * N) - 100$$

$$\begin{aligned} R_u &= 1.75\sqrt{22.61 * 1000} * \log(10 * 7) - 100 \\ &= 385.52 \text{ kips} \end{aligned}$$

WSDOT:

$$R_u = 6.6 * F_{eff} * E * \ln(10N)$$

$$\begin{aligned} R_u &= 6.6 * 1.6 * WH * \ln(10 * 7) \\ &= 307.39 \text{ kips} \end{aligned}$$

*4.2.3.4 Case Number 25-1, Site No. 25, Pile No. 1 (PDLT2000 No. MP22)*

- Location Hwy. 401 and Elgin Country Road 5, West Lorne
- Pile type Steel Tube 324 O.D. x 6.3 wall (metric), 12.75" x 0.25", the embedded length is 5.64(m), 18.50.ft total length 9.45(m), 31 ft.
- The Soil around the shaft was Silty Clay –Very Stiff to Stiff, The Soil under the tip, Silty Clay - Very Stiff
- The hammer type used to drive the pile was a Diesel Delmag D-12 with a max. Rated energy 30506 J/ Blow, 22.61 k-ft/Blow
- Final Set: 3 Blows/25mm, 3 Blows/in
- Based on the information provided, the driving logs and the load test results (applying Davisson's failure criterion), the static pile capacity was determined to be: 72.4 kips

Modified Gates:

$$R_u = 1.75\sqrt{E_n} * \log(10 * N) - 100$$

$$\begin{aligned} R_u &= 1.75\sqrt{22.61 * 1000} * \log(10 * 3) - 100 \\ &= 288.69 \text{ kips} \end{aligned}$$

WSDOT:

$$R_u = 6.6 * F_{eff} * E * \ln(10N)$$

$$\begin{aligned} R_u &= 6.6 * 1.6 * WH * \ln(10 * 3) \\ &= 246.08 \text{ kips} \end{aligned}$$

#### **4.2.4 MnDOT Research Panel Evaluation**

The research panel evaluated all cases reviewed in sections 4.2.2 and 4.2.3 and came to the conclusion that these cases of four pipe piles and three H piles are justified to be removed from the database as they were deemed irrelevant for MnDOT practices.

### **4.3 Re-Evaluation of Dynamic Equations Considering Outliers**

#### **4.3.1 Initial Analysis**

The Dynamic Equations were applied the same way as applied in the 2009 report, i.e. 75% energy for MnDOT, nominal energy for Modified Gates and the New MnDOT equations. Note; the  $W_r \cdot h$  was available for the CAPWAP databases but not for the static load test databases.

Tables 47 and 48 were developed by:

- a) Referring to the original analyses presented in Tables 5.2 (H piles) and 5.3 (Pipe piles) of Phase I (Paikowsky et al., 2009) report.
- b) Referring to the exclusion of the lowest outliers (unsafe cases where the prediction is greater than the measured capacity) reviewed by MnDOT and deemed irrelevant for MnDOT practice (four Pipe Pile outliers and three H Pile outliers outlined in section 4.2).
- c) Removing systematically cases of the highest outliers (safe cases where the prediction is lower than the measured capacity). Typically this procedure is completely acceptable for the range of beyond the mean and two standard deviations (five Pipe Pile cases and seven H pile cases).
- d) The analyses included, therefore, all previously analyzed equations for EOD cases and above (b) and (c) conditions using the same outliers for all cases.
- e) To easily follow the ramifications of the new analyses, examine the recommended resistance factor ( $\phi$ ) at the column before last along with its efficiency factor. The higher the efficiency factor, the more economical the method is as absolute  $\phi$  values are of limited significance. At the same time check the mean of the method as while one wants the method to be efficient, one expects the predicted values to be realistic (mean bias to be as close to 1.0 as possible), see highlighted cases in Tables 47 and 48.

From the dynamic measurements database provided by MnDOT and analyzed in Chapter 3, one can conclude that the ratio of measured energy ( $W_r \cdot h$ , where  $h$ =stroke observed in the field) to the nominal hammer energy for the  $n=126$  cases is mean = 0.763 and S.D. = 0.109. As such, the assumption made all along by MnDOT of observed energy being 75% of nominal energy (when stroke is not available) is correct. Additional six cases for the pipe piles are presented using the New MnDOT equations in which the nominal energy  $E_n$  was replaced by  $0.75E_n$ . These cases are also included in Table 48. Note, as the predicted capacity was artificially lowered (applying

0.75E<sub>n</sub> to an equation developed for E<sub>n</sub>) the equations will have to be adjusted (i.e. instead of using a coefficient of 30, a new coefficient of about 35, and instead of 35, a coefficient of about 40).

**Table 47. Dynamic equation predictions for H-Piles EOD condition only**

Equation	No. of Cases (n)	Mean Bias Measured/ Calculated (m <sub>λ</sub> )	Stand. Dev. (σ <sub>λ</sub> )	Coef. of Var. (COV <sub>λ</sub> )	Best Fit Line Equation (least square)	Coefficient of Determination (r <sup>2</sup> )	Resistance Factor φ β=2.33, p <sub>f</sub> =1%, Redundant			φ/λ Efficiency Factor (%)
							FOSM	MC <sup>3</sup>	Recom	
ENR	(a) 125	0.297	0.222	0.747	R <sub>u</sub> <sup>1</sup> =5.031* <sup>2</sup> R <sub>s</sub>	0.819	0.062	0.066	0.07	23.6
	(b) 122	0.301	0.224	0.742			0.064	0.067	0.07	23.3
	(c) 115	0.263	0.145	0.553			0.083	0.088	0.08	30.4
Gates	(a) 125	1.429	0.506	0.354	R <sub>u</sub> =0.626*R <sub>s</sub>	0.896	0.697	0.761	0.75	52.5
	(b) 122	1.451	0.491	0.338			0.732	0.805	0.75	51.7
	(c) 115	1.381	0.393	0.285			0.776	0.870	0.80	57.9
Modified Gates	(a) 125	0.813	0.323	0.397	R <sub>u</sub> =1.189*R <sub>s</sub>	0.893	0.361	0.393	0.40	49.2
	(b) 122	0.825	0.317	0.384			0.377	0.411	0.40	48.5
	(c) 115	0.770	0.225	0.293			0.426	0.475	0.45	58.4
WSDOT	(a) 125	0.874	0.329	0.377	R <sub>u</sub> =1.221*R <sub>s</sub>	0.900	0.406	0.443	0.45	51.5
	(b) 122	0.887	0.321	0.362			0.425	0.464	0.45	50.7
	(c) 115	0.850	0.281	0.331			0.435	0.480	0.45	52.9
MnDOT	(a) 125	0.984	0.650	0.660	R <sub>u</sub> =1.268*R <sub>s</sub>	0.833	0.247	0.260	0.25	25.4
	(b) 122	1.001	0.649	0.649			0.258	0.272	0.25	25.0
	(c) 115	0.886	0.410	0.463			0.342	0.368	0.35	39.5
New MnDOT (coef. 35) E=E <sub>n</sub>	(a) 125	1.016	0.360	0.354	R <sub>u</sub> =0.880*R <sub>s</sub>	0.896	0.495	0.542	0.55	54.1
	(b) 122	1.032	0.349	0.338			0.520	0.572	0.55	53.3
	(c) 115	0.982	0.280	0.285			0.552	0.619	0.60	61.1
New MnDOT (coef. 30) E=E <sub>n</sub>	(a) 125	1.186	0.420	0.354			0.578	0.632	0.60	50.6
	(b) 122	1.204	0.407	0.338			0.607	0.668	0.65	54.0
	(c) 115	1.146	0.326	0.285			0.644	0.722	0.70	61.1

Notes: 1. R<sub>u</sub> is the calculated capacity using each of the dynamic formulae.  
2. R<sub>s</sub> is the Static Capacity of the pile determined by Davisson's Failure Criterion.  
3. MC - Monte Carlo Simulation for 10,000 simulations  
(a) Original data presented in Phase I (Paikowsky et al., 2009) report, Table 5.2.  
(b) Low Outliers (removed 3 cases numbered: 23-3, 91-118-1, 37-6)  
(c) High Outliers (>2S.D.) (removed 7 cases numbered: 7-2, 100-60-1, CHB2, 91-118-2, FIA, 164-176-3, 103-38-1)



**Table 48. Dynamic equation predictions for Pipe Piles EOD condition only**

Equation	No. of Cases (n)	Mean Bias Measured/ Calculated ( $m_\lambda$ )	Stand. Dev. ( $\sigma_\lambda$ )	Coef. of Var. (COV $_\lambda$ )	Best Fit Line Equation (least square)	Coefficient of Determination ( $r^2$ )	Resistance Factor $\phi$ $\beta=2.33, p_f=1\%$ , Redundant			$\phi/\lambda$ Efficiency Factor (%)
							FOSM	MC <sup>3</sup>	Recom.	
ENR	(a) 99	0.331	0.348	1.052	$R_u=4.183*R_s^{-2}$	0.728	0.038	0.040	0.04	12.1
	(b) 95	0.342	0.351	1.026	$R_u=4.205*R_s$	0.733	0.042	0.043	0.04	11.7
	(c) 90	0.280	0.197	0.703			0.064	0.068	0.065	23.2
Gates	(a) 99	1.559	0.837	0.537	$R_u=0.573*R_s$	0.849	0.511	0.542	0.50	32.1
	(b) 95	1.613	0.812	0.503	$R_u=0.574*R_s$	0.861	0.570	0.610	0.60	37.2
	(c) 90	1.485	0.603	0.406			0.648	0.703	0.70	47.1
Modified Gates	(a) 99	0.878	0.549	0.626	$R_u=1.085*R_s$	0.839	0.238	0.251	0.25	28.5
	(b) 95	0.908	0.540	0.595	$R_u=1.088*R_s$	0.849	0.262	0.277	0.25	27.5
	(c) 90	0.815	0.351	0.431			0.337	0.363	0.35	42.9
WSDOT	(a) 99	0.816	0.493	0.604	$R_u=1.257*R_s$	0.862	0.231	0.244	0.25	30.6
	(b) 95	0.841	0.486	0.578	$R_u=1.258*R_s$	0.867	0.252	0.266	0.25	29.7
	(c) 90	0.782	0.414	0.530			0.260	0.276	0.25	32.0
MnDOT <sup>4</sup>	(a) 99 (96)	1.103 (0.961)	1.278 (0.738)	1.159 (0.767)	$R_u=1.142*R_s$	0.759	0.106 (0.193)	0.110 (0.204)	0.10 (0.20)	9.1 (20.8)
	(b) 95 (92)	1.141 (0.994)	1.291 (0.736)	1.132 (0.740)	$R_u=1.163*R_s$ ( $R_u=1.177*R_s$ )	0.756 (0.779)	0.115 (0.211)	0.119 (0.223)	0.20	18.7
	(c) 90 (89)	0.907 (0.913)	0.578 (0.578)	0.638 (0.633)			0.239 (0.243)	0.252 (0.257)	0.25	27.5
New MnDOT (coef. 35) $E=E_n$	(a) 99	1.109	0.595	0.537	$R_u=0.805*R_s$	0.849	0.364	0.385	0.35	31.6
	(b) 95	1.147	0.577	0.503	$R_u=0.807*R_s$	0.861	0.405	0.434	0.40	34.8
	(c) 90	1.056	0.429	0.406			0.461	0.500	0.50	47.3
New MnDOT (coef. 35) $E=0.75E_n$	(a) 99	1.280	0.688	0.537			0.420	0.445	0.40	31.3
	(b) 95	1.324	0.667	0.503			0.468	0.501	0.50	37.8
	(c) 90	1.219	0.495	0.406			0.532	0.577	0.55	45.1
New MnDOT (coef. 30) $E=E_n$	(a) 99	1.294	0.695	0.537			0.424	0.450	0.45	34.8
	(b) 95	1.338	0.673	0.503	$R_u=0.692*R_s$	0.861	0.473	0.506	0.50	37.4
	(c) 90	1.232	0.500	0.406			0.538	0.583	0.55	44.6
New MnDOT (coef. 30) $E=0.75E_n$	(a) 99	1.494	0.802	0.537			0.490	0.519	0.50	33.5
	(b) 95	1.545	0.778	0.503			0.546	0.584	0.55	35.6
	(c) 90	1.423	0.578	0.406			0.621	0.674	0.60	42.2

- Notes:
1.  $R_u$  is the calculated capacity using each of the dynamic formulae.
  2.  $R_s$  is the Static Capacity of the pile determined by Davisson's Failure Criterion.
  3. MC – Monte Carlo Simulation for 10,000 simulations.
  4. For the MnDOT equation results presented in parentheses, see section 5.6.3 of Aug 2009 report.
    - (a) Original data presented in Phase I (Paikowsky et al., 2009) report Table 5.3.
    - (b) Low Outliers (removed 4 cases numbered: 14-2, 22-3, 22-5, 25-1)
    - (c) High Outliers (>2S.D.) (removed 5 cases numbered: OD4T, OD4W, CH39, CH6-5B, CH95B)

Tables 49 and 50 summarize for each analyzed equation independently, the low and high end outliers relevant to each case for H and Pipe piles, respectively. In the case of the low range, the mean minus one standard deviation was taken as a general guideline, though due to the unsafe nature of these cases, each case history needs to be examined independently.

Table 51 provides the details of the additional lower end outliers identified in Table 50. These outliers were carefully examined as to their application to MnDOT practices. Due to the importance and difficulties encountered with the analyses of pipe piles, only lower end outliers of pipe piles are listed in Table 51. The following section provides details regarding the outlier case histories.

**Table 49. Summary of selective outlier references for H Piles**

Equation	Range of Outliers		Low Range Outliers	High Range Outliers	Comments
	Low (unsafe) cases Bias = $m_x - 1\sigma_x$	High (safe) cases Bias = $m_x + 2\sigma_x$			
Mod. Gates	0.490	1.459	GF412 $m_x=0.4281$ 1*-EOID $m_x=0.4325$		2 additional low outliers. All high outliers match criterion
WS DOT	0.545	1.532	SLFA-1 $m_x=0.3706$ ABUT1 $m_x=0.3872$ plus 12 more	63-136-2 $m_x=1.9303$ LTP-1 $m_x=1.8867$ LTP-2 $m_x=1.7221$ to be included Cases 91-118-2, 7-2, CHB2, and 164-176-3 to be excluded	14 additional low outlier cases. Three high outliers matched and three additional outlier cases to include
MnDOT	0.334	2.284	Cases 63-434-1 $m_x=0.2785$ , and ABUT1 $m_x=0.2895$ should be included Case 37-6 $m_x=0.3476$ should be excluded	Cases 69 $m_x=2.4673$ and FV10 $m_x=2.4069$ to be included. Case 164-176-3 $m_x=1.4285$ to be excluded	
New MnDOT coeff=35	0.656	1.736	Cases 25-9 28-2, 37-3, 39-2 GF412, GF413, 42-134-2, 63-138- 2, 1*-EOID to be included	Cases PX3 $m_x=1.9059$ 63-136-2 $m_x=1.7706$ and FMN2 $m_x=1.7653$ to be included Cases 100-60-1 $m_x=1.6310$ 7-2 $m_x=1.3800$ , and 103- 38-1 $m_x=1.5111$ to be excluded	9 additional low outliers to be included. 4 high outliers matched, and 3 additional high outliers to include
New MnDOT coeff=30	0.766	2.025	Cases 25-9 28-2, 37-3, 39-2 GF412, GF413, 42-134-2, 63-138- 2, 1*-EOID to be included	Cases PX3 $m_x=2.2235$ 63-136-2 $m_x=2.0657$ and FMN2 $m_x=2.0596$ to be included Cases 100-60-1 $m_x=1.9028$ 7-2 $m_x=1.6099$ , and 103- 38-1 $m_x=1.7630$ to be excluded	9 additional low outliers to be included. 4 high outliers matched, and 3 additional high outliers to include

**Table 50. Summary of selective outliers references for Pipe Piles**

Equation	Range of Outliers		Low Range Outliers	High Range Outliers	Comments
	Low (unsafe) cases	High (safe) cases			
	Bias = $m_x - 1\sigma_x$	Bias = $m_x + 2\sigma_x$			
Mod. Gates	0.329	1.976	Cases #25-6 $m_x=0.3265$ 2-5 $m_x=0.2852$ and 23-2 $m_x=0.2749$ to be included		Three additional low outliers
WS DOT	0.323	1.802		Cases BEL4-LTP4 $m_x=0.33559$ and DD29 $m_x=1.8117$ to be included. Cases OD4T $m_x=1.6136$ and OD4W $m_x=1.3769$ to be excluded from outliers.	All low outliers match criterion. From high outlier, 2 to be excluded and 2 others to be included
MnDOT	0	3.659	Cases 23-2 $m_x=0.2408$ and 2-5 $m_x=0.2604$ fall w/in range of other excluded cases	Case CH4 $m_x=3.8334$ to be included Cases OD4T $m_x=3.2473$ and OD4W $m_x=2.4829$ to be excluded	Due to high S.D., no low cases should be included other than when following same logic as for other equations
New MnDOT coeff=35	0.514	2.299	Cases 23-2, $m_x=0.3424$ 2-5 $m_x=0.3893$ 25-6 $m_x=0.3938$ 4-2 $m_x=0.4456$ 25-5 $m_x=0.4489$	Case SLT-B-1 $m_x=2.3019$	Five additional low outlier cases, and one additional high outlier case
New MnDOT coeff=30	0.599	2.684	Cases 23-2 $m_x=0.3995$ 2-5 $m_x=0.4542$ 25-6 $m_x=0.4595$ 4-2 $m_x=0.5199$ 25-5 $m_x=0.5237$		Five additional low outlier cases

**Table 51. Details of additional low end outliers encountered in the analyses of the Pipe Piles database**

No.	Pile Case No.	Refer. No.	Location	Pile Type	Total Length (ft)	Soil Type		Hammer Type	Rated Hammer Energy (kip-ft)	Hammer CED? OED?	Blow Count (BPI)	Davisson's Criterion (kips)	Mod. Gates Eq. (kips)	WS DOT Eq. (kips)	MnDOT Eq. (kips)	New MnDOT Eq. coeff=35 (kips)	New MnDOT Eq. coeff=30 (kips)
						Side	Tip										
MP8	2-5	45	Canada	CEP 12"	27	Sand	Gravelly sand	Delmag D-12	22.61	OED	60	180	631	463	691	462	396
MP15	4-2	45	Canada	CEP 12.75"	120	Silt	Clayey silt	Delmag D-12	22.61	OED	4.15	120	326	270	212	269	231
MP21	23-2	45	Canada	CEP 12.75"	15	Silty clay	Silty clay	Delmag D-12	22.61	OED	6.2	102	371	298	424	298	255
MP23	25-5	45	Canada	CEP 12.75"	75	Silty clay	Silty clay	Delmag D-12	22.61	OED	9	146	414	326	327	325	279
MP24	25-6	45	Canada	CEP 12.75"	36	Silty clay	Silty clay	Delmag D-12	22.61	OED	4	105	322	267	287	267	229

### **4.3.2 Evaluation of Outliers**

#### **4.3.2.1 General**

Five cases from the global database were considered for possible exclusion in the final formula analyses. These cases were listed in Table 51 and additional information relating to these five cases is provided below. Each case was discussed during a research panel meeting in some detail, after which time a decision was made as to include or exclude that case from future analyses.

#### **4.3.2.2 MP8 – Case 2-5**

A 12 inch shell pile driven open-ended, with a total length of 27ft but the pile was only embedded 19ft below grade. The wall thickness was 0.15 inches, which is very thin relative to MnDOT practice. The open-ended state was grounds for excluding this case from the closed-end pipe equation/database.

#### **4.3.2.3 MP15 – Case 4-2**

A 12.75 inch shell pile driven with a Delmag D-12 hammer (a small hammer for today's design in MnDOT practice.) The pile was driven to a depth (120ft) below the available borings, therefore, no information exists as to the soil profile at the pile toe. The pile was driven to 50bpf with relatively low loads. The hammer seemed undersized for the pile length and weight (the ram weight was approximately 2800 lbs, with a pile weight of about 4000 lbs).

#### **4.3.2.4 MP21 – Case 23-2**

A 12.75 inch shell pile driven 9.9ft below ground, which is a very short pile relative to MnDOT practice. In reviewing the boring logs for Borehole No. 7 (pg. 204 from the project information), cone penetration data went above 120kPa. One could wonder if the pile punched through a stiff layer. The soil had high silt content. This could lead to dilation of the soil, resulting in high resistance to driving but subsequent soil relaxation that led to reduced capacity at the time of load testing. The point/question of whether relaxation was common to MnDOT experience was discussed, with the consensus being that relaxation is not a common concern but that it could exist.

#### **4.3.2.5 MP23 and MP24**

These cases were both 12.75 inch pipe with 0.25 inch wall thicknesses, not unlike current MnDOT practice. The soils had high silt content near the plastic limit. No reason for exclusion was brought forward.

### 4.3.3 MnDOT Research Panel Evaluation

The panel evaluation of the cases presented in section 4.2.2 was:

1. MP8 – Case 2-5 – to exclude due to being an open-ended pipe pile.
2. MP15 – Case 4-2 – to exclude due to low field driving capacity relative to MnDOT practice.
3. MP21, MP23 and MP24 – to include after confirming that there were not conversion errors with respect to loading units.

## 4.4 Re-Evaluation of the New MnDOT Dynamic Equation for EOD and BOR Low and High Blow Count

### 4.4.1 Summary Tables

Summary Tables 52 to 59 present the performance of the new MnDOT equation presented in Phase I report) utilized with various coefficients (30, 35 and 40) and two variations of hammer energy;  $E = E_n$  and  $E = 0.75E_n$ . The statistical values in Tables 52 to 59 excluded all outliers described in sections 4.3.2 and 4.3.3, and in addition specific low and high removed outliers are detailed in the notes accompanied each table. The tables are categorized in the following way:

- Pipe Piles  
Table 52 EOD and Table 53 EOD with  $BC \leq 15BPI$  (capped resistance)  
Table 54 BOR and Table 55 BOR with  $BC \leq 15BPI$  (capped resistance)
- H Piles  
Table 56 EOD and Table 57 EOD with  $BC \leq 15BPI$  (capped resistance)  
Table 58 BOR and Table 59 BOR with  $BC \leq 15BPI$  (capped resistance)

### 4.4.2 Intermediate Conclusions

The results of the analyses presented in Tables 52 to 59 suggest that the use of the MnDOT equation developed in Phase I adjusted for the energy based on field observations (i.e.  $E = W_r \cdot h$  approximated as  $E = 0.75E_n$  when stroke measurements are not available) performed overall very well. The equation modification is in the form of:

$$R_u = R_n = 40\sqrt{W_r \cdot h} \log(10N) \quad (24)$$

**Table 52. Dynamic equation predictions for Pipe Piles EOD condition only**

Equation	No. of Cases (n)	Mean Bias Measured/ Calculated ( $m_\lambda$ )	Stand. Dev. ( $\sigma_\lambda$ )	Coef. of Var. ( $COV_\lambda$ )	Resistance Factor $\phi$ $\beta=2.33, p_f=1\%$ , Redundant			$\phi/\lambda$ Efficiency Factor (%)
					FOSM	MC <sup>3</sup>	Recom.	
New MnDOT (coef. 40) $E=E_n$	(a) 99	0.970	0.521	0.537	0.318	0.337		
	(b) 93	1.017	0.502	0.493	0.367	0.394		
	(c) 87	0.924	0.353	0.382	0.425	0.463		
New MnDOT (coef. 40) $E=0.75E_n$	(a) 99	1.120	0.602	0.537	0.367	0.389	<b>0.50</b>	
	(b) 93	1.175	0.579	0.493	0.424	0.455		
	(c) 87	1.067	0.407	0.382	0.490	0.534		
New MnDOT (coef. 35) $E=E_n$	(a) 99	1.109	0.595	0.537	0.364	0.385	0.35	31.6
	(b) 93	1.163	0.573	0.493	0.420	0.451		
	(c) 87	1.056	0.403	0.382	0.485	0.529		
New MnDOT (coef. 35) $E=0.75E_n$	(a) 99	1.280	0.688	0.537	0.420	0.445	0.40	31.3
	(b) 93	1.343	0.662	0.493	0.485	0.520		
	(c) 87	1.220	0.466	0.382	0.561	0.611		
New MnDOT (coef. 30) $E=E_n$	(a) 99	1.294	0.695	0.537	0.424	0.450	0.45	34.8
	(b) 93	1.356	0.669	0.493	0.490	0.525		
	(c) 87	1.232	0.471	0.382	0.566	0.617		
New MnDOT (coef. 30) $E=0.75E_n$	(a) 99	1.494	0.802	0.537	0.490	0.519	0.50	33.5
	(b) 93	1.566	0.772	0.493	0.565	0.607		
	(c) 87	1.423	0.543	0.382	0.654	0.712		

- Notes: 1.  $R_u$  is the calculated capacity using each of the dynamic formulae.  
2.  $R_s$  is the Static Capacity of the pile determined by Davisson's Failure Criterion.  
3. MC – Monte Carlo Simulation for 10,000 simulations.  
(a) Original data presented in Phase I (Paikowsky et al., 2009) report Table 5.3.  
(b) Low Outliers (removed 6 cases numbered: 14-2, 22-3, 22-5, 25-1, 2-5, and 4-2)  
(c) High Outliers ( $>2S.D.$ ) (removed 6 cases numbered: SLT-B-1, OD4T, OD4W, CH39, CH6-5B, CH95B)

**Table 53. Dynamic equation predictions for Pipe Piles EOD condition only blow count limited to max 15BPI (20 cases)**

Equation	No. of Cases (n)	Mean Bias Measured/ Calculated ( $m_\lambda$ )	Stand. Dev. ( $\sigma_\lambda$ )	Coef. of Var. ( $COV_\lambda$ )	Resistance Factor $\phi$ $\beta=2.33, p_f=1\%$ , Redundant			$\phi/\lambda$ Efficiency Factor (%)
					FOSM	MC <sup>3</sup>	Recom.	
New MnDOT (coef. 40) $E=E_n$	(a) 99	0.995	0.523	0.526	0.334	0.355		
	(b) 93	1.043	0.503	0.482	0.386	0.415		
	(c) 87	0.952	0.361	0.380	0.439	0.479		
New MnDOT (coef. 40) $E=0.75E_n$	(a) 99	1.149	0.604	0.526	0.386	0.410	<b>0.50</b>	
	(b) 93	1.205	0.581	0.482	0.446	0.479		
	(c) 87	1.099	0.417	0.380	0.507	0.553		
New MnDOT (coef. 35) $E=E_n$	(a) 99	1.138	0.598	0.526	0.382	0.406		
	(b) 93	1.192	0.575	0.482	0.441	0.474		
	(c) 87	1.087	0.413	0.380	0.502	0.547		
New MnDOT (coef. 35) $E=0.75E_n$	(a) 99	1.314	0.691	0.526	0.441	0.468		
	(b) 93	1.377	0.664	0.482	0.509	0.548		
	(c) 87	1.256	0.477	0.380	0.580	0.632		
New MnDOT (coef. 30) $E=E_n$	(a) 99	1.327	0.698	0.526	0.446	0.473		
	(b) 93	1.391	0.671	0.482	0.515	0.553		
	(c) 87	1.269	0.482	0.380	0.586	0.638		
New MnDOT (coef. 30) $E=0.75E_n$	(a) 99	1.533	0.806	0.526	0.515	0.547		
	(b) 93	1.606	0.775	0.482	0.594	0.639		
	(c) 87	1.465	0.556	0.380	0.676	0.737		

- Notes: 1.  $R_u$  is the calculated capacity using each of the dynamic formulae.  
2.  $R_s$  is the Static Capacity of the pile determined by Davisson's Failure Criterion.  
3. MC – Monte Carlo Simulation for 10,000 simulations.  
(a) Original data presented in Phase I (Paikowsky et al., 2009) report Table 5.3, cases with BC > 15BPI were assumed BC = 15BPI.  
(b) Low Outliers (removed 6 cases numbered: 14-2, 22-3, 22-5, 25-1, 2-5, and 4-2)  
(c) High Outliers (>2S.D.) (removed 6 cases numbered: BEL4-LTP4, OD4T, OD4W, CH39, CH6-5B, CH95B)



**Table 54. Dynamic equation predictions for Pipe Piles BOR condition only**

Equation	No. of Cases (n)	Mean Bias Measured/ Calculated ( $m_\lambda$ )	Stand. Dev. ( $\sigma_\lambda$ )	Coef. of Var. ( $COV_\lambda$ )	Resistance Factor $\phi$ $\beta=2.33, p_c=1\%$ , Redundant			$\phi/\lambda$ Efficiency Factor (%)
					FOSM	MC <sup>3</sup>	Recom.	
New MnDOT (coef. 40) E=E <sub>n</sub>	(a) 58	0.859	0.271	0.316	0.453	0.503		
	(b) 49	0.923	0.244	0.265	0.539	0.611		
	(c) 46	0.886	0.200	0.255	0.528	0.601		
New MnDOT (coef. 40) E=0.75E <sub>n</sub>	(a) 58	0.991	0.313	0.316	0.523	0.580	<b>0.60</b> potentially 0.70	
	(b) 49	1.066	0.282	0.265	0.623	0.706		
	(c) 46	1.023	0.230	0.255	0.609	0.694		
New MnDOT (coef. 35) E=E <sub>n</sub>	(a) 58	0.981	0.310	0.316	0.518	0.575		
	(b) 49	1.055	0.279	0.265	0.617	0.698		
	(c) 46	1.012	0.228	0.255	0.603	0.686		
New MnDOT (coef. 35) E=0.75E <sub>n</sub>	(a) 58	1.133	0.358	0.316	0.598	0.664		
	(b) 49	1.218	0.322	0.265	0.712	0.806		
	(c) 46	1.169	0.263	0.255	0.696	0.793		
New MnDOT (coef. 30) E=E <sub>n</sub>	(a) 58	1.145	0.362	0.316	0.604	0.671		
	(b) 49	1.231	0.326	0.265	0.719	0.815		
	(c) 46	1.181	0.266	0.255	0.704	0.801		
New MnDOT (coef. 30) E=0.75E <sub>n</sub>	(a) 58	1.322	0.417	0.316	0.698	0.774		
	(b) 49	1.421	0.376	0.265	0.830	0.941		
	(c) 46	1.364	0.307	0.255	0.813	0.925		

- Notes:
1.  $R_u$  is the calculated capacity using each of the dynamic formulae.
  2.  $R_s$  is the Static Capacity of the pile determined by Davisson's Failure Criterion.
  3. MC – Monte Carlo Simulation for 10,000 simulations.
  4. Low outliers arbitrarily removed to examine influence – need to be checked case by case.
    - (a) All BOR data
    - (b) Low Outliers ( $\leq 1S.D.$ ) removed (9 cases numbered FN4, FM12, TR131, EF167, CA3/8, ND50, LTP1-Restrike, B2, and CA24)
    - (c) High Outliers ( $>2S.D.$ ) removed (3 cases numbered DD23, FIB, and OD4W)

**Table 55. Dynamic equation predictions for Pipe Piles BOR condition only blow count limited to max 15 BPI (17 cases)**

Equation	No. of Cases (n)	Mean Bias Measured/ Calculated ( $m_\lambda$ )	Stand. Dev. ( $\sigma_\lambda$ )	Coef. of Var. ( $COV_\lambda$ )	Resistance Factor $\phi$ $\beta=2.33, p_f=1\%$ , Redundant			$\phi/\lambda$ Efficiency Factor (%)
					FOSM	MC <sup>3</sup>	Recom.	
New MnDOT (coef. 40) $E=E_n$	(a) 58	0.901	0.285	0.316	0.476	0.528		
	(b) 49	0.969	0.255	0.263	0.569	0.645		
	(c) 47	0.943	0.225	0.239	0.579	0.662		
New MnDOT (coef. 40) $E=0.75E_n$	(a) 58	1.040	0.329	0.316	0.549	0.609	<b>0.60</b> potentially 0.75	
	(b) 49	1.119	0.295	0.263	0.657	0.745		
	(c) 47	1.089	0.260	0.239	0.669	0.764		
New MnDOT (coef. 35) $E=E_n$	(a) 58	1.029	0.326	0.316	0.543	0.603		
	(b) 49	1.108	0.292	0.263	0.650	0.738		
	(c) 47	1.078	0.257	0.239	0.662	0.756		
New MnDOT (coef. 35) $E=0.75E_n$	(a) 58	1.189	0.376	0.316	0.628	0.696		
	(b) 49	1.279	0.337	0.263	0.750	0.851		
	(c) 47	1.244	0.297	0.239	0.764	0.873		
New MnDOT (coef. 30) $E=E_n$	(a) 58	1.201	0.380	0.316	0.634	0.704		
	(b) 49	1.292	0.340	0.263	0.758	0.860		
	(c) 47	1.257	0.300	0.239	0.772	0.882		
New MnDOT (coef. 30) $E=0.75E_n$	(a) 58	1.387	0.439	0.316	0.732	0.812		
	(b) 49	1.492	0.393	0.263	0.875	0.993		
	(c) 47	1.452	0.347	0.239	0.892	1.019		

- Notes:
1.  $R_u$  is the calculated capacity using each of the dynamic formulae.
  2.  $R_s$  is the Static Capacity of the pile determined by Davisson's Failure Criterion.
  3. MC – Monte Carlo Simulation for 10,000 simulations.
  4. Low outliers arbitrarily removed to examine influence – need to be checked case by case.
    - (a) All BOR data, cases with BC > 15BPI were assumed BC = 15BPI
    - (b) Low Outliers ( $\leq 1S.D.$ ) removed (9 cases numbered FN4, FM12, TR131, EF167, CA3/8, ND50, LTP1-Restrike, B2 and CA24)
    - (c) High Outliers ( $>2S.D.$ ) removed (2 cases numbered FIB and 120-Restrike)

**Table 56. Dynamic equation predictions for H-Piles EOD condition only**

Equation	No. of Cases (n)	Mean Bias Measured/ Calculated ( $m_\lambda$ )	Stand. Dev. ( $\sigma_\lambda$ )	Coef. of Var. ( $COV_\lambda$ )	Resistance Factor $\phi$ $\beta=2.33, p_r=1\%$ , Redundant			$\phi/\lambda$ Efficiency Factor (%)
					FOSM	MC <sup>3</sup>	Recom	
New MnDOT (coef. 40) E=E <sub>n</sub>	(a) 125	0.889	0.315	0.354	0.434	0.474		
	(b) 118	0.916	0.302	0.330	0.470	0.518		
	(c) 111	0.864	0.222	0.257	0.513	0.583		
New MnDOT (coef. 40) E=0.75E <sub>n</sub>	(a) 125	1.027	0.364	0.354	0.501	0.548	<b>0.60</b>	58.4
	(b) 118	1.058	0.349	0.330	0.543	0.599		56.7
	(c) 111	0.998	0.256	0.257	0.592	0.674		60.1
New MnDOT (coef. 35) E=E <sub>n</sub>	(a) 125	1.016	0.360	0.354	0.495	0.542	0.55	54.1
	(b) 118	1.047	0.346	0.330	0.537	0.592		
	(c) 111	0.988	0.254	0.257	0.586	0.667		
New MnDOT (coef. 35) E=0.75E <sub>n</sub>	(a) 125	1.174	0.416	0.354	0.573	0.626	0.60	51.1
	(b) 118	1.209	0.399	0.330	0.620	0.684		
	(c) 111	1.141	0.293	0.257	0.677	0.770		
New MnDOT (coef. 30) E=E <sub>n</sub>	(a) 125	1.186	0.420	0.354	0.578	0.632	0.60	50.6
	(b) 118	1.221	0.403	0.330	0.626	0.691		
	(c) 111	1.153	0.296	0.257	0.684	0.779		
New MnDOT (coef. 30) E=0.75E <sub>n</sub>	(a) 125	1.369	0.485	0.354	0.668	0.730	0.70	51.1
	(b) 118	1.410	0.466	0.330	0.723	0.798		
	(c) 111	1.331	0.342	0.257	0.790	0.899		

- Notes:
1.  $R_u$  is the calculated capacity using each of the dynamic formulae.
  2.  $R_s$  is the Static Capacity of the pile determined by Davisson's Failure Criterion.
  3. MC - Monte Carlo Simulation for 10,000 simulations
- (a) Original data presented in Phase I (Paikowsky et al., 2009) report, Table 5.2.  
(b) Low Outliers (removed 7 cases numbered: 23-3, 25-9, 28-2, 37-3, 37-6, 39-2, 91-118-1)  
(c) High Outliers (>2S.D.) (removed 7 cases numbered; 63-136-2, CHB2, 91-118-2, FMN2, FIA, 164-176-3, PX3)

**Table 57. Dynamic equation predictions for H-Piles EOD condition only blow count limited to max 15 BPI (50 cases)**

Equation	No. of Cases (n)	Mean Bias Measured/ Calculated ( $m_\lambda$ )	Stand. Dev. ( $\sigma_\lambda$ )	Coef. of Var. ( $COV_\lambda$ )	Resistance Factor $\phi$ $\beta=2.33, p_f=1\%$ , Redundant			$\phi/\lambda$ Efficiency Factor (%)
					FOSM	MC <sup>3</sup>	Recom	
New MnDOT (coef. 40) $E=E_n$	(a) 125	0.931	0.313	0.336	0.471	0.519		
	(b) 118	0.960	0.296	0.309	0.514	0.572		
	(c) 113	0.921	0.232	0.252	0.552	0.629		
New MnDOT (coef. 40) $E=0.75E_n$	(a) 125	1.075	0.361	0.336	0.544	0.599		
	(b) 118	1.108	0.342	0.309	0.593	0.660		
	(c) 113	1.063	0.267	0.252	0.637	0.726		
New MnDOT (coef. 35) $E=E_n$	(a) 125	1.064	0.358	0.336	0.539	0.593		
	(b) 118	1.097	0.339	0.309	0.587	0.654		
	(c) 113	1.052	0.265	0.252	0.630	0.718		
New MnDOT (coef. 35) $E=0.75E_n$	(a) 125	1.228	0.413	0.336	0.622	0.684		
	(b) 118	1.267	0.391	0.309	0.678	0.755		
	(c) 113	1.215	0.306	0.252	0.728	0.829		
New MnDOT (coef. 30) $E=E_n$	(a) 125	1.241	0.417	0.336	0.628	0.692		
	(b) 118	1.280	0.395	0.309	0.685	0.763		
	(c) 113	1.228	0.309	0.252	0.736	0.838		
New MnDOT (coef. 30) $E=0.75E_n$	(a) 125	1.433	0.482	0.336	0.726	0.799		
	(b) 118	1.478	0.456	0.309	0.791	0.881		
	(c) 113	1.418	0.357	0.252	0.850	0.968		

- Notes:
1.  $R_u$  is the calculated capacity using each of the dynamic formulae.
  2.  $R_s$  is the Static Capacity of the pile determined by Davisson's Failure Criterion.
  3. MC - Monte Carlo Simulation for 10,000 simulations
- (a) Original data presented in Phase I (Paikowsky et al., 2009) report, Table 5.2, cases with BC > 15BPI were assumed BC = 15BPI.
- (b) Low Outliers (removed 7 cases numbered: 23-3, 25-9, 28-2, 37-3, 37-6, 39-2, 91-118-1)
- (c) High Outliers (>2S.D.) (removed 5 cases numbered: CHB2, 91-118-2, FIA, 164-176-3, PX3)

**Table 58. Dynamic equation predictions for H-Piles BOR condition only**

Equation	No. of Cases (n)	Mean Bias Measured/ Calculated ( $m_\lambda$ )	Stand. Dev. ( $\sigma_\lambda$ )	Coef. of Var. ( $COV_\lambda$ )	Resistance Factor $\phi$ $\beta=2.33, p_f=1\%$ , Redundant			$\phi/\lambda$ Efficiency Factor (%)
					FOSM	MC <sup>3</sup>	Recom	
New MnDOT (coef. 40) $E=E_n$	(a) 34	0.817	0.499	0.611	0.228	0.241		
	(b) 30	0.890	0.486	0.546	0.286	0.303		
	(c) 28	0.781	0.262	0.335	0.396	0.436		
New MnDOT (coef. 40) $E=0.75E_n$	(a) 34	0.944	0.576	0.611	0.264	0.278		
	(b) 30	1.028	0.562	0.546	0.331	0.350		
	(c) 28	0.902	0.302	0.335	0.458	0.504		
New MnDOT (coef. 35) $E=E_n$	(a) 34	0.934	0.541	0.611	0.261	0.275		
	(b) 30	1.017	0.556	0.546	0.327	0.346		
	(c) 28	0.893	0.299	0.335	0.453	0.499		
New MnDOT (coef. 35) $E=0.75E_n$	(a) 34	1.078	0.659	0.611	0.301	0.318		
	(b) 30	1.175	0.642	0.546	0.378	0.400		
	(c) 28	1.031	0.345	0.335	0.523	0.576		
New MnDOT (coef. 30) $E=E_n$	(a) 34	1.090	0.666	0.611	0.304	0.321		
	(b) 30	1.187	0.648	0.546	0.382	0.404		
	(c) 28	1.042	0.349	0.335	0.529	0.582		
New MnDOT (coef. 30) $E=0.75E_n$	(a) 34	1.258	0.769	0.611	0.351	0.371		
	(b) 30	1.370	0.749	0.546	0.441	0.466		
	(c) 28	1.203	0.403	0.335	0.611	0.672		

- Notes:
1.  $R_u$  is the calculated capacity using each of the dynamic formulae.
  2.  $R_s$  is the Static Capacity of the pile determined by Davisson's Failure Criterion.
  3. MC - Monte Carlo Simulation for 10,000 simulations
  4. Low outliers arbitrarily removed to examine influence – need to be checked case by case.
    - (a) All BOR data
    - (b) Low Outliers ( $\leq 1S.D.$ ) removed (4 cases numbered 63S, 35-1, TRBH, and DW2)
    - (c) High Outliers ( $>2S.D.$ ) removed (2 cases numbered FIA, and PX3)

**Table 59. Dynamic equation predictions for H-Piles BOR condition only blow count limited to max 15 BPI (16 cases)**

Equation	No. of Cases (n)	Mean Bias Measured/ Calculated ( $m_\lambda$ )	Stand. Dev. ( $\sigma_\lambda$ )	Coef. of Var. ( $COV_\lambda$ )	Resistance Factor $\phi$ $\beta=2.33, p_t=1\%$ , Redundant			$\phi/\lambda$ Efficiency Factor (%)
					FOSM	MC <sup>3</sup>	Recom	
New MnDOT (coef. 40) $E=E_n$	(a) 34	0.982	0.472	0.481	0.364	0.391		
	(b) 32	1.014	0.469	0.463	0.391	0.421		
	(c) 29	0.881	0.212	0.241	0.539	0.615		
New MnDOT (coef. 40) $E=0.75E_n$	(a) 34	1.134	0.545	0.481	0.420	0.452		
	(b) 32	1.171	0.541	0.463	0.451	0.487		
	(c) 29	1.018	0.245	0.241	0.623	0.711		
New MnDOT (coef. 35) $E=E_n$	(a) 34	1.123	0.540	0.481	0.416	0.448		
	(b) 32	1.159	0.536	0.463	0.447	0.482		
	(c) 29	1.007	0.243	0.241	0.616	0.703		
New MnDOT (coef. 35) $E=0.75E_n$	(a) 34	1.296	0.623	0.481	0.480	0.517		
	(b) 32	1.338	0.619	0.463	0.516	0.556		
	(c) 29	1.163	0.280	0.241	0.711	0.812		
New MnDOT (coef. 30) $E=E_n$	(a) 34	1.310	0.630	0.481	0.486	0.522		
	(b) 32	1.352	0.625	0.463	0.521	0.562		
	(c) 29	1.175	0.283	0.241	0.719	0.821		
New MnDOT (coef. 30) $E=0.75E_n$	(a) 34	1.512	0.727	0.481	0.560	0.603		
	(b) 32	1.561	0.722	0.463	0.602	0.649		
	(c) 29	1.357	0.327	0.241	0.830	0.948		

- Notes:
1.  $R_u$  is the calculated capacity using each of the dynamic formulae.
  2.  $R_s$  is the Static Capacity of the pile determined by Davisson's Failure Criterion.
  3. MC - Monte Carlo Simulation for 10,000 simulations
  4. Low outliers arbitrarily removed to examine influence – need to be checked case by case.
    - (a) All BOR data, cases with BC > 15BPI were assumed BC = 15BPI
    - (b) Low Outliers ( $\leq 1S.D.$ ) removed (2 cases numbered FN1 and 63S)
    - (c) High Outliers ( $>2S.D.$ ) removed (3 cases numbered FIA, PX3 and PX2)

This equation was designated as MnDOT Pile Formula 2012 or abbreviated as MPF12. The statistical results of equation (24) were highlighted in Tables 52 to 59 and suggest the following:

1. For all pipe pile cases (EOD and BOR with and without limiting blow count) the bias of the equation varied between 0.991 to 1.205.
2. With removal of high and low outliers, the equation when applied for all pipe pile cases resulted with a bias varying between 1.023 to 1.099 with a Coefficient of Variation (COV) between 0.239 to 0.382.
3. For all H pile cases (EOD and BOR with and without limiting blow count) the bias of the equation varied between 0.902 to 1.171.
4. With removal of high and low outliers, the equation when applied for all H pile cases resulted with a bias varying between 0.902 to 1.063 with a COV between 0.241 and 0.335.

Based on the above, the following sections concentrate on the performance of the equation in the format presented in equation (24).

## **4.5 Evaluation of MPF12 and Resistance Factors Development**

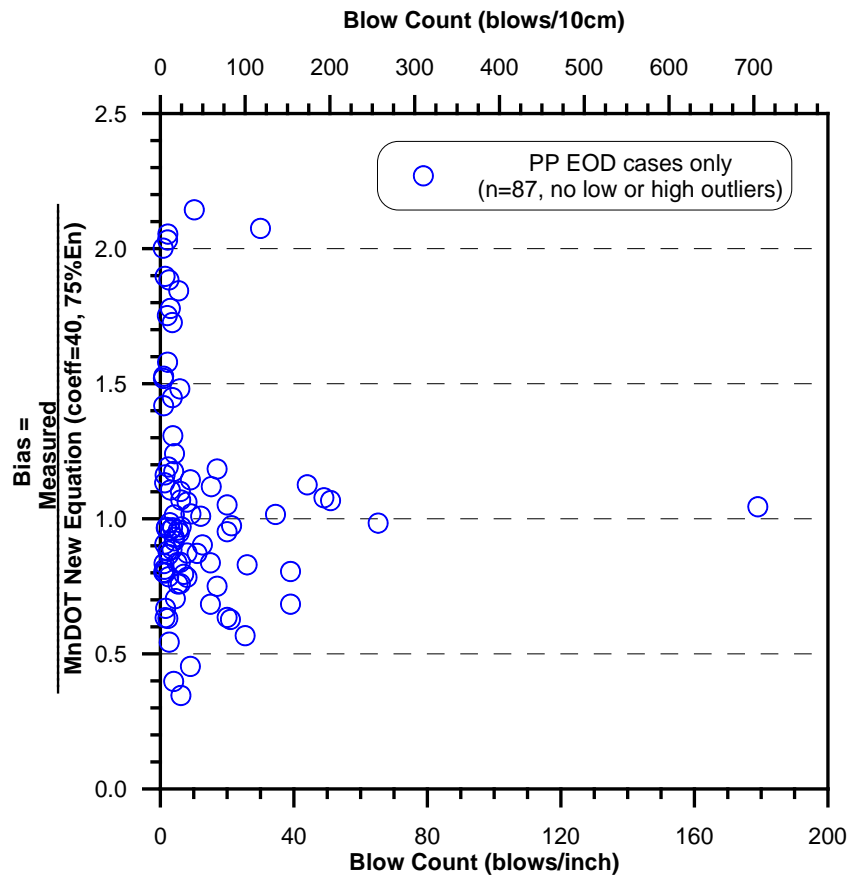
### **4.5.1 Graphical Presentation**

The performance of the MPF12, equation (24), is examined in Figures 86 to 94 in the form of the actual bias of the data (static measured capacity over dynamic equation prediction) vs. driving resistance (blow count) for the following groups:

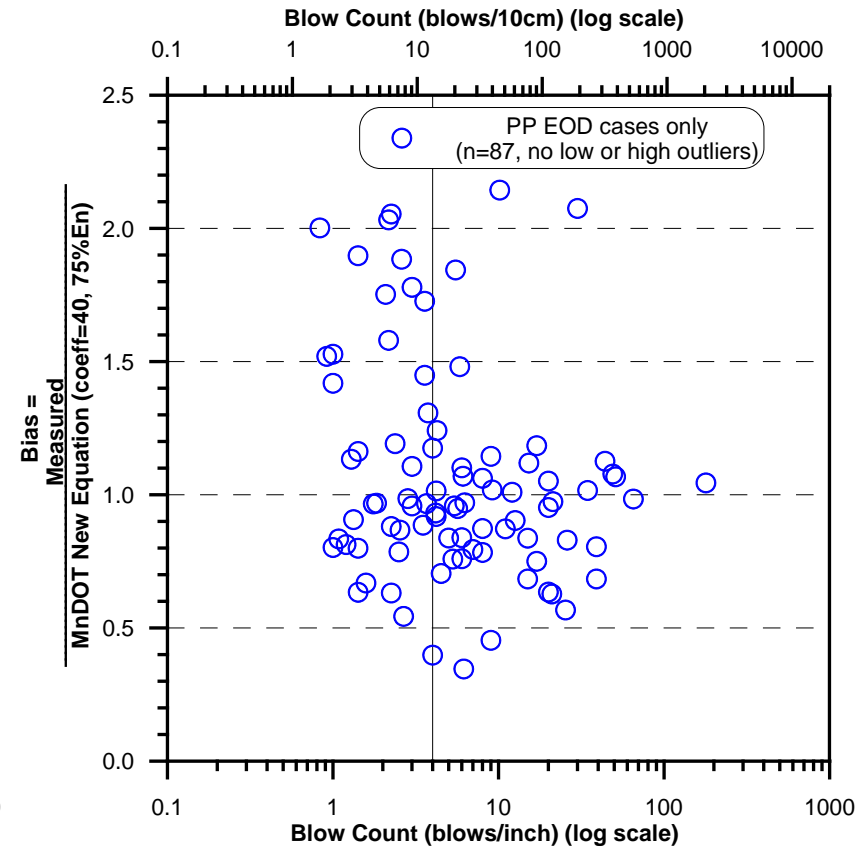
- a. Pipe Pile EOD (Figures 86 and 87)
- b. Pipe Piles BOR (Figures 88 and 89)
- c. H Piles EOD (Figures 90 and 91)
- d. H Piles BOR (Figures 92 and 93)
- e. H Piles EOD and BOR grouping the zones of driving resistance (Figure 94)

Each of the sets was presented in four ways:

- a. Bias vs. linear Blow Count
- b. Bias vs. log scale Blow Count
- c. Bias vs. linear Blow Count for the range of 0 to 16 BPI
- d. Mean and Standard Deviation of the Bias for 2BPI zones, e.g. 0-2, 2-4, etc.



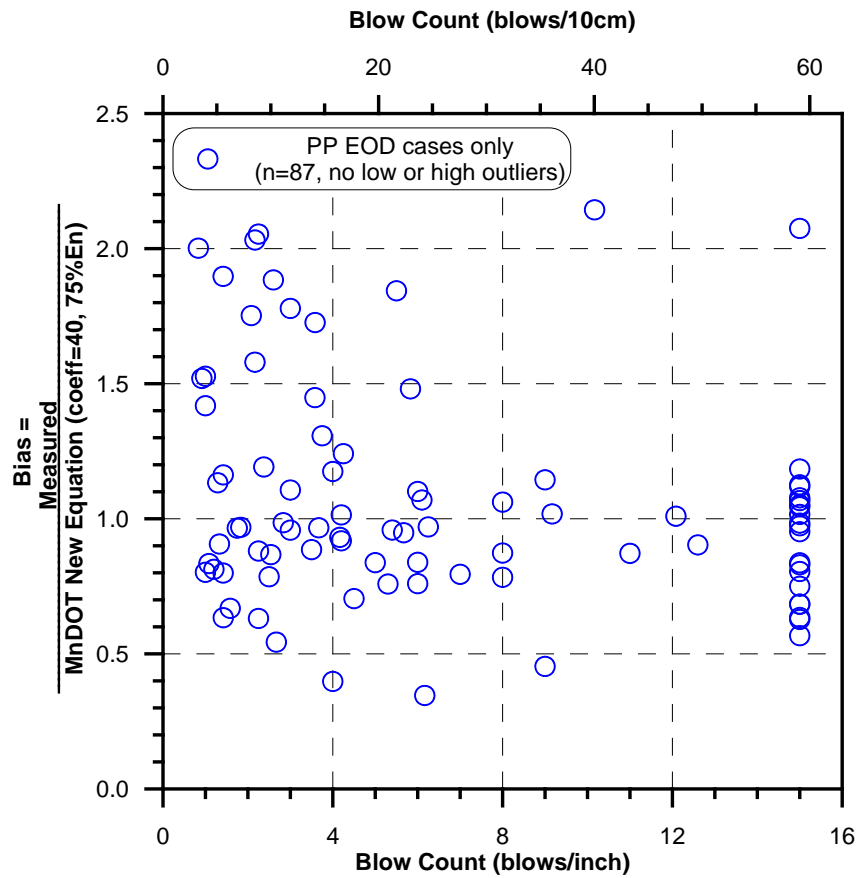
(a)



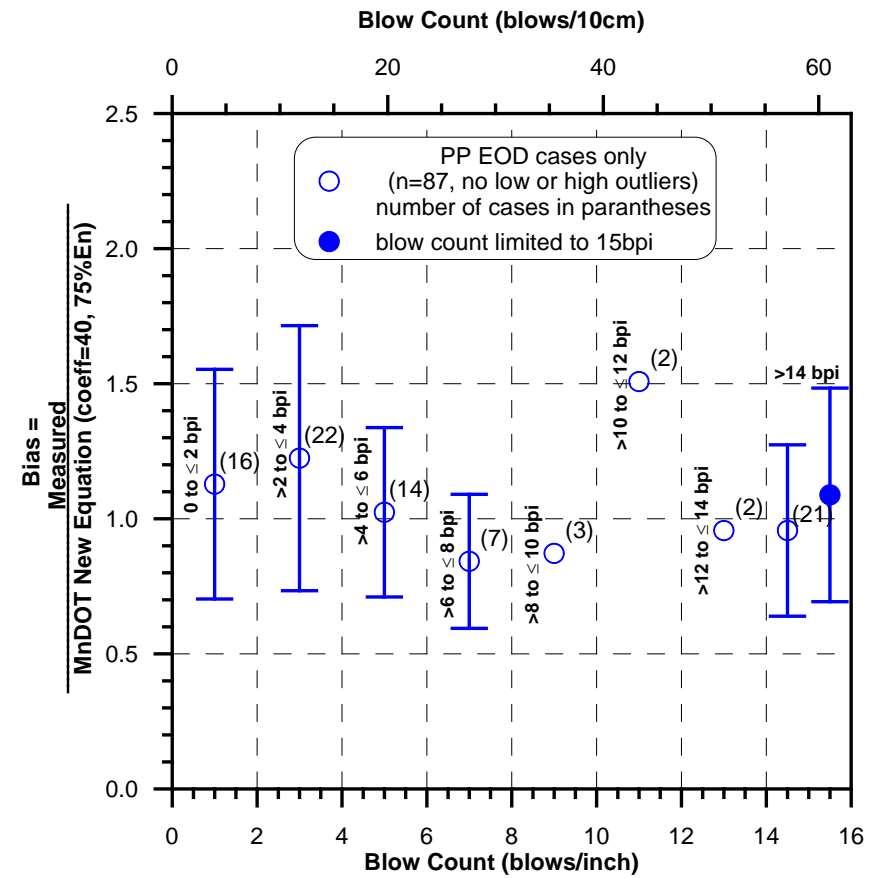
(b)

**Figure 86. Bias vs. blow count for Pipe Pile EOD cases only (low and high outliers removed) for the New MnDOT Equation (coefficient 40, 75% energy); (a) linear scale, and (b) log scale**



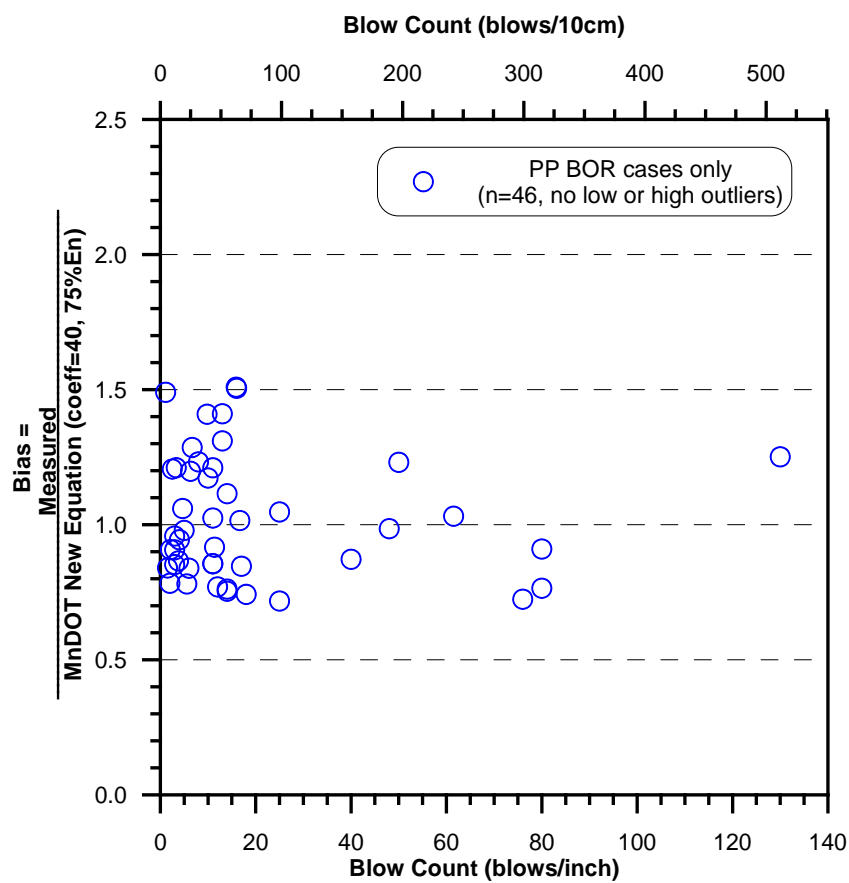


(a)

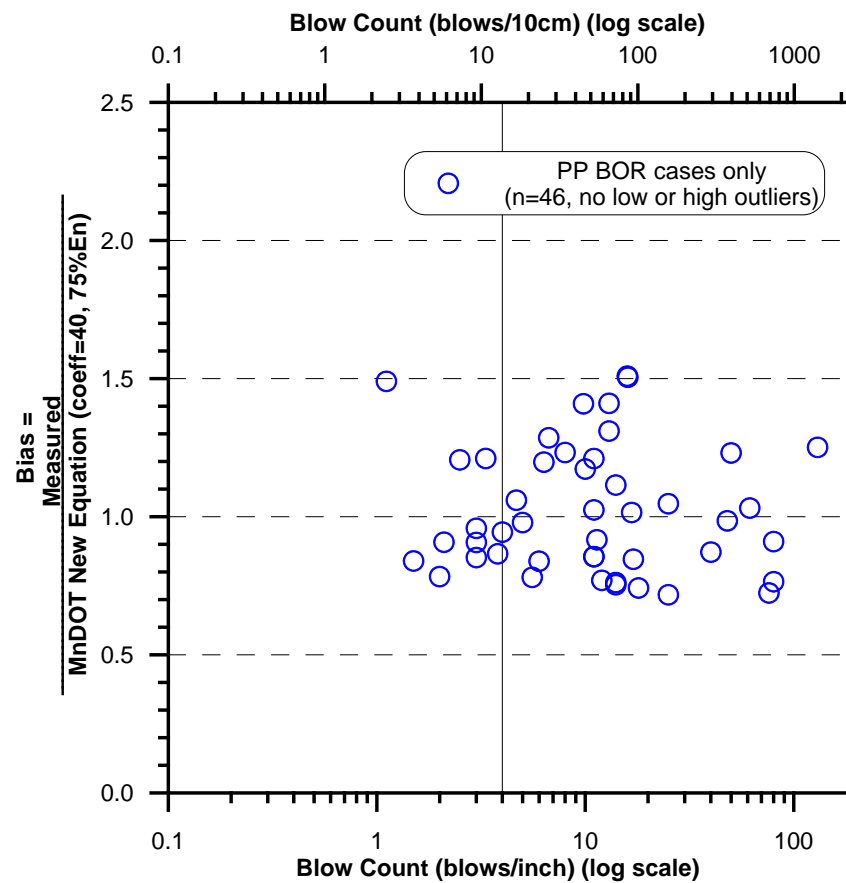


(b)

**Figure 87. Bias vs. blow count for Pipe Pile EOD cases only (low and high outliers removed) for the New MnDOT Equation (coefficient 40, 75% energy) where the blow count is limited to 15bpi maximum; (a) linear scale, and (b) average and standard deviation per 2bpi segments**

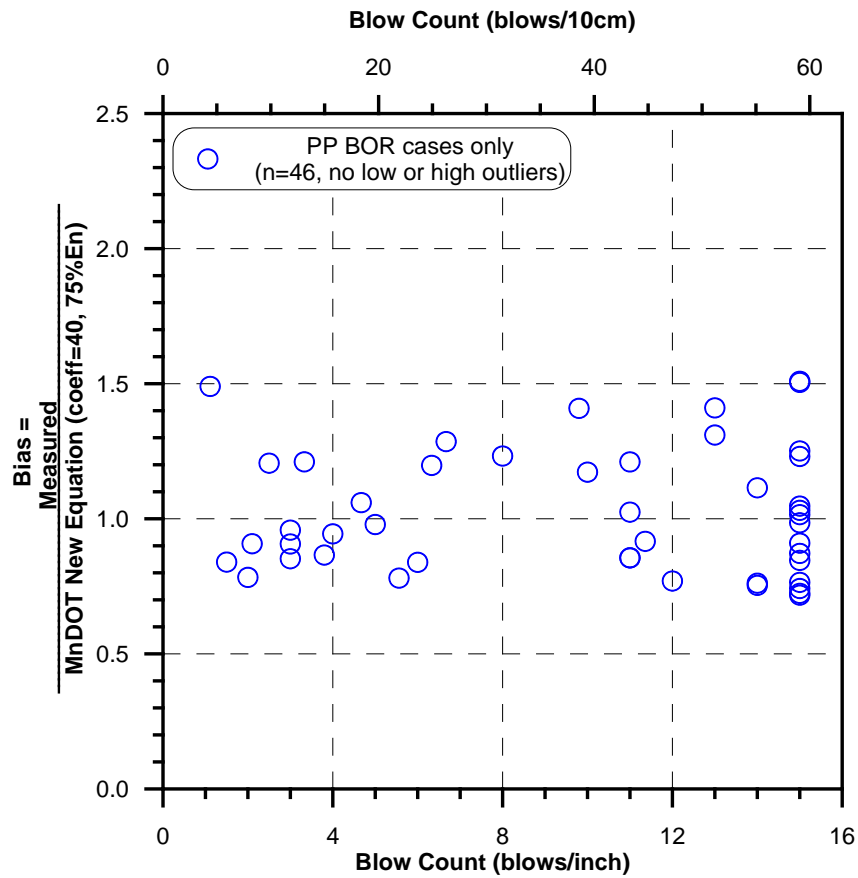


(a)

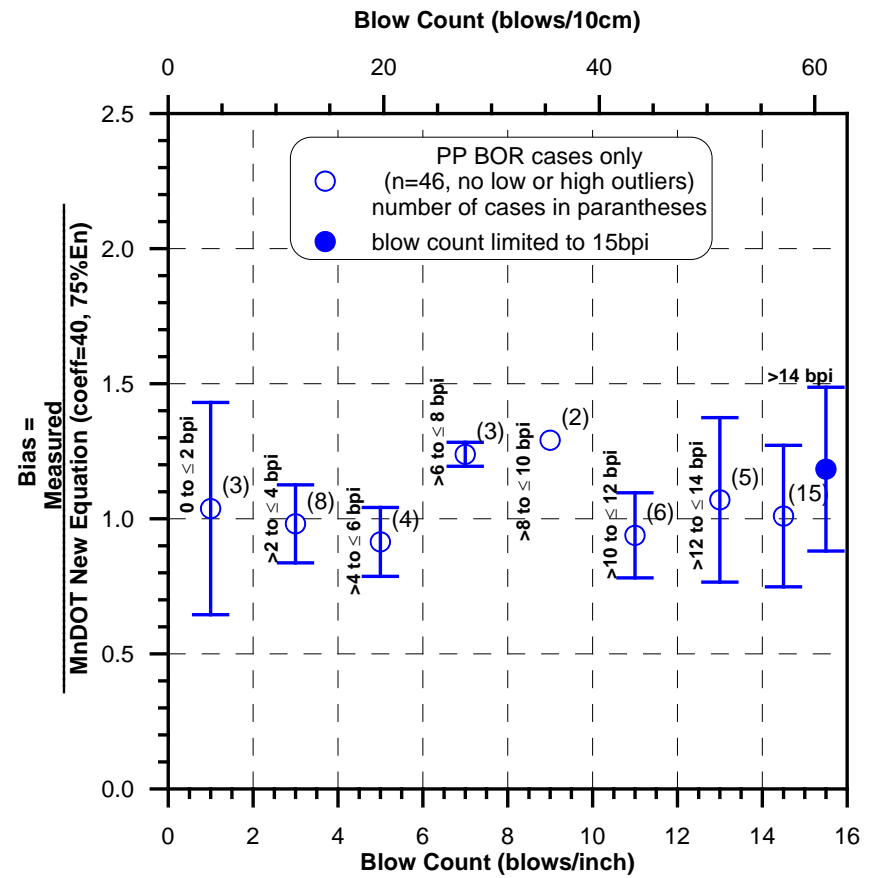


(b)

**Figure 88. Bias vs. blow count for Pipe Pile BOR cases only (low and high outliers removed) for the New MnDOT Equation (coefficient 40, 75% energy); (a) linear scale, and (b) log scale**

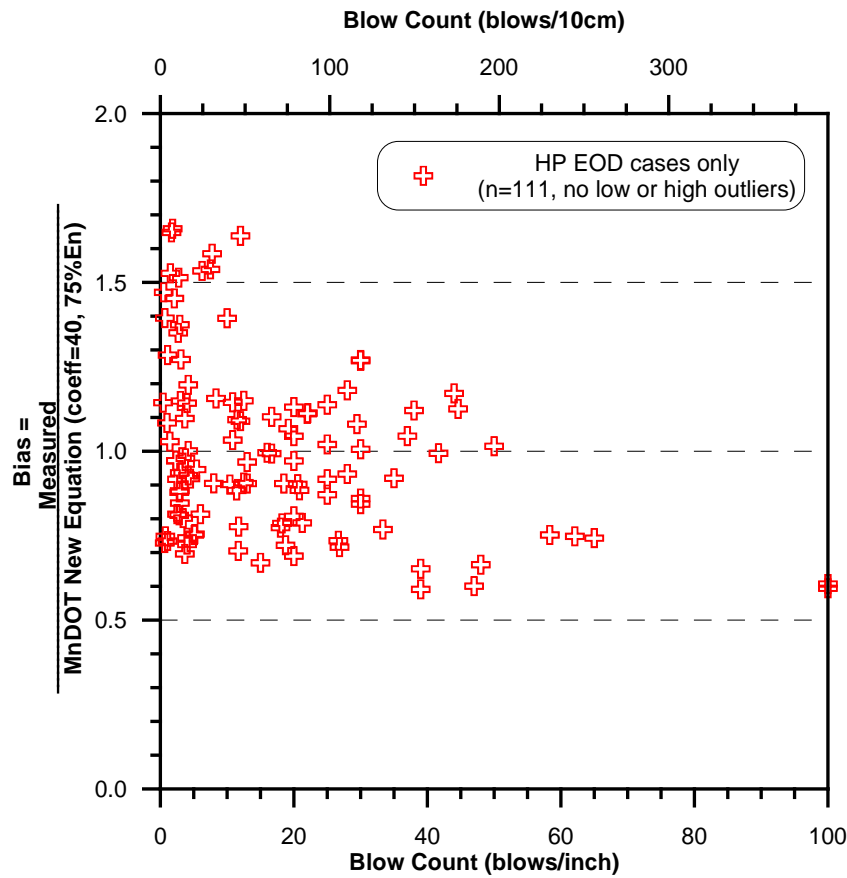


(a)

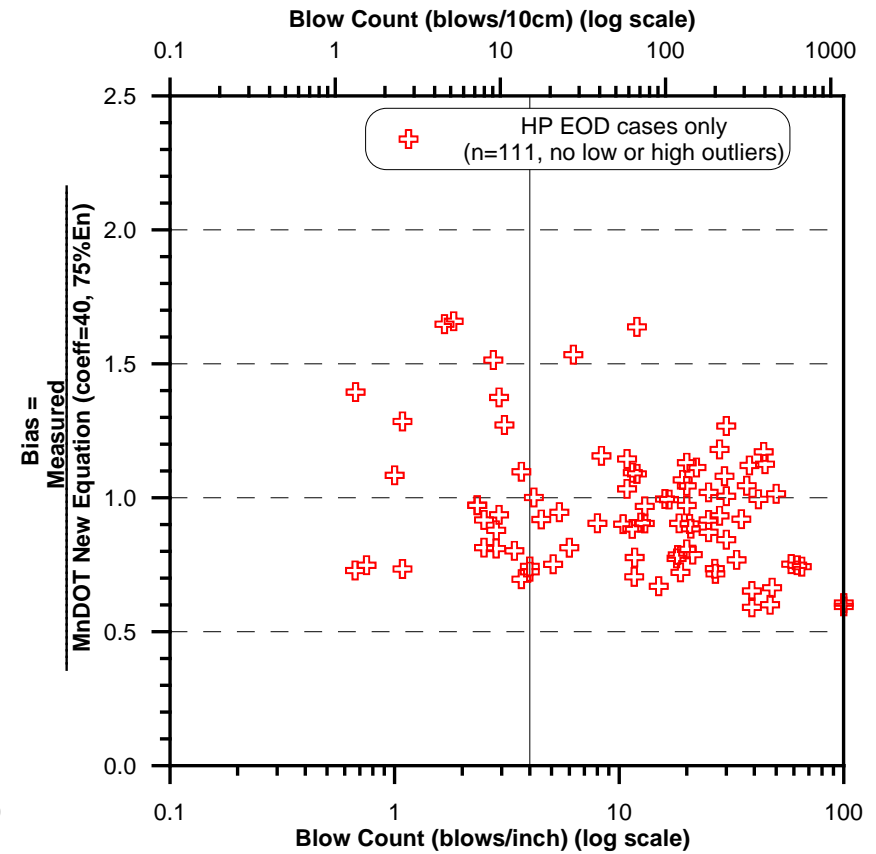


(b)

**Figure 89. Bias vs. blow count for Pipe Pile BOR cases only (low and high outliers removed) for the New MnDOT Equation (coefficient 40, 75% energy) where the blow count is limited to 15bpi maximum; (a) linear scale, and (b) average and standard deviation per 2bpi segments**

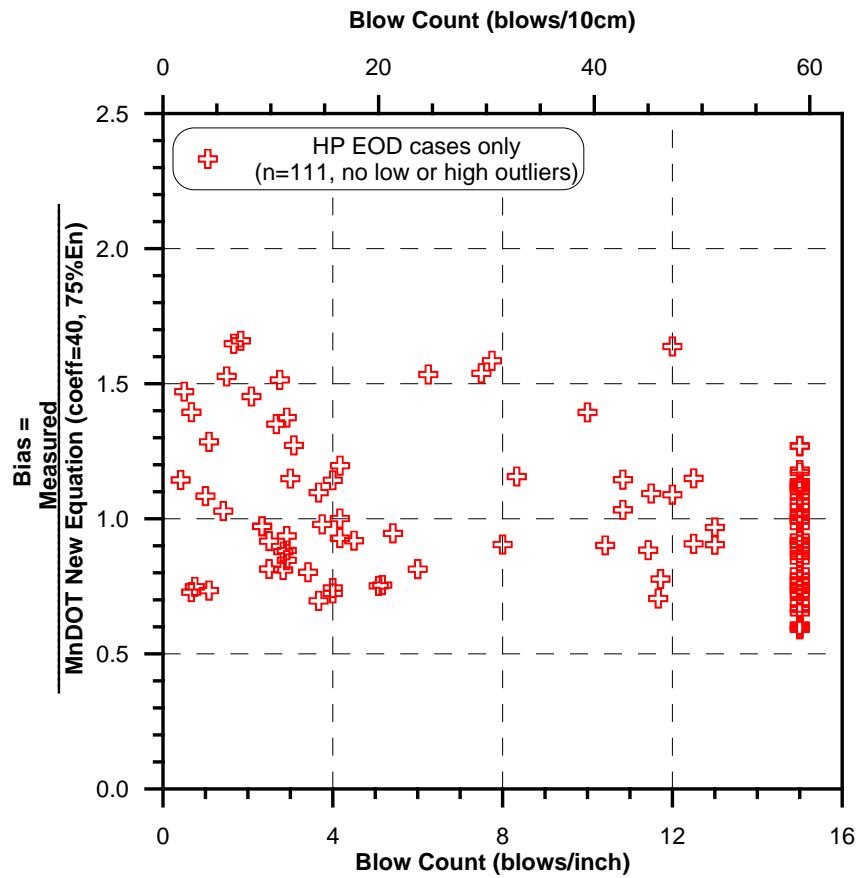


(a)

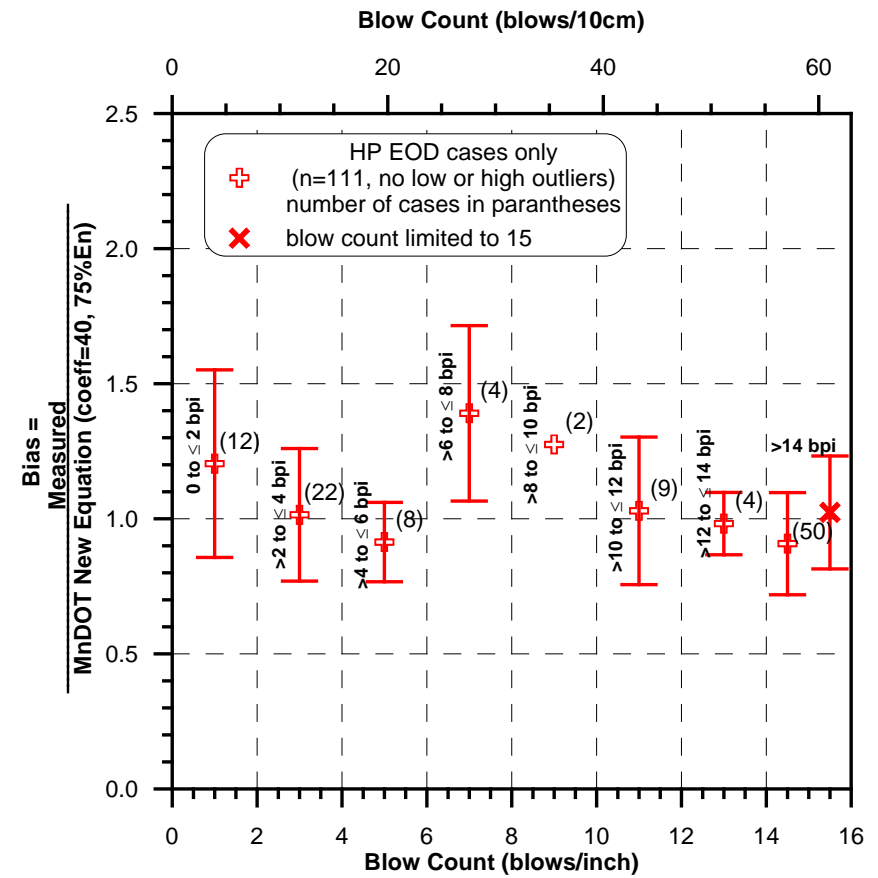


(b)

**Figure 90. Bias vs. blow count for H Pile EOD cases only (low and high outliers removed) for the New MnDOT Equation (coefficient 40, 75% energy); (a) linear scale, and (b) log scale**

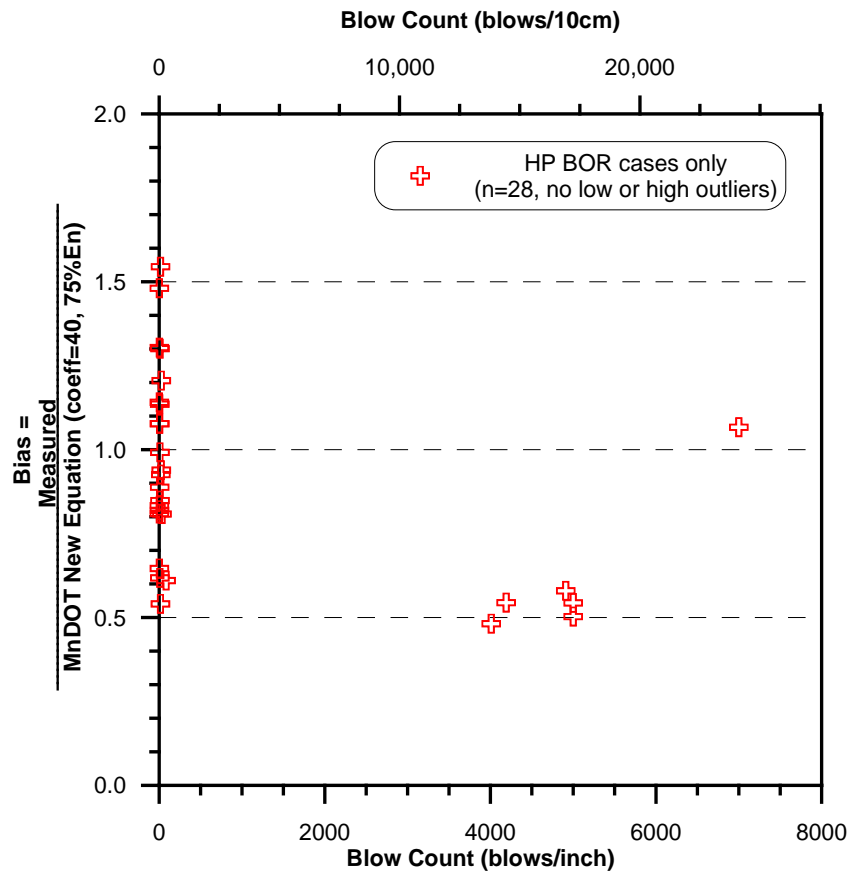


(a)

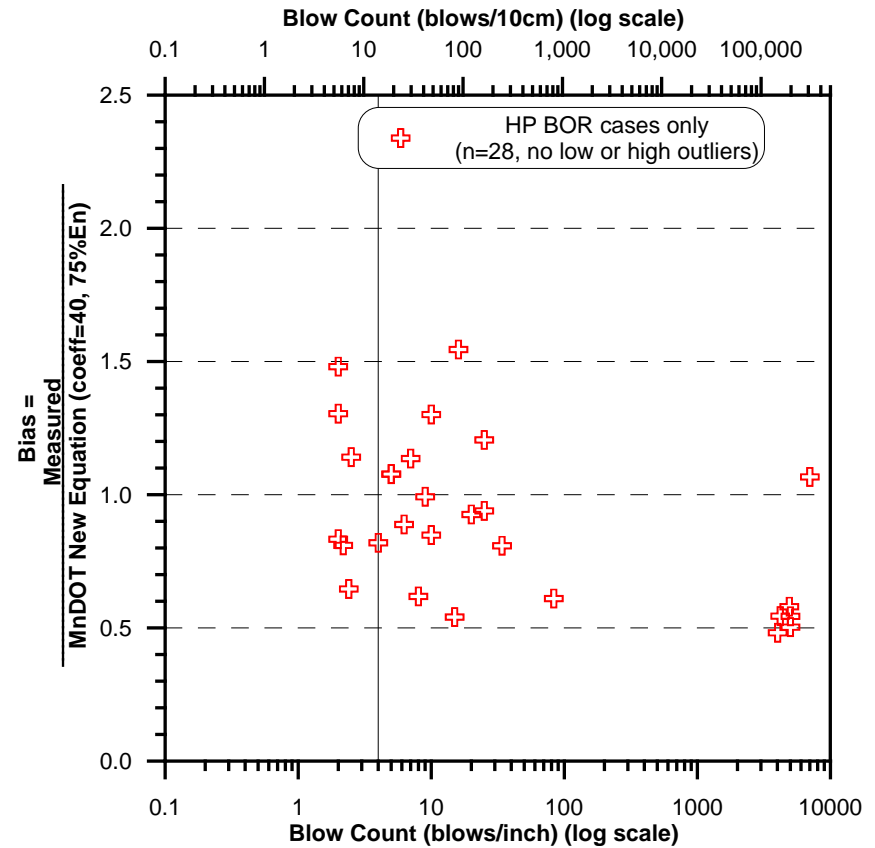


(b)

**Figure 91. Bias vs. blow count for H Pile EOD cases only (low and high outliers removed) for the New MnDOT Equation (coefficient 40, 75% energy) where the blow count is limited to 15bpi maximum; (a) linear scale, and (b) average and standard deviation per 2bpi segments.**

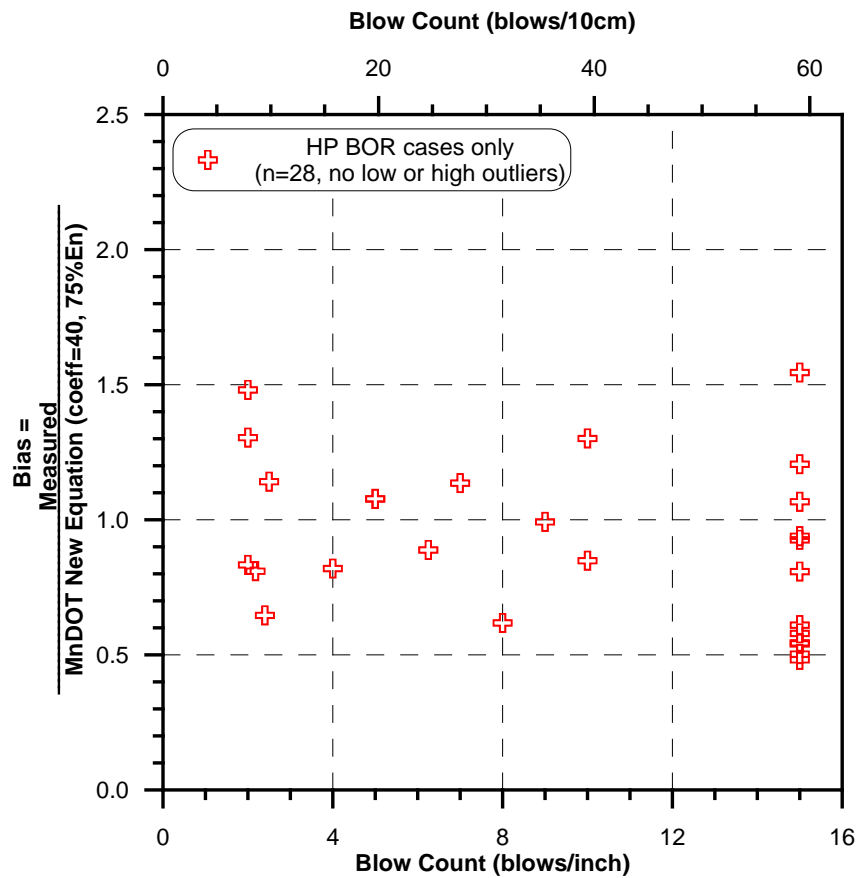


(a)

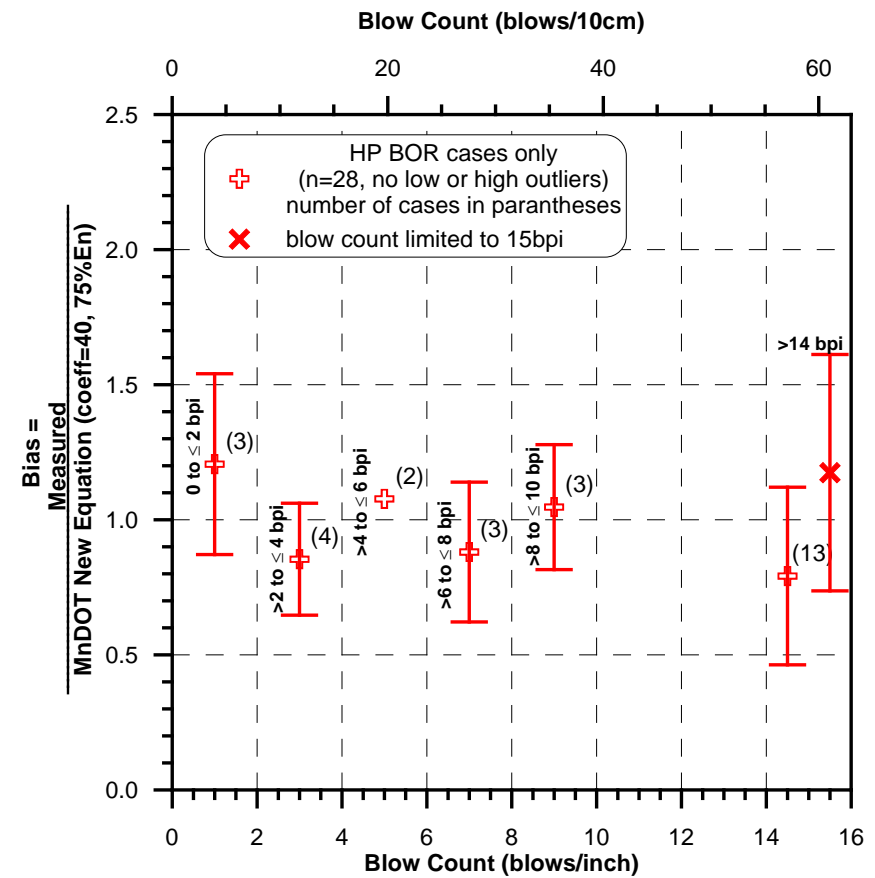


(b)

**Figure 92. Bias vs. blow count for H Pile BOR cases only (low and high outliers removed) for the New MnDOT Equation (coefficient 40, 75% energy); (a) linear scale, and (b) log scale**

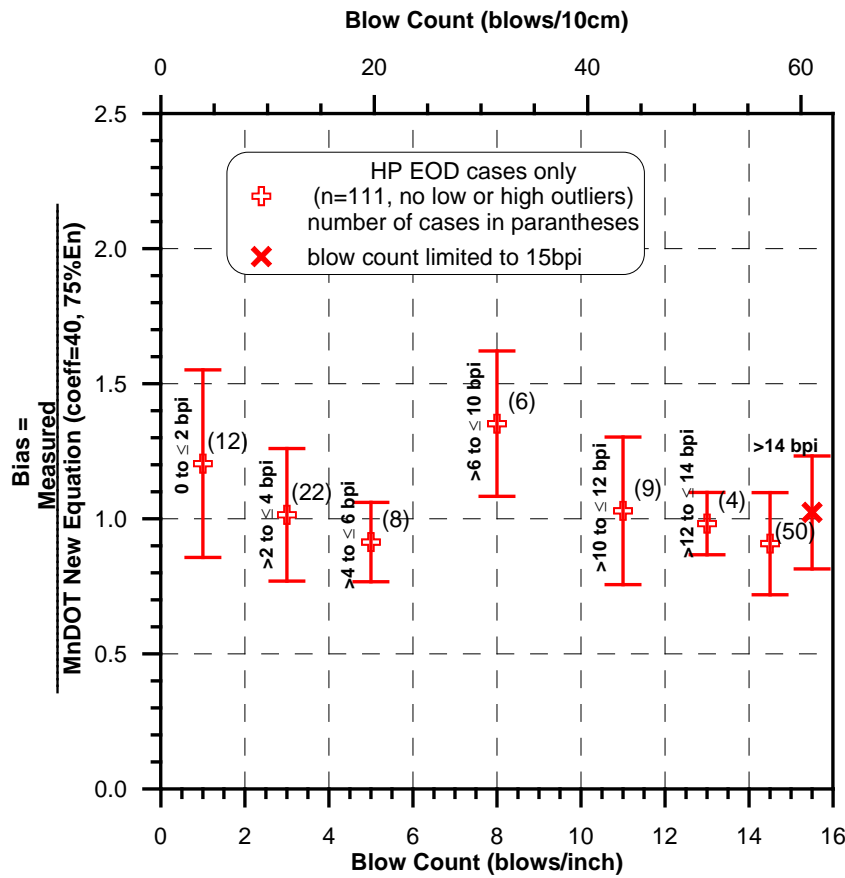


(a)

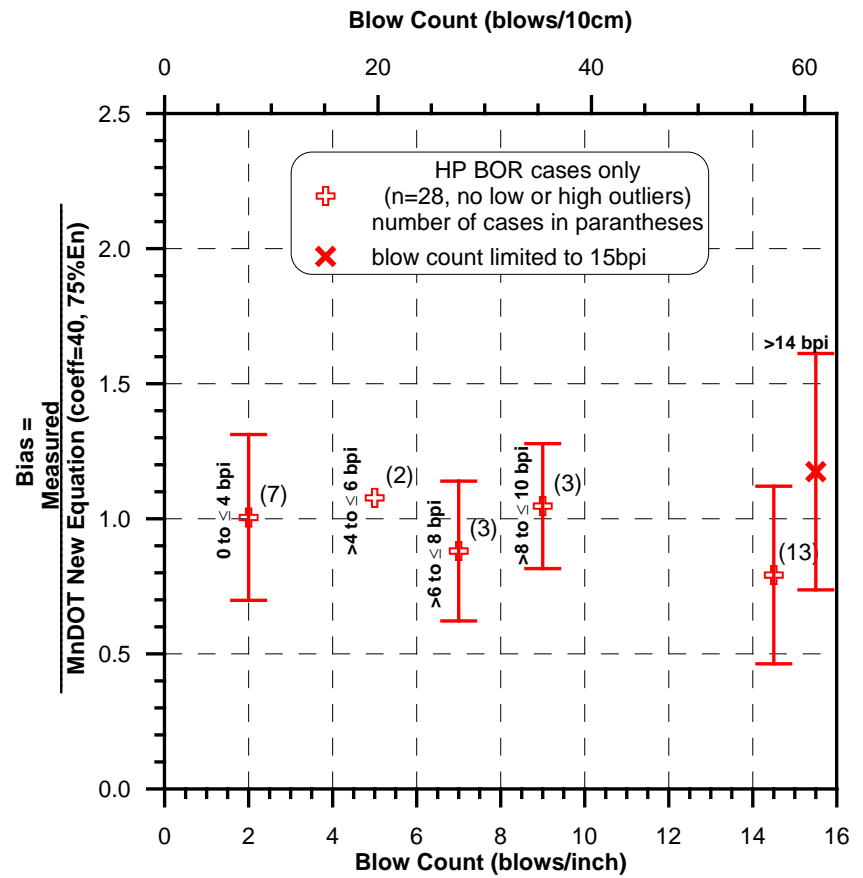


(b)

**Figure 93. Bias vs. blow count for H Pile BOR cases only (low and high outliers removed) for the New MnDOT Equation (coefficient 40, 75% energy) where the blow count is limited to 15bpi maximum; (a) linear scale, and (b) average and standard deviation per 2bpi segments**



(a)



(b)

**Figure 94. Average and standard deviation of the bias vs. blow count for H Pile cases (low and high outliers removed) for the New MnDOT Equation (coefficient 40, 75% energy) where the blow count is limited to 15bpi maximum; (a) EOD only, and (b) BOR only**



#### 4.5.2 Summary Tables

Tables 60 to 61 and Tables 62 to 63 present the performance of MPF12, equation (24), for pipe and H piles under EOD and BOR, respectively. The Tables summarize the performance of MPF12 under various assumptions associated with variation in driving resistance (blow count). All tables refer to the cases presented in Tables 52 to 59 for which the high and the low outliers were removed (case 3c in the notes associated with those tables).

All four tables show extremely accurate predictions in regard to the bias and the low coefficient of variations. Table 60 reveals the sensitivity of the dynamic analyses to the condition of large soil inertia effects. Closed pipe piles under easy driving conditions ( $< 4\text{bpi}$ ) present systematic under-prediction. These conditions are marginally relevant at BOR and of small relevance for H piles, only under very easy driving ( $< 2\text{bpi}$ ).

**Table 60. Statistical summary based on blow count of Pipe Pile EOD cases (low and high outliers removed) for the New MnDOT Equation (coefficient 40, 75% energy)**

Blow Count		No. of Cases	Avg. Bias ( $m_x$ )	Stand. Dev.	COV	$\phi$		
						FOSM	MC	Recom.
$BC \leq 4$	0 – 2	16	1.128	0.425	0.377	0.524	0.571	0.50
	2 – 4	22	1.224	0.491	0.401	0.540	0.587	
	0 – 4	38	1.184	0.461	0.389	0.536	0.583	
Actual $BC \geq 15$		21	0.957	0.317	0.332	0.489	0.539	
Limited $BC \geq 15 \Rightarrow BC=15$		21	1.088	0.395	0.363	0.597	0.675	
All – Actual BC		87	1.067	0.408	0.382	0.490	0.534	
All – Limited BC		87	1.099	0.417	0.380	0.501	0.545	

**Table 61. Statistical summary based on blow count of Pipe Pile BOR cases (low and high outliers removed) for the New MnDOT Equation (coefficient 40, 75% energy)**

Blow Count		No. of Cases	Avg. Bias ( $m_x$ )	Stand. Dev.	COV	$\phi$		
						FOSM	MC	Recom.
$BC \leq 4$	0 – 2	3	1.038	0.393	0.379	0.480	0.523	0.65
	2 – 4	8	0.981	0.144	0.147	0.702	0.842	
	0 – 4	11	0.997	0.215	0.216	0.638	0.741	
Actual $BC \geq 15$		15	1.010	0.262	0.259	0.597	0.679	
Limited $BC \geq 15 \Rightarrow BC=15$		15	1.184	0.303	0.256	0.704	0.801	
All – Actual BC		46	1.023	0.230	0.255	0.609	0.694	
All – Limited BC		47	1.089	0.260	0.239	0.669	0.764	

**Table 62. Statistical summary based on blow count of H Pile EOD cases (low and high outliers removed) for the New MnDOT Equation (coefficient 40, 75% energy)**

Blow Count		No. of Cases	Avg. Bias ( $m_x$ )	Stand. Dev.	COV	$\phi$		
						FOSM	MC	Recom.
BC $\leq 4$	0 – 2	12	1.204	0.347	0.288	0.673	0.753	0.60
	2 – 4	22	1.015	0.245	0.242	0.620	0.708	
	0 – 4	34	1.082	0.295	0.272	0.624	0.705	
Actual BC $\geq 15$		50	0.908	0.189	0.208	0.590	0.687	
Limited BC $\geq 15 \Rightarrow$ BC=15		50	1.024	0.209	0.204	0.669	0.782	
All – Actual BC		111	0.998	0.256	0.257	0.592	0.674	
All – Limited BC		113	1.063	0.267	0.252	0.637	0.726	

**Table 63. Statistical summary based on blow count of H Pile BOR cases (low and high outliers removed) for the New MnDOT Equation (coefficient 40, 75% energy)**

Blow Count		No. of Cases	Avg. Bias ( $m_x$ )	Stand. Dev.	COV	$\phi$		
						FOSM	MC	Recom.
BC $\leq 4$	0 – 2	3	1.206	0.335	0.278	0.687	0.774	0.60
	2 – 4	4	0.854	0.207	0.243	0.520	0.594	
	0 – 4	7	1.005	0.307	0.305	0.543	0.604	
Actual BC $\geq 15$		13	0.792	0.329	0.415	0.339	0.367	not to apply
Limited BC $\geq 15 \Rightarrow$ BC=15		13	1.174	0.438	0.373	0.550	0.600	0.60
All – Actual BC		28	0.902	0.302	0.335	0.458	0.504	not to apply
All – Limited BC		29	1.018	0.245	0.241	0.623	0.711	0.60

#### 4.5.3 Driving Resistance Bearing Graphs

The MPF12 was utilized to develop driving resistance curves (bearing graphs) presented in Figure 95 showing the variation of the calculated capacity vs. blow count for three nominal hammer energies ( $E_n = 60, 80, 100\text{kip-ft}$ ), including a suggested limiting blow count of 15 bpi.

#### 4.5.4 Calculated Resistance Factors

Tables 60 to 63 include the evaluation of the resistance factors for the different investigated conditions described in section 4.5.2. Both First Order Second Moment (FOSM) and Monte Carlo (MC) simulations were used for the evaluation with the load side statistical parameters and load factors following the methodology presented by Paikowsky et al. (2004) and reviewed in the Phase I report (Paikowsky et al., 2009). Tables 60 to 63 also include the recommended

resistance factors for each of the conditions. The calculated resistance factors lead to the following recommendations:

- For pipe piles, use  $\phi = 0.50$  for EOD,  $\phi = 0.65$  for BOR, keep  $2 < BC \leq 15$
- For H piles, use  $\phi = 0.60$  for EOD and BOR, keep  $BC \leq 15$

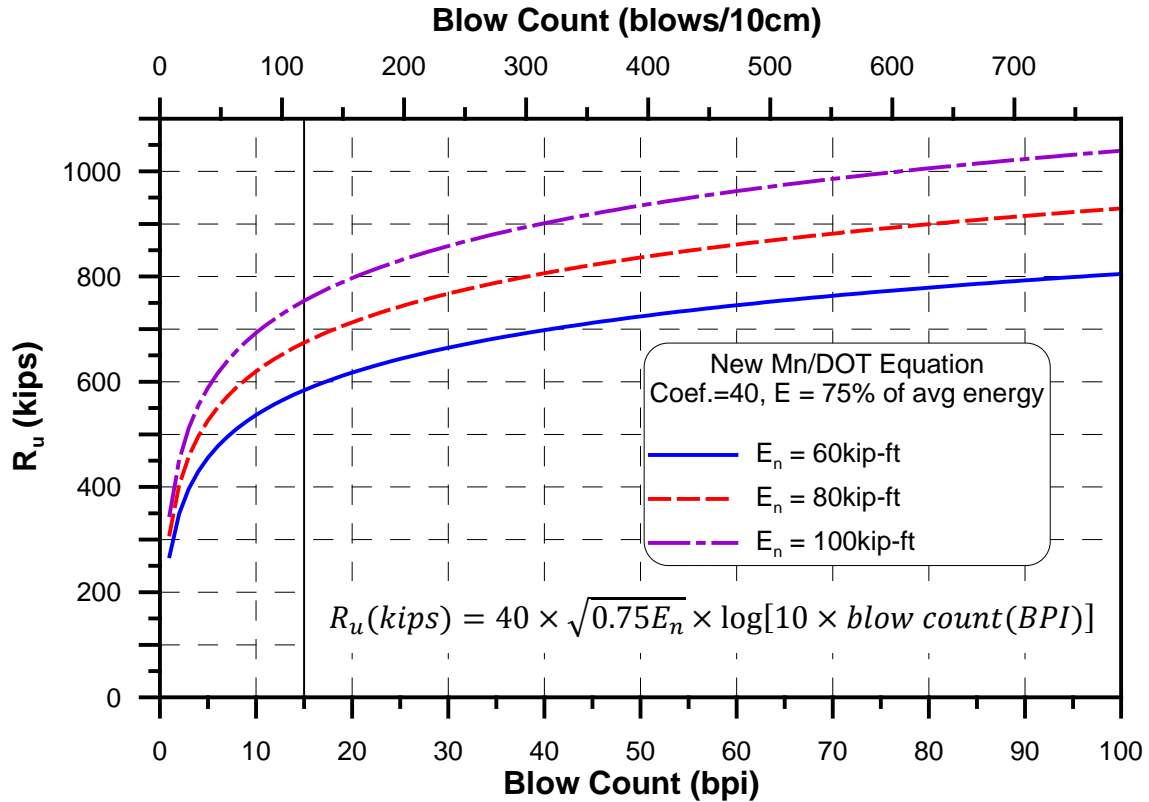


**Figure 95. New MnDOT equation vs. blow count for set energy values**

#### 4.6 MPF12 Final Format and Recommended Resistance Factors

Following the analyses presented in the previous section and attempting to maintain the engineering units format of the new equation in line with previous practices, the final format of MPF12 to be used by the MnDOT is:

$$R_n = 20 \sqrt{\frac{W \times H}{1,000}} \times \log\left(\frac{10}{s}\right) \quad (25)$$

in which

$R_n$  = nominal resistance (tons)

H = stroke (height of fall) (ft)

W = weight of ram (lbs)

s = set (pile permanent displacement per blow) (inch)

The value of the energy ( $W \cdot H$ ) used in the dynamic formula shall not exceed 85% of the manufacturer's maximum rated energy for the hammer used considering the settings used during driving. Equation (25) is to be used with the following Resistance Factors (RF) in order to obtain the factored resistance:

$$R_r = \phi \cdot R_n \quad (26)$$

where

for Pipe Piles,  $\phi = 0.50$ ,  $2 < BC \leq 15$

for H piles,  $\phi = 0.60$ ,  $2 < BC \leq 15$

## **5 EVALUATION OF MPF12 FOR PRECAST PRESTRESSED CONCRETE PILES**

### **5.1 Overview**

The MPF12 was investigated for application to precast prestressed concrete piles. As the case history database was diverse and extensive, it required looking at 24 combinations for establishing the resistance factors, but also allowed to expand the investigation in various ways:

1. The use of MPF12 for large/voided piles that would require equation modification, for the present research it can be resolved using a higher resistance factor as presented in the conclusions.
2. CAPWAP predictions were compared to static load test results and to MPF12. The performance of MPF12 is much better than that of CAPWAP for EOD and comparable to CAPWAP at BOR within the applicable pile sizes.

### **5.2 PSC Database Summary**

Table 64 outlines the database compiled for examining the application of MPF12 equation (Paikowsky et al., 2009) for the capacity evaluation of precast, prestressed concrete piles. Overall, 137 cases are available, related to 38 piles for which End of Driving (EOD) records are available in addition to 99 Beginning of Restrike (BOR) records.

Table 64 categorizes the piles by size and shape distinguishing between voided and un-voided shapes. Most of the un-voided EOD pile cases range from 14 to 24-inch size piles (20 of 26). Table 65 further subcategorizes the pile cases by referring to the driving resistance in the form of Blows Per Inch (BPI) of the EOD and BOR cases. Both tables provide the pile capacity ranges as established by a static load test using the Davisson's failure criterion.

**Table 64. Summary of PSC data set attributes**

Pile Type/Size (in)		No.	Capacity Range (kips)		Type of Data		Soil Types*		
					EOD	BOR	Soil Type	Side	Tip
Square/Cylindrical Concrete	10	9	64 - 270		0	9	Sand w/ Fines	77	45
	12	7	358 - 466		2	5			
	14	12	313 - 398		5	7			
	16	5	807 - 1006		2	3	Sand w/out Fines	26	62
	18	18	230 - 550		7	11			
	20	9	368 - 1360		1	8			
	24	28	453 - 1671		5	23			
	30	6	754 - 1590		3	3	Clay/Till	34	21
36	2	1140		1	1				
Voided Concrete	20	2	980		1	1	Rock/IGM	0	9
	24	13	400 - 817		4	9			
	30	7	511 - 900		1	6			
	36	10	540 - 542		2	8	Total:	137	137
	54	3	920 - 1430		1	2			
Octagonal Concrete	24	6	512 - 1140		3	3			
	Total:	137			38	99			

\*includes all cases, hence may refer multiple times to same pile.

**Table 65. PSC cases categorized by pile shape/size, time of driving and driving resistance**

Pile Type	All Cases	EOD Cases		BOR Cases		Static Capacity (kips)
		All	B.C. >2 bpi	All	B.C. >2 bpi	
10" sq	9	0	0	9	8	64 to 270
12" sq	7	2	2	5	5	358 to 466
14" cyl	2	1	1	1	1	313
14" sq	10	4	3	6	6	320 to 398
16" sq	5	2	1	3	3	807 to 1006
18" sq	18	7	6	11	11	230 to 550
20" hollow cyl.	2	1	1	1	1	980
20" sq	9	1	1	8	8	368 to 1360
24" oct	6	3	3	3	3	512 to 1140
24" hollow sq.	13	4	2	9	8	400 to 817
24" sq	28	5	5	23	23	453 to 1671
30" hollow sq.	7	1	0	6	5	511 to 900
30" sq	6	3	3	3	3	754 to 1590
36" hollow cyl.	10	2	1	8	8	540 to 542
36" sq	2	1	1	1	1	1140
54" hollow cyl.	2	1	1	1	1	1430
54" hollow sq.	1	0	0	1	1	920
<b>TOTAL:</b>	137	38	31	99	96	

### 5.3 Statistical Analysis

Table 66 provides the statistical analysis for the 24 investigated subgroups of the PSC database. Overall the database was broken down based on (a) pile type, distinguishing between full shape and voided piles (typically included in large size piles), (b) time of driving, EOD, BOR and combined, and (c) driving resistance, typically resistance greater than either 2 or 4 bpi. This detailed subdivision was recognized by investigating the data in various ways and reflects the large variability of the pile types.

Graphical presentation of the major subcategories (with a different notation for each pile type) comparing the measured (static load test) to the calculated capacities, are presented in Figures 96 through 99. Based on the analyses and graphs, the following major observations can be made:

1. For EOD, the bias of the unvoided piles is smaller than that of the voided piles ( $m_\lambda = 1.27$  for  $n = 28$  vs.  $m_\lambda = 1.53$  for  $n = 10$ ). This seems to be associated with size and capacity, i.e. the equation naturally under-predicts the capacities of the larger piles in size and capacity as it was originally not developed for these pile sizes. Figure 99 elucidates this fact by examining the bias for all tested pile sizes showing an overall trend of increased bias with the increase with pile size.
2. A substantial under-prediction with a large scatter exists in the low driving resistance range for which the blow count (BC) is smaller than 2BPI. This evidence becomes clear in the graphical presentation of the data in Figure 100.
3. The equation provides accurate prediction for the non-voided piles at BOR for all cases and in particular for the cases when the  $BC > 2BPI$  and outliers are removed, resulting with a mean bias of  $m_\lambda = 0.98$  for  $n = 66$  cases and a  $COV_\lambda = 0.33$ . The relationship between the bias and the driving resistance for the BOR cases is presented in Figure 101.
4. Figure 102 presents the relationship between the bias and the pile dimension for (a) EOD and (b) BOR. While for the piles equal or smaller than 24-inch, the bias ranges typically about 0.6 to 1.2. For sizes greater than 24-inch, the bias is typically above 1, suggesting the equation to under-predict consistently the higher pile dimensions and their associated higher capacities.

**Table 66. Summary of statistics and resistance factors for PSC piles categorized by pile shape/size, time of driving and driving resistance**

			# of Cases	$\sigma_\lambda$	$m_\lambda$	$COV_\lambda$	Resistance Factor $\phi$		
							FOSM	MC	Recom.
Cases w/out Hollow PSC	EOD	All Cases	28	0.55	1.27	0.43	0.52	0.56	0.50
		B.C. > 2 bpi	25	0.51	1.23	0.41	0.53	0.57	
		B.C. > 2 bpi & No Outliers <sup>1</sup>	22	0.40	1.10	0.36	0.53	0.58	
		B.C. > 4 bpi	18	0.54	1.27	0.43	0.53	0.57	
		B.C. > 4 bpi & No Outliers <sup>1</sup>	16	0.45	1.15	0.40	0.51	0.56	
	BOR	All Cases	72	0.42	1.05	0.40	0.46	0.50	0.50
		B.C. > 2 bpi	71	0.42	1.06	0.40	0.47	0.51	
		B.C. > 2 bpi & No Outliers <sup>2</sup>	66	0.32	0.98	0.33	0.50	0.56	
		B.C. > 4 bpi	65	0.42	1.09	0.39	0.50	0.54	
		B.C. > 4 bpi & No Outliers <sup>2</sup>	60	0.31	1.01	0.31	0.54	0.60	
Both	All Cases	100	0.47	1.11	0.42	0.47	0.51	0.50	
	B.C. >2 & No Outliers	88	0.34	1.01	0.34	0.51	0.56		
Hollow PSC Piles	EOD	All Cases	10	0.26	1.53	0.17	1.05	1.25	0.80
	BOR	All Cases	27	0.25	1.16	0.21	0.74	0.86	
	Both	All Cases	37	0.30	1.26	0.24	0.77	0.89	
		B.C. >2 & No Outliers	30	0.24	1.17	0.20	0.77	0.90	
All PSC Piles	EOD	All Cases	38	0.47	1.27	0.37	0.60	0.66	N/A
		B.C. >2.	31	0.51	1.27	0.40	0.56	0.61	
	BOR	All Cases	99	0.37	1.05	0.35	0.52	0.57	
		B.C. > 2 BPI	96	0.39	1.08	0.36	0.52	0.57	
		No Outliers <sup>3</sup>	93	0.30	1.02	0.30	0.56	0.62	
		B.C. > 4	88	0.38	1.09	0.35	0.54	0.60	
		B.C. $\geq$ 4 & No Outliers <sup>3</sup>	82	0.28	1.03	0.28	0.59	0.66	
	Both	All Cases	137	0.42	1.13	0.37	0.53	0.58	

Notes:

1. Omit all piles with bias > 2.10
2. Omit all piles with bias > 1.85
3. Omit all piles with bias > 1.74



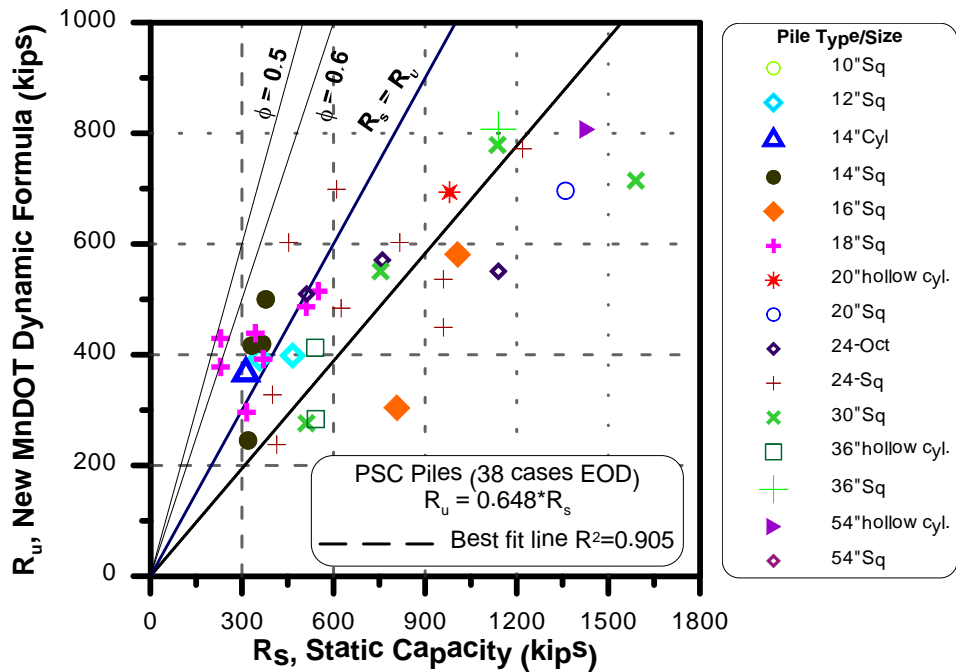


Figure 96. Measured static capacity vs. New MnDOT dynamic equation prediction for 38 EOD cases

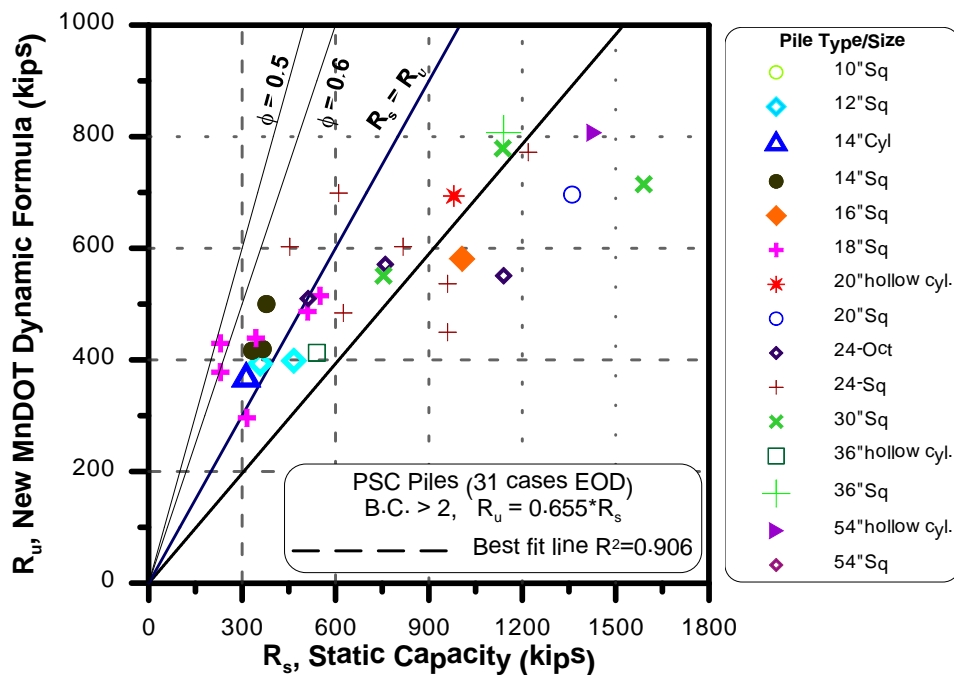


Figure 97. Measured static capacity vs. New MnDOT dynamic equation prediction for 31 EOD cases (B.C.  $\geq 2$  bpi)

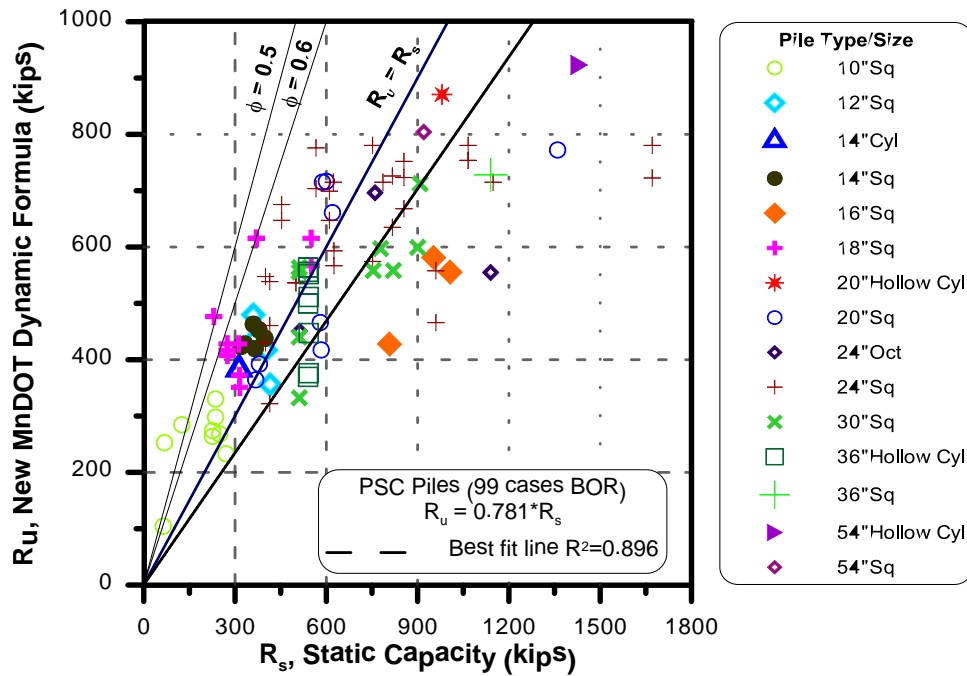


Figure 98. Measured static capacity vs. New MnDOT dynamic equation prediction for 99 BOR cases

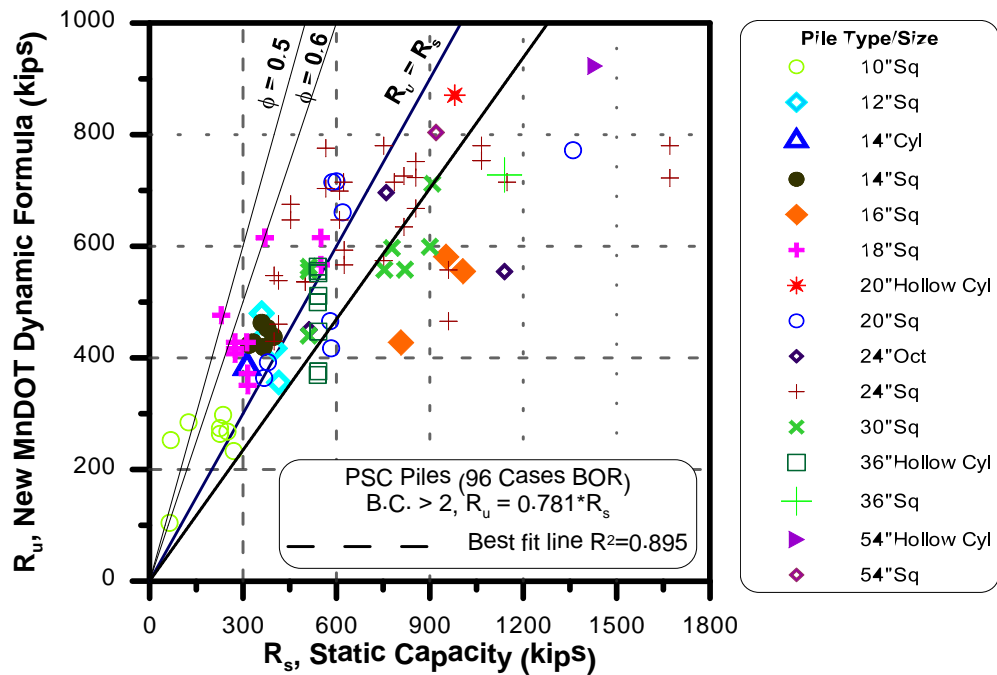
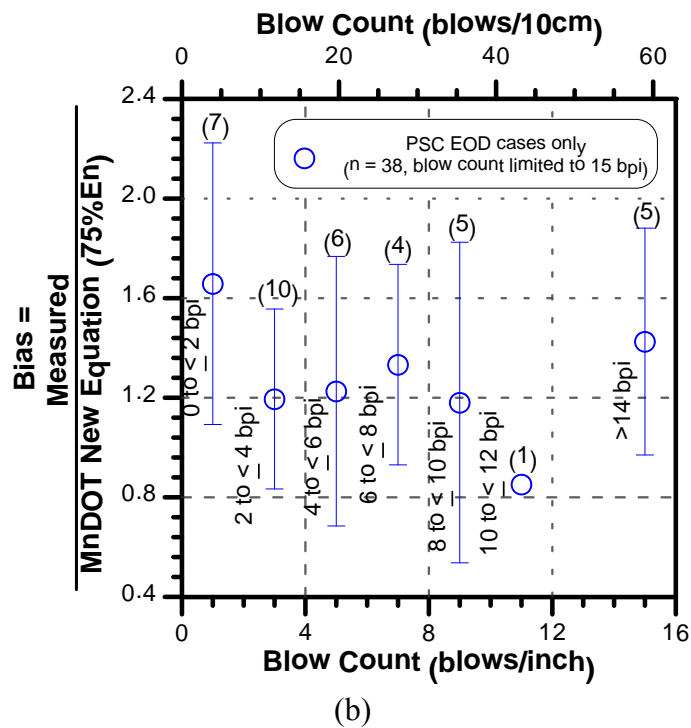
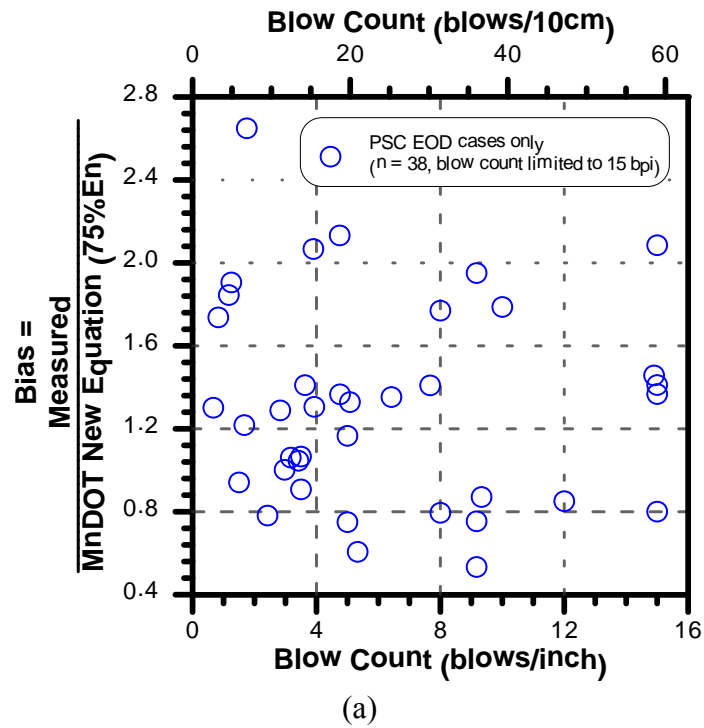
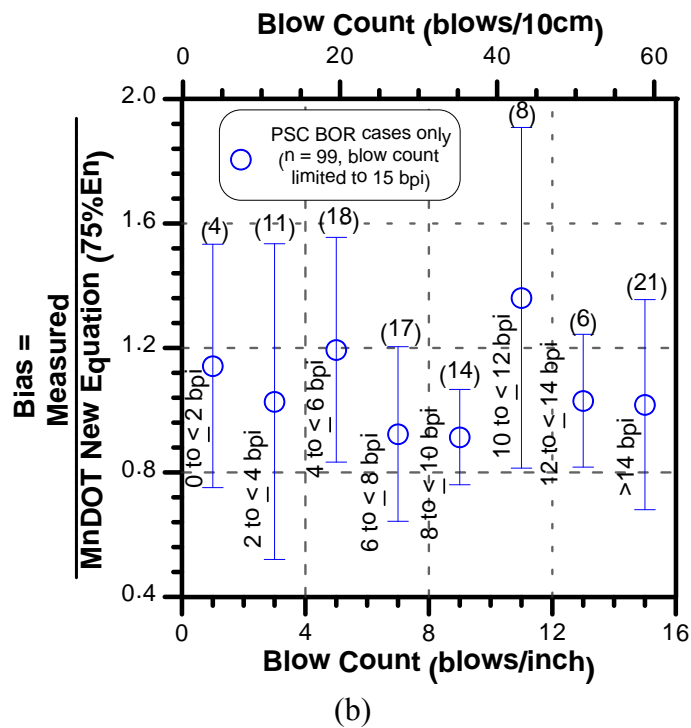
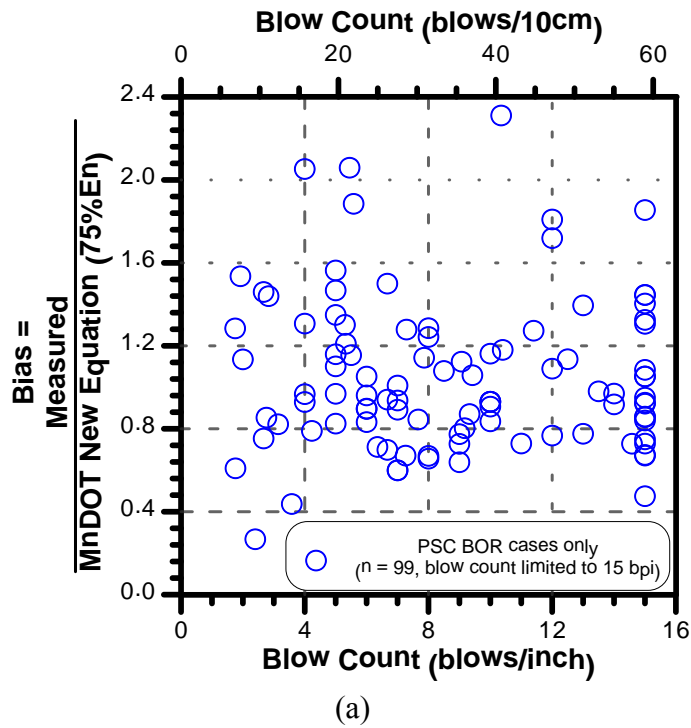


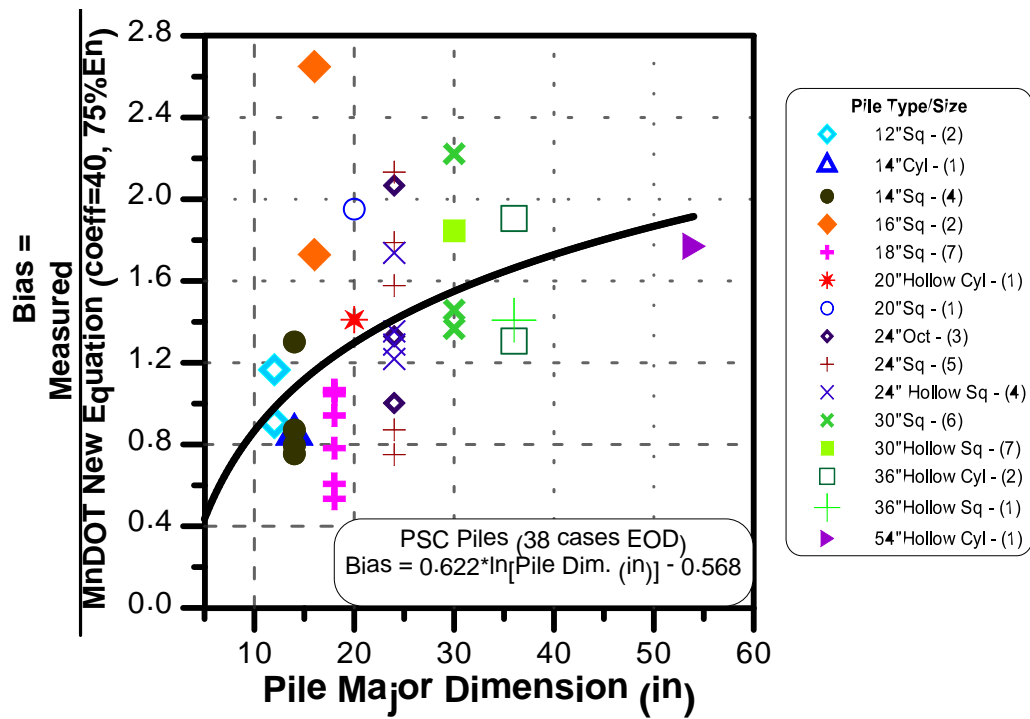
Figure 99. Measured static capacity vs. New MnDOT dynamic equation prediction for 96 BOR cases (B.C.  $\geq 2$  bpi)



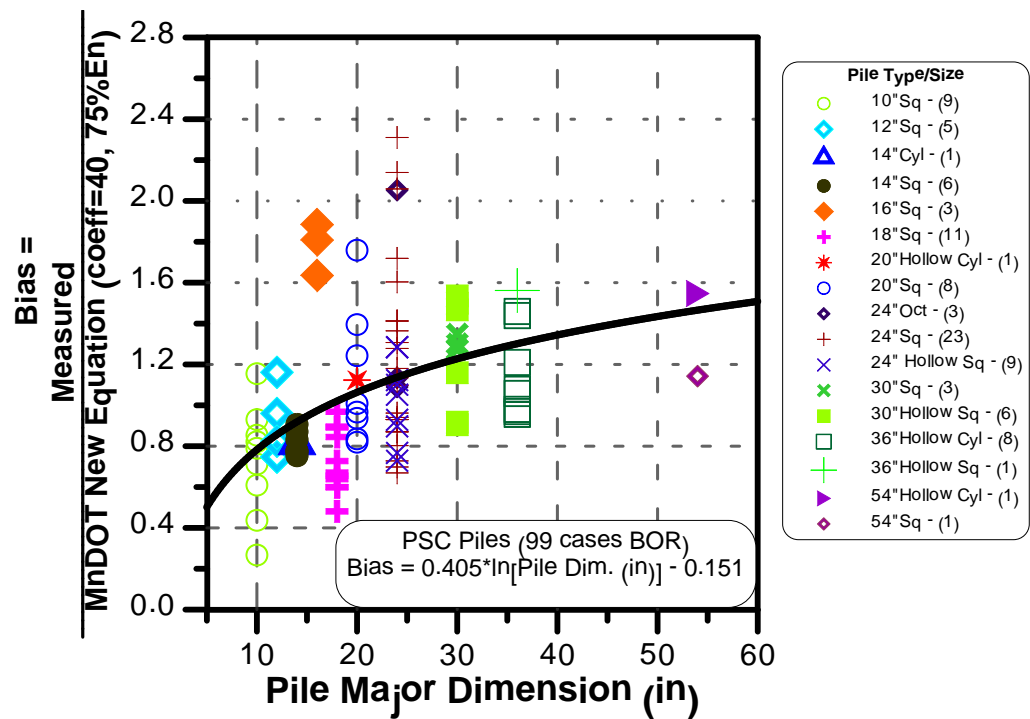
**Figure 100. Bias vs. blow count for PSC EOD cases for the New MnDOT Equation (75% energy) where the blow count is limited to 15bpi maximum; (a) linear scale, and (b) average and standard deviation per 2bpi segments**



**Figure 101. Bias vs. blow count for PSC BOR cases for the New MnDOT Equation (75% energy) where the blow count is limited to 15bpi maximum; (a) linear scale, and (b) average and standard deviation per 2bpi segments**



(a)



(b)

Figure 102. Bias versus PSC pile size (in) for (a) EOD cases and (b) BOR cases

## 5.4 Broader Examination of the MPF12 Equation

Additional analyses were carried out to gain better perspective of the aforementioned investigation of the MPF12 equation performance. The case histories that contained dynamic measurements and signal matching (CAPWAP) analyses were examined for the accuracy of the prediction and compared to MPF12 performance. Figures 103 and 104 contain comparisons between static load test capacity (Davisson's failure criterion) and CAPWAP predictions for EOD and BOR cases, respectively. Figures 105 and 106 present comparisons between the MPF12 and the CAPWAP predictions; note that  $R_s$  in these figures relate to CAPWAP prediction and not to static capacity. The data in Figures 103 to 106 lead to the following observations:

1. CAPWAP predictions at EOD provide systematically lower capacities when compared to the measured static capacities. On the average for the 35 examined cases, the bias was  $m_\lambda = 2.37$  and the  $COV_\lambda = 0.91$ . This is in contrast to the comparison in Figures 96 and 97, and the data in Table 66, suggesting significantly better pile capacity predictions by MPF12 than CAPWAP for the EOD examined cases. This observation may have been influenced by the nature of the cases where capacity gain with time had taken place.
2. Figure 104 shows a much better performance for the CAPWAP analyses when compared to the measured static capacity for the BOR cases. For the 99 cases (note, multiple restrikes on same piles), the mean bias  $m_\lambda = 1.22$  and the  $COV_\lambda = 0.35$ . The comparison in Figure 104 suggests the signal matching to perform comparably to the MPF12 for the BOR cases when compared to the relations presented in Figures 98 and 99 and Table 66 all BOR cases.
3. The data in Figure 105 related to EOD suggests that a somehow good agreement exists between MPF12 and CAPWAP for the range of pile capacities approximately lower than 300kips. For capacities between 300 and about 500kips, the MPF12 predictions are somehow conservative compared to the CAPWAP predictions (approximately  $\frac{2}{3}$ ) and for pile capacities in excess of 500kips the MPF12 capacities are under predicting significantly compared to CAPWAP (by approximately  $\frac{1}{2}$ ).
4. The data in Figure 106 related to BOR suggests that as both methods perform well in this category, overall a good agreement exists between the MPF12 and CAPWAP predictions over the entire range of capacities (i.e. ratio of 90%). However, graphical observation of the data shows that up to about 600kips the MPF12 capacity is typically higher than that of CAPWAP, between about 600kips and 900kips the MPF12 capacity is typically moderately lower than the CAPWAP predictions, while for capacity range beyond 900kips the MPF12 seriously under-predicts the pile capacities as compared to CAPWAP. Naturally this zone is dominated by large piles mostly voided with capacities beyond the range for which MPF12 was originally developed.

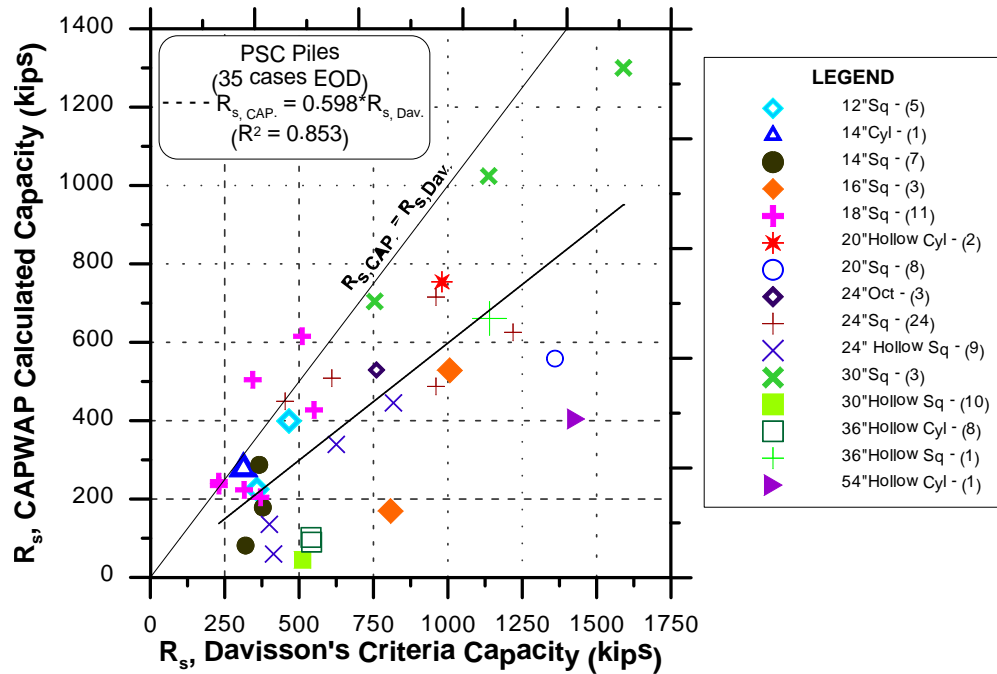


Figure 103. Davisson's criteria predicted static capacity versus CAPWAP prediction for 35 EOD cases

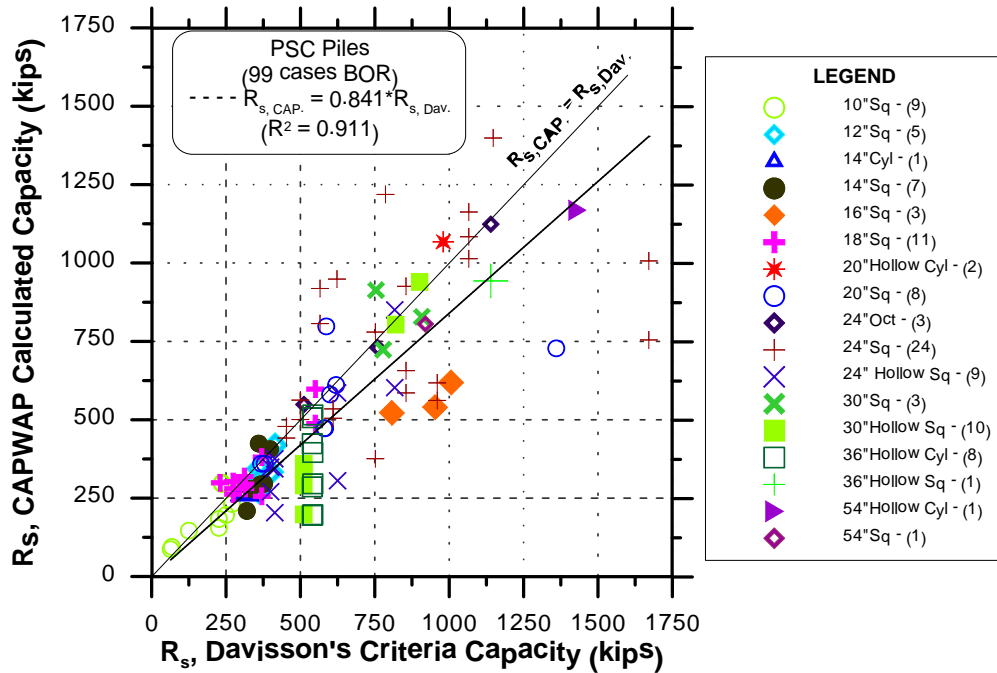


Figure 104. Davisson's criteria predicted static capacity versus CAPWAP prediction for 99 BOR cases

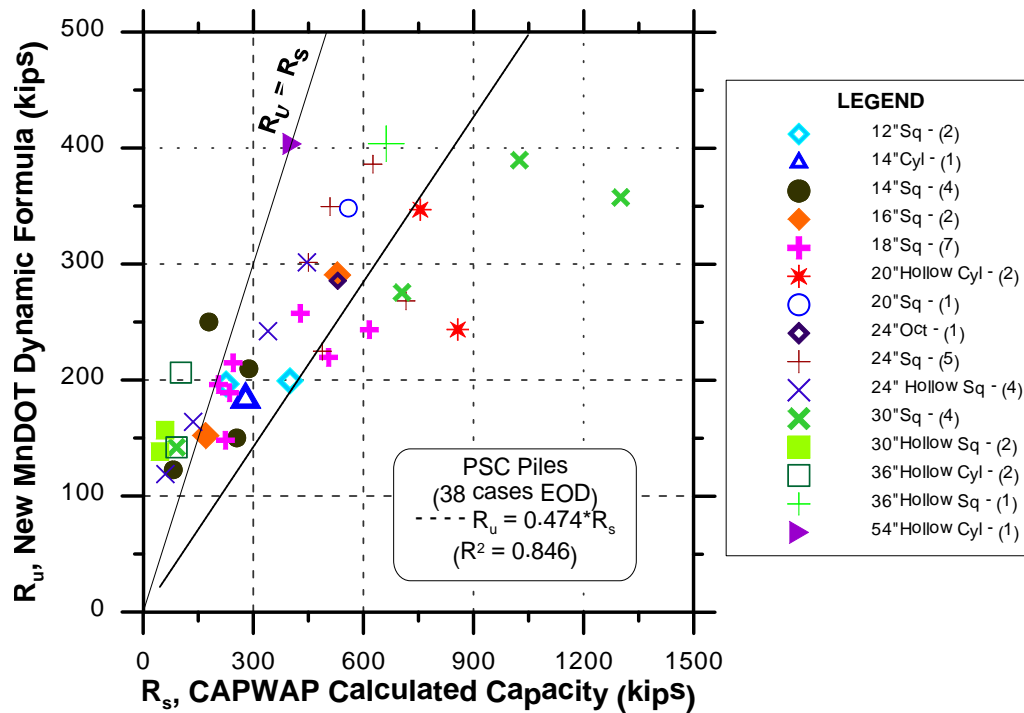


Figure 105. CAPWAP predicted static capacity versus New MnDOT dynamic equation prediction for 38 EOD cases

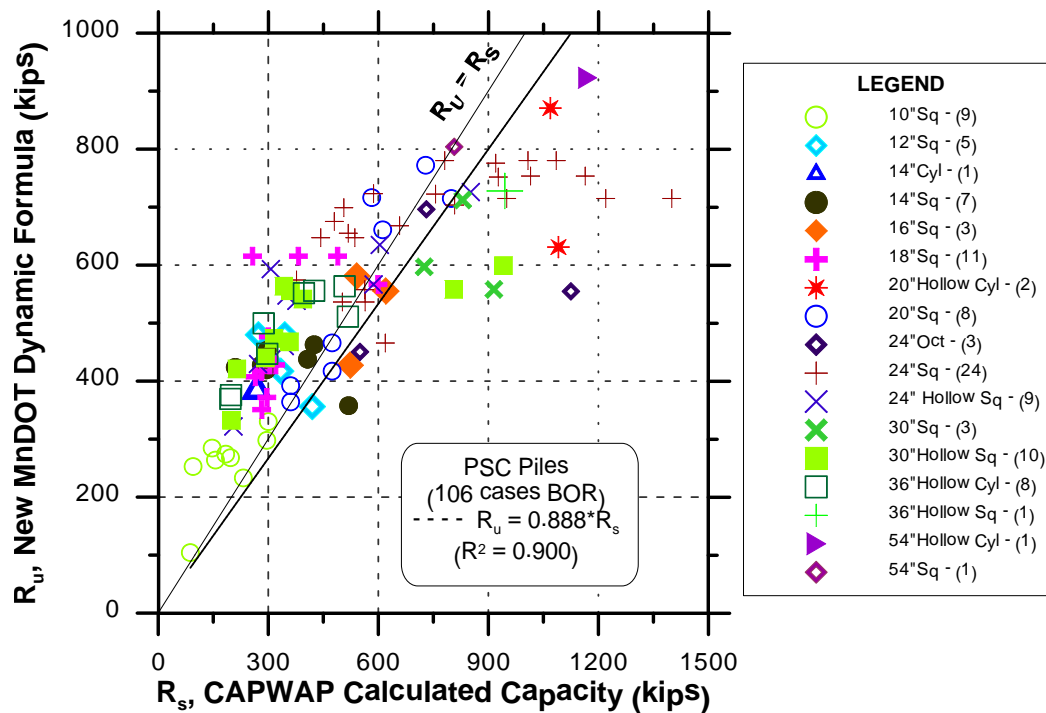


Figure 106. CAPWAP predicted static capacity versus New MnDOT dynamic equation prediction for 106 BOR cases



## 5.5 Resistance Factors

Table 66 summarizes the calculated and recommended resistance factors based on the above discussed sub categorization of the cases. Figures 96 to 99 present the application of resistance factors  $\phi = 0.5$  and  $\phi = 0.6$  to the analyzed data. It should be noted that with the factored load, the cases on the boundary are actually on the safe side (i.e. factored resistance greater than factored load).

## 5.6 Recommendations

The calculated resistance factors of Table 66 and the graphics representation of Figures 96 to 99 lead to the following recommendations:

1. For non-voided PSC Pile sizes  $\leq 24"$   
use the same recommendations as previously provided for steel pipes, i.e.:  
 $\phi = 0.5$  for EOD and BOR,  $2 < B.C. < 15BPI$  (see equation (25), section 4.6)
2. For voided PSC sizes  $20" \leq PSC \leq 54"$   
use  $\phi = 0.80$

Case 2 requires modification of the equation but as a first evaluation one can use  $\phi = 0.80$  for all cases.

## 6 EVALUATION OF MPF12 FOR TIMBER PILES

### 6.1 Overview

The MPF12 was investigated for application to timber piles. A total of 28 timber piles were examined and the appropriate resistance factor was developed based on 25 of the original 28 cases. Three cases were set aside as control cases. Due to large damping and loss of energy when impacting timber, it was proposed that the MPF12 equation be multiplied by 0.50 for a simplified format and accurate pile capacity predictions. The use of the Timber piles modified equation was calibrated resulting with a recommended resistance factor of  $\phi = 0.60$ .

### 6.2 Timber Pile Database

#### 6.2.1 Summary

Table 67 outlines the database compiled for examining the application of MPF12 equation (Paikowsky et al., 2009) for the capacity evaluation of timber piles. Overall, 25 cases are available for evaluating the efficacy of the MPF12 equation, related to 24 piles for which End of Driving (EOD) records are available in addition to one Beginning of Restrike (BOR) records. All cases were obtained from the Ontario Ministry of Transportation.

Results outlined in this report represent all relevant timber pile cases for both EOD and BOR times of driving. Three (3) additional cases (to the 25 timber piles) were set aside as control cases, primarily to examine the validity of the recommended MPF12 equation for timber piles and the associated resistance factors. Table 67 categorizes the piles by three common metric sizes: Size 30, 32, and 36 (in centimeters). Table 68 summarizes the range of tip/butt diameters (inch) and embedded lengths (ft) for each pile size. The driving resistances, in the form of Blows Per Inch (BPI), were limited to 15 BPI for all cases, where a total of three (3) cases exceeded this limit.

**Table 67. Summary of timber pile data set attributes**

Pile Size					Capacity Range (kips)
Type	Embedded Length (ft)			No.	
	Min.	Max.	Ave.		
Size 30	15	22	17	6	130-350
Size 32	n/a	n/a	24	1	150
Size 36	11	72	36	18	70-350
Total:				25	

Soil Type*		
	Side	Tip
Sand w/ Fines	10	11
Sand w/out Fines	2	4
Clay/Silt	16	12
Rock	0	1

\* Includes all cases, hence may refer multiple times to same pile.

**Table 68. Range of timber pile dimensions**

<b>Pile Type</b>	<b>Butt Diameter (in)</b>	<b>Tip Diameter (in)</b>	<b>Average Diameter (in)</b>	<b>Embedded Length (ft)</b>
Size 30	12.0	8.0 - 10.0	10.0 - 11.0	15.0 - 22.0
Size 32	12.8	8.5	10.6	24.0
Size 36	13.4 - 16.7	8.0 - 13.8	11.5 - 14.8	11.0 - 72.0

### **6.2.2 Pile Capacity Evaluation**

The capacity of driven piles is most appropriately defined by Davisson (1972) failure criterion. Paikowsky et al. (2004) had established the statistical validity of this criterion and, as such, all calibrations were conducted based on the load test results interpretations utilizing Davisson's criterion.

The application of Davisson's criterion requires the use of the pile's modulus of elasticity in order to establish the elastic deformation of a free standing pile (i.e. column) under load. In contrast to manmade materials (steel, concrete), timber modulus varies significantly based on the timber type, orientation of grain, etc. As such, Table 67 provides the pile capacity ranges as established by a static load test using the Shape of Curve failure analysis. The Shape of Curve analysis was preferable due to the general/plunging failure behavior of the timber piles and the ability to introduce judgment. A comparison of the static capacity based on the Shape of Curve and Davisson's Criterion is presented in Figure 107. For the majority of the cases a section modulus ( $E$ ) of 1500 ksi was assumed (Collin, 2002). A reduced modulus was assumed for those cases yielding a distinct under-prediction of static capacity based on Davisson's Criterion and is summarized as follows:  $E = 1100$  ksi for TS #33 Pile #5 and TS #35 Pile #7,  $E = 800$  ksi for TS #13 Pile #s 1, 2, 12, and 14. This subjective modulus application further augments the invalidity of applying Davisson's Failure Criterion for analyzing the static capacity of timber piles.

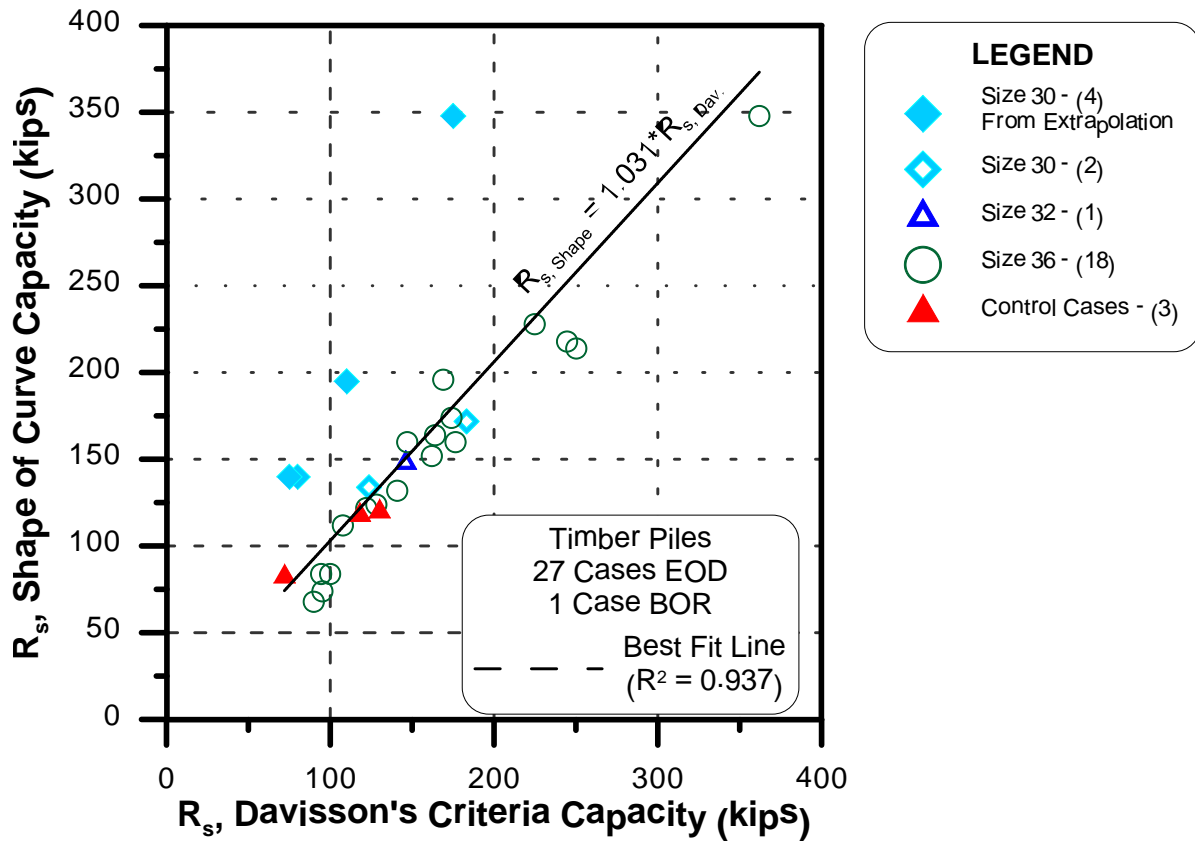


**Figure 107. Shape of Curve versus Davisson's Criteria for determining the static capacity of 28 timber piles**

### 6.2.3 Extrapolated Non-Failed Load Tests

The timber pile data set includes four (4) piles from one test site (TS #13) which were statically loaded but did not reach failure. Given the limited number of cases presented (25 combined EOD and BOR), an extrapolation procedure was performed to accurately predict the static capacity from the non-failed load tests. The extrapolation procedure followed is described in FHWA-RD-99-170 (Paikowsky and Tolosko, 1999). The resulting extrapolated curves are shown in Figures 108 through 111.

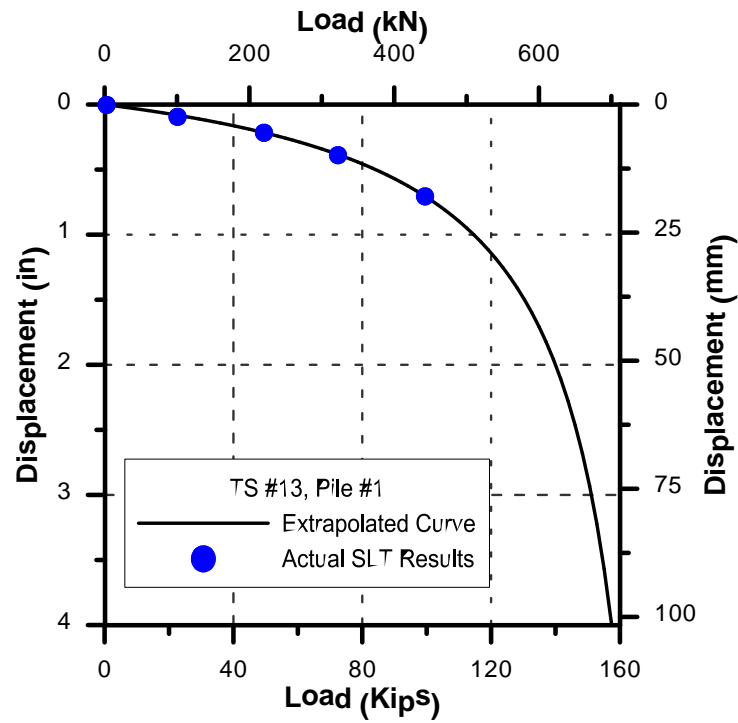


Figure 108. Extrapolated load-displacement curve for TS #13 Pile #1

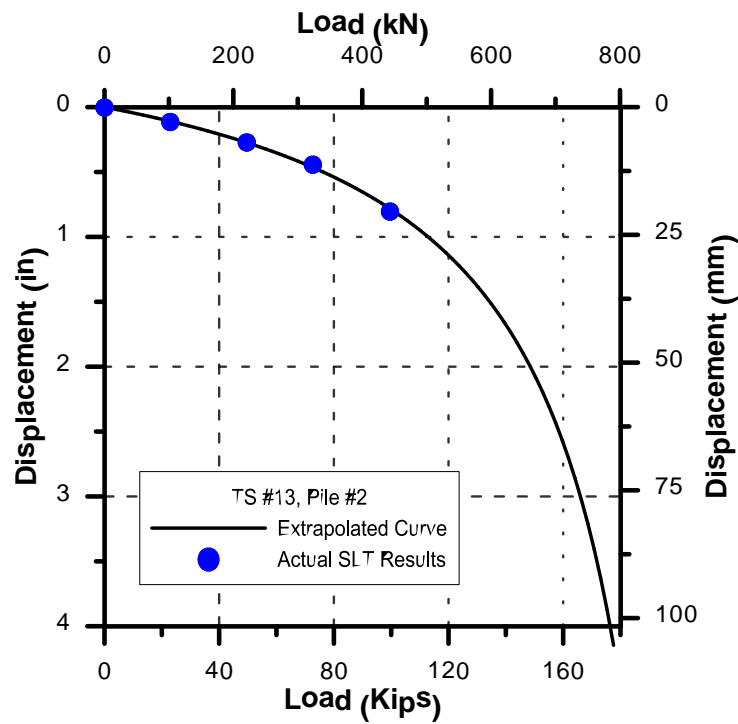


Figure 109. Extrapolated load-displacement curve for TS #13 Pile #2

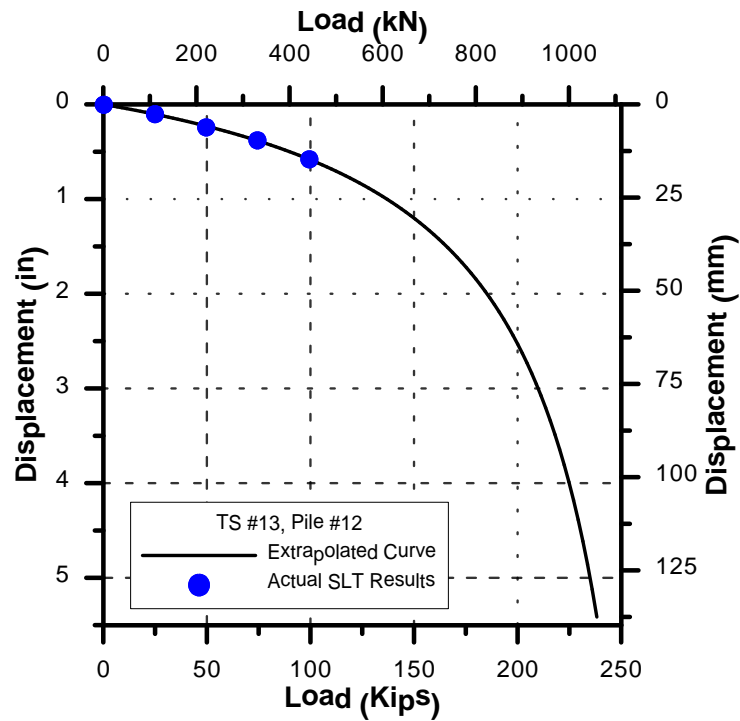


Figure 110. Extrapolated load-displacement curve for TS #13 Pile #12

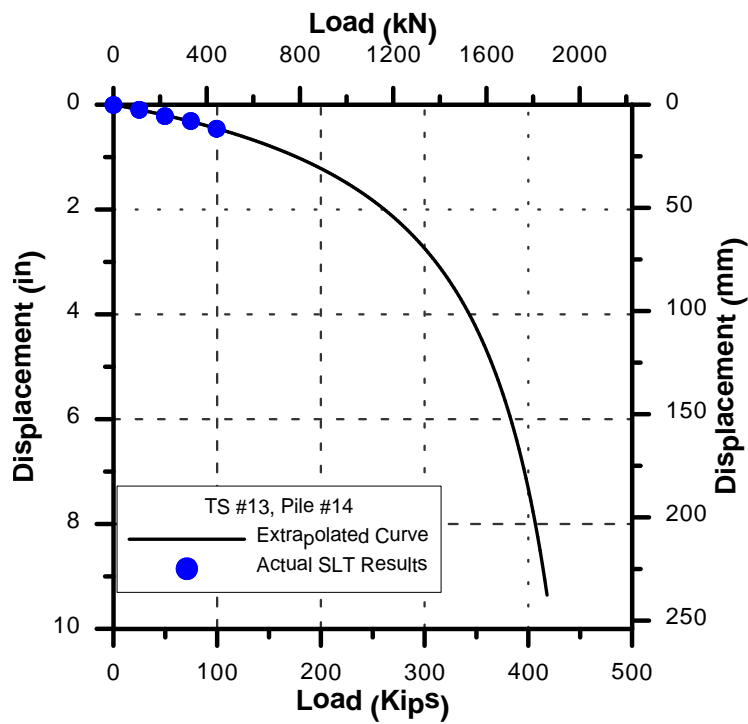


Figure 111. Extrapolated load-displacement curve for TS #13 Pile #14

## 6.3 Statistical Analysis

### 6.3.1 Equation Modification

Table 69 provides the statistical analysis for the 25 timber pile cases. The database was broken down based on driving resistance, typically resistance greater than 2 BPI, and resulting bias of measured versus predicted axial capacity. Under an initial investigation, the MPF12 equation in its current format yielded a high over-prediction of the piles' static capacity. This can be attributed to the nature of the wood where large energy is lost in impact and stress propagation, and as such, different from steel or concrete piles. The first three rows of Table 69 present, therefore, the statistical analysis in terms of a fixed reduction in the ultimate capacity determined from the MPF12 equation. Both a 50% and 75% reduction in the predicted capacity are presented. The  $(0.50) \times \text{MPF12}$  equation provides the most accurate predictions, while using a simplified factor (0.50) particularly when the  $\text{BC} \geq 2\text{BPI}$  and outliers are removed. This MPF12 format resulted with a mean bias of  $m_\lambda = 1.07$  for  $n = 25$  cases and a  $\text{COV}_\lambda = 0.28$ .

In principle one can use the MPF12 in its prevailing format and a reduced resistance factor (e.g.  $\phi = 0.30$ ). This will result with the same factored resistance but a nominal resistance (predicted capacity) of twice the actual magnitude. Such approach is unwarranted as it leads to unrealistic capacities instead of dealing with factored accurate predictions.

**Table 69. Summary of statistics and resistance factors for timber piles**

Equation	# of Cases	$m_\lambda$	$\sigma_\lambda$	$\text{COV}_\lambda$	Resistance Factor $\phi$			Comments <sup>1</sup>
					FOSM	MC	Recom.	
<b><math>(0.50) \times \text{MPF12}</math></b>	25	1.23	0.45	0.36	0.59	0.64	<b>0.60</b>	$m_\lambda > 1$ , Safe side
<b><math>(0.75) \times \text{MPF12}</math></b>	25	0.82	0.30	0.36	0.39	0.43	N/A	$m_\lambda < 1$ , Unsafe side
<b>MPF12</b>	25	0.61	0.22	0.36	0.29	0.32	N/A	$m_\lambda < 1$ , Unsafe side
<b><math>(0.50) \times \text{MPF12}</math></b>	23	1.14	0.33	0.29	0.64	0.71	<b>0.60</b>	Omit high outliers <sup>2</sup>
<b><math>(0.50) \times \text{MPF12}</math></b>	21	1.18	0.47	0.40	0.53	0.57		B.C. $\geq 2 \text{ bpi}$ <sup>3</sup>
<b><math>(0.50) \times \text{MPF12}</math></b>	19	1.07	0.30	0.28	0.60	0.67		B.C. $\geq 2 \text{ bpi}$ <sup>3</sup> ; Omit high outliers <sup>2</sup>

Notes:

<sup>1</sup> All results limited B.C. to 15 bpi

<sup>2</sup> Omit cases w/ S.D.  $\geq 1.90$ ; TS #13 Pile #14, TS #26 Pile #26

<sup>3</sup> Omit cases w/ B.C.  $< 2.0 \text{ bpi}$ ; TS #15 Pile #2, TS #26 Pile #9, TS #31 Pile #3, TS # 38 Pile #2

<sup>4</sup> Omit cases with S.D.  $\geq 1.60$ ; TS #26 Pile #6

### 6.3.2 Performance and Graphical Presentation

The remaining three rows of Table 69 refer, therefore, to the statistical analysis of the modified equation. Graphical presentation of the timber pile analysis is shown in Figures 112 and 113. Figure 112 displays all 25 cases used in the statistical analysis with three (3) additional control cases. Based on the presented results, the following conclusions can be made:

1. The calculated pile capacities are typically less than 60% of the measured static capacity. Based on the control cases, (0.50)\*MPF12 provided highly accurate predictions for two (2) cases and over-predicted the capacity of one (1) timber pile. Despite the over-prediction, with the appropriate load and resistance factors the factored resistance (allowable capacity) is safe (allowable capacity is less than the measured static capacity).
2. An under-prediction is evident for low driving resistance ( $BC \leq 2$ ), with a relatively large scatter in the bias throughout the driving resistances. The scatter in the bias is significantly diminished for high driving resistances. Relatively accurate predictions for those piles with high resistances are evident in Figure 113, where the mean bias is typically less than 1.4.

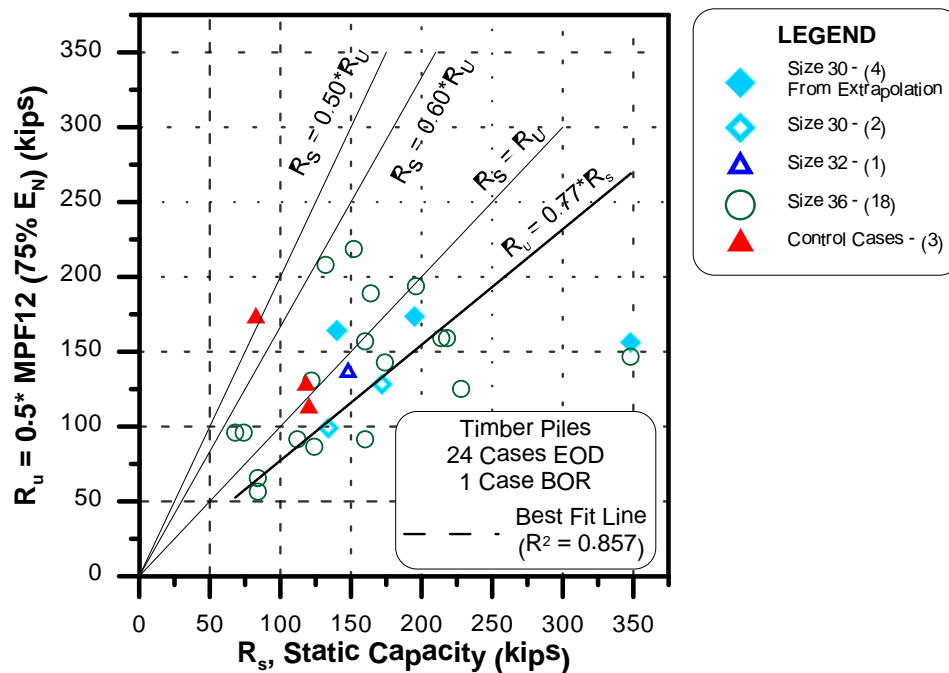


**Figure 112. Measured static capacity vs. New MnDOT dynamic equation prediction for 28 timber pile cases**



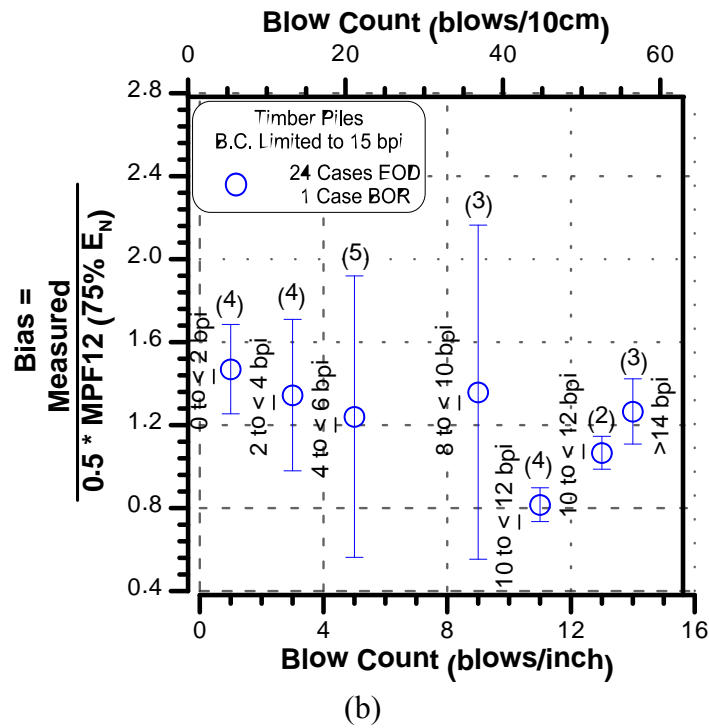
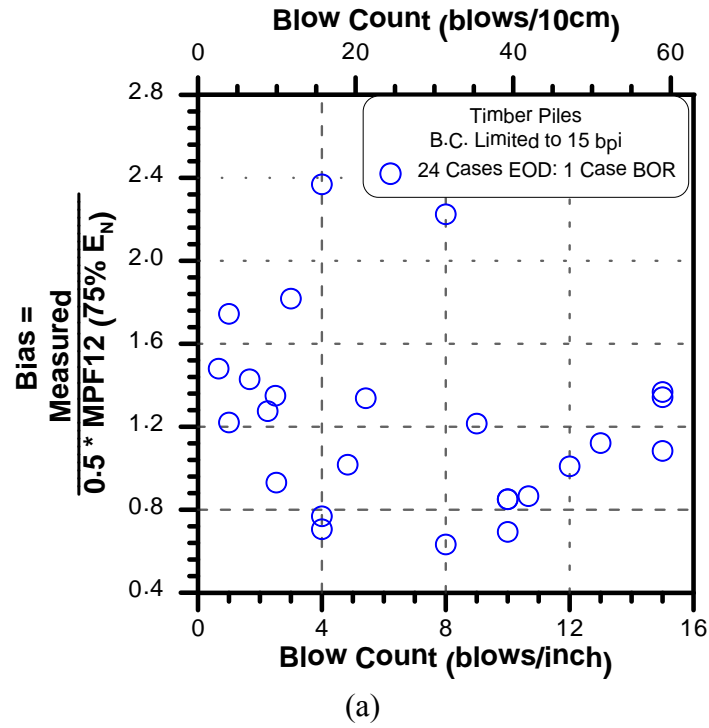


**Figure 113. Bias vs. blow count for timber pile cases for the (0.50)\*MPF12 (75% energy) where the blow count is limited to 15bpi maximum; (a) linear scale, and (b) average and standard deviation per 2bpi segments**

### 6.3.3 Control Cases

Table 70 summarizes the details and results of the control case. For two of the cases, a good match (bias of about 1.0) exists between the measured and calculated capacities. For one of the cases, the equation significantly over-predicts the pile capacity but remains safe when considering a resistance factor of 0.6 and a typical combination of load factors of  $\gamma_D = 1.25$   $\gamma_L = 1.75$  leading to the approximate relations of  $FS \approx 1.4167/\phi$  (Paikowsky et al. 2004).

**Table 70. Summary of timber pile control cases**

Case #	Pile Diameter (inch)	Hammer Type	Rated Hammer Energy (kip-ft)	Blow Count (bpi)	$R_s$ (kips)	0.5* MPF12, $R_u$ (kips)	$R_s/R_u$	0.60* $R_u$ (kips)
TS#23 Pile#1	12.00	D-12	22.50	12.70	82.50	172.85	0.48	103.71
TS#29 Pile#1	11.16	B225	25.00	2.00	120.00	112.67	1.07	67.60
TS#29 Pile#2	11.16	B225	25.00	3.00	118.00	127.92	0.92	76.75

## 6.4 Resistance Factors

Table 69 summarizes the calculated and recommended resistance factors. Figure 112 presents the application of resistance factors  $\phi = 0.5$  and  $\phi = 0.6$  to the analyzed data. A resistance factor of  $\phi = 0.6$  is recommended.

## 6.5 Recommendations

1. A multiplier of 0.50 should be used for MPF12 when applied to capacity evaluation of driven timber piles (refer to equation (25), section 4.6).

$$Rn = 10 \sqrt{\frac{WH}{1000}} \log\left(\frac{10}{s}\right) \quad (27)$$

2. A resistance factor of  $\phi = 0.6$  should be used with the modified equation.

## **7 MINNESOTA LOAD TESTING PROGRAM**

### **7.1 Overview**

The MnPILE Static Load Test program is a Load Testing Program Development project initiated and conducted by MnDOT. The program is promoted and directed by Mr. Derrick Dasenbrock from the MnDOT Foundations Unit. This chapter provides a summary of this effort in the form of two load test results at bridge locations. The chapter includes the presentation and interpretation of the results and the examination of the prediction methods, focusing on the MPF12.

Two static load tests (axial compression tests) were conducted during the contract period for this project. One load test was conducted in Victoria, Minnesota (state project no. 1002-89) in June 2012. The second was conducted in Arden Hills (Old Snelling Ave.), Minnesota (state project no. 6285-62716) in January 2013.

For each of these projects, and for subsequent projects for which load tests are scheduled, a significant effort has been made to develop and improve the load testing specifications and construction plans in hopes of greatly reducing the effort needed on future projects. Having a complete and accurate set of specifications and accompanying plans will allow future tests to be included early in project discussions, enabling greater ability to expedite the process and allow load tests to be performed more readily. Such upcoming projects as Dresbach and others, continue to improve and broaden the specification language and the plan documents to allow greater efficiency in the MnPILE program as it moves forward. Further discussion on the subject is presented in Chapter 8.

The intent of this chapter is threefold. First, to summarize the data obtained from the two load tests conducted thus far and to show the performance of the MPF12 formula relative to the original MnDOT Dynamic formula (the latter of which was specified for both projects since contracts preceded adoption of the new MPF12 formula developed during this project). Second, to establish the data needed from such load tests to develop a useful database which will allow further refinement of the MPF12 formula and the MnDOT pile driving practice in general. Third, to provide the data collected from the geotechnical subconsultants who performed the two static load tests described in this chapter, with reference to the most critical information from this documentation. The reports provided by the subcontractors are presented in the Appendices C and D.

## 7.2 TP1 Load Test at Victoria, MN

### 7.2.1 General

The load test at Victoria was the inaugural application of the 500 ton load frame designed and fabricated as part of the MnPILE Load Test Program. Figure 114 shows the load frame prior to the load test being conducted. The frame is supported by four reaction piles.



**Figure 114. 500 ton MnDOT load frame being used at Bridge 10003 in Victoria, Minnesota**

### 7.2.2 Static Capacity Evaluation

One traditional boring and ten cone penetration soundings were performed by MnDOT at the site in order to develop soil stratigraphy and to aid in foundation design. Based on the SPT data collected from the soil boring, a static capacity was estimated as a function of pile length using the FHWA DRIVEN software. Various CPT-based methods/models were also used to estimate pile capacity as a function of depth for the CPT data collected at the site. Figure 115 presents a summary of these static capacity predictions as a function of pile toe elevation. The average predicted pile capacity at the tip elevation at which the load test was conducted was about 125 tons, consistent for most of the seven models evaluated. Twelve inch diameter closed-end pipe piles were used for the project, having a wall thickness (w.t.) of 0.25 inches. The piles were comprised of Grade 3 steel, with a minimum yield stress of 45ksi required.

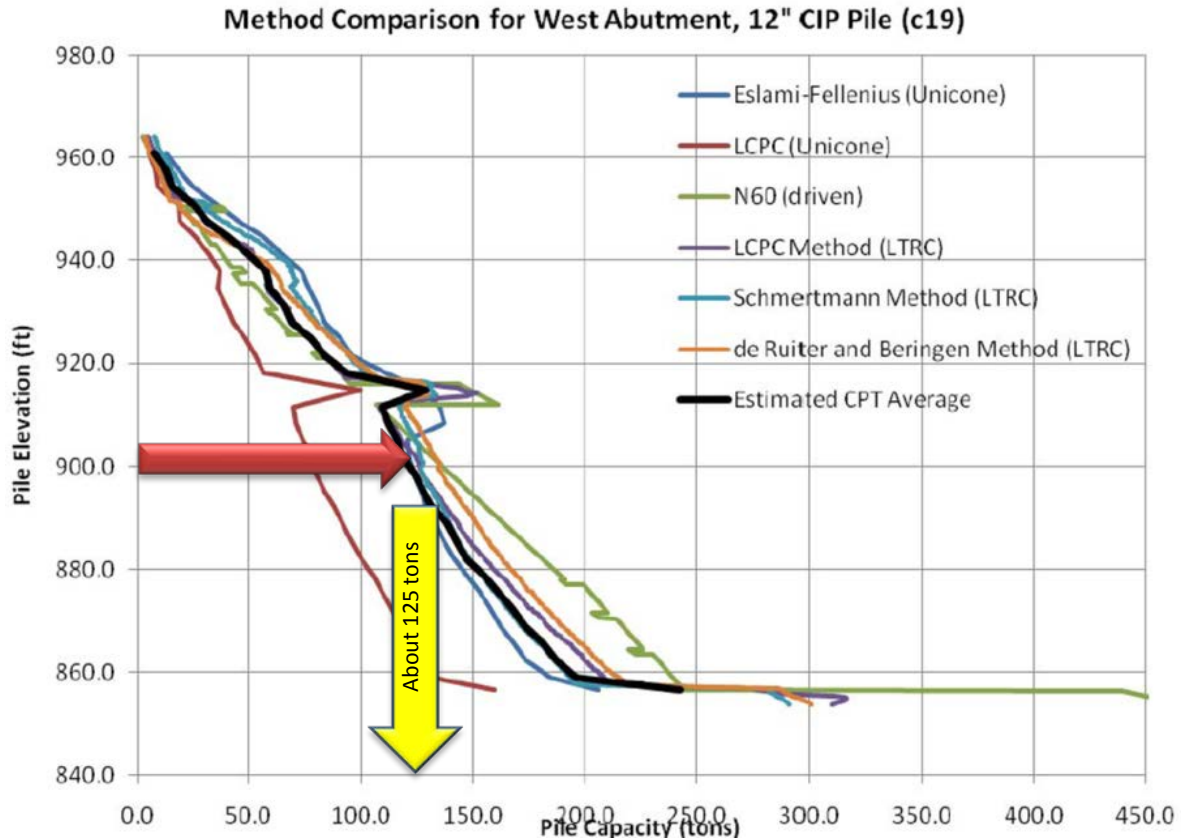


**Figure 115. Static pile capacity predictions for Bridge 10003 in Victoria, Minnesota**

### 7.2.3 Load and Resistance

The factored design load for Bridge 10003 piles was 99.2 tons/pile, based on Strength I Load Combination as presented in Table 71. Table 71 also shows a summary of the Required Nominal Resistance values for each of the field control methods.

Required Nominal Pile Bearing Resistance values ( $R_n$ ) were approximately 250 tons/pile, 180 tons/pile and 125 tons/pile for the original (old) MnDOT Dynamic Formula, Energy Approach using the PDA and the Static Load Test field control methods, respectively, as presented in Table 71 as well. Using the new MPF12 formula and the associated resistance factor of 0.5 would have required a nominal resistance of approximately 200 tons/pile.

**Table 71. Computed pile load and required nominal pile bearing resistances for Bridge 10003 in Victoria, Minnesota (per project plans)**

West Abutment Computed Pile Load (Tons/Pile)	
Factored Dead Load + Earth Pressure	82.8
Factored Live Load	16.4
*Factored Design Load	99.2

\*Based on Strength I load combination

West Abutment Required Nominal Pile Bearing Resistance $R_n$ (Tons/Pile)		
Field Control Method	$\phi$ dyn	* $R_n$
MnDOT Nominal Resistance Formula	0.40	247.9
Energy Approach	0.55	180.4
MPF12	0.50	198.4
Static Load Test	0.80	124.0

\* $R_n = (\text{Factored Design Load})/\phi$  dyn

#### 7.2.4 Dynamic Observations, Predictions, and Static Load Test Results

Detailed static and dynamic load test results were reported by Minnowa Construction, Inc. and prepared by Braun Intertec Corporation are presented in Appendix C. The pile 12 inch diameter and 0.25 inch w.t. was driven 63 ft with a diesel hammer D19-42. Table 72 presents a summary of the field and office capacity prediction methods at the end of drive (EOD) and subsequent restrikes. Note; the second restrike was carried out after the static load test. The estimated capacity of the pile at the end of initial drive was approximately 222 tons, significantly higher than the measured capacity but below the required 250 tons for the resistance factor of 0.4 per past practice. The new formula (MPF12) at 168 tons estimated more accurately the measured bearing but is also below the required 198 tons for the resistance factor of 0.5. CAPWAP analysis based on dynamic records at the end of initial drive estimated a nominal geotechnical resistance of 138 tons, which is the best match to the nominal resistance measured at the load test but still less than the required 153 tons with a resistance factor of 0.65.

Figure 116 shows the load test data. The load-displacement relations indicating a maximum applied load of 134 tons and suggesting a general shear mode failure under a small tip resistance. A Static Load test capacity of 132 tons can be interpreted based on Davisson's criterion, which met the required 124 ton capacity using a resistance factor of 0.8.

Table 73 presents the nominal and factored resistances of the various testing methods for TP1. Based on EOD, MPF12, Old MnDOT equation and CAPWAP would have required the pile to be driven a deeper into the soil in order to gain capacity (unless restrikes were used to show increased capacity due to setup.) The Energy Approach would have shown at the EOD the pile capacity as valid and hence is highlighted as the best match for factored resistance at the EOD. The estimated static capacity of 125tons (see section 7.2.2) based on field investigation, matched

exceptionally well the static load test results, but when applied with a resistance factor of 0.45, would result with unacceptable pile penetration and would require a significantly deeper penetration design.

For the 3 day restrike (BOR3), the factored resistance obtained from the MPF12 formula best match the required resistance and along with the Energy Approach at BOR3 would indicate the pile to be valid. The CAPWAP and the old MnDOT equation while indicating the same are unsafe as they significantly over predict. The Energy Approach CAPWAP and MPF12 predict well for the restrike after the load test with the factored CAPWAP resistance for the last BOR matching well the factored resistance of the EA at EOD. The old MnDOT equation systematically shows unsafe nominal and factored resistances at both restrikes.

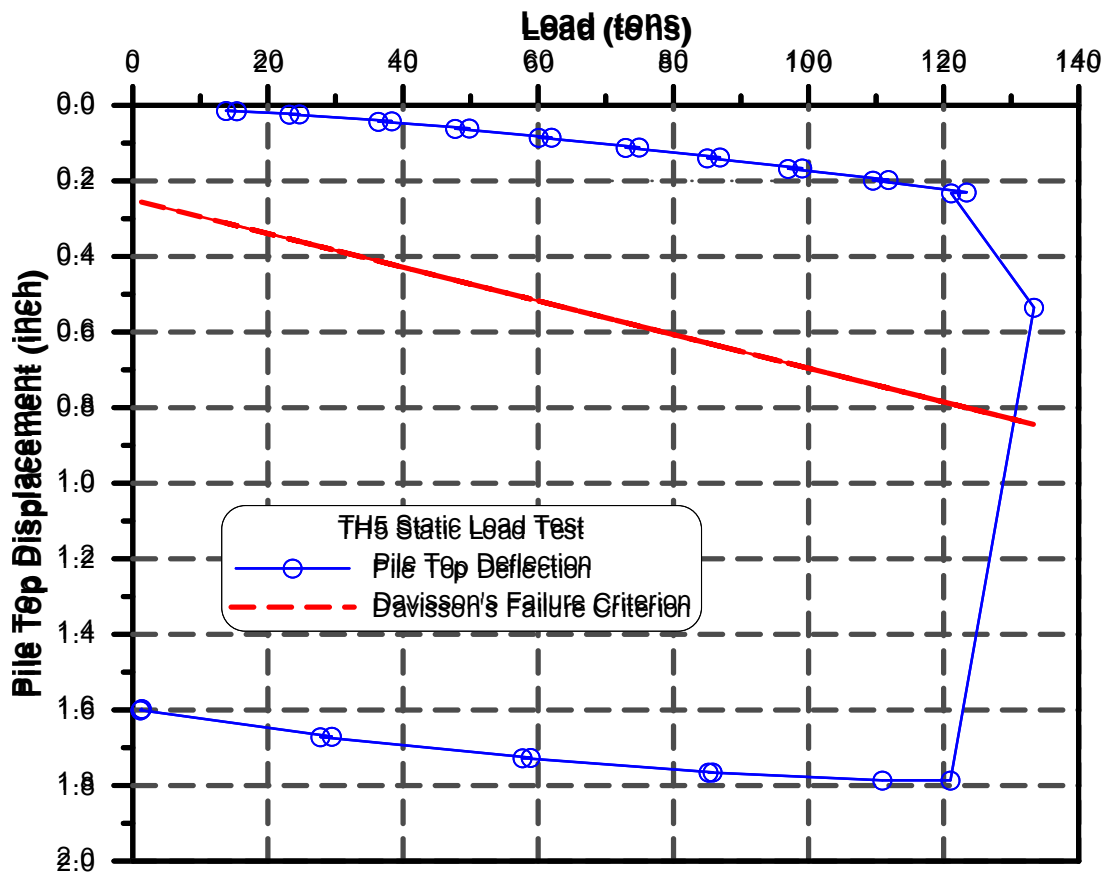


Figure 116. Additional load vs. displacement of pile top – static load test results for Bridge 10003 in Victoria, Minnesota

**Table 72. Nominal resistances from dynamic analyses of the test pile TP1**

Driving <sup>1</sup> State	Date <sup>1</sup>	Driving <sup>1</sup> Resistance (BPF)	Field <sup>1</sup> Observation of Hammer Stroke (feet)	EMX <sup>1</sup> (kip-ft)	DMX <sup>1</sup> (inch)	Maximum <sup>1</sup> Case Method Capacity (tons)	Signal Match <sup>1</sup> CAPWAP (tons)	Energy Approach <sup>2</sup> EA (tons)	MPF12 <sup>3</sup> (tons)	Old MnDOT <sup>4</sup> formula (ton)
EOD	6-15-2012	30 <sup>5</sup>	7.75	21.0	0.90	143	138	194	156	222
BOR3	6-18-2012	80 <sup>5</sup>	9.5	28.2	0.96	242	244	305	221	465
BOR11 After SLT	6-26-2012	240 <sup>5</sup>	8.0	15.3	0.65	223	219	262	247	548

Notes:

1. See Appendix C report by Minnowa Construction, Inc., dated July 25, 2012.
2. See Table 40, equation 1. See Paikowsky et al. (2004) for performance and LRFD calibration.
3. See section 4.6 equation (25) including limiting energy and blow count.
4. Using the general equation Table 40, equation 6, with  $W_r = 4015\text{lb}$ ,  $M = 2984\text{lb}$ .
5. Equivalent BPF values calculated from BPI observations.

**Table 73. Nominal and factored resistances of the various testing methods**

Factored Design Load (tons)	Driving State	CAPWAP			EA			MPF12			Old MnDOT Eq.			SLT		
		$R_n$ (tons)	$\phi^1$	$R_r$ (tons)	$R_n$ (tons)	$\phi^1$	$R_r$ (tons)	$R_n$ (tons)	$\phi^2$	$R_r$ (tons)	$R_n$ (tons)	$\phi^3$	$R_r$ (tons)	$R_n$ (tons)	$\phi$	$R_r$ (tons)
99.2	EOD	138	0.65	88	194	0.55	107	156	0.50	78	222	0.40	88	134	0.80	107
	BOR3	244	0.65	159	305	0.40	122	221	0.50	110	465	0.40	186			
	BOR11 After SLT	219	0.65	108	262	0.40	105	247	0.50	123	548	0.40	219			

Notes:

1. See Paikowsky et al. (2004) for calibrations and R.F. recommendations.
2. See section 4.6 and adoption by MnDOT.
3. Un-calibrated R.F. as used by MnDOT when adopting LRFD.



Best match for factored resistance



Best match for nominal resistance



## **7.3 TP2 Load Test at Arden Hills (Old Snelling)**

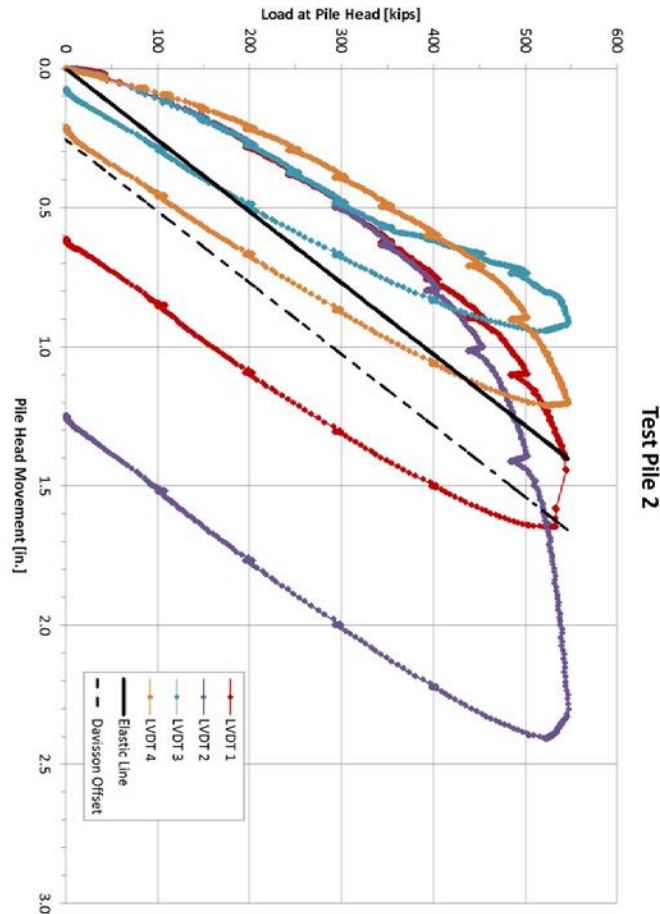
### **7.3.1 General**

The same load frame used at the Victoria load test on TP1 was also used at Arden Hills for load test TP2 conducted in January 2013. The Geotechnical Subconsultant for this load test was American Engineering Testing, Inc. and the submitted report is presented in Appendix D. At this site, 12.75 inch diameter closed-end pipe piles with 0.25 inch wall thickness were used. The contractor indicated that the steel had a yield strength of 60 ksi.

### **7.3.2 Static Load Test**

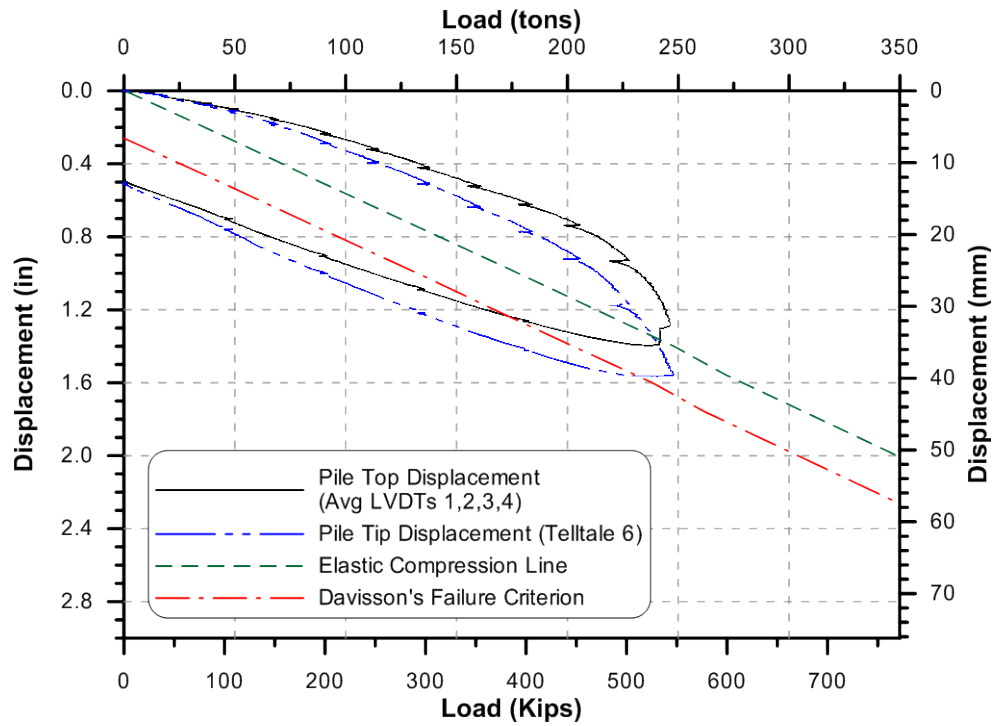
The test pile was driven on December 19, 2012 with APE D25-32 Diesel hammer to a penetration depth of 63 ft. The pile was not filled with concrete prior to the static load test, which was conducted on January 14, 2013. Thus, almost one month had passed from the end of initial drive to the time of the load testing. The 500 ton load frame was installed and the load test plan was to fail the pile geotechnically in order to establish the static capacity. The load versus pile head movement for each of the four LVDT's used for monitoring the pile's top is presented in Figure 117. As the pile was loaded to around 275 tons, the pile yielded structurally near the pile top and the load test was stopped. Data collected indicate that the pile was on a verge of failure (geotechnically). Figure 117 suggests that according to two LVDT's (1 and 2), pile capacity is about 268 tons. The data in Figure 117 also suggested that either the load application was not vertical or the pile was not installed vertically, hence, with the increased loading and with lack of concrete in the section, the developed moments resulted with the structural failure of the pile.

Figure 118 presents the average pile top displacement based on the data presented in Figure 117. As the measured displacements in Figure 117 suggest uneven pile top displacement, the relations presented in Figure 118 are speculative and assuming even average pile top movement though it was clearly not the case. The displacement values for the top of the pile in Figure 118 were developed by averaging all LVDT's (1 – 4) readings. The pile's tip displacement against the applied load is also presented in Figure 118. The fact that the pile tip displacement exceeds the average of all LVDT's suggest that either (a) the average of the four top displacements don't represent correctly the pile top movement, or (b) the pile tip displacement is not accurate due to several possibilities (one of which is the bending in the pile), or the combination of both. The relationships in Figure 117 were re-analyzed by averaging only LVDT's 1 and 2 that seem to better represent the actual pile top movement. The results are presented in Figure 119, which seem to present a better load-displacement behavior when judged by the pile tip movement, though still not correct relations between the two.



**Figure 117. Load versus pile head movement for each of the pile's top LVDT sensors of Test Pile 2 (per Report No. 22-01025 submitted to MnDOT by American Engineering Testing, Inc.)**

The relations between load and displacement in Figures 118 and 119 were re-evaluated and the procedure proposed by Paikowsky and Tolosko (1999) was applied in order to estimate the pile behavior beyond the maximum applied load. Figures 120 and 121 present the outcome of this procedure suggesting the pile capacity to be as high as 288 tons, or more realistically, 265 tons. Due to the relatively small gap between the two, an average value of 277 tons was chosen as a representative of the capacity of test pile TP2, its nominal resistance. Without having the actual static load test geotechnical capacity, comparisons to dynamic formula are made in the next section assuming the capacity is 277 tons and knowing the limitation of this value. The load test did serve as a proof test, showing that the 125 tons required nominal resistance for a resistance factor of 0.8 (based on a static load test as construction control) was met. The measured load of around 275 tons at structural failure, while less than the geotechnical capacity anticipated, was more than twice the factored load for the project.



**Figure 118. Load-displacement relations for TP2 based on top displacement of LVDT 1-4 and tip displacement based on LVDT 6**

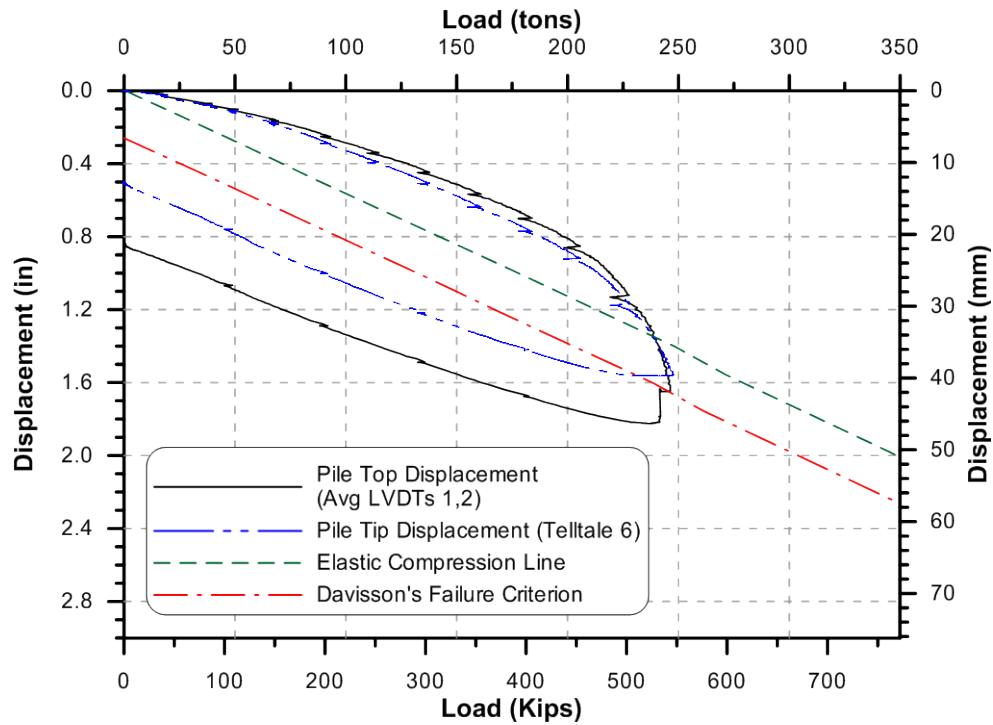


**Figure 119. Load-displacement relations for TP2 based on top displacement of LVDT 1-2 and tip displacement based on LVDT 6**

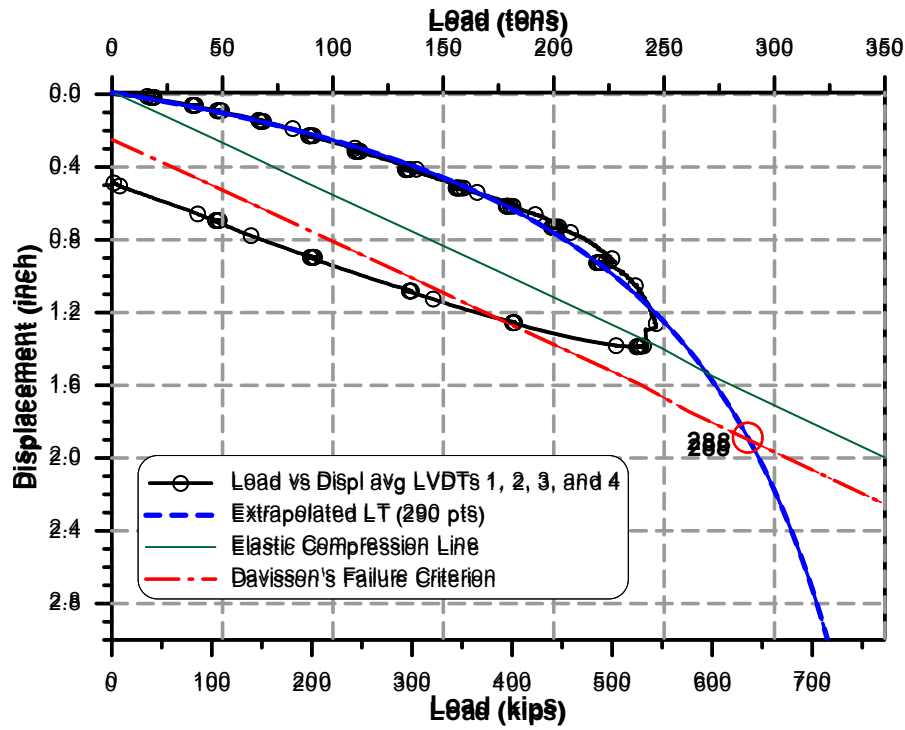


Figure 120. Measured and extrapolated load-displacement relations for TP2 based on LVDT's 1 - 4

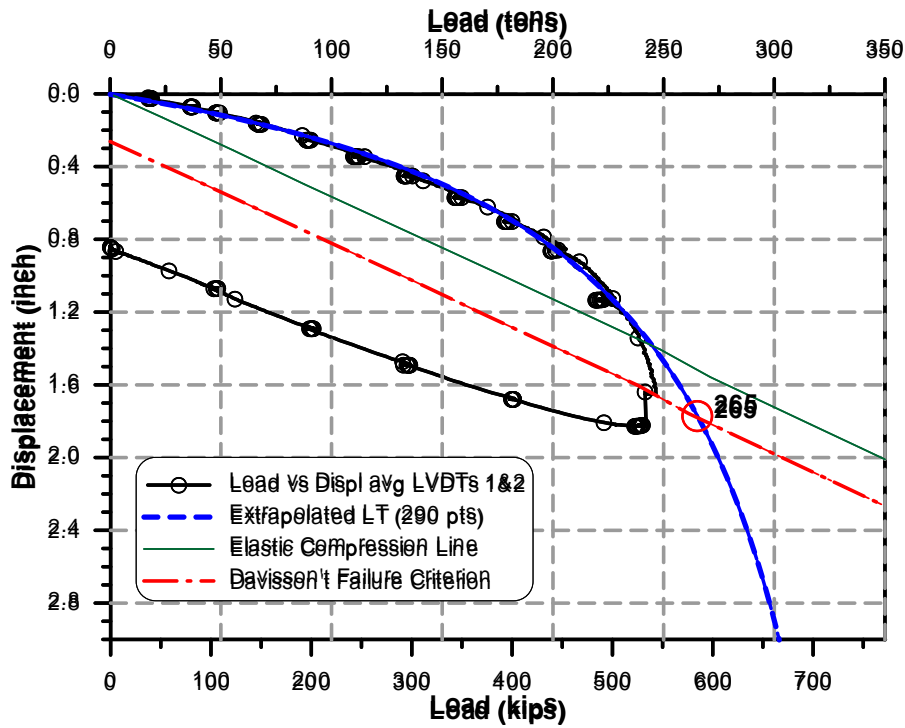


Figure 121. Measured and extrapolated load-displacement relations for TP2 based on LVDT's 1 - 2

### **7.3.3 *Dynamic Observations and Predictions***

Detailed static and dynamic load test results were reported by American Engineering Testing, Inc. and are presented in Appendix D. The pile 12 inch diameter and 0.25 inch w.t. was driven with a diesel hammer, APE D25-32. Table 74 presents a summary of the field and office capacity prediction methods at the end of drive (EOD) and subsequent restrikes. Note: the second restrike was carried out after the static load test. The estimated capacity of the pile at the end of initial drive was approximately 326 to 386 tons (depending on the stroke), significantly higher than the measured or estimated capacity and exceeding the required 313 tons for the resistance factor of 0.4 per past practice. The new formula (MPF12) at 261 tons estimated more accurately the measured/estimated bearing and matches well the required 250 tons for the resistance factor of 0.5. CAPWAP analysis based on dynamic records at the end of initial drive estimated a nominal geotechnical resistance of 141 tons, which is about half of the nominal resistance measured at the load test and a factored resistance less than half of the required 192 tons with a resistance factor of 0.65.

Table 75 presents the nominal and factored resistances of the various testing methods for TP2. Based on EOD, the EA and in particular CAPWAP the pile would have been required to be driven deeper into the soil in order to gain capacity (unless restrikes were used to show increased capacity due to setup.) The dynamic formulae MPF12 and Old MnDOT equation would have shown at the EOD the pile capacity as valid and hence is highlighted as the best match for factored resistance at the EOD. In contrast to the extreme over-prediction of the previous MnDOT formula, the estimated static capacity of 261 tons based on MPF12, matched exceptionally well the static load test results and was the best prediction of all the dynamic methods.

For the 1 day restrike (BOR1), the factored resistance obtained from the MPF12 formula and CAPWAP best match the required factored resistance also at BOR27, which would indicate the pile to be valid. The old MnDOT equation consistently predicts unsafe capacity as it significantly over-predicts. The Energy Approach and MPF12 predict well the nominal capacity in comparison to all other methods.

**Table 74. Nominal resistances from dynamic analyses of the test pile TP2**

Driving <sup>1</sup> State	Date <sup>1</sup>	Driving <sup>1</sup> Resistance (BPF)	Field <sup>1,7</sup> Observation of Hammer Stroke (feet)	EMX <sup>1</sup> (kip-ft)	DMX <sup>1</sup> (inch)	Maximum <sup>1,2</sup> Case Method Capacity (tons)	Signal Match <sup>1</sup> CAPWAP (tons)	Energy Approach <sup>3</sup> EA (tons)	MPF12 <sup>4</sup> (tons)	Old MnDOT <sup>5</sup> formula (ton)
EOD	12-19-2012	240 <sup>6</sup>	6.0/7.1	19.9	1.107	145	141	206	250/272	326/386
BOR1	12-20-2012	320 <sup>6</sup>	9.9	29.9	1.370	202	199	255	306	567
BOR27 After SLT	1-15-2013	960 <sup>6</sup>	9.1	28.5	1.190	484	223	284	306	582

Notes:

1. See Appendix D report by American Eng Testing Inc., dated January 30, 2013.
2. Case method evaluation at each stage was calculated using a different  $J_c$  factor.
3. See Table 40, equation 1. See Paikowsky et al. (2004) for performance and LRFD calibration.
4. See section 4.6 equation (25) including limiting energy and blow count.
5. Using the general equation Table 40, equation 6, with  $W_r = 5512\text{lb}$ ,  $M = 2386\text{lb}$ .
6. Equivalent BPF values calculated from BPI observations.
7. Read by field inspector / PDA calculation.

**Table 75. Nominal and factored resistances of the various testing methods**

Factored Design Load (tons)	Driving State	CAPWAP			EA			MPF12			Old MnDOT Eq.			SLT		
		$R_n$ (tons)	$\phi^1$	$R_r$ (tons)	$R_n$ (tons)	$\phi^1$	$R_r$ (tons)	$R_n$ (tons)	$\phi^2$	$R_r$ (tons)	$R_n$ (tons)	$\phi^3$	$R_r$ (tons)	$R_n$ (tons)	$\phi$	$R_r$ (tons)
125.0	EOD	141	0.65	92	206	0.55	113	261	0.50	130	346	0.40	138	277 (265-288)	0.80	212 (230)
	BOR1	199	0.65	129	255	0.40	102	306	0.50	153	567	0.40	227			
	BOR27 After SLT	223	0.65	145	284	0.40	114	306	0.50	153	582	0.40	333			

Notes:

1. See Paikowsky et al. (1004) for calibrations and R.F. recommendations.
2. See section 4.6 and adoption by MnDOT.
3. Un-calibrated R.F. as used by MnDOT when adopting LRFD.



Best match for factored resistance



Best match for nominal resistance

## **7.4 Comparisons Between Statically Measured and Dynamically Predicted Capacity**

### **7.4.1 *Nominal Resistance***

Figure 122 is a graphical presentation of the data contained in Tables 73 and 75 in the form of nominal measured and predicted resistances of TP1 and TP2 for EOD condition (Figure 122a) and BOR condition (Figure 122b). The data in Figure 122a shows the excellent match of MPF12 for the EOD condition, while the old MnDOT formula performs consistently as the most unsafe over-prediction. The data in Figure 122b again illustrates the extreme unsafe over-prediction of the old MnDOT equation and the robustness of MPF12 and the dynamic methods that are based on dynamic measurements.

The presentation in Figure 122 shows similar trend to the large database analysis presented in the Phase I report (Paikowsky et al., 2009) and in Chapters 3 and 4 of this manuscript. The presented two cases are the first ones that contain Minnesota SLT data and systematically compare the new MPF12 formula to static and dynamic measurements. It is emphasized that the databases used originally for developing MPF12 did not include any data from Minnesota and the dynamic measurements data used for its evaluation in Phase II did not include any static load test results from Minnesota. These tests are, therefore, extremely important and their continuation is vital for establishing MPF12's applicability to local conditions.

### **7.4.2 *Factored Resistance***

Figure 123 is a graphical presentation of the data contained in Tables 73 and 75 in the form of factored measured and predicted resistances of TP1 and TP2 for EOD condition (Figure 123a) and BOR condition (Figure 123b). The data in Figure 123a shows a relatively good match of all the methods for TP1, and a consistent match of all for TP2. Figure 123b shows a large scatter of the data with the old MnDOT equation consistently over-predicting on the unsafe side, at times in the extreme zone of over-prediction.

The MPF12 was proven very accurate for TP1, and under-predicts similarly to the methods based on dynamic measurements (i.e. CAPWAP and Energy Approach). Considering the limited available data from Minnesota (thus far), the use of the MPF12 formula appears to be valuable, reporting typically more accurate but lower capacities than the old MnDOT formula. The previous formula provided a false sense of security due to the high (but inaccurate) capacities at the end of driving, especially for high driving resistances.

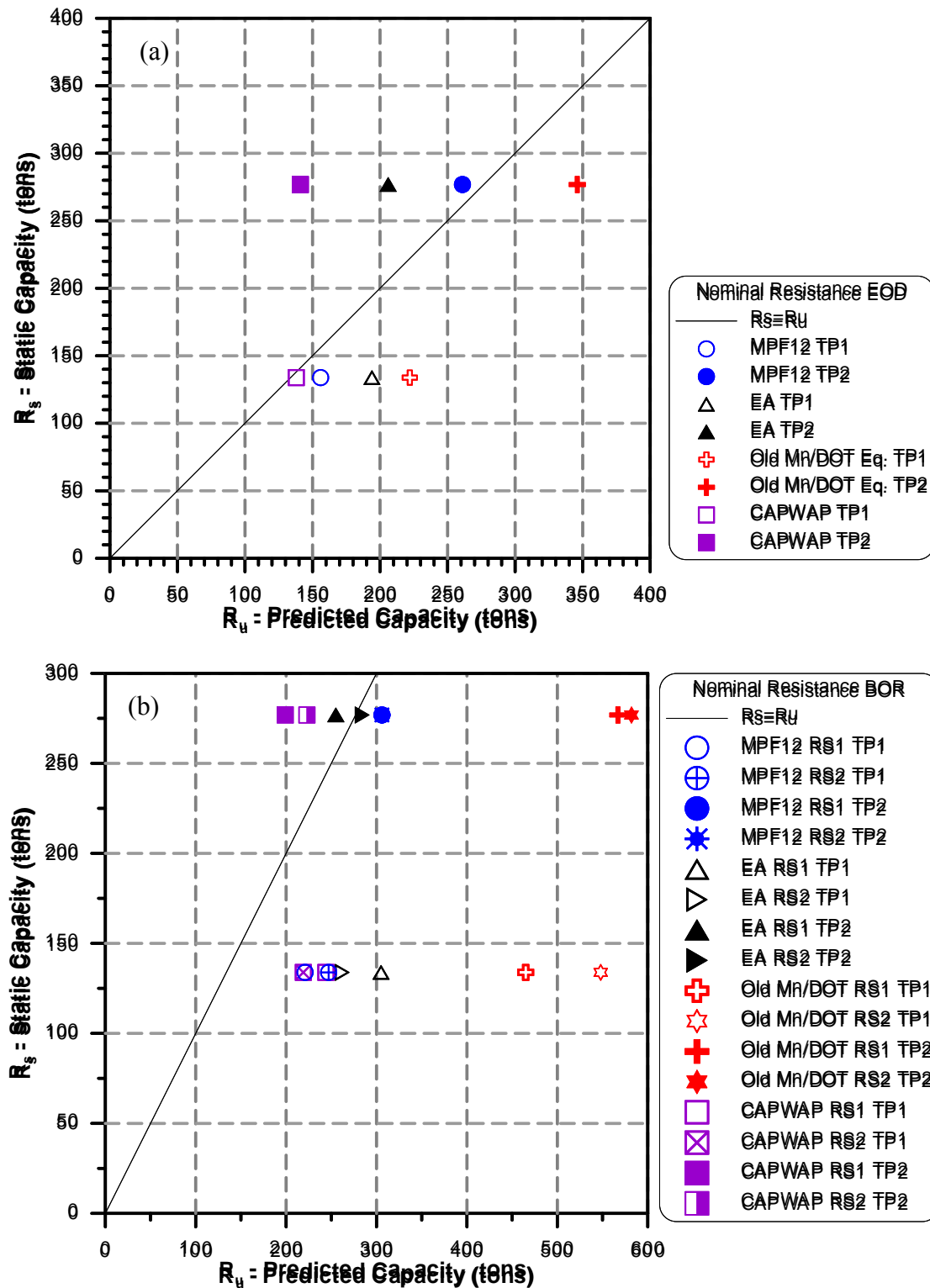


Figure 122. Nominal resistance static capacity ( $R_s$ ) vs. predicted dynamic capacity ( $R_u$ ): (a) EOD and (b) restrikes



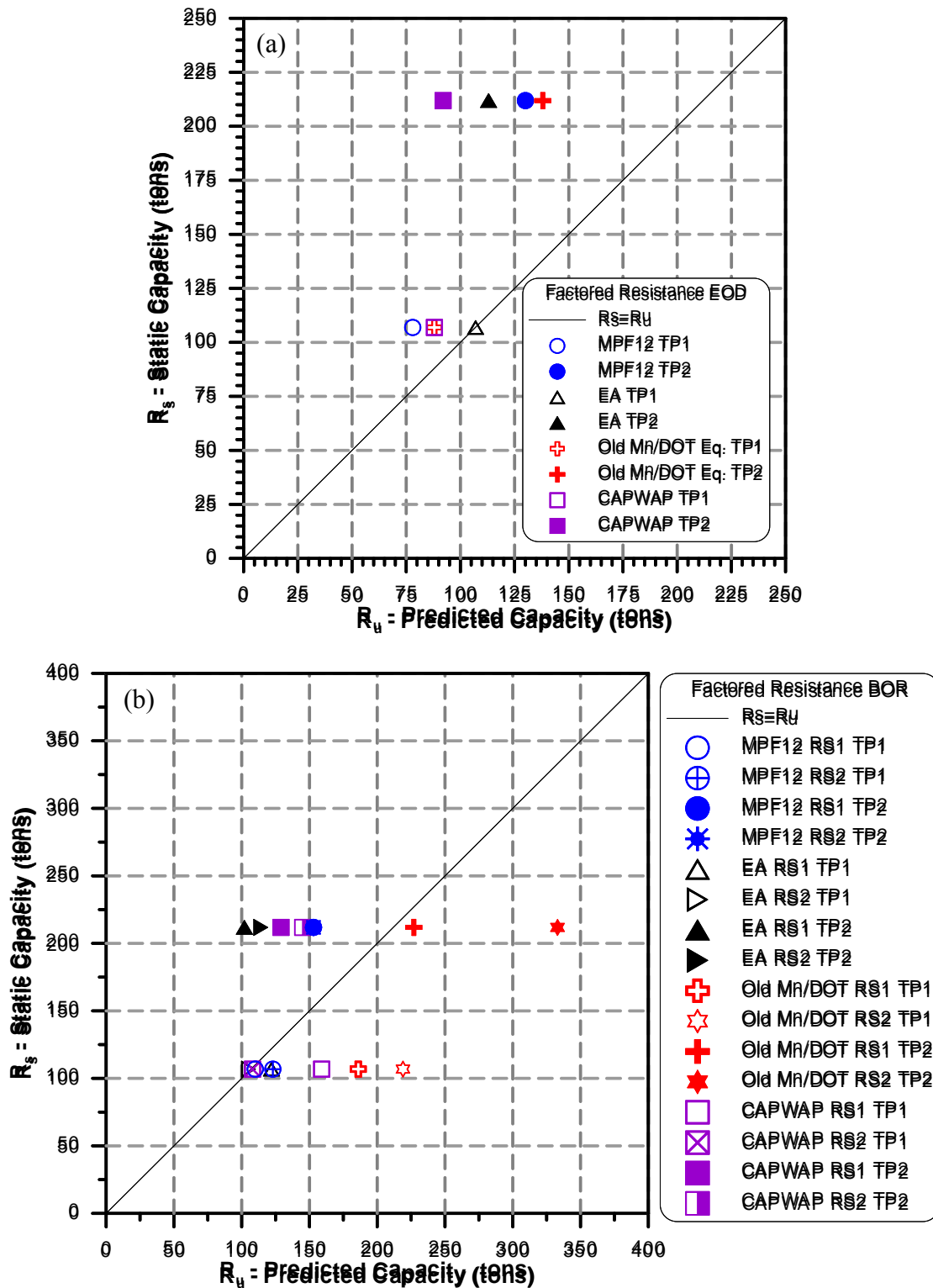


Figure 123. Factored resistance of the nominal static capacity ( $R_s$ ) vs. the factored predicted dynamic capacity ( $R_u$ ): (a) EOD and (b) restrikes

## **8 WEAP ANALYSIS (WAVE EQUATION ANALYSIS PROGRAM)**

### **8.1 Overview**

This chapter comes to address the use of a wave equation analysis simulating the pile driving during design and construction and its utilization in qualifying pile hammers. The modern application of the numerical solution to the one dimensional wave equation (1-D W.E.) for piles under impact was proposed by Smith (1960) with relatively small substantive changes since. The commonly used program in the USA to conduct the analyses is the WEAP (Wave Equation Analysis Program) by GRL/Pile Dynamics Inc. (PDI, 2010).

GRL/Pile Dynamics includes the following description, warnings and suggestions.

“The GRLWEAP program simulates the behavior of a pile driven by either an impact hammer or a vibratory hammer. The program is based on mathematical models, which describe motion and forces of hammer, driving system, pile and soil under the hammer action. Under certain conditions, the models only crudely approximate, often complex, dynamic situations. A wave equation analysis generally relies on input data, which represents normal situations. In particular, the hammer data file supplied with the program assumes that the hammer is in good working order. All of the input data selected by the user may be the best available information at the time when the analysis is performed. However, input data and therefore results may significantly differ from actual field conditions. Therefore, the program authors recommend prudent use of the GRLWEAP results. Soil response and hammer performance should be verified by static and/or dynamic testing and measurements. Estimates of bending or other local non-axial stresses and prestress effects must also be accounted for by the user. The calculated capacity - blow count relationship, i.e. the bearing graph, should be used in conjunction with observed blow counts for the capacity assessment of a driven pile. Soil setup occurring after pile installation may produce bearing capacity values that differ substantially from those expected from a wave equation analysis due to soil setup or relaxation. This is particularly true for pile driven with vibratory hammers. The GRLWEAP user must estimate such effects and should also use proper care when applying blow counts from restrike because of the variability of hammer energy, soil resistance and blow count during early restriking. Finally, the GRLWEAP capacities are ultimate values. They MUST be reduced by means of an appropriate factor of safety to yield a design or working load. The selection of a factor of safety should consider the quality of the construction control, the variability of the site conditions, uncertainties in the loads, the importance of building and other factors.”

## **8.2 Design and Construction Process of Deep Foundations**

Figure 124 presents a flow chart depicting the design and construction process of deep foundations. Commonly, design starts with site investigation and soil parameter evaluation, assessments that vary in quality and quantity according to the importance of the project and complexity of the subsurface. Possible foundation schemes are identified based on the results of the investigation, load requirements, and local practice. All possible schemes are evaluated via static analyses. Schemes for driven piles also require dynamic analysis (drivability) using WEAP for hammer evaluation, feasibility of installation, and structural adequacy of the pile. In sum, the design stage combines, therefore, structural and geotechnical analyses to determine the best prebidding design. This process leads to estimated quantities to appear in construction bidding documents.

Upon construction initiation, static load testing and/or dynamic testing, or dynamic analysis based on driving resistance (using dynamic formulas or wave-equation) are carried out on selected elements (i.e., indicator piles) of the original design. Pile capacity is evaluated based on the construction phase testing results, which determine the assigned capacity and final design specifications. In large or important projects, the pile testing may also be used as part of the design. Two requirements are evident from this process: (1) pile evaluation is carried out at both the design and the construction stage, and (2) these two evaluations should result in foundation elements of the same reliability but possibly different number and length of elements depending on the information available at each stage.

Figure 125 summarizes the above process in a flow chart describing in detail the utilization of WEAP in the design and construction of driven piles. The following sections address various stages associated with the process depicted in Figure 125.

## **8.3 The Accuracy of WEAP for Capacity Evaluation**

Paikowsky et al. (2004) evaluated the accuracy of WEAP in evaluating driven piles' capacity based on driving resistance observed in the field. The evaluation of WEAP effectiveness for capacity predictions is difficult, as a large range of input parameters is possible and the results are greatly affected by the actual field conditions. Examination of the method through analyses making use of default values is therefore the best avenue unless a local database exists where specific soil parameters for modeling had been established and static load tests database exists. Other evaluations, including WEAP analysis adjustments following dynamic measurements (e.g., matching energy), seem to be impractical in light of the other methods available and lead to questionable results regarding their quality and meaning (Rausche et al., 1997; Rausche, 2000). The WEAP analysis was evaluated by Paikowsky et al. (2004) as a dynamic method for pile

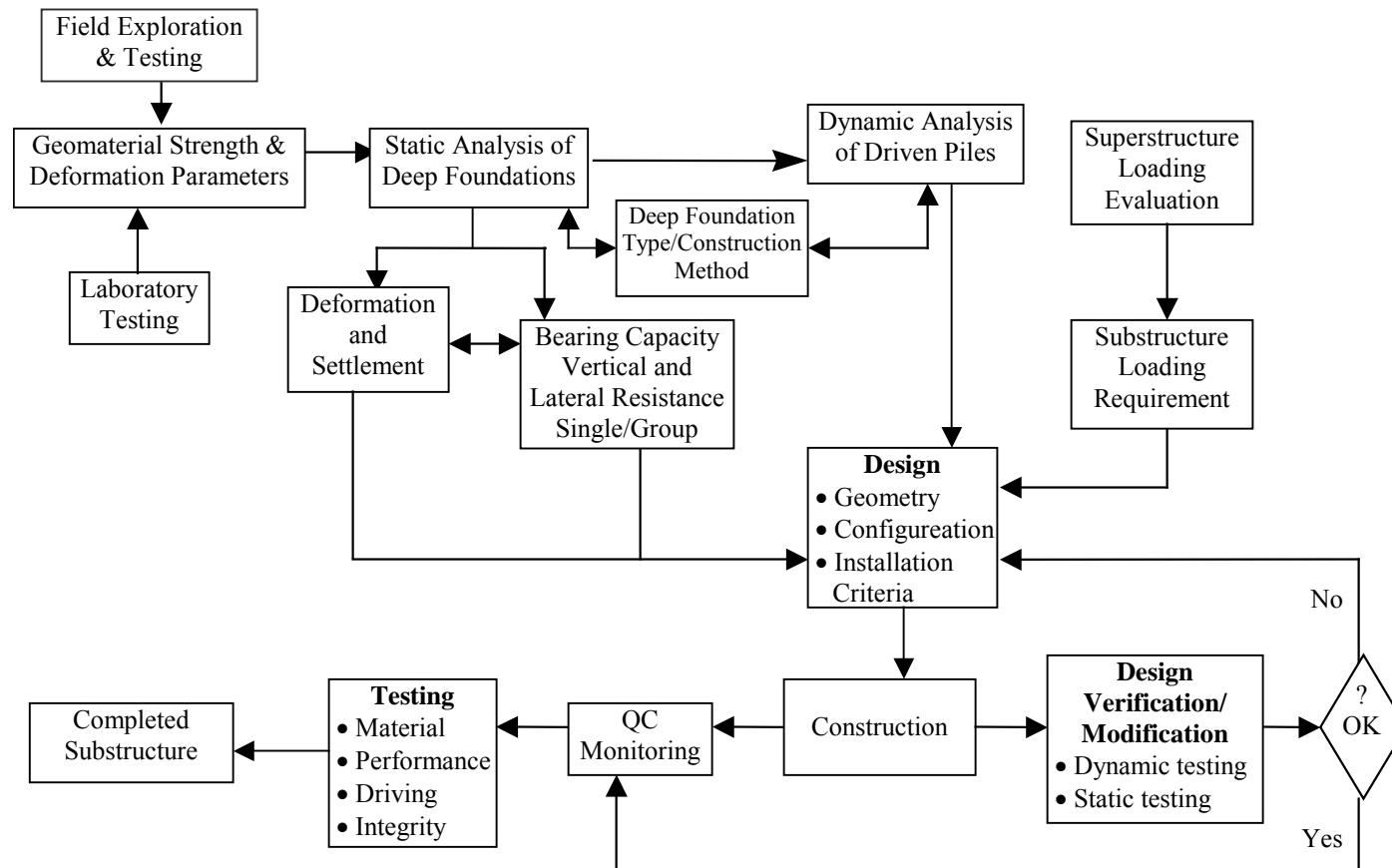


**Figure 124. Design and construction process for deep foundations (Paikowsky et al., 2004)**

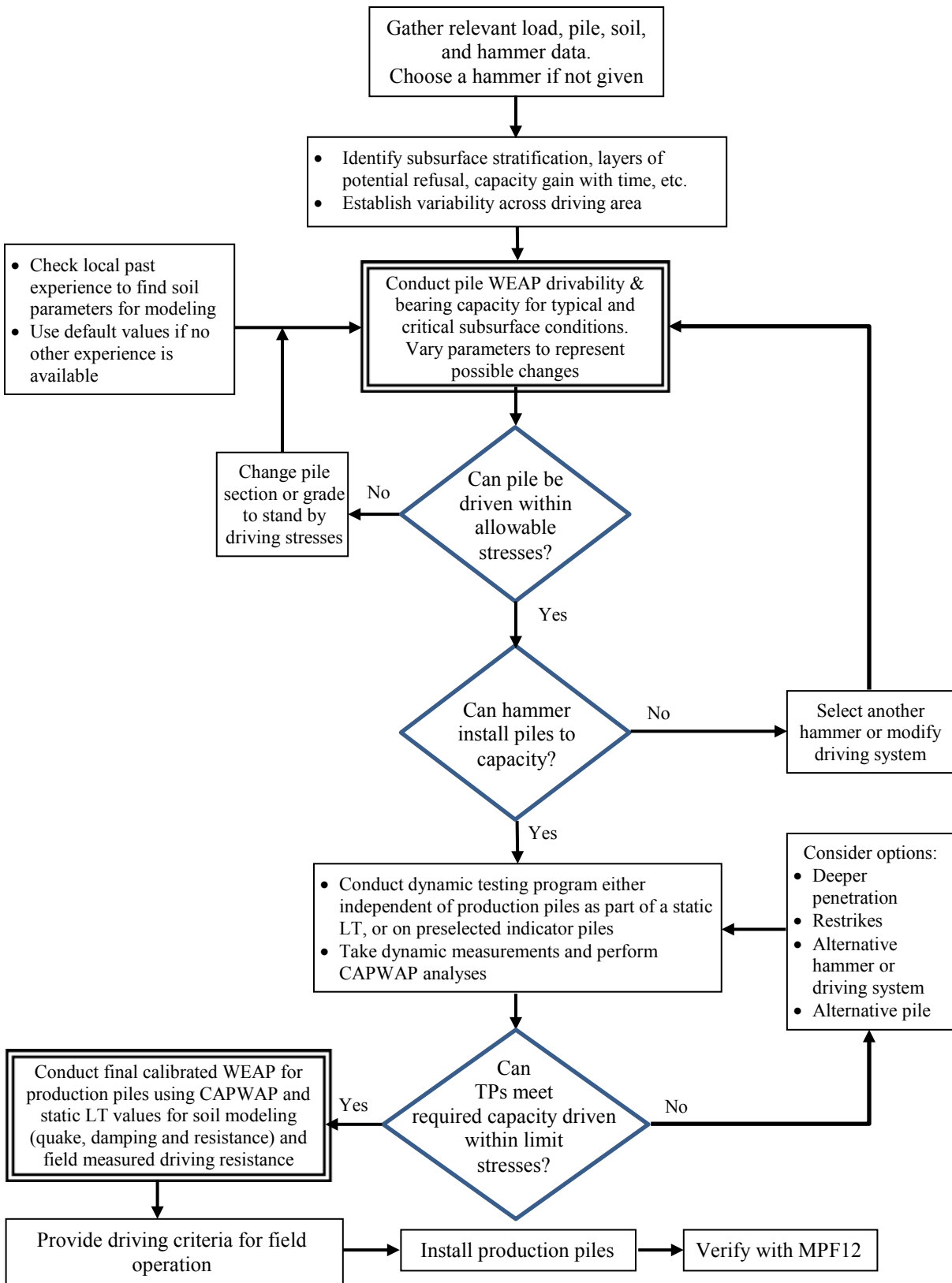


**Figure 125. WEAP utilization in the design and construction process of driven piles**

capacity prediction. The use of the method for the evaluation of pile capacity was examined through the comparison of WEAP results for default input values and the blow count at the EOD with static load test results. The data presented were provided by GRL Inc. (Hannigan et al., 1996). A comparison between the performance of WEAP to other methods is summarized in Table 76. For the construction category, the dynamic analyses methods without dynamic measurements included in Table 76, is the MPF12 performance as describes in previous chapters. The methods with dynamic measurements are CAPWAP and the Energy Approach. The dynamic methods are broken down into subsets based on time of driving, driving resistance, and area ratios. Judgment and statistical guidelines were used for the inclusion or exclusion of cases. For example, extreme CAPWAP under-predictions (beyond 2 standard deviations) were observed at EOD at one site. All the case histories on that site included easy driving and large area ratios; if included in the general population of the data, the EOD statistics would have become  $1.861 \pm 1.483$  (mean  $\pm$  1 S.D.). This site is included only in the subcategory of blow count  $< 16$  BP10cm and  $A_R < 350$ .

Observing the statistical information presented in Table 76, one can come to the following conclusions regarding the WEAP analysis as a method for predicting pile capacity:

- a. Using default soil modeling values in the design stage, the WEAP analysis results performs very poorly as a capacity predictor based on driving resistance. Overall it shows a great under-prediction (on the average 60% of the actual value) with a large scatter. This fact should not detract from the need of conducting WEAP analysis for structural and drivability reasons.
- b. MPF12 provides a much better method for capacity prediction, developing a driving resistance-capacity relationship.
- c. Both Energy Approach in the field and CAPWAP following analysis provide good capacity estimations as presented in previous chapters.
- d. Though never examined in a systematic way and on a large scale, the correction of WEAP following dynamic and/or static tests provide a means for improving the field prediction of capacity and will be further discussed.

**Table 76. The performance of the dynamic methods: statistical summary and resistance factors (Paikowsky et al., 2004) compared to MPF12 performance**

Method		Time of Driving	No. of Cases	Mean	Standard Deviation	COV	Resistance Factors for a given Reliability Index, $\beta$		
							2.0	2.5	3.0
Dynamic Measurements	CAPWAP	General	377	1.368	0.620	0.453	0.68	0.54	0.43
		EOD	125	1.626	0.797	0.490	0.75	0.59	0.46
		EOD - AR < 350 & Bl. Ct. < 16 BP10cm	37	2.589	2.385	0.921	0.52	0.35	0.23
		BOR	162	1.158	0.393	0.339	0.73	0.61	0.51
	Energy Approach	General	371	0.894	0.367	0.411	0.48	0.39	0.32
		EOD	128	1.084	0.431	0.398	0.60	0.49	0.40
		EOD - AR < 350 & Bl. Ct. < 16 BP10cm	39	1.431	0.727	0.508	0.63	0.49	0.39
		BOR	153	0.785	0.290	0.369	0.46	0.38	0.32
	WEAP	EOD	99	1.656	1.199	0.724	0.48	0.34	0.25
	MPF 12	H EOD	111	0.998	0.256	0.257	0.60	$\beta = 2.33$	
		H BOR	28	1.018	0.245	0.241	0.60		
		Pipe EOD	87	1.099	0.417	0.380	0.50		
		Pipe BOR	46	1.023	0.230	0.255	0.65		

Notes: EOD = End of Driving; BOR = Beginning of Restrike; AR = Area Ratio;  
 Bl. Ct. = Blow Count; ENR = Engineering News Record Equation;  
 BP10cm = Blows per 10cm; COV = Coefficient of Variation;  
 Mean = ratio of the static load test results (Davisson's Criterion) to the predicted capacity =  $K_{SX} = \lambda$  = bias

## 8.4 WEAP Analyses for Typical MnDOT Pile Driving Conditions

### 8.4.1 Overview

Following the process depicted in Figure 125, WEAP analyses were conducted based on MnDOT typical piles, hammers and soil conditions as described in our initial report of August 3, 2009. Section 9.4 presents and discusses these analyses. A summary table of representative cases was prepared and analyzed. Utilizing the extensive detailed results, simplified driving resistances relations were developed. The following section provides the driving resistance graphs for each typical case and “average” summary graphs for several cases. The average graphs are then compared to the MPF12 when assuming 75% hammer efficiency or for the average stroke calculated by WEAP as part of the analysis. Conclusions are derived and the results are put in perspective of other information.

#### **8.4.2 Typical WEAP Analyses for MnDOT Conditions**

Table 77 summarizes the typical pile sizes, soil profiles and hammer types used in MnDOT projects reviewed and summarized in our initial report by Paikowsky et al. (2009). Variations in pile length, based on the previously reviewed projects, were included as the pile's length affects the energy transfer and the driving resistance. Each of the seventy (70) identified cases (with range of loads for each) was analyzed using the WEAP program and default soil model parameter values. A summary of all analyzed cases, each identified by a case number, along with the soil parameters used in the analyses and the figure number presenting the results are shown in Table 78. The note section below Table 78 also presents the structure of each case number.

#### **8.4.3 Driving Resistance Charts**

Figures 126 to 132 are each comprised of two figures. One provides the driving resistance graphs for each typical case presented in Table 78, and the other presents “average” representative summary graphs for several cases. The average graphs are then compared to the MPF12 when assuming 75% hammer efficiency and when using the average stroke calculated by WEAP as part of the analysis. Reviewing the graphs presented in Figures 126 to 132, one can conclude the following:

1. The graphs provide easy representation in the design stage of the WEAP performance under ‘typical’ MnDOT cases and, hence, can serve as a first approximation as well as a basis for comparison with site specific and/or other analyses.
2. In almost all cases within typical driving resistances at or below 8bpi, the capacity associated with a given driving resistance is lower (often significantly) compared to that obtained by us in MPF12. This fact matches the statistics shown in Table 76 suggesting WEAP to typically under-predict capacity by 60% of the actual value.
3. The above observation suggests that the hammer/pile/soil combinations used in MnDOT projects were adequate and based on long term experience rather than some inadequacy indicated by WEAP.
4. The cases for which a better match exists between the WEAP results and the MPF12 curves are typically those for shorter end bearing piles where the energy loss is small and the displacements are small.
5. The MPF12 should be used for developing resistance curves at the design stage in addition to the field calculation of capacity as a result of driving.



**Table 77. WEAP plan of study for MnDOT prevailing driving conditions**

Pile Type	Length ft	Soil		Percent End Bearing (%)	Hammer Type <sup>1</sup>				Load kips	Quake <sup>2</sup>		Damping <sup>2</sup>	
		Side	Tip		D-12	D-19	D-25	D-30		Side	Tip	Side	Tip
CEP 12"x0.25"	35	Sand/Silt	Till	60%	x				160 (120-200)	0.1	0.04	0.05	0.15
	70	Sand/Silt	Till	50%	x					0.1	0.04	0.05	0.15
	105	Sand/Silt	Till	25%		x	x			0.1	0.04	0.05	0.15
	140	Sand/Silt	Till	25%		x	x			0.1	0.04	0.05	0.15
CEP 12"x0.25"	35	Clay	Till	80%	x				160 (120-200)	0.1	0.04	0.2	0.15
	70	Clay	Till	75%	x					0.1	0.04	0.2	0.15
	105	Clay	Till	50%		x	x			0.1	0.04	0.2	0.15
	140	Clay	Till	50%		x	x			0.1	0.04	0.2	0.15
CEP 12"x0.25"	35	Sand/Silt	Sand	50%	x				160 (120-200)	0.1	0.1	0.05	0.15
	70	Sand/Silt	Sand	50%	x					0.1	0.1	0.05	0.15
	105	Sand/Silt	Sand	25%		x	x			0.1	0.1	0.05	0.15
	140	Sand/Silt	Sand	25%		x	x			0.1	0.1	0.05	0.15
CEP 12"x0.25"	35	Clay	Sand	75%	x				160 (120-200)	0.1	0.1	0.2	0.15
	70	Clay	Sand	75%	x					0.1	0.1	0.2	0.15
	105	Clay	Sand	50%		x	x			0.1	0.1	0.2	0.15
	140	Clay	Sand	50%		x	x			0.1	0.1	0.2	0.15
CEP 12"x0.25"	35	Clay	Clay	20%	x				160 (120-200)	0.1	0.2	0.2	0.15
	70	Clay	Clay	20%	x					0.1	0.2	0.2	0.15
	105	Clay	Clay	10%		x	x			0.1	0.2	0.2	0.15
	140	Clay	Clay	10%		x	x			0.1	0.2	0.2	0.15
CEP 16"x0.3125"	50	Sand/Silt	Till	50%				x	250 (200-300)	0.1	0.04	0.05	0.15
	60	Sand/Silt	Till	50%				x		0.1	0.04	0.05	0.15
	70	Sand/Silt	Till	50%				x		0.1	0.04	0.05	0.15
CEP 16"x0.3125"	50	Clay	Till	85%				x	250 (200-300)	0.1	0.04	0.2	0.15
	60	Clay	Till	85%				x		0.1	0.04	0.2	0.15
	70	Clay	Till	85%				x		0.1	0.04	0.2	0.15
CEP 16"x0.3125"	50	Sand/Silt	Sand	50%				x	250 (200-300)	0.1	0.13	0.05	0.15
	60	Sand/Silt	Sand	50%				x		0.1	0.13	0.05	0.15
	70	Sand/Silt	Sand	50%				x		0.1	0.13	0.05	0.15
CEP 16"x0.3125"	50	Clay	Sand	75%				x	250 (200-300)	0.1	0.13	0.2	0.15
	60	Clay	Sand	75%				x		0.1	0.13	0.2	0.15
	70	Clay	Sand	75%				x		0.1	0.13	0.2	0.15

Note: <sup>1</sup>Default hammer set-up

<sup>2</sup>Default soil parameters

**Table 77 (cont'd.). WEAP plan of study for MnDOT prevailing driving conditions**

Pile Type	Length ft	Soil		Percent End Bearing (%)	Hammer Type <sup>1</sup>				Load kips	Quake <sup>2</sup>		Damping <sup>2</sup>	
		Side	Tip		D-12	D-19	D-25	D-30		Side	Tip	Side	Tip
CEP 16"x0.3125"	50	Clay	Clay	50%				x	250 (200-300)	0.1	0.27	0.2	0.15
	60	Clay	Clay	50%				x		0.1	0.27	0.2	0.15
	70	Clay	Clay	50%				x		0.1	0.27	0.2	0.15
HP 12x53	30	Sand/Silt	Till	40%	x				150, 160 & 170	0.1	0.04	0.05	0.15
	40	Sand/Silt	Till	40%		x	x			0.1	0.04	0.05	0.15
	50	Sand/Silt	Till	40%		x	x			0.1	0.04	0.05	0.15
HP 12x53	30	Clay	Till	70%	x				150, 160 & 170	0.1	0.04	0.2	0.15
	40	Clay	Till	70%		x	x			0.1	0.04	0.2	0.15
	50	Clay	Till	70%		x	x			0.1	0.04	0.2	0.15
HP 12x53	30	Sand/Silt	Sand	50%	x				150, 160 & 170	0.1	0.1	0.05	0.15
	40	Sand/Silt	Sand	50%		x	x			0.1	0.1	0.05	0.15
	50	Sand/Silt	Sand	50%		x	x			0.1	0.1	0.05	0.15
HP 12x53	30	Clay	Sand	80%	x				150, 160 & 170	0.1	0.1	0.2	0.15
	40	Clay	Sand	80%		x	x			0.1	0.1	0.2	0.15
	50	Clay	Sand	80%		x	x			0.1	0.1	0.2	0.15
HP 12x53	30	Clay	Clay	10%	x				150, 160 & 170	0.1	0.2	0.2	0.15
	40	Clay	Clay	10%		x	x			0.1	0.2	0.2	0.15
	50	Clay	Clay	10%		x	x			0.1	0.2	0.2	0.15

Note: <sup>1</sup>Default hammer set-up

<sup>2</sup>Default soil parameters

**Table 78. Summary of typical pile, hammer and soil conditions for MnDOT pile driving to be used in WEAP analysis**

Pile Type	CASE	Group	Length	Soil		Percent End Bearing (%)	Hammer Type <sup>1</sup>				Load kips	Quake <sup>2</sup>		Damping <sup>2</sup>	
			ft	Side	Tip		D-12 <sup>3</sup>	D-19	D-25	D-30		Side	Tip	Side	Tip
HP 12x53	3-A-1-A	Figure 1. - Group 1.	30	Sand/Silt	Till	40%	x				150, 160 & 170	0.1	0.04	0.05	0.15
	3-A-3-B & 3-A-3-C	Figure 2. - Group 1. / Figure 3. - Group 1.	40	Sand/Silt	Till	40%		x	x			0.1	0.04	0.05	0.15
	3-A-4-B & 3-A-4-C	Figure 2. - Group 1. / Figure 3. - Group 1.	50	Sand/Silt	Till	40%		x	x			0.1	0.04	0.05	0.15
HP 12x53	3-B-1-A	Figure 1. - Group 2.	30	Clay	Till	70%	x				150, 160 & 170	0.1	0.04	0.2	0.15
	3-B-3-B & 3-B-3-C	Figure 2. - Group 2. / Figure 3. - Group 2.	40	Clay	Till	70%		x	x			0.1	0.04	0.2	0.15
	3-B-4-B & 3-B-4-C	Figure 2. - Group 2. / Figure 3. - Group 2.	50	Clay	Till	70%		x	x			0.1	0.04	0.2	0.15
HP 12x53	3-C-1-A	Figure 1. - Group 1.	30	Sand/Silt	Sand	50%	x				150, 160 & 170	0.1	0.1	0.05	0.15
	3-C-3-B & 3-C-3-C	Figure 2. - Group 1. / Figure 3. - Group 1.	40	Sand/Silt	Sand	50%		x	x			0.1	0.1	0.05	0.15
	3-C-4-B & 3-C-4-C	Figure 2. - Group 1. / Figure 3. - Group 1.	50	Sand/Silt	Sand	50%		x	x			0.1	0.1	0.05	0.15
HP 12x53	3-D-1-A	Figure 1. - Group 2.	30	Clay	Sand	80%	x				150, 160 & 170	0.1	0.1	0.2	0.15
	3-D-3-B & 3-D-3-C	Figure 2. - Group 2. / Figure 3. - Group 2.	40	Clay	Sand	80%		x	x			0.1	0.1	0.2	0.15
	3-D-4-B & 3-D-4-C	Figure 2. - Group 2. / Figure 3. - Group 2.	50	Clay	Sand	80%		x	x			0.1	0.1	0.2	0.15
HP 12x53	3-E-1-A	Figure 1. - Group 3.	30	Clay	Clay	10%	x				150, 160 & 170	0.1	0.2	0.2	0.15
	3-E-3-B & 3-E-3-C	Figure 2. - Group 3. / Figure 3. - Group 3.	40	Clay	Clay	10%		x	x			0.1	0.2	0.2	0.15
	3-E-4-B & 3-E-4-C	Figure 2. - Group 3. / Figure 3. - Group 3.	50	Clay	Clay	10%		x	x			0.1	0.2	0.2	0.15
CEP 12"x0.25"	1-A-2-A	Figure 4. - Group 1.	35	Sand/Silt	Till	60%	x				160 (120-200)	0.1	0.04	0.05	0.15
	1-A-6-A	Figure 4. - Group 1.	70	Sand/Silt	Till	50%	x					0.1	0.04	0.05	0.15
	1-A-7-B & 1-A-7-C	Figure 5. - Group 1. / Figure 6. - Group 1.	105	Sand/Silt	Till	25%		x	x			0.1	0.04	0.05	0.15
	1-A-8-B & 1-A-8-C	Figure 5. - Group 1. / Figure 6. - Group 1.	140	Sand/Silt	Till	25%		x	x			0.1	0.04	0.05	0.15
CEP 12"x0.25"	1-B-2-A	Figure 4. - Group 2.	35	Clay	Till	80%	x				160 (120-200)	0.1	0.04	0.2	0.15
	1-B-6-A	Figure 4. - Group 2.	70	Clay	Till	75%	x					0.1	0.04	0.2	0.15
	1-B-7-B & 1-B-7-C	Figure 5. - Group 2. / Figure 6. - Group 2.	105	Clay	Till	50%		x	x			0.1	0.04	0.2	0.15
	1-B-8-B & 1-B-8-C	Figure 5. - Group 2. / Figure 6. - Group 2.	140	Clay	Till	50%		x	x			0.1	0.04	0.2	0.15
CEP 12"x0.25"	1-C-2-A	Figure 4. - Group 1.	35	Sand/Silt	Sand	50%	x				160 (120-200)	0.1	0.1	0.05	0.15
	1-C-6-A	Figure 4. - Group 1.	70	Sand/Silt	Sand	50%	x					0.1	0.1	0.05	0.15
	1-C-7-B & 1-C-7-C	Figure 5. - Group 1. / Figure 6. - Group 1.	105	Sand/Silt	Sand	25%		x	x			0.1	0.1	0.05	0.15
	1-C-8-B & 1-C-8-C	Figure 5. - Group 1. / Figure 6. - Group 1.	140	Sand/Silt	Sand	25%		x	x			0.1	0.1	0.05	0.15
CEP 12"x0.25"	1-D-2-A	Figure 4. - Group 2.	35	Clay	Sand	75%	x				160 (120-200)	0.1	0.1	0.2	0.15
	1-D-6-A	Figure 4. - Group 2.	70	Clay	Sand	75%	x					0.1	0.1	0.2	0.15
	1-D-7-B & 1-D-7-C	Figure 5. - Group 2. / Figure 6. - Group 2.	105	Clay	Sand	50%		x	x			0.1	0.1	0.2	0.15
	1-D-8-B & 1-D-8-C	Figure 5. - Group 2. / Figure 6. - Group 2.	140	Clay	Sand	50%		x	x			0.1	0.1	0.2	0.15

Note:

1. Default Hammer Set-up
2. Default Soil Parameters

First Pile Type - 1 = CEP 12"x0.25", 2= CEP 16"x0.3125", & 3 = HP 12x 53  
 Second Soil Type - A=Sand/Silt Till, B=Clay Till, C=Sand/Silt Sand, D= Clay Sand, E= Clay Clay  
 Third Pile Length - 1 = 30, 2=35, 3=40, 4=50, 5=60, 6=70, 7=105, 8=140  
 Fourth Hammer Type - A=D-12, B=D-19, C=D-25, D=D-30

**Table 78 (cont'd). Summary of typical pile, hammer and soil conditions for MnDOT pile driving to be used in WEAP analysis**

Pile Type	CASE	Group	Length	Soil		Percent End Bearing (%)	Hammer Type <sup>1</sup>				Load kips	Quake <sup>2</sup>		Damping <sup>2</sup>	
			ft	Side	Tip		D-12 <sup>3</sup>	D-19	D-25	D-30		Side	Tip	Side	Tip
CEP 12"x0.25"	1-E-2-A	Figure 4. - Group 3.	35	Clay	Clay	20%	x				160 (120-200)	0.1	0.2	0.2	0.15
	1-E-6-A	Figure 4. - Group 3.	70	Clay	Clay	20%	x					0.1	0.2	0.2	0.15
	1-E-7-B & 1-E-7-C	Figure 5. - Group 2. / Figure 6. - Group 2.	105	Clay	Clay	10%		x	x			0.1	0.2	0.2	0.15
	1-E-8-B & 1-E-8-C	Figure 5. - Group 2. / Figure 6. - Group 2.	140	Clay	Clay	10%		x	x			0.1	0.2	0.2	0.15
CEP 16"x0.3125"	2-A-4-D	Figure 7. - Group 1.	50	Sand/Silt	Till	50%				x	250 (200-300)	0.1	0.04	0.05	0.15
	2-A-5-D	Figure 7. - Group 1.	60	Sand/Silt	Till	50%				x		0.1	0.04	0.05	0.15
	2-A-6-D	Figure 7. - Group 1.	70	Sand/Silt	Till	50%				x		0.1	0.04	0.05	0.15
CEP 16"x0.3125"	2-B-4-D	Figure 7. - Group 2.	50	Clay	Till	85%				x	250 (200-300)	0.1	0.04	0.2	0.15
	2-B-5-D	Figure 7. - Group 2.	60	Clay	Till	85%				x		0.1	0.04	0.2	0.15
	2-B-6-D	Figure 7. - Group 2.	70	Clay	Till	85%				x		0.1	0.04	0.2	0.15
CEP 16"x0.3125"	2-C-4-D	Figure 7. - Group 1.	50	Sand/Silt	Sand	50%				x	250 (200-300)	0.1	0.13	0.05	0.15
	2-C-5-D	Figure 7. - Group 1.	60	Sand/Silt	Sand	50%				x		0.1	0.13	0.05	0.15
	2-C-6-D	Figure 7. - Group 1.	70	Sand/Silt	Sand	50%				x		0.1	0.13	0.05	0.15
CEP 16"x0.3125"	2-D-4-D	Figure 7. - Group 2.	50	Clay	Sand	75%				x	250 (200-300)	0.1	0.13	0.2	0.15
	2-D-5-D	Figure 7. - Group 2.	60	Clay	Sand	75%				x		0.1	0.13	0.2	0.15
	2-D-6-D	Figure 7. - Group 2.	70	Clay	Sand	75%				x		0.1	0.13	0.2	0.15
CEP 16"x0.3125"	2-E-4-D	Figure 7. - Group 3.	50	Clay	Clay	50%				x	250 (200-300)	0.1	0.27	0.2	0.15
	2-E-5-D	Figure 7. - Group 3.	60	Clay	Clay	50%				x		0.1	0.27	0.2	0.15
	2-E-6-D	Figure 7. - Group 3.	70	Clay	Clay	50%				x		0.1	0.27	0.2	0.15

Note:

- |                            |        |   |
|----------------------------|--------|---|
| 3. Default Hammer Set-up   | First  | Pile Type - 1 = CEP 12"x0.25", 2= CEP 16"x0.3125", & 3 = HP 12x 53                      |
| 4. Default Soil Parameters | Second | Soil Type - A=Sand/Silt Till, B=Clay Till, C=Sand/Silt Sand, D= Clay Sand, E= Clay Clay |
|                            | Third  | Pile Length - 1 = 30, 2=35, 3=40, 4=50, 5=60, 6=70, 7=105, 8=140                        |
|                            | Fourth | Hammer Type - A=D-12, B=D-19, C=D-25, D=D-30  |

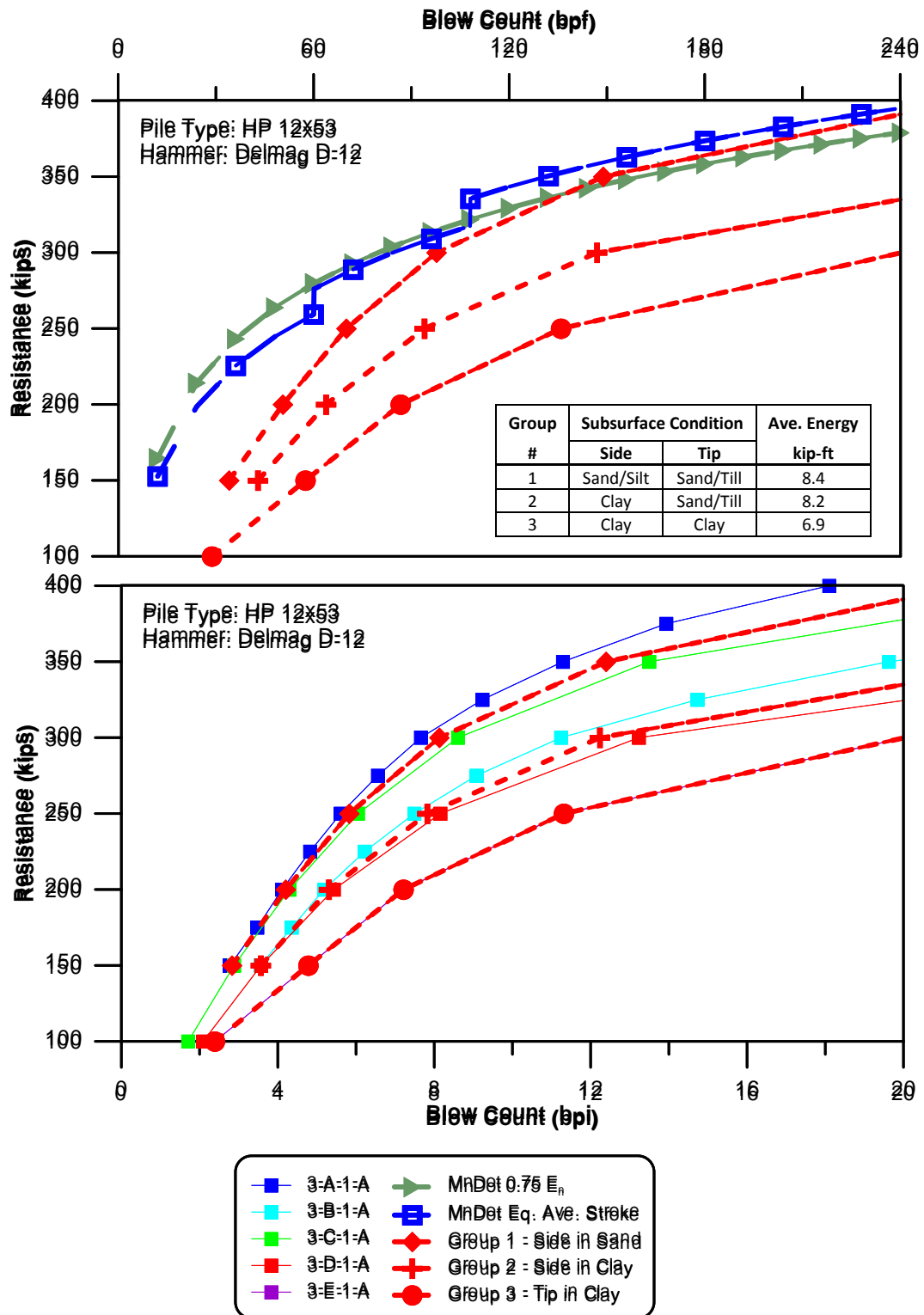


Figure 126. WEAP analysis results presenting static capacity vs. driving resistances for HP 12x53 piles driven by a D-12 hammer (a) detail graphs based on typical case studies (b) representative cases of (a) compared to MPF12 with assumed 75% hammer performance and strokes as indicated by the WEAP analysis

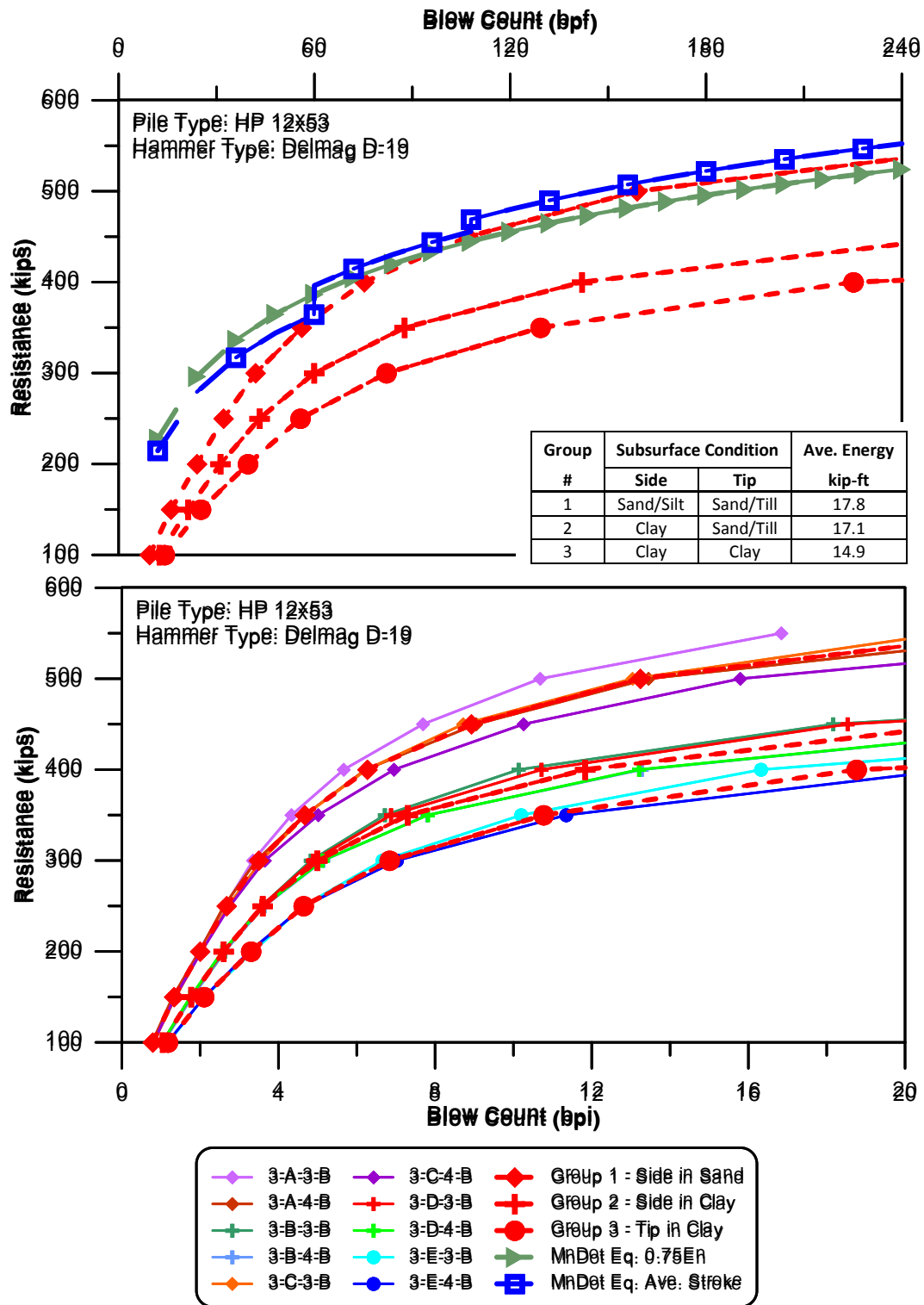


Figure 127. WEAP analysis results presenting static capacity vs. driving resistances for HP 12x53 piles driven by a D-19 hammer (a) detail graphs based on typical case studies (b) representative cases of (a) compared to MPF12 with assumed 75% hammer performance and strokes as indicated by the WEAP analysis

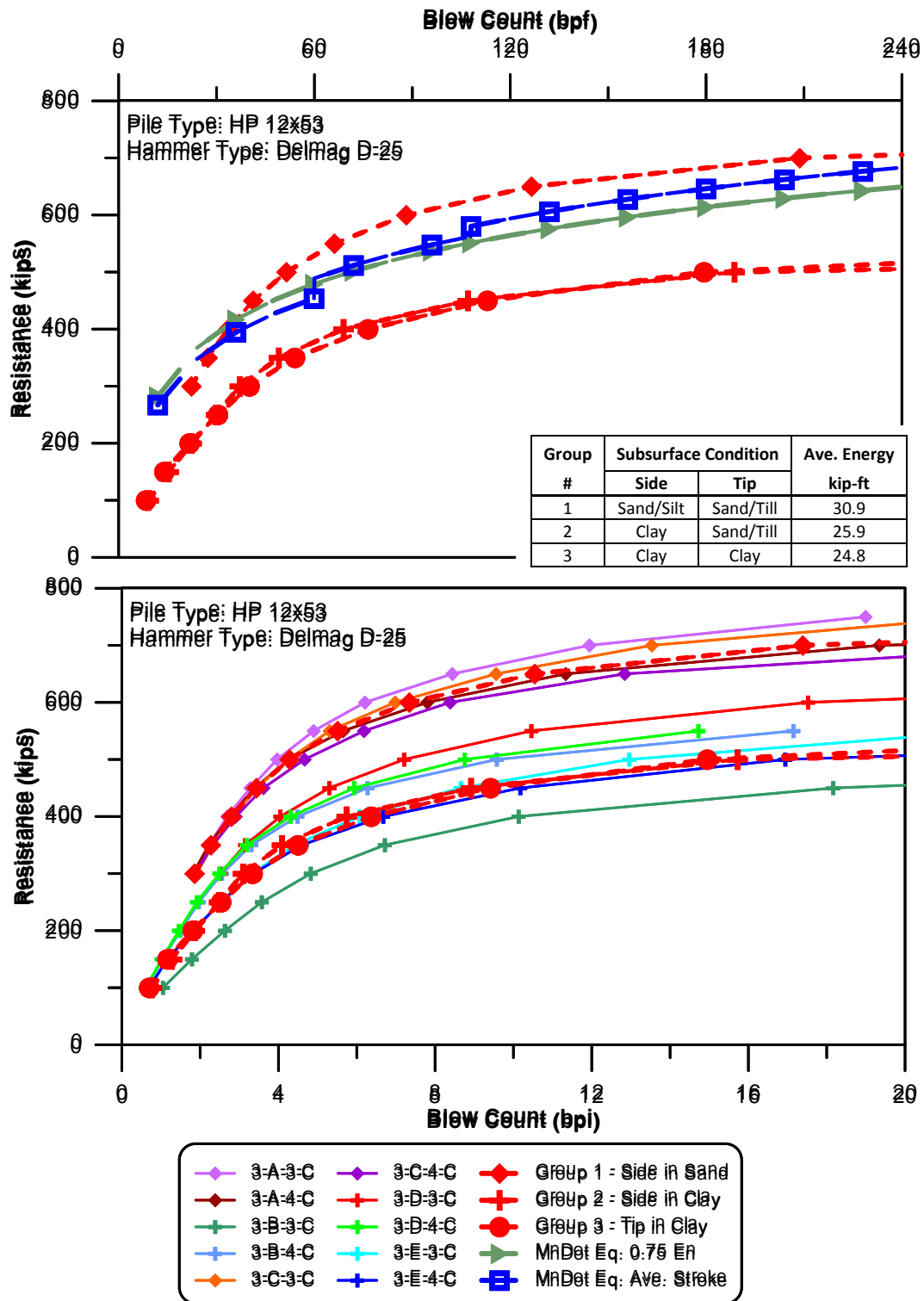
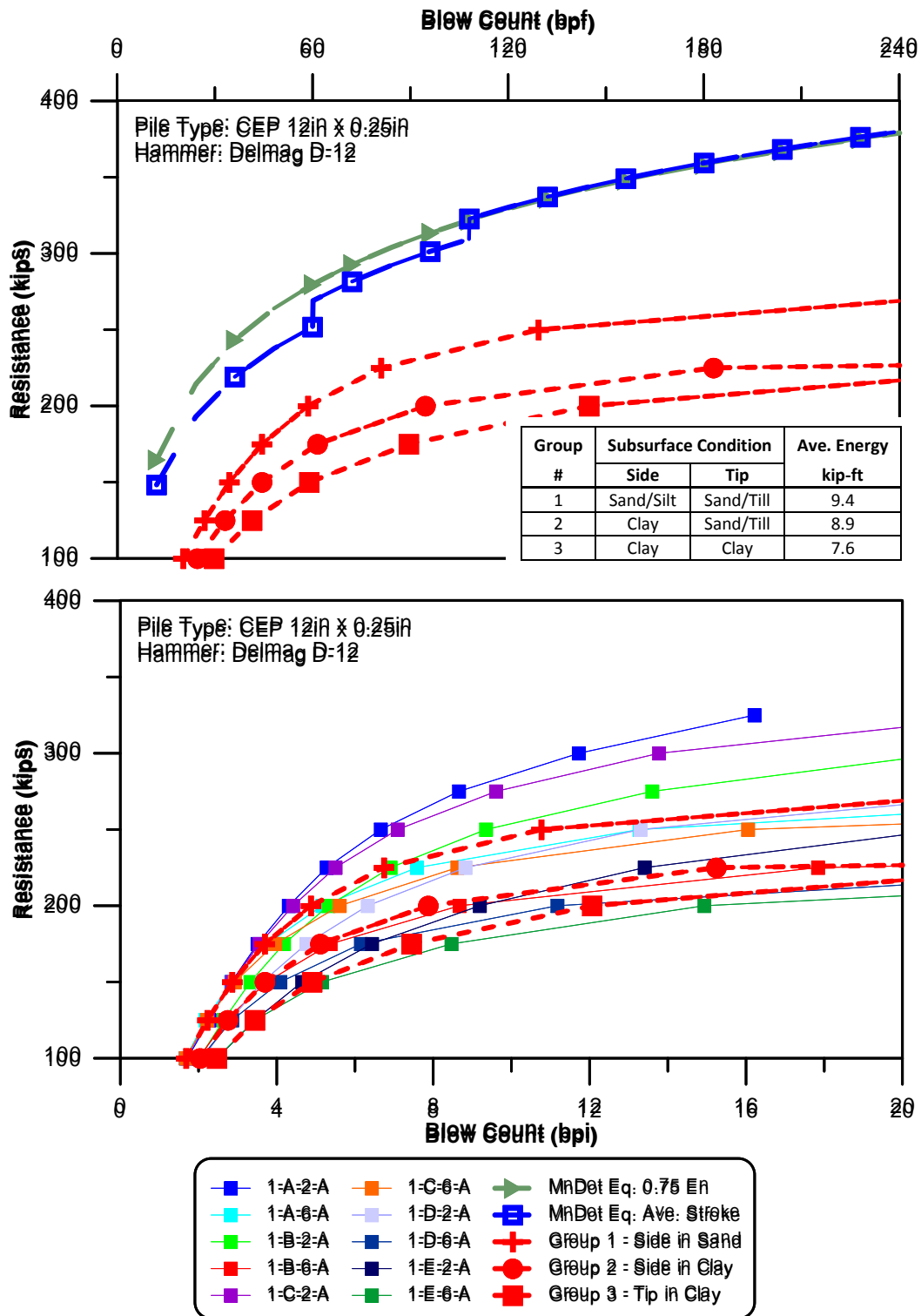


Figure 128. WEAP analysis results presenting static capacity vs. driving resistances for HP 12x53 piles driven by a D-19 hammer (a) detail graphs based on typical case studies (b) representative cases of (a) compared to MPF12 with assumed 75% hammer performance and strokes as indicated by the WEAP analysis



**Figure 129. WEAP analysis results presenting static capacity vs. driving resistances for CEP 12in x 0.25in piles driven by a D-12 hammer (a) detail graphs based on typical case studies (b) representative cases of (a) compared to MPF12 with assumed 75% hammer performance and strokes as indicated by the WEAP analysis**



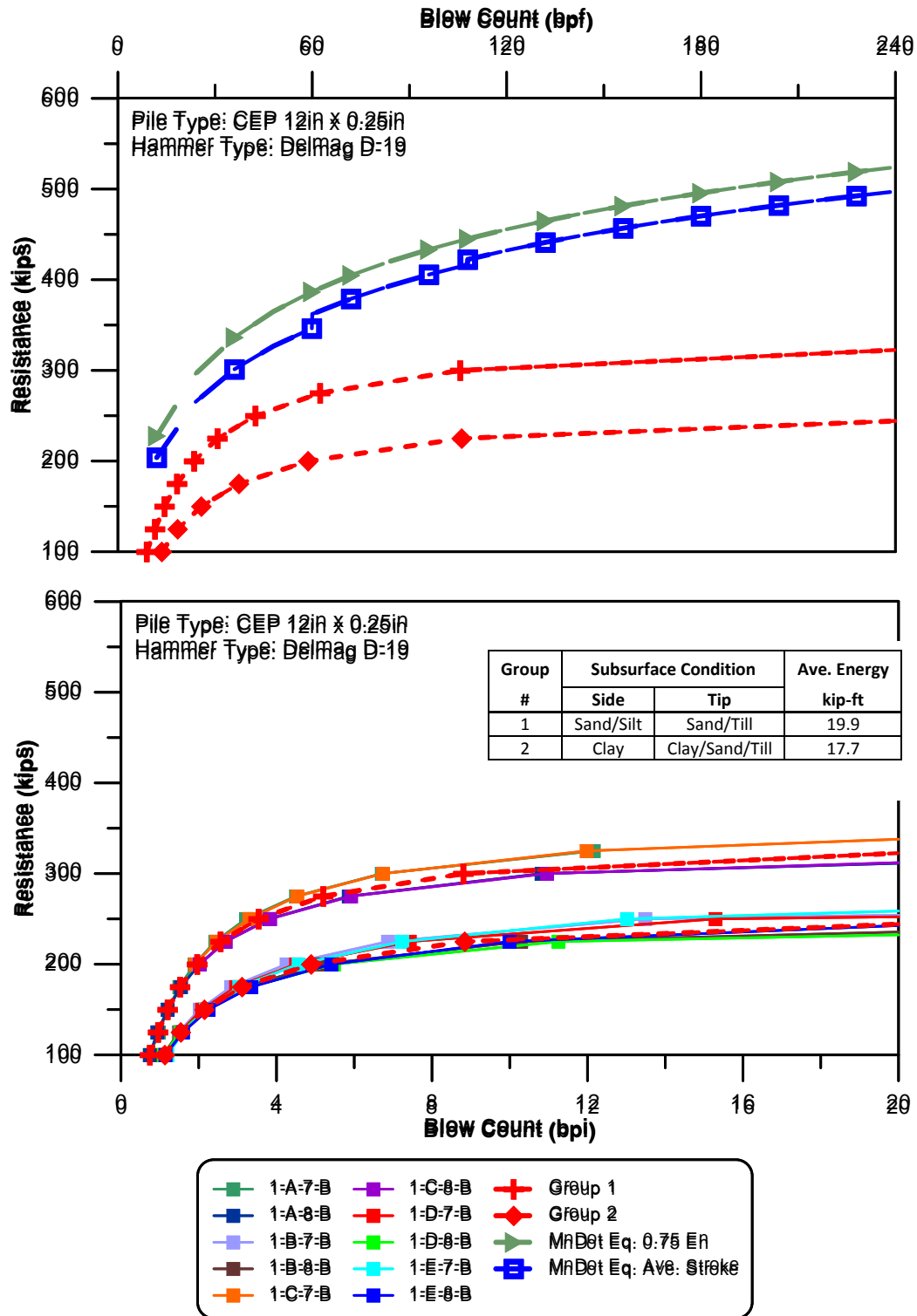


Figure 130. WEAP analysis results presenting static capacity vs. driving resistances for CEP 12in x 0.25in piles driven by a D-19 hammer (a) detail graphs based on typical case studies (b) representative cases of (a) compared to MPF12 with assumed 75% hammer performance and strokes as indicated by the WEAP analysis

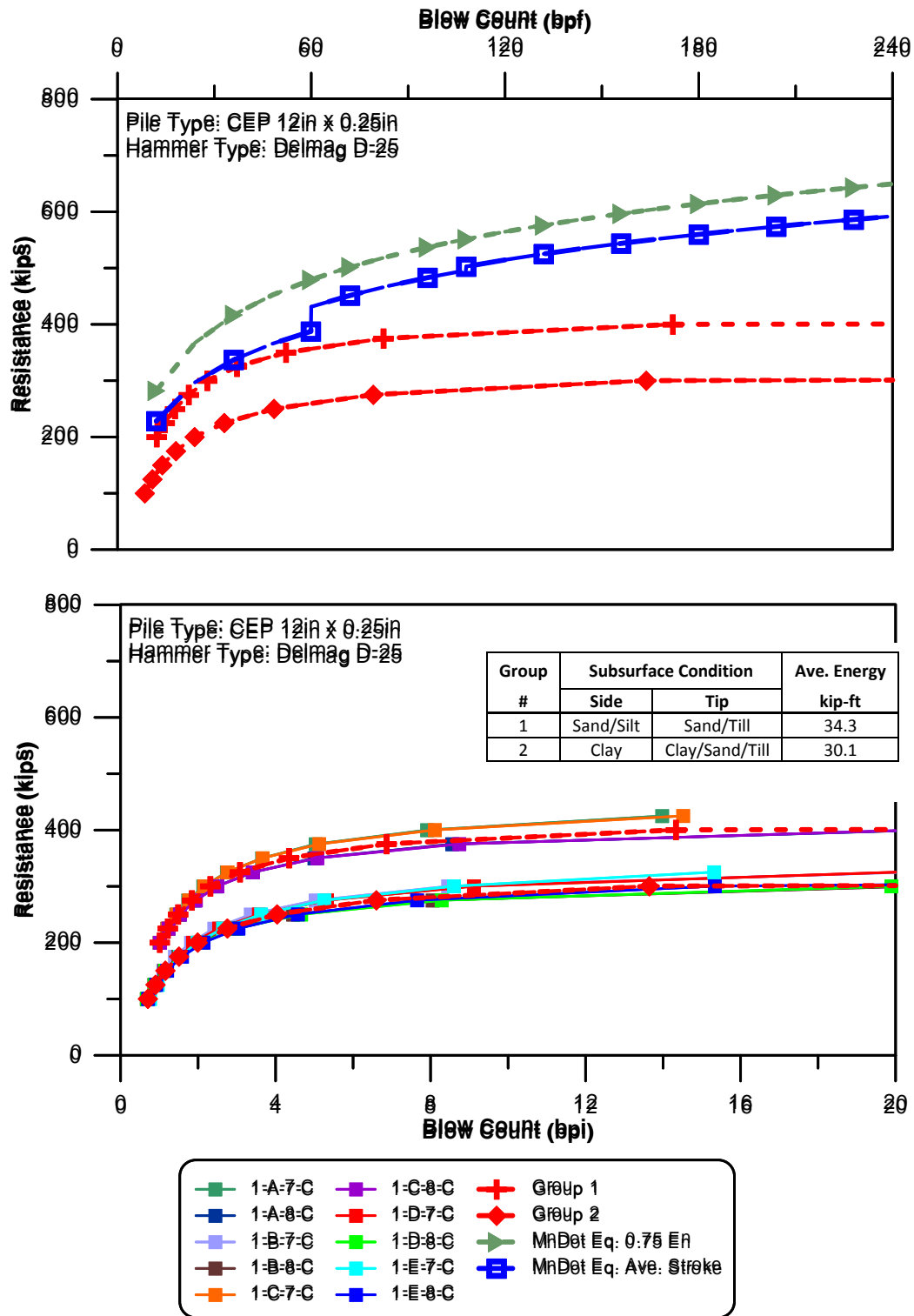


Figure 131. WEAP analysis results presenting static capacity vs. driving resistances for CEP 12in x 0.25in piles driven by a D-25 hammer (a) detail graphs based on typical case studies (b) representative cases of (a) compared to MPF12 with assumed 75% hammer performance and strokes as indicated by the WEAP analysis

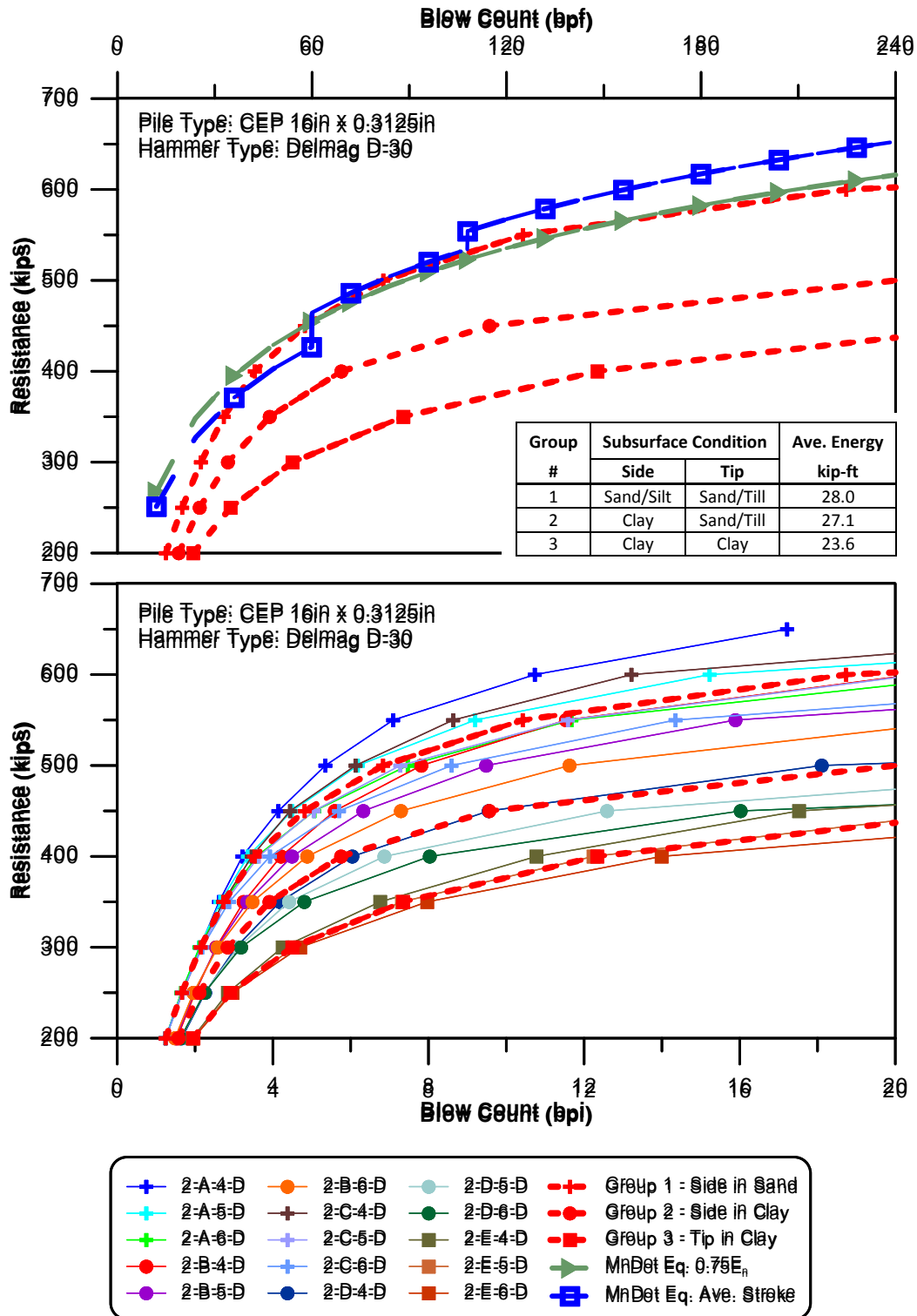


Figure 132. WEAP analysis results presenting static capacity vs. driving resistances for CEP 16in x 0.3125in piles driven by a D-30 hammer (a) detail graphs based on typical case studies (b) representative cases of (a) compared to MPF12 with assumed 75% hammer performance and strokes as indicated by the WEAP analysis

## **8.5 WEAP Adjustment Following Dynamic Measurements**

### **8.5.1 Overview – Victoria Load Test**

Section 7.2 describes the static load test (on pile TP1) carried out by MnDOT for bridge 10003 in Victoria, Minnesota. The present section examines the WEAP submittal prior to testing and the adjustment of the WEAP using the information becoming available during the dynamic and the static testing.

### **8.5.2 Subsurface Conditions**

Figures 133 and 134 provide the bridge longitudinal cross-section of subsurface conditions based on a drilled boring with SPT (T05) and on CPT soundings, respectively, as provided by Johnson et al. (2011). The subsurface at the site is described based on borings T05 (see Figure 135 for the boring log) in the following way:

“The SPT boring (T05), that was drilled later to supplement the CPT soundings, was located on the Lake Minnetonka LRT Regional Trail approximately 28 feet below the bridge. The boring was approximately in the middle of the bridge, located 37 and 59 feet from the east and west abutments, respectively.

The upper 3.5 feet of the T05 boring consisted of soft clay loam. Below this layer, there was approximately 94 feet of plastic sandy loam with pebbles which had a 14 foot layer of dense loamy sand beginning at elevation 913.5 feet. A dense layer of sand and coarse sand with gravel was discovered at the bottom of the boring. The N-value blow counts were slightly higher than the CPT interpreted values, but seemed to correlate relatively well. Due to the similar nature between the T05 boring and the CPT values acquired at the east abutment, this boring was used for pile analysis only at the east abutment. Water was encountered at an elevation of 953 feet.”

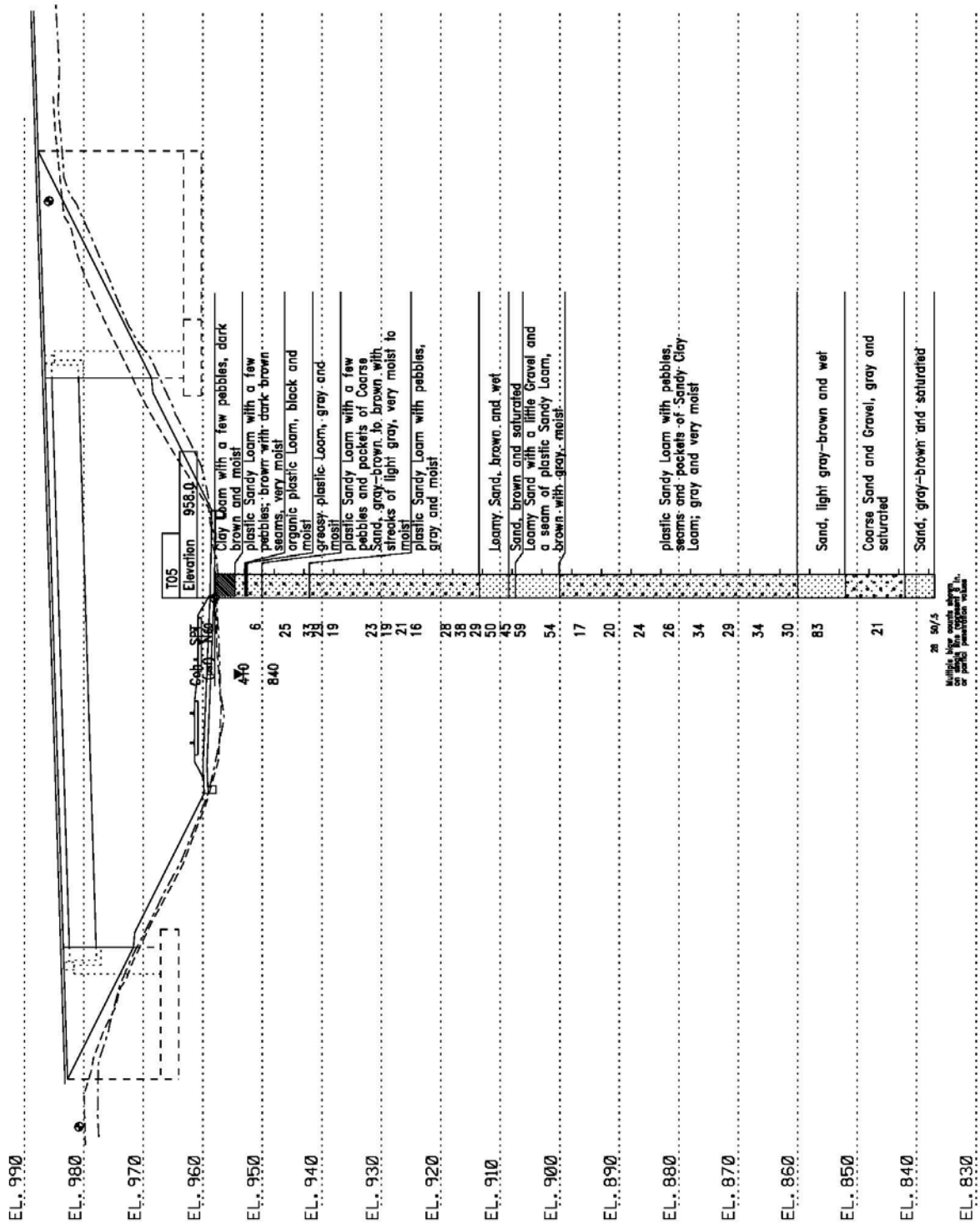
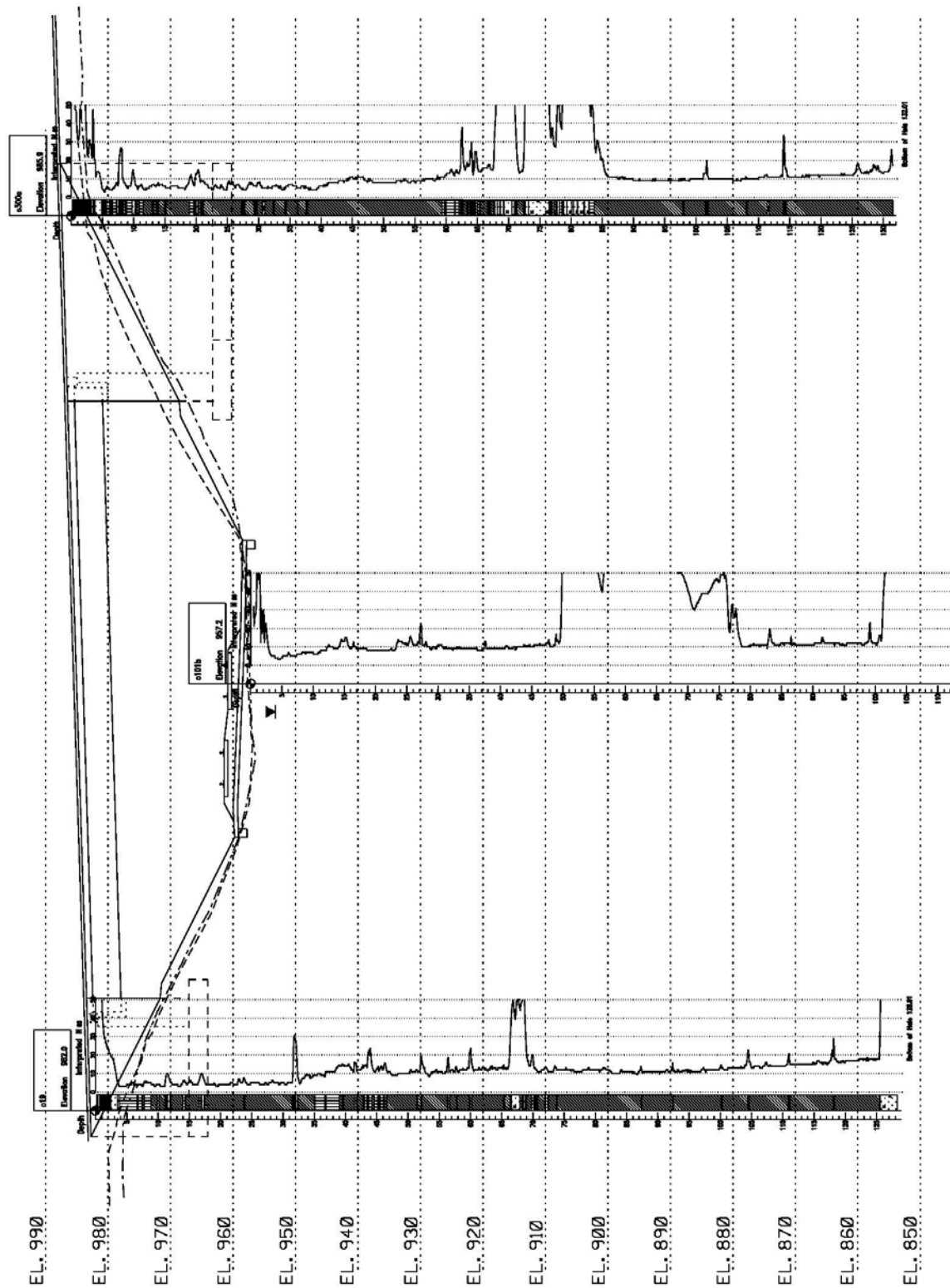


Figure 133. Victoria, Minnesota Bridge 10003 longitudinal cross-section of subsurface conditions based on drilled SPT boring (T05) (Johnson et al., 2011)



**Figure 134. Victoria, Minnesota Bridge 10003 longitudinal cross-section of subsurface conditions based on drilled CPT boring (T05) (Johnson et al., 2011)**

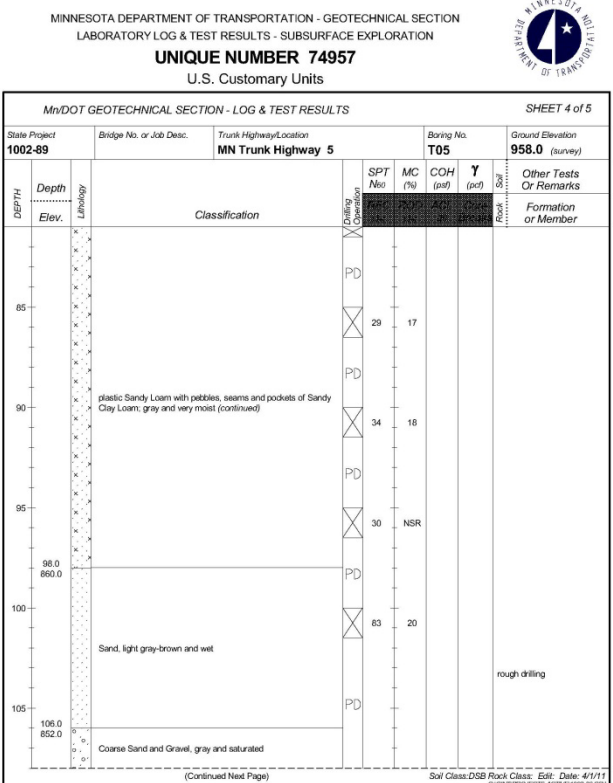
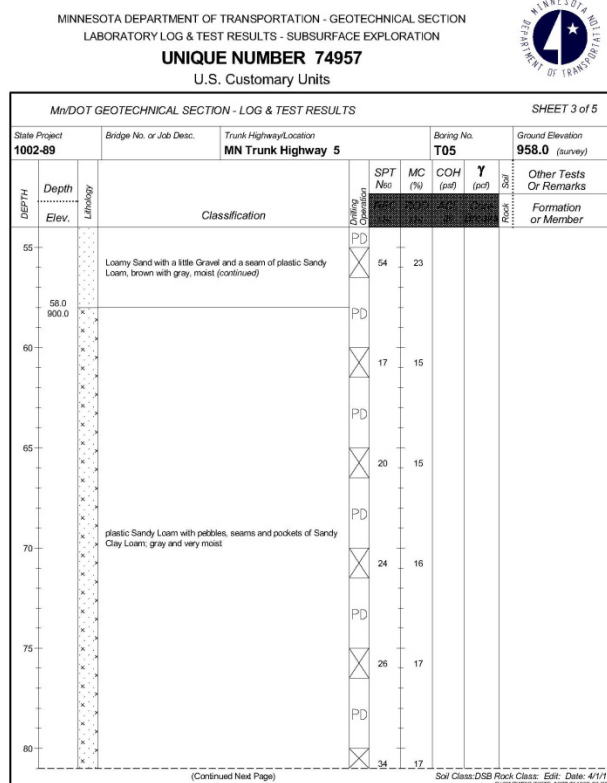
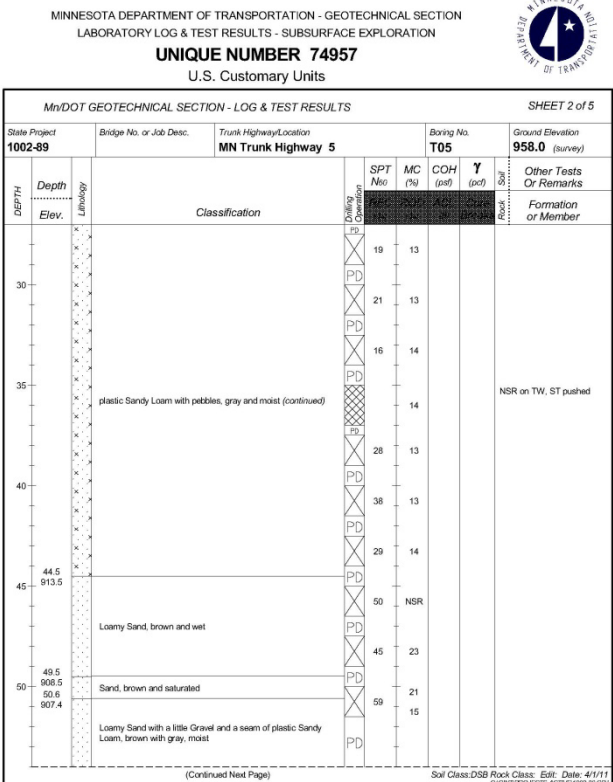
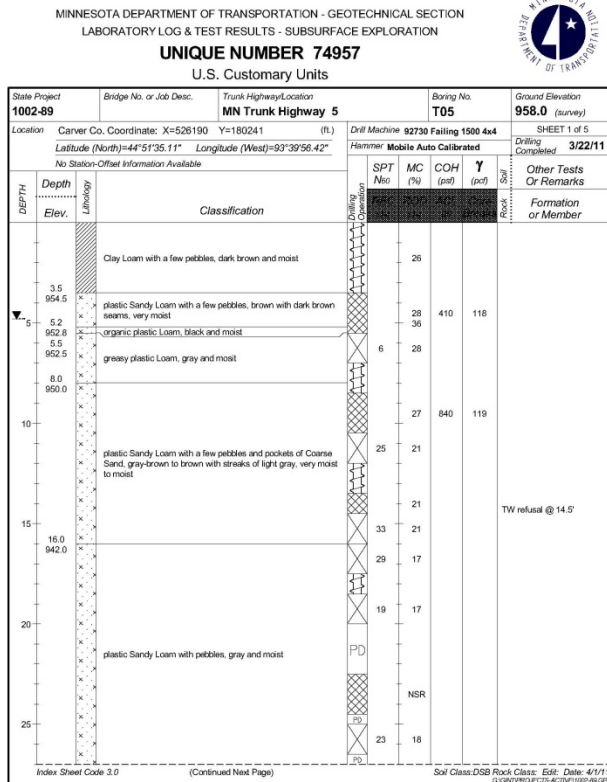


Figure 135. Boring T05 (Johnson et al., 2011)



WEAP input file dated April 20, 2012 was provided by Engineer Corwin Reese of Braun Interfer Corp. of Minneapolis, MN. The analysis was performed for drivability. The subsurface resistance distribution table and graph are presented in Figure 136. Figure 137 presents the input file for the drivability analysis and the resistance distribution along the pile based on the input file of Figure 136. Figure 138 and Table 79 present the drivability analysis results. Note that although Figures 136 to 138 and Table 79 contain in their heading the name GeoDynamica Inc., the data and analyses are based on a WEAP input file provided by others and only run through GeoDynamica licensed software. The analysis results suggest that the pile capacity increases with depth to a capacity of 250kips at a penetration depth of 65ft and the expected blow count at the end of driving is 3.5bpi (42.3bpf) but high driving resistance/refusal of 55bpi (661bpf) is expected at the depth of about 60ft.



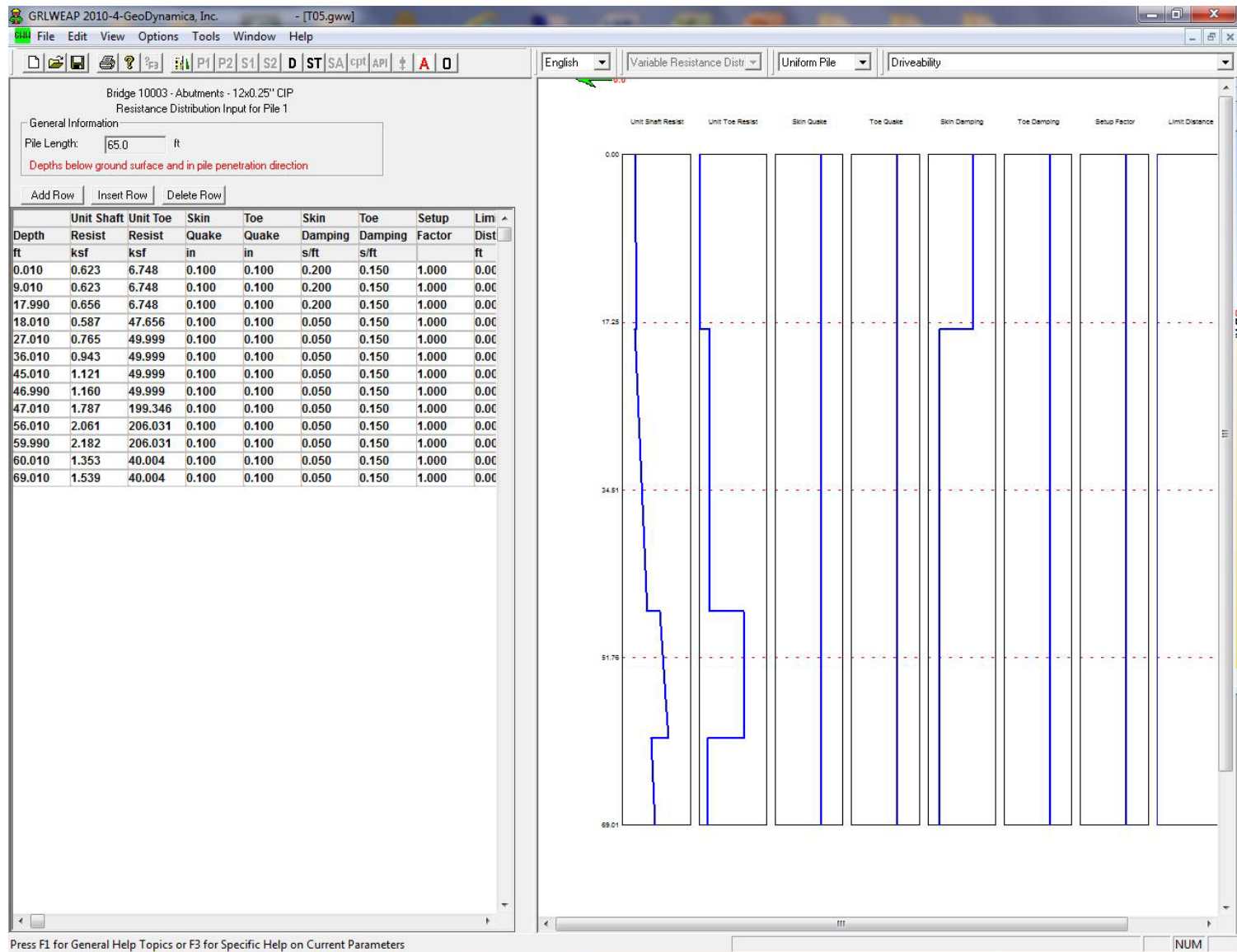
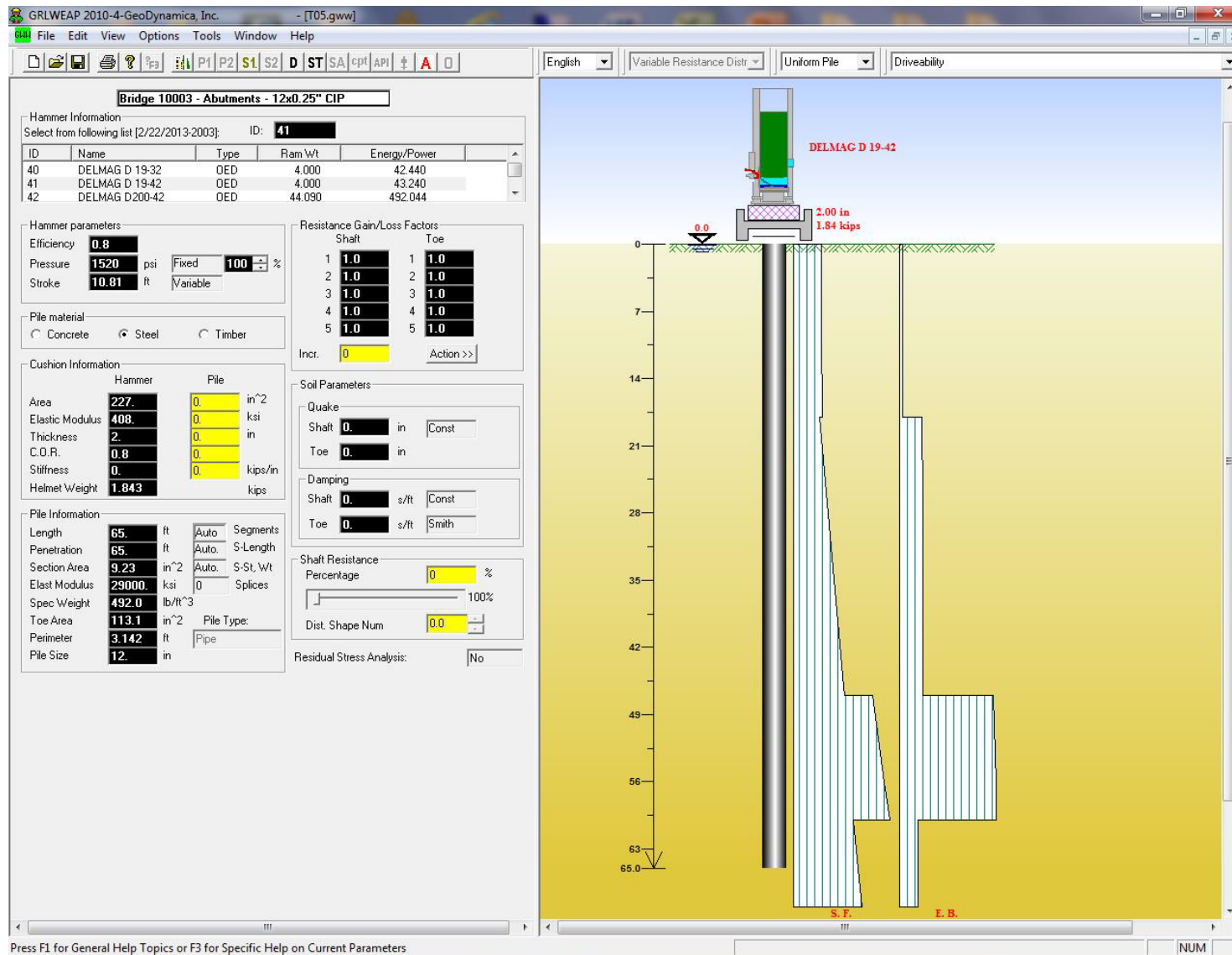
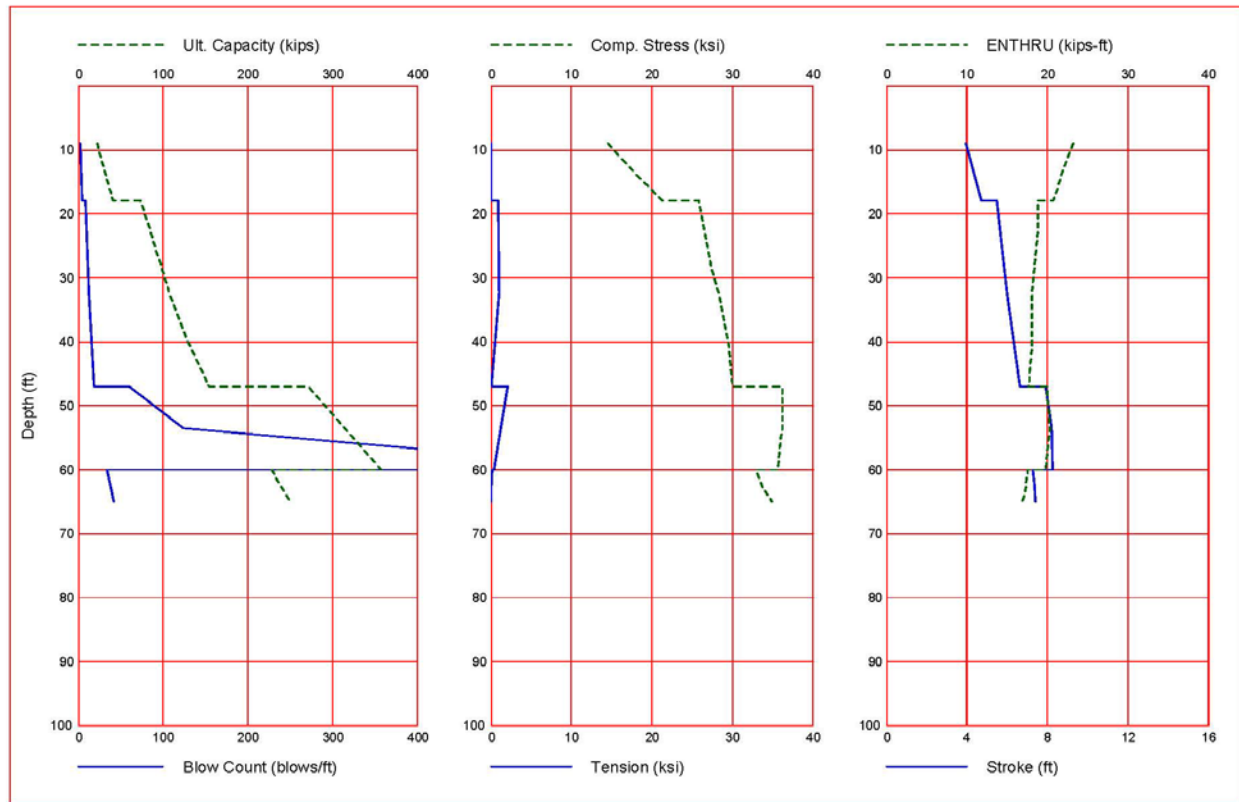


Figure 136. Resistance distribution input file – Victoria L.T. design stage



**Figure 137. Input file for drivability analysis and resistance distribution along the pile based on the input table presented in Figure 136**

Gain/Loss 1 at Shaft and Toe 1.000 / 1.000



**Figure 138. Drivability analysis results**

**Table 79. Drivability analysis results table**

Gain/Loss 1 at Shaft and Toe 1.000 / 1.000

Depth ft	Ultimate Capacity kips	Friction kips	End Bearing kips	Blow Count blows/ft	Comp. Stress ksi	Tension Stress ksi	Stroke ft	ENTHRU kips-ft
9.0	22.9	17.6	5.3	2.3	14.522	0.000	3.93	23.2
18.0	40.9	35.6	5.3	4.7	21.289	0.000	4.72	20.7
18.0	73.2	35.7	37.4	8.8	25.902	-0.858	5.47	18.8
32.5	108.2	69.0	39.3	12.8	28.358	-1.040	6.01	18.1
47.0	154.5	115.2	39.3	18.5	30.056	0.000	6.62	17.7
47.0	272.0	115.4	156.6	60.1	36.211	-2.108	7.93	20.0
53.5	314.2	153.8	160.4	123.9	36.208	-1.275	8.23	20.3
60.0	358.0	196.2	161.8	685.3	35.633	-0.411	8.27	19.8
60.0	227.9	196.4	31.4	33.6	33.063	-0.212	7.26	17.5
62.5	238.6	207.1	31.4	37.6	33.628	-0.011	7.34	17.3
65.0	249.8	218.4	31.4	42.4	34.899	0.000	7.42	16.9

Total Continuous Driving Time 92.00 minutes; Total Number of Blows 3847

**Figure 139. Driving log of TP1 Victoria static load test**

The dedicated WEAP analysis results presented in Figure 138 and Table 79 can initially be compared to the “typical” MnDOT conditions analyzed in section 9.4. Case 1-C-7B of Table 78 refers to a pipe pile 12 × 0.25 inch driven by D-19 in sand/silt/sand conditions. Figure 130 suggests that for a resistance of about 250kips the expected blow count is about 45bpf (Group #1 typical behavior) or when using MPF12 250kips translates to about 18bpf. Note that while the WEAP in figure 130 was developed for a 102ft pile, the MPF12 equation is independent of the pile’s length.

The drivability analysis results can be compared to the pile driving in the field using the driving log presented in Figure 139. Note that some site, dates and hammer details on the original log were corrected per communication with Derrick Dasenbrock (2013). The design stage drivability analysis is compared to the field records, dynamic measurements and static LT (see section 7.2) in Table 80 and suggests the following:

1. The driving log suggests a relatively uniform driving from a penetration depth of about 42ft with driving resistances varying between 21 to 27bpf.
2. The actual test pile driving was as follows:
  - EOD - 6-15-2012 pen = 62.25ft (895.75) 30bpf
  - 3DR - 6-18-2012 pen = 62.50ft (895.50) 80bpf (eq.)
  - 1 day following LT 6-26-2012 Pen = 62.50ft (895.50) 240bpf (eq.)

Note that while Figure 139 suggests 26bpf at EOD, the load test report specifies the numbers presented in Tables 72 and 80.
3. Table 79 shows WEAP predication of 238.6kips at the depth of 62.50ft and a blow count of 37.6bpf with energy of 17.3kip-ft (ENTHRU)
4. Considering that the static capacity of the pile was determined to be 268kips (see section 7.2), a relatively close match was achieved other than in the transferred energy.

**Table 80. Summary of WEAP predicted and measured during pile driving**

Analysis	Date	Pen (ft)	El. (ft)	BC (bpf)	Energy (kip-ft)	Capacity (kip)	Comment	Reference
WEAP	4/20/2012	62.50	895.50	37.6	17.3	238.6	Static analysis & drivability	Figure 138 Table 79
Typical WEAP	N/A	102.00	N/A	45.0	19.9	250.0	General relations	Figure 130
EOD	6/15/2012	62.25	895.75	30.0*	21.0	276.0	CAPWAP	Table 72 App. C
3DR	6/18/2012	62.50	895.50	80.0	28.2	488.0	CAPWAP	Table 72 App. C
Static LT	6/25/2012	62.50	895.50	N/A	N/A	268.0	failure	Table 72 App. C

\*the driving resistance is based on the LT report and the field PDA measurements while the driving log suggests 26bpf as shown in Figure 139.

In Summary it can be concluded that while the drivability analysis with depth was not accurate, the final match between the blow count and the resistance was very good. It is important, however, to notice that the match was achieved with the calculated transferred energy by WEAP being about 20% lower than the one measured in the driving.

#### **8.5.4 Construction Stage WEAP Analysis**

A signal matching analysis was carried out following the dynamic measurements obtained during the installation of TP1. The summary of the results are presented in Table 72 while the details are provided in Appendix C. Figure 140 provides the input data file for abutment W with penetrations similar to the load test pile. Figure 141 and Table 81 provide the results of this analysis. The parameters used in this analysis were influenced by the EOD CAPWAP analysis of the test pile provided in Appendix C for blow number 783. The analysis is noted as being carried out on July 12, 2012. While the CAPWAP analysis had resulted with the use of quakes of  $Q_s = 0.04\text{inch}$  and  $Q_t = 0.465\text{inch}$  for shaft and toe, respectively. The WEAP analysis made use of  $Q_s = 0.039\text{inch}$  and  $Q_t = 0.522\text{inch}$ . Similarly, while the CAPWAP had resulted with damping factors of  $J_s = 0.087\text{s/ft}$  and  $J_t = 0.024\text{s/ft}$ , the WEAP analysis was conducted for  $J_s = 0.111\text{s/ft}$  and  $J_t = 0.024\text{s/ft}$  and shaft resistance being 83%. The analysis of Figures 140, 141 and Table 81 while being a 'modified' WEAP following the dynamic testing are not clearly following the procedure. The driving resistance relations in Figure 140 can be further evaluated as to the driving resistance and ultimate capacity suggesting that the graph does not reflect the field driving condition and the match to the static load test. Table 82 summarizes the soil parameters used in the WEAP analysis prior to construction, the CAPWAP analyses for the dynamic measurements and the WEAP analysis for the West abutment following CAPWAP.

#### **8.5.5 GeoDynamica Modified WEAP for the Construction Stage**

Signal matching analysis (CAPWAP) has many more unknowns than equations to satisfy. As such, there is a large number of combinations that would lead to the signal match solution. With this fact in mind, several observations are known to be valid (i) the variation between the solution of one user (of the program) to the other usually, does not exceed 10% in the obtained total capacity, and (ii) the total capacity remains accurate while the distribution of tip and friction resistances (especially at the lower part of the pile) can vary quite a bit.

The issue of CAPWAP accuracy is therefore of less significance when dealing with capacity alone, but is important when trying to use a modified WEAP analysis based on a CAPWAP match. For example, the EOD and 3DR analyses have resulted with significant differences

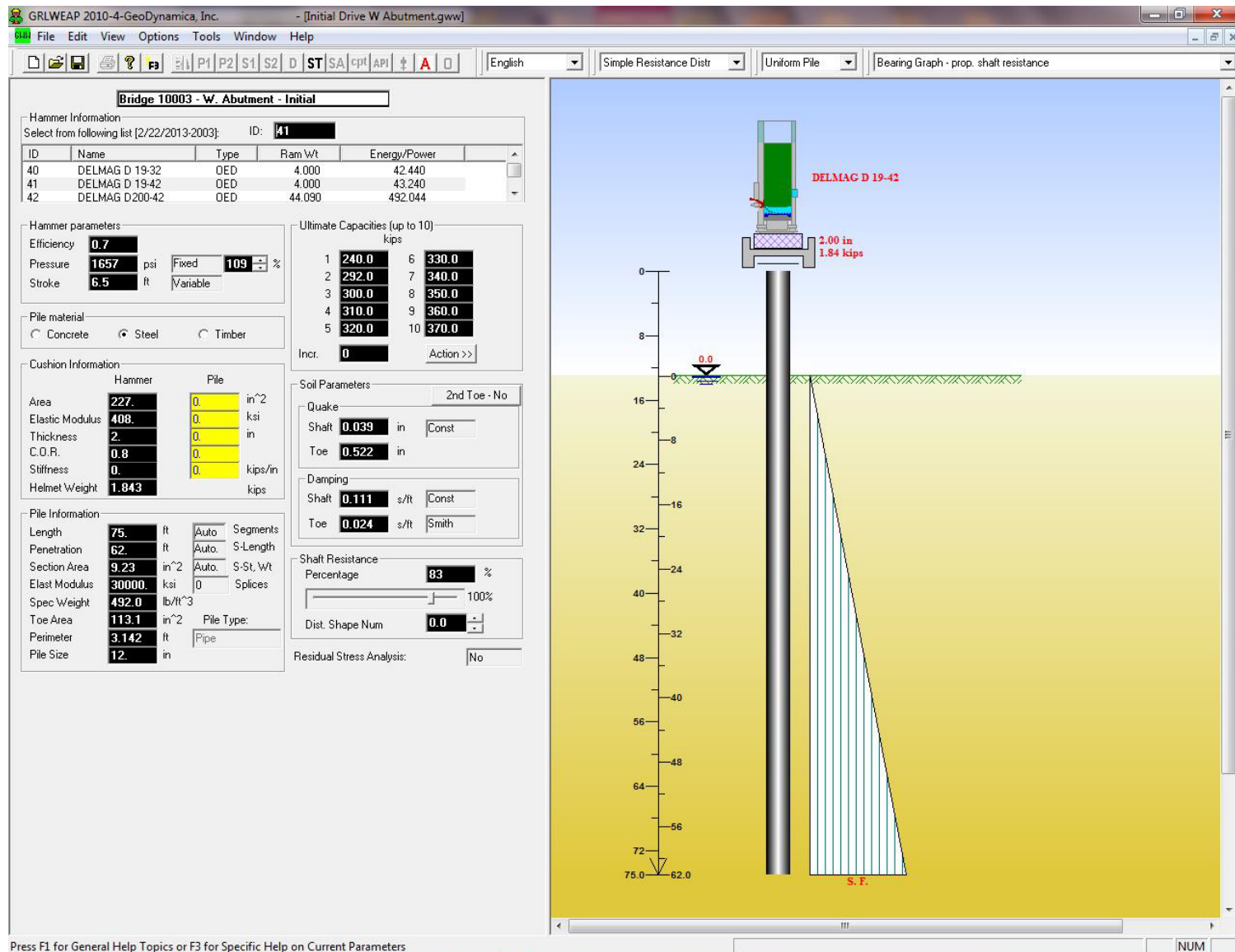
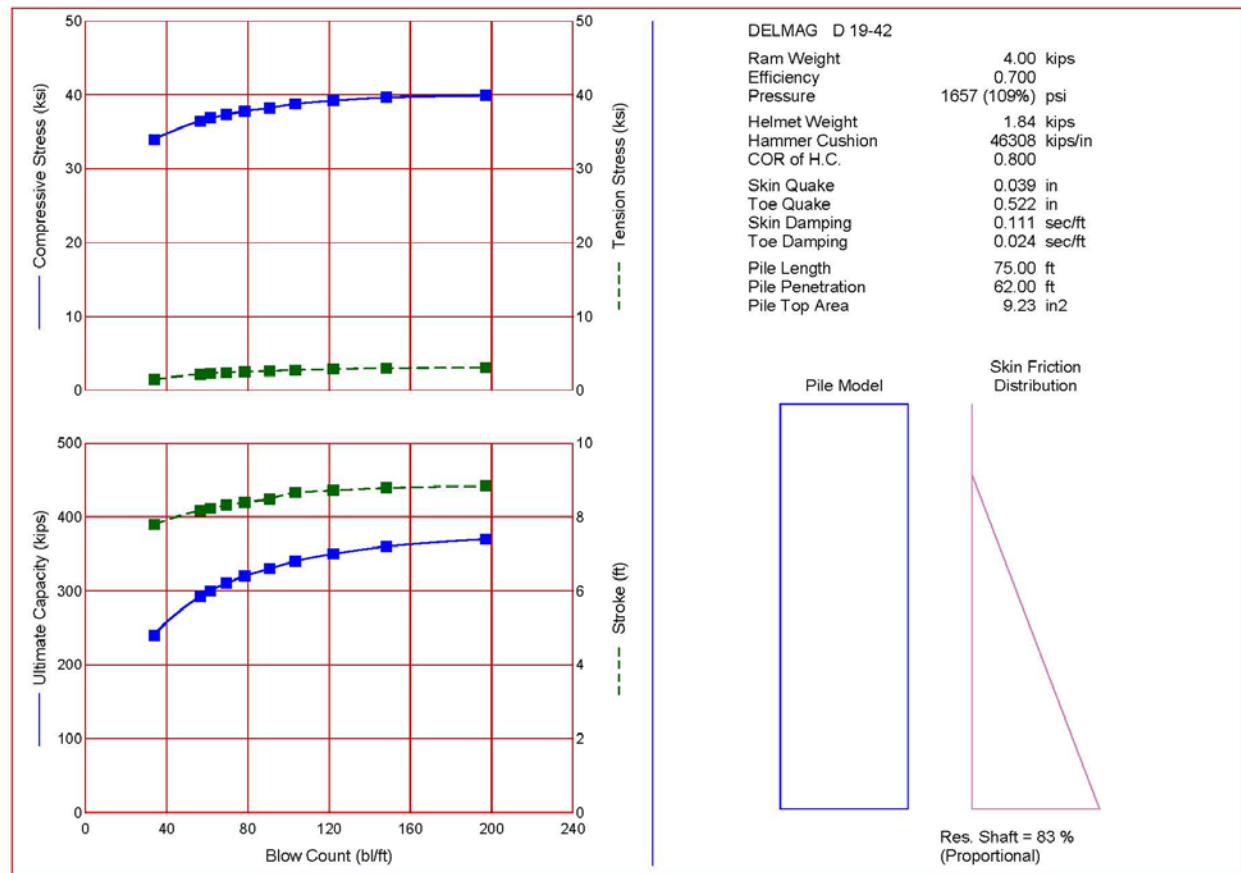


Figure 140. Abutment W input file





**Figure 141. Abutment W driving resistance graph**

**Table 81. Abutment W driving resistance table**

GeoDynamica, Inc.  
Bridge 10003 - W. Abutment - Initial

01-Nov-2013  
GRLWEAP Version 2010

Ultimate Capacity kips	Maximum Compression Stress ksi	Maximum Tension Stress ksi	Blow Count bl/ft	Stroke ft	Energy kips-ft
240.0	33.94	1.48	34.0	7.80	19.33
292.0	36.45	2.20	56.5	8.17	19.64
300.0	36.86	2.32	61.5	8.23	19.76
310.0	37.31	2.41	69.4	8.32	19.86
320.0	37.80	2.53	78.4	8.40	20.02
330.0	38.22	2.63	90.7	8.49	20.10
340.0	38.78	2.76	103.4	8.66	20.39
350.0	39.24	2.90	122.0	8.72	20.55
360.0	39.67	3.02	148.2	8.79	20.68
370.0	39.94	3.08	197.0	8.84	20.61



**Table 82. Summary table for WEAP parameters prior and post construction along with CAPWAP parameters**

Analysis	Date	Qs (in)	Qt (in)	Js (s/ft)	Jt (s/ft)	Load Distribution	Comment
WEAP	4/20/201	0.100	0.100	0.050	0.150	15.2% tip	Braun Interfer Corp. prior to driving
CAPWAP EOD	6/15/2012	0.040	0.465	0.087	0.024	7.5% tip	Braun Interfer Corp.
CAPWAP 3DR	6/18/2012	0.129	0.064	0.240	0.439	22.3% tip	Braun Interfer Corp.
WEAP W abutment	6/26/2012	0.039	0.522	0.111	0.024	17.0% tip	Braun Interfer Corp. post CAPWAP
GeoDynamica WEAP	11/15/2013	0.040	0.465	0.087	0.024	7.5% tip	Example using EOD CAPWAP

between the soil parameters (see Table 82 and Appendix C) and as such, two questions need to be answered: (i) are the differences truly reflecting variation in the soil property over time, and (ii) what should be used for the modified WEAP? The answer to these questions is awareness when conducting the CAPWAP to try and maintain consistent and “reasonable” values for the soil parameters as a requirement around which the value of other parameters can be shifted. With that in mind, GeoDynamica had used the model parameters from CAPWAP EOD to perform a modified WEAP serving as an example. Table 83 presents the parameters used in the analysis and Figure 142 presents the input file including the detailed copy of the load distribution along the pile shaft and tip, which was obtained in the EOD signal matching analysis. Table 83 provides the driving resistance for that analysis and Figure 143 presents the driving resistance graph to be used in the field. The comparison of this graph, presenting the ultimate capacity vs. driving resistance (blow count) for the modified WEAP, with the MPF12 and the load test data are summarized in Figure 144. The relations in Figure 144 suggest a remarkable agreement between the MPF12 (using the ram’s stoke measured in the field), the modified WEAP following the dynamic measurements, and the static load test results. These curves are the driving resistance curves that should be used in the field along with the curves obtained by using MPF12 for the specific pile.



**Table 83. GeoDynamica modified WEAP driving resistance table**

GeoDynamica, Inc.  
Bridge 10003 - W. Abutment - Initial

03-Dec-2013  
GRLWEAP Version 2010

Ultimate Capacity kips	Maximum Compression Stress ksi	Maximum Tension Stress ksi	Blow Count blows/in	Stroke ft	Energy kips-ft
100.0	28.23	3.42	0.6	5.87	22.28
150.0	31.88	1.27	1.1	6.79	21.39
200.0	35.38	0.01	1.6	7.29	20.35
250.0	38.90	0.27	2.2	7.75	20.86
300.0	41.97	0.55	3.1	8.20	21.46
350.0	44.95	0.68	4.6	8.69	22.30
400.0	47.26	0.73	8.1	8.97	22.62
450.0	49.52	0.99	20.1	9.34	23.47
470.0	50.56	0.89	44.4	9.43	23.59
500.0	51.61	0.83	9999.0	9.54	23.64

GeoDynamica, Inc.  
Bridge 10003 - W. Abutment - Initial

03-Dec-2013  
GRLWEAP Version 2010

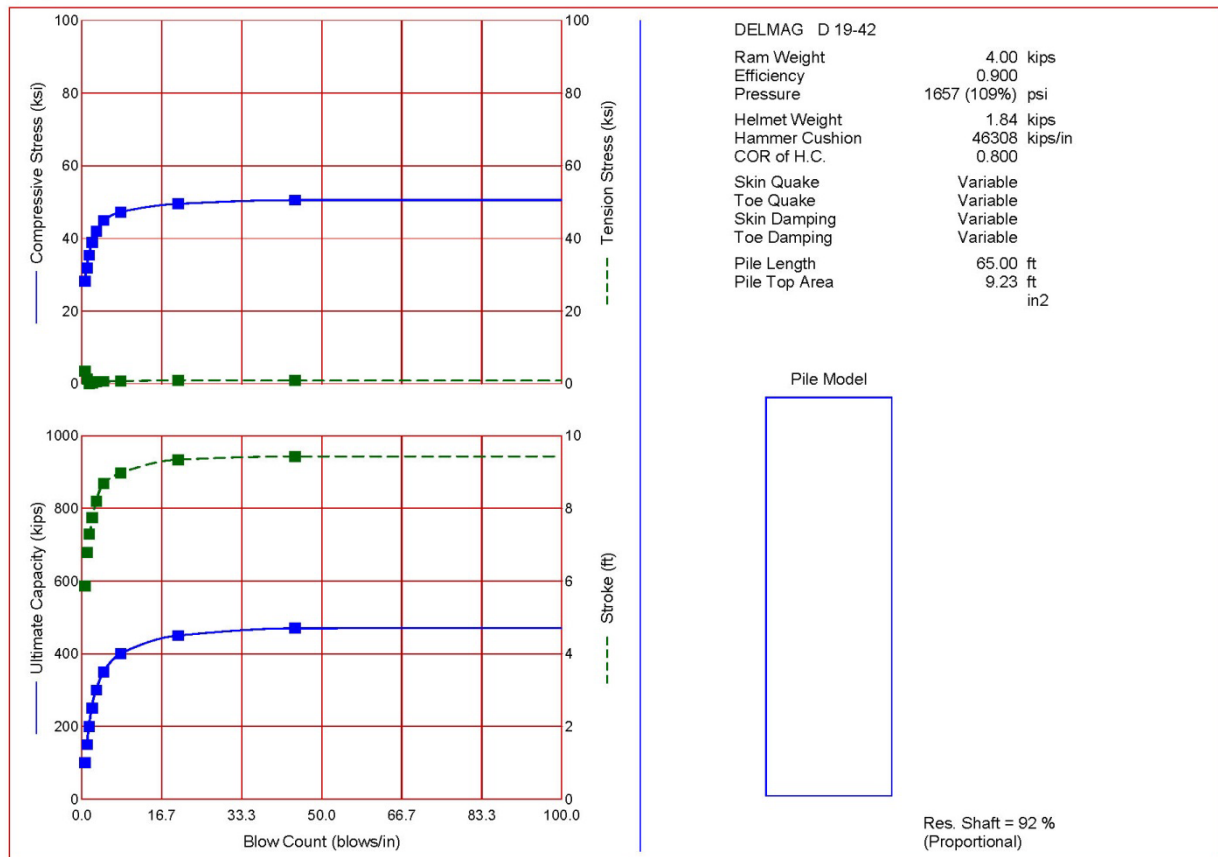


**Figure 143. GeoDynamica modified WEAP driving resistance graph**

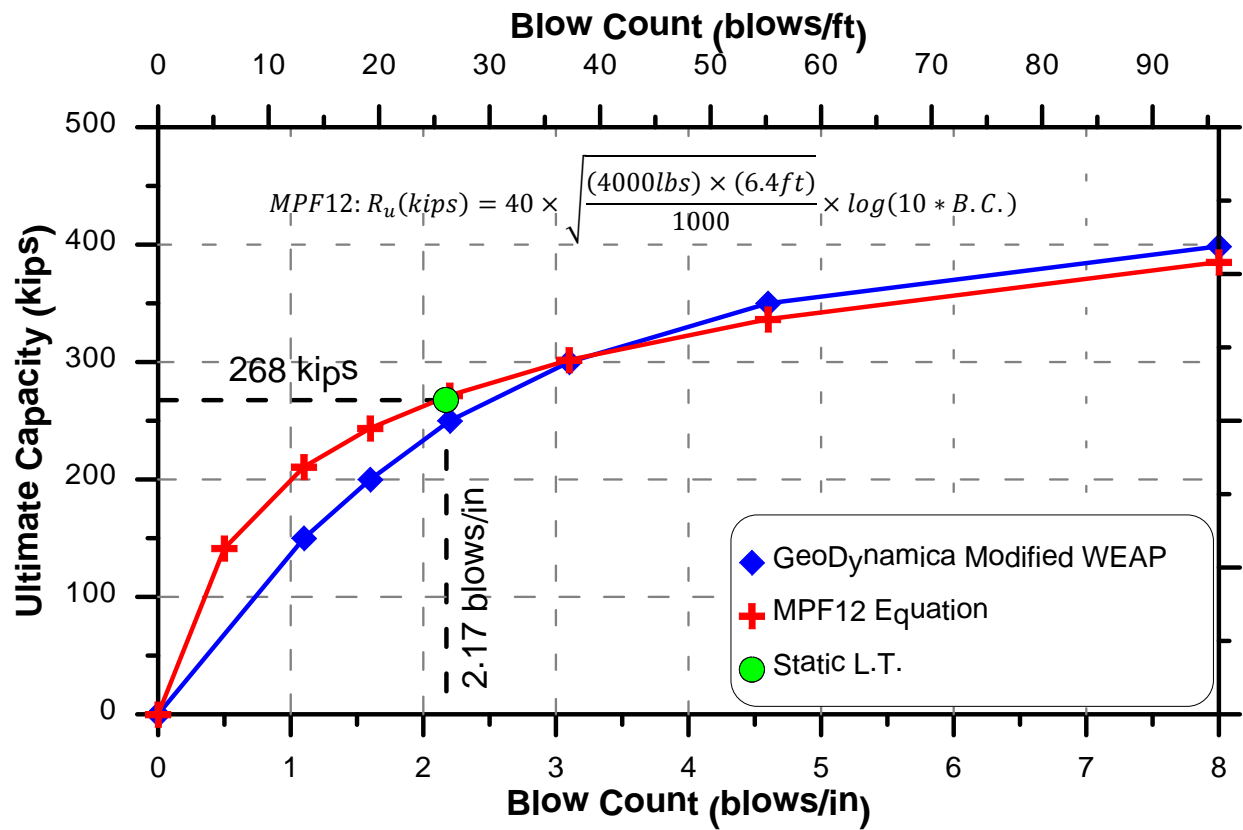


**Figure 144. Driving resistance summary of Geodynamica modified WEAP, MPF12 and the static load test results**

#### 8.5.6 Instructions for WEAP Modifications Following Dynamic Measurements

Stroke or bounce chamber pressure and transferred energy should be compared between the WEAP and field measurements. Often transferred energy values are lower than calculated and adjustment of hammer efficiency alone may improve energy agreement but need to be checked that driving stresses and capacity remain in agreement requiring the cushion stiffness or coefficient of restitution adjustment. Due to the many variables, matching of measured values can be difficult and matching stresses and transferred energies within 10% of the observed or measured quantities are sufficient.

The following procedure is recommended by the FHWA (2006) and requires that wave equation input parameters for hammer, driving system, and soil resistance are adjusted and then wave equation analyses are run for the CAPWAP calculated capacity. The following data preparation steps and successive input parameter adjustments generally lead to an acceptable solution.

- a. Set up a table with the observed stroke or bounce chamber pressure for diesel hammers, and measured values of compressive stresses and transferred energy, both at the measurement location. Include in this table for concrete piles the PDA calculated maximum tension stresses. These values should be averages over several consistent blows of pile installation or the earliest consistent blows of restrike testing. Additional matching quantities are CAPWAP calculated capacity and penetration resistance.
- b. Set up a wave equation model to run bearing graphs for the actual hammer, pile, and driving system with total capacity, resistance distribution, quake, and damping from CAPWAP.
- c. Run wave equation analyses and compare results with table values from step a. Adjust hammer efficiency (for diesel hammers, also maximum combustion pressure) until agreement between measured and wave equation computed compressive stress and transferred energy (for diesel hammers, also stroke) is within 10%. For steel piles, occasionally the hammer cushion stiffness, and for concrete piles modifications of the pile cushion stiffness, may also be needed. In rare cases, it is necessary to change the cushion coefficients of restitution.
- d. After an initial agreement has been achieved for transferred energy and pile top compressive stress, compare calculated penetration resistance for CAPWAP capacity and associated maximum tension stresses. For steel piles, adjust hammer cushion stiffness and coefficient of restitution, and for concrete piles adjust the equivalent pile cushion parameters together with efficiency to improve agreement of penetration resistance and tension stresses within the 10% tolerance.
- e. Adjust the hammer efficiency to values not greater than 0.95 and not less than 50% of the standard recommended hammer efficiency values for that hammer type. The exceptions are hammers whose stroke input is based on measured impact velocity. Efficiency values greater than 0.95 are then possible. Adjust cushion coefficients of restitution between 0.25 and 1.0.
- f. If penetration resistance and stresses cannot be simultaneously matched by adjusting hammer and driving system parameters, change the shaft and toe damping and the toe quake simultaneously and proportionately to achieve agreement between measured and computed penetration resistance. Under certain conditions, it may also be necessary to change the wave equation damping model from Smith to Smith-Viscous.

## **8.6 WEAP – Wave Equation Analysis of Piles – Submittal**

### **8.6.1 Description**

The submittal consists of conducting Wave Equation Analysis of Piles (WEAP) at each substructure or location specified on the contract plans, using the latest version of the WEAP software program. The analyses assumptions and driving recommendation shall be provided to

the Engineer for review and approval, to establish the pile acceptance criteria and ensure the proposed driving system will not overstress the piles.

### **8.6.2 Submittals**

The Contractor shall submit the wave equation analysis results and driving recommendations to the Engineer for review and approval. The wave equation analysis shall be conducted by an Engineer experienced in the use of the WEAP program and selection of the geotechnical and hammer input parameters.

As a minimum, the Contractor shall submit the following analysis assumptions:

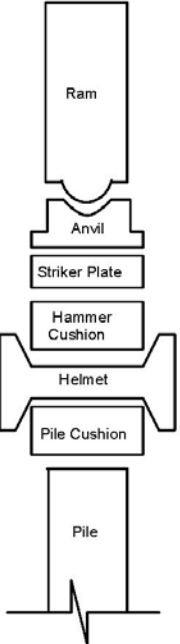
1. The pile type and size analyzed at each location.
2. The Nominal Required Bearing specified at each location.
3. The test pile bearing when test pile(s) are specified.
4. The batter angle(s) of any piles specified to be driven in a non-vertical alignment.
5. The proposed or anticipated total pile length and length above ground at end of driving.
6. Ground surface elevation during driving.
7. The assumed subsurface soil profile layer depths and thicknesses, location of water table, soil type and strength parameters.
8. Borings numbers used to develop the design soil profile.
9. Explanation of why any input values were selected that differ from the default values recommend by the program.
10. A completed "Hammer Data Form" documenting the proposed hammer, helmet and cushion information, see Figure 145 or see <http://www.pile.com/pdi/users/GRLWEAP/equipdatafrm-en.pdf>

The recommendations to be included in the submittal are to include:

1. An assessment of the proposed hammer driving system(s) ability of drive the test, production and batter piles to their required bearings at a penetration rate between 2 and 10 blows per inch.
2. The expected stress levels in the piles at the maximum expected hammer energy and any recommended limitations on hammer energy or fuel settings to ensure the pile stresses do not exceed 90% of the pile yield stress.
3. A pile inspector's charts showing hammer stroke (ft) or Energy versus pile penetration rate (blows/inch) at the nominal required bearing, batter pile bearing and test pile bearing for each substructure specified.

## Pile Driving Equipment Data Form

Structure Number: \_\_\_\_\_ - \_\_\_\_\_  
 Pile Driving Contractor: \_\_\_\_\_  
 Abutment / Pier Number(s): \_\_\_\_\_ Route: \_\_\_\_\_  
 Pile Type & Size(s): \_\_\_\_\_ Section: \_\_\_\_\_  
 Nominal Required: \_\_\_\_\_ County: \_\_\_\_\_  
 Production Pile Length(s): \_\_\_\_\_ Closest Boring(s): \_\_\_\_\_ Contract: \_\_\_\_\_  
 Hammer Manufacturer: \_\_\_\_\_ Model No: \_\_\_\_\_  
 Type (diesel, air/steam hydraulic, etc.): \_\_\_\_\_ Ram Stroke Type (fixed or Variable): \_\_\_\_\_  
 Maximum Operating Energy: \_\_\_\_\_ Minimum Operating Energy: \_\_\_\_\_

	<p>             Maximum Recommended Stroke: _____              Minimum Measurable Stroke: _____              Ram Weight: _____              Anvil Weight: _____              Modifications to Hammer (if any): _____              Striker Plate              Diameter: _____              Thickness: _____              Weight: _____              Hammer Cushion Material 1              Material Type: _____              Diameter: _____              Thickness per Plate: _____              No. of Plates: _____              Total Hammer Cushion Thickness: _____              Hammer Cushion Material 2 (if composite)              Material Type: _____              Diameter: _____              Thickness per Plate: _____              No. of Plates: _____              Helmet (Drive Head, Pile Cap) Weight (including bonnet insert if any): _____              Pile Cushion (precast concrete piles only)              Material: _____              Thickness Per Sheet: _____              Area: _____              No. of Sheets: _____              Thickness Total: _____           </p>
--	--

Double Acting/Differential Acting Air or Steam  
 Hammers Net Weight: \_\_\_\_\_  
 Cylinder Net Weight: \_\_\_\_\_  
 Piston Area: \_\_\_\_\_

Attach Bounce Chamber Pressure vs. Equivalent Energy Graphs (Closed-End Diesel Hammers Only): \_\_\_\_\_

Hammer Data Completed by: \_\_\_\_\_ Contact Phone Number: \_\_\_\_\_  
 Date Completed: \_\_\_\_\_

**Figure 145. Sample pile driving equipment data form**

A new analysis is required if the contractor makes driving system changes from what is proposed in the approved analysis.

## **8.7 MnDOT Specifications**

The following specification summary was proposed by Eng. Derrick Dasenbrock based on review of documents and discussions with Samuel Paikowsky and Aaron Budge.

### **C.1 Requirements for Pile Hammers**

Use pile driving equipment approved by the Engineer. The Engineer will use the contractor-provided Driving System Submittal (C.1.1) as the basis for approval of equipment. Acceptance of the pile driving equipment does not relieve the Contractor of the responsibility to properly install the piling. If in the opinion of the Engineer the accepted driving system fails to perform satisfactorily during actual driving, the Engineer reserves the right to revise the driving criteria and/or require change of equipment.

#### **C.1.1 Driving System Submittal**

The driving system submittal must be sealed and signed by a professional engineer, licensed in the State of Minnesota. Allow 10 business days for the Department's review. Allow an additional 10 business days for the review of any resubmittals. No variations in the driving system will be permitted without the Engineer's written approval. Submit a Revised Driving System Submittal if the hammers or other driving system components change from those shown in the original approved submittal. Use the same pile hammer to drive test piles and to drive the piles authorized by the Engineer based on the results of the test pile driving. Any variation needs to be authorized by the engineer.

For the Driving System Submittal, perform drivability studies as follows for each hammer and pile type:

1. Model the proposed driving system including hammers, striker plate, hammer cushion, helmet, and pile cushions based on a wave equation analysis.
2. Include in the analysis pile length variation to account for driven length variation, stickup length, and other considerations appropriate to construction requirements. As appropriate, include soil parameter variations to account for geotechnical uncertainties at the project site as well as possible range of hammer energy.
3. Use the last version of an authorized computer program (GRL WEAP or similar program).
4. When a follower is used, include (1) an analysis of the driving system with the follower and (2) an analysis of the driving system without the follower.
5. When adding weld on sections, provide set-up analysis and redrive assessment considering capacity change during driving recess and the effect of the additional pile section.

Include in the Driving System Submittal:

1. Results of the drivability analysis showing that all proposed driving systems will install piles to the specified tip elevation or nominal pile bearing resistance shown on plans. The system should be adequate to overcome the greatest expected driving resistance or a minimum of 155% of the factored design load and account for end of initial driving, interruptions in driving, and restrike conditions, as appropriate. Driving systems must generate sufficient energy to drive the piles with compressive and tensile stresses not more than 90 percent of the yield strength of a steel pile as driven.
2. The Engineer will only accept pile driving equipment, as determined by the wave equation analysis, capable of operating from 30 blows per ft to 180 blows per ft [10 blows per 0.1 m to 60 blows per 0.1 m] at the above conditions.
3. Include with relevant ranges when applicable scaled graphs depicting:
  - 3.1 Pile compressive stress versus blows per foot.
  - 3.2 Pile tensile stress vs. blows per foot.



- 3.3 Nominal driving resistance vs. blows per foot.
- 4. Complete description of:
  - 4.1 Soil parameters used, including soil quake and damping coefficients, skin friction distribution, and ratio of shaft resistance to total resistance.
  - 4.2 Assumptions made regarding the formation of soil plugs, drilling through the center of open ended steel shells, pre-augering, pre-boring, jetting, use of vibratory or other systems to advance the pile other than impact hammers, and the use of closure plates, shoes, and other tip treatment.
- 5. List of all hammer operation parameters assumed in the analysis, including fuel settings, stroke limitations, and hammer efficiency.
- 6. Copies of all test results from any previous pile load tests, dynamic monitoring, and all driving records used in the analyses.
- 7. Completed Pile and Driving Data Form along with manufacturer's specifications for pile driving system components. Driving system components will be confirmed by the Engineer upon delivery of the hammer to the project site.
- 8. An electronic copy of the WEAP input files.

## **9 STATIC LOAD TEST – PROCEDURES, INTERPRETATIONS AND SPECIFICATIONS**

### **9.1 Background**

#### **9.1.1 Overview**

Traditional static axial load test is performed by a slow application of a force produced against independent reaction, imitating structural loading. It is the most reliable method to determine the pile's performance as commonly required under typical service conditions, and hence, remains as the 'benchmark' for pile behavior monitoring and capacity determination. The major limitations of the static load testing are: (i) high cost associated with set-up, test duration, interpretation and construction delays, (ii) often carried out to a limited load (typically to twice the design load) and hence serves as a "proof test", which does not provide meaningful information for possible savings or future design, and (iii) inability to obtain information about the pile-soil interaction along the pile without additional testing means (e.g. tell tales, strain gauges, etc.). These limitations are acute when high capacity foundations are involved.

Alternative methods to the standard static load testing have been developed in two avenues:

- i. Static loading by methods that either do not require independent, external reaction for load application (e.g. Osterberg cells – Osterberg, 1989), or short duration, pseudo-static loading procedures (e.g. Static-Cyclic Testing; Paikowsky et al., 1999), and
- ii. Dynamic testing in which the pile is exposed to dynamic effects i.e., a varying stress with time is generated at the top of the pile through the impact of a mass or its combination with explosion

The dynamic testing methods include the generation of low and high strain waves as well as impacts that produce short and long relative wavelengths. The methods that produce a relatively long wavelength (e.g. Statnamics, Birmingham and Janes, 1990) are most appropriately termed kinetic testing (Holeyman, 1992). These testing methods encounter difficulties in wave resolution with depth, and hence in interpretation of test results based on wave mechanics, as explained below. The traditional impact tests in which a falling mass strikes the pile top (driving hammers or drop weight systems) become, therefore, an attractive testing solution due to physics principles and economical advantages.

Paikowsky (2004, 2013) outlines the basic methodology for understanding the underlying principles of the dynamic and static testing methods in the framework of wave length. This leads to the testing categorization as well as the description and the analyses of the tests themselves.

### 9.1.2 Principles

A simplified mechanical model was introduced (Paikowsky 2004, 2013), producing a relationship between force and velocity at pile top vs. impact time. That allows to examine the relationship between the produced wave length and the ability to analyze the pile-soil system. Such a measure can be done through the relationship between the wavelength and the pile length, introducing the relative wavelength  $\Lambda$ :

$$\Lambda = \text{Length of the force pulse} / \text{double length of the pile } (2L)$$

The relationship between pile acceleration, force duration, and relative wavelength (which represents the sharpness and duration of the force pulse) for different pile tests is presented in Figure 146. To understand a relative wavelength, one needs to follow the propagation of a force pulse through a pile realizing the importance of the pulse sharpness and its length relative to the pile's length.

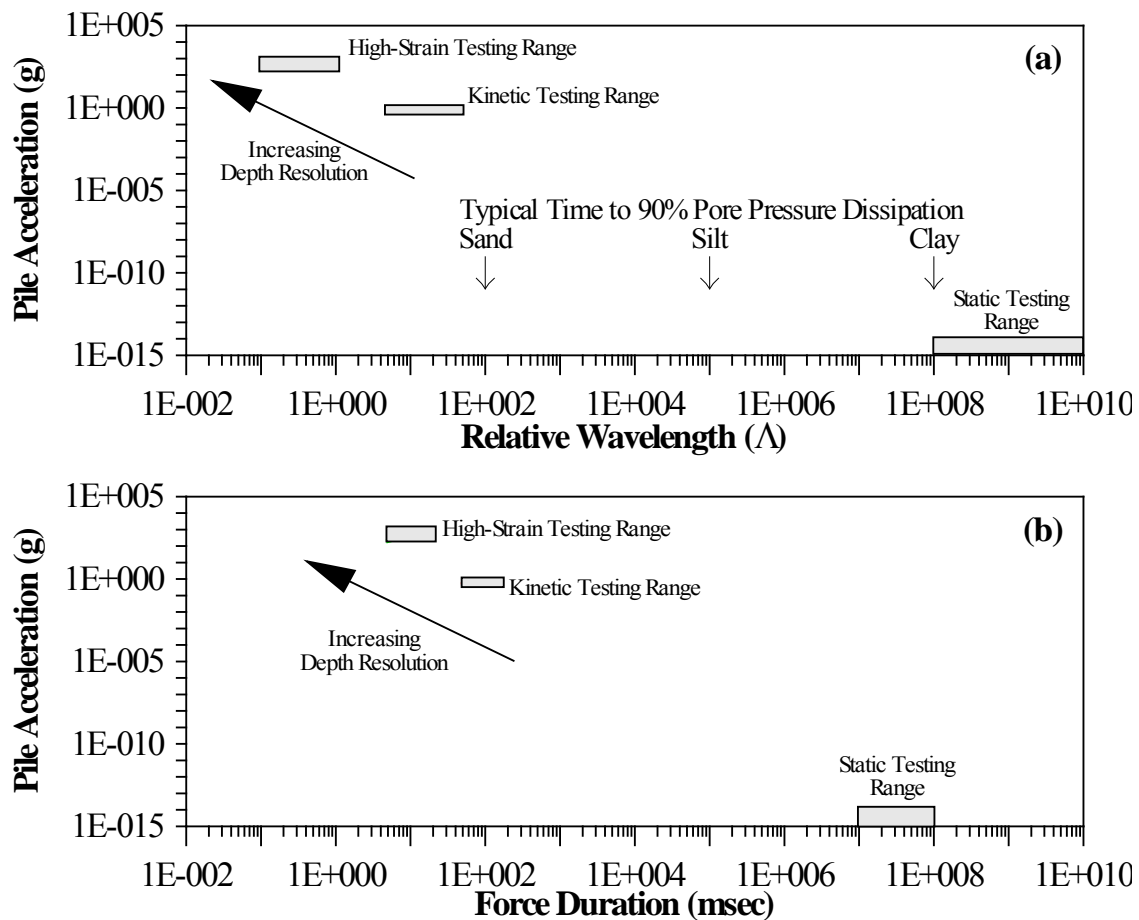


**Figure 146. Typical load testing values for Pile A acceleration vs. (a) relative wavelength, and (b) force duration (after Holeyman, 1992)**

When a compressive force pulse propagates down the pile, it will be reflected whenever there is a change in the pile impedance (e.g. change in cross-section) or as a result of external forces (i.e. friction), generating two waves; a compressive wave up and a tension wave down, which combines with the initial pulse. Upon reaching the pile toe (under easy or normal driving conditions, say less than 8 BPI) the resulting downward compressive wave is reflected upward and reversed (compression becomes tension) with a compressive offset corresponding to the mobilized toe resistance. On its way up toward the pile head, the wave interacts again with (and activates) the shaft resistance, and impedance changes, arriving back to the pile top after time  $t = 2L/c$  in which  $L$  is the pile's length and  $c$  speed of wave propagation. This depiction of wave mechanism results in the understanding that:

- i. A shorter pulse duration enables higher resolution of the propagating waves and the combined reflections,
- ii. The number and complexity of the waves depends on the changes of the cross-section of the pile, and
- iii. The reflecting wave is affected by the interaction of the pile with the soil (shaft and end resistances) allowing the interpretation of the soil's resistance along the shaft.

### ***9.1.3 Pile Testing in Light of Pulse Duration and Relative Wavelength***

Following the above, one can examine the different dynamic testing in light of the produced relative wavelength and possible interpretation. Integrity testing that utilizes reflection techniques of low strain, short duration pulse, is typically characterized by a relative wave length of 0.1, which provides for maximum depth resolution. Dynamic testing during driving is typically characterized by a relative wavelength of 1, associated with force duration of 5 to 20 milliseconds. These relations allow for depth resolution for typical piles while providing high strain testing. Further enhancement of the depth resolution is possible with additional internal measurement near the pile's tip (e.g. Smart Pile System, Frederick, 1996, or McVay et al., 2004). Dynamic Fast Penetration (or Kinetic Testing) such as Statnamic (Birmingham and Janes, 1990), as well as Dynatest or Fundex, are characterized by a relative wave length  $\Lambda$  of 10 or higher and, therefore, do not allow for depth resolution. The produced pulse duration is about 50 to 200 milliseconds (about an order of magnitude larger than that of impact dynamic testing), and practically the front of the wave's reflection from the tip arrives back to the top before the main portion of the wave propagates through the pile.

Although these tests resort to inertial actions on masses to generate their extended force pulse, they can be referred to as "Kinetic Tests" or "Dynamic Fast Penetration" as the inertial forces within the pile are small compared to the force being applied, and as a result of their high relative wave length, the interpretation of these tests cannot make use of the wave equation form of analysis, hence, different from tests which can be categorized as Dynamic Wave Action tests (e.g. impact hammer). This fact does not affect the ability to determine the total

capacity/resistance of shafts from kinetic tests using other techniques or diminishes their distinctive advantages such as mobility and the ability to produce high-energy impacts to mobilize the resistance of very high capacity shafts.

The above discussion leads to the categorization of pile testing based on the nature of the loading and its duration relative to the pile itself. The relative wave length ( $\Lambda$ ) explains the relationship between the loading, the transfer of the loading in the pile, the importance of dynamic effects, and the ability to analyze the pile-soil interaction as a result of measurements recorded at the pile's top. Table 84 outlines the different tests based on this categorization and their relevant method of analysis.

**Table 84. Typical Key Attributes of Different Types of Pile Tests (Holeyman, 1992)**

Attributes	Integrity Testing	High-Strain Dynamic Testing	Kinetic Testing	Static Testing
Mass of Hammer	0.5 - 5kg	2,000 - 10,000 kg	2,000 - 5,000 kg	N/A
Pile Peak Strain	2 - 10 $\mu$ str	500 - 1,000 $\mu$ str	1,000 $\mu$ str	1,000 $\mu$ str
Pile Peak Velocity	10 - 40 mm/s	2,000 - 4,000 mm/s	500 mm/s	$10^{-3}$ mm/s
Peak Force	2 - 20 kN	2,000 - 10,000 kN	2,000 - 10,000 kN	2,000 - 10,000 kN
Force Duration	0.5 - 2 ms	5 - 20 ms	50 - 200ms	$10^7$ ms
Pile Acceleration	50 g	500 g	0.5 - 1 g	$10^{-14}$ g
Pile Displacement	0.01 mm	10 - 30 mm	50 mm	>20 mm
Relative Wave Length	0.1	<1.0	>10	$10^8$

A comprehensive testing program illustrating the above concept was carried out on a test pile cluster at a bridge reconstruction site in Newbury, Massachusetts. The research at the site was conducted by the Geotechnical Engineering Research Laboratory at the University of Massachusetts Lowell, as part of a long-term research sponsored by the Massachusetts Highway Department (see e.g. Paikowsky and Chen, 1998, and Paikowsky and Hajduk, 1999).

Figure 147 presents magnitudes and durations of load measurements during some of the testing conducted on a 14-inch square, 80 foot long pre-stressed, pre-cast concrete pile. The pile was instrumented and subjected to various testing over a long period of time; relevant information is provided by Paikowsky and Hajduk (2004), Hajduk et al. (2000), and Hajduk et al. (1998). The data in Figure 147 demonstrates the principles previously discussed. The driving system produced an impact of about 5 milliseconds in wave length, the Statnamic test produced a wave length of about 60 milliseconds, a Static-Cyclic load test was carried out at about 15 minutes a cycle while a short duration static testing was about 8 hours. A slow maintained load test that was carried out at the site was not included in Figure 147, as it adversely affected the time scale. The data in Figure 147 clearly demonstrates the different time ranges phenomena associated with the different tests.

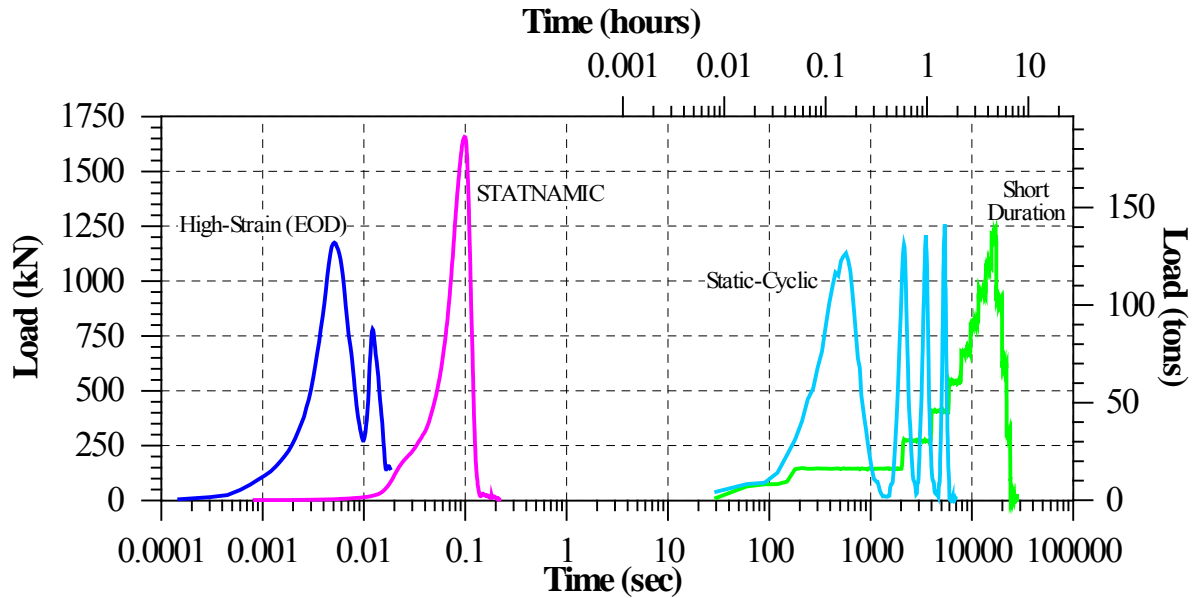


**Figure 147. Typical loading durations for various tests performed on Test Pile #3 by the Geotechnical Engineering Research Laboratory of the University of Massachusetts Lowell, at the Newbury test site**

## 9.2 Review of Static Pile Load Testing Methods

### 9.2.1 ASTM Procedures

#### *Overview*

The American Standard for Testing and Materials (ASTM) provides three designated standards for static load test procedures:

D1142/1143M-07 (Reapproved 2013) “Standard Test Methods for Deep Foundations Under Static Axial Compressive Load”

D3689/D3689M-07 (Reapproved 2013) “Standard Test Methods for Deep Foundations Under Static Axial Tensile Load”

D3966/D3966M-07 (Reapproved 2013) “Standard Test Methods for Deep Foundations Under Lateral Load

The tests for axial compressive loading outlines five procedures, and that of tensile (uplift) loading outlines six procedures that are described briefly below. The overlapping procedures for compression and tension are presented together. For more details, refer to ASTM D1143-07 and D3689-07 (both reapproved in 2013). Table 85 and Figure 148 summarize these procedures.

**Table 85. Summary of static load test procedures**

Code	Test Name	Loading		Hold Time at Max. Load	Unloading		Hold Time at Zero Load
		Increments	Hold Time		Decrements	Hold Time	
<b>ASTM D1142/1143</b>	Proc A Quick LT	5%	4-15min	-	5-10 steps	Instantaneous	0hr
	Proc. B Maintained LT Standard Loading Proc.	25%	0.01"/hr	24hr	25%	1hr & 0.01"/hr	1hr
	Proc. G Cyclic Loading	50%, 100%, 150%, 200%	1hr 0.33hr	0hr 12-24hr	50% 25%	0.33hr 1hr	1hr 0hr
	Proc. E Constant Rate of Penetration	0.01-0.05"/min	0hr	-	-	-	-
<b>MassDOT</b>	Short Duration	25%	0.5hr	1hr	25%	0.25hr	1hr
	Maintained LT	50%	2hr	12-24hr	25%	4hr	4hr
	Quick LT	10-20kips	2.5min	5min	25% of max	2.5min	15min
	Static-Cyclic LT	Continuous loading at 20-40kips/min			Continuous at 60-80kips/min		Carry out 3 cycles of load to failure and unload

Notes:

1. ASTM – American Standard for Testing and Materials
2. MassDOT – Massachusetts Department of Transportation
3. All percentages relate to the design load of the pile.
4. The loading increment for the standard test is based on the assumed bearing capacity of the pile.

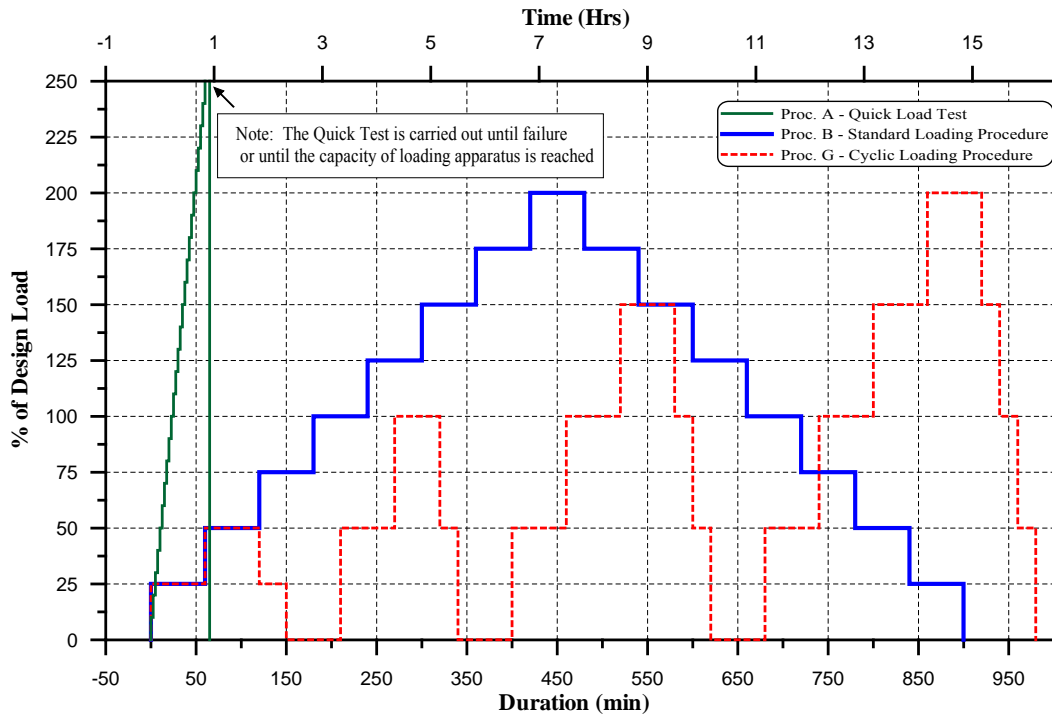


**Figure 148. Static pile load testing procedures according to ASTM (Paikowsky et al., 1999)**

***Procedure A – Quick Load Test Method for Individual Piles or Pile Groups (ASTM D1143 and ASTM D3689 section 8.1.2)***

The load is applied continuously (delay at every increment for a consistent interval of 4 to 15 minutes for readings only) in increments of 5% of the anticipated failure load. Load increments are added until reaching failure or the safe structural limit, i.e. continuous jacking is required to hold the test load or practically until the specified capacity of the loading device is reached. After one of these criteria is reached, the load is removed from the pile in 5 to 10 approximately equal increments. The procedure recommends considering longer time intervals for the failure load and the final zero without specific guidelines.

***Procedure B – Maintained Load Test Standard Loading Procedure (ASTM D1143 and D3689 section 8.1.3)***

The traditional (standard) ASTM method calls for single piles to be loaded to 200% of the anticipated design load and pile groups to 150% of the design load unless failure occurs first. The load is applied in increments of 25% of the design load. Each load increment will be held until the rate of settlement is not greater than 0.01 inches per hour (0.25mm/hr) but no longer than two hours per increment. In the event the pile has not failed, the total load is held on the test pile or pile group for 24 hours. If failure occurs during loading, the maximum load is maintained until the total settlement equals 15% of the pile diameter. After completing the final load increment, the load is removed in decrements of 25% of the maximum test load with one hour between decrements.

***Procedure C – Maintained Load Test in Excess of Procedure B (ASTM D1143 and D3689 section 8.1.4)***

Following the loading and unloading of Procedure B, the pile or pile group is loaded to the maximum maintained load in increments of 50% of the design load allowing 20 minutes between load increments and then applying additional load in increments of 10% of the design load until reaching the maximum required load or failure. If failure does not occur, the maximum load is held for 2 hours and then removed in four equal decrements allowing 20 minutes between decrements. If failure occurs, the pile is continued to be loaded until the settlement equals 15% of the pile diameter.

***Procedure D – Constant Time Interval Loading (ASTM D3689 section 8.1.5)***

Using procedure B but applying the load in increments of 20% of the design load with 1 hour between load increments. Unload in decrements of 25% of the maximum test load with 1 hour between decrements.



***Procedure E – Constant Rate of Penetration or Uplift (ASTM D1143 and D3689 section 8.1.6)***

The pile is loaded at a constant rate of penetration 0.01 to 0.05 in/min (0.3 to 1.3 mm/min) for cohesive soils or 0.03 to 0.1 in/min (0.75 to 2.5 mm/hr) for granular soils. For uplift, maintain a pile uplift rate of 0.02 to 0.04 inch/min (0.5 to 1.0 mm/min). In the compression test, the pile is continually loaded until no further increase in load is necessary for the constant rate of penetration of the pile under the predetermined rate or the capacity of the pile is reached. If the pile continues to settle under the constant load, the load is held until the pile has moved at least 15% of the average pile diameter and then the pile is gradually unloaded completely. If maximum capacity of the pile is reached before failure, the total load is released.

***Procedure F – Compression Constant Movement Increment Test (ASTM D1143 section 8.1.7)***

Load is applied in increments required to produce pile top movement increments equal to approximately 1% of the average pile diameter/width. The load is varied as necessary to maintain each movement. The pile is continued to be loaded until the load movement equals 15% of the average pile diameter/width. The load is then removed in four equal decrements.

***Procedure F Uplift and G Compression – Cyclic Loading Test (ASTM D1143 section 8.1.8 and D3689 section 8.1.7)***

The pile is loaded in a series of four cycles up to 50%, 100%, 150% and 200% of the design load (50% and 100% for pile groups). Each cycle follows the loading procedure described in Procedure B, e.g. the first cycle is loaded in increments of 25% of the total design load up to 50% and each load increment is held for one hour, at 50% the pile is unloaded in decrements of 25% until the entire load is removed from the pile with 20 minutes between decrements. Cycles two, three, and four are loaded to 100%, 150%, and 200%, respectively in increments of 50% of the total design load. Each load increment is held for one hour during each cycle. Once the maximum load is reached per cycle, the pile is unloaded to zero in decrements of 50% of the maximum applied load with 20 minutes between each unloading.

***9.2.2 Massachusetts Department of Transportation (MassDOT) Procedures***

***Overview***

The Massachusetts Department of Transportation described in its standard specifications for Highways and Bridges – 1988 English edition (see also 1995, 1998 and 2006) load test procedures similar to the previous generation ASTM methods. The procedures described by the MassDOT encompass the short duration test, maintained load test, and the quick load test. The procedures are described in detail by the MassDOT (1995) and were supplemented by a new load test procedure, Static-Cyclic (Express) load test as appears in the Supplemental

Specifications of 2012. All procedures are briefly described below and summarized in Table 85 and Figure 149.

### ***Short Duration Test***

Massachusetts Highway Department requires the load to be applied up to 200% of the design load to the load transferring 100% of the design load to the bearing layer as determined by tell-tales, but not to exceed 90% of the reaction load. The load is to be applied in increments of 25% of the design load. Each load increment is held for half an hour. Once the maximum applied load is achieved, it is held for one hour and until the settlement rate is less than 0.01 inch per hour (25 mm/hr). After both of the above criteria are met, the load is removed in decrements of 25% of the design load every 15 minutes until zero load is reached. Finally, zero load is held for one hour to complete the test.

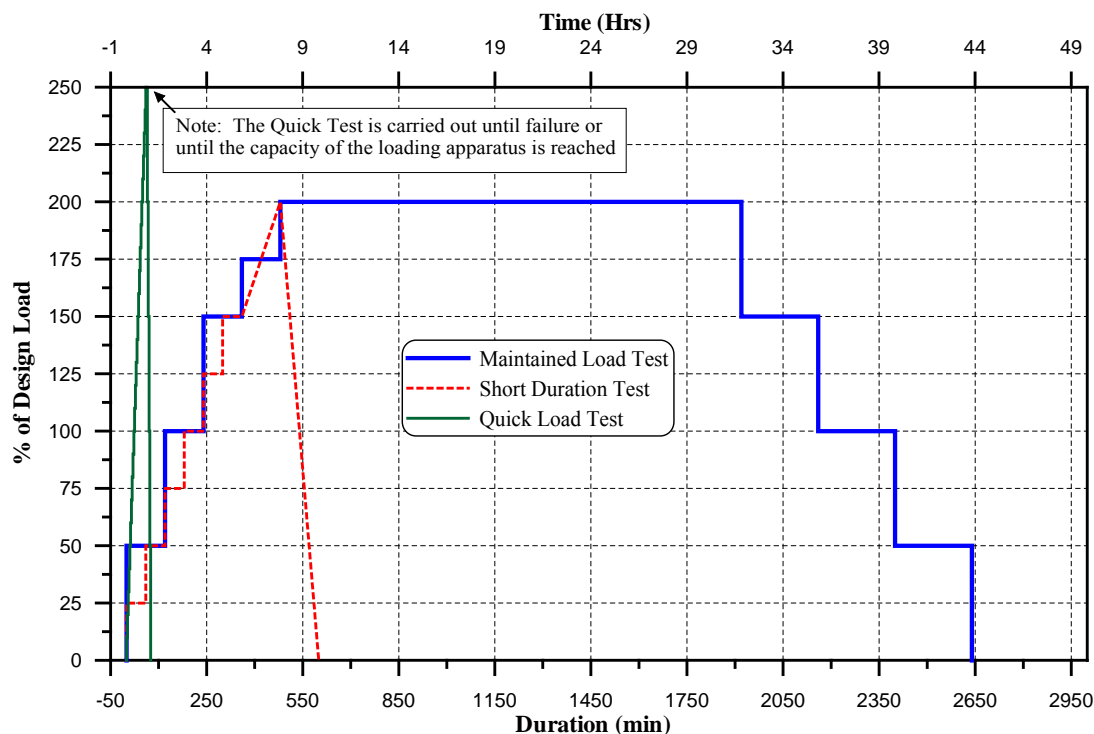


**Figure 149. Static pile load testing procedures according to MassDOT (Paikowsky et al., 1999)**

### ***Maintained Load Test***

The pile is tested under load increments equal to 50, 100, 150, 175, and 200% of the design load and maintained for a period of two hours. Once the maximum load is achieved, it is held until the settlement does not exceed 0.02 inches (0.5 millimeters) in a 12-hour time period or until the pile failed. The loading period for twice the design load is held no less than 24 hours. After

completion of the loading, the unloading is conducted in decrements not exceeding one quarter of the total test load and maintained for a period of four hours each.

### ***Quick Load Test***

The test shall be applied in increments of 5 to 10 tons not to exceed 10% of the design load and maintained for 2.5 minutes until continuous jacking is required to maintain the test load. The final load increment shall be held for no more than five minutes and then unloaded in four equal decrements.

### ***9.2.3 Static-Cyclic (Express) Load Test***

This load test procedure was proposed by Paikowsky et al. (1997) and appears as part of the Massachusetts Department of Transportation supplemental Specifications to the 1988 English Standard Specifications and 1995 metric standard specifications (see MassDOT, 2012). The following language is a direct quotation of the MassDOT specifications.

This load test can apply to a compression test, tension test, or both, on a pile and provide the ultimate capacity of the pile. The load test is carried out in four “loading-unloading” cycles, at a constant loading rate, conducted continuously without allowing for settlement stabilization. The loading frame should be designed to handle at least two times the estimated ultimate pile capacity. The displacement and load readings from the top of the pile are to be taken continually by a data acquisition system. The load sequence shall be as follows:

- a. For a compression test; apply continuously a load at a rate between 20 to 40 kips/minute (100 to 200 kN/minute) until failure is observed and an additional settlement equal to 0.1 inches (2.5 mm) is achieved with total pile settlement equal or exceeding 1 inch (25 mm). A failure is defined when displacement increases without an increase in the pile’s load at or below the ratio of 0.1 kips/0.1 inch/foot (0.67 kN/mm/meter) pile embedment for all compression tests. Unload the pile at a constant rate between 60 to 80 kips/minute (300 to 350 kN/minute) until zero load. Carry out additional three load-unload cycles to the maximum load that was achieved in the first cycle.
- b. For a tension test, apply a load at a rate of 15 to 30 kips/minute (75 to 150 kN/minute) and unload at a rate of 30 to 60 kips/minute (150 to 300 kN/minute). Failure is defined when displacement increases without an increase in the pile’s load at or below the ratio of 0.05 kips/0.1 inches/foot (0.33 kN/mm/meter) pile embedment for all tension tests.
- c. For all tests, pile top load and displacement are measured at intervals of loads equal to 1/10 of the estimated ultimate pile capacity but no more than 20 kips (100 kN) for a compression test and 10 kips (50 kN) for a tension test. The readings need to allow for accurate definition of the load-unload interception. The use of electronic data acquisition

is recommended. If dial gages are used, the gages should not be adjusted at the end of the first cycle and the zero load reading at the end of the first cycle (first zero reading of the second cycle) will be subtracted from the readings of the second cycle.

The pile design load on this test is based on the measured ultimate capacity of the pile. The ultimate capacity of the pile is defined as the average of the three intersection points formed by the load-unload curves.

### **9.3 Static Pile Load Test Interpretation Procedures**

#### **9.3.1 Overview**

Various methods are available for interpreting static load test results in order to determine the pile's bearing capacity. The methods are based on different principles related to a limiting settlement, maximum load, ratio of load to settlement, shape of curve, and so on. Davisson's failure criterion (Davisson, 1972) is typically being adopted to provide a single unique value when determining a driven pile's bearing capacity based on a load test to failure. However, judgment must be used in evaluating this value as well. Detailed description of interpretation procedures and the analyses are presented by Paikowsky et al. (1994). The following brief description summarizes major methods to consider. Load test results on a 65 ft (19.8 m)-long, 24 inch square, pre-stressed concrete pile driven 63 ft into a silty sand in Alabama is used to demonstrate the different interpretation methods (see case no. 5 Paikowsky and Tolosko, 1999).

#### **9.3.2 Consistent Presentation of Load-Settlement Relationship**

For consistent visual judgment and interpretation of a load test load-settlement curve, a common scale needs to be implemented. The scale is based on the elastic deformation of the pile as proposed by Vesic, (1977). When plotting the load-settlement curve, the elastic deformation of a fixed end free standing frictionless pile (i.e., a column) is expressed as:

$$\delta = PL/EA \quad (28)$$

where:  $\delta$  = calculated elastic deformation of the pile  
P = applied load  
L = pile length  
E = elastic modulus of the pile's material  
A = cross-sectional area of the pile

The elastic compression obtained by equation 28 is based on the assumption that the entire load applied to the pile top is transferred to the pile tip. To implement a scale proportional to all settlement curves, the elastic compression line is kept inclined at an angle of approximately 20 degrees to the load axis. Figure 150 shows an example of a scaled load-settlement curve using

the above criterion. Note that observing the load-displacement relations in the non-scaled load-settlement relations would lead to an erroneous conclusion as to the ‘failure’ load if judged by the curve shape appearance alone.

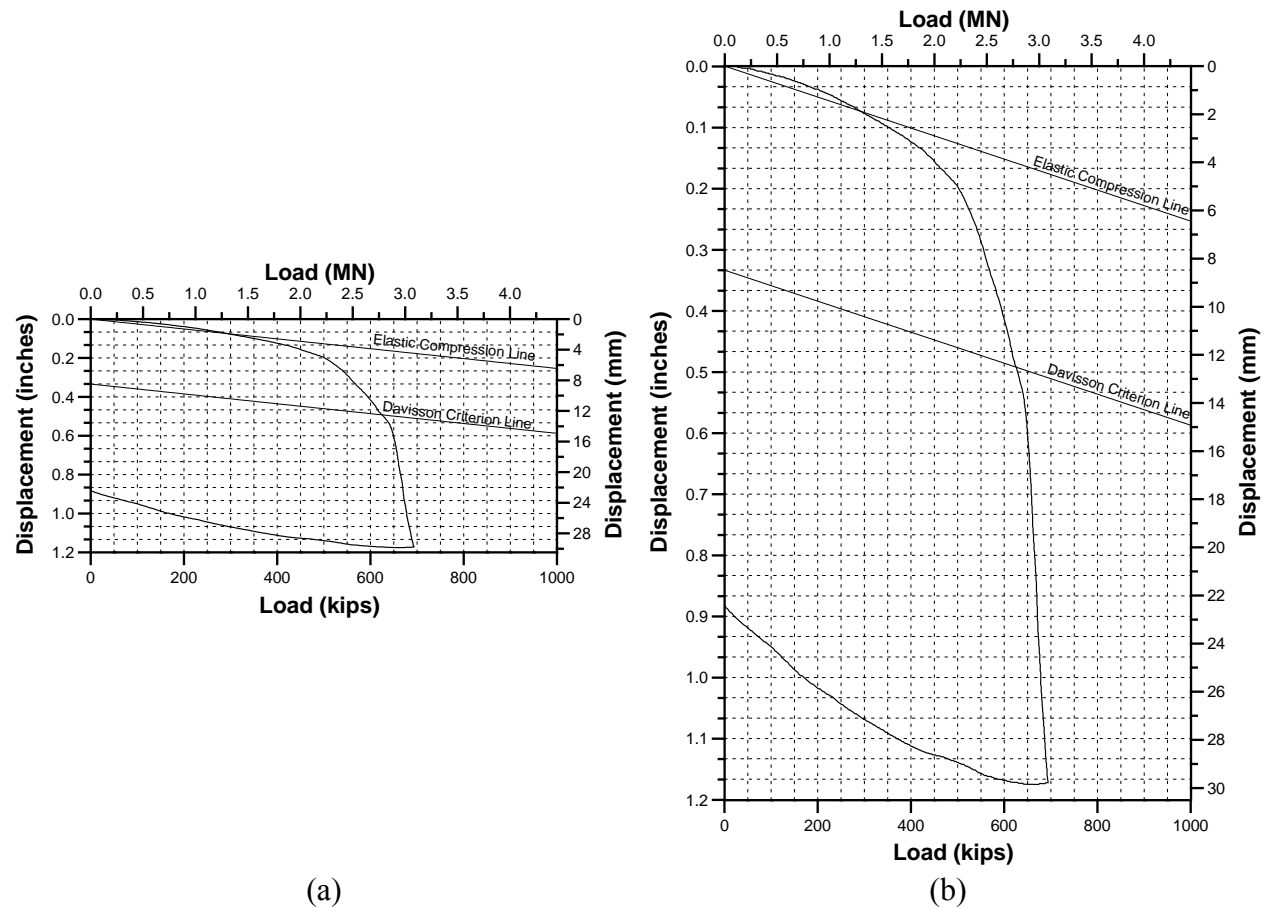


**Figure 150. Load-settlement curve with (a) a non-specific scale for Pile Case No. 5, and (b) with the elastic compression line inclined at 20 degrees (Paikowsky et al., 1994)**

### 9.3.3 Davisson's Criterion

Davisson's Criterion (Davisson, 1972), or the offset limits, defines the failure load of a pile as the load corresponding to the settlement that exceeds the elastic compression of the pile ( $\delta$ ) by an offset ( $X$ ) equal to 0.15 inches (3.8 mm) plus the pile diameter (in inches) divided by 120;

$$X = 0.15 + B/120 \quad (29)$$

where:  $X$  = Offset displacement of the elastic compression line (inches)  
 $B$  = diameter of the pile in inches.

The Davisson's Criterion line is parallel to the elastic compression line. The intersection of Davisson's line with the load-settlement curve provides the ultimate capacity of the pile. Figure

151 illustrates the use of Davisson's failure criterion for load-settlement relations for the pile described in section 9.3.1 yielding a capacity of 625 kips. Davisson's Criterion has the advantage of being deterministic (and hence objective), while being able to consider the pile properties and geometry, hence the influence of the tip size on the failure zone.

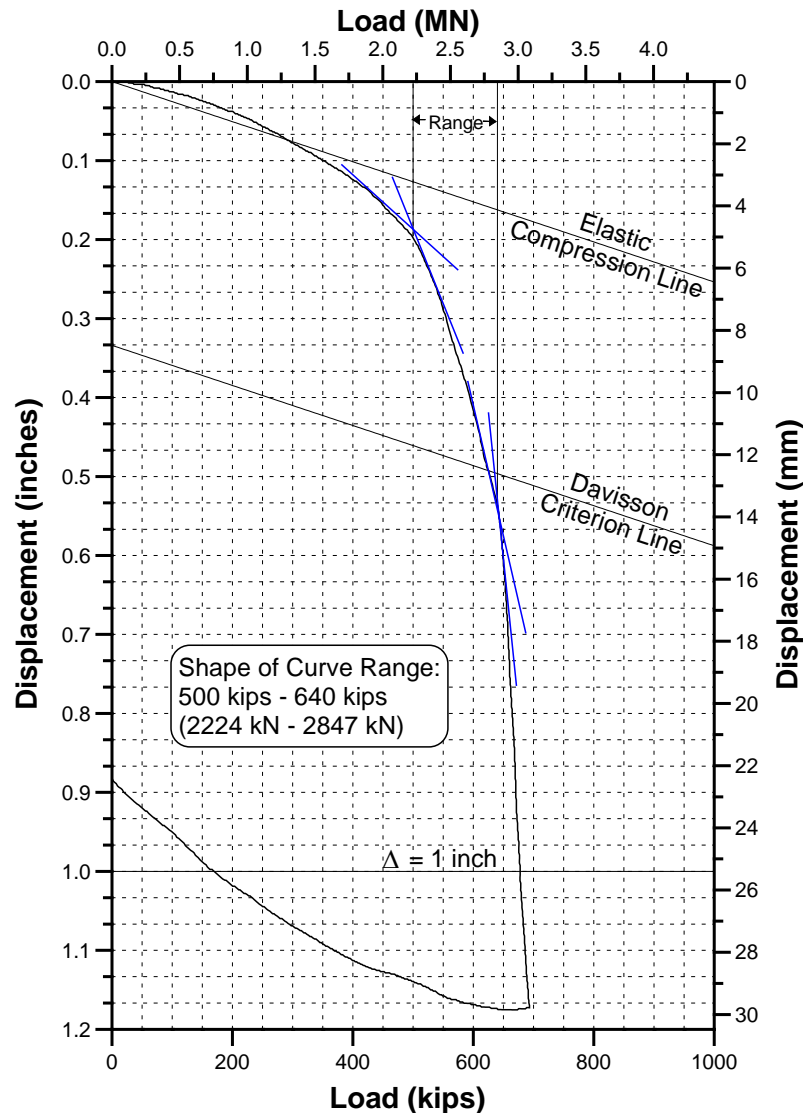


**Figure 151. Load-settlement curve for Pile Case No. 5 of the PD/LT data set with the elastic compression line inclined at 20 degrees and different ultimate capacity interpretation methods (Paikowsky et al., 1994)**

#### **9.3.4 Shape of Curve**

The Shape of Curve Method is a failure load approximation that usually yields a range of values over which the pile is considered at or near failure. The boundaries of this range can be determined by examining the minimum curvature in the load-settlement curve through lines drawn tangent to the load-settlement curve (similar to the method proposed by Butler and Hoy, 1977). The failure range is relatively easy to define for load-settlement curves that exhibit general failure or plunging failure (rapid settlement with slightly increased loads). Piles that experience local failure, or non-plunging failure, are difficult to analyze using the shape-of-curve method because of the uniform changes in the slope of the lines drawn tangent to the curve. Figure 151 illustrates the use of the shape-of-curve procedure, yielding an estimated capacity ranges of 500 kips to 640 kips with a representative average of 570 kips for the concrete pile for which Davisson's criterion resulted with 626 kips.

#### **9.3.5 Limited Total Settlement Methods**

The limited total settlement methods define the failure load as the load corresponding to the settlements of one inch ( $\Delta=1$  inch) and 0.1 times the pile diameter ( $\Delta=0.1B$ ) (Terzaghi, 1942). These methods are not applicable in many cases most likely due to the changes in the piles employed since 1942. For example, the elastic compression for a very long steel pile often exceeds 1 inch and/or  $0.1B$  without inducing plastic deformation in the soil at the tip and the lower portion of the pile. Figure 151 presents the load-settlement curve for the concrete pile that experiences a plunging failure well before a displacement of 1 inch is achieved but due to the plunging, the  $\Delta = 1$  inch criterion provides a failure of 679 kips. Also, it is obvious in this case that a settlement of  $0.1B$ , or 2.4 inches, does not represent the failure load of this pile, and therefore, is not applicable. In contrast, Paikowsky et al. (2004) had shown that the use of the FHWA failure criterion for drilled shafts ( $\Delta = 0.05B$ ) is the most suitable for such deep foundations.

#### **9.3.6 DeBeer's Log-Log Method**

DeBeer defines the failure load as the load corresponding to the intersection of two distinct slopes created by the load-settlement data plotted using logarithmic scales (DeBeer, 1970). Figure 152 illustrates the use of DeBeer's criterion for the same load-settlement curve (24 inch Pre-Stressed Concrete Pile) presented in Figure 150, resulting in an estimated capacity of 648 kips. The two slopes are especially visible for piles that experience plunging failures, yet when using DeBeer's method on piles that undergo local failures, the result may be a range of values.

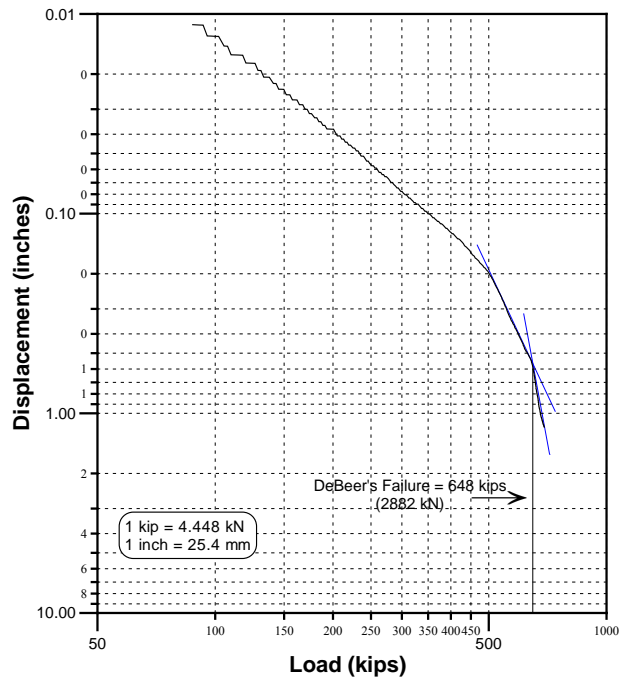


**Figure 152. Load-settlement data plotted on a logarithmic scale for Pile Case No. 5 to determine the failure load according to DeBeer's method (Paikowsky et al., 1994)**

### 9.3.7 Representative Static Capacity

The capacity results from Davisson's criterion, the Shape of the Curve, Limited Total Settlement methods, and DeBeer's method for the specific case history shown in Figures 150 to 152 yields the following values:

- Davisson's = 645 kips
- Shape of Curve = 500-640 kips, 570 kips representative
- $\Delta = 1$  inch = 679 kips
- $\Delta = 0.1B$  = not applicable
- DeBeer's = 648 kips

Excluding the  $\Delta = 1$  inch settlement method, which is clearly beyond failure and the  $\Delta = 0.1B$  method, which does not apply, the average of all acceptable criteria leads to a final representative static capacity of 614 kips.

Other interpretation methods like Chin (1971) and Brinch-Hansen (1963) methods are not widely used in practice and would result with failure capacities of 748 kips and 603 kips, respectively.

Paikowsky et al. (2004) used the above methods to independently evaluate the capacity of each pile of a large data set. After considering the pile type, size, and the load test procedure, unrealistic results were eliminated and the acceptable values were averaged, yielding a final



(representative) static pile capacity. These values were then employed against the individual interpretation procedure in order to establish a nominal strength and its uncertainty as detailed in section 9.5.

## **9.4 Full Scale Pile Testing Examining Testing Methods and Driven Piles Capacity Evaluation**

### **9.4.1 Overview**

The presented detailed case studies are aimed at demonstrating the previously discussed load test procedures as well as the interpretation method in order to allow for recommendations to be made for the MnDOT load test procedures. A fully instrumented test pile cluster was tested during a research project by the Geotechnical Engineering Research Laboratory of UMass Lowell for the Massachusetts Highway Department (currently MassDOT) as part of a bridge reconstruction site in Newbury, MA. The test pile cluster consisted of two 12-inch diameter close-ended steel pipe piles and one 14 inch, square, pre-cast concrete pile. The test piles were labeled as test piles #1, #2, and #3. Figure 153 shows the soil profile and test pile depths for the bridge reconstruction site in Newbury. The site generally consisted of a 4 ft top layer of a miscellaneous fill followed by a thin organic layer, a 3 ft overconsolidated clay layer, a 5 ft soft normally consolidated clay layer, a 5 ft normally consolidated clay layer, a 2 ft sand layer between two interbedded silt, sand and clay layers, a 2 ft fine to medium sand, followed by 4 ft of fine to coarse gravel/till, underlain by bedrock at a depth of 98 ft from the ground surface. For a detailed description of the soil properties at the Newbury bridge reconstruction site, refer to Paikowsky and Chen, (1998).

Figure 153 shows the magnitude of the instrumentation and depths associated with each test pile. The vibrating wire strain gages (VWSG) inside each pile are used to monitor the load distributions under the static load tests. For a more detailed description of the piles and their instrumentation refer to Paikowsky and Hajduk (1999 and 2004). All static load testing information presented in this section is based on Hajduk (2006), a graduate research student of the Geotechnical Engineering Research Laboratory at UMass Lowell.

### **9.4.2 Static Load Test Set-Up**

Figure 154 presents a plan view of the test piles and reaction piles location. The load frame entails 12-reaction piles setup in a triangular pattern. Depending on which pile is tested, a large steel reaction beam is placed across the reaction piles. For example, the reaction beam is placed across reaction piles three to six to statically load test pile #3. Figure 155 is a photograph of the driving of test pile #1 with the static load-testing frame on the perimeter.

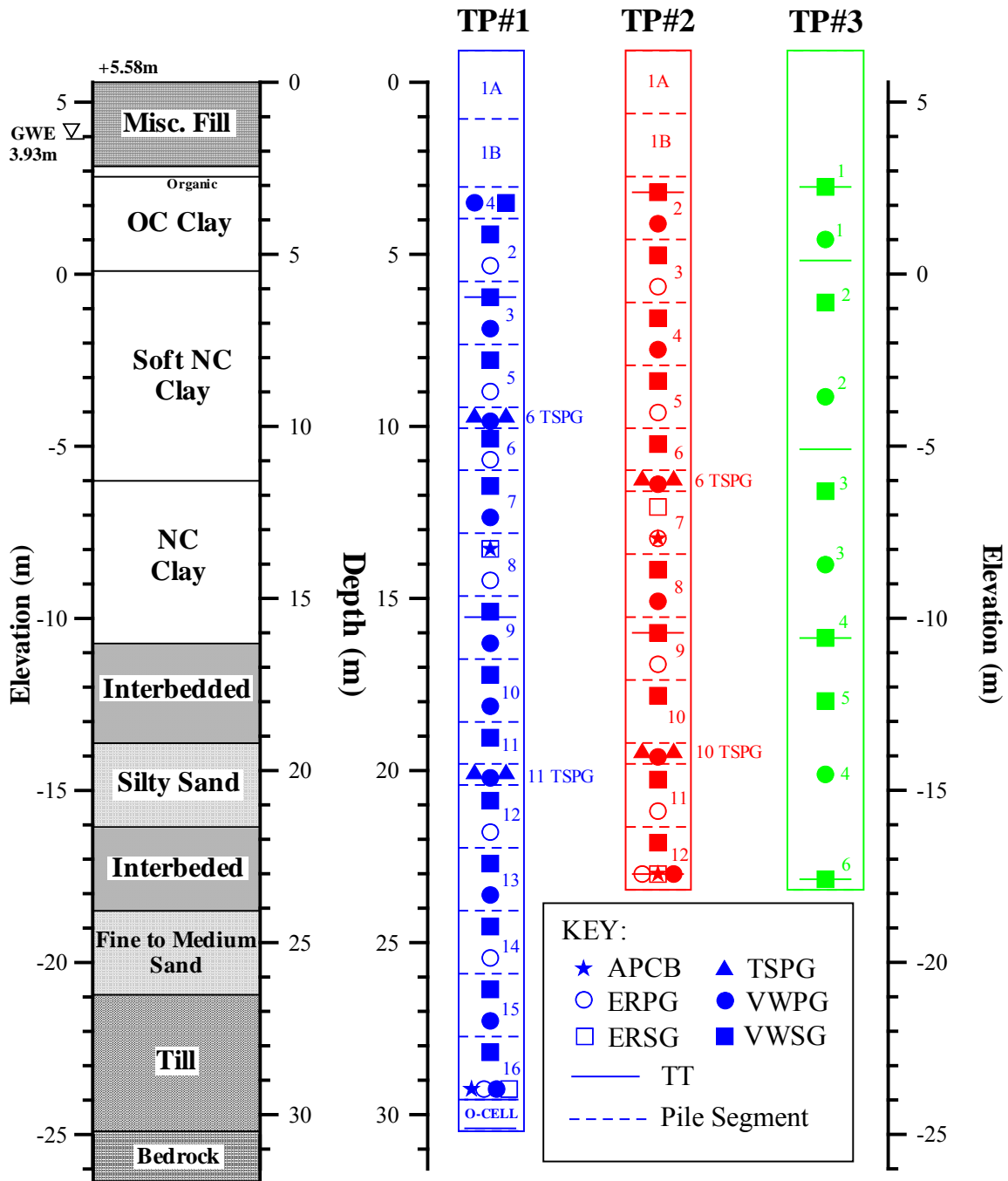
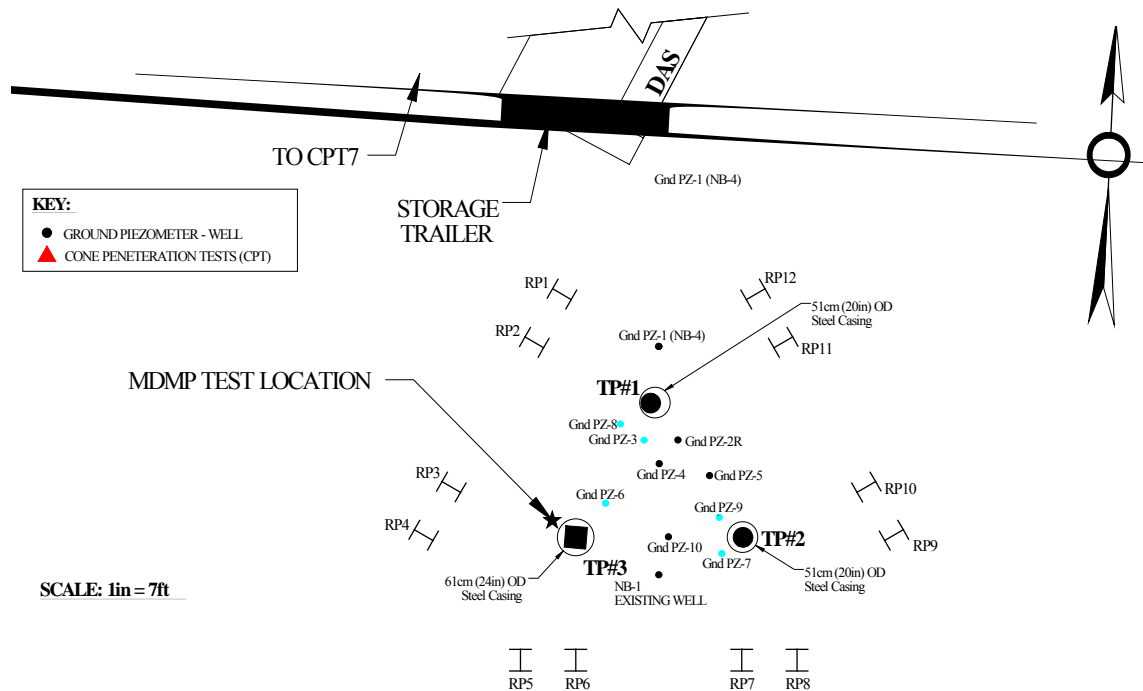


Figure 153. General soil profile and planned test pile layouts (Paikowsky and Hajduk, 2004)



**Figure 154. Plan view of test pile layout and reaction piles (Paikowsky and Hajduk, 1999)**



**Figure 155. Static load test frame used for test pile cluster in Newbury, MA (Paikowsky & Hajduk, 1999)**

### 9.4.3 Static Load Testing Procedures and Records

Each pile was tested using three load-testing procedures: (i) short duration (ii) maintained load test and (iii) static cyclic load test. The applied load to the pile was recorded using the pressure gage on the pump (which is supplying the hydraulic fluid to the jack), and via a load is recorded using a load cell and a Data Acquisition System (DAS). The DAS recorded the output from the instrumentation on and in the piles, for more details see Paikowsky & Hajduk, (1999 and 2004). The pressure in the hydraulic jack was also recorded by the DAS. The movement of the piles was recorded using two methods, one via four dial gauges placed on the pile top, and the second using several direct current differential transformers (DCDT's) connected to the data acquisition system. The dial gauges and DCDT's were setup in accordance with ASTM standard D1143. Table 86 summarizes the different static load tests and the dates in which they are conducted on the Newbury test pile cluster.

**Table 86. Summary of static load tests conducted on Newbury test pile cluster (Paikowsky and Hajduk, 1999)**

Test Pile #	Test Type	Date Conducted
1	Short Duration (Osterberg Cell)	12/11/1997
	Static Cyclic (Osterberg Cell)	12/12/1997
	Short duration	1/11/1998
	Incremental Static Cyclic	1/12/1998
	Static Cyclic	1/12/1998
2	Slow Maintained	10/2/1997
	Short Duration	10/27/1997
	Static Cyclic	10/28/1997
3	Slow Maintained	12/2/1997
	Short Duration	12/4/1997
	Static Cyclic	12/5/1997

### 9.4.4 Test Pile #1

#### Overview

Test pile #1 is a 12-inch diameter, 103 ft long, 0.5 inch wall thickness, close-ended steel pipe pile drive to 98 ft. with the tip of the pile resting on bedrock. An Osterberg load cell is attached to the tip of test pile #1 allowing to perform static load tests by pushing the pile up from the bottom. For more details on the Osterberg load cell configuration and testing method refer to Paikowsky and Hajduk (1999).

#### Static Load Test

The first two static load tests were conducted using the Osterberg load cell located at the pile tip. The Osterberg load cell tests the piles in compression from the bottom up with a movement

upwards, similar to a tension test conducted on the pile top. The test was completed when the peak skin friction of the pile was overcome. The first Osterberg load test conducted was a short duration test. Figure 156 shows the applied load versus displacement, applied load versus time, and displacement versus time for the Osterberg short duration test. The figure is graphed using the load from the Osterberg load cell and the displacement from an average of three DCDT's on the pile top. The ultimate compressive load for this test is around 81 tons. The second Osterberg static load test was the static cyclic test. Figure 157 shows the applied load versus displacement, applied load versus time, and displacement versus time for this load test. Figure 158 shows the applied load versus displacement in an enlarged scale to provide clarification of the load-unload intersection point.

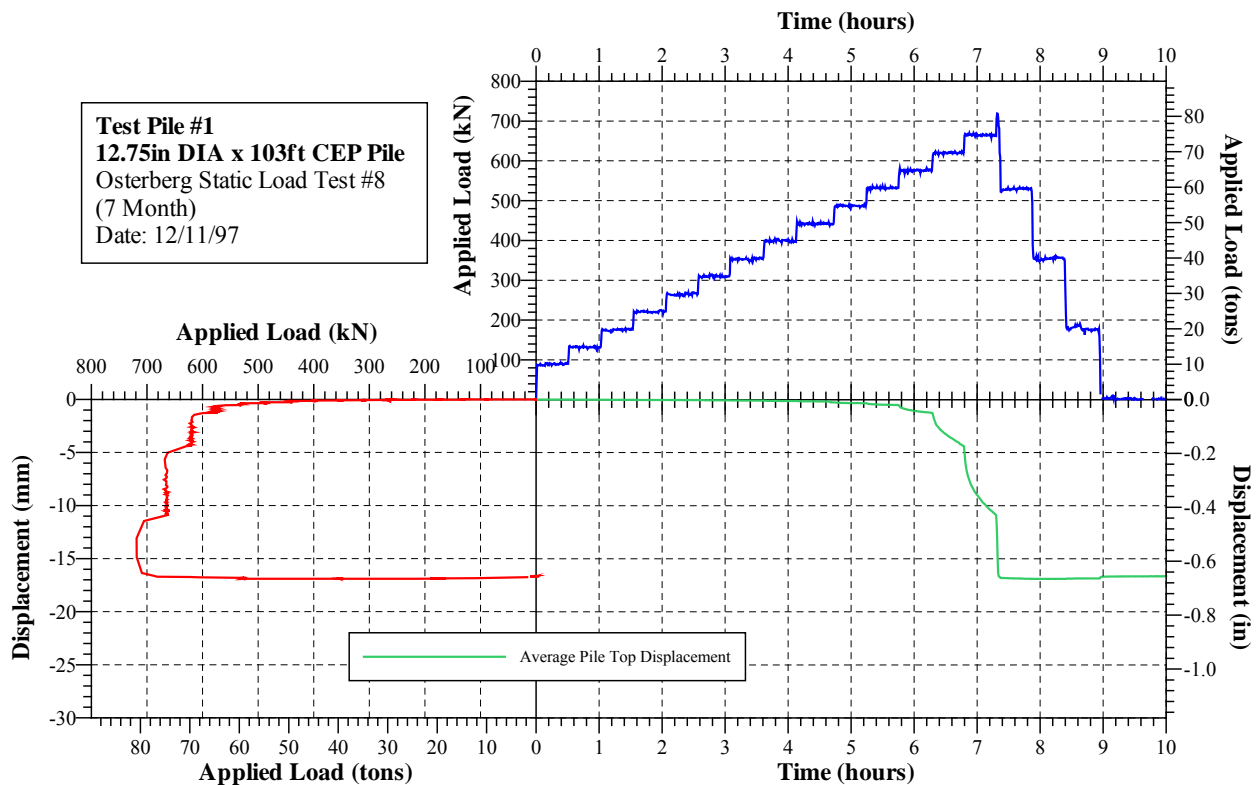


**Figure 156. Short duration test plots: (a) load vs. time, (b) displacement vs. time, and (c) load vs. displacement (Paikowsky and Hajduk, 1999)**

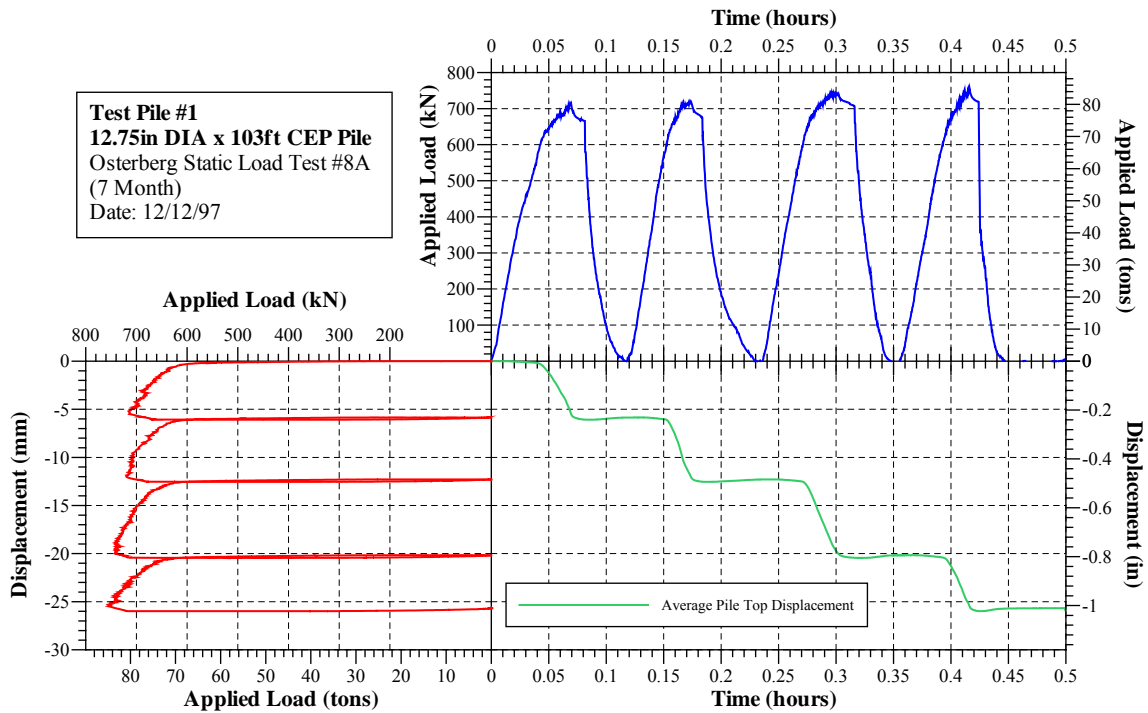


Figure 157. Osterberg static-cyclic test plots: (a) load vs. time, (b) displacement vs. time, and (c) load vs. displacement (Paikowsky and Hajduk, 1999)

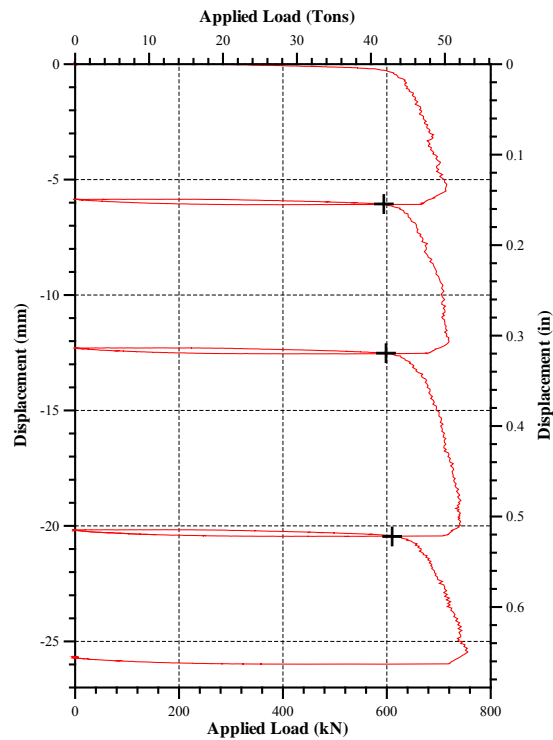


Figure 158. Test Pile #1 load vs. displacement for static cyclic test (Paikowsky and Hajduk, 1999)

**Test Pile #1**  
**12.75in DIA x 103ft CEP Pile**  
 Static Load Test 9  
 (8 Month Top Inc. Static-Cyclic)  
 Date: 1/12/98

**Applied Load (kN)**

**Displacement (mm)**

**Applied Load (tons)**

**Time (hours)**

**Applied Load (tons)**

**Displacement (in)**

--- Elastic Compression  
 — Davison's Criteria

220

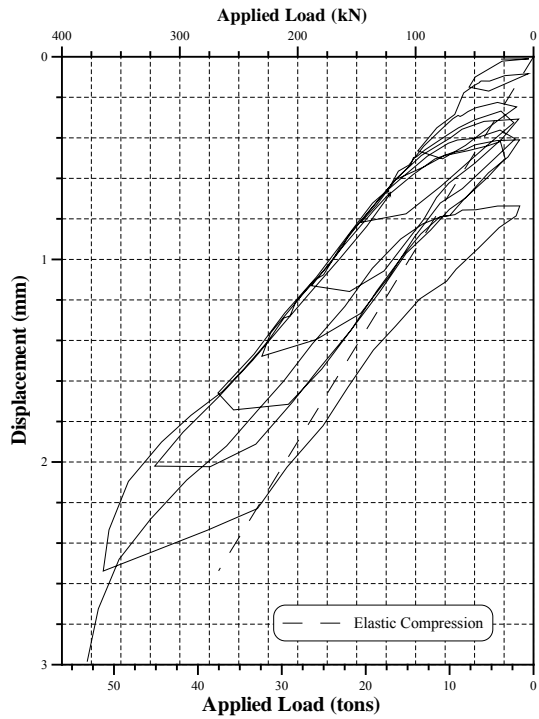


**Figure 160. Details of the load vs. displacement relationship for Test Pile #1 (Paikowsky and Hajduk, 1999)**

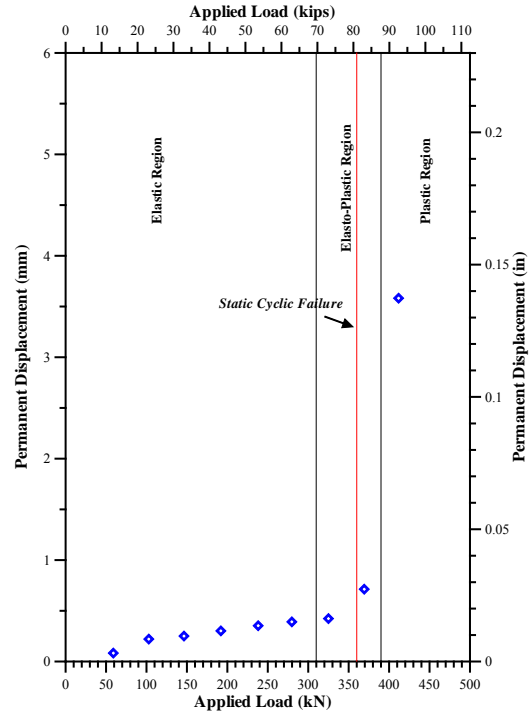


**Figure 161. Applied load vs. permanent displacement of incremental static cyclic test (Paikowsky and Hajduk, 1999)**

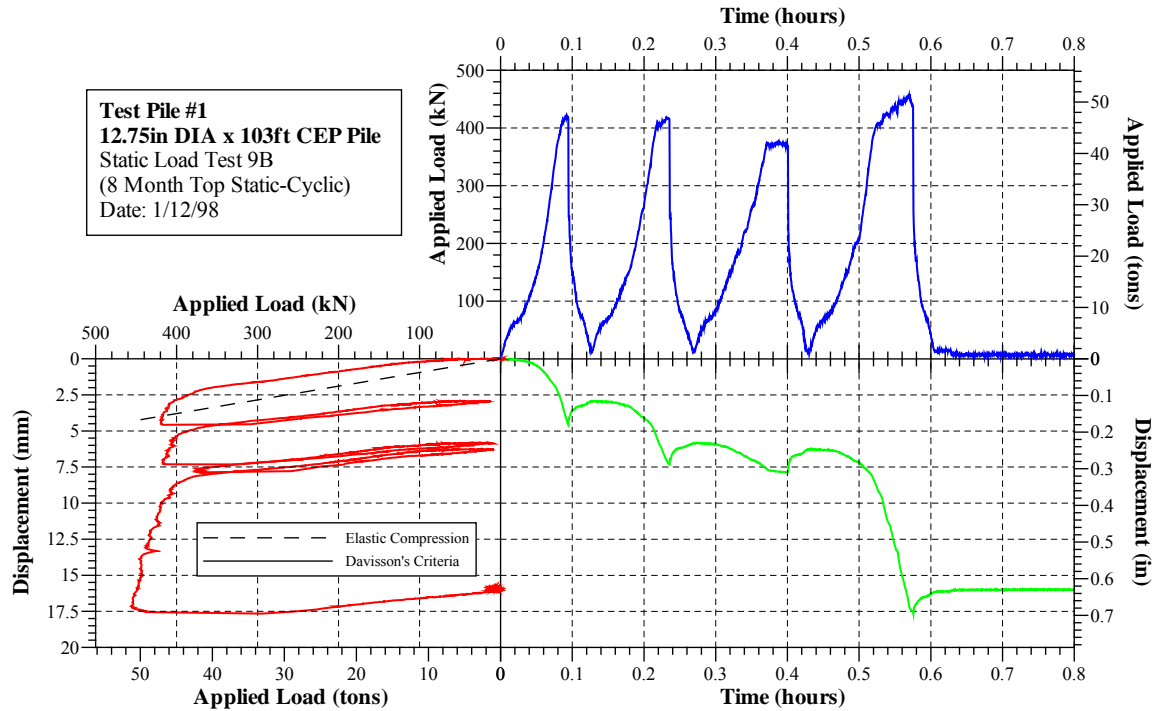


**Figure 162. Static-cyclic test plots: (a) load vs. time, (b) displacement vs. time, and (c) load vs. displacement (Paikowsky and Hajduk, 1999)**



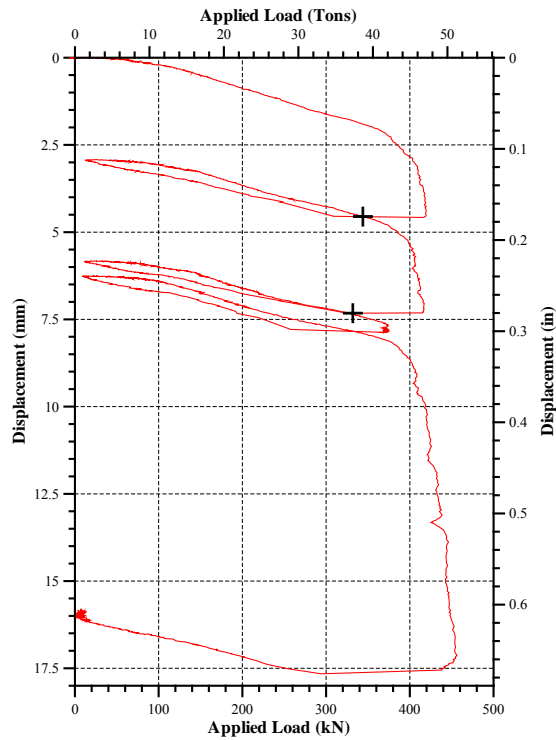


**Figure 163. Test Pile #1 load vs. displacement for static cyclic test (Paikowsky and Hajduk, 1999)**

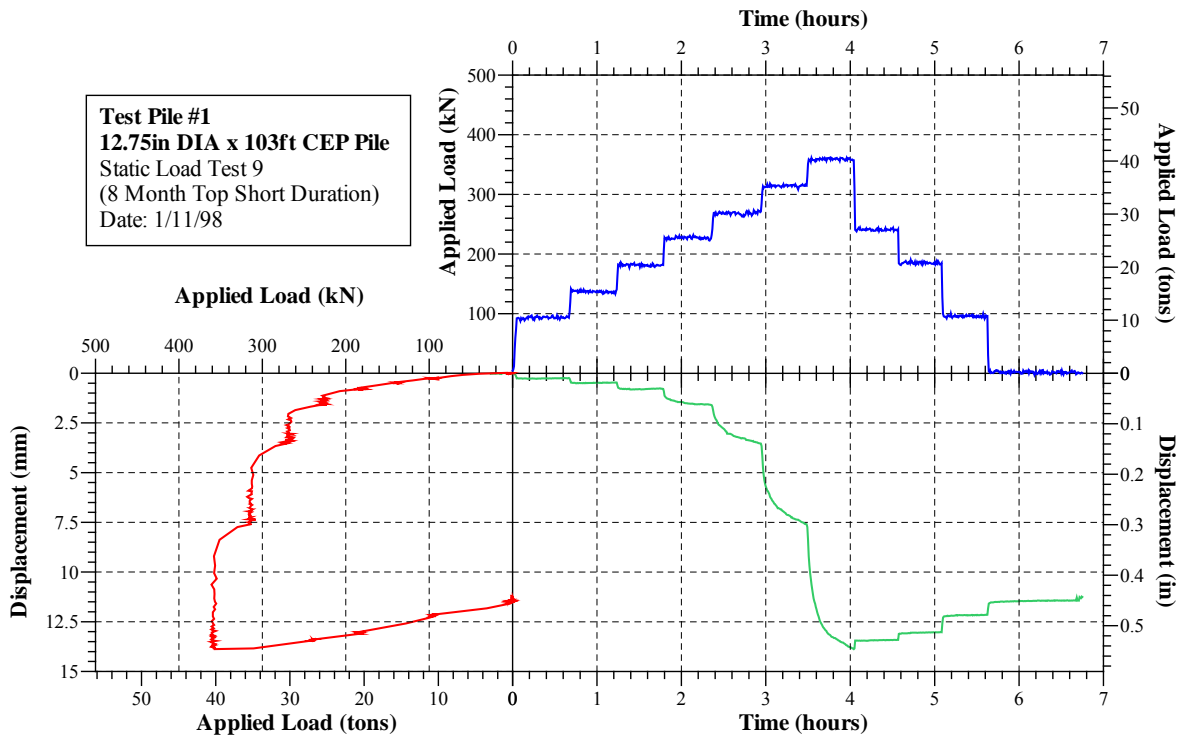


**Figure 164. Short duration test plots: (a) load vs. time, (b) displacement vs. time, and (c) load vs. displacement**

### ***Intermediate Summary***

The static cyclic failure point is based on the fundamental mechanism of the soil/pile interaction. The failure point is defined by the intersection of the load-unload portions of the load versus displacement graphs. The static cyclic failure point is correlated with the transition from the elastic to plastic regions of the soil/pile mechanism. Figure 161 displays the three regions, elastic, elasto-plastic, and plastic, based on the results from Figure 159. The soil/pile mechanism behaves elastically until approximately 70 kips. From there the mechanism is a combination between elastic and plastic behavior ranging from 70 to 88 kips. After 88 kips, the soil/pile system behaves plastically. Figure 161 clearly shows the transition of the soil/system from one region to the next.

#### ***9.4.5 Test Pile #2***

##### ***Overview***

Test pile #2 is a 12-inch diameter, 80 ft long, 0.5 inch wall thickness, close-ended steel pipe pile. The pile penetrated through overconsolidated clay, normally consolidate clay, and interbedded silt, sand, and clay layers. The tip of the pile was in an interbedded layer of silt, sand, and clay.

##### ***Static Load Tests***

Three tests were carried out on test pile #2, a slow maintained test, short duration test, and a static cyclic test. The short duration and slow maintained tests were analyzed using four traditional pile capacity interpretation methods, (i) DeBeer, (ii) Limited Total Settlement, (iii) Shape of Curve, and (iv) Davisson, and the intersection of the load-unload loops determines the failure for the static cyclic test. Figure 165 presents a graph describing the results of the slow maintained test, which was carried out first. The ultimate compressive load and maximum displacement on the pile were 96 tons and 1.3 inches, respectively. The representative static capacity based on the average of the above four interpretation methods was 83 tons (741 kN). Table 87 summarizes the failure loads for each method and the representative static pile capacity based on the average of the four methods. Figure 166 describes the short duration test results, which were carried out next. The ultimate compressive load and maximum displacement on the pile were 90 tons and 1.0 inches, respectively. The representative static capacity based on the average of the three applied methods was 81 tons and is tabulated in Table 87. The limited total settlement method was not applicable to this test because the pile top was not displaced 10% of the pile diameter. The third test conducted was the static cyclic test. Figure 167 shows the load versus displacement, load versus time, and displacement versus time for the static cyclic test. The test was conducted in three loops and the average point of intersection of the loops, i.e. the failure point, was 75 tons shown in detail in Figure 168. Figure 169 provides a comparison of the load versus displacement curves for the three static load tests conducted on test pile #2. The

static cyclic test was compared to the two traditional tests in the last column of Table 87. The ratio between the representative static capacities and the static cyclic test for the short duration and slow maintained tests were 1.12 and 1.11, respectively.

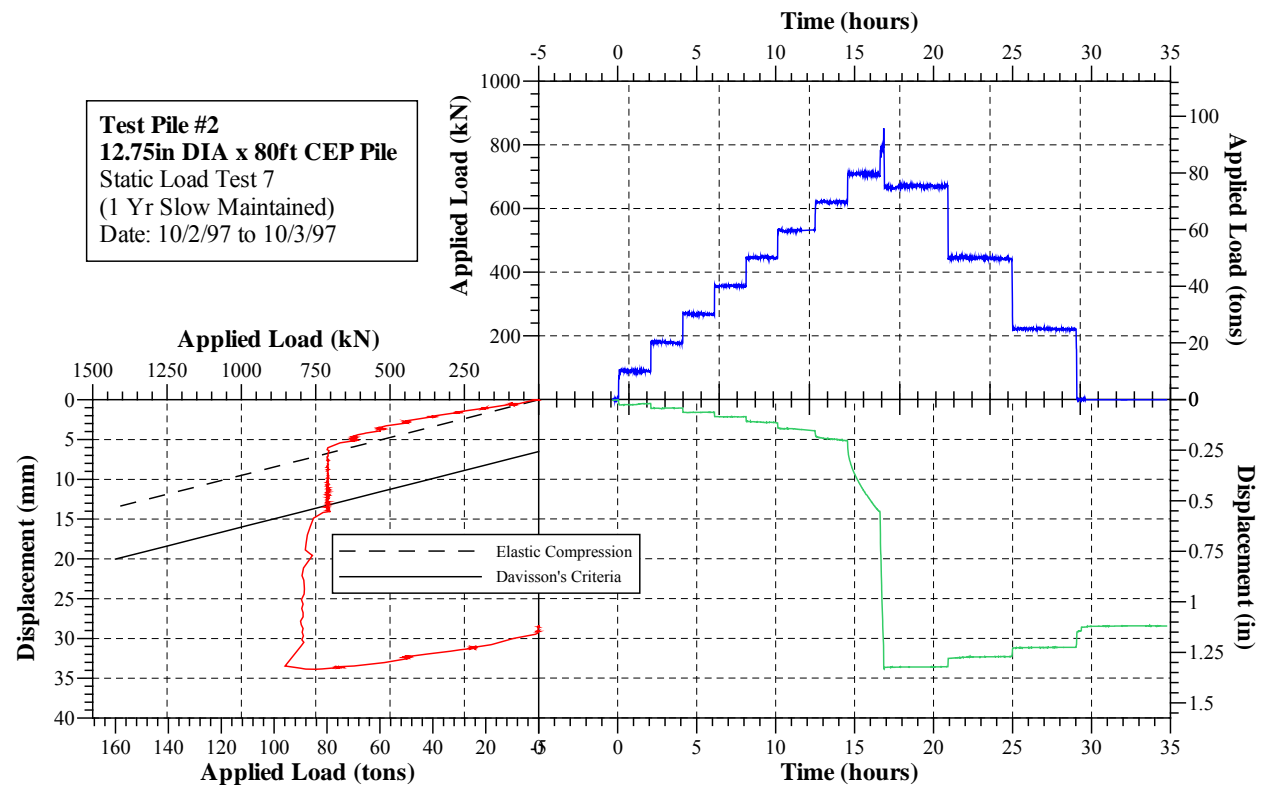


**Figure 165. Slow maintained test plots: (a) load vs. time, (b) displacement vs. time, and (c) load vs. displacement (Paikowsky and Hajduk, 1999)**

**Table 87. Summary of pile capacity interpretation for Test Pile #2 (Paikowsky and Hajduk, 1999)**

Test Type	DeBeer (kN)	Limited Total Settlement (kN)	Shape of Curve (kN)	Davisson (kN)	Representative Static Capacity (kN)	Static Cyclic Capacity (kN)	$P_s/P_{cyc}$
Short Duration	720	-	738	791	750	-	1.12
Slow Maintained	715	796	745	709	741	-	1.11
Static Cyclic	-	-	-	-	-	668	-

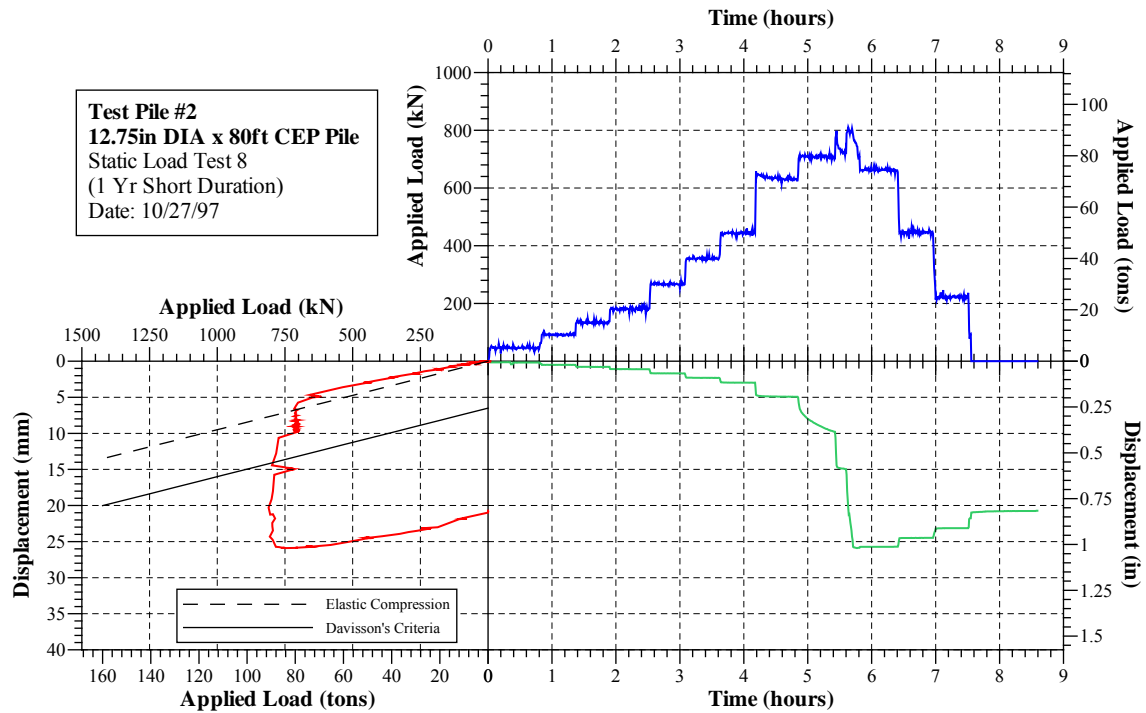


**Figure 166. Short duration test plots: (a) load vs. time, (b) displacement vs. time, and (c) load vs. displacement (Paikowsky and Hajduk, 1999)**

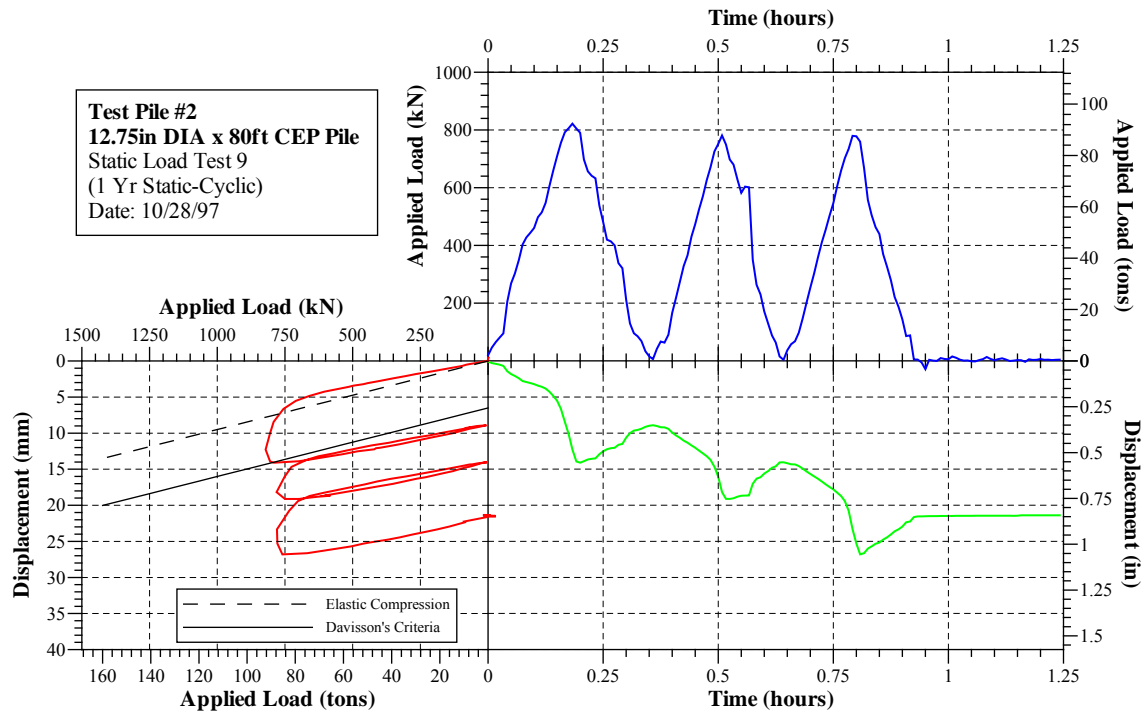


**Figure 167. Static-cyclic test plots: (a) load vs. time, (b) displacement vs. time, and (c) load vs. displacement (Paikowsky and Hajduk, 1999)**

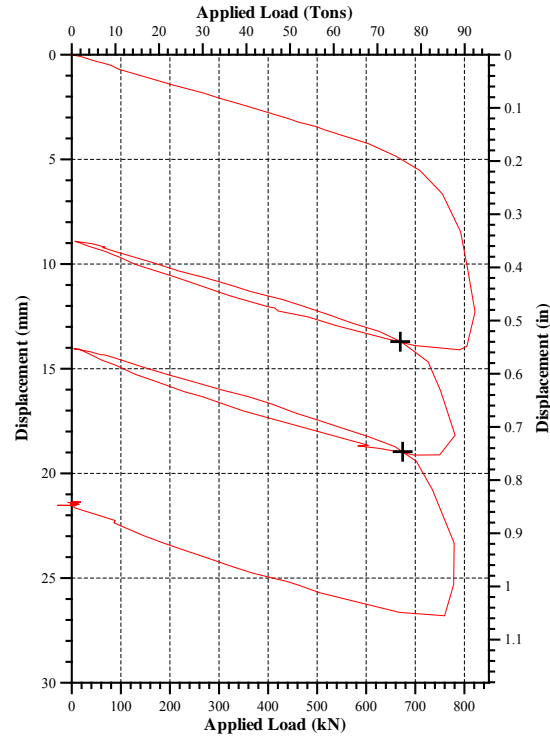


**Figure 168. Test Pile #2 load vs. displacement for static cyclic test (Paikowsky and Hajduk, 1999)**

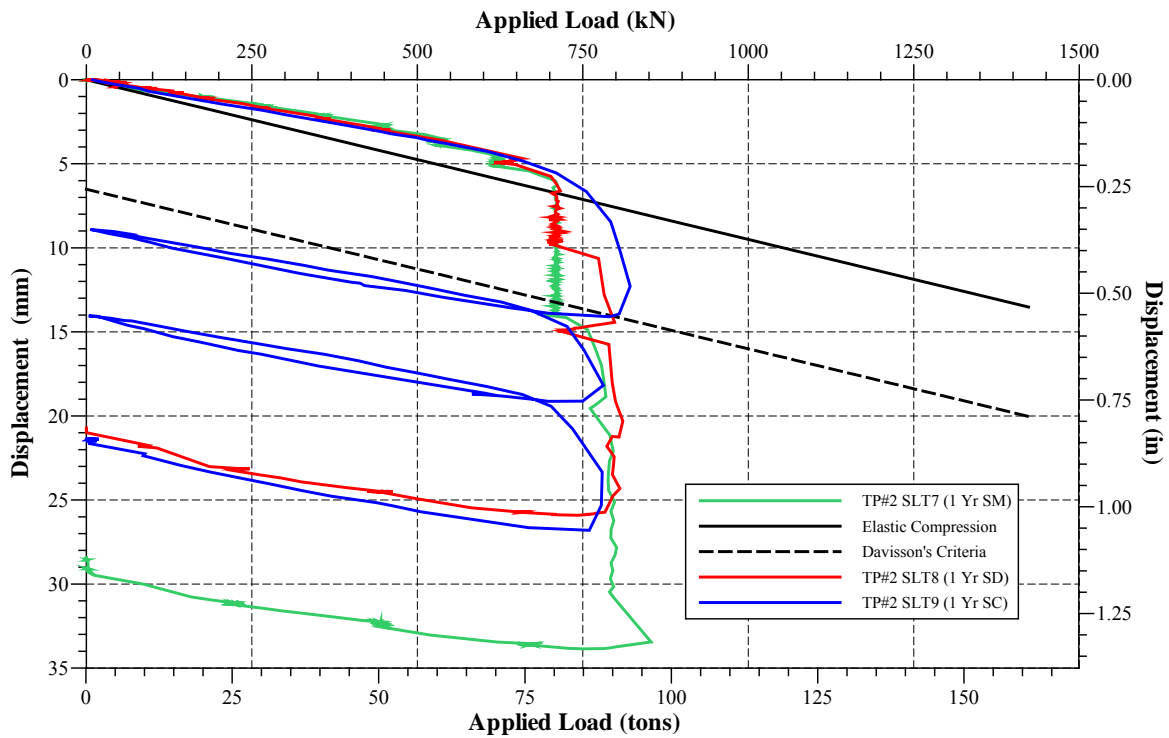


**Figure 169. Comparison of load vs. displacement for various tests on TP#2 (Paikowsky and Hajduk, 1999)**

## Load Distributions

The load distributions for the three static load tests carried out on test pile #2 were measured using 10 vibrating wire strain gages (VWSG) and the load cell on the pile top.

Figure 170 shows the load distribution for the short duration test indicating the location of each strain gage along the length of the pile in relation to the soil profile. The distribution of load was based on an average at each strain gage location during the duration of the time the load was held at each of the 10 loading increments. The maximum load was recorded using the load cell on the pile top. Table 88 shows the ratio of the load carried at the pile tip from the applied load on the pile top for each loading increment during the short duration test. The ratio of  $P_{tip}/P_{top}$  for this test was initially 0% under the first loading increment and increased up to 20% for the final loading increment.

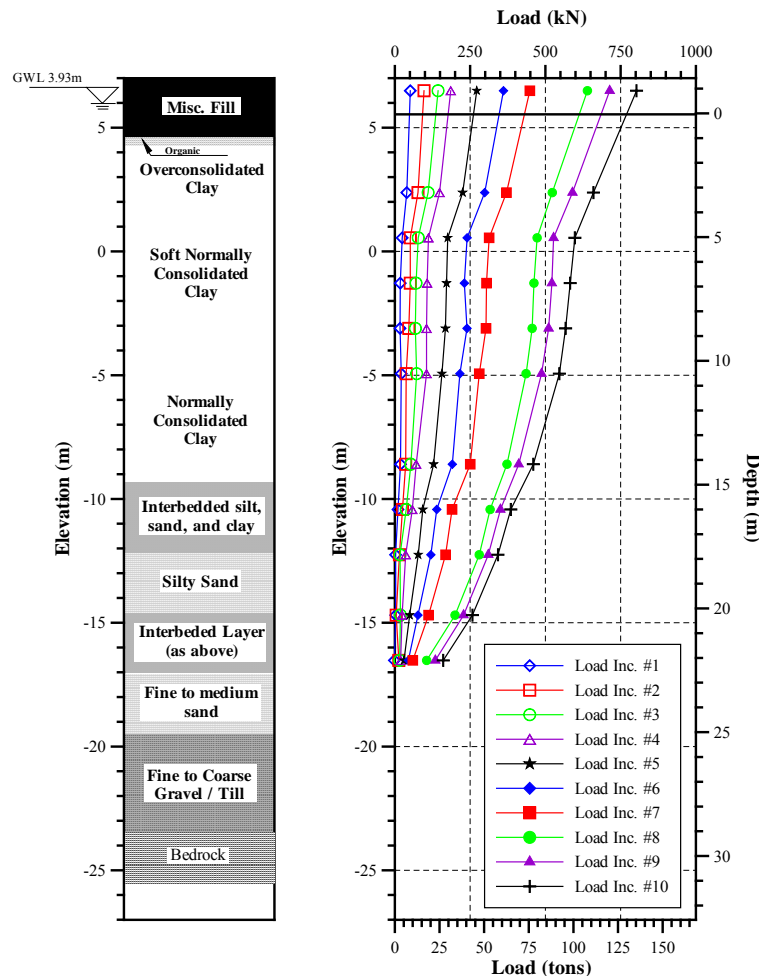


**Figure 170. Test Pile #2 short duration test load distribution (Paikowsky and Hajduk, 1999)**

**Table 88. Relations between tip and applied loads for test pile #2 distribution analysis (Paikowsky and Hajduk, 1999)**

Load Increment #	Short Duration $P_{tip}/P_{top}$ (%)	Slow Maintained $P_{tip}/P_{top}$ (%)	Static Cyclic $P_{tip}/P_{top}$ (%)
1	0	0	13 (Elastic-2)
2	13	8	20 (Intersection-2)
3	11	9	19 (Peak-2)
4	10	9	-
5	11	11	-
6	13	12	-
7	13	15	-
8	17	17	-
9	18	19	-
10	20	19	-

Figure 171 shows the load distribution for the slow maintained test indicating the location of each strain gage along the length of the pile in relation to the soil profile. The distribution of load was based on an average at each strain gage location for the entire time the load was maintained for each of the 10 loading increments. The maximum load was recorded using the load cell on the pile top. Table 88 shows the ratio of the load carried at the pile tip from the applied load on the pile top for each loading increment during the slow maintained test. The ratio of  $P_{tip}/P_{top}$  for this test was initially 0% under the first loading increment and increased up to 19% for the final loading increment.

Figure 172 shows the load distribution for the static cyclic load test on test pile #2. Three loading points were used to produce the distribution presented in Figure 172 during the three soil/pile regions, (i) a point along the elastic compression line, (ii) the second point is the intersection between the load-unload load-displacement relations in the elasto-plastic region, and (iii) the third point is the peak compressive load on the pile for the second loading cycle in the plastic region. The elastic condition (load point) was taken for a 0.38 inches pile top displacement, the intersection point was at 0.54 inches of pile top displacement, and the peak compressive load was taken at 0.71 inches of the pile's top displacement. Table 88 shows the ratio of the load carried out by the pile tip to the load applied at the pile top for each point during the static cyclic test. The ratio of  $P_{tip}/P_{top}$  for the elastic, intersection, and peak points were 13%, 20%, and 19%, respectively. The number two next to the labels signifies that the second loading loop was used to produce indicated values. Figures 173 & 174 were created to compare the load distributions between the short duration and the static cyclic test and the slow maintained test and the static cyclic test, respectively. Figure 173 presents a comparison between the load distribution along the length of the pile during the short duration test (five loading conditions) to that observed during the static cyclic test. Figure 174 presents a comparison between the load distribution along the length of the pile during the slow maintained test (five loading conditions) to that

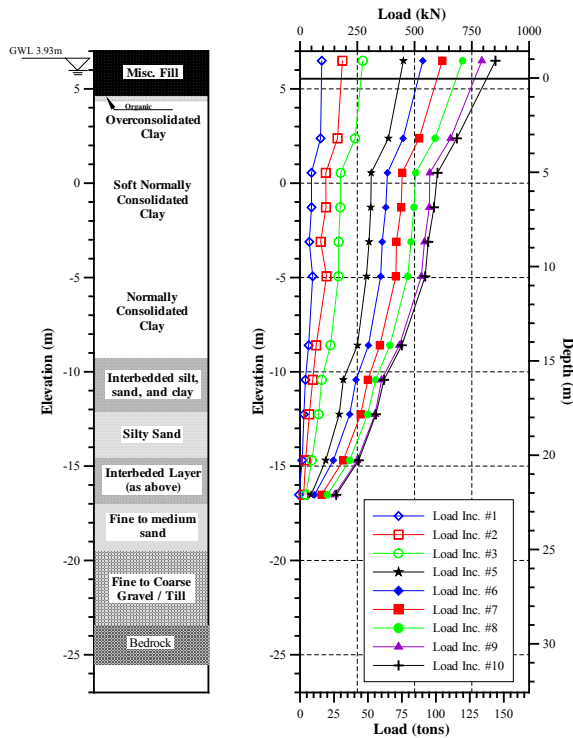


Figure 171. Test Pile #2 slow maintained test load distribution (Paikowsky and Hajduk, 1999)

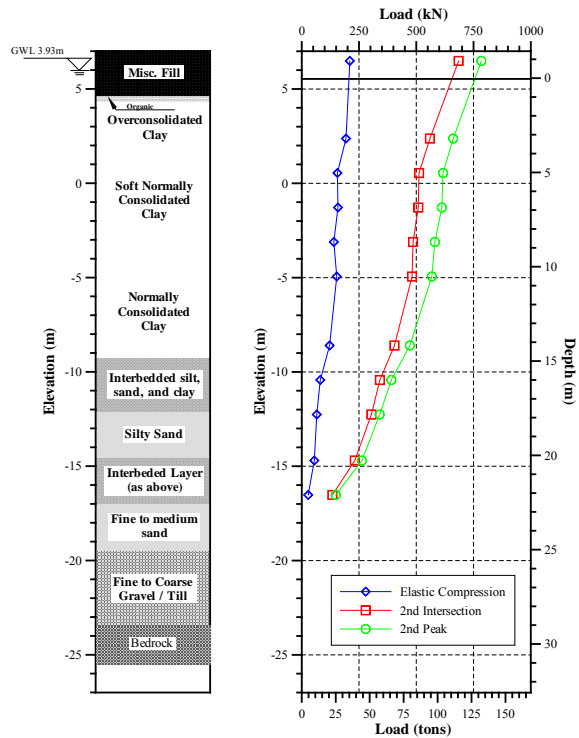


Figure 172. Test Pile #2 static cyclic test load distribution (Paikowsky and Hajduk, 1999)

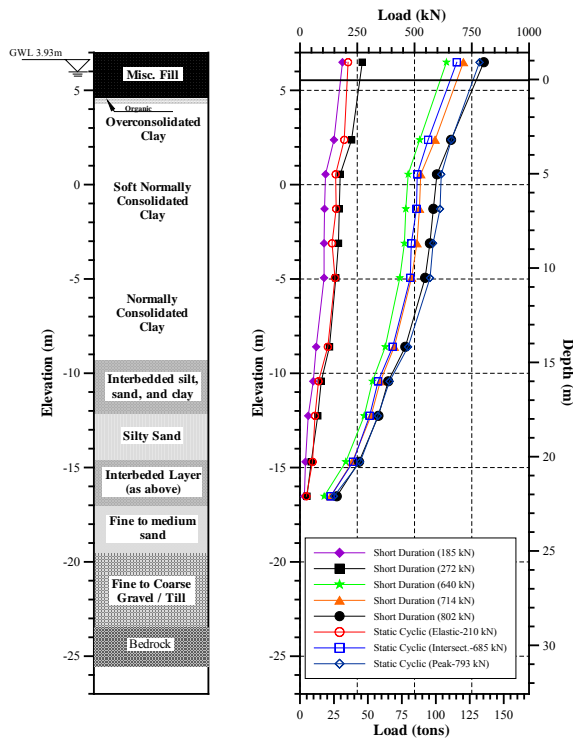


Figure 173. Test Pile #2 short duration & static cyclic comparison of load distributions (Paikowsky and Hajduk, 1999)

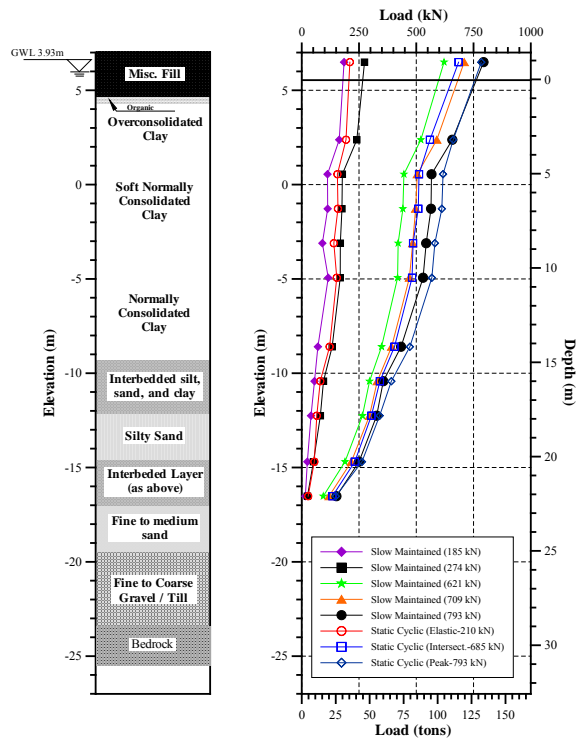


Figure 174. Test Pile #2 slow maintained & static cyclic comparison of load distributions (Paikowsky and Hajduk, 1999)



observed during the static cyclic test. The data of Figures 173 and 174 lead to two important observations/conclusions regarding the load distribution differences between the static cyclic test and the two traditional load tests (slow maintained and short duration): (i) effect of rate of loading, and (ii) magnitude of loads. The load distributions of the static cyclic tests are identical to the traditional methods yielding that the rate of loading does not affect the distribution of load along the length of the pile. Finally, the magnitudes of the loads produced under the static cyclic test correspond to the magnitudes of load produced by traditional methods.

#### **9.4.6 Test Pile #3**

##### ***Overview***

Test pile #3 is a 14 inch, square, 80-foot long precast concrete pile. The shaft of the pile was in overconsolidated clay, normally consolidate clay, and interbedded silt, sand, and clay layers. The tip of the pile was in an interbedded layer of silt, sand, and clay.

##### ***Static Load Tests***

Three tests were carried out on test pile #3, a slow maintained, short duration, and a static cyclic. The short duration and slow maintained tests were analyzed using four traditional pile capacity interpretation methods, (i) DeBeer, (ii) Limited Total Settlement, (iii) Shape of Curve, and (iv) Davisson, and the intersection of the load-unload loops determines the failure for the static cyclic test. Figure 175 presents a graph describing the results of the slow maintained test, which was carried out first. The ultimate compressive load and maximum displacement on the pile were 152 tons and 1.4 inches, respectively. The representative static capacity based on the average of the above four interpretation methods is 132 tons. Table 89 summarizes the failure loads for each method and the representative static pile capacity based on the average of the four methods. Figure 176 presents a graph describing the short duration test results, which were carried out next. The ultimate compressive load and maximum displacement on the pile were 135 tons and 1.1 inches, respectively. The representative static capacity based on the average of the three applied methods is 122 tons and are tabulated in Table 89. The limited total settlement method is not applicable to this test because the pile top was not displaced 10% of the pile diameter. The third test conducted was the static cyclic test. Figure 177 shows the load versus displacement, load versus time, and displacement versus time for the static cyclic test. The test was conducted in four loops and the average point of intersection of the loops, i.e. the failure point, is 117 tons shown in detail in Figure 178. Figure 179 provides a comparison of the load versus displacement curves for the three static load test conducted on test pile #3. The static cyclic test is compared to the two traditional tests in the last column of Table 89. The ratio between the representative static capacities and the static cyclic test for the short duration and slow maintained tests are 1.05 and 1.13, respectively.

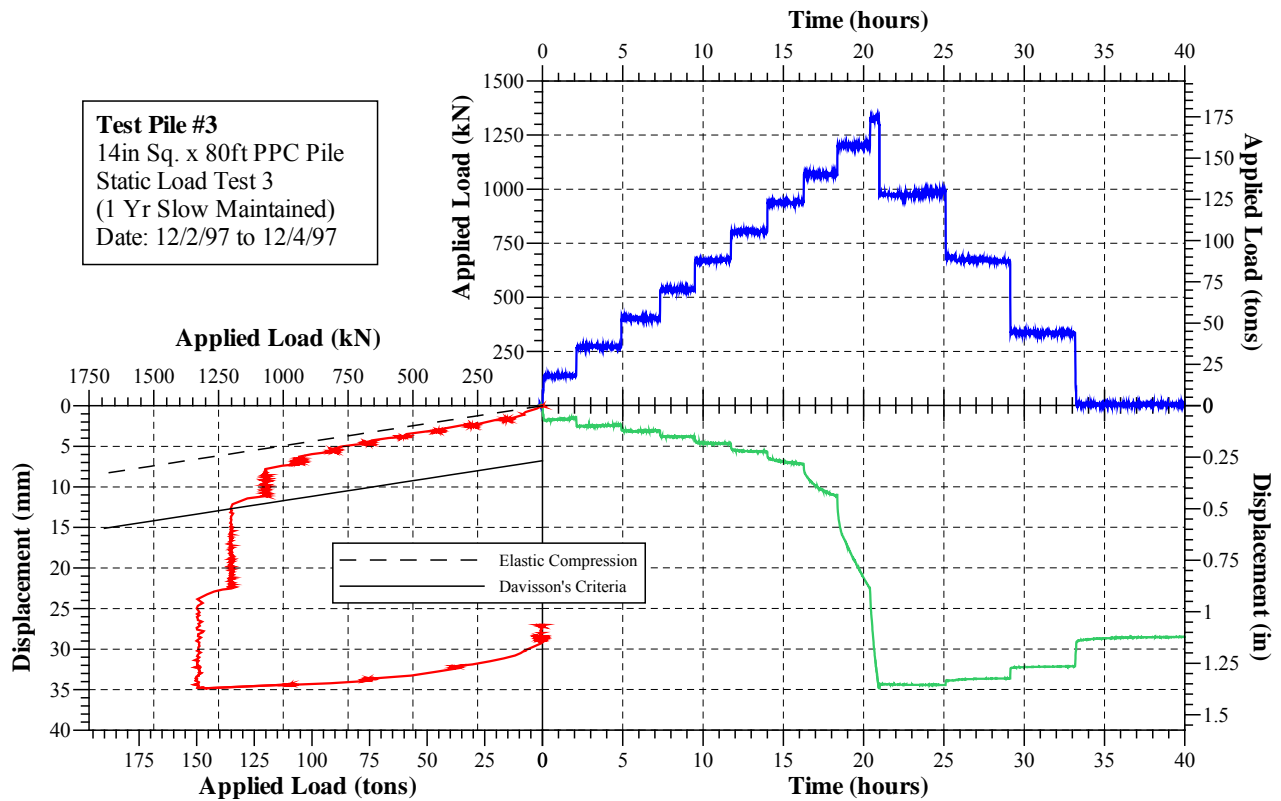


**Figure 175. Slow maintained test plots: (a) load vs. time, (b) displacement vs. time, and (c) load vs. displacement (Paikowsky and Hajduk, 1999)**

**Table 89. Summary of pile capacity interpretation for Test Pile #3 (Paikowsky and Hajduk, 1999)**

Test Type	DeBeer (kN)	Limited Total Settlement (kN)	Shape of Curve (kN)	Davisson (kN)	Representative Static Capacity (kN)	Static Cyclic Capacity (kN)	$P_s/P_{cyc}$
Short Duration	1070	-	1126	1070	1089	-	1.05
Slow Maintained	1050	1325	1133	1195	1176	-	1.13
Static Cyclic	-	-	-	-	-	1037	

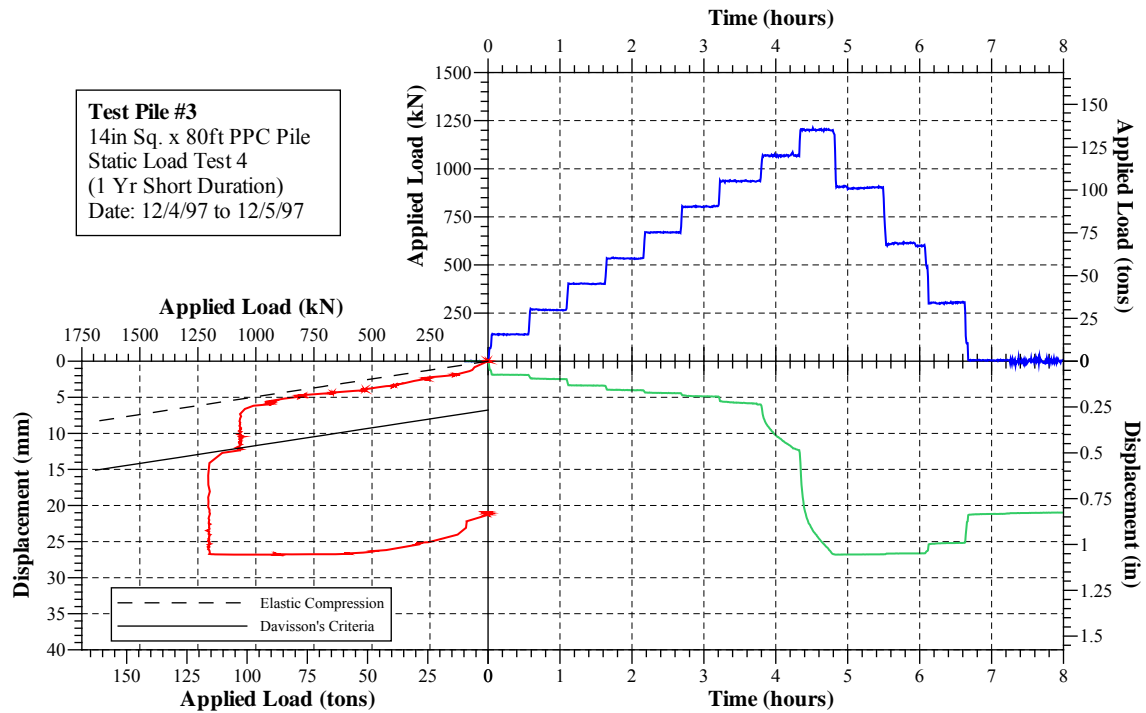


**Figure 176. Short duration test plots: (a) load vs. time, (b) displacement vs. time, and (c) load vs. displacement (Paikowsky and Hajduk, 1999)**

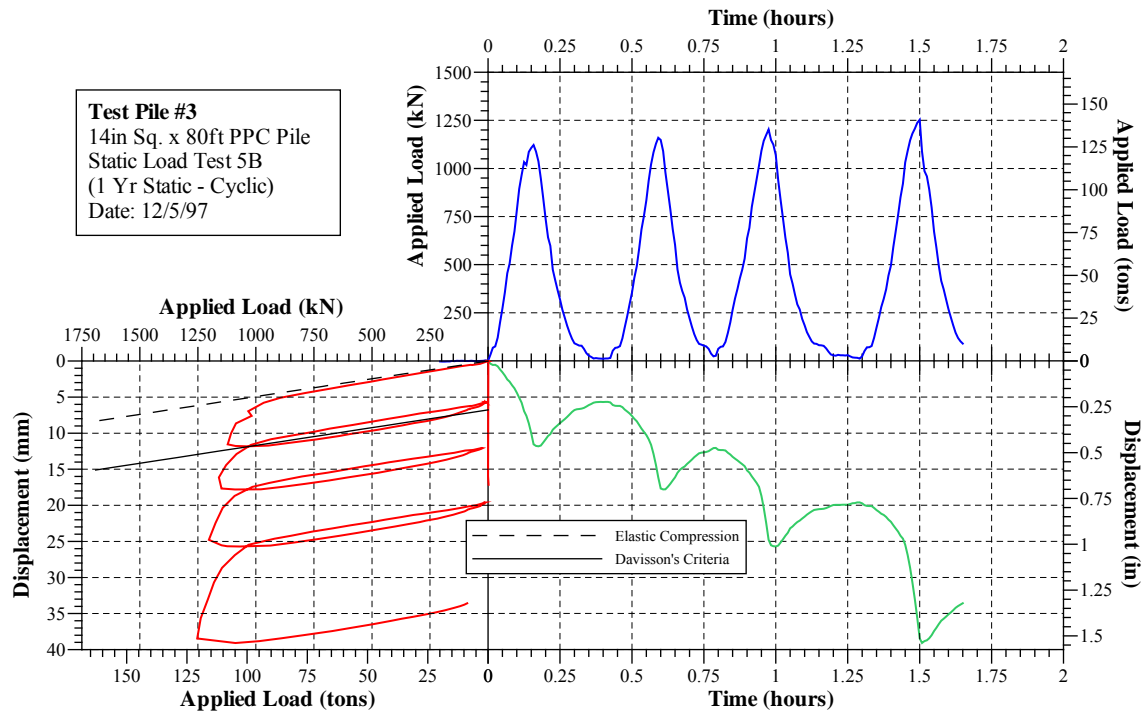


**Figure 177. Static-cyclic test plots: (a) load vs. time, (b) displacement vs. time, and (c) load vs. displacement (Paikowsky and Hajduk, 1999)**

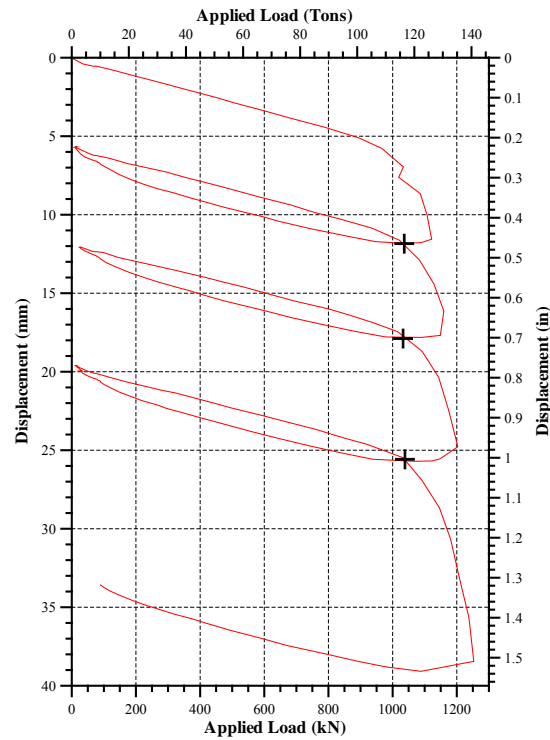


**Figure 178. Test Pile #3 load vs. displacement for static cyclic test (Paikowsky and Hajduk, 1999)**

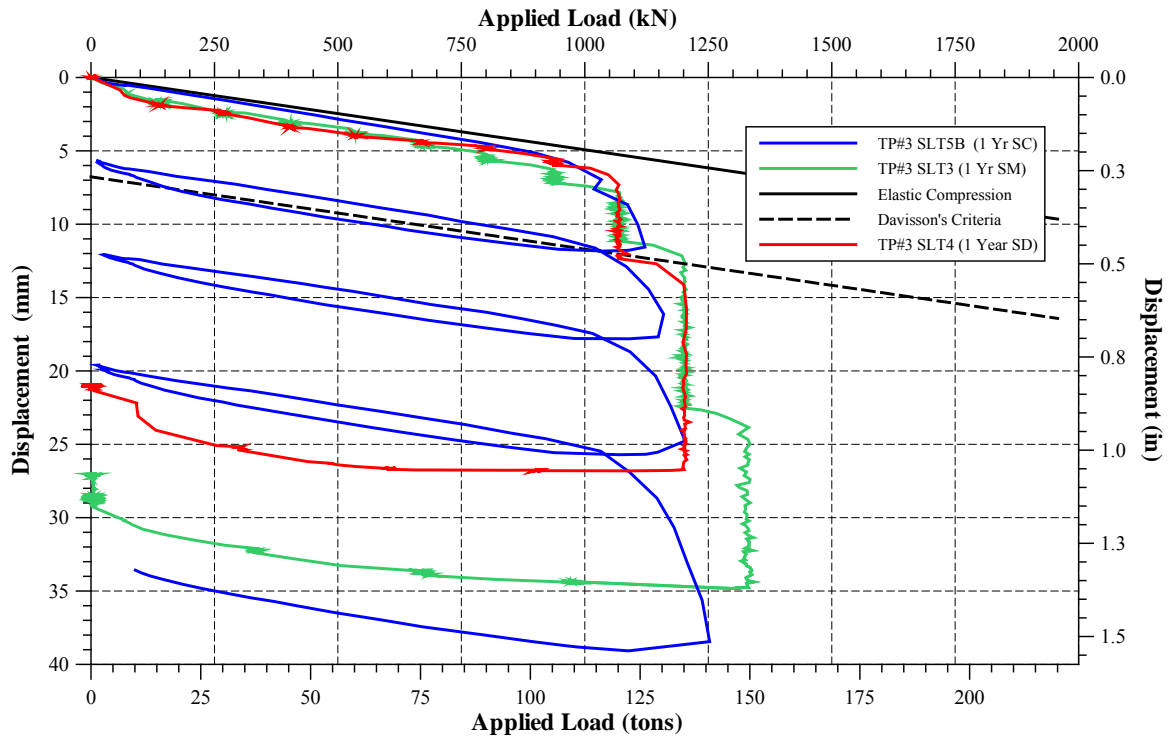


**Figure 179. Comparison of load vs. displacement for various tests on TP#3 (Paikowsky and Hajduk, 1999)**

## Load Distributions

The load distributions for the three static load tests on test pile #3 were measured using six vibrating wire strain gauges (VWSG) and the load cell on the top of the pile.

Figure 180 shows the load distribution for the short duration test indicating the location of each strain gage along the length of the pile in relation to the soil profile. The distribution of load is based on an average at each strain gage location during the duration of the time the load is held at each of the 10 loading increments. The maximum load was recorded using the load cell on the pile top. Table 90 shows the ratio of the load carried at the pile tip from the applied load on the pile top for each loading increment during the short duration test. The ratio of  $P_{tip}/P_{top}$  for this test is initially 10% under the first loading increment and increases up to 14% for the final loading increment.

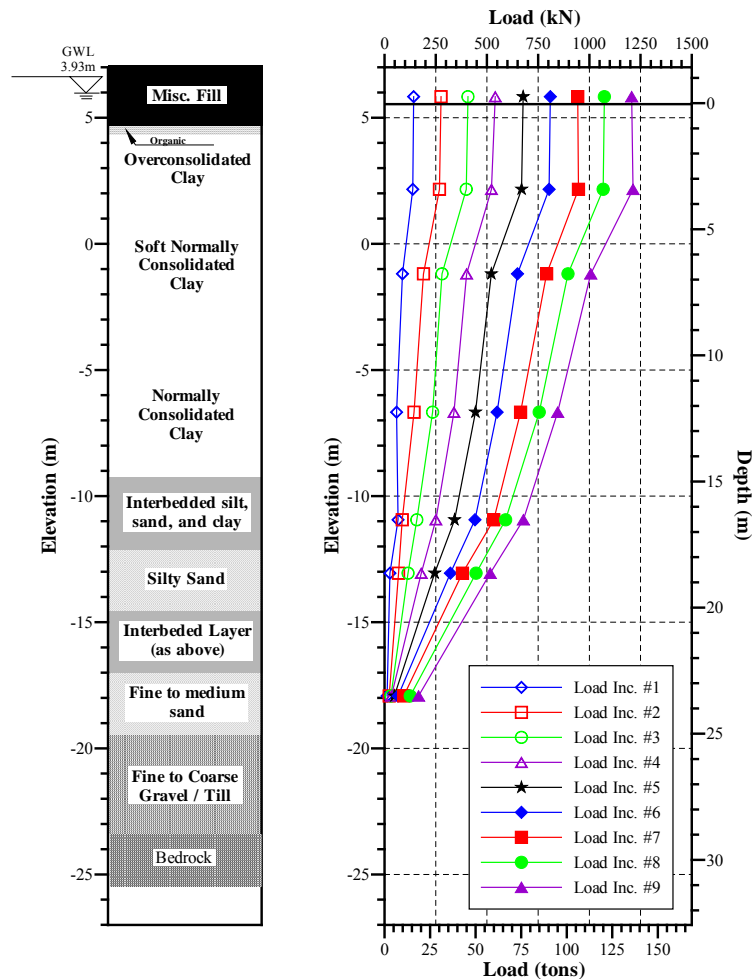


**Figure 180. Test Pile #3 slow maintained test load distributions (Paikowsky and Hajduk, 1999)**

**Table 90. Relations between tip and applied loads for test pile #3 distribution analysis (Paikowsky and Hajduk, 1999)**

Load Increment #	Short Duration $P_{tip}/P_{top}$ (%)	Slow Maintained $P_{tip}/P_{top}$ (%)	Static Cyclic $P_{tip}/P_{top}$ (%)
1	9	10	9 (Elastic-2)
2	8	10	13 (Intersection-2)
3	8	9	12 (Peak-2)
4	6	9	-
5	7	11	-
6	8	12	-
7	10	12	-
8	12	13	-
9	14	14	-
10	-	-	-

Figure 181 shows the load distribution for the slow maintained test indicating the location of each strain gage along the length of the pile in relation to the soil profile. The distribution of load is based on an average at each strain gage location for the entire time the load is maintained for each of the 10 loading increments. The maximum load was recorded using the load cell on the pile top. Table 90 shows the ratio of the load carried at the pile tip from the applied load on the pile top for each loading increment during the slow maintained test. The ratio of  $P_{tip}/P_{top}$  for this test is initially 9% under the first loading increment and increases up to 14% for the final loading increment.

Figure 182 shows the load distribution for the static cyclic load test on test pile #3. Three loading points were used to produce the distribution presented in Figure 182 during the three soil/pile regions, (i) a point along the elastic compression line, (ii) the second point is the intersection between the load-unload load-displacement relations in the elasto-plastic region, and (iii) the third point is the peak compressive load on the pile for the second loading cycle in the plastic region. The elastic condition (load point) is taken for a 0.38 inches pile top displacement, the intersection point is at 0.70 inches of pile top displacement, and the peak compressive load is taken at 0.70 inches of the pile's top displacement. Table 90 shows the ratio of the load carried out by the pile tip to the load applied at the pile top for each point during the static cyclic test. The ratio of  $P_{tip}/P_{top}$  for the elastic, intersection, and peak points are 9%, 13%, and 12%, respectively. The number two next to the labels signifies that the second loading loop is used to produce indicated values. Figures 183 & 184 were created to compare the load distributions between the short duration and the static cyclic test and the slow maintained test and the static cyclic test, respectively. Figure 183 presents a comparison between the load distribution along the length of the pile during the short duration test (five loading conditions) to that observed during the static cyclic test. Figure 184 presents a comparison between the load distribution along the length of the pile during the slow maintained test (five loading conditions) to that

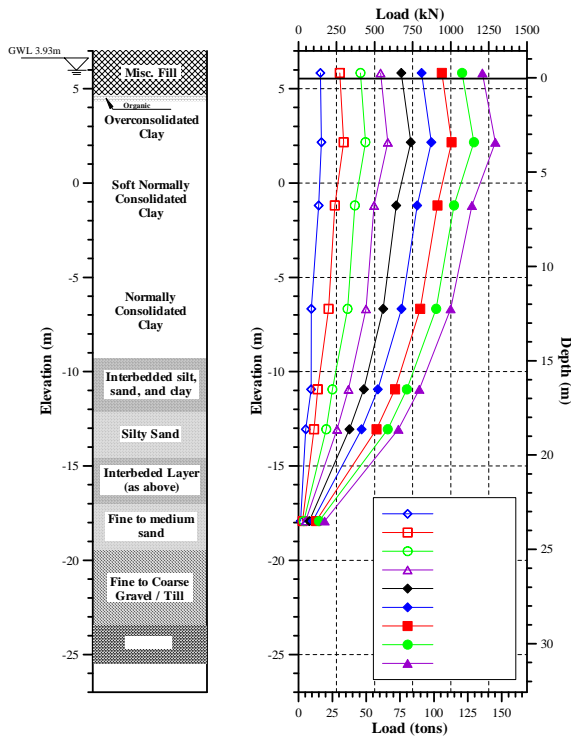


Figure 181. Test Pile #3 short duration test load distributions (Paikowsky and Hajduk, 1999)

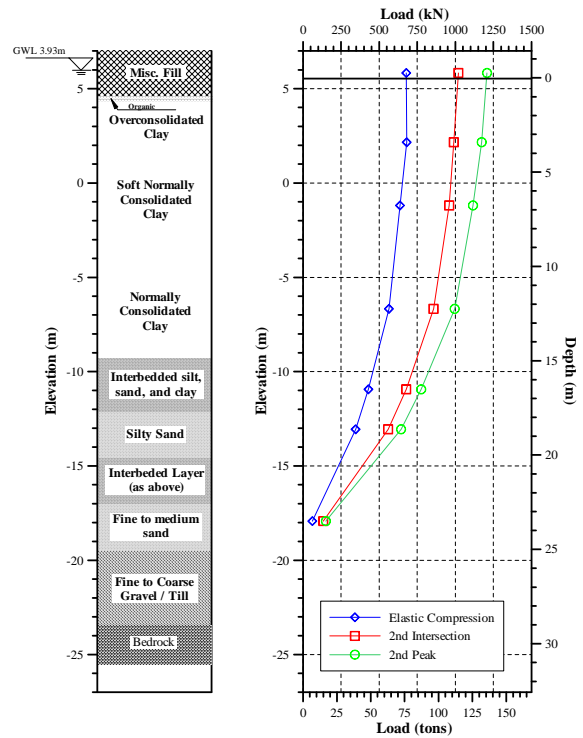


Figure 182. Test Pile #3 static cyclic test load distribution (Paikowsky and Hajduk, 1999)

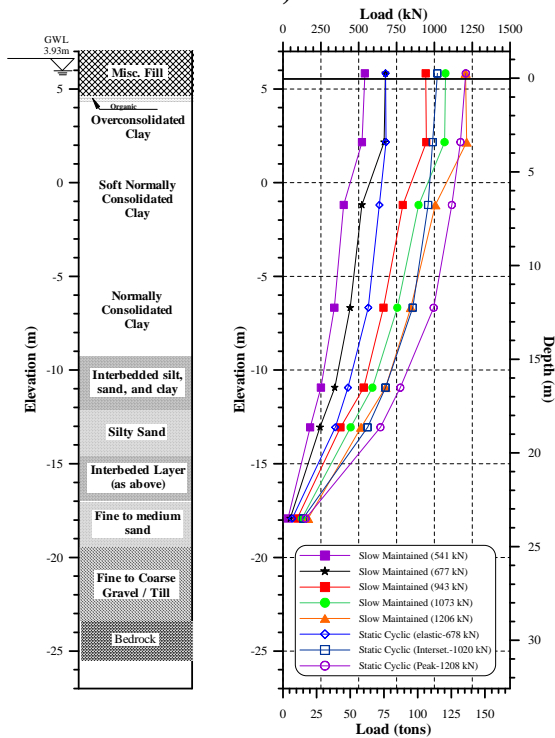


Figure 183. Test Pile #3 slow maintained test & static cyclic comparison of load distributions (Paikowsky and Hajduk, 1999)

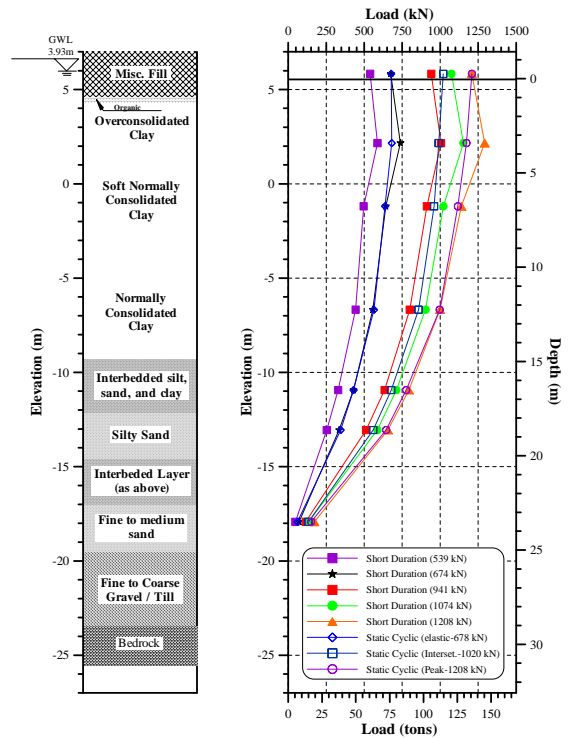


Figure 184. Test Pile #3 short duration test & static cyclic comparison of load distributions (Paikowsky and Hajduk, 1999)

observed during the static cyclic test. Figures 183 and 184 lead to two important conclusions regarding the load distribution comparison of the static cyclic test and the two traditional load tests (slow maintained and short duration): (i) effect of rate of loading, and (ii) magnitude of loads. The load distributions of the static cyclic tests are identical to the traditional methods yielding that the rate of loading does not affect the distribution of load along the length of the pile. Finally, the magnitudes of the loads produced under the static cyclic test correspond to the magnitudes of load produced by traditional methods.

#### **9.4.7 Conclusions**

The figures presented in the above sections provide the following conclusions: (i) the failure load by static cyclic loading is very similar (between 5 and 12%) to the average failure load from traditional interpretation methods based on traditional tests, (ii) the loading rate does not affect the distribution or magnitude of load along the length of the pile, and (iii) and the ability to conduct full-scale pile load tests is important to determine the pile capacity based on an accurate and cost effective static load test.

### **9.5 Deep Foundations Nominal Strength for Reliability Based Design**

#### **9.5.1 Overview**

Probabilistic calibration of resistance factors for any predictive method utilizing a database is possible when the nominal geotechnical pile strength (i.e. static pile capacity) is defined and compared to the outcome of the calibrated prediction method. The definition of ultimate static capacity given static load test results (load-displacement relations) is not unique, and as discussed in section 9.3.1, the use of the term “reference static capacity for calibration” (may include judgment) is more appropriate than “nominal strength”. The static load test results depend on the load testing procedures and the applied interpretation method, often being subjective. The following sections examine each of these factors and its influence on the reference static capacity, concluding with a recommended unique procedure to be followed in the calibration.

#### **9.5.2 The Uncertainty of the Various Failure Criteria**

Section 9.3 has resorted to a representative static pile capacity based on the assessment by five interpretation methods; (1) Davisson’s Criterion (Davisson, 1972), (2) Shape of Curve (similar to the procedure proposed by Butler and Hoy, 1977), (3) Limiting Total Settlement to 1 inch, (4) Limiting Total Settlement to 0.1B (Terzaghi, 1942), and (5) the DeBeer log-log method (DeBeer, 1970).



A single representative capacity value was then calculated for the analyzed case as the average of the methods considered relevant (i.e. provided reasonable value). The development of a calibration in a framework suitable for future modifications requires that the evaluated resistance factors in LRFD design be based on an objective, reproducible procedure. In order to do so, the static capacity of each pile in database PD/LT2000 (Paikowsky and Stenersen, 2000, and Paikowsky et al., 2004) was evaluated according to all five aforementioned criteria and a representative capacity was assigned for each pile. The mean and standard deviations of the ratio of the representative pile capacity to the capacity given by the method being evaluated was then determined. Table 91 presents a summary of the uncertainty results for the investigated methods. Details of the analyses and their results are presented in Appendix B of Paikowsky et al. (2004). Figure 185 shows the histogram and calculated distributions (normal and lognormal) for Davisson's failure criterion in which  $K_{SD}$  is the ratio of the designated static capacity to that defined by Davisson's failure criterion. The data presented in Figure 185 and Table 91 demonstrates that: (1) a small bias exists in the static capacity being used as a reference for the evaluation of the methods predicting the capacity of driven piles, and (2) this bias (and other considerations) needs to be accounted for when evaluating the resistance factor to be used for field static load tests.

Davisson's criterion was found to perform the best overall and was therefore chosen as the single method to be used when analyzing load-displacement curves and when establishing the nominal strength for LRFD calibration of the uncertainty in pile capacity evaluation (either for dynamic or static evaluation methods). Davisson's method provides an objective failure criterion and was also found to perform well for piles exceeding a diameter of 24 inch, examined through 30 pile cases as described below.

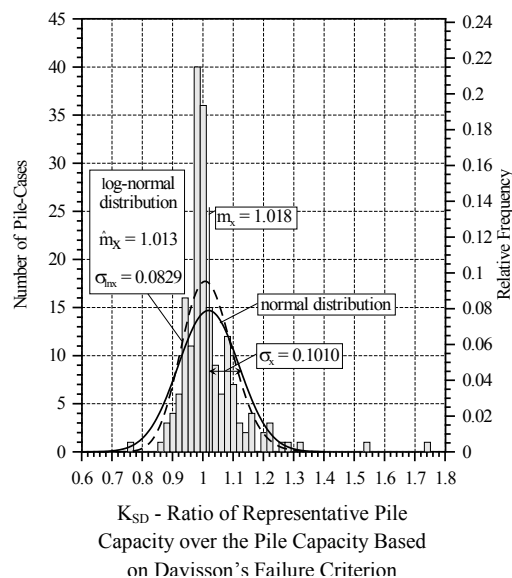


**Figure 185. Histogram and frequency distributions of  $K_{SD}$  for 186 PD/LT2000 pile cases in all types of soils (Paikowsky and Stenersen, 2000)**

**Table 91. Summary of the interpretation methods applied to the static load test curves in PD/LT2000 (Paikowsky et al., 2004)**

Interpretation Method	# of Valid Cases	Mean Ratio $K_{SX}$	Stand. Dev.	Max Value Of $K_{SX}$	Min Value of $K_{SX}$	# of Cases for the Range of $K_{SX}$ from 0.95 to 1.05	# of Cases for the Range of $K_{SX}$ from 0.90 to 1.10	Non-Applicable Cases and Reason why they are non-applicable
<b>Davisson's Criteria</b>	186	1.018	0.101	1.734	0.766	111	161	9 - max settlement less than failure criterion 1 - load below the failure range
<b>DeBeer</b>	187	1.033	0.088	1.429	0.750	119	153	9 - no clear failure point on log - log graph of load settlement curve
<b><math>\Delta = 0.1B</math></b>	90	0.938	0.114	1.367	0.647	39	59	106 - max settlement less than failure criterion
<b><math>\Delta = 1''</math></b>	161	0.971	0.098	1.538	0.714	73	120	35 - max settlement less than failure criterion
<b>Shape of Curve</b>	193	1.019	0.066	1.600	0.833	145	179	3 - load settlement curve did not have a clear failure point
<b>Representative Pile Capacity</b>	196	1.000	0.000	1.000	1.000	196	196	0

Notes:  $K_{SX}$  – The ratio between the representative pile capacity to the capacity obtained by the examined method

### 9.5.3 Evaluation of a Modification for Davisson's Criterion

#### *The Common Modification*

Davisson's Criterion as concluded above is the method that should be used to analyze static load test curves if only one method of analysis needs to be used. Static load tests on large diameter piles require larger settlements to develop the toe resistance, therefore, Kyfor et al., (1992), proposed that for large diameter piles (diameter greater than 24 inch), the offset to be used for Davisson's criterion should be:

$$X = \frac{B}{30} \quad (30)$$

Where B is the pile diameter in the units consistent with the calculated elastic deformation. This procedure was adopted by AASHTO. The following section presents an evaluation of the proposed criterion.

### ***The Performance of the Proposed Modification***

Thirty-one (31) piles of database PD/LT2000 belong to the large diameter pile category, for which the load-settlement curves were reanalyzed based on the modified criterion and new pile capacities were determined. Figure 186 presents the normal and lognormal distributions of the  $K_{SD}$  and  $K_{SLD}$  values for the large diameter piles in PD/LT2000.  $K_{SLD}$  represents the ratio of the representative pile capacity to the capacity determined by the Davisson's criterion method using the offset given in Equation 30 for the large diameter piles. Of the 31 piles that fall into the large diameter pile category only 20 meet the Davisson's failure criterion using the modified offset. Using the original offset there was only one pile that did not meet the Davisson's failure criterion. Using the modified offset caused ten additional cases (out of the 31) to be excluded from the Davisson's failure criterion. These were excluded because the settlement of the pile did not reach the failure criterion. This information alone raises doubts about the applicability of the modified offset for large diameter piles as it significantly decreases the number of piles that meet the failure criterion. As shown in Figure 186 for the thirty-one large diameter piles, the mean  $K_{SLD}$  is 0.920, while the mean  $K_{SD}$  is 0.994, which is much better. The standard deviation of the  $K_{SLD}$  values is 0.0714, which is slightly better than that of the standard deviation for the  $K_{SD}$  values, 0.0749. The lognormal distribution statistics also show that the original offset gives better results than the modified offset based on the 31 large diameter piles. The bar chart, which shows the actual data for the  $K_{SLD}$  values compares relatively well with the normal and lognormal distributions, with the exception being the two ranges from 0.970 to 0.990 and 0.990 to 1.010 with large numbers of  $K_{SLD}$  values, 36 and 31, respectively. Figure 187 shows that there is no correlation between the  $K_{SLD}$  value and the pile diameter. The results of this analysis has lead Paikowsky et al. (2004) to the conclusion that the single method of choice for analyzing static load test results is the Davisson's criterion method and the correction for large diameter piles should not be used.

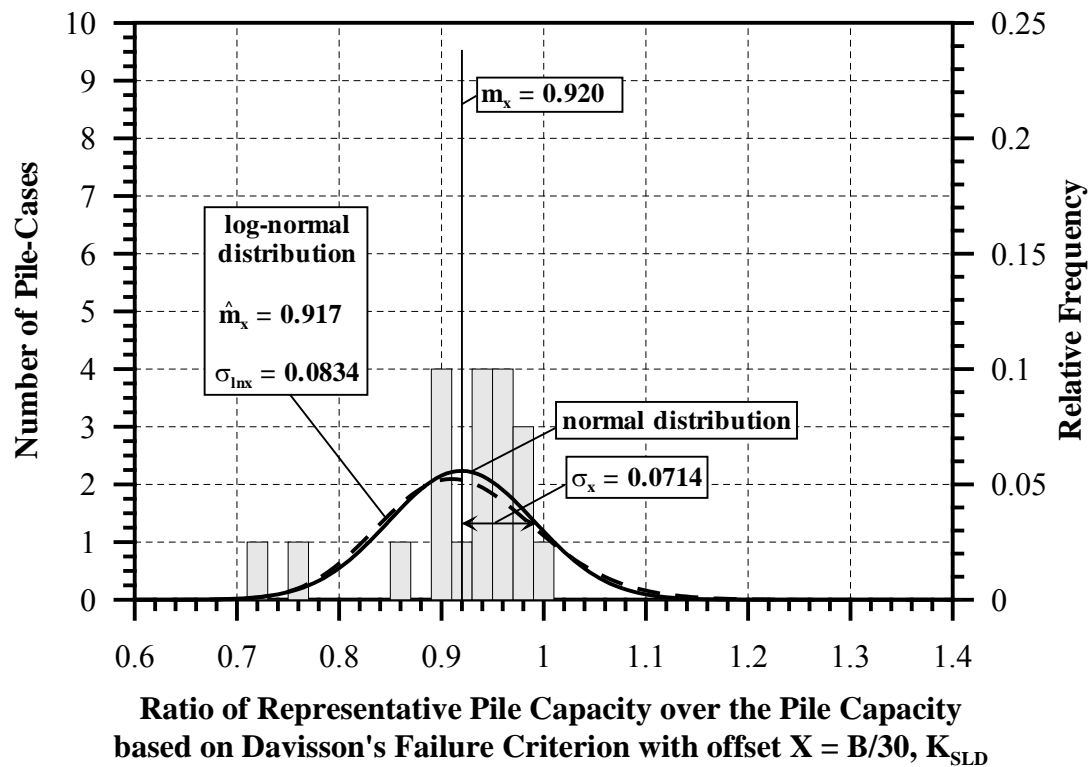
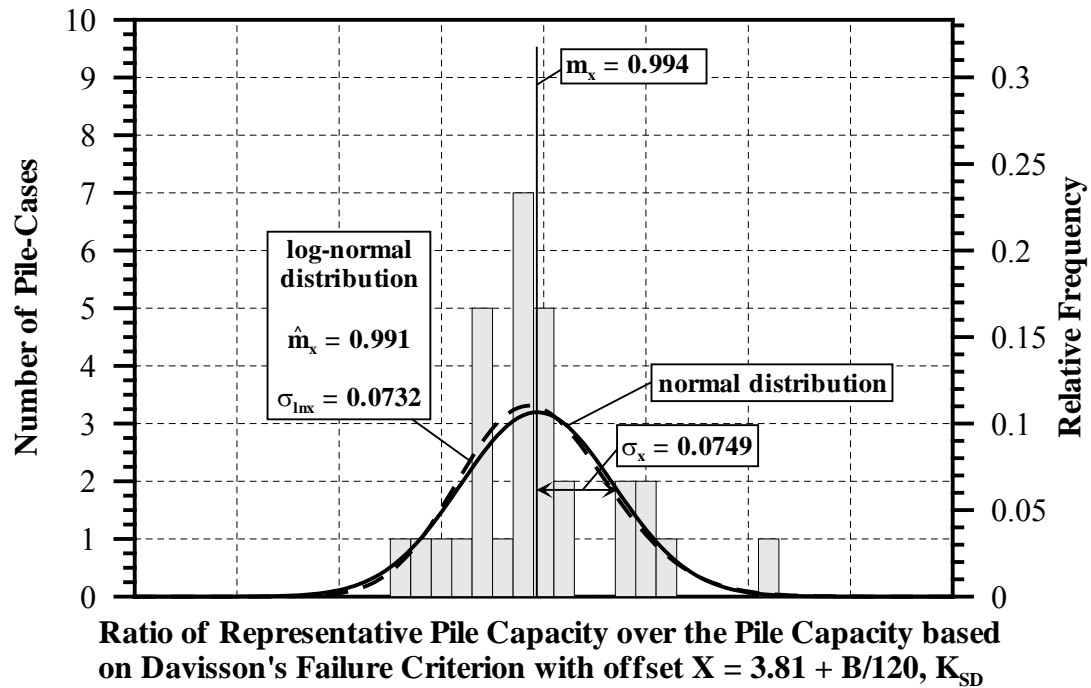
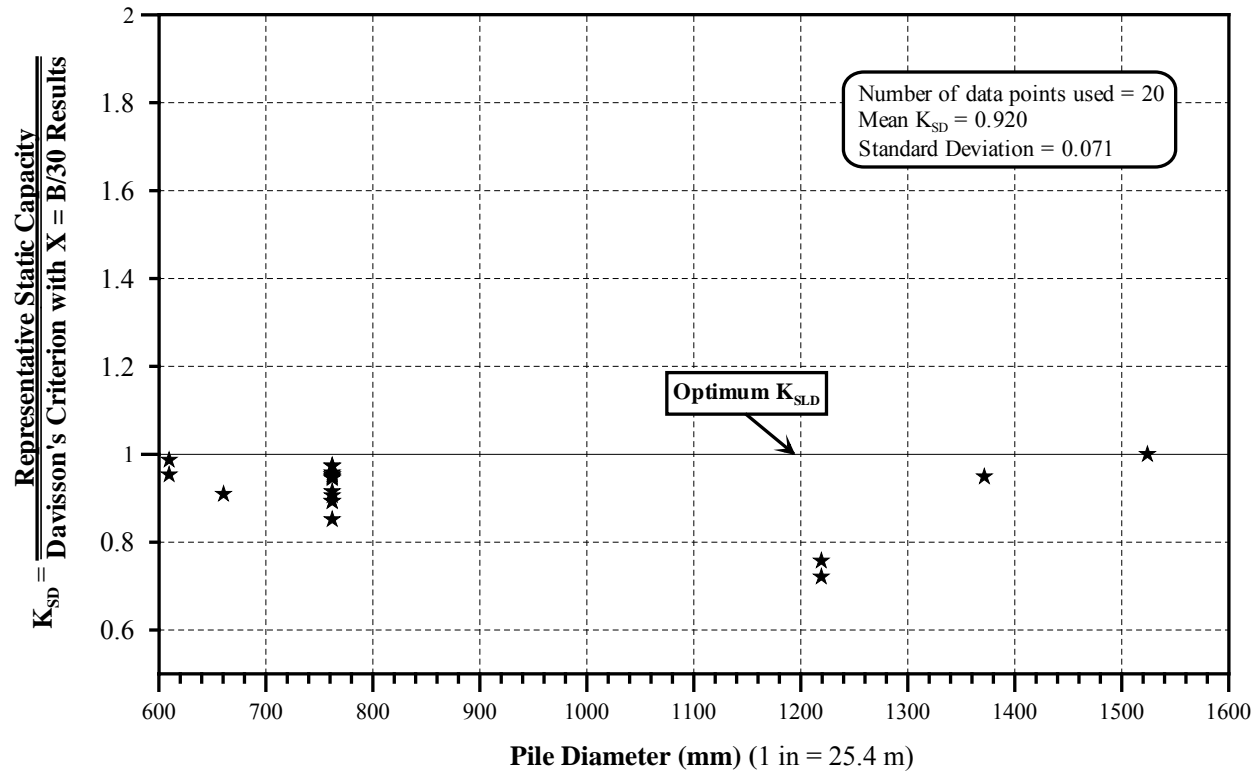


Figure 186. Histogram and frequency distributions of  $K_{SD}$  and  $K_{SLD}$  for 30 and 20 PD/LT2000 pile-cases, respectively, in all types of soils (Paikowsky et al., 2004)



**Figure 187.  $K_{SLD}$  values vs. pile diameter for all large diameter PD/LT2000 pile-cases, all types of soils (Paikowsky et al., 2004)**

#### 9.5.4 Load Test Procedure for Statically Loaded Driven Piles

The influence of the static load testing procedure (loading rate) on the designated pile capacity was examined in two ways: an evaluation of detailed case histories from a research site in Newburyport, Massachusetts (as presented in section 9.4), and via a database from the Ukraine comparing static cyclic to slow maintained load test results on 75 piles.

Two pipe piles and prestressed concrete heavily instrumented friction pile were tested over a lengthy period at a bridge reconstruction site. Both piles were tested using three types of static load testing procedures: slow maintained (testing duration of about 45 hrs), short duration (testing duration of about 6 to 8 hrs), and static cyclic (testing duration of about 15 min.). Details about the piles and the testing are presented in section 9.4 with more details provided by Paikowsky and Hajduk (1999, 2000) and Paikowsky et al. (1999). The interpretation of the load-displacement relationships in both cases suggested that the test type had an insignificant influence on the pile capacity (referring to a failure criterion irrespective of the displacement).

The effect of the test type was further investigated utilizing a database containing information related to 75 piles tested under slow maintained and static-cyclic load testing procedures. In the static-cyclic procedure, the piles were loaded to failure using a high loading rate and then

unloaded. The process was repeated for four cycles. The testing procedure and its interpretation method are presented by Paikowsky et al. (1999). A comparison between the pile capacity based on Davisson's failure criterion for the slow maintained tests and the static-cyclic capacity is presented in Figure 188. The obtained relations and the associated statistical information suggest that there is no significant influence on the static pile capacity based on the applied static load rate.

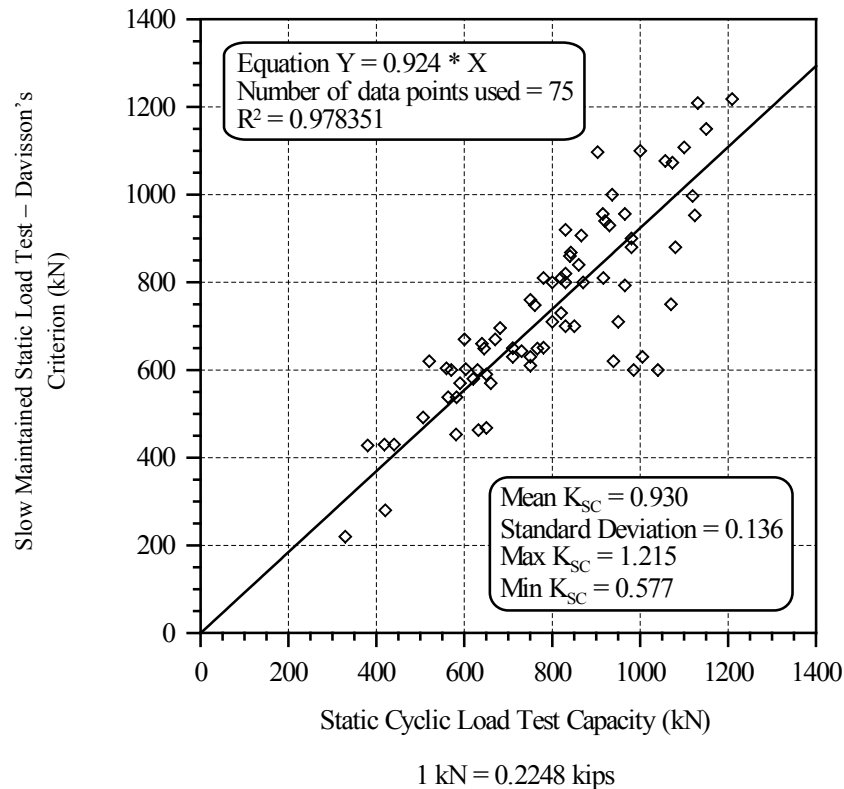


**Figure 188. Comparison between pile capacity based on davisson's criterion for slow maintained load tests and static cyclic load test capacity for 75 piles (Paikowsky et al., 1999)**

The static cyclic load test results were also compared to the representative static pile capacity (based on the aforementioned five methods), resulting in a mean  $K_{SC}$  of 1.023 and a standard deviation of 0.057. These evaluations led to the conclusion that Davisson's pile failure criterion can be used to determine the reference pile capacity for driven piles irrespective of the pile's diameter and the static load-testing procedure.

## **9.6 Extrapolation of Non—Failed Static Load Test**

### **9.6.1 Background**

Static pile load test to failure is the ultimate procedure available to examine the capacity and integrity of deep foundations. Being expensive and time-consuming, the procedure is often substituted for the application of a load to a certain factor (most often two) times the contemplated design load. Even for tests aimed at failure, the actual capacity often exceeds the anticipated one. In fact, only a proof test is mostly carried out while the ultimate capacity and actual safety margin remains unknown. This procedure results in an uneconomic foundation solution, unknown capacity when modifications are required, and the inability of the engineer to gain insight into the controlling mechanism for improved design.

A practical analytical method was developed by Paikowsky and Tolosko (1999) capable of extrapolating the measured load-settlement relations beyond the maximum tested load. The proposed procedure was examined through a database of 63 driven piles load-tested to failure. Loading was assumed to be known for only 25%, 33%, 50%, 75%, and 100% of the entire load-settlement data point. The limited “known” data is then extrapolated using the different methods and the obtained bearing capacity was compared to the actual measurements. For consistency, only one failure criterion (Davisson) was applied. The obtained results were analyzed statistically to evaluate the accuracy of the developed extrapolation method. The following sections outline shortly the methodology and present the reliability of the method.

### **9.6.2 Paikowsky and Tolosko (1999) Extrapolation Method**

Given the load versus settlement results from the load test to failure, each displacement value is divided by its corresponding load. Values of displacement divided by load are plotted versus displacement ( $\Delta/P$  vs.  $\Delta$ ). After some initial scatter, the values eventually form a straight line. These relationships for the load-displacement curve of Figure 150 are presented in Figure 189.

The data are then subjected to a linear regression analysis to determine the best-fit line ratio and the coefficient of regression. The value of displacement divided by the load ( $x$ ) is considered the controlled variable, while the displacement ( $y$ ) is considered to be the dependent variable. The coefficient of regression ( $r^2$ ) is a measure of the dependence of  $y$  on  $x$ . The best-fit line was developed by Gauss and the line is fitted through the given points such that the sum of the squares of the distances to those points from the straight line is minimal (Grossman, 1984). The distance from the point to the line is measured in vertical direction.

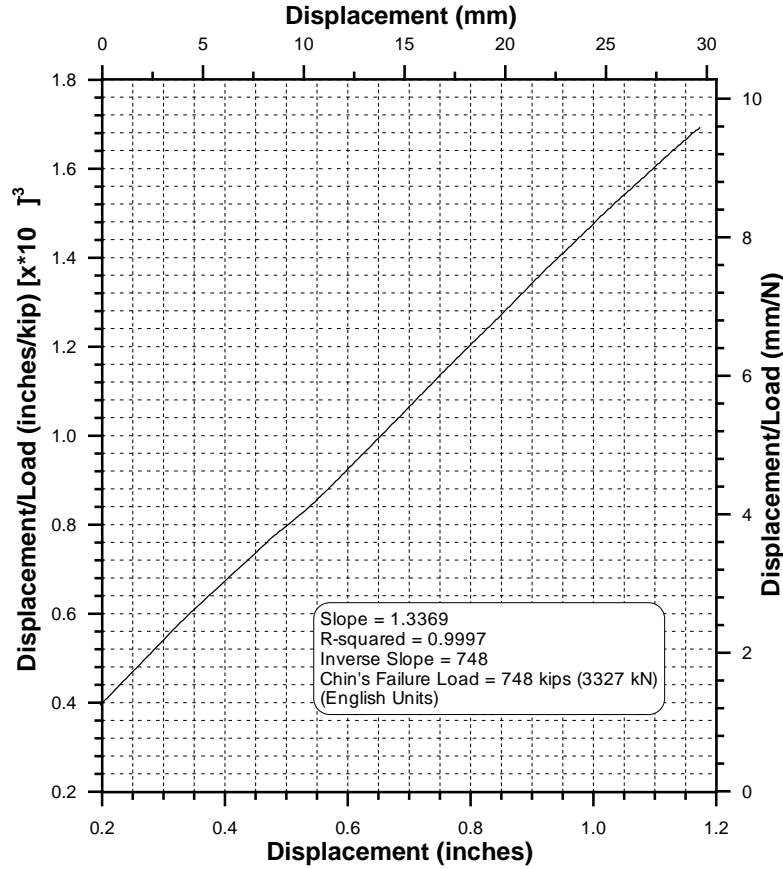


**Figure 189. Displacement over load versus displacement for Pile Case No. 5 according to chin's failure determination method (Paikowsky and Tolosko, 1999)**

The coefficient of regression varies between zero and 1, with zero indicating that no line is obtainable and 1 being a perfect best-fit line. Data points at the beginning of the plotted line (from the plot of displacement divided by load versus displacement) are eliminated until a regression coefficient of 0.8 or greater is produced.

With a coefficient of regression of 0.8 or greater, the general obtained equation of the line is:

$$y = ax + b \quad (31)$$

And 
$$y = \frac{\Delta}{P} \quad (32)$$

$$x = \Delta \quad (33)$$

where:  $y$  = displacement divided by load  
 $a$  = slope of the line  
 $x, \Delta$  = displacement of pile top  
 $b$  = intercept of the best-fit line through the y-axis



P = load corresponding to the displacement

Substituting gives:

$$\frac{\Delta}{P} = a\Delta + b \quad (34)$$

$\Delta$ , yields:

$$\Delta = \frac{b}{\left(\frac{1}{P} - a\right)} \quad (35)$$

The slope (m) and intercept (c) values are obtained from the linear best-fit analysis. Using equation (35) load values (from the original load test) were used and the equation was solved for the displacement of the pile ( $\Delta$ ) for the 100%, 75%, 50%, 33%, and 25% cases for both the percent of data and the percent static load case.

Since Davisson's criterion is often used and its rationale allows for pile geometry considerations, Equation (34) was used in conjunction with Davisson's criterion to mathematically determine the pile's ultimate capacity based on the constructed load-settlement relations and Davisson's criterion. From Davisson's analysis, the equation of Davisson's line is known to be:

$$\Delta = X + SP_{\text{METH}} \quad (36)$$

where  $\Delta$  = displacement of pile top at the capacity associated with Davisson's criterion  
 $X$  =  $0.15 + B/120$  (offset)  
 $S$  =  $L/EA$   
 $P_{\text{METH}}$  = extrapolated pile's ultimate capacity load based on Davisson's criterion  
 $B$  = pile diameter (inches)  
 $L$  = pile length  
 $E$  = elastic compression of the pile material  
 $A$  = cross-sectional area of the pile

Substituting equation (36) into equation (35), and solving for  $P_{\text{METH}}$  (Davisson's ultimate capacity), yields:

$$P_{\text{METH}} = \frac{-B \pm \sqrt{B^2 + 4AX}}{2A} \quad (37)$$

where  $P_{\text{METH}}$  = Davisson's ultimate capacity  
 $B$  =  $aX + b - S$   
 $A$  =  $aS$

The resultant  $P_{\text{METH}}$  was compared to the static load as actually measured in the original load test. The accuracy of the method  $P_{\text{METH}}$  is discussed below. Note that when applying the method to a non-failed load test, the above procedure is carried out to the limit of the load-displacement

relations. When developing the extrapolated load displacement relations using equation 35, arbitrary loads  $P$  are applied and  $\Delta$  is calculated till failure appears and equation 37 can be implemented.

### ***9.6.3 Evaluation of the Extrapolation Method***

#### ***Overview***

The load-test extrapolation method was examined utilizing the pile cases in data set PD/LT (Paikowsky and Tolosko, 1999). The analyses were carried out in the following stages:

1. Determination of the ultimate capacity based on the ratios of available load-test data and ratios of the designated known ultimate capacity
2. Examination of the correlation between the prediction ratio of the results from the extrapolation method and the designated pile capacity and varying factors such as pile stiffness and pile slenderness.
3. Statistical analyses of the obtained results, evaluating the performance of the proposed method and the associated risk of application, allowing the establishment of conclusions and recommendations.

#### ***The Analyzed Load Ranges***

During a typical proof test, the actual capacity of the pile remains unknown. Therefore, the amount of load-displacement data necessary to complete the load test and the load test graph (the plot of load versus displacement) remains unknown as well. To account for this unknown, data were decreased from the original data (the 100% case) to ranges of the load and displacement data. The proposed method was repeated for each subsequent decrease in the range of data or load. The calculated capacity extrapolated for each range was then compared to the designated static capacity.

The performance evaluation of the proposed method was carried out in five ranges related to: (1) available data points for the entire load-settlement relations and (2) the designated ultimate capacity. The ranges include 25%, 33%, 50%, 75% and 100% of either all the load-test data or the data related to the designated capacity only. For the data related cases, the 100% analysis means that the entire load-displacement relations were used. The 75% case under this category means that 75% of the available data points were used arbitrarily, regardless of its meaning in relation to the load-displacement relations. The other ranges of 50%, 33% and 25% follow the same logic.

For the capacity-related cases, the 100% analysis means that the load-displacement data up to the designated static capacity was used. The 75% case under this category means that the data related to the load settlement relationship from the start of the loading to the value of 75% of the

designated pile capacity were used for the analysis. The other ranges of 50%, 33% and 25% follow the same logic regardless of the actual number of data points associated with the analyzed loading level.

### Example

Figures 190 and 191 refer to extrapolated cases related to designated data ranges and load ranges, respectively for an 18-inch square prestressed concrete pile driven to a depth of 75ft in Alabama. The effectiveness of the extrapolation method is evident by the graphical presentation. For more details refer to Paikowsky and Tolosko (1999), while statistical evaluation follow.

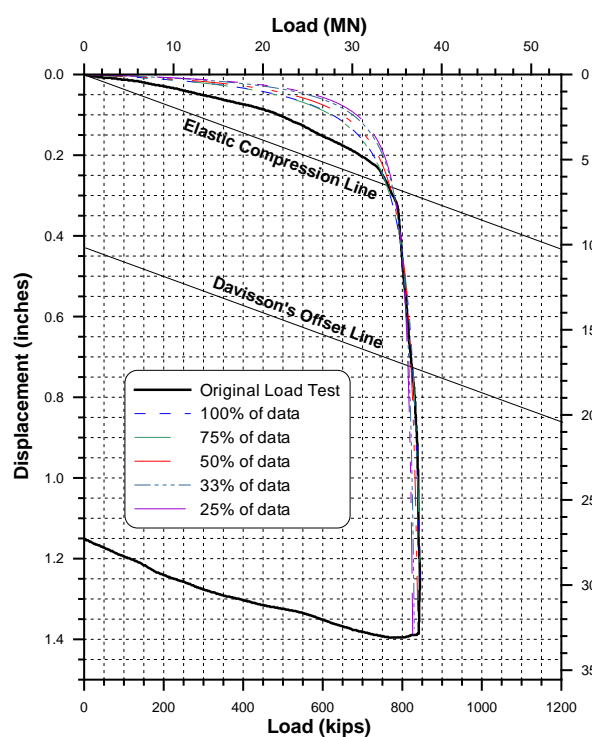


**Figure 190. Actual and extrapolated load-settlement relations for the re-analysis of Pile Case No. 14 using ranges of available data (Paikowsky and Tolosko, 1999)**

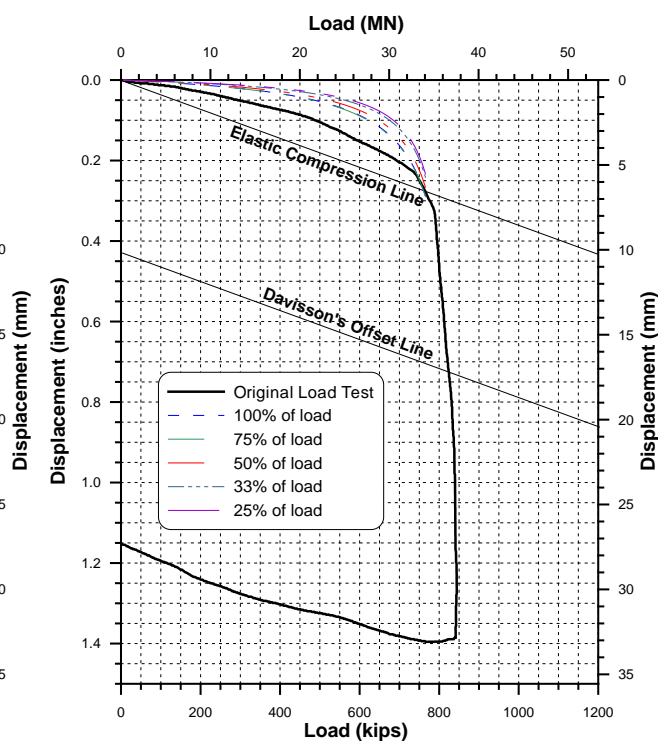


**Figure 191 actual and extrapolated load-settlement relations for the analysis of Pile Case No. 14 using ranges of the designated static capacity (Paikowsky and Tolosko, 1999)**

### Statistical Analysis

Table 92 presents the results of the statistical analysis for the extrapolation method using ranges of load-displacement data points. Rows 4 and 5 list the mean and standard deviation for each range of data analyzed. The average values for the 100% to 75% cases are nearly 1.0, indicating almost perfect agreement with the actual load test results. As expected, the 25% case was the

least accurate, with an average value of 0.78. The standard deviation for all cases ranged from 0.21 for the 100% case to 0.33 for the 25% case. The mean values for the five ranges of data analyzed were all below 1.0, indicating that the proposed method is conservative in its results and, hence, consistently on the safe side.

**Table 92. Mean and standard deviation of the ratio between the extrapolated capacity based on the extrapolation method and the actual capacity (both determined by Davisson's Criterion) using ranges of load-settlement data (Paikowsky and Tolosko, 1999)**

Range of Data	100%	75%	50%	33%	25%
No. of Cases	63	63	63	62	60
Range	0.13 – 1.52	0.38 – 1.54	0.31 – 1.92	0.26 – 1.82	0.24 – 1.94
Mean	0.96	0.99	0.96	0.87	0.78
Standard Deviation	0.21	0.21	0.27	0.30	0.30

Table 93 presents the results of the statistical analysis for the extrapolation method using ranges of the static capacity. Again, rows 4 and 5 list the mean and standard deviation for each range of analyzed load. The mean value for the 100% case is slightly greater than one. The mean for the 75% case is nearly one, with the mean values falling further from one as the percentages of static load decreases. The mean value is least in the 25% case. The standard deviations are similar to those obtained when analyzing ranges of load data.

**Table 93. Mean and standard deviation of the ratio between the extrapolated capacity based on the extrapolation method and the actual capacity (both determined by Davisson's Criterion) using ranges of designated static capacity (Paikowsky and Tolosko, 1999)**

Range of Data	100%	75%	50%	33%	25%
No. of Cases	63	62	61	54	48
Range	0.26 – 1.72	0.47 – 2.06	0.47 – 2.74	0.34 – 2.87	0.23 – 2.73
Mean	1.02	0.99	0.89	0.74	0.64
Standard Deviation	0.21	0.26	0.41	0.46	0.44

The statistical analysis presented in Tables 92 and 93 suggest the following:

1. The extrapolation method is very accurate and can be used with any available data.
2. The accuracy of the prediction decreases with the decrease of the available loading range compared to the failure load.
3. The extrapolated values are conservative, and hence, even when predicting four times the tested load, these values can be used safely.

Additional insight of the method is presented in the following sections through detailed statistical analysis and a correlation study. Paikowsky and Tolosko (1999) followed these statistics and examined the risk associated with using the extrapolation method.

## ***Summary***

It was shown that the accuracy of the extrapolation method was  $0.99 \pm 0.21$  (1S.D.),  $0.96 \pm 0.27$ ,  $0.87 \pm 0.30$ , and  $0.78 \pm 0.33$  when assuming 75%, 50%, 33%, and 25% of the data points to be known and  $0.99 \pm 0.26$  (1S.D.),  $0.89 \pm 0.41$ ,  $0.74 \pm 0.46$ , and  $0.64 \pm 0.44$  when assuming 75%, 50%, 33%, and 25% of the bearing capacity to be known, respectively. The obtained results for the 63 database cases suggested that even when the predicted ultimate capacity was four times the maximum actual tested load, the associated risk was zero for exceeding the design load, when using the extrapolated value with a factor of safety of 2.0. All the case histories used in the research related to driven piles. Even though it was expected to be valid, a detailed examination of the method is required before its safe application to cast-in-place piles.

### ***9.6.4 Extrapolation Implementation in MnDOT Load Test Database and Program***

Implementation of the extrapolation technique presented in this section has been presented earlier in this report. Section 6.2.3 presents the use of extrapolated load test results for four timber piles when constructing the timber pile database. Section 7.3.2 presents the extrapolation of TP2 load test carried out at Arden Hills site (1/14/2013, state project no. 6285-62716) by the MnDOT.

## **9.7 Recommended Load Test Procedures and Submittals for the MnDOT**

### ***9.7.1 Recommended Load Test Procedures and Interpretation***

## ***Summary***

Based on experience gathered by the first author, two procedures are recommended for MnDOT static load tests; Procedure A of ASTM D1143 described in section 9.2.1 and modified as detailed below, and the static-cyclic load test procedure adopted by MassDOT and presented in section 9.2.3.

### ***Proposed Modifications for Procedure A of ASTM D1143 – Quick Load Test***

1. Design the load-test to geotechnical failure or at least to 300% of the design load.
2. Carry the load to geotechnical failure or structural limit or set-up loading limit, whichever is obtained first.
3. Require maintaining longer time intervals under constant loads for the following load levels: (a) design load, (b) 150% of the design load, (c) 200% of the design load, (d) 250% of the design load, (e) at failure, and (f) zero load upon unloading.
4. At each of the above stages, keep the load until a displacement rate of 0.01 inch/hr is achieved or if the settlement criterion is not met, for the minimum of the following: (a)

15 minutes for 150% and 250% of the design load, at failure and zero load upon unloading, and (b) 30 minutes for 200% of the design load.

5. Use Davisson's criterion for capacity interpretation. Examine Shape of Curve and other failure interpretation methods to ensure 'logical' result.

### ***Static-Cyclic Load Test***

See procedures as adopted by MassDOT and presented in section 9.2.3. Note the load test needs to be carried out to failure in four cycles with the failure load determined by the intersection of the load-unload cycles and the average of those intersections is taken as the representative failure load. Comparison can be made with the failure load obtained by applying Davisson's failure criterion. Follow examples in Section 9.4 for the load-displacement relations and comparisons between the static-cyclic load test results and other test results.

### ***9.7.2 Pre Load-Test Submittal Requirements***

The following is expected to be submitted prior to a load test:

1. Contractors and subcontractors responsibilities. Detailing the contractor in charge and the subcontractors to conduct and analyze the tests. Provide specific names, addresses, contact details and responsibilities for each. For example: access roads, subsurface drilling, pile installation, pile instrumentation, load frame design and construction, load test set-up, load application, test monitoring, data reduction, etc.
2. Location plan including test location and subsurface conditions based on at least one boring log not to exceed 25 ft away from the test pile location.
3. Site preparation details including access roads, site leveling, drainage, fencing, load test coverage (protection), electricity supply, lighting, field office, safety procedures, etc.
4. Static load test preparation including shop drawings of test set-up, reaction evaluation including geotechnical and structural calculations and design, loading set-up specifications and arrangements including type and size of hydraulic jacks, pile top set-up, load cells and swivel set-up, etc.
5. Static load test set-up including list and drawings of instrumentation and back-up readings, e.g. electronic gauges: 3 displacement transducers on top of pile, 2 displacement transducers horizontally normal to the pile (North and East), and 3 displacement transducers for tell tales. Backup systems: 3 dial gauges for top of the pile and 2 dial gauges for lateral movement, a level to monitor test pile and reaction pile movements, wire and mirror system.
6. Test pile details, structure, strength, length, etc. Include instrumentation location (including tell tales).
7. Instrumentation details: required ranges, type, manufacturer, specifications, layout and numbering system. Installation details.

8. Data acquisition set-up: type, allocation of channels, and frequency of readings. Manual back-up readings, equipment to be used and frequency of readings.
9. Load test plan: based on the required procedure, a table listing the planned loading stages and timing of the entire load test detailing expected jack pressure and allocating space for manual readings.
10. Test pile installation details, including driving equipment, WEAP analysis (see WEAP submittal requirements in section 8.6), expected stresses, equipment/instrumentation protection, dynamic measurements.
11. Time schedule for the entire testing program including procurement, shop installation, calibration, field installation and reaction set-up, test set-up, load test execution and break-down, initial and final reporting.

### **9.7.3 Load Test Reporting**

The load test final reporting requires all of the above information provided in the pre-testing submittal, updated with the actual details of as built, instrumentation serial numbers and calibrations, and the test records and their interpretations. Specifically, the load test submittal should include:

1. Executive summary providing the major findings of the testing including dynamic capacity predictions and static load test results, highlighting the major goals and results.
2. Background information addressing:
  - a. The project
  - b. Contractors details and responsibilities
  - c. Site location and conditions, boring log and subsurface description including relevant soil test results.
  - d. Site set-up
3. Detailed time table of the load test preparation and execution stages.
4. Test pile and reaction set-up and construction.
5. Instrumentation details including serial number, calibration sheets and installation details.
6. Pile installation details including: driving logs, records of dynamic measurements, dynamic testing reports of analyses and interpretations, pile capacities based on MnDOT dynamic equation (MPF12), field Case Method, Energy Approach and CAPWAP analyses. Electronic records of the measured data should be part of the submittal.
7. Static load test set-up including photograph and sketches detailing all the locations and setting of the instrumentations in and outside the pile.
8. All electronic records of the raw data organized at the way it was recorded before any reduction analysis or interpretation takes place. That includes instrumentation in and out of the pile and load application system.
9. All electronic and printout records of the reduced data including at least: time step, load cell reading(s), jack pressure gauge readings and corresponding loads, individual

- displacement readings and the average reading at the pile top, lateral movement readings of pile top.
10. Copies of all field raw manual readings including dial gauges, pressure gauge, level and mirror/wire movement.
  11. All electronic input of the manual readings.
  12. Presentation of the static load test results in the following format:
    - a. A combined plot of load-displacement and time (see e.g. Figure 176)
    - b. Detailed load-displacement relations in a scale where the elastic compression line is approximately 20° of the load (x) axis (see e.g. Figure 179). This graph should include the elastic compression line and Davisson's failure criterion.
    - c. If telltale readings are taken, add to the above, a plot of the top load vs. tip displacement relationship on the same figure along with the top load and top displacement relationship.
    - d. Load distribution with depth for various loading levels (e.g. see Figure 171).
    - e. Detailed graphs of the vertical applied load vs. lateral displacements providing both measurements (East and North) vs. the applied load.
    - f. Pile top load-displacement relations based on level reading and dial-gauge manual readings.
    - g. Records and plots if relevant of reaction pile movements relative to the applied load.
  13. Discussion of the testing including problems, special observations, and comments.

#### **9.7.4 Database/Data Requirements for MnDOT Load Testing Program**

As the MnPILE Load Testing Program moves forward, MnDOT desires to ensure that all load tests conducted obtain the appropriate data to be useful in developing a local database of pile capacities which can be used to further refine the dynamic formula adopted (MPF12) along with improving MnDOT pile driving practice in general. Beyond the detailed submittals presented in the above sections 9.7.2 and 9.7.3, the database items should include the following:

- General site/project information including subsurface profile and boring log (available from MnDOT project plans and foundation reports) and test pile coordinates and ground elevations.
- Test pile physical details, length at installation, EOID, BOR and static testing, section, strength, penetration at end of driving, testing penetration, etc.
- Required Nominal Resistance Values (for MPF12, PDA and SLT – per project plan sheets)
- Driving Records for EOID and BOR (available from MnDOT inspectors)
- Complete digital PDA records and dynamic testing reports including capacity estimates and calculated parameters including EMX, DMX and DFN enabling to calculate the Energy Approach (available from Geotechnical Subconsultants)



- Complete SLT records and Davisson failure capacity (available from Geotechnical Subconsultants)
- Appropriate project information (driving and testing timeline, etc. – available from Geotechnical Subconsultants and/or MnDOT records)

Based on this information, a table providing the necessary details for the database can be developed for each MNPILE Static Load Test conducted. As additional tests are performed, the MPF12 formula can be evaluated and refined using local data, since it was developed based on a global database restricted to MnDOT practice but with no MnDOT data included.

## 10 SUMMARY CONCLUSIONS AND RECOMMENDATIONS

### 10.1 Summary

#### *General*

MnDOT used its own pile driving formula; however, its validity and accuracy has never been thoroughly evaluated. Systematic probabilistic-based evaluation of a resistance factor requires quantifying the uncertainty of the investigated method. As the investigated analysis method (the model) contains large uncertainty itself (in addition to the parameters used for the calculation), doing so requires:

- (i) Knowledge of the conditions in which the method is being applied, and
- (ii) A database of case histories allowing comparison between the calculated value to one measured.

The first phase of the research addressed these needs via:

- (i) Establishing the MnDOT state of practice in pile design and construction, and
- (ii) Compilation of a database of driven pile case histories (including field measurements and static load tests to failure) relevant to Minnesota design and construction practices.

The first phase of the study was presented in a research report by Paikowsky et al. (2009). Phase I concentrated on establishing MnDOT practices, developing databases related to these practices and examining different dynamic equations as well as developing new equations. The proposed resistance factors developed in Phase I for the driving of pipe piles were assessed to be conservative in light of the MnDOT traditional design and construction practices, and hence, Phase II of the research was initiated.

A comprehensive investigation of the Phase I findings were conducted. The studies lead to the development of dynamic formula suitable for MnDOT foundation practices, its calibrated resistance factors and its application to concrete and timber piles.

Phase II of the study also expanded on related issues associated with Wave Equation analyses and static load tests assisting the MnDOT in establishing requirements and specifications.

Phase II of the study was established to:

1. Re-evaluate resistance factors for the Load Resistance Factor Design (LRFD) implementation as obtained in the Phase I study,
2. Examine other dynamic pile driving formulae and other Midwest states practices,
3. Recommend to MnDOT an appropriate formula (and associated resistance factors) for implementation,

4. Examine the recommended formula in use with timber and prestressed precast concrete piles,
5. Examine WEAP analyses procedures for MN conditions and recommend procedures to be implemented, and
6. Examine load test procedures, interpretations and submittals.

### ***Alternative Formulas and Midwest Practices***

Pile driving practices and research carried out in Illinois, Wisconsin, Iowa and Washington were reviewed and analyzed along with the Gates (1957) and modified Gates equations. A critical review revealed both deficiencies in the data and limitation in the developed analyses leading to results of limited validity. In depth investigation of the equations prepared by Gates (1957), Olson and Flaate (1967) modified Gates, and FHWA modified Gates (USDOT 1988) had been carried out. While all variations of the Gates formulae provide a relatively good correlation to the piles capacity, none have a mean bias close to 1.0 and some have many format variations not easily implemented or justified.

### ***Evaluation of MnDOT Bridge Office Data***

A database containing dynamic measurements and signal matching analyses was provided by MnDOT. The data were used for examining typical energy transfer values and compare the performance of various dynamic equations to the signal matching analysis results. The updated pile data suggests that the most common pile used by MnDOT is a 16 in CEP (0.3125" and 0.25" wall thickness) installed at about 55% of the total foundation length. The typical pile is 83 ft long. Around 80% of the piles were driven beyond 4 BPI at EOD.

The statistical analysis and correlations obtained from comparing the signal matching analyses (CAPWAP) to various dynamic equations showed unequivocally that the equation developed specifically for the MnDOT in Phase I of the study outperformed all other equations.

### ***Reassessment and LRFD Calibration of MPF12***

The evaluation described in the previous section included modifications of the MnDOT equation developed in Phase I to better represent field practices in MN (e.g. using measured stroke rather than nominal energy). In depth reassessment was carried out by systematic evaluation of the data and case by case examination of outliers. MnDOT TAP review, excluded cases deemed irrelevant to MnDOT practices (e.g. pile sizes and use, driving conditions, etc.) and hence enabled the statistical data to better match the conditions the developed equation is going to be applied to. In addition to the re-evaluation of the data and the resulting statistics and dynamic

formula development, additional equations were examined in parallel. The final format of the recommended Minnesota Pile Formula 2012 (MPF12) is:

$$R_n = 20 \sqrt{\frac{W \times H}{1,000}} \times \log\left(\frac{10}{s}\right)$$

in which

- $R_n$  = nominal resistance (tons)
- $H$  = stroke (height of fall) (ft)
- $W$  = weight of ram (lbs)
- $s$  = set (pile permanent displacement per blow) (inch)

The value of the energy ( $W \cdot H$ ) used in MPF12 shall not exceed 85% of the manufacturer's maximum rated energy for the hammer used considering the settings used during driving. MPF12 is to be used with the following Resistance Factors (RF) in order to obtain the factored resistance:

$$R_r = \phi \cdot R_n$$

where

- for Pipe Piles,  $\phi = 0.50$ ,  $2 < BC \leq 15$
- for H piles,  $\phi = 0.60$ ,  $2 < BC \leq 15$

### ***Evaluation of MPF12 for PPC Piles***

The MPF12 was investigated for its application to precast prestressed concrete piles using 137 cases. As the case history database was diverse and extensive, it required looking at 24 combinations for establishing the resistance factors, but also allowed to expand the investigation in various ways:

1. The use of MPF12 for large/voided piles that would require equation modification. For the present research it can be resolved using a higher resistance factor as presented below.
2. CAPWAP predictions were compared to static load test results and to MPF12. The performance of MPF12 is much better than that of CAPWAP for EOD and comparable to CAPWAP at BOR within the applicable pile sizes.

The calculated resistance factors lead to the following recommendations:

1. For non-voided PSC Pile sizes  $\leq 24"$   
use the above recommendations provided for steel pipes, i.e.:  
 $\phi = 0.5$  for EOD and BOR,  $2 < B.C. < 15BPI$

2. For voided PSC sizes  $20'' \leq \text{PSC} \leq 54''$   
use  $\phi = 0.80$

Case 2 requires modification of the equation but as a first evaluation one can use  $\phi = 0.80$  for all cases.

### ***Evaluation of MPF12 for Timber Piles***

The MPF12 was investigated for its application to timber piles. A total of 28 timber piles were examined and the appropriate resistance factor was developed based on 25 of the original 28 cases. Three cases were set aside as control cases. Due to large damping and loss of energy when impacting timber, it was proposed that the MPF12 equation be multiplied by 0.50 for a simplified format and accurate pile capacity predictions. The recommended resulting equation and resistance factors to be used with the Timber piles are:

$$R_n = 10 \sqrt{\frac{WH}{1000}} \log\left(\frac{10}{s}\right)$$
$$\phi = 0.6$$

### ***Minnesota Load Testing Program***

Two axial compression static load tests carried out by MnDOT were included as part of the study. One test was carried out in Victoria, Minnesota in June 2012 (state project 1002-89) and the other in Arden Hills, Minnesota in January 2013 (state project 6285-62716). TP1 at the Victoria test was carried out on 12 in O.D., 0.25 in wall thickness closed ended pipe 63 ft penetration. A good match was obtained between the factored pile measured static capacity to that of CAPWAP at BOR after the test and to the factored resistances of the Energy Approach at EOD and BOR and the MPF12 at BOR. While the MPF12 factored resistance was lower than the SLT factored resistance, the old MnDOT equation was found to be very unsafe in BOR.

TP2 at the Arden Hills test site was carried out on a 12.75 in, 0.25 in wall thickness closed ended pile driven to a penetration of 63 ft. An extrapolation procedure was carried out to estimate the failure capacity of the pile. A good match was obtained between the nominal capacities of the SLT, Energy Approach BOR, and MPF12 all stages. While CAPWAP nominal resistance under predicted the capacity, the old MnDOT equation over predicted significantly the piles' capacity. A good match was also found between the factored resistances of CAPWAP BOR and MPF12 EOD.

### ***WEAP Analysis***

The use of WEAP in driven pile design and construction processes was presented in flow charts (Figures 124 and 125). The accuracy of the method for pile capacity prediction was reviewed. The use of the WEAP with default soil model parameters was shown to be extremely conservative (mean bias 1.66) compared, for example, to MPF12 for H and pipe piles (mean bias 1.01). WEAP analyses were run for 70 cases representing MnDOT practice. Mean driving resistance charts were developed and compared to MPF12 capacity-driving resistance relationship.

The process of WEAP adjustment following the analysis of dynamic measurements and static load tests were presented and demonstrated via the Victoria test pile. The comparison between the WEAP modified analysis, the MPF12 and the static load test were found to be extremely precise as demonstrated in Figure 144. The last section of Chapter 8 presents the submittals that should be required for the WEAP analysis along with MnDOT Specifications for that end.

### ***Static Load Test***

Following a presentation of the principle of testing and examining static and dynamic tests in context, Chapter 9 present procedures for carrying out static load tests and methods for pile capacity interpretation. A detailed full scale pile field testing is then used for providing examples for testing methods and interpretations.

The concept of piles' static capacity nominal strength and its uncertainty is presented along with the investigation of Davisson's failure criterion modification for piles exceeding 24 inch in diameter. Evaluation of the rate in which static load tests are being carried out leads to the conclusion that slow tests have limited advantages and can be focused on specific load levels only.

An extrapolation method and its accuracy are reviewed in detail and references are made to its use in the study. Finally, recommendations are made for static load testing procedures to be adopted by the MnDOT along with pile load test submittal and load test reporting requirements, both as part of a project and for the MnDOT database.

## **10.2 Conclusions**

The operative findings in Phase II relevant to the dynamic pile formula to be used by the MnDOT are summarized in Table 94.

The independent examination of the developed equations against an independent data, dynamic measurements in MN and load tests conducted by the MnDOT, affirmed the effectiveness and

accuracy of the proposed equations. Further monitoring and calibration is recommended by following the outcome of piles installed during construction, utilizing dynamic measurements and conducting static load tests for MnDOT typical design practices.

**Table 94. Summary of the final formulation known as MPF12 (Minnesota Pile Formula 2012) adopted for use**

Application	Format	Variables	$\phi$ Resistance Factor	Comments
Pipe, Concrete and H Piles	$R_n = 20 \sqrt{\frac{W \times H}{1,000}} \times \log\left(\frac{10}{s}\right)$	$R_n$ = nominal resistance (tons) $H$ = stroke (height of fall) (ft) $W$ = weight of ram (lbs) $s$ = set (pile permanent displacement per blow) (inch)	$R_r = \phi \times R_n$  For pipe and concrete piles $\phi = 0.50, 2 < BC \leq 15BPI$  For H piles $\phi = 0.60, 2 < BC \leq 15BPI$	The value of the energy ( $W \cdot H$ ) used in the dynamic formula shall not exceed 85% of the manufacturer's maximum rated energy for the hammer used considering the settings used during driving.
Timber Piles	$R_n = 10 \sqrt{\frac{W \times H}{1,000}} \times \log\left(\frac{10}{s}\right)$		$\phi = 0.60$	

Note: Although the equations were developed for hammers with  $Eh \leq 165$  kip-ft, its use should be applicable for hammers with higher energies but this was not verified directly in the study.



### **10.3 Recommendations**

The current study is only a major first step in advancing the bridge foundation design and construction practices carried out by the MnDOT. To fully realize the potential of this study, the following is recommended:

1. Expand the static load test program for building up a database related to MN. Such expansion should include (according to priority of usage) various pile types, sizes and subsurface conditions.
2. Conduct routinely dynamic measurements on indicator piles in all projects, and retain a database for capacity predictions of the cases, comparing MPF12, Energy Approach, and Case Method in the field to CAPWAP results for EOD and BOR.
3. Retain a systematic database of piles monitored in the field and the associated calculated capacities.
4. Conduct within one or two years a re-evaluation and adjustment of the current study based on the above.

## REFERENCES

- Allen, T.M. (2007). “Development of a New Pile Driving Formula and Its Calibration for Load and Resistance Factor Design”, *Proc. 86th Transportation Research Board Annual Meeting*, January 21-25, 2007, Washington, DC.
- Allen, T.M. (2005). *Development of the WSDOT Pile Driving Formula and Its Calibration for Load and Resistance Factor Design (LRFD)*. Final Research Report submitted to Washington State Department of Transportation, Olympia, WA, March.
- ASTM C670-90a (1990). *Standard Practice for Preparing Precision and Bias Statements for Test Methods for Construction Materials*, American Standard for Testing and Materials, Washington, DC, see also updated standard ASTM C670-13.
- ASTM D1143/D1143M-07 (2013). *Standard Test Methods for Deep Foundations Under Static Axial Compression Load*, American Standard for Testing and Materials, Washington, DC.
- ASTM D3689/D3689M-07 (2013). *Standard Test Methods for Deep Foundations Under Static Axial Tensile Load*, American Standard for Testing and Materials, Washington, DC.
- ASTM D3966/D3966M-07 (2013). *Standard Test Methods for Deep Foundations Under Lateral Load*, American Standard for Testing and Materials, Washington, DC.
- Barker, R., Duncan, J., Rojiani, K., Ooi, P., Tan, C., and Kim, S. (1991). *NCHRP Report 343: Manuals for the Design of Bridge Foundations*. TRB, National Research Council, Washington, DC.
- Brinch-Hansen, J. (1963). “Hyperbolic Stress-Strain Response: Cohesive Soils” Discussion, *American Society of Civil Engineers Journal of the Soil Mechanics and Foundation Division*, Vol. 89, No. SM4, pp. 241-242.
- Butler, H.D., and Hoy, H.E. (1977). *Users Manual for the Texas Quick-Load Method for Foundation Load Testing*. FHWA-IP-77-8. FHWA, Office of Development, Washington, DC.
- Chin, F.K. (1971). “Estimation of the Ultimate Load of Piles Not Carried to Failure.” *Proceedings of the 2<sup>nd</sup> Southeast Asian Conference on Soil Engineering*, pp. 81-90.
- Collin, J. G. (2002). *Timber Pile Design and Construction Manual*, Timber Piling Council American Wood Preservers Institute, 2002, Fairfax, VA.
- Cornell, C. (1969). “A Probability Based Structural Code”, *Journal of American Conc. Institute*, Vol. 66, No. 12, pp. 974-985.
- Dasenbrock, D. (2013). Email communication on 11/4/2013.
- Davisson, M. (1972). “High Capacity Piles”, *Proceedings, Soil Mechanics Lecture Series on Innovations in Foundation Construction*, ASCE, Illinois Section, Chicago, IL, pp. 81–112.

- Davidson, J.L, and Townsend, F.C. (1996). “Reliability and Limitations of Dynamic Methods for Predicting Capacity and Settlement of Driven Piles”, Final report submitted to Florida Department of Transportation, University of Florida, Gainesville, FL, June, pp.141.
- Davidson, J.L., Townsend, F.C., Ruesta, P.F., and Caliendo, J.A. (1994). "Pile Load Test Database and an Evaluation of the Program SPT91", *International Conf. on Design and Construction of Deep Foundations*, Orlando, FL, December 1994, FHWA, Vol. II, pp.759-773.
- DeBeer, E. (1970). Proefondervindelijke bijdrage tot de studie van het grandsdraagvermogen van zand onder funderinger op staal. English version. *Geotechnique*, Vol. 20, No. 4, pp. 387-411.
- Eslami, A., (1996). “Bearing capacity of piles from cone penetrometer test data”, Ph.D. Thesis, University of Ottawa, Department of Civil Engineering, Ottawa, ON, Canada.
- FHWA (1995). *Design and Construction of Driven Pile Foundations I, II* FHWA Contract No. DTFH61-93-C-00115, Federal Highway Administration, Research and Procurement, Washington, D.C.
- FHWA (2006).
- Flaate, K. (1964). *An Investigation of the Validity of Three Pile-Driving Formulae in Cohesionless Material*, Norwegian Geotechnical Institute, Publication 56, Oslo, Norway.
- Fragaszy, R.J., Argo, D., and Higgins, J.D. (1989). “Comparison of Formula Predictions with Pile Load Test”, *Transportation Research Record No. 1219, Geotechnical Engineering*, Transportation Research Board, Washington, DC.
- Fragaszy, R.J., Higgins, J.D., and Argo, D.E. (1988). *Comparison of Methods for Estimating Pile Capacity*, Washington State Department of Transportation Research Report WA-RD 163.1, and in cooperation with U.S. Department of Transportation FHWA, Olympia, WA.
- Gates, M. (1982). “Generic Driven Pile Specification”, *Geotechnical Guideline No.13*, Federal Highway Administration, Washington, DC
- Gates, Marvin (1957). “Empirical Formula for predicting Pile Capacity”, *Journal of the Soil Mechanics and Foundations Division*, ASCE, Volume 27-3, March 1957, pp. 65-66.
- Grossman, S.I. (1984). *Calculus, 3<sup>rd</sup> Edition*, Academic Press, Inc., London.
- Hannigan, R., Goble, G., Thendean, G., Likins, G., and Rausche, F. (1996). *Design and Construction of Driven Piles Foundations—Volume II (Working Draft)*. U.S. DOT, FHWA. Washington, DC.
- Hajduk, E.L. (2006). “Full Scale Field Testing Examination of Pile Capacity Gain with Time”, Doctorate of Engineering, Civil and Environmental Engineering Dept., University of Massachusetts Lowell, Summer 2006, Lowell, MA.

- Johnson, K., Dasenbrock, and D., Person, G. (2011). Minnesota Department of Transportation Memo on S.P. 1002-89 Bridge 10003 (Replacing 6654) Foundation Investigation and Recommendations and Recommendation for Static Load Testing at this site, Office of Materials & Road Research Geotechnical Eng. Section, Maplewood, MN, April 12, 2011.
- Kyfor, Z.G., Schnore, A.S., Carlo, T.A. and Baily, D.F. (1992). *Static Testing of Deep Foundations*. Report No. FHWA-SA-91-042, U.S. Department of Transportation, Federal Highway Administration, Office of Technology Applications, Washington, DC, p. 174
- Long, J.H. and Maniaci, M. (2000). *Friction Bearing Design of Steel H-Piles*, Final report no. ITRC FR 94-5 Illinois Transportation Research Center, December, 2000, University of Illinois at Urbana-Champaign, Urbana, IL.
- Long, J.H., Hendrix, J., and Baratta, A. (2009a). *Evaluation/Modification of IDOT Foundation Piling Design and Construction Policy*, Report FHWA-ICT-09-0037 Illinois Department of Transportation, 58 pp., Illinois Center for Transportation, Rantoul, IL.
- Long, J.H., Hendrix, J., and Jaromin, D. (2009b). *Comparison of Five Different Methods for Determining Pile Bearing Capacities*, Report #0092-07-04 Wisconsin Department of Transportation, 166p., Wisconsin Highway Research Program, Madison, WI.
- MassDOT (2012). *Supplemental Specifications to the 1988 English Standard Specifications for Highways and Bridges and the 1995 Metric Standard Specifications for Highways and Bridges*, June 15, 2012, Massachusetts Department of Transportation, Boston, MA.
- Massachusetts Highways Department (2006). *Supplemental Specifications to the 1988 Standard Specifications for Highways and Bridges*, English units, Massachusetts Highway Department, Boston, MA.
- Massachusetts Highway Department (1995). *Standard Specifications for Highways and Bridges*, Metric Edition, Massachusetts Highway Department, Boston, MA.
- Massachusetts Highway Department (1988). *Standard Specifications for Highways and Bridges*, English Edition, Massachusetts Highway Department, Boston, MA
- Olsen, R.E., and Flaate, K.S. (1967). "Pile-Driving Formulas for Friction Piles in Sand", *ASCE Journal of Soil Mechanics and Foundations*, Volume 92, No. 6, pp. 279-297.
- Paikowsky, S.G. (2013). "Dynamic Load Testing of Drilled Deep Foundations", invited keynote paper, Swiss Geotechnic Annual Meeting, Freiburg, Switzerland, 2 May 2013, Vol.166, pp.1-52.
- Paikowsky, S.G. (2004). "Drop Weight Dynamic Testing of Drilled Deep Foundations", Invited Special Lecture, *Proceedings of the 7th International Conference on the Application of Stress Wave Theory to Piles*, Kuala Lumpur Malaysia, August 9-11, 2004, pp.13-84.
- Paikowsky, S.G. (1982). "Use of Dynamic Measurements to Predict Pile Capacity under Local Conditions", M.Sc. Thesis, Technion, Israel Institute of Technology, July, Haifa, Israel.

- Paikowsky, S.G. with contributions by Birgission G., McVay M., Nguyen T., Kuo C., Baecher G., Ayyub B., Stenerson K., O'Mally K., Chernauskas L., and O'Neill M. (2004). *NCHRP Report 507 Load and Resistance Factor Design (LRFD) for Deep Foundations*, National Cooperative Highway Research Program report for Project NCHRP 24-17, TRB, Washington, DC, 2004, [http://onlinepubs.trb.org/onlinepubs/nchrp/nchrp\\_rpt\\_507.pdf](http://onlinepubs.trb.org/onlinepubs/nchrp/nchrp_rpt_507.pdf)
- Paikowsky, S.G. and Chen, Y.L. (1998). "Field and Laboratory Study of the Physical Characteristics and Engineering Parameters of the Subsurface at the Newbury Bridge Site", Research Report submitted to the Massachusetts Highway Department, Geotechnical Section, Boston, Massachusetts.
- Paikowsky, S.G. and Hajduk, E.L. (1999). *Design and Construction of an Instrumented Test Pile Cluster*: Research Report submitted to the Massachusetts Highway Department, September, 1999. University of Massachusetts – Lowell, MA.
- Paikowsky, S.G. and Hajduk, E.L. (2000). *Theoretical Evaluation and Full Scale Field Testing Examination of Pile Capacity Gain with Time*: Research Report submitted to the Massachusetts Highway Department, December, University of Massachusetts – Lowell, MA.
- Paikowsky, S.G. and Hajduk, E.L. (2004). "Design and Construction of Three Instrumented Test Piles to Examine Time Dependent Pile Capacity Gain", *ASTM Geotechnical Testing Journal*, Vol. 27, No.6, pp. 515 – 531.
- Paikowsky, S.G., Honjo, Y., Faraji, S., Yoshida, I., and Ye, L. (2005). "Interim Progress Report Project NCHRP 12-66 AASHTO LRFD Specifications for Serviceability in the Design of Bridge Foundations", submitted to the National Cooperative Highway Research Program for Project NCHRP 12-66 AASHTO LRFD Specifications for Serviceability in the Design of Bridge Foundations, GTR, Inc., North Chelmsford, MA.
- Paikowsky, S.G., Lesny, K., Amatya, S., Kisse, A., Muganga, R. and Canniff, M. (2010). *NCHRP Report 651 LRFD Design and Construction of Shallow Foundations for Highway Bridge Structures*, National Cooperative Highway Research Program Report for Project NCHRP 24-31, TRB, Washington, DC, June 2010, [http://onlinepubs.trb.org/onlinepubs/nchrp/nchrp\\_rpt\\_651.pdf](http://onlinepubs.trb.org/onlinepubs/nchrp/nchrp_rpt_651.pdf)
- Paikowsky, S.G., Marchionda, C.M., O'Hearn, C.M., and Canniff, M.C. (2009). *Developing a Resistance Factor for Mn/DOT's Pile Driving Formula*, final research report submitted to Minnesota Department of Transportation in cooperation with Minnesota State University-Mankato, University of Massachusetts, Lowell, MA. <http://www.lrrb.org/pdf/200937.pdf>
- Paikowsky, S., Operstein, V., and Bachand, M. (1999). *Express Method of Pile Testing by Static Cyclic Loading*. Research Report submitted to the Massachusetts Highway Department, October, University of Massachusetts – Lowell, MA.
- Paikowsky, S.G., Regan, J.E., and McDonnell, J.J. (1994). *A Simplified Field Method for Capacity Evaluation of Driven Piles*, FHWA research report. No. RD - 94-042, 1994, 291pp (HNR publication), Federal Highway Administration, Washington, DC.

- Paikowsky, S.G., and Stenersen, K.L. (2000). "The Performance of the Dynamic Methods, their Controlling Parameters and Deep Foundation Specifications", Keynote lecture in the *Proceeding of the Sixth International Conference on the Application of Stress-Wave Theory to Piles*, Niyama S. and Beim J. ed., September 11- 13, São Paulo, Brazil, A.A. Balkema Publishers, The Netherlands, pp.281-304.
- Paikowsky, S., and Tolosko, T. (1999). *Extrapolation of Pile Capacity From Non-Failed Load Tests*, FHWA Report No. FHWA-RD-99-170, December, 1999, Federal Highway Administration, Washington, DC.  
<http://ntl.bts.gov/lib/16000/16000/16053/PB2000102368.pdf>
- PDI. (2010). *GRLWEAP Wave Equation Analysis of Pile Driving*, ver.2010-4, Pile Dynamics, Inc., Cleveland, OH.
- Rausche, F. (2000). Personal communication. February 2000.
- Rausche, F., Thendean, F., Abou-matar, H., Likins, G., and Goble, G. (1997). *Determination of Pile Driveability and Capacity from Penetration Tests. Vol. 1-3, Final Report*. FHWA-RD-96-179, FHWA.
- Rausche, F., Thendean, G., Abou-matar, H., Likins, G.E., and Goble, G.G. (1996). *Determination of Pile Driveability and Capacity from Penetration Tests*, Final Report, U.S. Department of Transportation, Federal Highway Administration, Washington, DC.
- Rowekamp, P. (2011). Email communication Monday, April 11, 2011 at 10:47AM to A. Budge and S. Paikowsky, from [paul.rowekamp@state.mn.us](mailto:paul.rowekamp@state.mn.us).
- Smith, E.A.L. (1960). Pile Driving Analysis by the Wave Equation, *ASCE J. Soil Mech. And Found. Div.*, 86(4): 35-61.
- Terzaghi, K. (1942). Discussion of the Progress Report of the Committee on the Bearing Value of Pile Foundations. *Proceedings, ASCE*. Vol. 68, pp. 311-323.

## **Appendix A**

### **Summary Tables**

**Table A-1 Mn/DOT - Details of Selected Representative Bridges**

Case No.	Bridge Name	MN Bridge Number	Bridge Type	Notation	# of Spans	Span Lengths (ft)	Total Length (ft)	Width (ft)	Construction Type	Year Built
<b>1</b>	York Ave over Promnade Trail	27B66	Continuous, single-span	SS-C	1	30	30	43	Concrete slab	2009
<b>2</b>	BNSF over TH12	27R14	Continuous, multi-span	MS-C	2	91,91	183	21	Steel plate girders	2009
<b>3</b>	TH121 over I494	27V63	Continuous, multi-span	MS-C	4	52,96,96,64	312	140	Steel plate girders	2009
<b>4</b>	NB 35W to NB TH121	27V65	Continuous, multi-span	MS-C	4	140,200,200,130	670	43	Precast segmental box	2007
<b>5</b>	Ramp 35W to TH 62	27V66	Continuous, multi-span	MS-C	3	150,200,150	509	34	Precast segmental box	2007
<b>6</b>	EB TH 62 over TH 121 & 35W	27V68	Continuous, multi-span	MS-C	4	195,210,220,240	865	27-111	Steel plate girders	2007
<b>7</b>	TH 121 to TH 62	27V69	Simple, multi-span	MS-S	2	65,80	145	43	Prestressed concrete beams	2007
<b>8</b>	Ramp From EB TH62 to NB 35W	27V71	Simple, single-span	SS-S	1	118	118	152-155	Prestressed concrete beams	2007
<b>9</b>	EB TH62 over TH121	27V72	Simple, single-span	SS-S	1	118	118	66-76	Prestressed concrete beams	2007
<b>10</b>	Ramp 35W to TH 62	27V73	Continuous, multi-span	MS-C	3	120,170,120	419	33	Precast segmental box	2007
<b>11</b>	TH 62 & 35W over CP RR	27V74	Simple, single-span	SS-S	1	58	58	285	Prestressed concrete beams	2007
<b>12</b>	Ramp over Nicollet Ave.	27V75	Continuous, multi-span	MS-C	6	130,200(x4),120	1089	43	Precast segmental box	2007
<b>13</b>	TH62 Over 35W & Nicollet Ave	27V76	Continuous, multi-span	MS-C	5	121,161,190,190,140	811	45	Precast segmental box	2007
<b>14</b>	TH 62 over Nicollet Ave.	27V78	Simple, single-span	SS-S	1	85	85	57-60	Prestressed concrete beams	2007
<b>15</b>	Ramp over 35W / TH 62	27V79	Continuous, multi-span	MS-C	7	114,180(x5),110	1159	45	Precast segmental box	2007
<b>16</b>	Ramp From SB TH35W to TH 62	27V80	Simple, single-span	SS-S	1	90	60	90	Prestressed concrete beams	2007
<b>17</b>	Diamond Lake Road over 35W	27V84	Continuous, multi-span	MS-C	2	103,103	208	75	Steel plate girders	2007
<b>18</b>	SB 35W over Nicollet Ave	27V85	Simple, single-span	SS-S	1	88	88	63	Prestressed concrete beams	2007
<b>19</b>	NB 35W over Nicollet Ave	27V86	Simple, single-span	SS-S	1	86	86	90-93	Prestressed concrete beams	2007
<b>20</b>	CSAH 14 over Prairie River	01531	Simple, multi-span	MS-S	3	57,57,57	173	50	Prestressed concrete beams	2009
<b>21</b>	Hanson Blvd. over TH10	02567	Continuous, multi-span	MS-C	2	94,94	189	165	Steel plate girders	2007
<b>22</b>	35W Under City Rd J	02571	Simple, multi-span	MS-S	2	156,156	315	138	Prestressed concrete beams	2006
<b>23</b>	35W under CSAH 23	02817	Simple, multi-span	MS-S	2	138,138	284	118	Prestressed concrete beams	2007
<b>24</b>	CSAH 12 over DM&E RR	07589	Simple, multi-span	MS-S	2	85,125	219	78-84	Prestressed concrete beams	2009
<b>25</b>	CSAH 11 over Cottonwood Riv.	08552	Simple, multi-span	MS-S	3	127,127,127	388	43	Prestressed concrete beams	2009
<b>26</b>	TH 95 over 35	13809	Simple, multi-span	MS-S	2	99.99	203	115	Prestressed concrete beams	2010
<b>27</b>	Ped. Bridge over Ski Trail	16523	Continuous, single-span	SS-C	1	99	99	12	Steel truss	2009
<b>28</b>	TWP Rd 99 over Root River	23579	Continuous, multi-span	MS-C	3	42,56,42	140	29	Concrete slab	2009
<b>29</b>	CSAH 19 over Shell Rock River	24545	Continuous, multi-span	MS-C	3	31,60,31	125	43	Concrete slab	2009
<b>30</b>	CSAH 6 over BNSF RR	27199	Simple, multi-span	MS-S	4	66,102,92,125	391	114	Prestressed concrete beams	2007
<b>31</b>	TH 12 over Unstable Soil	27296	Simple, multi-span	MS-S	17	111,112,112,115(x4), 109(x10)	1885	61	Prestressed concrete beams	2007



Case No.	Bridge Name	MN Bridge Number	Bridge Type	Notation	# of Spans	Span Lengths (ft)	Total Length (ft)	Width (ft)	Construction Type	Year Built
32	SB 35W over Minnehaha Creek	27405	Continuous, multi-span	MS-C	2	105,135	248	89	Steel plate girders	2007
33	CSAH 7 Between Lakes Ida & Little Sand	29528	Continuous, single-span	SS-C	1	49	49	37	Concrete slab	2007
34	CSAH 9 over Schoolcraft River	29529	Continuous, multi-span	MS-C	3	25,31,25	84	39	Concrete slab	2008
35	CSAH 6 over Stanchfield Creek	30515	Simple, single-span	SS-S	1	82	82	39	Prestressed concrete beams	2009
36	CSAH 20 over City Ditch #3	32564	Continuous, multi-span	SS-C	1	75	75	39	Concrete slab	2006
37	TH 107 over Snake River	33002	Simple, multi-span	MS-S	3	72,72,72	218	43	Prestressed concrete beams	2009
38	CSAH 1 over Two Rivers	35536	Continuous, multi-span	MS-C	3	42,54,42	141	39	Concrete slab	2008
39	CSAH 8 over Yellow Medicine River	42565	Continuous, multi-span	MS-C	3	30,38,30	101	39	Concrete slab	2009
40	TH 23 over Rum River	48030	Simple, multi-span	MS-S	3	53,53,53	161	70	Prestressed concrete beams	2009
41	Concord St. over Otter Tail Riv.	56540	Continuous, multi-span	MS-C	3	27,35,27	91	55	Concrete slab	2009
42	CSAH 9 over JD-7	65562	Continuous, multi-span	MS-C	3	28,34,28	93	43	Concrete slab	2009
43	TH 3 over UP RR	66002	Simple, multi-span	MS-S	2	147,147	303	51	Prestressed concrete beams	2008
44	TH 89 over Roseau River	68003	Simple, single-span	SS-S	1	77	77	43	Prestressed concrete beams	2009
45	CSAH 24 Over Roseau River	68540	Simple, multi-span	MS-S	3	75,75,75	226	43	Prestressed concrete beams	2009
46	TH 71 over Crow River	73045	Simple, single-span	SS-S	1	76	76	51	Prestressed concrete beams	2009
47	TH 14 under CSAH 12	81006	Simple, multi-span	MS-S	2	105,105	214	65	Prestressed concrete beams	2008
48	CSAH 27 over TH 14	81007	Simple, multi-span	MS-S	2	108,108	220	43	Prestressed concrete beams	2008
49	TH 14 under CSAH 5	81008	Simple, multi-span	MS-S	2	108,108	219	39	Prestressed concrete beams	2008
50	CSAH 3 over Le Sueur River	81530	Simple, multi-span	MS-S	3	47,47,47	142	43	Prestressed concrete beams	2009
51	TH 74 over Whitewater River	85024	Simple, multi-span	MS-S	2	84,84	169	43	Prestressed concrete beams	2006

### Table A-2 MN Bridge Construction Classification of Details

Bridge Type	Superstructure Type	
1	2	3
Multispan Simple Supported	Steel Girders	Multiple Beam/Girders
		Box Girders
	Concrete	Prestressed Girders
		CIP Box Girders
		Concrete Slab
Multispan Continuous	Steel Girders	Multiple Beam/Girders
		Box Girders
	Concrete	Prestressed Girders
		CIP Box Girders
		Concrete Slab
Single Span Simple 1.1.1.1.1.1	Steel Girders	Multiple Beam/Girders
		Box Girders
	Concrete	Prestressed Girders
		CIP Box Girders
		Concrete Slab

Bridge Type	Superstructure Type	
1	2	3
Integral Abutment Simple Span	Steel Girders	Multiple Beam/Girders
		Box Girders
	Concrete	Prestressed Girders
		CIP Box Girders
		Concrete Slab
Integral Abutment Multispan	Steel Girders	Multiple Beam/Girders
		Box Girders
	Concrete	Prestressed Girders
		CIP Box Girders
		Concrete Slab
Specify Others if Relevant to New Design		

Typical Mn/DOT construction practice:

1. Multi-span simple supported prestressed concrete girders bridge with a typical span of 100ft semi-stub abutment and column bent pier.
2. Single-span simple supported prestressed concrete girders bridge with a typical span of 100ft (up to 150ft) semi-stub abutment.
3. Multi-span continuous steel girders with a typical span of 120ft semi-stub abutment and column bent pier.
4. Multi-span integral abutment bridges steel girders with a typical span of 100ft and prestressed concrete girders with a typical span of 50ft, pile supported integral abutment and pile bent with encasement wall piers

Notes:

A. Abutment Type	
A1	Gravity
A2	U
A3	Cantilever
A4	Full Height
A5	Stub
A6	Semi Stub
A7	Counter Fort
A8	Pile Bent
A9	Reinforced Earth System
A10	Spill-through
A11	Pile Supported Integral
A12	Others, please specify

B. Bearing Type	
B1	Elastomeric Bearings
B2	Seismic Isolaters
B3	Rocker Bearings
B4	Roller Bearings
B8	Siding Plate Bearing
B6	Pot Bearing
B7	Spherical Bearing
B8	Lead Rubber
B9	Others, please specify

1 C. Bearing Function	
C1	Fixed Allows Rotation only
C2	Expansion Allows Rotation and Horizontal Translation
C3	Expansion allows Rotation and Vertical + Horizontal Translation

D. Pier Type	
D1	Hammerhead S/M
D2	Column Bent
D3	Pile Bent
D4	Solid Wall
D5	Integral Pier
D6	Others, please specify

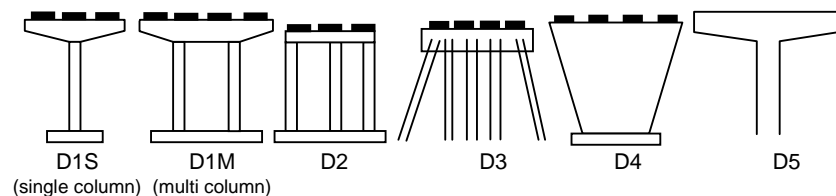


**Table A-3 Mn/DOT Foundation Details of Selected Representative Bridges**

Case No	Bridge Name	MN Bridge No.	General Soil Condition									Foundation Type		Foundation Size						
			Abutments				Piers					Abutments	Piers	Piers						
			Designation	Soil	Designation	Soil	1	2	3	4	5			1	2	3	4	5		
1	York Ave over Promenade Trail	27B66	North Abut	Silty Sand, Sandy Clay	South Abut	No Info.	-	-	-	-	-	CIPC Pipe	-	North 12" CIPC 5/16" Wall 16 piles (+6 wing wall) 30 ft long	South 12" CIPC 5/16" Wall 14 piles (+6 wing wall) 30 ft long	-	-	-	-	-
2	BNSF over TH 12	27R14	North Abut	Sandy Clay Loam	South Abut	Sandy Clay Loam	Sandy Clay Loam	-	-	-	-	CIPC Pipe	CIPC Pipe	North 16" CIPC 5/16" Wall 62 piles 60 ft long	South 16" CIPC 5/16" Wall 62 piles 60 ft long	16" CIPC 5/16" Wall 37 piles 60 ft long	-	-	-	-
3	NB 35W to NB TH 121	27V63	North Abut	Sand	South Abut	Sand	Sand	Loamy Sand, Sand	Sand	-	-	CIPC Pipe	CIPC Pipe	North 12" CIPC 1/4" Wall 164 piles 60 ft long	South 12" CIPC 1/4" Wall 148 piles 60 ft long	12" CIPC 5/16" Wall 96 piles 60 ft long	12" CIPC 5/16" Wall 48 piles 60 ft long	12" CIPC 5/16" Wall 96 piles 60 ft long	-	-
4	Ramp 35W to TH 62	27V65	North Abut	Loamy Fine Sand	South Abut	Loamy Sand, Sand	Fine Sand, Sand	Fine Sand	Loamy Sand, Sand	-	-	CIPC Pipe	CIPC Pipe	North 12" CIPC 1/4" Wall 24 piles 75 ft long	South 12" CIPC 1/4" Wall 148 piles 95 ft long	12" CIPC 5/16" Wall 36 piles 85 ft long	12" CIPC 5/16" Wall 36 piles 85 ft long	16" CIPC 5/16" Wall 36 piles 75 ft long	-	-
5	Ramp 35W to TH 62	27V66	North Abut	Sand	South Abut	Sand	Sand	Sand	-	-	-	CIPC Pipe	CIPC Pipe	North 16" CIPC 5/16" Wall 30 piles 70 ft long	South 16" CIPC 5/16" Wall 34 piles 80 ft long	16" CIPC 5/16" Wall 30 piles 80 ft long	16" CIPC 5/16" Wall 30 piles 70 ft long	-	-	-
6	EB TH 62 over TH 121 & 35W	27V68	West Abut	Fine & Coarse Sand	East Abut	Loamy Sand, Sandstone	Loamy Sand, Sand, Sandy Loam	Sand & Gravel, Sand, Sandstone	Sand, Sandstone, Sandy Loam	-	-	CIPC Pipe/H Piles	CIPC Pipe/H Piles	West 12" CIPC 1/4" Wall 45 piles 70 ft long	East HP 14x73 78 piles 70 ft long	12" CIPC 1/4" Wall 64 piles 60 ft long	HP 14x73 46 piles 80 ft long	HP 14x73 34 piles 80 ft long	-	-
7	TH 121 to TH 62	27V69	West Abut	Loose Sand	East Abut	Loose Sand, Clay	Peat, Sand	-	-	-	-	CIPC Pipe	CIPC Pipe	West 12" CIPC 1/4" Wall 12 piles (+5 wing wall) 70 ft long	East 12" CIPC 1/4" Wall 11 piles (+4 wing wall) 80 ft long	12" CIPC 1/4" Wall 18 piles 80 ft long	-	-	-	-
8	Ramp From EB TH 62 to NB 35W	27V71	West Abut	Loamy Sand, Fine Sand	East Abut	Fine Sand, Coarse Sand	-	-	-	-	-	H-Pile	-	West HP 12x53 63 piles 50 ft long	East HP 12x53 63 piles 50 ft long	-	-	-	-	-
9	EB TH 62 over TH121	27V72	West Abut	Loamy Sand, Fine Sand	East Abut	Fine Sand, Sand	-	-	-	-	-	H-Pile	-	West HP 12x53 34 piles 50 ft long	East HP 12x53 29 piles 50 ft long	-	-	-	-	-
10	Ramp 35W to TH 62	27V73	West Abut	Loose Sand	East Abut	Fine Sand, Gravel	Loose Sand	Fine Sand, Gravel	-	-	-	H-Pile	H-Pile	West HP 14x73 23 piles 55 ft long	East HP 14x73 33 piles 50 ft long	HP 14x73 20 piles 50 ft long	HP 14x73 20 piles 50 ft long	-	-	-

**Table A-3 Mn/DOT Foundation Details of Selected Representative Bridges (Cont. page 2/6)**

Case No	Bridge Name	MA Bridge No.	General Soil Condition									Foundation Type		Foundation Size						
			Abutments				Piers					Abutments	Piers	Piers						
			Designation	Soil	Designation	Soil	1	2	3	4	5/6			1	2	3	4	5/6		
11	TH 62 & 35W over CP RR	27V74	West Abut	Fine Sand, Sand	East Abut	Fine Sand, Sand & Gravel	-	-	-	-	-	CIPC Pipe	-	West 16" CIPC 5/16" Wall 151 piles 50 ft long	East 12" CIPC 5/16" Wall 150 piles 50 ft long	-	-	-	-	-
12	Ramp Over Nicollet Ave.	27V75	West Abut	Fine Sand, Org.	East Abut	Fine Sand, Org.	Fine Sand, Gravel	Fine Sand, Gravel	Fine Sand, Gravel	Fine Sand, Gravel	Fine Sand, Gravel	CIPC Pipe	CIPC Pipe	West 16" CIPC 5/16" Wall 56 piles 65 ft long	East 16" CIPC 5/16" Wall 42 piles 70 ft long	16" CIPC 5/16" Wall 36 piles 65 ft long	16" CIPC 5/16" Wall 40 piles 65 ft long	16" CIPC 5/16" Wall 45 piles 70 ft long	16" CIPC 5/16" Wall 40 piles 70 ft long	16" CIPC 5/16" Wall 40 piles 70 ft long
13	TH 62 over 35W & Nicollet Ave	27V76	West Abut	Fine Sand, Sand	East Abut	Fine Sand, Sand & Gravel	Loamy Fine Sand, Fine Sand	No Info.	Sand, Loamy Sand	Sand	-	CIPC Pipe	CIPC Pipe	West 16" CIPC 5/16" Wall 51 piles 70 ft long	East 16" CIPC 5/16" Wall 29 piles 85 ft long	16" CIPC 5/16" Wall 30 piles 65 ft long	16" CIPC 5/16" Wall 32 piles 80 ft long	16" CIPC 5/16" Wall 36 piles 70 ft long	16" CIPC 5/16" Wall 32 piles 70 ft long	-
14	TH 62 Over Nicollet Ave.	27V78	West Abut	Fine Sand, Gravel	East Abut	Fine Sand, Gravel	-	-	-	-	-	CIPC Pipe	-	West 16" CIPC 1/4" Wall 34 piles 60 ft long	East 16" CIPC 1/4" Wall 34 piles 60 ft long	-	-	-	-	-
15	Ramp over 35W / TH 62	27V79	East Abut	Loose Sand, Fine Sand, some Clay	West Abut	Fine Sand, Gravel	Loose Sand, Fine Sand	Loose Sand, Fine Sand	Loose Sand, Fine Sand	Loose Sand, Fine Sand, Gravel	Loose Sand, Fine Sand, Gravel	CIPC Pipe	CIPC Pipe	East 16" CIPC 5/16" Wall 24 piles 40 ft long	West 16" CIPC 5/16" Wall 43 piles 70 ft long	16" CIPC 5/16" Wall 36 piles 30 ft long	16" CIPC 5/16" Wall 36 piles 30 ft long	16" CIPC 5/16" Wall 45 piles 75 ft long	16" CIPC 5/16" Wall 38 piles 65 ft long	16" CIPC 5/16" Wall 36/36 piles 60/60 ft long
16	Ramp from SB 35W to TH 62	27V80	South Abut	Fine Sand, Plastic Loams	North Abut	Fine Sand, Loamy Fine Sand, Clay	-	-	-	-	-	H-Pile	-	South HP 12x53 23 piles (+4 wing wall) 75 ft long	North HP 12x53 22 piles (+4 wing wall) 75 ft long	-	-	-	-	-
17	Diamond Lake Road	27V84	West Abut	Loose Sand, Sand and Gravel, some Clay	East Abut	Loose Sand, Sand and Gravel, some Clay	Loose Sand, Sand and Gravel, some Clay	-	-	-	-	CIPC Pipe	CIPC Pipe	West 12" CIPC 1/4" Wall 64 piles 60 ft long	East 12" CIPC 1/4" Wall 44 piles 60 ft long	12" CIPC 1/4" Wall 36 piles 65 ft long	-	-	-	-
18	SB 35W over Nicollet Ave	27V85	West Abut	Fine Sand, Coarse Sand	East Abut	Loamy Very Fine Sand, Coarse Sand	-	-	-	-	-	CIPC Pipe	-	West 16" CIPC 5/16" Wall 37 piles 55 ft long	East 16" CIPC 5/16" Wall 36 piles 75 ft long	-	-	-	-	-
19	NB 35W over Nicollet Ave	27V86	West Abut	Sand, Loamy Sand	East Abut	No Info.	-	-	-	-	-	CIPC Pipe	-	West 16" CIPC 5/16" Wall 44 piles 65 ft long	East 16" CIPC 5/16" Wall 44 piles 65 ft long	-	-	-	-	-

**Table A-3 Mn/DOT Foundation Details of Selected Representative Bridges (Cont. page 3/6)**

Case No	Bridge Name	MA Bridge No.	General Soil Condition									Foundation Type		Foundation Size							
			Abutments				Piers					Abutments	Piers	Piers							
			Designation	Soil	Designation	Soil	1	2	3	4	5/6			1	2	3	4	5/6			
20	CSAH 14 over Prairie River	01531	North Abut	Sand, Silty Sand	South Abut	Sand	No. Info	No. Info	-	-	-	CIPC Pipe	CIPC Pipe	North 16" CIPC 5/16" Wall 7 piles 85 ft long	South 16" CIPC 5/16" Wall 7 piles 85 ft long	16" CIPC 5/16" Wall 9 piles 100 ft long	16" CIPC 5/16" Wall 9 piles 100 ft long	-	-	-	
21	Hanson Blvd over TH 10	02567	South Abut	Loamy Sand, Silty Clay Loam	North Abut	Sand, Silty Clay Loam	Sandy Loam, Silty Loam	-	-	-	-	CIPC Pipe	CIPC Pipe	South 12" CIPC 5/16" Wall 128 piles 40 & 80 ft long	North 12" CIPC 5/16" Wall 128 piles 50 ft long	12" CIPC 5/16" Wall 90 piles 70 ft long	-	-	-		
22	35W under City Rd J	02571	West Abut	Loamy Sand, Clay, Sand	East Abut	Sand, Sandy Clay Loam	North Sand, Silt Loam	South Sand, Silt Loam	-	-	-	CIPC Pipe	CIPC Pipe	West 12" CIPC 5/16" Wall 103 piles 40 ft long	East 12" CIPC 5/16" Wall 102 piles 70 ft long	North 12" CIPC 5/16" Wall 53 piles 40 ft long	South 12" CIPC 5/16" Wall 51 piles 40 ft long	-	-	-	
23	35W under CSAH 23	02817	South Abut	Sandy Clay, Sand	North Abut	Sand, Loamy Sand	Sandy Clay Loam, Sand	-	-	-	-	CIPC Pipe	CIPC Pipe	South 12" CIPC 1/4" Wall 55 piles 55 ft long	North 12" CIPC 1/4" Wall 55 piles 55 ft long	12" CIPC 1/4" Wall 43 piles 50 ft long	-	-	-		
24	CSAH 12 over DM&E RR	07589	South Abut	Clayey Sand, Sandy Lean Clay	North Abut	Sandy Lean Clay, Clayey Sand	Sandy Lean Clay, Clayey Sand	-	-	-	-	CIPC Pipe	CIPC Pipe	South 12" CIPC 5/16" Wall 76 piles 106 ft long	North 12" CIPC 5/16" Wall 91 piles 117 ft long	12" CIPC 5/16" Wall 51 piles 85 ft long	-	-	-		
25	CSAH 11 over Cottonwood River	08552	South Abut	Sand, Fat Clay	North Abut	Sand, Fat Clay, Shale	No Info.	No Info.	-	-	-	H-pile	H-Pile	South HP 12x53 17 piles 70 ft long	North HP 12x53 17 piles 70 ft long	HP 12x53 24 piles 40 ft long	HP 12x53 24 piles 40 ft long	-	-	-	
26	TH 95 over 35	13809	West Abut	Sand, Silt Loam	East Abut	Fine Sand, Silt Loam	Fine Sand, Clay	-	-	-	-	CIPC Pipe	Spread Footing	West 12" CIPC 1/4" Wall 56 piles (+4 wing wall) 45 ft long	East 12" CIPC 1/4" Wall 56 piles (+4 wing wall) 50 ft long	Spread Footing	-	-	-	-	
27	Ped Bridge over Ski Trail	16523	South Abut	Silty Sand, Lean Clay	North Abut	Silty Sand, Silty Clay	-	-	-	-	-	H-pile	-	South HP 10x42 4 piles 70 ft long	North HP 10x42 4 piles 70 ft long	-	-	-	-	-	
28	TWP Rd 99 over Root River	23579	West Abut	Gravel w/ Clay, Shale	East Abut	Gravel w/ Sand, Shale	No Info.	No Info.	-	-	-	H-pile	H-Pile	West HP 10x57 4 piles 50 ft long	East HP 10x57 4 piles 65 ft long	HP 10x57 6 piles 55 ft long	HP 10x57 6 piles 60 ft long	-	-	-	
29	CSAH 19 over Shell Rock River	24545	West Abut	Sand, Sandy Lean Clay	East Abut	Sand, Sandy Lean Clay	No Info.	No Info.	-	-	-	CIPC Pipe	CIPC Pipe	West 12" CIPC 5/16" Wall 5 piles 110 ft long	East 12" CIPC 5/16" Wall 5 piles 110 ft long	16" CIPC 5/16" Wall 9 piles 120 ft long	16" CIPC 5/16" Wall 9 piles 120 ft long	-	-	-	

**Table A-3 Mn/DOT Foundation Details of Selected Representative Bridges (Cont. page 4/6)**

Case No	Bridge Name	MN Bridge No.	General Soil Condition									Foundation Type		Foundation Size						
			Abutments				Piers					Abutments	Piers	Abutments		Piers				
			Designation	Soil	Designation	Soil	1	2	3	4	5					1	2	3	4	5
30	CSAH 6 over BNSF RR	27199	West Abut	Sandy Clay, Plastic Sandy Loam	East Abut	No Info.	No Info.	Silty Clay,	Plastic Sandy Loam, Loamy Sand	-	-	CIPC Pipe	CIPC Pipe	West 12" CIPC 5/16" Wall 32 piles 70 ft long	East 12" CIPC 5/16" Wall 33 piles 70 ft long	12" CIPC 5/16" Wall 40 piles 60 ft long	12" CIPC 5/16" Wall 44 piles 60 ft long	12" CIPC 5/16" Wall 50 piles 60 ft long	-	-
31	TH 12 over Unstable Soil	27296	West Abut	Plastic Sandy Loam, Loamy Sand	East Abut	Plastic Sandy Loam, Sandy Clay	Piers 1-5, 7-16 No Info.	Pier 6 Clay, Peat, Sandy Loam				CIPC Pipe	CIPC Pipe	West 12" CIPC 5/16" Wall 15 piles 80 ft long	East 12" CIPC 5/16" Wall 13 piles 80 ft long	Piers 1-7 16" CIPC 5/16" Wall 13 piles 85 ft long	Piers 8-10 16" CIPC 5/16" Wall 12 piles 85 ft long	Piers 11-16 16" CIPC 5/16" Wall 11 piles 85 ft long	-	-
32	SB 35W over Minnehaha Creek	27405	South Abut	Sand, Loam	North Abut	Sand, Sandy Loam	No Info.	-	-	-	-	CIPC Pipe	Drilled Shaft	South 16" CIPC 5/16" Wall 52 piles 55 ft long	North 16" CIPC 5/16" Wall 49 piles 55 ft long	Drilled Shaft	-	-	-	-
33	CSAH 7 between Lakes Ida & Little Sand	29528	South Abut	Poorly Graded Sand	North Abut	Poorly Graded Sand	-	-	-	-	-	CIPC Pipe	-	South 12" CIPC 5/16" Wall 8 piles 90 ft long	North 12" CIPC 5/16" Wall 8 piles 90 ft long	-	-	-	-	-
34	CSAH 9 over Schoolcraft River	29529	West Abut	Sand, Hemic Peat	East Abut	Sand, Hemic Peat, Sandy Silt	No Info.	No Info.	-	-	-	CIPC Pipe	CIPC Pipe	West 12" CIPC 1/4" Wall 4 piles 85 ft long	East 12" CIPC 1/4" Wall 4 piles 85 ft long	12" CIPC 1/4" Wall 6 piles 75 ft long	12" CIPC 1/4" Wall 6 piles 75 ft long	-	-	-
35	CSAH 6 over Stanchfield Creek	30515	West Abut	Sandy Lean Clay, Silty Sand, Sandstone	East Abut	Clayey Sand, Sandy Lean Clay, Sandstone	-	-	-	-	-	CIPC Pipe	-	West 12" CIPC 1/4" Wall 6 piles 90 ft long	East 12" CIPC 1/4" Wall 6 piles 90 ft long	-	-	-	-	-
36	CSAH 20 over City Ditch #3	32564	West Abut	Lean Clay, Sandy Lean Clay	East Abut	Lean Clay	-	-	-	-	-	CIPC Pipe	-	West 12" CIPC 1/4" Wall 5 piles 70 ft long	East 12" CIPC 1/4" Wall 5 piles 70 ft long	-	-	-	-	-
37	TH 107 over Snake River	33002	South Abut	Loamy Fine Sand, Sandy Loam	North Abut	Loamy Fine Sand	No Info.	Slightly Plastic Sandy Loam	-	-	-	H-pile	CIPC Pipe	South HP 10x42 7 piles 50 ft long	North HP 10x42 7 piles 50 ft long	16" CIPC 5/16" Wall 8 piles 45 ft long	16" CIPC 5/16" Wall 8 piles 45 ft long	-	-	-
38	CSAH 1 over Two Rivers	35536	South Abut	Lean Clay, Silty Sand	North Abut	Sandy Lean Clay, Fat Clay	Lean Clay, Silty Sand	Sandy Lean Clay, Fat Clay	-	-	-	H-pile	H-pile	South HP 10x42 5 piles 42 ft long	North HP 10x42 5 piles 42 ft long	HP 12x53 7 piles 42 ft long	HP 12x53 7 piles 42 ft long	-	-	-



Table A-3 Mn/DOT Foundation Details of Selected Representative Bridges (Cont. page 5/6)

Case No	Bridge Name	MN Bridge No.	General Soil Condition								Foundation Type		Foundation Size							
			Abutments				Piers				Abutments	Piers	Abutments		Piers					
			Designation	Soil	Designation	Soil	1	2	3	4					5	1	2	3	4	5
39	CSAH 8 over Yellow Medicine River	42565	South Abut	Silty Sand, Fat Clay	North Abut	Sandy Lean Clay, Silty Sand	No info.	No info.	-	-	-	CIPC Pipe	CIPC Pipe	South 12" CIPC 1/4" Wall 5 piles 60 ft long	North 12" CIPC 1/4" Wall 5 piles 60 ft long	12" CIPC 1/4" Wall 5 piles 60 ft long	12" CIPC 1/4" Wall 5 piles 60 ft long	-	-	-
40	TH 23 over Rum River	48030	West Abut	Loamy Sand, Fine Sand	East Abut	Loamy Sand, Loamy Fine Sand	No info.	No info.	-	-	-	CIPC Pipe	CIPC Pipe	West 12" CIPC 1/4" Wall 10 piles 40 ft long	East 12" CIPC 1/4" Wall 10 piles 40 ft long	16" CIPC 5/16" Wall 14 piles 45 ft long	16" CIPC 5/16" Wall 14 piles 45 ft long	-	-	-
41	Concord St over Otter Tail River	56540	South Abut	Poorly Graded Sand, Sandy Lean Clay	North Abut	Poorly Graded Sand, Silty Sand	No info.	No info.	-	-	-	CIPC Pipe	CIPC Pipe	South 12" CIPC 1/4" Wall 6 piles 65 ft long	North 12" CIPC 1/4" Wall 6 piles 65 ft long	16" CIPC 5/16" Wall 7 piles 75 ft long	16" CIPC 5/16" Wall 7 piles 75 ft long	-	-	-
42	CSAH 9 over JD-7	65562	South Abut	No info.	North Abut	No info.	Sandy Lean Clay	Sandy Lean Clay	-	-	-	H-Pile	H-Pile	South HP 10x57 4 piles 45 ft long	North HP 10x57 4 piles 45 ft long	HP 10x57 6 piles 50 ft long	HP 10x57 6 piles 50 ft long	-	-	-
43	TH 3 over UP RR	66002	East Abut	Sandy Clay Till, St. Peter	West Abut	Sand & Gravel, St. Peter	Sandy Clay Till, St. Peter	-	-	-	-	H-Pile	H-Pile	East HP 14x73 26 piles 45 ft long	West HP 14x73 26 piles 65 ft long	HP 14x73 16 piles 45 ft long	-	-	-	-
44	TH 89 over Roseau River	68003	North Abut	Plastic Sandy Loam, Fine Sand	South Abut	Loamy Sand, Loamy Fine Sand	-	-	-	-	-	CIPC Pipe	-	North 12" CIPC 5/16" Wall 5 piles 30 ft long	South 12" CIPC 5/16" Wall 5 piles 35 ft long	-	-	-	-	-
45	CSAH 24 Over Roseau River	68540	North Abut	No info.	South Abut	Clay, Sand	No info.	No info.	-	-	-	H-Pile	H-Pile	North HP 10x42 7 piles 80 ft long	South HP 10x42 7 piles 80 ft long	HP 10x57 9 piles 95 ft long	5 HP 10x57 9 piles 95 ft long	-	-	-
46	TH 71 over Crow River	73045	South Abut	Sandy Loam	North Abut	Sandy Loam, Loam	-	-	-	-	-	CIPC Pipe	-	South 12" CIPC 3/8" Wall 7 piles 75 ft long	North 12" CIPC 3/8" Wall 7 piles 100 ft long	-	-	-	-	-
47	TH 14 under CSAH 12	81006	West Abut	Sandy Clay	East Abut	Loam	Loam	-	-	-	-	CIPC Pipe	CIPC Pipe	West 12" CIPC 1/4" Wall 28 piles 80 ft long	East 12" CIPC 1/4" Wall 28 piles 80 ft long	12" CIPC 1/4" Wall 27 piles 70 ft long	-	-	-	-
48	CSAH 27 over TH 14	81007	South Abut	Clay, Sandy Loam	North Abut	Loam, Silty Loam, Clayey Loam	Clay, Loam, Silty Loam	-	-	-	-	CIPC Pipe	CIPC Pipe	South 12" CIPC 1/4" Wall 18 piles 110 ft long	North 12" CIPC 1/4" Wall 18 piles 80 ft long	12" CIPC 1/4" Wall 20 piles 90 ft long	-	-	-	-

**Table A-3 Mn/DOT Foundation Details of Selected Representative Bridges (Cont. page 6/6)**

Case No	Bridge Name	MN Bridge No.	General Soil Condition									Foundation Type		Foundation Size							
			Abutments				Piers					Abutments	Piers	Abutments		Piers					
			Designation	Soil	Designation	Soil	1	2	3	4	5					1	2	3	4	5	
49	TH 14 under CSAH 15	81008	South Abut	Clayey Loam, Loamy Sand	North Abut	Clayey Loam, Loamy Sand, Loam	Clayey Loam, Loamy Sand	-	-	-	-	CIPC Pipe	CIPC Pipe	South 12" CIPC 1/4" Wall 22 piles 75 ft long	North 12" CIPC 1/4" Wall 22 piles 75 ft long	12" CIPC 1/4" Wall 18 piles 60 ft long	-	-	-	-	
50	CSAH 3 over Le Sueur River	81530	South Abut	Sandy Lean Clay	North Abut	Sandy Lean Clay	No info.	No info.	-	-	-	CIPC Pipe	CIPC Pipe	South 12" CIPC 1/4" Wall 6 piles 90 ft long	North 12" CIPC 1/4" Wall 6 piles 90 ft long	12" CIPC 1/4" Wall 5 piles 100 ft long	12" CIPC 1/4" Wall 5 piles 100 ft long	-	-	-	
51	TH 74 over Whitewater River	85024	West Abut	Sand and Gravel, Coarse Sand and Gravel	East Abut	Sand and Gravel, Coarse Sand and Gravel	Sand and Gravel, Coarse Sand and Gravel	-	-	-	-	H-Pile	H-Pile	West HP 10x42 10 piles 40 ft long	East HP 10x42 10 piles 40 ft long	* * * HP 12x53 9 piles 50 ft long	-	-	-	-	



**Table A-4 Mn/DOT Pile, Soil, and Hammer Details of Selected Representative Bridges**

Case No.	Bridge	Pile Type	Wall Thickness (in)	Length (ft)	Side	Tip	Hammer type	Rated Energy (lbs-ft)	Weight of Ram (lbs)	Final Stroke (ft)	Final Energy (lbs-ft)	CAPWAP (kips)	Energy Approach (kips)	WSDOT (kips)	MnDOT Equation (kips)	New MnDOT Equation (35) (kips)	New MnDOT Equation (30) (kips)
1	27B66	CIP 12.75"	5/16	50	L	SCL	DELMAG D19-32	42440	4000	7.5	30000	-	-	386	492	411	352
2	27B66	CIP 12.75"	5/16	50	-	-	DELMAG D19-32	42440	4000	9.0	36000	-	-	452	565	401	344
3	27R14	CIP 16"	5/16	78.7	-	-	APE D30-42	91088	6615	9.1	60197	324	932	595	559	462	396
4	27R14	CIP 16"	5/16	60.2	SC	LFS	APE D30-42	91088	6615	10.4	68796	497	942	896	1141	609	522
5	27V63	CIP 12.75"	1/4	73.2	S	S	DELMAG D19-32	42440	4000	7.2	28680	307	640	423	521	471	404
6	27V63	CIP 12.75"	1/4	74.2	S	S	DELMAG D19-32	42440	4000	8.1	32360	275	642	462	550	456	391
7	27V63	CIP 12.75"	5/16	78.8	S	S	DELMAG D25-32	66340	5513	8.3	45703	188	468	532	632	464	398
8	27V63	CIP 12.75"	5/16	75.9	S	S	DELMAG D25-32	66340	5513	9.1	50113	289	483	466	435	371	318
9	27V63	CIP 12.75"	5/16	90.5	S	S	APE D19-42	42820	4190	8.1	33939	322	566	442	500	418	358
10	27V63	CIP 12.75"	5/16	90.8	S	S	APE D19-42	42820	4190	7.8	32850	333	559	469	564	458	393
11	27V63	CIP 12.75"	1/4	73.3	S	L	APE D19-42	42820	4190	7.4	30922	209	337	302	257	313	268
12	27V65	CIP 16"	5/16	110	LS, S	LS	APE D30-42	91088	6615	10.3	68135	504	887	1073	1435	736	631
13	27V65	CIP 16"	5/16	100	S, S&G, FS	LS	DELMAG D36-32	90560	7930	8.3	65581	404	624	609	494	433	371
14	27V65	CIP 16"	5/16	100	plFSL, FS	plSL	DELMAG D36-32	90560	7930	8.3	65978	476	564	613	497	433	371
15	27V65	CIP 16"	5/16	100	S, L	S	APE D30-42	91088	6615	9.4	62446	486	645	726	766	544	466
16	27V66	CIP 16"	5/16	118	LS, CL	SL	APE D30-42	91088	6615	8.9	58675	313	234	703	775	560	480
17	27V66	CIP 16"	5/16	100	LS, CL	CL	APE D30-42	91088	6615	9.9	65621	434	844	825	995	588	504
18	27V66	CIP 16"	5/16	124.5	LS, SL	SL	DELMAG D36-31	90560	7930	9.9	78111	566	707	780	686	466	399
19	27V66	CIP 16"	5/16	124.5	LS, SL	LS	DELMAG D36-32	90560	7930	8.1	64233	454	677	654	588	475	407
20	27V66	CIP 16"	5/16	83	LS, SL	LS	APE D30-42	91088	6615	9.9	65158	451	951	886	1127	636	545
21	27V66	CIP 16"	5/16	130	LS, S	S	APE D30-42	91088	6615	9.5	62843	468	736	818	947	609	522
22	27V66	CIP 16"	5/16	136	LS, S	S	APE D30-42	91088	6615	10.4	68598	326	393	506	317	345	296
23	27V68	CIP 12"	1/4	98	CL, LS, S	CL	APE D25-32	57880	5513	7.3	40245	340	495	488	600	452	388
24	27V68	CIP 12"	1/4	60	LS, SL, ORG	LS	DELMAG D19-32	42440	4190	7.6	31844	301	511	411	552	412	353
25	27V69	CIP 12"	1/4	109	PT, S, CL	CL	APE D19-42	42820	4190	7.7	32431	343	501	492	628	487	417
26	27V69	CIP 12"	1/4	101	PT, S, CL	CL	APE D19-42	42820	4190	7.8	32682	420	498	496	647	487	417
27	27V69	CIP 12"	1/4	105	LS, CL, S	S	APE D19-42	42820	4190	8.2	34190	355	421	415	464	389	334
28	27V69	CIP 12"	1/4	104.5	LS, CL, S	LS	APE D19-42	42820	4190	8.6	35992	317	452	437	485	389	334
29	27V74	CIP 16"	5/16	60	FS, S&G	S&G	DELMAG D25-32	66340	5513	11.0	60643	617	1208	920	1327	606	519
30	27V74	CIP 16"	5/16	60	FS, S&G	S&G	DELMAG D25-32	66340	5513	10.2	56177	510	853	803	1127	570	489
31	27V74	CIP 16"	5/16	63	FS, S&G	LS	DELMAG D25-32	66340	5513	8.5	46695	438	919	767	1040	656	562
32	27V74	CIP 16"	5/16	63	CrS, FS	SL	DELMAG D25-32	66340	5513	9.1	50334	470	1007	719	934	570	489
33	27V74	CIP 16"	5/16	65	CrS, FS	SL	DELMAG D30-32	75440	6600	8.8	58014	376	568	573	598	421	361
34	27V74	CIP 16"	5/16	61	LS, SL, CL	CL	DELMAG D30-32	75440	6600	9.5	62436	376	618	580	572	396	339
35	27V74	CIP 16"	5/16	60	LFS, S&FG	plFSL	DELMAG D25-32	66340	5513	10.3	56839	479	999	712	908	500	428

**Table A-4 Mn/DOT Pile, Soil, and Hammer Details of Selected Representative Bridges (Cont. page 2/4)**

Case No.	Bridge	Pile Type	Wall Thickness	Length (ft)	Side	Tip	Hammer type	Rated Energy	Weight of Ram	Stroke (ft)	Final Energy	CAPWAP (kips)	Energy Approach	WSDOT (kips)	MnDOT Equation	New MnDOT Equation (35)	New MnDOT Equation (30)
36	27V74	CIP 16"	5/16	60	LFS, S&FG	plFSL	DELMAG D25-32	66340	5513	11.7	64723	520	1114	982	1416	606	519
37	27V74	CIP 16"	5/16	62	LFS, S&FG	plFSL	DELMAG D30-32	75440	6600	12.3	81180	624	1499	1334	1939	700	600
38	27V74	CIP 16"	5/16	62	FS, S&G	CL	DELMAG D30-32	75440	6600	12.2	80652	508	1369	1014	1288	535	459
39	27V74	CIP 16"	5/16	70	FS, S&G	CL	DELMAG D30-32	75440	6600	10.5	69036	646	944	1048	1558	646	554
40	27V74	CIP 16"	5/16	71	FS, S&G	SiCL	DELMAG D30-32	75440	6600	11.3	74448	612	1168	1064	1535	608	521
41	27V74	CIP 16"	5/16	68.3	FS, S&G	SiCL	DELMAG D30-32	75440	6600	11.0	72732	601	1221	1195	1817	700	600
42	27V75	CIP 16"	1/4	85	FS	S&G	APE D30-42	91088	6615	10.0	66150	505	546	757	833	535	459
43	27V75	CIP 16"	1/4	85	FS	spl SL	APE D30-42	91088	6615	9.7	63901	496	588	714	765	522	448
44	27V75	CIP 16"	5/16	75	S, LS	LS	APE D30-42	91088	6615	8.5	56426	476	500	563	542	467	400
45	27V75	CIP 16"	5/16	75	S, LS	LS	APE D30-42	91088	6615	9.7	64099	476	672	778	924	568	486
46	27V75	CIP 16"	5/16	90	S, LS, SL	LS	APE D30-42	91088	6615	9.1	59998	542	639	754	883	588	504
47	27V75	CIP 16"	5/16	90	S, LS, SL	LS	APE D30-42	91088	6615	9.1	60064	527	624	729	826	568	486
48	27V76	CIP 16"	1/4	101	S, FS	plSL	APE D30-42	91088	6615	10.0	66216	482	710	832	1004	588	504
49	27V76	CIP 16"	5/16	90	S&G, FS, S	S&G	APE D30-42	91088	6615	9.4	61983	551	678	779	912	588	504
50	27V76	CIP 16"	5/16	90	S&G, FS, S	S&G	APE D30-42	91088	6615	9.3	61652	529	652	748	848	568	486
51	27V76	CIP 16"	5/16	92.5	S, L	Sandstone	APE D30-42	91088	6615	7.6	50274	538	813	763	998	710	608
52	27V78	CIP 16"	1/4	70	S&G, LVFS, S	pl L&S	DELMAG D25-32	66340	5513	10.1	55902	397	737	741	1031	529	453
53	27V78	CIP 16"	1/4	70	S&G, LVFS, S	pl L&S	DELMAG D25-32	66340	5513	9.3	51326	521	678	652	876	507	434
54	27V79	CIP 16"	5/16	90	S, LS, FLS	FLS	APE D30-42	91088	6615	9.5	62710	497	740	737	809	550	471
55	27V79	CIP 16"	5/16	90	S, LS, FLS	FLS	APE D30-42	91088	6615	8.9	59138	430	858	695	763	550	471
56	27V79	CIP 16"	5/16	95	S, FS	CL	DELMAG D36-32	90560	7930	8.7	69070	551	875	1048	1339	708	607
57	27V79	CIP 16"	5/16	91	S, FS	CL	DELMAG D36-32	90560	7930	8.6	68357	534	804	830	920	566	485
58	27V79	CIP 16"	5/16	92	S, FS, SL	S	DELMAG D30-32	75440	6600	8.6	57024	478	797	838	1083	626	536
59	27V79	CIP 16"	5/16	92	S, FS, SL	SL	DELMAG D30-32	75440	6600	7.4	48576	441	834	842	1117	738	632
60	27V79	CIP 16"	5/16	71	S, S&G, plSL	S	DELMAG D36-32	90560	7930	8.3	65819	482	929	858	1065	608	521
61	27V84	CIP 12"	1/4	70	S, CL	SL	DELMAG D19-42	43240	4190	7.9	33101	325	407	349	371	340	291
62	27V84	CIP 12"	1/4	70	-	-	APE D19-42	42820	4190	8.3	34777	337	458	411	492	379	325
63	27V84	CIP 12"	1/4	70	-	-	APE D19-42	42820	4190	8.4	35196	332	486	517	731	471	404
64	27V84	CIP 12.75"	1/4	71	S, CrS	VFS	DELMAG D19-42	43240	4190	7.5	31425	356	531	416	551	427	366
65	27V85	CIP 16"	1/4	70	FS, S&G, S	plSL	DELMAG D25-32	66340	5513	8.1	44490	360	680	580	726	520	446
66	27V85	CIP 16"	1/4	89	LVFS, CrS	S	DELMAG D25-32	66340	5513	8.3	45537	327	666	680	875	596	511
67	27V85	CIP 16"	1/4	90	LVFS, CrS	S	DELMAG D25-32	66340	5513	8.3	45537	411	673	647	810	567	486
68	27V86	CIP 16"	1/4	75	FS, S	spl SL	DELMAG D25-32	66340	5513	8.4	46530	416	691	610	756	523	448
69	27V86	CIP 16"	1/4	75	LS, S, S&G, C	LS	DELMAG D25-32	66340	5513	8.5	46805	368	841	691	922	589	505
70	27V86	CIP 16"	1/4	75	LS, S, S&G, C	LS	DELMAG D25-32	66340	5513	9.2	50554	458	912	831	1138	656	562

**Table A-4 Mn/DOT Pile, Soil, and Hammer Details of Selected Representative Bridges (Cont. page 3/4)**

Case No.	Bridge	Pile Type	Wall Thickness	Length (ft)	Side	Tip	Hammer type	Rated Energy	Weight of Ram	Stroke (ft)	Final Energy	CAPWAP (kips)	Energy Approach	WSDOT (kips)	MnDOT Equation	New MnDOT Equation (35)	New MnDOT Equation (30)
71	27V86	CIP 16"	1/4	80	-	-	DELMAG D25-32	66340	5513	10.4	57170	458	937	868	1152	606	519
72	27V86	CIP 16"	1/4	80	-	-	DELMAG D25-32	66340	5513	8.0	43994	393	690	723	975	656	562
73	27V86	CIP 16"	1/4	80	-	-	DELMAG D25-32	66340	5513	7.8	42726	397	666	660	882	617	529
74	1531	CIP 16"	1/4	50.4	S	SiL	DELMAG D19-42	43240	4000	8.5	34000	-	-	426	581	404	346
75	1531	CIP 16"	1/4	110.4	-	-	DELMAG D19-42	43240	4000	9.6	38200	-	-	580	696	489	419
76	1531	CIP 16"	1/4	95.4	S, SiL, SiC	SiL	DELMAG D19-42	43240	4000	9.6	38200	-	-	558	696	471	403
77	2567	CIP 12.75"	1/4	62.0	S, SL	SL	DELMAG D19-32	42440	4000	6.0	24000	249	327	291	343	387	332
78	2567	CIP 12.75"	1/4	105	S, SL, SiCL	SiL	DELMAG D19-32	42440	4000	5.9	23600	193	319	253	231	342	293
79	2567	CIP 12.75"	1/4	104	S, SL, SiCL	SiL	DELMAG D19-32	42440	4000	6.5	26000	222	429	362	422	445	381
80	2571	CIP 12.75"	1/4	52.9	S, LS, SiL	SiC	DELMAG D25-32	66340	5513	8.8	48514	451	319	612	869	503	431
81	2571	CIP 12.75"	1/4	60	S, SCL, Si	S	DELMAG D25-32	66340	5513	9.0	49617	462	648	722	1108	581	498
82	2817	CIP 12"	1/4	65	S, SCL, CL	S	APE D25-32	57880	5513	7.9	43608	431	623	576	764	493	422
83	2817	CIP 12"	1/4	65	S, SCL, LS	S	APE D25-32	57880	5513	7.7	42230	527	567	593	820	524	449
84	7589	CIP 12"	5/16	110	SC, SLC	SC	APE D25-32	57880	5513	8.3	45758	276	402	425	374	346	297
85	7589	CIP 12"	5/16	110	SC, SLC	SC	APE D25-32	57880	5513	11.0	60643	465	758	736	868	452	388
86	7589	CIP 12"	5/16	120	SC, SLC	SC	APE D25-32	57880	5513	10.0	55130	334	655	572	555	387	331
87	13809	CIP 12.75"	1/4	62	FS, pISL, S	FS	APE D19-42	42820	4190	7.9	33143	451	671	503	703	487	417
88	13809	CIP 12.75"	1/4	62	FS, pISL, S	FS	APE D19-42	42820	4190	7.8	32473	253	702	423	541	418	358
89	24545	CIP 16"	1/4	100.0	-	-	DELMAG D19-42	43240	4000	10.3	41320	-	-	679	862	530	454
90	24545	CIP 12.75"	1/4	110.0	SiL, S, SLC	S	DELMAG D19-42	43240	4000	8.2	32920	-	-	500	616	489	419
91	27199	CIP 12"	1/4	85.4	pISL, SCL	SCL	DELMAG D19-42	43240	4000	9.1	36360	478	568	676	991	599	513
92	27199	CIP 12"	1/4	60.4	pISL, SCL	SCL	DELMAG D19-42	43240	4000	6.3	25240	254	600	415	679	530	454
93	27296	CIP 12"	1/4	90.4	pISL, SCL	LS	APE D19-42	42820	4190	8.2	34232	398	-	563	753	527	452
94	27296	CIP 16"	1/4	102.4	PT, C, spl SL	CL	DELMAG D30-32	75440	6600	9.7	63888	510	880	1006	1485	670	574
95	27296	CIP 16"	1/4	103	-	-	DELMAG D30-32	75440	6600	11.1	73392	687	-	1079	1588	626	536
96	27296	CIP 16"	1/4	101.9	SCL, LS, pISL	pISL	DELMAG D30-32	75440	6600	8.4	55374	458	-	669	839	514	441
97	27405	CIP 16"	1/4	69.5	S, SL	SL	DELMAG D30-32	75440	6600	8.1	53658	432	758	699	942	555	475
98	27405	CIP 16"	1/4	70	S, SL	S	DELMAG D30-32	75440	6600	8.1	53658	438	-	699	941	555	475
99	29528	CIP 12.75"	1/4	98.3	ORG, S, S&G	S&G	DELMAG D19-32	42440	4190	5.5	23045	-	-	323	385	447	384
100	29529	CIP 12"	1/4	95.3	S, PT	S	MKT DE-40	32000	4000	8.0	32000	-	-	503	689	435	373
101	29529	CIP 16"	1/4	80.2	S, PT	S	MKT DE-40	32000	4000	8.0	32000	-	-	512	678	443	380
102	30515	CIP 12.75"	1/4	100	SLC, Si, SiL	Sandstone	DELMAG D19-42	43240	4000	8.7	34800	-	-	687	807	637	546
103	32564	CIP 12.75"	1/4	80	SLC, LC	SLC	DELMAG D19-32	42440	4000	6.8	27200	-	-	300	326	352	302
104	32564	CIP 16"	1/4	75.7	-	-	DELMAG D19-32	42440	4000	7.7	30600	-	-	437	527	456	391
105	33002	CIP 16"	5/16	50	LFS, spl SL	spl SL	DELMAG D19-42	43240	4000	9.5	38000	-	-	529	686	449	385

**Table A-4 Mn/DOT Pile, Soil, and Hammer Details of Selected Representative Bridges (Cont. page 4/4)**

Case No.	Bridge	Pile Type	Wall Thickness	Length (ft)	Side	Tip	Hammer type	Rated Energy	Weight of Ram	Stroke (ft)	Final Energy	CAPWAP (kips)	Energy Approach	WSDOT (kips)	MnDOT Equation	New MnDOT Equation (35)	New MnDOT Equation (30)
106	33002	CIP 16"	5/16	50.1	LFS, spl SL	spl SL	DELMAG D19-42	43240	4000	9.00	36000	-	-	469	580	420	360
107	42565	CIP 12"	1/4	50	SLC, S	SiL	MVE M-19	49380	4015	8.62	34597	-	-	545	893	542	465
108	48030	CIP 16"	5/16	50	-	-	DELMAG D19-42	43240	4000	9.00	36000	-	-	452	538	405	347
109	48030	CIP 16"	5/16	50	-	-	DELMAG D19-42	43240	4000	9.50	38000	-	-	499	616	424	363
110	48030	CIP 12"	1/4	50	LS, S, LFS	LFS	DELMAG D19-42	43240	4000	8.50	34000	-	-	413	484	391	335
111	56540	CIP 12.75"	1/4	80	SLC, SiL, LC	SiL	ICE I-30V2	90824	6615	9.90	65489	-	-	591	573	421	361
112	56540	CIP 16"	1/4	99	SLC, SiL, LC	SiL	ICE I-30V2	90824	6615	10.20	67473	-	-	772	884	534	458
113	68003	CIP 12"	5/16	45	spl SL, C	LS	MKT DE-42/35	42000	4200	9.50	39900	-	-	613	867	488	418
114	68003	CIP 12"	5/16	45	LS, LFS, plSL	LS	MKT DE-42/35	42000	4200	9.50	39900	-	-	620	880	494	423
115	73045	CIP 12"	3/8	86	SL, C	SL	DELMAG 30-02	66200	6600	8.00	52800	-	-	594	652	448	384
116	73045	CIP 12"	3/8	100	SL, L, SiCL	SL	DELMAG 30-02	66200	6600	8.20	54120	-	-	696	838	513	440
117	81006	CIP 12.75"	1/4	128	SCL, plSL	-	DELMAG D25-32	66340	5513	8.32	45868	-	-	557	597	484	415
118	81006	CIP 12.75"	1/4	128	SCL, plSL	-	DELMAG D25-32	66340	5513	8.27	45610	-	-	553	594	484	415
119	81007	CIP 12.75"	1/4	120	CL, SL, L	SL, L	DELMAG D25-32	66340	5513	9.40	51822	557	-	852	1099	656	562
120	81007	CIP 12.75"	1/4	110	CL, SL, L	L, SiL	DELMAG D25-32	66340	5513	7.44	41014	-	-	493	546	480	411
121	81008	CIP 12.75"	1/4	88.8	CL, SL, L	LS	DELMAG D25-32	66340	5513	7.23	39859	-	-	605	825	606	519
122	81008	CIP 12.75"	1/4	59.8	CL, SL, LS	LS, SL	DELMAG D25-32	66340	5513	7.60	41899	336	-	689	1028	656	562
123	81010	CIP 12.75"	1/4	99.5	CL, SL, L	SL, L	DELMAG D25-32	66340	5513	9.70	53476	554	603	964	1291	719	616
124	81011	CIP 12.75"	1/4	120	CL, L, SL	S, LS	DELMAG D25-32	66340	5513	9.40	51822	555	627	651	735	502	430
125	81530	CIP 20"	3/8	115	S, SLC, SiL	SLC	DELMAG D25-32	66340	5513	7.92	43663	-	-	663	703	606	519
126	81530	CIP 12"	1/4	100	S, SLC, SiL	SLC	DELMAG D19-42	66340	5513	7.92	43663	-	-	541	741	494	424

S = Sand

SC = Sandy Clay

LFS = Loamy Fine Sand

L = Loam

plSL = Plastic Sandy Loam

SCL = Sandy Clay Loam

ORG = Organics

C = Clay

LS = Loamy Sand

plFSL = Plastic Fine Sandy Loams

FS = Fine Sand

S&G = Sand and Gravel

CL = Clayey Loam

PT = Peat

CrS = Coarse Sand

SiCL = Silty Clay Loam

pl L&S = plastic Loam and Sand

VFS = Very Fine Sand

SiL = Silty Loam

SCL = Sandy Clay Loam

SLC = Sandy Lean Clay

S&FG = Sand and Fine Gravel

spl SL = Slightly Plastic Sandy Loam

LVFS = Loamy Very Fine Sand

SiC = Silty Clay

SiCL = Silty Clay Loam

Si = Silt

LC = Lean Clay

## **Appendix B**

### **Hammer Specifications**

# APE Model D19-42 Single Acting Diesel Impact Hammer

*D19-42 driving H-beam.*



## MODEL D19-42 (1.9 metric ton ram)

### SPECIFICATIONS

Stroke at maximum rated energy	135 in (343 cm)
Maximum rated energy (Setting 4)	47,335 ft-lbs (64,177 Nm)
Setting 3	37,868 ft-lbs (51,341 Nm)
Setting 2	31,715 ft-lbs (42,999 Nm)
Minimum rated energy (Setting 1)	22,721 ft-lbs (2,567 Nm)
<i>(Variable throttle allows for lower minimum energy and infinite fuel settings.)</i>	
Maximum obtainable stroke	150 in (381 cm)
Maximum obtainable energy	52,362 ft-lbs (70,992 Nm)
Speed (blows per minute)	34-52

### WEIGHTS

Ram	4,189 lbs (798 kg)
Anvil	749 lbs (340 kg)
Anvil cross sectional area	124.42 sq in (316.02 sq-cm)
Hammer weight (includes trip device)	8,400 lbs (3,810 kg)
Typical operating (weight with DB26 and H-beam insert)	11,052 lbs (5,013 kg)

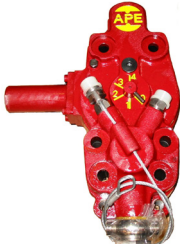
### CAPACITIES

Fuel tank (runs on diesel or bio-diesel)	8.3 gal (31.41 liters)
Oil tank	2.3 gal (8.7 liters)

### CONSUMPTION

Diesel or Bio-diesel fuel	1.3 gal/hr (6.6 liters/hr)
Lubrication	.13 gal/hr (.49 liters/hr)
Grease	8 to 10 pumps every 45 minutes of operation time.

*Optional Variable Throttle.*



### STRIKER PLATE FOR DB 26

Weight	628 lbs (284 kg)
Diameter	22.5 in (57.15 cm)
Area	471 sq-in (696 sq-cm)
Thickness	6 inches (15.24 cm)

### STRIKER PLATE FOR DB 20

Weight	440 lbs (199 kg)
Diameter	17 3/4 in (45.08 cm)
Area	247 sq-in (628 sq-cm)
Thickness	6 inches (15.24 cm)

### CUSHION MATERIAL

Type	Monocast MC 904
Diameter-DB26	22.5 in (57.15 cm)
Diameter-DB20	17.3/4 in (45.08 cm)
Thickness	2 inches (5.08 cm)
Elastic-modulus	285 ksi (1,965 mpa)
Coeff. of restitution	.8

*Drive Base Assembly.*



### DRIVE CAP

DB 26:	1,076 lbs (488 kg)
DB 20:	750 lbs (340 kg)

### INSERT WEIGHT

H-Beam insert for 12" (305 mm) and 14" (355 mm):	948 lbs (430 kg)
Large pipe insert for sizes 12" to 24" diameter:	1,830 lbs (830 kg)

### MINIMUM BOX LEAD SIZE/OPERATING LENGTH

Minimum box leader size	8 in x 21 in (3.14 cm x 53.34 cm)
Operating length w/ base and insert	348 in (884 cm)



Corporate Offices  
7032 South 196th  
Kent, Washington 98032 USA  
(800) 248-8498 & (253) 872-0141  
(253) 872-8710 Fax

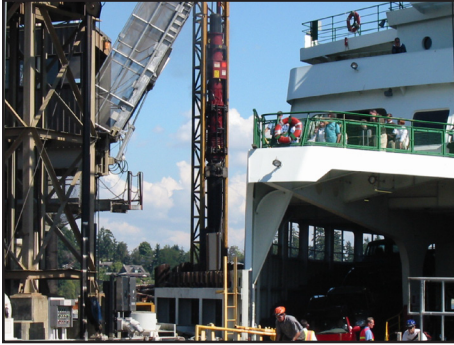
Visit our WEB site:  
[www.apevibro.com](http://www.apevibro.com)  
e-mail: [ape@apevibro.com](mailto:ape@apevibro.com)

*Note: All specifications are subject to change without notice 03-10-10*



# APE Model D30-42 Single Acting Diesel Impact Hammer

D30-42 Finishing Dolphin Piles.



## MODEL D30-42 (3.0 metric ton ram)

### SPECIFICATIONS

Stroke at maximum rated energy	135 in (343 cm)
Maximum rated energy (Setting 4)	74,750 ft-lbs (101,346 Nm)
Setting 3	67,274 ft-lbs (91,210 Nm)
Setting 2	55,315 ft-lbs (72,284 Nm)
Minimum rated energy (Setting 1)	37,824 ft-lbs (51,282 Nm)
<i>(Variable throttle allows for lower minimum energy and infinite fuel settings.)</i>	
Maximum obtainable stroke	157 in (381 cm)
Maximum obtainable energy	86,546 ft-lbs (117,339 Nm)
Speed (blows per minute)	34-53

### WEIGHTS

Ram	6,615 lbs (3,000 kg)
Anvil	1,358 lbs (616 kg)
Anvil cross sectional area	214.49 sq in (544.8 sq-cm)
Hammer weight (includes trip device)	13,571 lbs (6,154 kg)
Typical operating (weight with DB26 and H-beam insert)	16,223 lbs (7,357 kg)

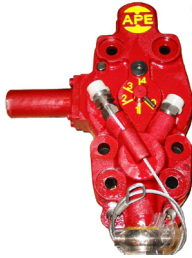
### CAPACITIES

Fuel tank (runs on diesel or bio-diesel)	17.4 gal (65 liters)
Oil tank	5 gal (19 liters)

### CONSUMPTION

Diesel or Bio-diesel fuel	2.6 gal/hr (9.84 liters/hr)
Lubrication	.26 gal/hr (1 liters/hr)
Grease	8 to 10 pumps every 45 minutes of operation time.

Optional Variable Throttle Control.



### STRIKER PLATE FOR DB 26

Weight	628 lbs (284 kg)
Diameter	22.5 in (57.15 cm)
Area	471 sq-in (696 sq-cm)
Thickness	6 inches (15.24 cm)

### CUSHION MATERIAL

Type/Qty	Micarta/2 ea
Diameter-DB26	22.5 in (57.15 cm)
Thickness	1 in (25.4 mm)
Type/Qty	Aluminum/3 ea
Thickness	1/2 in (12.7 mm)
Diameter	25 in (57.15 cm)
Total Combined Thickness	3.5 inches (8.89 cm)
Area	471 sq-in (696 sq-cm)
Elastic-modulus	285 ksi (1,965 mpa)
Coeff. of restitution	.8

Drive Base Assembly.



### DRIVE CAP

DB 26:	1,076 lbs (488 kg)
--------	--------------------

### INSERT WEIGHT

H-Beam insert for 12" (305 mm) and 14" (355 mm):	948 lbs (430 kg)
Large pipe insert for sizes 12" to 24" diameter:	1,830 lbs (830 kg)

### MINIMUM BOX LEAD SIZE/OPERATING LENGTH

Minimum box leader size	8 in x 26 in (3.14 cm x 66 cm)
Operating length as described above	354 in (9 m)



Corporate Offices  
7032 South 196th  
Kent, Washington 98032 USA  
(800) 248-8498 & (253) 872-0141  
(253) 872-8710 Fax

Visit our WEB site:  
[www.apevibro.com](http://www.apevibro.com)  
e-mail: [ape@apevibro.com](mailto:ape@apevibro.com)

Note: All specifications are subject to change without notice 03-10-10

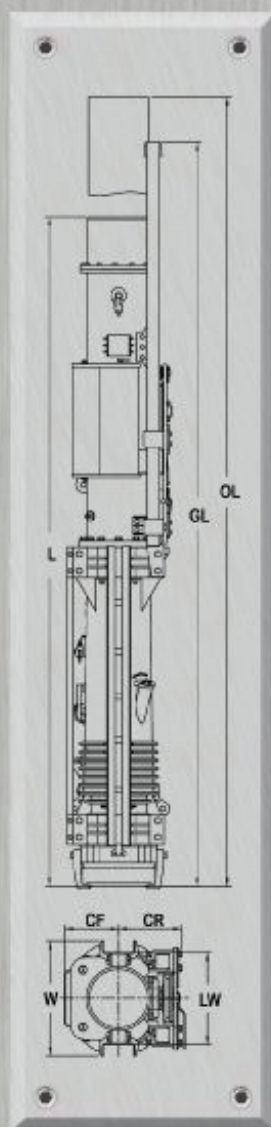


International Construction Equipment  
301 Warehouse Drive  
Matthews, NC 28104  
Phone: 704 821-8200  
Email [info@iceusa.com](mailto:info@iceusa.com)

## ICE® MODEL I-30<sup>V2</sup> SINGLE-ACTING DIESEL PILE HAMMER

Simple, reliable design  
Automatic lubrication  
Optional variable fuel control  
Optional hydraulic trip

Equipped with ICE® Box leads guides  
Uses standard ICE® drive caps  
Swinging, fixed and sliding leads available  
Spotters available for precise pile positioning



### Working Specifications

Ram weight	6,615 lbs	3000 kg
Rated energy (fuel setting 4)	76,070 ft-lbs	103 135 Nm
Stroke at rated energy (fuel setting 4)	11.50 feet	3505 mm
Energy at fuel setting 3	69,435 ft-lbs	94 145 Nm
Energy at fuel setting 2	62,925 ft-lbs	85 315 Nm
Energy at fuel setting 1	56,415 ft-lbs	76 490 Nm
Energy at maximum stroke	83,370 ft-lbs	113 030 Nm
Geometric maximum stroke	12.60 feet	3840 mm
Blows per minute	35-52	

### Weights

Bare hammer with trip	13,440 lbs	6095 kg
Hammer with box lead guides	14,750 lbs	6690 kg
Drive cap base	DCB-1HD	
Drive cap base weight	1,245 lbs	565 kg
Striker plate	460 lbs	209 kg
Cushion material	110 lbs	25 kg
Pile insert	DCH-1	
Pile insert weight	780 lbs	345 kg
Operating weight with drive cap above	17,345 lbs	7834 kg

### Capacities

Fuel tank	16.8 gal	63.5 l
Lube oil tank	4.6 gal	17.5 l

### Dimensions

Hammer length (L)	16.9 ft	5160 mm
Length with trip guides (GL)	20.8 ft	6325 mm
Length at max stroke (OL)	24.4 ft	7445 mm
Overall width (W)	32.3 in	820 mm
Standard leads width (LW)	26 in	660 mm
Overall depth (CR + CF)	34.0 in	863 mm
Centerline to rear (CR)	18.8 in	477 mm
Centerline to front (CF)	15.2 in	386 mm

III-1-30 Sept-2010

**INTERNATIONAL CONSTRUCTION EQUIPMENT, INC.**

Corporate offices: 301 Warehouse Drive, Matthews, NC USA  
Phones: 888 ICEUSA1, 704 821-8200

[info@iceusa.com](mailto:info@iceusa.com)  
[www.iceusa.com](http://www.iceusa.com)



# ICE® MODEL I-30<sup>v2</sup>

## SINGLE-ACTING DIESEL PILE HAMMER

### BEARING CHART



888-ICE-USA1  
sales@iceusa.com  
www.iceusa.com

Blows per Minute	Ram Stroke (feet)	Hammer Energy (ft-lbs)	Pile Set (Blows per inch)																			
			2	3	4	5	6	7	8	9	10	11	12	13	14	15	16	17	18	19	20	
33	13.22	87,471	287	332	365	390	410	427	442	456	468	478	488	497	505	513	520	527	534	540	545	
34	12.46	82,401	277	321	352	377	397	413	428	441	452	463	472	481	489	497	504	510	516	522	528	
35	11.76	77,760	267	310	341	365	384	400	414	427	438	448	457	466	474	481	488	494	500	506	511	
36	11.11	73,500	259	300	330	353	372	388	401	414	424	434	443	451	459	466	473	479	485	491	496	
37	10.52	69,581	250	291	320	342	360	376	389	401	412	421	430	438	445	452	459	465	471	476	481	
38	9.97	65,967	242	282	310	332	350	365	378	389	399	409	417	425	432	439	445	451	457	462	467	
39	9.47	62,627	235	273	301	322	339	354	367	378	388	397	405	413	420	427	433	438	444	449	454	
40	9.00	59,535	228	265	292	313	330	344	356	367	377	386	394	401	408	415	421	426	431	437	441	
41	8.57	56,666	221	258	284	304	320	334	346	357	367	375	383	390	397	403	409	415	420	425	429	
42	8.16	54,000	215	250	276	295	312	325	337	347	357	365	373	380	386	392	398	404	409	413	418	
43	7.79	51,518	208	243	268	287	303	316	328	338	347	355	363	370	376	382	388	393	398	403	407	
44	7.44	49,202	203	237	261	280	295	308	319	329	338	346	354	360	367	372	378	383	388	392	397	
45	7.11	47,040	197	230	254	272	287	300	311	321	330	337	345	351	357	363	368	373	378	382	387	
46	6.81	45,017	192	224	247	265	280	293	303	313	321	329	336	342	348	354	359	364	369	373	377	
47	6.52	43,122	186	218	241	259	273	285	296	305	313	321	328	334	340	345	350	355	360	364	368	
48	6.25	41,344	181	213	235	252	266	278	289	298	306	313	320	326	332	337	342	347	351	355	359	
49	6.00	39,673	177	207	229	246	260	272	282	291	299	306	312	318	324	329	334	339	343	347	351	
50	5.76	38,102	172	202	224	240	254	265	275	284	292	299	305	311	317	322	326	331	335	339	343	
51	5.54	36,623	168	197	218	234	248	259	269	277	285	292	298	304	309	314	319	323	328	332	335	
52	5.33	35,228	164	193	213	229	242	253	263	271	278	285	291	297	302	307	312	316	320	324	328	
53	5.13	33,911	160	188	208	224	237	247	257	265	272	279	285	291	296	301	305	309	313	317	321	

Constant improvement and engineering progress make it necessary that ICE®, Inc. reserve the right to make specification changes without notice. Please consult ICE® for the latest available information.

This chart is based on the FHWA-modified version of the Gates Formula for pile bearing and is provided as a convenience only for those applications where this formula is specified. ICE® has no preference for this particular formula over any other.

$$R_u = \frac{1}{2} [1.75 \sqrt{E} \log(10 N) - 100]$$

Where:

$R_u$  = Pile bearing (tons)

$E$  = rated hammer energy in ft-lbs, or (ram weight × stroke) if lower fuel setting

$N$  = Blow Count per 1 in

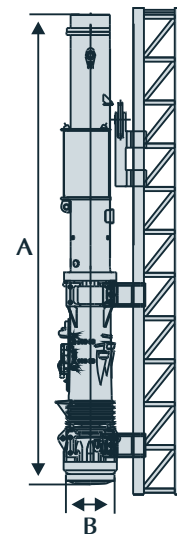
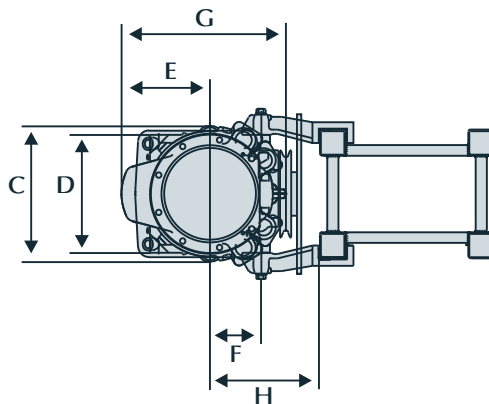
CAUTION: Driving at ten blows per inch is considered practical refusal. Driving in excess of ten blows per inch for more than six inches of driving or driving in excess of 20 blows per inch at all is considered improper use and will void the hammer warranty.

© INTERNATIONAL CONSTRUCTION EQUIPMENT, INC. ALL RIGHTS RESERVED.

"Due to improvements to ICE manufactured products and the EPA mandated Tier III emission regulations, unit specifications are subject to change without notice. Please contact ICE engineering department to confirm possible changes."

Technical data		D25-32	D30-32	D36-32	D46-32
Impact weight (piston)	lbs	5510	6610	7940	10140
Energy per blow, max.	ft-lbs	66380	75970	90720	122435
Energy per blow, min.	ft-lbs	29500	35400	41300	52370
Number of blows	min <sup>-1</sup>	35-52	36-52	36-53	35-53
Suitable for driving piles (depending on soil and pile)	lbs	3530-16535	4410-19840	5510-26455	6610-35270
<b>Consumption</b>					
Diesel oil	gal/h	1,65	2,2	2,53	3,52
Lubricant	gal/h	0,13	0,22	0,33	0,33
<b>Tank capacity</b>					
Diesel oil tank	gal	17,7	17,7	23,5	23,5
Lube tank	gal	5	5	4,5	4,5
Max. rope diameter for deflector sheave of tripping device	in	0,87	0,87	1,5	1,5
<b>Weight</b>					
Tripping device	lbs	410	410	992	992
Diesel pile hammer	lbs	12500	13600	18060	20485
Max. inclined pile driving without / with extension		1:5 / 1:1	1:5 / 1:1	1:5 / 1:1	1:5 / 1:1

Dimensions					
A	Length of Diesel pile hammer without extension	in	216,5	216,5	215,4
B	Outer diameter of impact block	in	22	22	26
C	Width of Diesel pile hammer	in	26,4	26,4	31,4
D	Width for connection of guide jaws	in	21,3	21,3	25,2
E	Center of hammer to pump guard	in	16	16	17,5
F	Center of hammer to center of threads for guide jaw bolts	in	9,3	9,3	10,8
G	Depth of Diesel pile hammer	in	30,7	30,7	37,4
H	Standard distance from center of Diesel pile hammer up to the face of lead	in	17,1	17,1	19,7



## **Appendix C**

**Load Testing Report – TP1 in Victoria, MN, July 2012**

**Minnowa Construction, Inc.**

# Static and Dynamic Load Test Results – SLT Pile

State Project 1002-89 – Bridge 10003  
Trunk Highway 5 over Trail  
Victoria, Minnesota

*Prepared for*

**Minnowa Construction, Inc.**

## **Professional Certification:**

I hereby certify that this plan, specification, or report was prepared by me or under my direct supervision and that I am a duly Licensed Professional Engineer under the laws of the State of Minnesota.



Corwin R. Reese, P.E.  
Project Engineer  
License Number: 49192  
July 25, 2012



Project BL-12-00434

Braun Intertec Corporation

July 25, 2012

Project BL-12-00434

Mr. Brian Connell  
Minnowa Construction, Inc.  
850 Wickett Drive NW  
Harmony, MN 55939

Re: Dynamic and Static Load Test Results – TH 5 Static Load Test Pile  
State Project 1002-89 – Bridge 10003  
Trunk Highway 5 over Trail  
Victoria, Minnesota

Dear Mr. Connell:

We have completed the high-strain dynamic pile tests, static load test and evaluations for the static load test (SLT) pile as part of the Bridge 10003 piling installation for State Project 1002-89 in Victoria, Minnesota. The purpose of this report is to summarize the high-strain dynamic pile test results, the Case method results using the PDILOT computer program, the wave matching results and the static load test results.

## Project Information

This portion of the project consists of performing dynamic and static load testing of a 12-inch, outer-diameter, closed-end pipe pile. According to Section SB-10.4.4 of the project special provisions, the plan tip elevation of the SLT pile is the same as for the production piling. According to Plan Sheet 4 of 53, the production piling length is 65 feet and the factored design load is 99.2 tons (198.4 kips) per pile. Based on a  $\phi_{dyn}$  of 0.80 for performing a static load test on-site, the required nominal resistance is 124.0 tons (248.0 kips) per pile. The SLT pile is included in the abutment as structural support after the load test.

## Geotechnical Information

Boring T05, performed in-between the east and west abutments, has a surface elevation of about 958 feet. The ground-surface elevation near the SLT pile is about 958. The boring generally encountered clay loam to elevation 953, underlain with plastic sandy loam and loamy sand to elevation 860. The relative density of this material is generally medium dense with a dense layer between approximate elevations 913 and 900. Underlying the loamy sand, the boring encountered medium dense to very dense sand and coarse sand and gravel to its termination elevation of about 838.

## Dynamic Load Test Results

### Pile Driving Hammer

Minnowa Construction, Inc. (Minnowa) installed the SLT pile and four reaction piles using a Delmag model D19-42 open-ended diesel hammer. The manufacturer's literature indicates this model of hammer has a nominal ram weight of 4,015 pounds and a maximum rated energy of 43,225 foot-pounds. The hammer has a variable fuel injection system and Minnowa operated the hammer on fuel setting 4 of 4.

## Pile

The SLT pile and four reaction piles were 12-inch, outer-diameter, closed-end pipe pile with a wall thickness of 1/4 inch. Minnowa drove the piles with a 3/4-inch thick flat steel plate welded to the toe and spliced sections of piling together using traditional welding methods. According to the mill stamp on the piles, they meet the requirements of ASTM A252 Grade 3 steel, which requires a minimum yield stress of at least 45 kips per square inch (ksi).

## High-Strain Dynamic Pile Testing

We performed dynamic testing using a model PAX Pile Driving Analyzer (PDA) manufactured by Pile Dynamics, Inc. (PDI). The PDA processes analog signals obtained from strain transducers and accelerometers attached to the pile. The purpose of high-strain dynamic pile testing is to measure the pile-driving stresses, hammer energy transfer, and to aid in evaluating the pile's load-carrying capacity and pile integrity. We used the PDIPlot computer program to summarize the results of the PDA test and are attaching them for your review and records.

The PDIPlot shows results in graphical and columnar form and includes: blow number, pile depth, penetration resistance as blows per foot (bpf), maximum force, maximum transferred energy, maximum and average compression stress at the pile top, compression stress near the pile toe, hammer stroke, the energy transfer ratio based on measured stroke, and predicted nominal pile capacity by the Case method. Table 1 summarizes the results of the high-strain dynamic pile testing for the SLT pile and reaction piles (RP) 1 through 4.

**Table 1: High-Strain Dynamic Test Results Summary**

Pile	Drive Type	Analyzed Depth (feet)	Approximate Pile Toe Elevation (feet)	Penetration Resistance (BPF)	Hammer Stroke (feet)	Maximum Case Method Capacity (kips)
RP-1	Initial Drive (6-15-12)	62	896	30	8	258
	3-Day Redrive (6-18-12)	62	896	120 (equivalent)	8 1/2	344
RP-2	Initial Drive (6-15-12)	62 1/4	895 3/4	23	7 1/2	184
	3-Day Redrive (6-18-12)	62 1/2	895 1/2	69 (equivalent)	9	437
RP-3	Initial Drive (6-15-12)	62	896	40	8	323
	3-Day Redrive (6-18-12)	62 1/4	895 3/4	120 (equivalent)	9 1/4	477
RP-4	Initial Drive (6-15-12)	62	896	30	7 3/4	276
	3-Day Redrive (6-18-12)	62 1/4	895 3/4	60 (equivalent)	9	418
SLT	Initial Drive (6-15-12)	62 1/4	895 3/4	30	7 3/4	286
	3-Day Redrive (6-18-12)	62 1/2	895 1/2	80 (equivalent)	9 1/2	483
	1-Day After SLT (6-26-12)	62 1/2	895 1/2	240 (equivalent)	8	446

With the exception of the redrive test performed on June 26, 2012, we performed the tests on piles not filled with concrete. Since the installation of vibrating wire strain gauges in the SLT pile required placing concrete in the pile, we performed the redrive test on June 26, 2012 on a partially-concrete-filled pile. Due to site and time constraints, Minnowa did not fill the upper 3 feet of the pile section. We observed pile-top buckling during this 10-blow redrive.

### Wave Matching

To estimate the soil resistance parameters, we performed wave-matching evaluations of the dynamic data collected in the field with the PDA using the Case Pile Wave Analysis Program (CAPWAP). CAPWAP uses an iterative process to compare the computed force and velocity to the measured pile data, while modifying the soil resistance parameters until obtaining a reasonable best fit of the soil model for the particular pile tested. The wave-matching evaluations also provide an estimated nominal pile resistance, referred to by the program as the CAPWAP capacity, at the time of testing and differentiate the estimated end bearing and skin friction components of the total pile capacity.

We performed wave-matching evaluations on selected hammer blows near the end-of-initial drive and beginning of each redrive for the SLT pile and each reaction pile. Table 2 summarizes the results of our wave-matching evaluations, which we are also attaching for your review and records.

**Table 2: Wave Matching Results Summary**

Test Pile	Drive Type	Analyzed Depth (feet)	Estimated Skin Friction (kips)	Estimated End Bearing (kips)	Estimated Total Capacity (kips)
RP-1	Initial Drive (6-15-12)	62	225	42	267
	3-Day Redrive (6-18-12)	62	274	51	325
RP-2	Initial Drive (6-15-12)	62 1/4	142	37	179
	3-Day Redrive (6-18-12)	62 1/2	390	22	412
RP-3	Initial Drive (6-15-12)	62	260	73	333
	3-Day Redrive (6-18-12)	62 1/4	392	91	483
RP-4	Initial Drive (6-15-12)	62	223	50	273
	3-Day Redrive (6-18-12)	62 1/4	325	107	432
SLT	Initial Drive (6-15-12)	62 1/4	254	21	275
	3-Day Redrive (6-18-12)	62 1/2	378	109	487
	1-Day After SLT (6-26-12)	62 1/2	189	249	438

Please refer to the 'Discussion' portion of this report for additional comments on the results of the dynamic redrive we performed on June 26, 2012.

## **Static Load Test Results**

### **Procedure and Equipment**

We performed a static load test on the SLT pile in general accordance with ASTM D1143-07 on June 25, 2012. Based on the results of the dynamic redrive testing, we anticipated a failure load of around 225-250 tons (450-500 kips). Therefore, we loaded the SLT pile in increments of 12.5 tons (25 kips) with 10-minute hold times at each loading increment.

We used a calibrated pressure gauge, hydraulic jack and load cell with working ranges in excess of 500 tons (1000 kips). We are attaching the calibration records for the pressure gauge, hydraulic jack and load cell for your review and records.

On June 18, 2012, we placed four vibrating wire 'sister-bar' strain gauges in the SLT pile. We placed a pair of gauges approximately 6 inches from the bottom of the pile, one gauge approximately 10 feet from the bottom and one gauge approximately 20 feet from the bottom. The Minnesota Department of Transportation (MnDOT) supplied the gauges that we placed 10 and 20 feet from the bottom. We attached the pair of gauges placed near the bottom to opposite sides of a metal ring and we attached the single gauges placed around 10 and 20 feet from the bottom to centralizers. We connected the four vibrating wire strain gauges to a four-channel data logger and connected the logger to an on-site computer. Therefore, we were able to observe the strain-gauge readings in "real-time". We set the data logger to record a reading every 10 seconds. We are attaching the calibration records for the vibrating wire strain gauges and the four-channel data logger for your review and records.

Minnowa placed concrete in the pile on June 19, 2012. Minnowa directed the concrete slowly down the side of the pile to limit the disturbance to the vibrating wire strain gauges.

We placed three linear variable differential transformers (LVDT's) on the steel plate placed between the SLT pile-top and the hydraulic jack. We attached the LVDT's to digital readout boxes and manually recorded the LVDT readings prior to and after each loading increment. We are attaching the calibration records for the LVDT's for your review and records.

### **Load Test Results**

At the 125-ton (250-kip) load increment, we observed an average pile-top movement of approximately 1/4-inch and micro-strain gauges placed 20 feet from the bottom, 10 feet from the bottom and the average of the pair near the bottom of 93, 33 and 19, respectively. We noticed a decrease in the load cell reading of about 2 tons during the 10-minute hold at the 125-ton (250-kip) load, which is consistent with our observations made during the loading increments up to this point.

As we increased the load up to the 137.5-ton (275-kip) load increment, we observed the pile-top plunge into the ground. We observed a maximum reading on the load-cell read-out box of 134.7 tons and as the pile plunged, we observed readings of between 120-125 tons.



## Discussion

After reviewing our results of wave matching evaluations and the results of the static load test, we conferred with Mr. Garland Likins with GRL Engineers, Inc. through emails to validate our wave matching models. The results of the SLT pile indicate that the pile was likely compromised and likely does not indicate the nominal resistance this pile type can achieve in the soils at this site.

The static load test plunged into the ground earlier, and at less pile-top movement, than we anticipated. The load-movement curve appears linear up to the plunge point. We anticipated a more gradual failure, which brings up the possibility of the pile section yielding rather than soil yielding. Also, around the plunge point, the strain gauge 10 feet from the bottom of the pile and one of the pair of strain gauges near the bottom of the pile indicated a reduction in strain, while the strain gauge 20 feet from the bottom of the pile and the other strain gauge near the bottom maintained a strain reading near their maximum values. This may be caused by “de-bonding” of the sister-bar strain gauge from the concrete at this point or indicative of compromised concrete.

Due to the un-expected strain reduction in two of the strain gauges, and the shape of the curves of the “tangent modulus vs. micro strain” graphs, the reliability of these two gauges is questionable beyond the 87.5-ton load increment. Also, due to the potentially compromised pile section above the bottom of the pile, the readings of the non-debonded strain gauge are not likely reflective of the actual load on the soil. Therefore, only the gauge placed 20 feet from the bottom of the pile appears to provide reliable results for the entire range of recorded values. We are attaching load versus depth curves plotting all four gauges.

We evaluated the strain gauge results based on both strain-dependant modulus theory presented by Bengt H. Fellenius in ‘From Strain Measurements to Load in an Instrumented Pile’, (2001) and constant-modulus theory using the unconfined compressive design concrete strength. The strain-dependant modulus theory indicates a total load-shedding of up to 45 tons (90 kips) in the upper 42 feet of the pile, whereas assuming a constant-modulus indicates a total load-shedding of up to 107 tons (214 kips) in the upper 42 feet. These values equate to average unit skin friction resistances of about 0.7 kips per square foot (ksf) and 1.6 ksf, respectively. The average unit skin friction resistance for the dynamic redrives performed on the reaction piles and the SLT pile (prior to the static load test) to a depth of 42 feet is about 1.5 ksf. Although the constant-modulus method of analysis produces results that are closer to the dynamic test results for this project, the variation in the results confirm the need for considering different methods when attempting to quantify nominal resistance values.

The dynamic test results from the redrive performed on June 26, 2012 appear suspect due to the pile profile during testing. With the upper 3 feet of the pile section open and then concrete-filled below that point, the impact from the hammer may have caused partial separation of the steel shell from the concrete-filled core. Such separation would affect the energy flow down the pile which, in turn, affects the resistance distribution measured with the PDA. The pile model we input into the CAPWAP program indicates separation of the steel from the concrete to a depth of 10 feet, partial separation between 10 and 20 feet and then a composite pile section from 20 feet to the pile toe.

## General Remarks

In performing its services, Braun Intertec used that degree of care and skill ordinarily exercised under similar circumstances by reputable members of its profession currently practicing in the same locality. No warranty, express or implied, is made.

We appreciate the opportunity to be of assistance on this project. Should you have any questions regarding the contents of this report, please call Corey Reese at 952.995.2382 or Matt Glisson at 314.569.9883.

Sincerely,

BRAUN INTERTEC CORPORATION



Corey R. Reese, PE  
Project Engineer



Matthew R. Glisson, PE  
Associate Principal-Senior Engineer

Attachments:

PDILOTS

CAPWAP Results

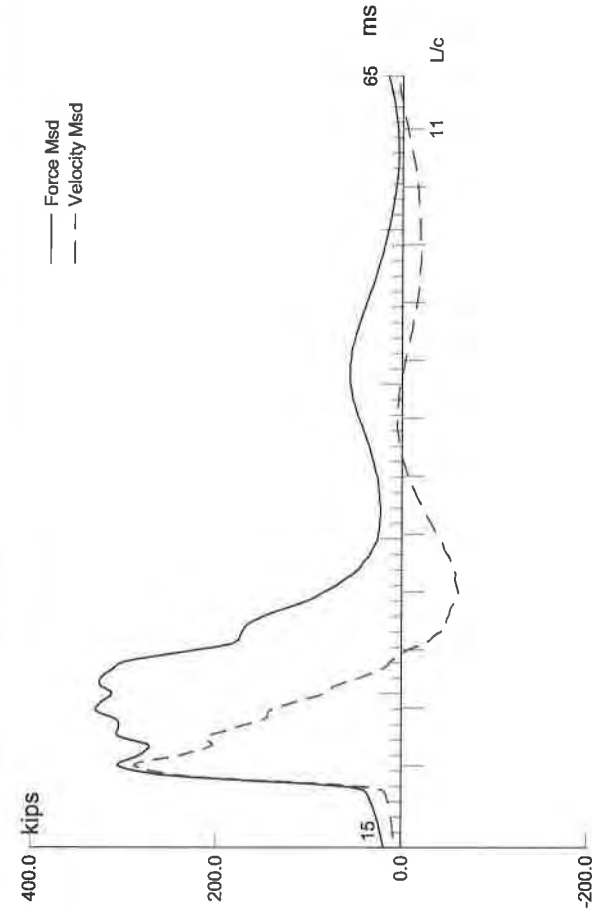
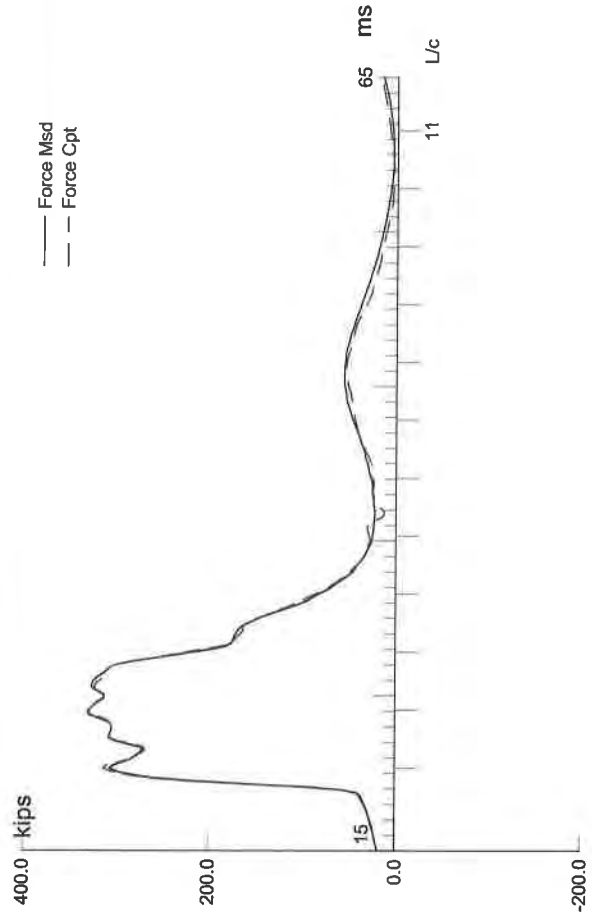
Static Load Test Spreadsheet

Load vs. Pile-top Movement Graph

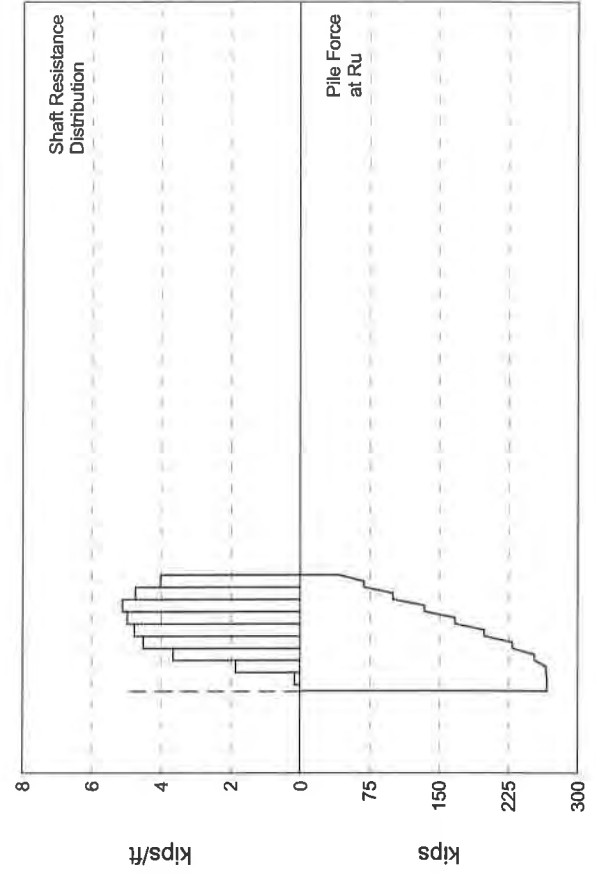
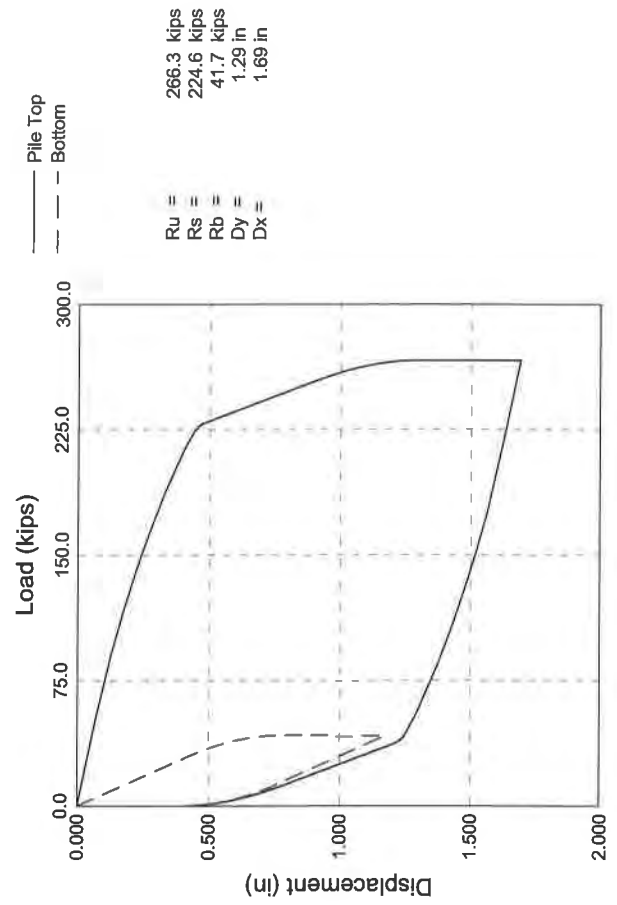
Load vs. Depth Graph – Strain-dependant modulus

Load vs. Depth Graph – Assumed constant-modulus

Equipment Calibrations



C-8



Bridge 10003; Pile: Reaction File 1 Initial  
 12" x 1/4" CIP, D19-42; Blow: 464  
 Braun Intertec Corp.

Test: 12-Dec-2011 13:11:  
 CAPWAP (R) 2006-3  
 OP: KAA

# CAPWAP SUMMARY RESULTS

Total CAPWAP Capacity: 266.3; along Shaft 224.6; at Toe 41.7 kips

Soil Sgmt No.	Dist. Below Gages ft	Depth Below Grade ft	Ru kips	Force in Pile kips	Sum of Ru kips	Unit Resist. (Depth) kips/ft	Unit Resist. (Area) ksf	Smith Damping Factor s/ft
				266.3				
1	9.9	8.8	1.1	265.2	1.1	0.13	0.04	0.103
2	16.6	15.4	12.4	252.8	13.5	1.87	0.60	0.103
3	23.2	22.0	24.3	228.5	37.8	3.66	1.17	0.103
4	29.8	28.7	30.0	198.5	67.8	4.52	1.44	0.103
5	36.5	35.3	31.7	166.8	99.5	4.78	1.52	0.103
6	43.1	41.9	33.0	133.8	132.5	4.98	1.58	0.103
7	49.7	48.6	33.9	99.9	166.4	5.11	1.63	0.103
8	56.4	55.2	31.5	68.4	197.9	4.75	1.51	0.103
9	63.0	61.8	26.7	41.7	224.6	4.03	1.28	0.103
Avg. Shaft			25.0			3.63	1.16	0.103
Toe			41.7				53.09	0.024

## Soil Model Parameters/Extensions

		Shaft	Toe
Quake	(in)	0.040	0.593
Case Damping Factor		1.402	0.062
Damping Type			Smith
Unloading Quake	(% of loading quake)	30	30
Reloading Level	(% of Ru)	100	100
Unloading Level	(% of Ru)	0	
Resistance Gap (included in Toe Quake) (in)			0.050
Soil Plug Weight	(kips)		0.23
Soil Support Dashpot		2.440	0.000
Soil Support Weight	(kips)	2.18	0.00

CAPWAP match quality = 1.66 (Wave Up Match) ; RSA = 0  
 Observed: final set = 0.400 in; blow count = 30 b/ft  
 Computed: final set = 0.438 in; blow count = 27 b/ft  
 max. Top Comp. Stress = 36.6 ksi (T= 24.3 ms, max= 1.085 x Top)  
 max. Comp. Stress = 39.7 ksi (Z= 16.6 ft, T= 25.1 ms)  
 max. Tens. Stress = -0.46 ksi (Z= 16.6 ft, T= 100.0 ms)  
 max. Energy (EMX) = 21.4 kip-ft; max. Measured Top Displ. (DMX) = 0.95 in

Bridge 10003; Pile: Reaction Pile 1 Initial  
 12" x 1/4" CIP, D19-42; Blow: 464  
 Braun Intertec Corp.

Test: 12-Dec-2011 13:11:  
 CAPWAP (R) 2006-3  
 OP: KAA

#### EXTREMA TABLE

Pile Sgmt No.	Dist. Below Gages ft	max. Force kips	min. Force kips	max. Comp. Stress ksi	max. Tens. Stress ksi	max. Trnsfd. Energy kip-ft	max. Veloc. ft/s	max. Displ. in
1	3.3	337.9	-4.0	36.6	-0.43	21.38	17.0	0.914
2	6.6	347.1	-4.0	37.6	-0.44	21.12	16.8	0.884
3	9.9	354.6	-4.2	38.4	-0.45	20.86	16.3	0.854
4	13.3	359.3	-4.2	38.9	-0.45	20.45	15.9	0.824
5	16.6	366.8	-4.2	39.7	-0.46	20.19	15.0	0.794
6	19.9	353.0	-3.9	38.2	-0.42	18.51	14.4	0.767
7	23.2	361.5	-3.9	39.2	-0.42	18.31	13.5	0.741
8	26.5	327.5	-3.2	35.5	-0.34	15.74	12.7	0.718
9	29.8	328.3	-3.3	35.6	-0.36	15.61	11.9	0.698
10	33.2	291.4	-2.5	31.6	-0.27	12.94	11.1	0.684
11	36.5	299.8	-2.5	32.5	-0.27	12.89	10.3	0.671
12	39.8	255.3	-1.5	27.7	-0.16	10.32	9.5	0.658
13	43.1	244.5	-1.3	26.5	-0.14	10.28	8.8	0.646
14	46.4	200.6	-0.4	21.7	-0.04	7.79	8.3	0.635
15	49.7	211.9	-0.5	23.0	-0.05	7.76	8.8	0.628
16	53.1	172.3	0.0	18.7	0.00	5.33	8.9	0.620
17	56.4	165.5	0.0	17.9	0.00	5.31	8.7	0.612
18	59.7	101.6	-0.1	11.0	-0.01	3.08	8.7	0.605
19	63.0	86.4	-0.1	9.4	-0.01	1.07	9.3	0.597
Absolute	16.6			39.7			(T = 25.1 ms)	
	16.6				-0.46		(T = 100.0 ms)	

#### CASE METHOD

J =	0.0	0.1	0.2	0.3	0.4	0.5	0.6	0.7	0.8	0.9
RP	418.1	399.7	381.3	362.9	344.5	326.0	307.6	289.2	270.8	252.4
RX	418.1	399.7	381.3	362.9	344.5	326.0	307.6	289.2	270.8	252.4
RU	418.1	399.7	381.3	362.9	344.5	326.0	307.6	289.2	270.8	252.4

RAU = 32.0 (kips); RA2 = 309.9 (kips)

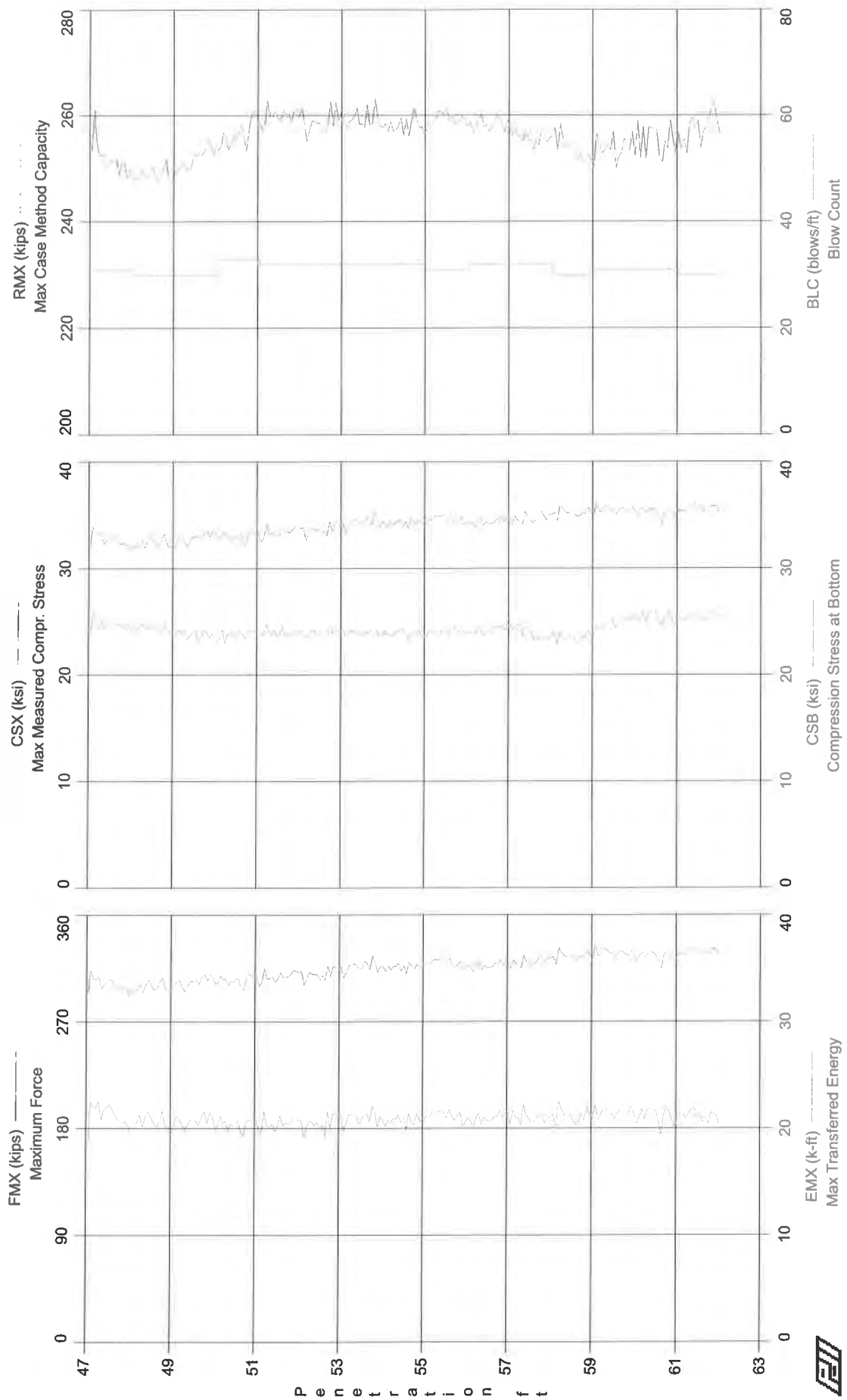
Current CAPWAP Ru = 266.3 (kips); Corresponding J(RP)= 0.82; J(RX) = 0.82

VMX	TVP	VT1*Z	FT1	FMX	DMX	DFN	SET	EMX	QUS
ft/s	ms	kips	kips	kips	in	in	in	kip-ft	kips
17.77	20.52	292.7	309.5	332.1	0.948	0.394	0.400	21.7	386.4

Bridge 10003; Pile: Reaction Pile 1 Initial  
 12" x 1/4" CIP, D19-42; Blow: 464  
 Braun Intertec Corp.

Test: 12-Dec-2011 13:11:  
 CAPWAP (R) 2006-3  
 OP: KAA

PILE PROFILE AND PILE MODEL				
Depth ft	Area in <sup>2</sup>	E-Modulus ksi	Spec. Weight lb/ft <sup>3</sup>	Perim. ft
0.00	9.23	29992.2	492.000	3.142
63.00	9.23	29992.2	492.000	3.142
Toe Area		0.785	ft <sup>2</sup>	
Top Segment Length		3.32 ft,	Top Impedance	16.47 kips/ft/s
Pile Damping		1.0 %,	Time Incr	0.197 ms, Wave Speed
				16807.9 ft/s, 2L/c
				7.5 ms



Bridge 10003 - Reaction Pile 1 Initial  
OP: KAA

12" x 1/4" CIP, D19-42  
Test date: 12-Dec-2011

AR: 9.23 in^2  
LE: 63.00 ft  
WS: 16,807.9 f/s

SP: 0.492 k/ft3  
EM: 30,000 ksi  
JC: 0.82

FMX: Maximum Force  
EMX: Max Transferred Energy  
CSX: Max Measured Compr. Stress  
CSI: Max F1 or F2 Compr. Stress  
CSB: Compression Stress at Bottom

STK: O.E. Diesel Hammer Stroke  
ETH: Energy Transfer Ratio - Stroke  
RX5: Max Case Method Capacity (JC=0.5)  
RMX: Max Case Method Capacity

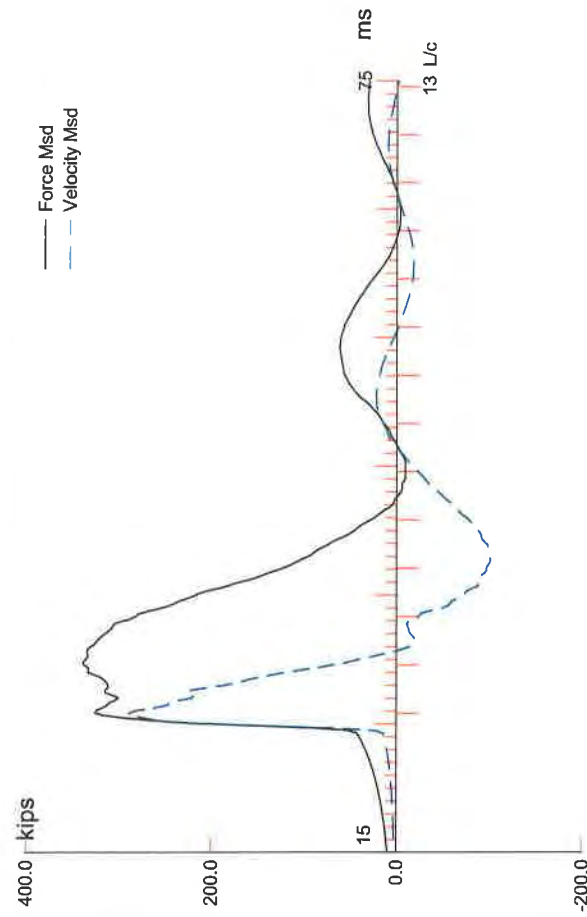
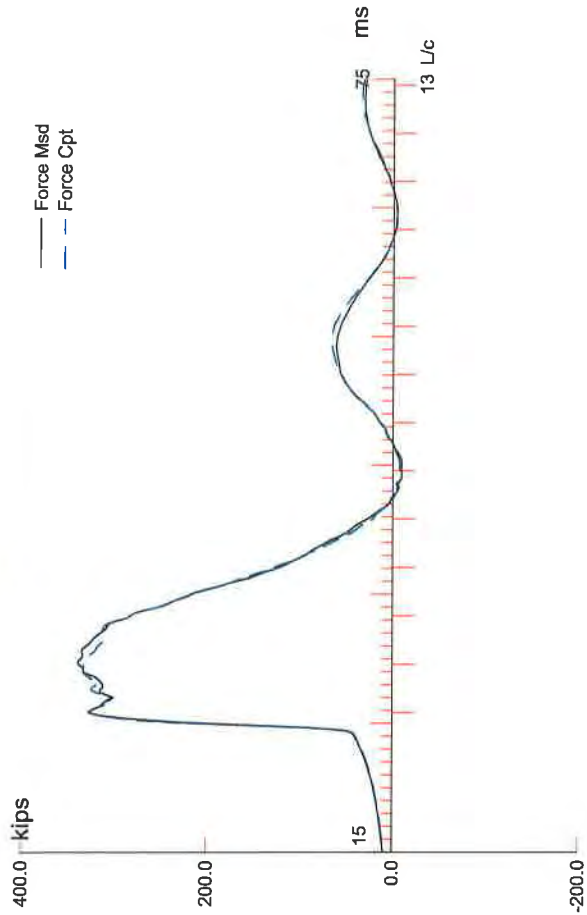
BL#	depth	BLC	TYPE	FMX	EMX	CSX	CSI	CSB	STK	ETH	RX5	RMX
end	ft	bl/ft		kips	k-ft	ksi	ksi	ksi	ft	(%)	kips	kips
31	48.00	31	AV31	302	21.4	32.7	34.2	24.9	7.7	69.0	297	252
61	49.00	30	AV30	299	20.7	32.4	35.9	24.4	7.5	68.5	291	249
91	50.00	30	AV30	304	20.7	32.9	36.8	23.9	7.6	68.5	291	252
124	51.00	33	AV33	305	20.4	33.0	36.6	23.8	7.6	67.4	297	256
156	52.00	32	AV32	309	20.5	33.4	36.4	24.0	7.6	67.7	300	260
188	53.00	32	AV32	311	20.5	33.7	35.9	24.0	7.6	67.1	301	259
220	54.00	32	AV32	317	21.0	34.4	35.8	24.0	7.7	67.8	305	259
252	55.00	32	AV32	316	20.8	34.3	35.5	23.9	7.7	67.2	304	258
283	56.00	31	AV31	320	21.2	34.6	36.4	24.1	7.8	67.8	306	259
315	57.00	32	AV32	318	21.0	34.4	37.4	24.3	7.8	67.1	307	259
347	58.00	32	AV32	321	21.0	34.7	38.1	24.0	7.9	66.6	306	256
377	59.00	30	AV30	325	21.2	35.3	39.8	23.6	8.0	66.5	307	254
408	60.00	31	AV31	328	21.5	35.6	39.7	24.9	8.1	66.7	314	254
439	61.00	31	AV31	325	21.1	35.2	37.8	25.4	8.0	66.3	315	255
469	62.00	30	AV30	329	21.2	35.6	36.3	25.5	8.0	66.2	318	258

Time Summary

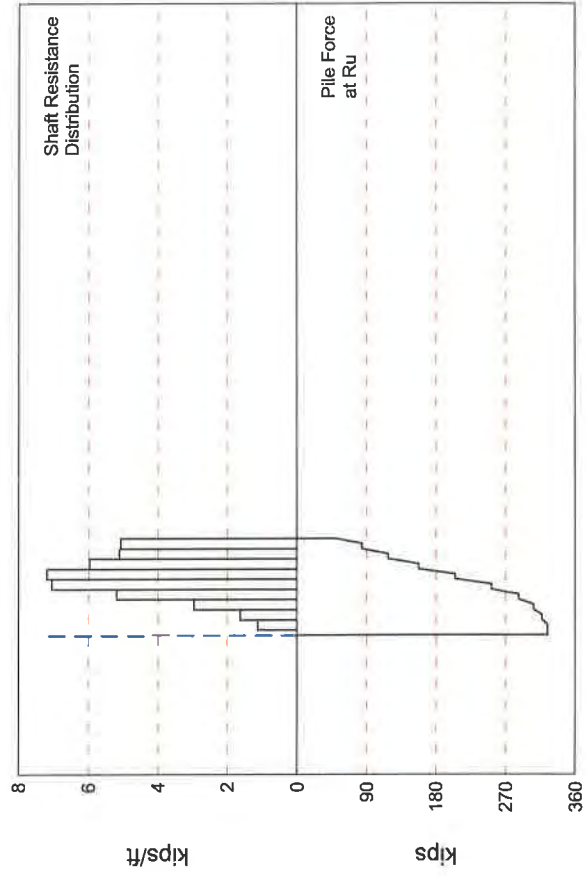
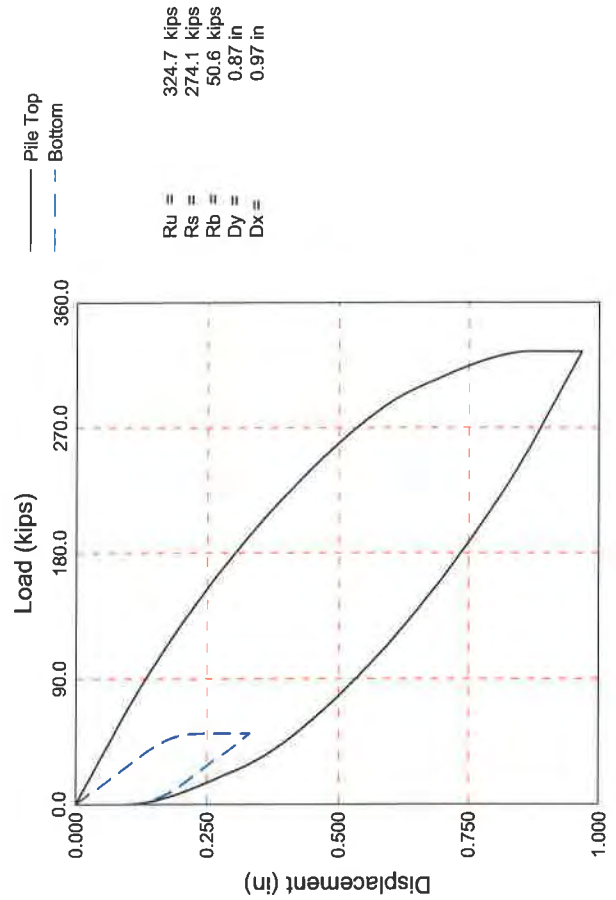
Drive 11 minutes 3 seconds

1:00:42 PM - 1:11:45 PM (12/12/2011) BN 1 - 469





C-14



Bridge 10003; File: Reaction Pile 1 Restrike  
 12" x 1/4" CIP, D19-42; Blow: 4  
 Braun Intertec Corp.

Test: 18-Jun-2012 07:49:  
 CAPWAP (R) 2006-3  
 OP: KAA

# CAPWAP SUMMARY RESULTS

Total CAPWAP Capacity: 324.7; along Shaft 274.1; at Toe 50.6 kips

Soil Sgmt No.	Dist. Below Gages ft	Depth Below Grade ft	Ru kips	Force in Pile kips	Sum of Ru kips	Unit Resist. (Depth) kips/ft	Unit Resist. (Area) ksf	Smith Damping Factor s/ft
				324.7				
1	9.9	9.0	7.5	317.2	7.5	0.83	0.26	0.164
2	16.6	15.7	10.8	306.4	18.3	1.63	0.52	0.164
3	23.2	22.3	19.7	286.7	38.0	2.97	0.95	0.164
4	29.8	28.9	34.4	252.3	72.4	5.19	1.65	0.164
5	36.5	35.6	46.8	205.5	119.2	7.06	2.25	0.164
6	43.1	42.2	47.7	157.8	166.9	7.19	2.29	0.164
7	49.7	48.8	39.6	118.2	206.5	5.97	1.90	0.164
8	56.4	55.5	33.9	84.3	240.4	5.11	1.63	0.164
9	63.0	62.1	33.7	50.6	274.1	5.08	1.62	0.164
Avg. Shaft			30.5			4.41	1.41	0.164
Toe			50.6				64.43	0.025

## Soil Model Parameters/Extensions

		Shaft	Toe
Quake	(in)	0.066	0.177
Case Damping Factor		2.731	0.075
Unloading Quake	(% of loading quake)	30	90
Reloading Level	(% of Ru)	100	100
Unloading Level	(% of Ru)	10	
Soil Plug Weight	(kips)		0.14

CAPWAP match quality = 1.40 (Wave Up Match) ; RSA = 0  
 Observed: final set = 0.100 in; blow count = 120 b/ft  
 Computed: final set = 0.132 in; blow count = 91 b/ft  
 max. Top Comp. Stress = 37.9 ksi (T= 29.4 ms, max= 1.085 x Top)  
 max. Comp. Stress = 41.1 ksi (Z= 23.2 ft, T= 29.2 ms)  
 max. Tens. Stress = -1.77 ksi (Z= 16.6 ft, T= 45.2 ms)  
 max. Energy (EMX) = 18.5 kip-ft; max. Measured Top Displ. (DMX)= 0.80 in

Bridge 10003; File: Reaction Pile 1 Restrike  
 12" x 1/4" CIP, D19-42; Blow: 4  
 Braun Intertec Corp.

Test: 18-Jun-2012 07:49:  
 CAPWAP (R) 2006-3  
 OP: KAA

# EXTREMA TABLE

File Sgmnt No.	Dist. Below Gages ft	max. Force kips	min. Force kips	max. Comp. Stress ksi	max. Tens. Stress ksi	max. Trnsfd. Energy kip-ft	max. Veloc. ft/s	max. Displ. in
1	3.3	349.8	-10.8	37.9	-1.17	18.51	17.0	0.759
2	6.6	359.8	-13.1	39.0	-1.42	17.88	16.7	0.712
3	9.9	373.4	-15.3	40.4	-1.66	17.22	16.1	0.664
4	13.3	367.9	-14.6	39.9	-1.58	15.50	15.6	0.617
5	16.6	379.5	-16.3	41.1	-1.77	14.89	14.7	0.572
6	19.9	368.8	-14.7	40.0	-1.59	13.14	13.8	0.530
7	23.2	379.5	-16.1	41.1	-1.74	12.69	12.7	0.490
8	26.5	349.5	-11.6	37.9	-1.26	10.62	11.5	0.454
9	29.8	358.1	-13.0	38.8	-1.41	10.25	10.2	0.418
10	33.2	303.9	-4.3	32.9	-0.46	7.85	9.0	0.387
11	36.5	312.4	-5.4	33.8	-0.59	7.57	7.7	0.356
12	39.8	246.2	0.0	26.7	0.00	5.34	7.0	0.330
13	43.1	245.8	0.0	26.6	0.00	5.15	5.8	0.305
14	46.4	176.6	0.0	19.1	0.00	3.46	5.3	0.284
15	49.7	179.8	0.0	19.5	0.00	3.34	4.6	0.264
16	53.1	130.5	0.0	14.1	0.00	2.20	4.5	0.248
17	56.4	132.3	0.0	14.3	0.00	2.13	4.3	0.232
18	59.7	90.5	0.0	9.8	0.00	1.32	4.7	0.220
19	63.0	94.1	0.0	10.2	0.00	0.56	4.6	0.208
Absolute	23.2			41.1			(T =	29.2 ms)
	16.6				-1.77		(T =	45.2 ms)

# CASE METHOD

J =	0.0	0.1	0.2	0.3	0.4	0.5	0.6	0.7	0.8	0.9
RP	461.7	446.2	430.7	415.1	399.6	384.1	368.6	353.0	337.5	322.0
RX	462.2	446.6	431.0	415.4	399.8	384.2	368.6	353.0	337.5	322.0
RU	520.8	511.1	501.5	491.9	482.2	472.6	463.0	453.4	443.7	434.1

RAU = 5.4 (kips); RA2 = 385.7 (kips)

Current CAPWAP Ru = 324.7 (kips); Corresponding J(RP)= 0.88; J(RX) = 0.88

VMX	TVP	VT1*Z	FT1	FMX	DMX	DFN	SET	EMX	QUS
ft/s	ms	kips	kips	kips	in	in	in	kip-ft	kips
17.67	26.04	291.1	326.0	340.2	0.802	0.096	0.100	19.1	507.1

Bridge 10003; Pile: Reaction Pile 1 Restrike  
 12" x 1/4" CIP, D19-42; Blow: 4  
 Braun Intertec Corp.

Test: 18-Jun-2012 07:49:  
 CAPWAP (R) 2006-3  
 OP: KAA

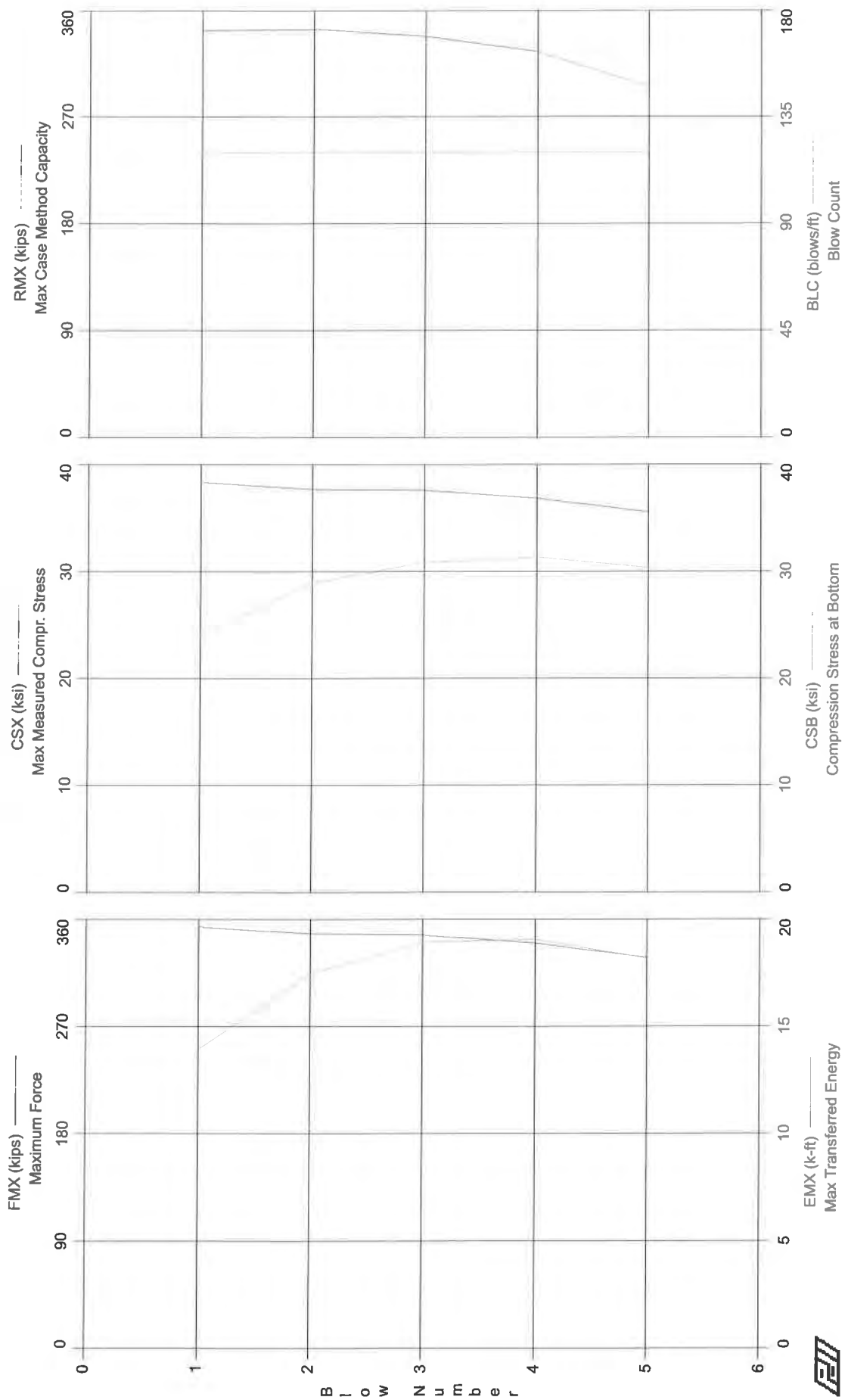
PILE PROFILE AND PILE MODEL				
Depth ft	Area in <sup>2</sup>	E-Modulus ksi	Spec. Weight lb/ft <sup>3</sup>	Perim. ft
0.00	9.23	29992.2	492.000	3.142
63.00	9.23	29992.2	492.000	3.142

Toe Area 0.785 ft<sup>2</sup>

Top Segment Length 3.32 ft, Top Impedance 16.47 kips/ft/s

Pile Damping 1.0 %, Time Incr 0.197 ms, Wave Speed 16807.9 ft/s, 2L/c 7.5 ms

Bridge 10003 - Reaction Pile 1 Restrike



Bridge 10003 - Reaction Pile 1 Restrike  
OP: KAA

12" x 1/4" CIP, D19-42  
Test date: 18-Jun-2012

AR: 9.23 in^2  
LE: 63.00 ft  
WS: 16,807.9 f/s

SP: 0.492 k/ft3  
EM: 30,000 ksi  
JC: 0.88

FMX: Maximum Force  
EMX: Max Transferred Energy  
CSX: Max Measured Compr. Stress  
CSI: Max F1 or F2 Compr. Stress  
CSB: Compression Stress at Bottom

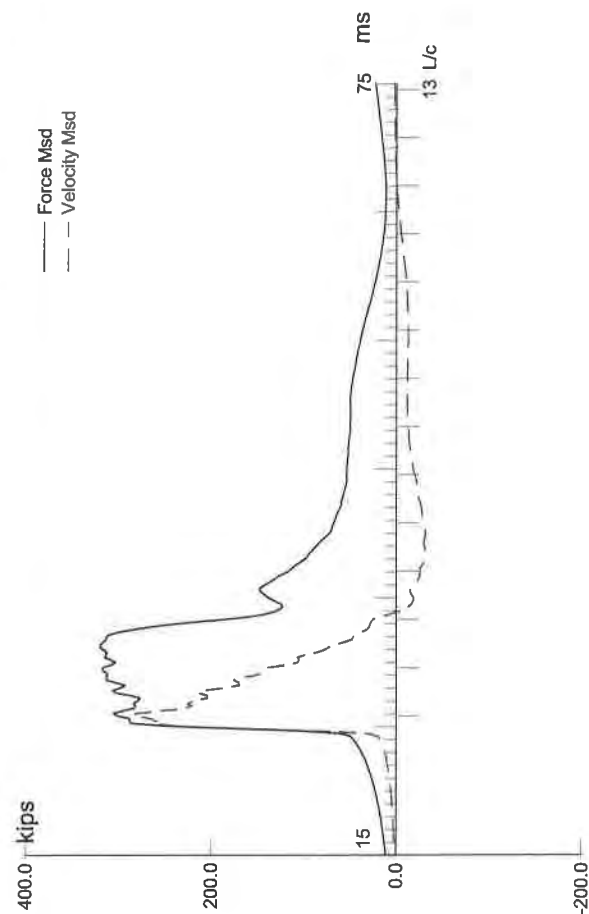
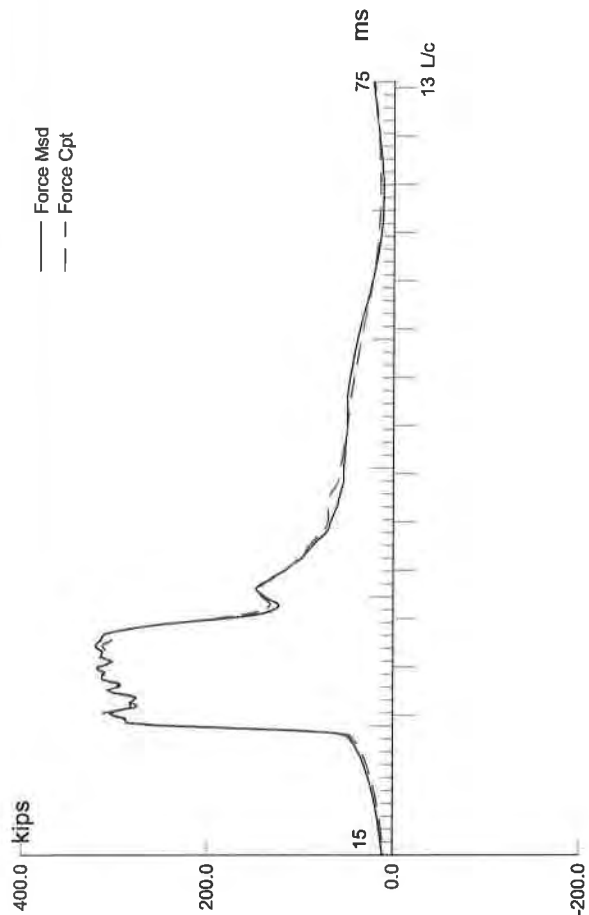
STK: O.E. Diesel Hammer Stroke  
ETH: Energy Transfer Ratio - Stroke  
RX5: Max Case Method Capacity (JC=0.5)  
RMX: Max Case Method Capacity

BL#	depth	BLC	TYPE	FMX	EMX	CSX	CSI	CSB	STK	ETH	RX5	RMX
end	ft	bl/ft		kips	k-ft	ksi	ksi	ksi	ft	(%)	kips	kips
1	62.07	120	AV1	354	14.0	38.4	44.1	24.0	7.8	44.8	369	343
2	62.08	120	AV1	348	17.5	37.7	42.4	29.0	8.6	50.9	389	344
3	62.08	120	AV1	347	18.9	37.6	40.9	30.9	8.5	55.5	394	338
4	62.09	120	AV1	340	19.1	36.9	41.2	31.4	8.7	54.8	384	325
5	62.10	120	AV1	328	18.2	35.6	42.3	30.4	8.7	52.3	357	295

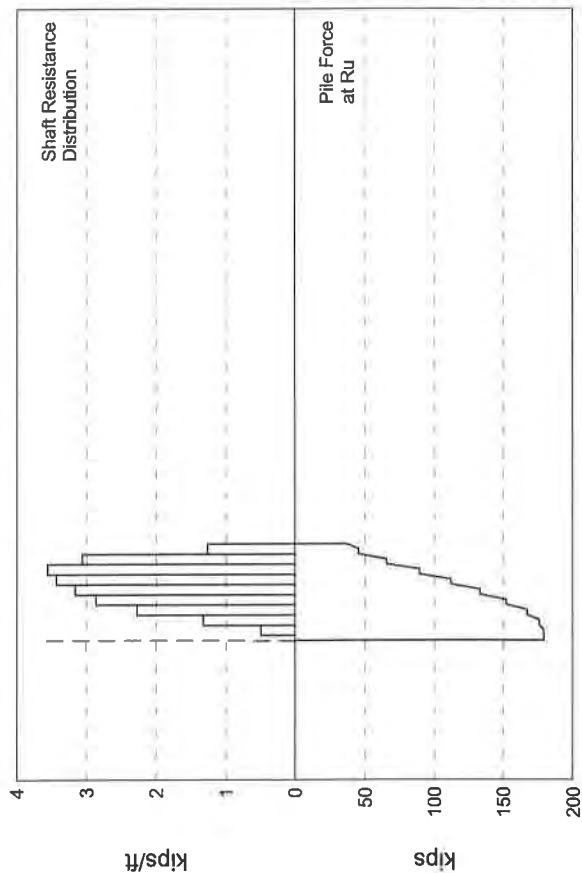
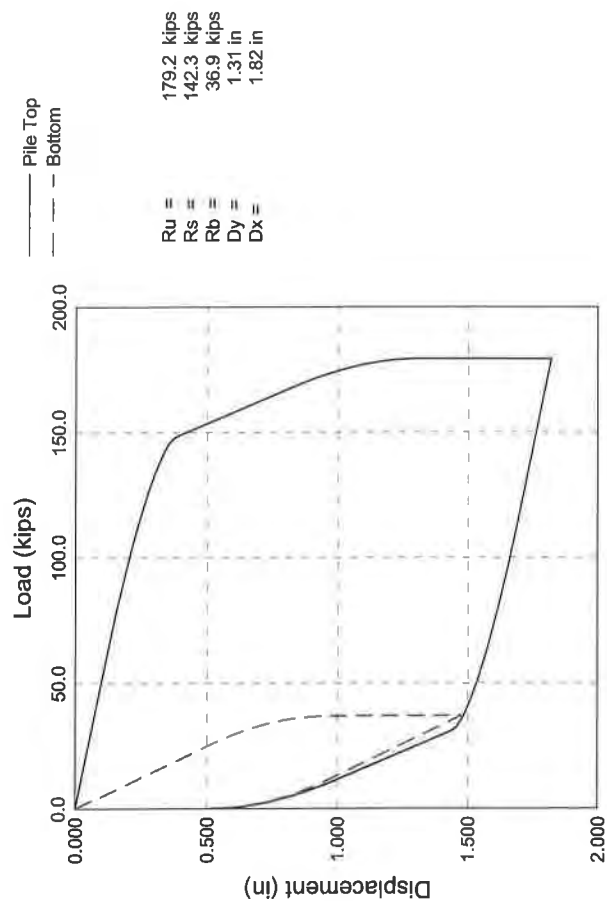
Time Summary

Drive 6 seconds

7:49:27 AM - 7:49:33 AM (6/18/2012) BN 1 - 5



C-20



Bridge 10003; File: Reaction File 2 Initial  
 12" x 1/4" CIP, D19-42; Blow: 73  
 Braun Intertec Corp.

Test: 15-Jun-2012 09:43:  
 CAPWAP (R) 2006-3  
 OP: KAA

# CAPWAP SUMMARY RESULTS

Total CAPWAP Capacity: 179.2; along Shaft 142.3; at Toe 36.9 kips

Soil Sgmt No.	Dist. Below Gages ft	Depth Below Grade ft	Ru kips	Force in Pile kips	Sum of Ru kips	Unit Resist. (Depth) kips/ft	Unit Resist. (Area) ksf	Smith Damping Factor s/ft
				179.2				
1	9.9	9.1	3.3	175.9	3.3	0.36	0.12	0.171
2	16.6	15.8	8.8	167.1	12.1	1.33	0.42	0.171
3	23.2	22.4	15.1	152.0	27.2	2.28	0.72	0.171
4	29.8	29.0	19.0	133.0	46.2	2.87	0.91	0.171
5	36.5	35.6	21.0	112.0	67.2	3.17	1.01	0.171
6	43.1	42.3	22.8	89.2	90.0	3.44	1.09	0.171
7	49.7	48.9	23.6	65.6	113.6	3.56	1.13	0.171
8	56.4	55.5	20.3	45.3	133.9	3.06	0.97	0.171
9	63.0	62.2	8.4	36.9	142.3	1.27	0.40	0.171
Avg. Shaft			15.8			2.29	0.73	0.171
Toe			36.9				46.98	0.259

Soil Model Parameters/Extensions			Shaft	Toe
Quake	(in)		0.099	0.738
Case Damping Factor			1.481	0.580
Damping Type				Smith
Unloading Quake	(% of loading quake)		230	113
Reloading Level	(% of Ru)		100	100
Unloading Level	(% of Ru)		49	
Resistance Gap (included in Toe Quake)	(in)			0.088
Soil Plug Weight	(kips)			0.25
Soil Support Dashpot			2.389	0.000
Soil Support Weight	(kips)		2.18	0.00

CAPWAP match quality = 2.05 (Wave Up Match) ; RSA = 0  
 Observed: final set = 0.514 in; blow count = 23 b/ft  
 Computed: final set = 0.508 in; blow count = 24 b/ft  
 max. Top Comp. Stress = 35.3 ksi (T= 29.8 ms, max= 1.058 x Top)  
 max. Comp. Stress = 37.3 ksi (Z= 16.6 ft, T= 29.8 ms)  
 max. Tens. Stress = 0.00 ksi (Z= 3.3 ft, T= 0.0 ms)  
 max. Energy (EMX) = 22.6 kip-ft; max. Measured Top Displ. (DMX)= 0.98 in



Bridge 10003; Pile: Reaction Pile 2 Initial  
 12" x 1/4" CIP, D19-42; Blow: 73  
 Braun Intertec Corp.

Test: 15-Jun-2012 09:43:  
 CAPWAP (R) 2006-3  
 OP: KAA

EXTREMA TABLE

Pile Sgmt No.	Dist. Below Gages ft	max. Force kips	min. Force kips	max. Comp. Stress ksi	max. Tens. Stress ksi	max. Trnsfd. Energy kip-ft	max. Veloc. ft/s	max. Displ. in
1	3.3	325.4	0.0	35.3	0.00	22.59	16.5	0.994
2	6.6	333.7	0.0	36.1	0.00	22.44	16.2	0.971
3	9.9	339.4	0.0	36.8	0.00	22.29	15.7	0.948
4	13.3	339.8	0.0	36.8	0.00	21.48	15.3	0.925
5	16.6	344.3	0.0	37.3	0.00	21.32	14.5	0.902
6	19.9	332.8	0.0	36.1	0.00	19.66	14.0	0.880
7	23.2	336.5	0.0	36.5	0.00	19.52	13.1	0.859
8	26.5	312.4	0.0	33.8	0.00	17.13	12.5	0.840
9	29.8	319.2	0.0	34.6	0.00	17.03	11.7	0.822
10	33.2	283.7	0.0	30.7	0.00	14.37	11.1	0.807
11	36.5	290.2	0.0	31.4	0.00	14.30	10.4	0.792
12	39.8	252.8	0.0	27.4	0.00	11.60	9.8	0.782
13	43.1	245.3	0.0	26.6	0.00	11.58	10.0	0.772
14	46.4	204.7	0.0	22.2	0.00	8.81	10.0	0.764
15	49.7	210.3	0.0	22.8	0.00	8.79	10.7	0.755
16	53.1	174.6	0.0	18.9	0.00	6.02	10.9	0.749
17	56.4	168.2	0.0	18.2	0.00	6.01	10.6	0.745
18	59.7	129.3	0.0	14.0	0.00	3.61	11.0	0.742
19	63.0	110.1	0.0	11.9	0.00	2.50	11.5	0.739
Absolute	16.6			37.3			(T =	29.8 ms)
	3.3				0.00		(T =	0.0 ms)

CASE METHOD

J =	0.0	0.1	0.2	0.3	0.4	0.5	0.6	0.7	0.8	0.9
RP	372.3	350.0	327.7	305.4	283.1	260.8	238.5	216.2	193.9	171.6
RX	372.3	350.0	327.7	305.4	283.1	260.8	238.5	216.2	195.4	178.7
RU	368.1	349.0	329.9	310.8	291.7	272.6	253.5	234.4	215.3	196.2

RAU = 69.9 (kips); RA2 = 309.6 (kips)

Current CAPWAP Ru = 179.2 (kips); Corresponding J(RP) = 0.87; J(RX) = 0.90

VMX	TVP	VT1*Z	FT1	FMX	DMX	DFN	SET	EMX	QUS
ft/s	ms	kips	kips	kips	in	in	in	kip-ft	kips
17.56	26.04	289.3	306.2	320.8	0.983	0.531	0.514	22.6	363.0

Bridge 10003; Pile: Reaction Pile 2 Initial  
 12" x 1/4" CIP, D19-42; Blow: 73  
 Braun Intertec Corp.

Test: 15-Jun-2012 09:43:  
 CAPWAP (R) 2006-3  
 OP: KAA

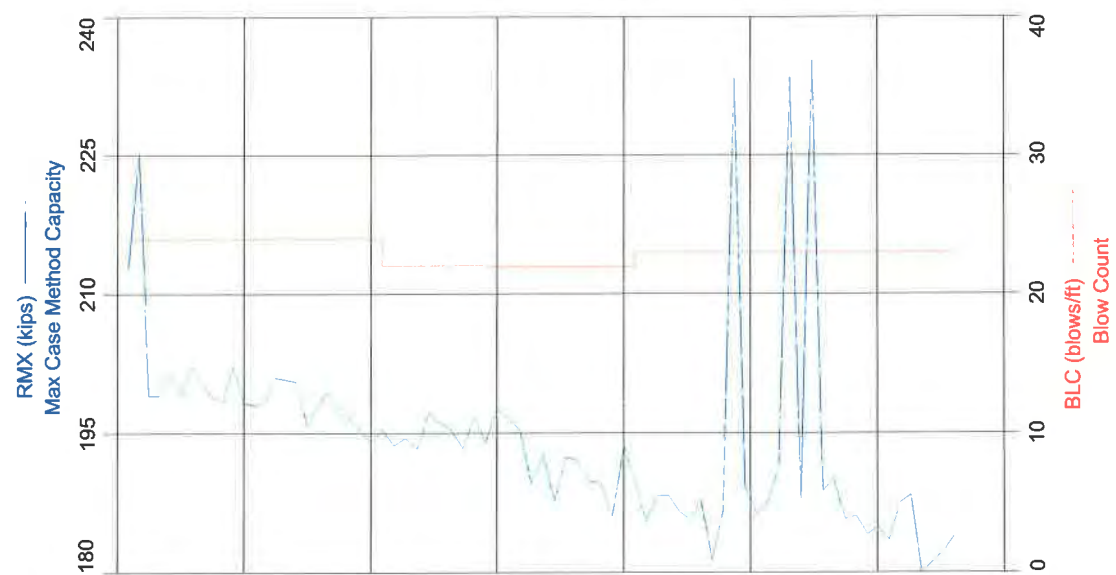
PILE PROFILE AND PILE MODEL

Depth ft	Area in <sup>2</sup>	E-Modulus ksi	Spec. Weight lb/ft <sup>3</sup>	Perim. ft
0.00	9.23	29992.2	492.000	3.142
63.00	9.23	29992.2	492.000	3.142

Toe Area 0.785 ft<sup>2</sup>

Top Segment Length 3.32 ft, Top Impedance 16.47 kips/ft/s

Pile Damping 1.0 %, Time Incr 0.197 ms, Wave Speed 16807.9 ft/s, 2L/c 7.5 ms



Bridge 10003 - Reaction Pile 2 Initial  
OP: KAA

12" x 1/4" CIP, D19-42  
Test date: 15-Jun-2012

AR: 9.23 in^2  
LE: 63.00 ft  
WS: 16,807.9 f/s

SP: 0.492 k/ft^3  
EM: 30,000 ksi  
JC: 0.90

FMX: Maximum Force  
EMX: Max Transferred Energy  
CSX: Max Measured Compr. Stress  
CSI: Max F1 or F2 Compr. Stress  
CSB: Compression Stress at Bottom

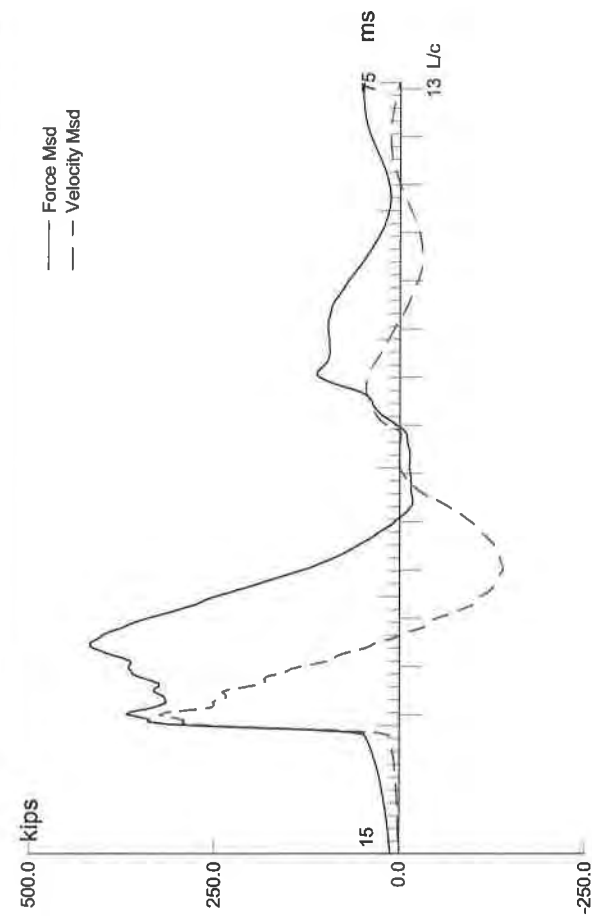
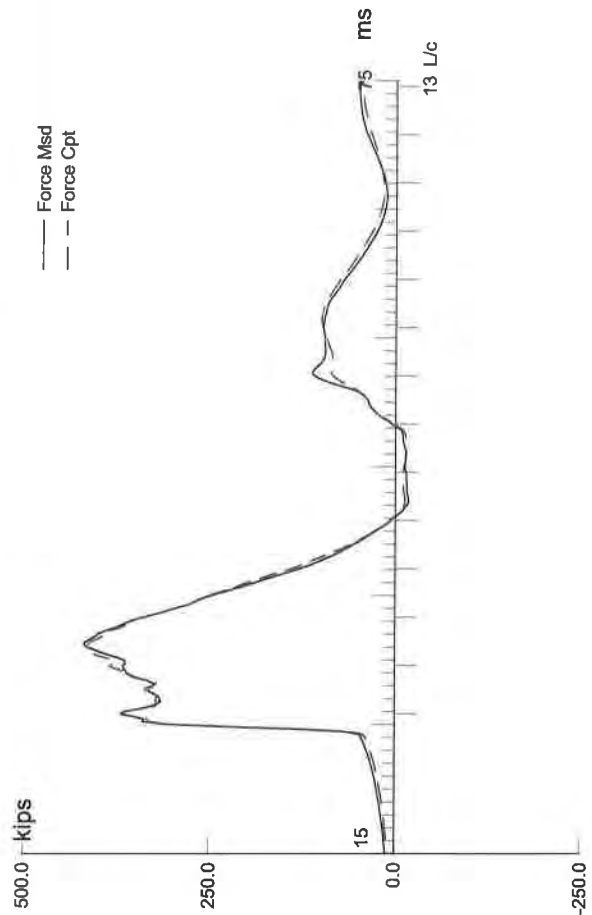
STK: O.E. Diesel Hammer Stroke  
ETH: Energy Transfer Ratio - Stroke  
RX5: Max Case Method Capacity (JC=0.5)  
RMX: Max Case Method Capacity

BL#	depth	BLC	TYPE	FMX	EMX	CSX	CSI	CSB	STK	ETH	RX5	RMX
end	ft	bl/ft		kips	k-ft	ksi	ksi	ksi	ft	(%)	kips	kips
24	60.00	24	AV24	308	20.1	33.4	44.5	22.0	7.2	69.5	261	201
46	61.00	22	AV22	319	21.2	34.5	43.6	21.9	7.4	71.4	263	193
69	62.00	23	AV23	320	21.2	34.7	42.7	22.4	7.4	72.2	262	193
76	62.30	23	AV7	314	21.1	34.1	47.1	23.0	7.5	70.3	261	184

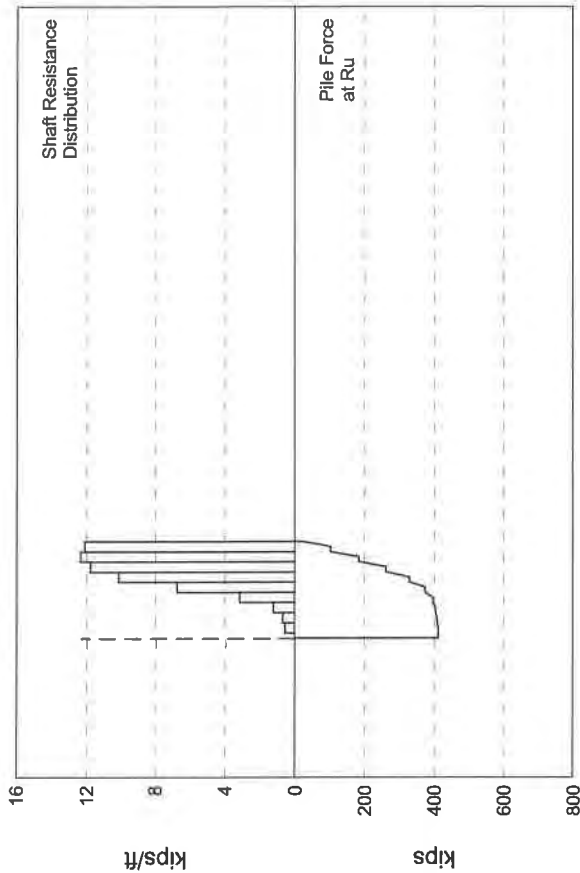
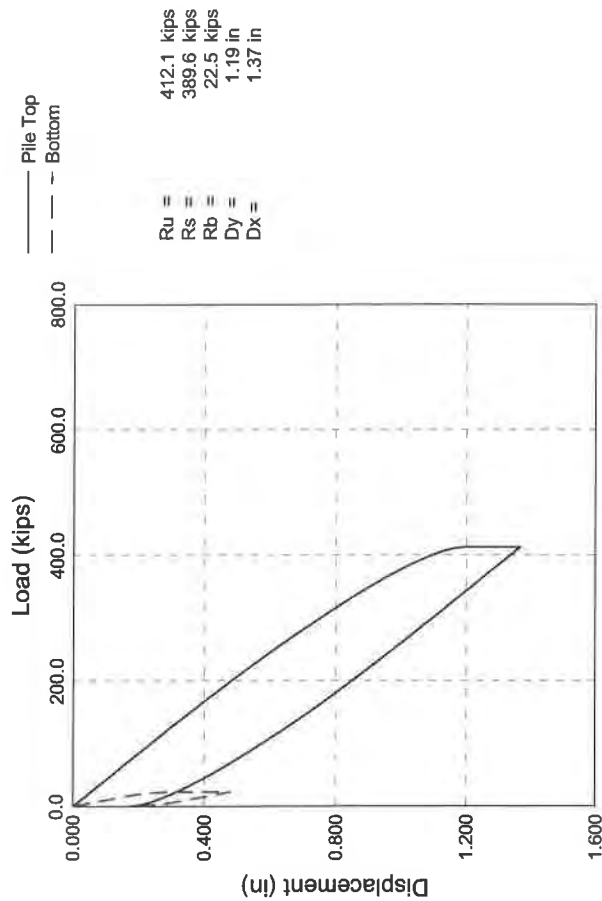
Time Summary

Drive 1 minute 44 seconds

9:41:59 AM - 9:43:43 AM (6/15/2012) BN 1 - 76



C-26



Bridge 10003; Pile: Reaction Pile 2 Restrike  
 12" x 1/4" CIP, D19-42; Blow: 4  
 Braun Intertec Corp.

Test: 18-Jun-2012 08:23:  
 CAPWAP (R) 2006-3  
 OP: KAA

#### CAPWAP SUMMARY RESULTS

Total CAPWAP Capacity:		412.1; along Shaft		389.6; at Toe		22.5 kips			
Soil Sgmnt No.	Dist. Below Gages ft	Depth Below Grade ft	Ru kips	Force in Pile kips	Sum of Ru kips	Unit Resist. (Depth) kips/ft	Unit Resist. (Area) ksf	Smith Damping Factor s/ft	Quake in
				412.1					
1	9.9	9.4	3.7	408.4	3.7	0.39	0.12	0.264	0.276
2	16.6	16.1	4.6	403.8	8.3	0.69	0.22	0.264	0.276
3	23.2	22.7	8.1	395.7	16.4	1.22	0.39	0.264	0.276
4	29.8	29.3	20.9	374.8	37.3	3.15	1.00	0.264	0.276
5	36.5	36.0	44.9	329.9	82.2	6.77	2.16	0.264	0.276
6	43.1	42.6	67.1	262.8	149.3	10.12	3.22	0.264	0.276
7	49.7	49.2	78.1	184.7	227.4	11.78	3.75	0.264	0.276
8	56.4	55.9	81.9	102.8	309.3	12.35	3.93	0.264	0.264
9	63.0	62.5	80.3	22.5	389.6	12.11	3.85	0.264	0.235
Avg. Shaft			43.3			6.24	1.98	0.264	0.265
Toe			22.5				28.65	0.024	0.235

Soil Model Parameters/Extensions			Shaft	Toe
Case Damping Factor			6.239	0.033
Unloading Quake (% of loading quake)			30	117
Reloading Level (% of Ru)			100	100
Unloading Level (% of Ru)			23	
Resistance Gap (included in Toe Quake) (in)				0.035
Soil Plug Weight (kips)				0.31

CAPWAP match quality	=	2.42	(Wave Up Match) ; RSA = 0
Observed: final set	=	0.175 in;	blow count = 69 b/ft
Computed: final set	=	0.200 in;	blow count = 60 b/ft
max. Top Comp. Stress	=	45.3 ksi	(T= 31.4 ms, max= 1.050 x Top)
max. Comp. Stress	=	47.5 ksi	(Z= 23.2 ft, T= 31.0 ms)
max. Tens. Stress	=	-4.19 ksi	(Z= 23.2 ft, T= 43.6 ms)
max. Energy (EMX)	=	25.4 kip-ft;	max. Measured Top Displ. (DMX)= 0.98 in

Bridge 10003; Pile: Reaction Pile 2 Restrike  
 12" x 1/4" CIP, D19-42; Blow: 4  
 Braun Intertec Corp.

Test: 18-Jun-2012 08:23:  
 CAPWAP (R) 2006-3  
 OP: KAA

# EXTREMA TABLE

Pile Sgmnt No.	Dist. Below Gages ft	max. Force kips	min. Force kips	max. Comp. Stress ksi	max. Tens. Stress ksi	max. Trnsfd. Energy kip-ft	max. Veloc. ft/s	max. Displ. in
1	3.3	418.0	-19.9	45.3	-2.15	25.38	19.2	0.956
2	6.6	422.9	-25.3	45.8	-2.74	24.44	18.9	0.899
3	9.9	428.8	-30.0	46.5	-3.25	23.48	18.4	0.842
4	13.3	429.4	-31.1	46.5	-3.37	21.58	18.0	0.785
5	16.6	438.0	-35.1	47.5	-3.81	20.67	17.3	0.730
6	19.9	434.9	-35.2	47.1	-3.81	18.83	16.7	0.675
7	23.2	438.8	-38.7	47.5	-4.19	17.98	15.2	0.621
8	26.5	429.0	-35.9	46.5	-3.89	15.93	14.3	0.570
9	29.8	432.1	-38.6	46.8	-4.19	15.16	12.9	0.519
10	33.2	397.7	-27.8	43.1	-3.01	12.35	11.4	0.472
11	36.5	401.2	-29.4	43.5	-3.19	11.77	9.5	0.428
12	39.8	331.0	-8.4	35.9	-0.91	8.56	8.2	0.391
13	43.1	333.8	-10.2	36.2	-1.10	8.20	6.3	0.356
14	46.4	250.3	-0.0	27.1	-0.00	5.52	5.5	0.328
15	49.7	253.0	-0.0	27.4	-0.00	5.33	4.4	0.302
16	53.1	177.1	-0.0	19.2	-0.00	3.41	3.7	0.283
17	56.4	178.6	-0.0	19.4	-0.00	3.31	3.2	0.264
18	59.7	117.0	-0.0	12.7	-0.00	1.87	3.5	0.250
19	63.0	118.7	-0.0	12.9	-0.00	0.21	3.2	0.235
Absolute	23.2			47.5			(T =	31.0 ms)
	23.2				-4.19		(T =	43.6 ms)

# CASE METHOD

J =	0.0	0.1	0.2	0.3	0.4	0.5	0.6	0.7	0.8	0.9
RP	522.9	511.1	499.3	487.4	475.6	463.8	452.0	440.2	428.4	416.6
RX	544.9	529.1	513.3	497.4	481.6	465.8	450.0	434.2	419.8	405.7
RU	543.2	530.1	517.0	503.9	490.9	477.8	464.7	451.6	438.5	425.4

RAU = 0.0 (kips); RA2 = 446.7 (kips)

Current CAPWAP Ru = 412.1 (kips); Corresponding J(RP)= 1.00; J(RX) = 0.85

VMX	TVP	VT1*Z	FT1	FMX	DMX	DFN	SET	EMX	QUS
ft/s	ms	kips	kips	kips	in	in	in	kip-ft	kips
19.98	26.04	297.8	343.2	420.2	0.979	0.175	0.175	26.5	551.9

Bridge 10003; Pile: Reaction Pile 2 Restrike  
 12" x 1/4" CIP, D19-42; Blow: 4  
 Braun Intertec Corp.

Test: 18-Jun-2012 08:23:  
 CAPWAP (R) 2006-3  
 OP: KAA

PILE PROFILE AND PILE MODEL

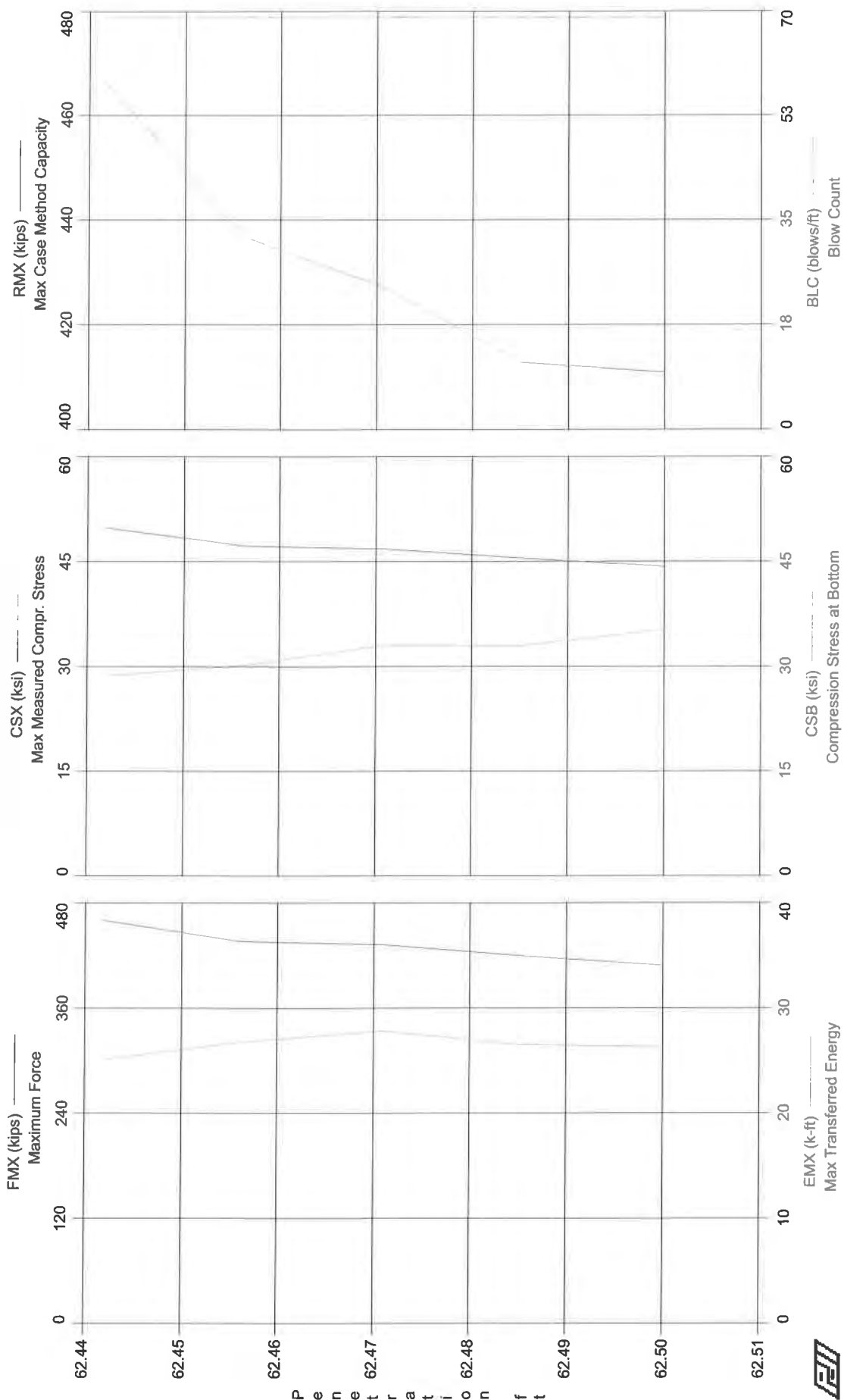
Depth ft	Area in <sup>2</sup>	E-Modulus ksi	Spec. Weight lb/ft <sup>3</sup>	Perim. ft
0.00	9.23	29992.2	492.000	3.142
63.00	9.23	29992.2	492.000	3.142

Toe Area 0.785 ft<sup>2</sup>

Segmnt Number	Dist. B.G. ft	Impedance kips/ft/s	Imped. Change %	Tension Slack in	Eff.	Compression Slack in	Eff.	Perim. ft	Soil Plug kips
1	3.32	16.47	0.00	0.000	0.000	0.000	0.000	3.142	0.00
2	6.63	16.47	0.00	0.000	0.000	0.000	0.000	3.142	0.01
19	63.00	16.47	0.00	0.000	0.000	0.000	0.000	3.142	0.01

Pile Damping 1.0 %, Time Incr 0.197 ms, Wave Speed 16807.9 ft/s, 2L/c 7.5 ms





Bridge 10003 - Reaction Pile 2 Restrike  
OP: KAA

12" x 1/4" CIP, D19-42  
Test date: 18-Jun-2012

AR: 9.23 in^2  
LE: 63.00 ft  
WS: 16,807.9 f/s

SP: 0.492 k/ft<sup>3</sup>  
EM: 30,000 ksi  
JC: 0.85

FMX: Maximum Force  
EMX: Max Transferred Energy  
CSX: Max Measured Compr. Stress  
CSI: Max F1 or F2 Compr. Stress  
CSB: Compression Stress at Bottom

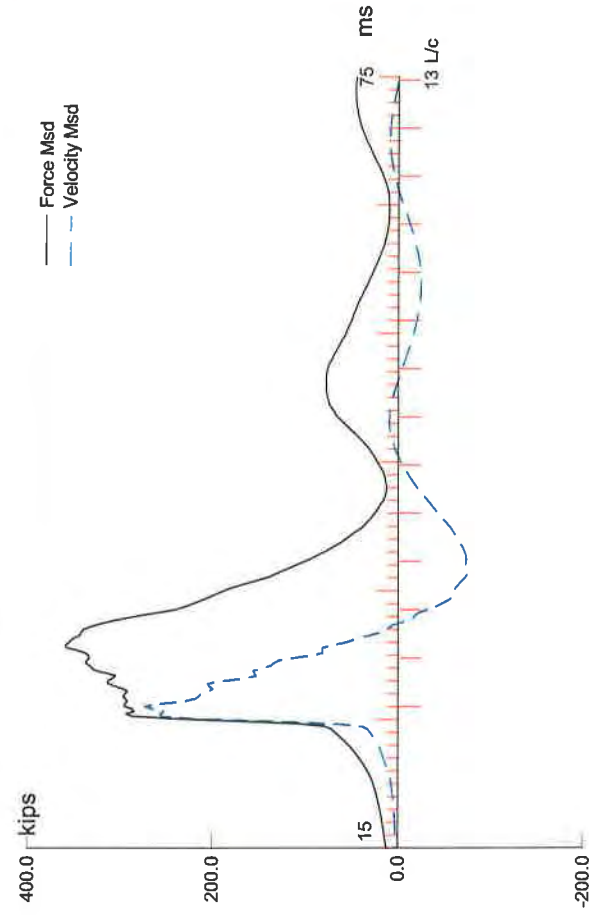
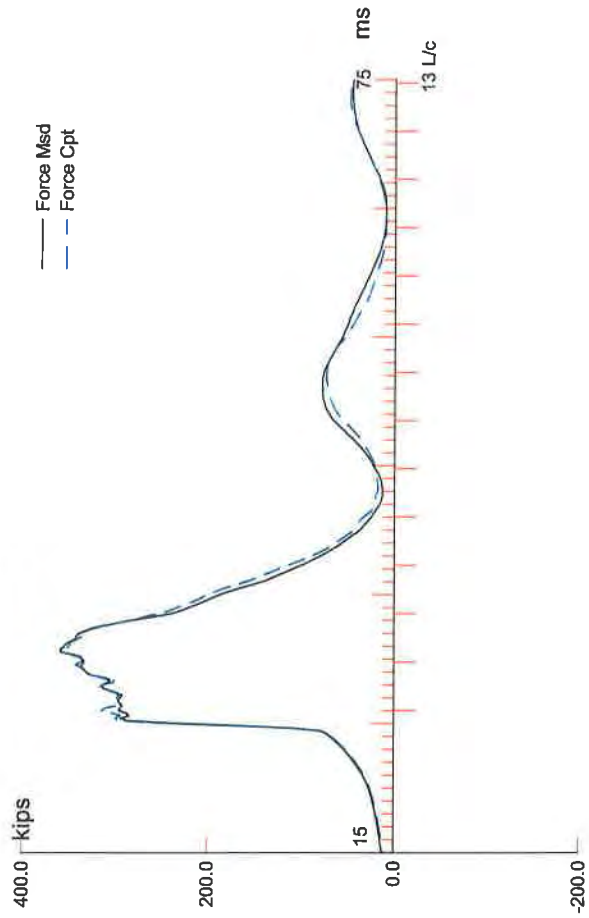
STK: O.E. Diesel Hammer Stroke  
ETH: Energy Transfer Ratio - Stroke  
RX5: Max Case Method Capacity (JC=0.5)  
RMX: Max Case Method Capacity

BL#	depth	BLC	TYPE	FMX	EMX	CSX	CSI	CSB	STK	ETH	RX5	RMX
end	ft	bl/ft		kips	k-ft	ksi	ksi	ksi	ft	(%)	kips	kips
1	62.44	69	AV1	461	25.1	49.9	57.1	28.6	8.4	74.7	492	466
2	62.46	69	AV1	436	26.8	47.3	51.6	30.2	9.1	73.7	478	437
3	62.47	69	AV1	433	27.8	46.9	50.9	33.1	9.3	75.1	477	427
4	62.49	69	AV1	420	26.5	45.5	48.6	33.0	9.0	73.5	466	413
5	62.50	69	AV1	409	26.3	44.3	46.8	35.4	9.0	73.3	468	411

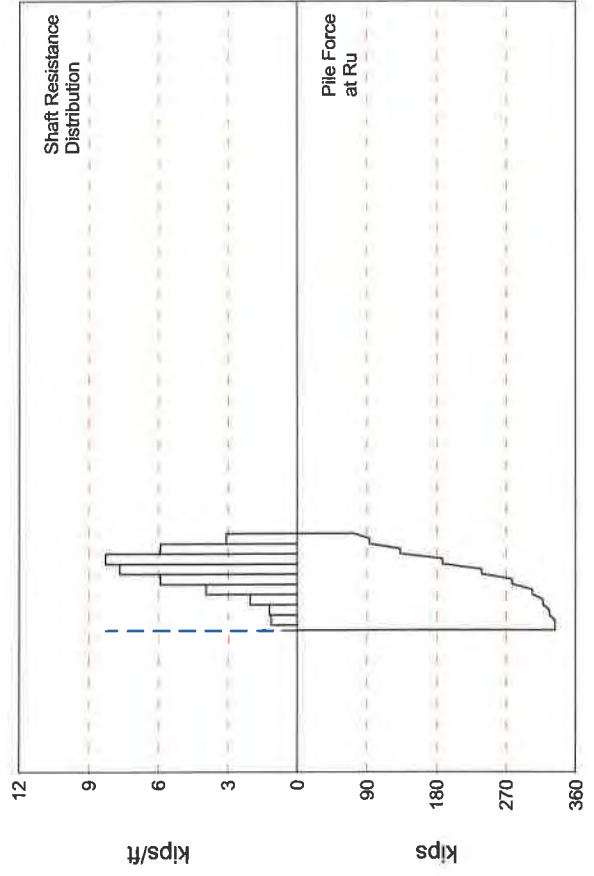
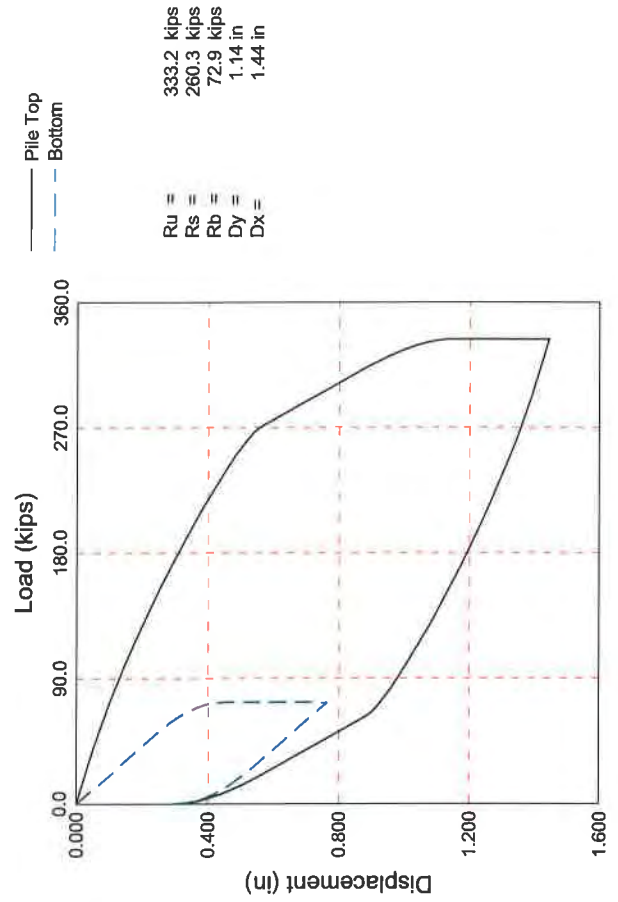
Time Summary

Drive 6 seconds

8:22:56 AM - 8:23:02 AM (6/18/2012) BN 1 - 5



C-32



Bridge 10003; File: Reaction File 3 Initial  
 12" x 1/4" CIP, D19-42; Blow: 549  
 Braun Intertec Corp.

Test: 15-Jun-2012 12:12:  
 CAPWAP (R) 2006-3  
 OP: KAA

#### CAPWAP SUMMARY RESULTS

Total CAPWAP Capacity:		333.2; along Shaft	260.3; at Toe	72.9 kips				
Soil Sgmt No.	Dist. Below Gages ft	Depth Below Grade ft	Ru kips	Force in Pile kips	Sum of Ru kips	Unit Resist. (Depth) kips/ft	Unit Resist. (Area) ksf	Smith Damping Factor s/ft
				333.2				
1	9.9	8.9	7.6	325.6	7.6	0.85	0.27	0.144
2	16.6	15.6	8.0	317.6	15.6	1.21	0.38	0.144
3	23.2	22.2	13.6	304.0	29.2	2.05	0.65	0.144
4	29.8	28.8	26.2	277.8	55.4	3.95	1.26	0.144
5	36.5	35.5	39.3	238.5	94.7	5.93	1.89	0.144
6	43.1	42.1	50.9	187.6	145.6	7.68	2.44	0.144
7	49.7	48.7	54.9	132.7	200.5	8.28	2.64	0.144
8	56.4	55.4	39.3	93.4	239.8	5.93	1.89	0.144
9	63.0	62.0	20.5	72.9	260.3	3.09	0.98	0.144
Avg. Shaft			28.9			4.20	1.34	0.144
Toe			72.9				92.82	0.024

Soil Model Parameters/Extensions		Shaft	Toe
Quake	(in)	0.040	0.355
Case Damping Factor		2.276	0.106
Damping Type			Smith
Unloading Quake	(% of loading quake)	30	100
Reloading Level	(% of Ru)	100	100
Unloading Level	(% of Ru)	17	
Resistance Gap (included in Toe Quake)	(in)		0.000
Soil Plug Weight	(kips)		0.17
Soil Support Dashpot		3.800	0.000
Soil Support Weight	(kips)	2.18	0.00

CAPWAP match quality = 2.68 (Wave Up Match) ; RSA = 0  
 Observed: final set = 0.300 in; blow count = 40 b/ft  
 Computed: final set = 0.265 in; blow count = 45 b/ft  
 max. Top Comp. Stress = 39.4 ksi (T= 31.2 ms, max= 1.033 x Top)  
 max. Comp. Stress = 40.7 ksi (Z= 9.9 ft, T= 31.4 ms)  
 max. Tens. Stress = 0.00 ksi (Z= 3.3 ft, T= 0.0 ms)  
 max. Energy (EMX) = 20.5 kip-ft; max. Measured Top Displ. (DMX)= 0.91 in

Bridge 10003; Pile: Reaction Pile 3 Initial  
 12" x 1/4" CIP, D19-42; Blow: 549  
 Braun Intertec Corp.

Test: 15-Jun-2012 12:12:  
 CAPWAP (R) 2006-3  
 OP: KAA

EXTREMA TABLE

File Sgmt No.	Dist. Below Gages ft	max. Force kips	min. Force kips	max. Comp. Stress ksi	max. Tens. Stress ksi	max. Trnsfd. Energy kip-ft	max. Veloc. ft/s	max. Displ. in
1	3.3	363.7	0.0	39.4	0.00	20.46	15.1	0.870
2	6.6	371.5	0.0	40.3	0.00	19.90	14.8	0.826
3	9.9	375.6	0.0	40.7	0.00	19.36	14.4	0.783
4	13.3	369.7	0.0	40.1	0.00	17.77	13.9	0.741
5	16.6	375.1	0.0	40.6	0.00	17.29	13.6	0.700
6	19.9	366.5	0.0	39.7	0.00	15.86	13.0	0.661
7	23.2	372.5	0.0	40.3	0.00	15.43	12.5	0.622
8	26.5	354.0	0.0	38.4	0.00	13.72	11.7	0.585
9	29.8	357.4	0.0	38.7	0.00	13.35	10.9	0.550
10	33.2	321.0	0.0	34.8	0.00	11.09	10.0	0.518
11	36.5	328.6	0.0	35.6	0.00	10.84	8.8	0.488
12	39.8	274.6	0.0	29.8	0.00	8.45	7.9	0.467
13	43.1	266.3	0.0	28.8	0.00	8.33	6.6	0.446
14	46.4	199.5	0.0	21.6	0.00	5.92	6.0	0.428
15	49.7	198.0	0.0	21.5	0.00	5.85	5.4	0.413
16	53.1	130.9	0.0	14.2	0.00	3.65	5.4	0.398
17	56.4	129.2	0.0	14.0	0.00	3.58	5.4	0.383
18	59.7	98.3	0.0	10.6	0.00	2.03	5.6	0.370
19	63.0	95.0	0.0	10.3	0.00	1.18	5.3	0.358
Absolute	9.9			40.7			(T =	31.4 ms)
	3.3				0.00		(T =	0.0 ms)

CASE METHOD

J =	0.0	0.1	0.2	0.3	0.4	0.5	0.6	0.7	0.8	0.9
RP	436.4	424.1	411.8	399.5	387.2	374.9	362.6	350.3	338.0	325.7
RX	436.4	424.1	411.8	399.5	387.2	374.9	362.6	350.3	338.0	325.7
RU	438.5	426.4	414.3	402.2	390.1	378.0	365.9	353.8	341.7	329.6

RAU = 24.8 (kips); RA2 = 359.6 (kips)

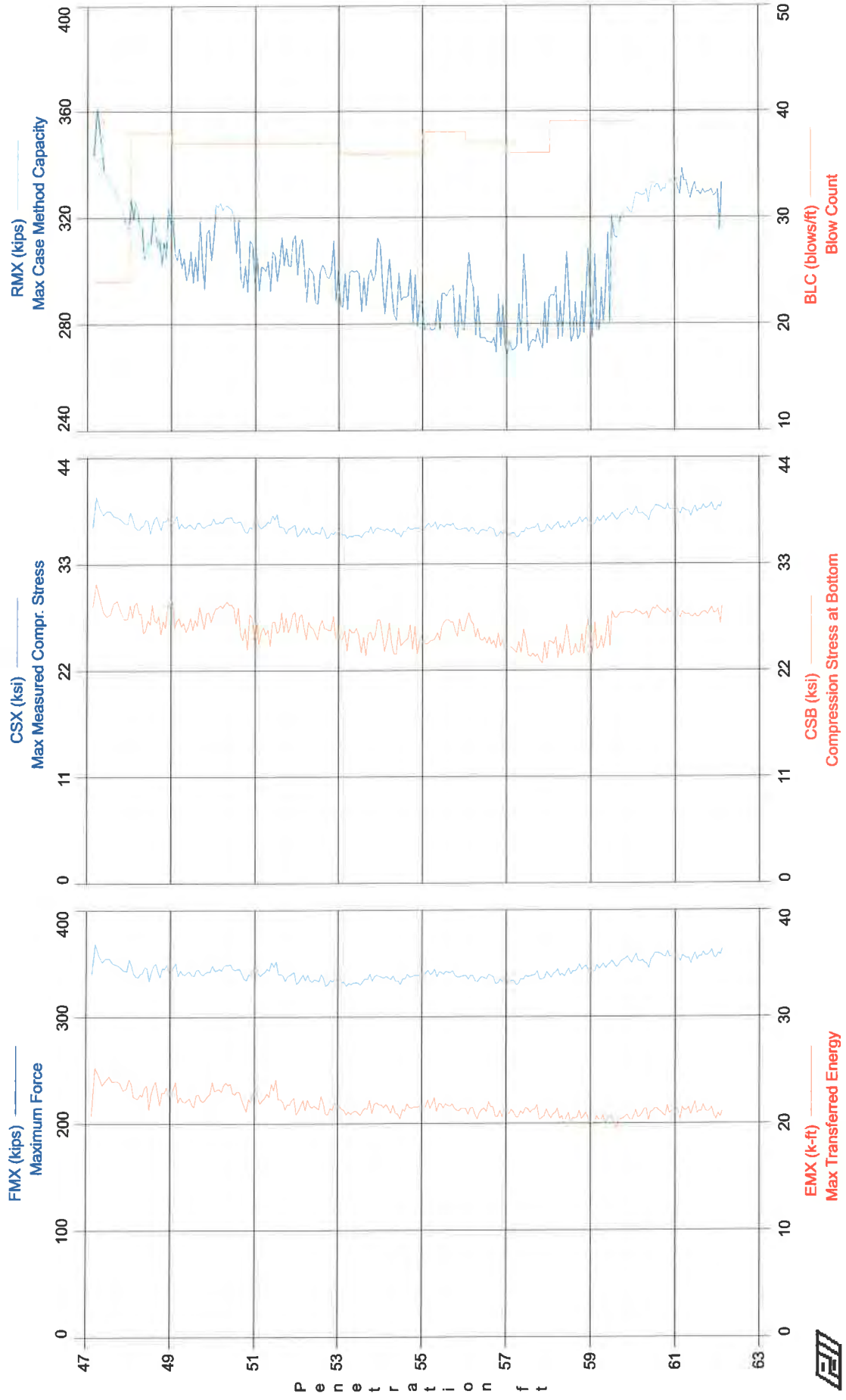
Current CAPWAP Ru = 333.2 (kips); Corresponding J(RP) = 0.84; J(RX) = 0.84

VMX	TVP	VT1*Z	FT1	FMX	DMX	DFN	SET	EMX	QUS
ft/s	ms	kips	kips	kips	in	in	in	kip-ft	kips
16.85	26.24	262.4	297.0	360.5	0.907	0.287	0.300	21.0	417.9

Bridge 10003; Pile: Reaction Pile 3 Initial  
 12" x 1/4" CIP, D19-42; Blow: 549  
 Braun Intertec Corp.

Test: 15-Jun-2012 12:12:  
 CAPWAP (R) 2006-3  
 OP: KAA

PILE PROFILE AND PILE MODEL				
Depth ft	Area in <sup>2</sup>	E-Modulus ksi	Spec. Weight lb/ft <sup>3</sup>	Perim. ft
0.00	9.23	29992.2	492.000	3.142
63.00	9.23	29992.2	492.000	3.142
Toe Area	0.785	ft <sup>2</sup>		
Top Segment Length	3.32 ft,	Top Impedance	16.47 kips/ft/s	
File Damping	1.0 %,	Time Incr	0.197 ms,	Wave Speed 16807.9 ft/s, 2L/c 7.5 ms



Bridge 10003 - Reaction Pile 3 Initial  
OP: KAA

12" x 1/4" CIP, D19-42  
Test date: 15-Jun-2012

AR: 9.23 in^2  
LE: 63.00 ft  
WS: 16,807.9 f/s

SP: 0.492 k/ft^3  
EM: 30,000 ksi  
JC: 0.84

FMX: Maximum Force  
EMX: Max Transferred Energy  
CSX: Max Measured Compr. Stress  
CSI: Max F1 or F2 Compr. Stress  
CSB: Compression Stress at Bottom

STK: O.E. Diesel Hammer Stroke  
ETH: Energy Transfer Ratio - Stroke  
RX5: Max Case Method Capacity (JC=0.5)  
RMX: Max Case Method Capacity

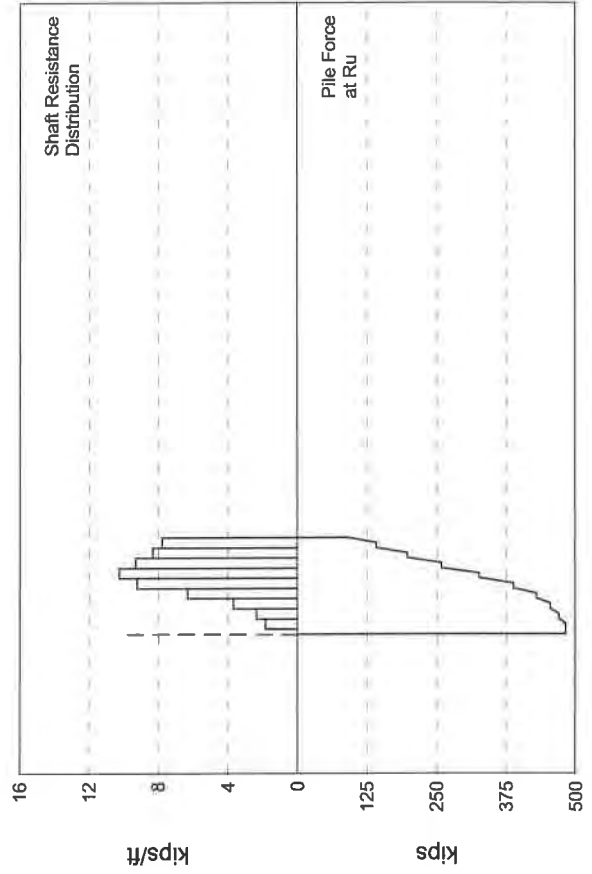
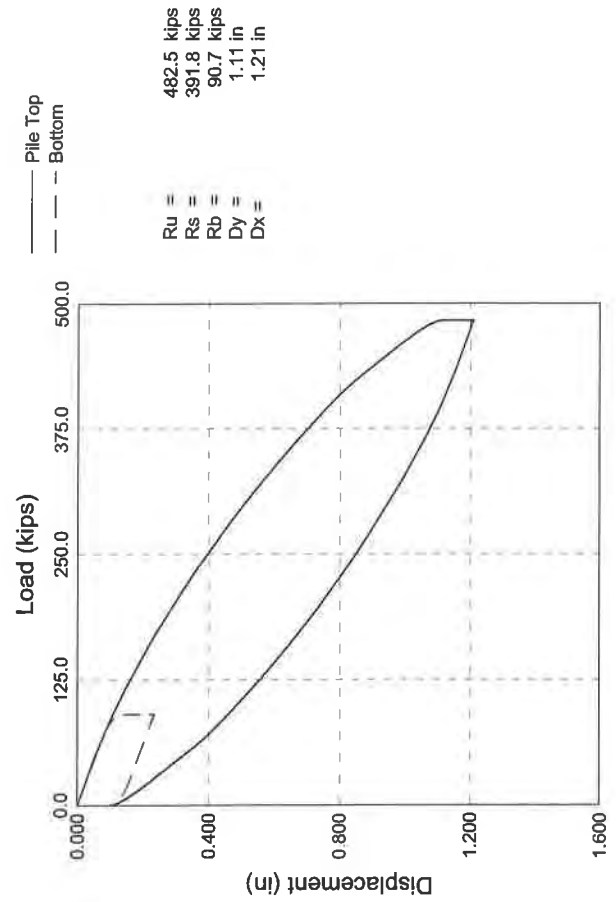
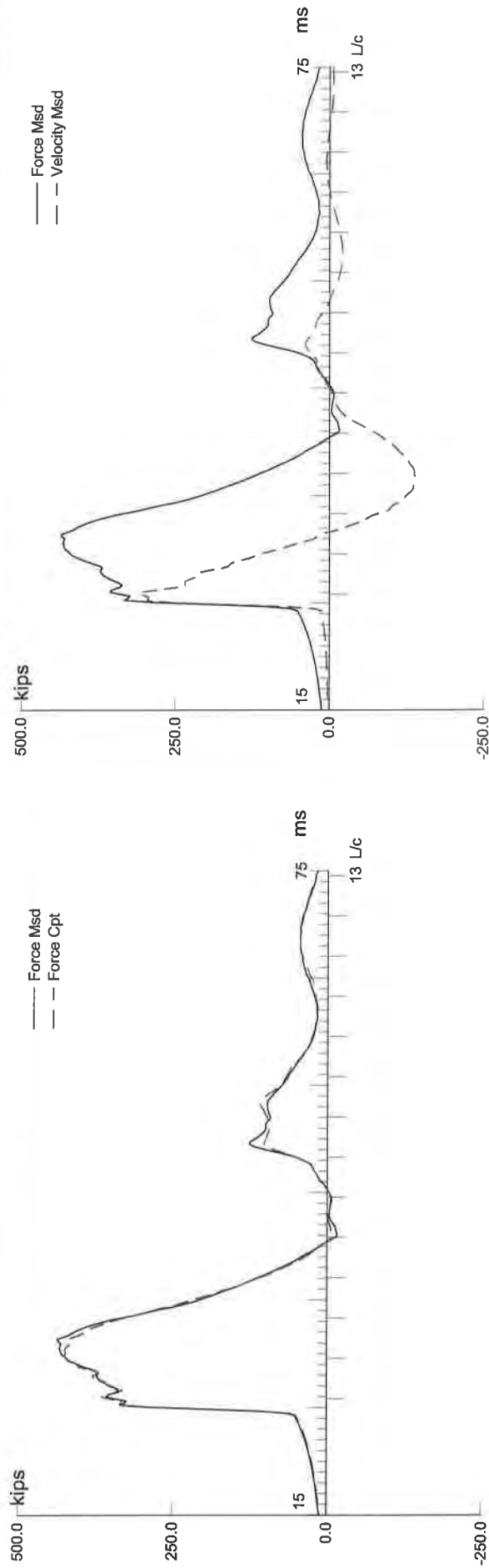
BL#	depth	BLC	TYPE	FMX	EMX	CSX	CSI	CSB	STK	ETH	RX5	RMX
end	ft	bl/ft		kips	k-ft	ksi	ksi	ksi	ft	(%)	kips	kips
22	48.00	24	AV22	351	23.7	38.1	40.3	28.5	8.0	74.1	380	334
60	49.00	38	AV38	344	22.9	37.3	38.6	27.6	7.9	72.6	362	315
97	50.00	37	AV37	343	22.5	37.1	39.9	27.2	7.8	72.0	354	306
134	51.00	37	AV37	344	22.9	37.3	40.3	27.5	7.9	72.0	358	313
171	52.00	37	AV37	342	22.4	37.1	42.6	26.4	7.9	70.7	346	303
208	53.00	37	AV37	335	21.6	36.3	42.4	26.5	7.9	68.5	343	300
244	54.00	36	AV36	334	21.4	36.2	43.0	25.6	7.9	67.3	337	297
280	55.00	36	AV36	337	21.4	36.5	43.4	25.1	8.0	67.0	333	291
318	56.00	38	AV38	341	21.6	36.9	43.0	26.0	8.1	66.8	333	284
355	57.00	37	AV37	336	21.2	36.4	42.4	25.6	8.0	65.9	331	281
391	58.00	36	AV36	337	21.0	36.5	42.3	24.0	8.0	65.8	328	277
430	59.00	39	AV39	343	20.6	37.1	43.4	24.8	7.9	65.0	334	287
469	60.00	39	AV39	350	20.3	37.9	44.5	26.6	7.9	64.4	349	305
509	61.00	40	AV40	356	21.1	38.5	43.9	28.0	8.0	65.9	373	331
549	62.00	40	AV40	357	21.2	38.7	41.7	27.8	8.0	65.9	373	331
553	62.10	40	AV4	360	20.8	39.0	40.9	27.7	8.0	65.2	365	323

Time Summary

Drive 13 minutes 10 seconds

11:59:04 AM - 12:12:14 PM (6/15/2012) BN 1 - 553





Bridge 10003; Pile: Reaction Pile 3 Restrike  
 12" x 1/4" CIP, D19-42; Blow: 1  
 Braun Intertec Corp.

Test: 18-Jun-2012 08:44:  
 CAPWAP(R) 2006-3  
 OP: KAA

#### CAPWAP SUMMARY RESULTS

Total CAPWAP Capacity:			482.5; along Shaft		391.8; at Toe		90.7 kips		
Soil Sgmnt No.	Dist. Below Gages	Depth Below Grade	Ru	Force in Pile	Sum of Ru	Unit Resist. (Depth)	Unit Resist. (Area)	Smith Damping Factor	Quake
	ft	ft	kips	kips	kips	kips/ft	ksf	s/ft	in
				482.5					
1	9.9	9.1	12.3	470.2	12.3	1.35	0.43	0.167	0.040
2	16.6	15.7	15.7	454.5	28.0	2.37	0.75	0.167	0.040
3	23.2	22.4	24.5	430.0	52.5	3.69	1.18	0.167	0.040
4	29.8	29.0	41.9	388.1	94.4	6.32	2.01	0.167	0.040
5	36.5	35.6	61.2	326.9	155.6	9.23	2.94	0.167	0.040
6	43.1	42.3	68.0	258.9	223.6	10.25	3.26	0.167	0.040
7	49.7	48.9	61.6	197.3	285.2	9.29	2.96	0.167	0.040
8	56.4	55.5	55.1	142.2	340.3	8.31	2.64	0.167	0.040
9	63.0	62.2	51.5	90.7	391.8	7.77	2.47	0.167	0.029
Avg. Shaft			43.5			6.30	2.01	0.167	0.038
Toe			90.7				115.48	0.390	0.104
Soil Model Parameters/Extensions						Shaft	Toe		
Case Damping Factor						3.981	2.150		
Unloading Quake			(% of loading quake)			30	30		
Reloading Level			(% of Ru)			100	100		
Unloading Level			(% of Ru)			23			
Soil Plug Weight			(kips)				0.31		
Soil Support Dashpot						7.973	0.000		
Soil Support Weight			(kips)			2.18	0.00		
CAPWAP match quality			=	1.93	(Wave Up Match) ; RSA = 0				
Observed: final set			=	0.100 in;	blow count	=	120 b/ft		
Computed: final set			=	0.117 in;	blow count	=	103 b/ft		
max. Top Comp. Stress			=	47.1 ksi	(T= 30.4 ms, max= 1.035 x Top)				
max. Comp. Stress			=	48.8 ksi	(Z= 9.9 ft, T= 30.4 ms)				
max. Tens. Stress			=	-2.76 ksi	(Z= 9.9 ft, T= 41.8 ms)				
max. Energy (EMX)			=	24.6 kip-ft;	max. Measured Top Displ. (DMX)= 0.90 in				

Bridge 10003; Pile: Reaction Pile 3 Restrike  
 12" x 1/4" CIP, D19-42; Blow: 1  
 Braun Intertec Corp.

Test: 18-Jun-2012 08:44:  
 CAPWAP(R) 2006-3  
 OP: KAA

EXTREMA TABLE

Pile Sgmt No.	Dist. Below Gages ft	max. Force kips	min. Force kips	max. Comp. Stress ksi	max. Tens. Stress ksi	max. Trnsfd. Energy kip-ft	max. Veloc. ft/s	max. Displ. in
1	3.3	434.7	-14.1	47.1	-1.53	24.62	17.7	0.862
2	6.6	443.2	-20.4	48.0	-2.21	23.61	17.1	0.803
3	9.9	450.1	-25.5	48.8	-2.76	22.60	16.5	0.743
4	13.3	435.9	-21.4	47.2	-2.32	19.65	15.8	0.686
5	16.6	440.6	-25.2	47.7	-2.73	18.69	15.0	0.628
6	19.9	421.8	-18.7	45.7	-2.02	15.85	14.1	0.573
7	23.2	428.3	-21.8	46.4	-2.36	14.97	12.9	0.517
8	26.5	398.2	-11.0	43.1	-1.20	12.03	11.7	0.465
9	29.8	398.9	-14.4	43.2	-1.56	11.26	10.0	0.413
10	33.2	352.2	0.0	38.2	0.00	8.26	8.8	0.367
11	36.5	355.4	-0.4	38.5	-0.04	7.70	7.1	0.323
12	39.8	297.6	0.0	32.2	0.00	5.21	6.2	0.285
13	43.1	301.0	0.0	32.6	0.00	4.81	5.0	0.248
14	46.4	242.1	0.0	26.2	0.00	3.11	4.3	0.216
15	49.7	244.3	0.0	26.5	0.00	2.85	3.5	0.187
16	53.1	193.7	0.0	21.0	0.00	1.85	3.1	0.162
17	56.4	195.1	0.0	21.1	0.00	1.69	2.5	0.139
18	59.7	148.9	0.0	16.1	0.00	1.11	2.0	0.121
19	63.0	150.7	0.0	16.3	0.00	0.65	1.3	0.104
Absolute	9.9			48.8			(T =	30.4 ms)
	9.9				-2.76		(T =	41.8 ms)

CASE METHOD

J =	0.0	0.1	0.2	0.3	0.4	0.5	0.6	0.7	0.8	0.9
RP	538.0	527.6	517.2	506.9	496.5	486.1	475.8	465.4	455.0	444.6
RX	539.7	527.6	517.2	506.9	496.5	486.1	475.8	465.4	455.0	444.6
RU	563.4	555.5	547.7	539.9	532.0	524.2	516.4	508.5	500.7	492.9

RAU = 1.5 (kips); RA2 = 477.9 (kips)

Current CAPWAP Ru = 482.5 (kips); Corresponding J(RP)= 0.54; J(RX) = 0.54

VMX	TVP	VT1*Z	FT1	FMX	DMX	DFN	SET	EMX	QUS
ft/s	ms	kips	kips	kips	in	in	in	kip-ft	kips
19.05	26.04	301.3	340.4	438.7	0.897	0.080	0.100	25.2	606.2

Bridge 10003; Pile: Reaction Pile 3 Restrike  
 12" x 1/4" CIP, D19-42; Blow: 1  
 Braun Intertec Corp.

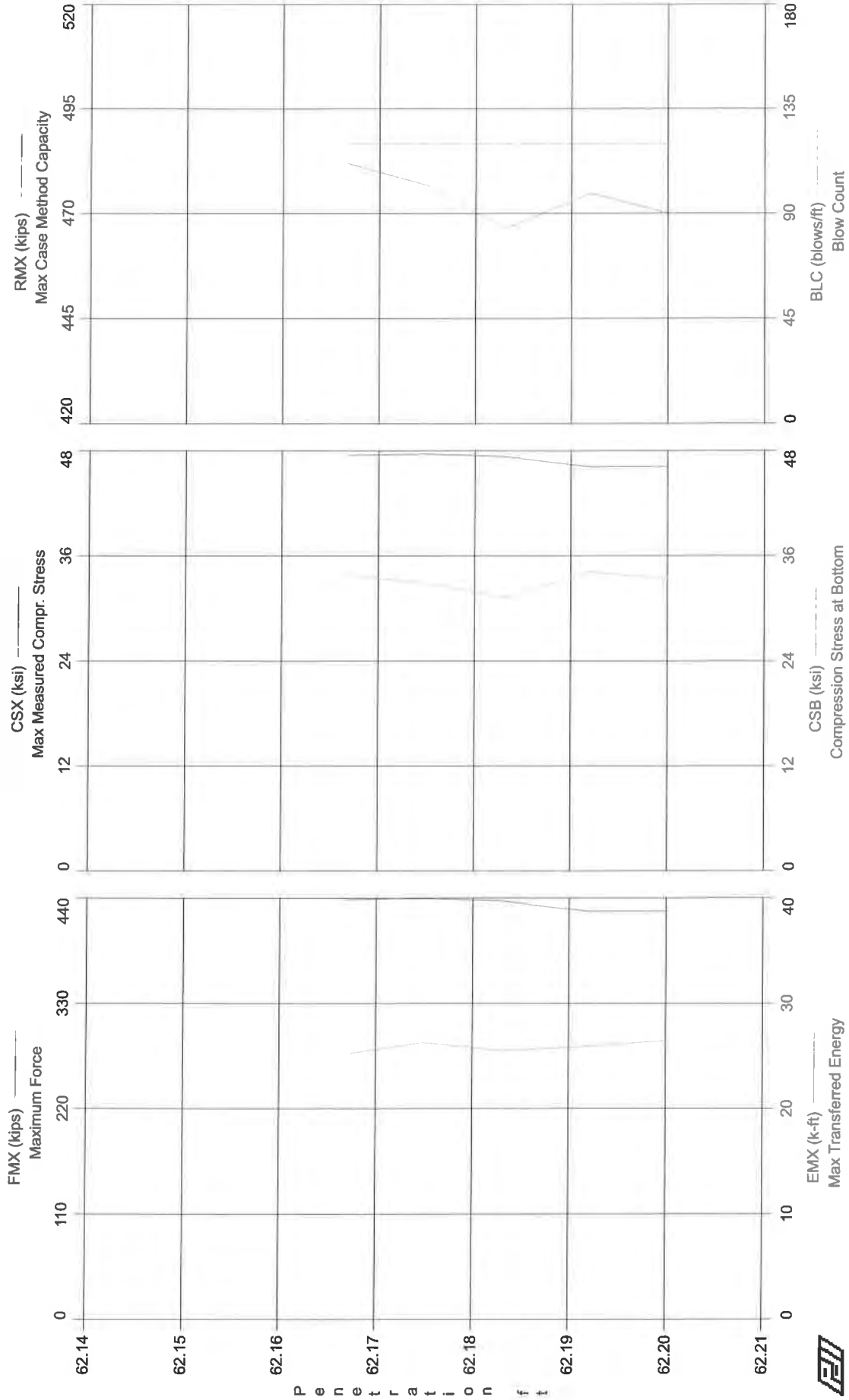
Test: 18-Jun-2012 08:44:  
 CAPWAP (R) 2006-3  
 OP: KAA

FILE PROFILE AND PILE MODEL				
Depth ft	Area in <sup>2</sup>	E-Modulus ksi	Spec. Weight lb/ft <sup>3</sup>	Perim. ft
0.00	9.23	29992.2	492.000	3.142
63.00	9.23	29992.2	492.000	3.142
Toe Area 0.785 ft <sup>2</sup>				
Top Segment Length 3.32 ft, Top Impedance 16.47 kips/ft/s				
Pile Damping 1.0 %, Time Incr 0.197 ms, Wave Speed 16807.9 ft/s, 2L/c 7.5 ms				

Braun Intertec Corp. - Case Method Results

Test date: 18-Jun-2012

Bridge 10003 - Reaction Pile 3 Restrike



Braun Intertec Corp.  
Case Method Results

Page 1 of 1  
PDILOT Ver. 2010.2 - Printed: 11-Jul-2012

Bridge 10003 - Reaction Pile 3 Restrike  
OP: KAA

12" x 1/4" CIP, D19-42  
Test date: 18-Jun-2012

AR: 9.23 in^2  
LE: 63.00 ft  
WS: 16,807.9 f/s

SP: 0.492 k/ft3  
EM: 30,000 ksi  
JC: 0.54

FMX: Maximum Force  
EMX: Max Transferred Energy  
CSX: Max Measured Compr. Stress  
CSI: Max F1 or F2 Compr. Stress  
CSB: Compression Stress at Bottom

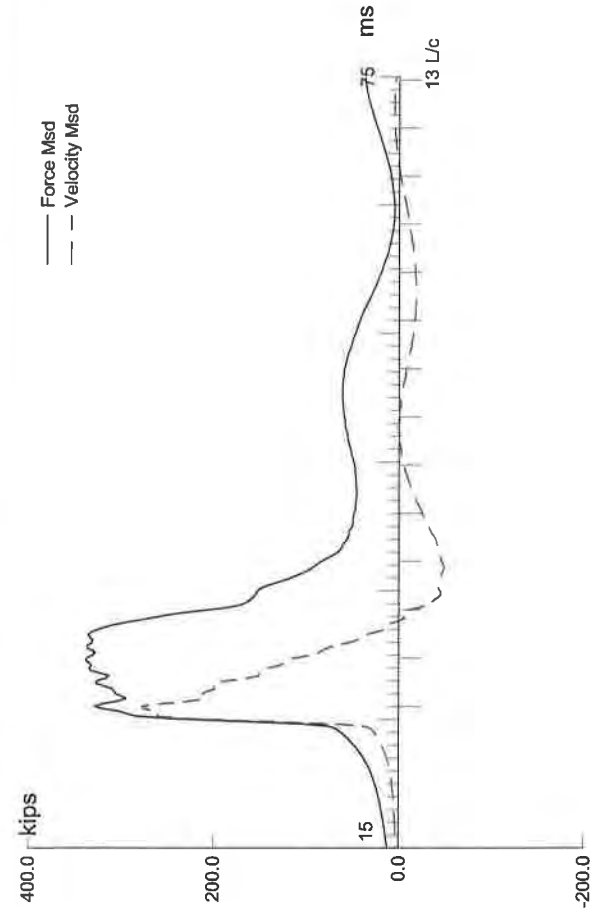
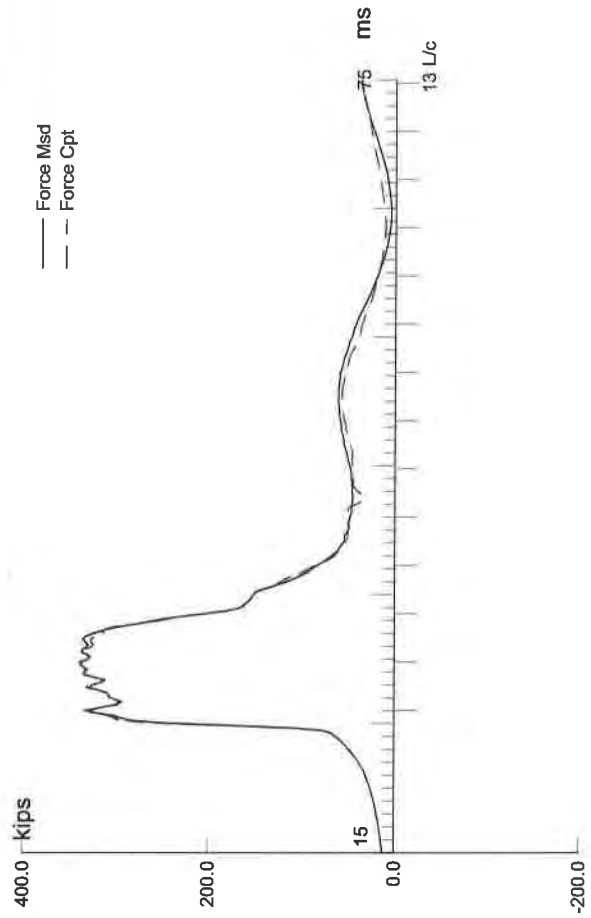
STK: O.E. Diesel Hammer Stroke  
ETH: Energy Transfer Ratio - Stroke  
RX5: Max Case Method Capacity (JC=0.5)  
RMX: Max Case Method Capacity

BL#	depth	BLC	TYPE	FMX	EMX	CSX	CSI	CSB	STK	ETH	RX5	RMX
end	ft	bl/ft		kips	k-ft	ksi	ksi	ksi	ft	(%)	kips	kips
1	62.17	120	AV1	439	25.2	47.5	49.2	33.8	8.9	70.5	486	482
2	62.18	120	AV1	440	26.3	47.7	48.7	32.9	9.2	71.2	482	477
3	62.18	120	AV1	437	25.5	47.4	49.0	31.3	9.1	70.0	471	466
4	62.19	120	AV1	426	25.9	46.2	47.7	34.2	8.9	72.9	479	475
5	62.20	120	AV1	427	26.4	46.3	47.2	33.4	9.2	71.7	475	470

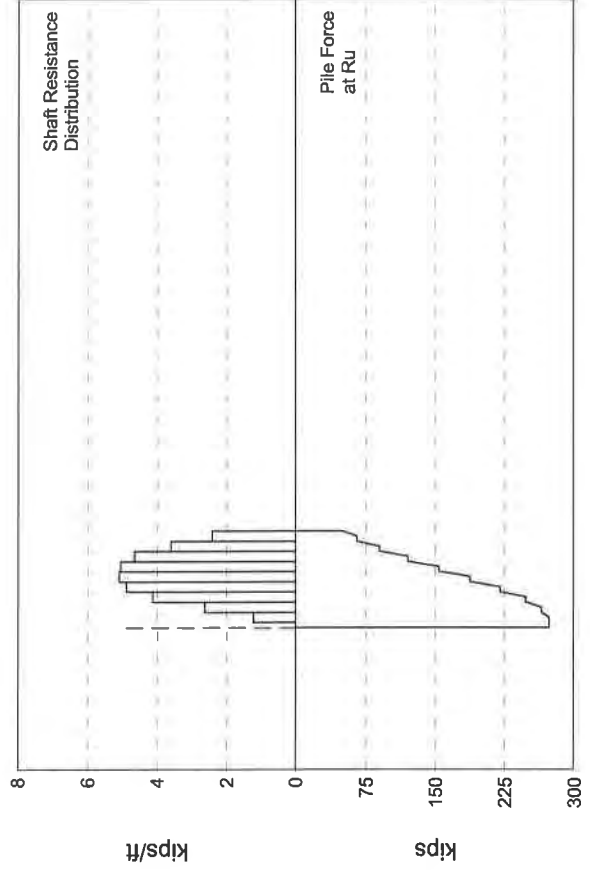
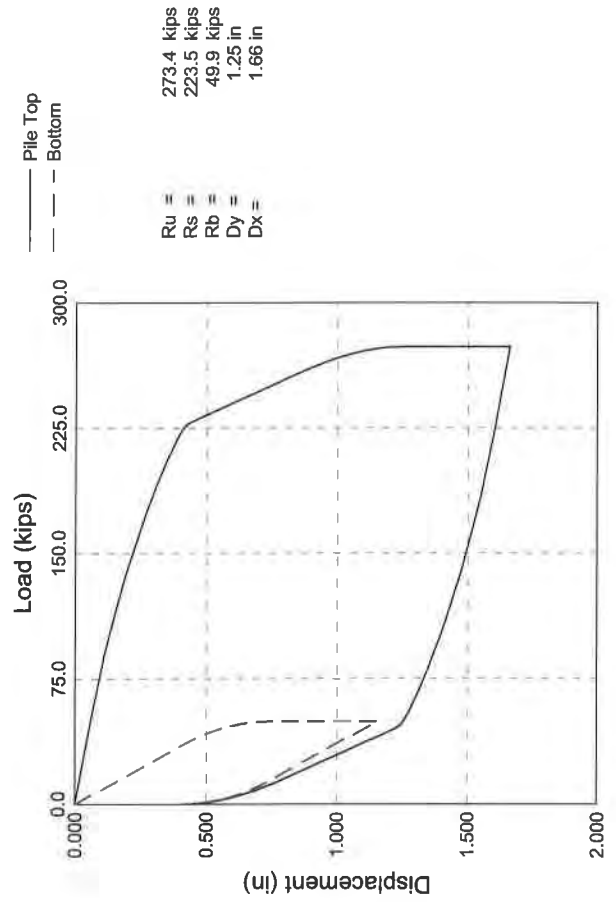
Time Summary

Drive 6 seconds

8:44:33 AM - 8:44:39 AM (6/18/2012) BN 1 - 5



C-44



Bridge 10003; File: Reaction File 4 Initial  
 12" x 1/4" CIP, D19-42; Blow: 382  
 Braun Intertec Corp.

Test: 15-Jun-2012 11:40:  
 CAPWAP (R) 2006-3  
 OP: KAA

#### CAPWAP SUMMARY RESULTS

Total CAPWAP Capacity: 273.4; along Shaft 223.5; at Toe 49.9 kips								
Soil Sgmt No.	Dist. Below Gages ft	Depth Below Grade ft	Ru kips	Force in Pile kips	Sum of Ru kips	Unit Resist. (Depth) kips/ft	Unit Resist. (Area) ksf	Smith Damping Factor s/ft
				273.4				
1	9.9	8.7	8.1	265.3	8.1	0.93	0.29	0.094
2	16.6	15.4	17.4	247.9	25.5	2.62	0.84	0.094
3	23.2	22.0	27.4	220.5	52.9	4.13	1.32	0.094
4	29.8	28.6	32.5	188.0	85.4	4.90	1.56	0.094
5	36.5	35.3	33.8	154.2	119.2	5.10	1.62	0.094
6	43.1	41.9	33.5	120.7	152.7	5.05	1.61	0.094
7	49.7	48.5	30.9	89.8	183.6	4.66	1.48	0.094
8	56.4	55.2	23.9	65.9	207.5	3.60	1.15	0.094
9	63.0	61.8	16.0	49.9	223.5	2.41	0.77	0.094
Avg. Shaft			24.8			3.62	1.15	0.094
Toe			49.9				63.53	0.028

Soil Model Parameters/Extensions		Shaft	Toe
Quake	(in)	0.040	0.571
Case Damping Factor		1.272	0.086
Damping Type			Smith
Unloading Quake	(% of loading quake)	30	35
Reloading Level	(% of Ru)	100	100
Unloading Level	(% of Ru)	0	
Resistance Gap (included in Toe Quake)	(in)		0.000
Soil Plug Weight	(kips)		0.24
Soil Support Dashpot		4.900	0.000
Soil Support Weight	(kips)	2.18	0.00

CAPWAP match quality = 2.18 (Wave Up Match) ; RSA = 0  
 Observed: final set = 0.414 in; blow count = 29 b/ft  
 Computed: final set = 0.460 in; blow count = 26 b/ft  
 max. Top Comp. Stress = 37.5 ksi (T= 30.0 ms, max= 1.049 x Top)  
 max. Comp. Stress = 39.4 ksi (Z= 16.6 ft, T= 29.0 ms)  
 max. Tens. Stress = 0.00 ksi (Z= 3.3 ft, T= 0.0 ms)  
 max. Energy (EMX) = 21.4 kip-ft; max. Measured Top Displ. (DMX)= 0.92 in



Bridge 10003; Pile: Reaction Pile 4 Initial  
 12" x 1/4" CIP, D19-42; Blow: 382  
 Braun Intertec Corp.

Test: 15-Jun-2012 11:40:  
 CAPWAP (R) 2006-3  
 OP: KAA

# EXTREMA TABLE

Pile Sgmnt No.	Dist. Below Gages ft	max. Force kips	min. Force kips	max. Comp. Stress ksi	max. Tens. Stress ksi	max. Trnsfd. Energy kip-ft	max. Veloc. ft/s	max. Displ. in
1	3.3	346.5	0.0	37.5	0.00	21.36	16.2	0.881
2	6.6	355.2	0.0	38.5	0.00	21.12	15.8	0.853
3	9.9	360.6	0.0	39.1	0.00	20.88	15.3	0.824
4	13.3	354.4	0.0	38.4	0.00	19.66	14.7	0.796
5	16.6	363.6	0.0	39.4	0.00	19.44	13.9	0.769
6	19.9	340.3	0.0	36.9	0.00	17.43	13.3	0.745
7	23.2	350.1	0.0	37.9	0.00	17.25	12.4	0.720
8	26.5	312.8	0.0	33.9	0.00	14.60	11.8	0.699
9	29.8	320.8	0.0	34.8	0.00	14.48	10.9	0.678
10	33.2	275.8	0.0	29.9	0.00	11.73	10.3	0.662
11	36.5	286.3	0.0	31.0	0.00	11.66	9.5	0.646
12	39.8	242.4	0.0	26.3	0.00	9.05	8.9	0.634
13	43.1	235.4	0.0	25.5	0.00	9.01	8.6	0.622
14	46.4	188.3	0.0	20.4	0.00	6.55	8.5	0.611
15	49.7	196.7	0.0	21.3	0.00	6.51	9.4	0.600
16	53.1	164.8	0.0	17.9	0.00	4.30	9.6	0.591
17	56.4	156.6	0.0	17.0	0.00	4.28	9.4	0.583
18	59.7	111.1	0.0	12.0	0.00	2.57	9.4	0.578
19	63.0	97.8	0.0	10.6	0.00	1.38	10.0	0.571
Absolute	16.6			39.4			(T =	29.0 ms)
	3.3				0.00		(T =	0.0 ms)

# CASE METHOD

J =	0.0	0.1	0.2	0.3	0.4	0.5	0.6	0.7	0.8	0.9
RP	417.4	403.4	389.4	375.5	361.5	347.5	333.6	319.6	305.6	291.7
RX	414.6	395.4	377.3	359.5	341.7	324.0	306.2	288.5	270.7	252.9
RU	426.6	410.3	393.9	377.5	361.1	344.8	328.4	312.0	295.6	279.2

RAU = 53.5 (kips); RA2 = 318.4 (kips)

Current CAPWAP Ru = 273.4 (kips); Corresponding J(RP)= 1.00; J(RX) = 0.78

VMX	TVP	VT1*Z	FT1	FMX	DMX	DFN	SET	EMX	QUS
ft/s	ms	kips	kips	kips	in	in	in	kip-ft	kips
17.16	26.24	265.6	291.5	338.8	0.915	0.395	0.414	21.6	390.3

Bridge 10003; Pile: Reaction Pile 4 Initial  
 12" x 1/4" CIP, D19-42; Blow: 382  
 Braun Intertec Corp.

Test: 15-Jun-2012 11:40:  
 CAPWAP(R) 2006-3  
 OP: KAA

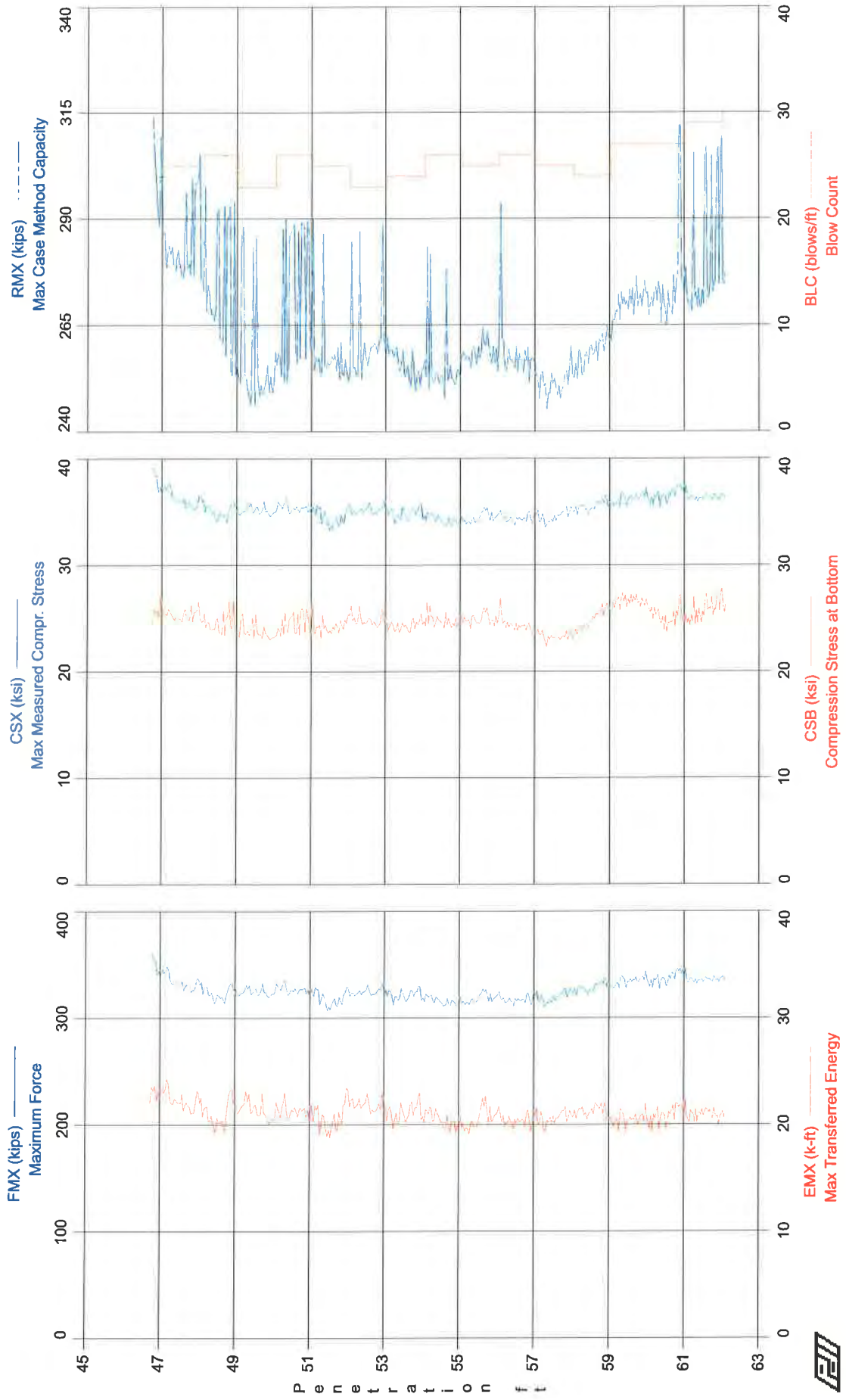
FILE PROFILE AND PILE MODEL

Depth ft	Area in <sup>2</sup>	E-Modulus ksi	Spec. Weight lb/ft <sup>3</sup>	Perim. ft
0.00	9.23	29992.2	492.000	3.142
63.00	9.23	29992.2	492.000	3.142

Toe Area 0.785 ft<sup>2</sup>

Top Segment Length 3.32 ft, Top Impedance 16.47 kips/ft/s

Pile Damping 1.0 %, Time Incr 0.197 ms, Wave Speed 16807.9 ft/s, 2L/c 7.5 ms



Bridge 10003 - Reaction Pile 4 Initial  
OP: KAA

12" x 1/4" CIP, D19-42  
Test date: 15-Jun-2012

AR: 9.23 in^2  
LE: 63.00 ft  
WS: 16,807.9 f/s

SP: 0.492 k/ft^3  
EM: 30,000 ksi  
JC: 0.78

FMX: Maximum Force  
EMX: Max Transferred Energy  
CSX: Max Measured Compr. Stress  
CSI: Max F1 or F2 Compr. Stress  
CSB: Compression Stress at Bottom

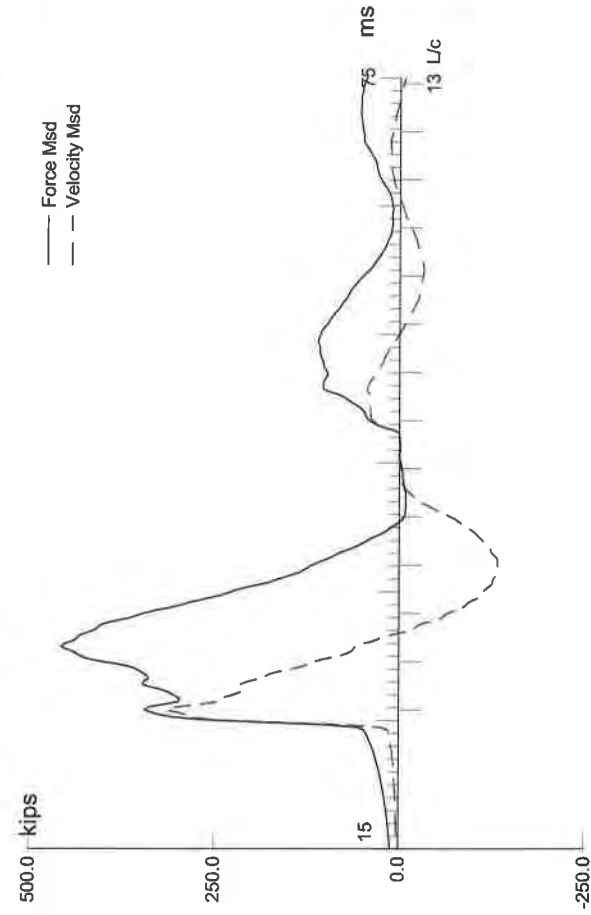
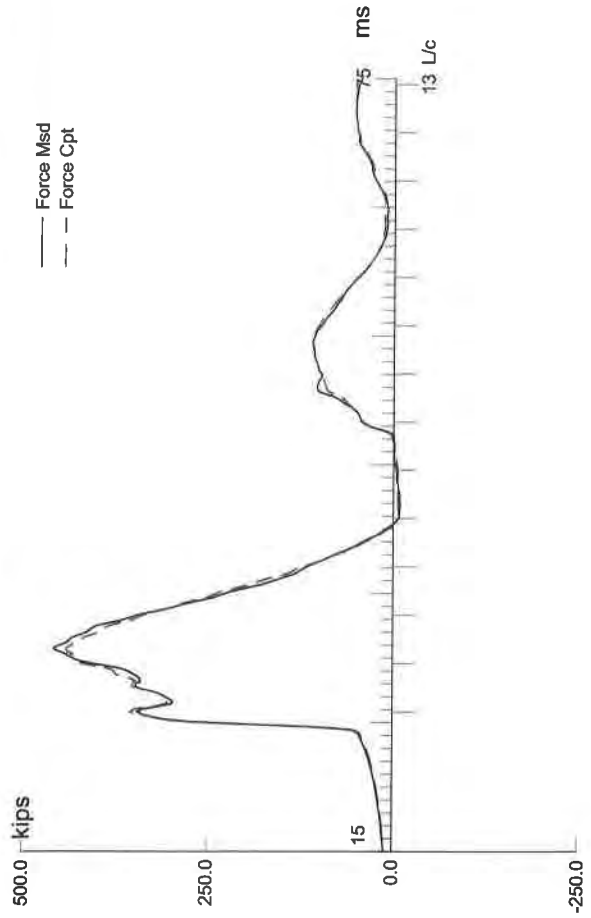
STK: O.E. Diesel Hammer Stroke  
ETH: Energy Transfer Ratio - Stroke  
RX5: Max Case Method Capacity (JC=0.5)  
RMX: Max Case Method Capacity

BL#	depth	BLC	TYPE	FMX	EMX	CSX	CSI	CSB	STK	ETH	RX5	RMX
end	ft	bl/ft		kips	k-ft	ksi	ksi	ksi	ft	(%)	kips	kips
7	47.00	24	AV7	351	23.0	38.0	49.4	25.6	7.6	75.3	343	299
32	48.00	25	AV25	335	22.4	36.3	51.5	25.4	7.6	73.2	330	285
58	49.00	26	AV26	325	21.2	35.2	46.3	24.6	7.4	71.5	317	273
81	50.00	23	AV23	325	21.5	35.2	49.5	23.8	7.4	72.3	304	257
107	51.00	26	AV26	327	21.3	35.5	48.6	24.5	7.5	71.5	315	271
132	52.00	25	AV25	319	20.7	34.6	49.6	24.3	7.4	70.2	304	258
155	53.00	23	AV23	325	21.9	35.2	53.0	24.9	7.7	71.4	309	262
179	54.00	24	AV24	322	21.2	34.9	52.5	24.4	7.6	70.1	303	256
205	55.00	26	AV26	317	20.5	34.3	52.3	24.8	7.5	68.5	302	256
230	56.00	25	AV25	319	20.6	34.5	52.1	24.9	7.5	68.2	305	259
256	57.00	26	AV26	318	20.5	34.4	52.4	24.4	7.5	68.3	305	259
281	58.00	25	AV25	320	20.7	34.6	52.8	23.3	7.6	68.1	300	252
305	59.00	24	AV24	328	21.3	35.6	55.0	24.9	7.7	68.6	307	259
332	60.00	27	AV27	335	20.5	36.3	53.0	26.6	7.6	67.6	315	270
359	61.00	27	AV27	338	20.9	36.6	51.7	25.2	7.7	68.2	318	274
388	62.00	29	AV29	336	21.0	36.4	46.9	25.8	7.7	67.9	326	282
391	62.10	30	AV3	337	21.1	36.5	45.6	26.0	7.8	67.9	324	276

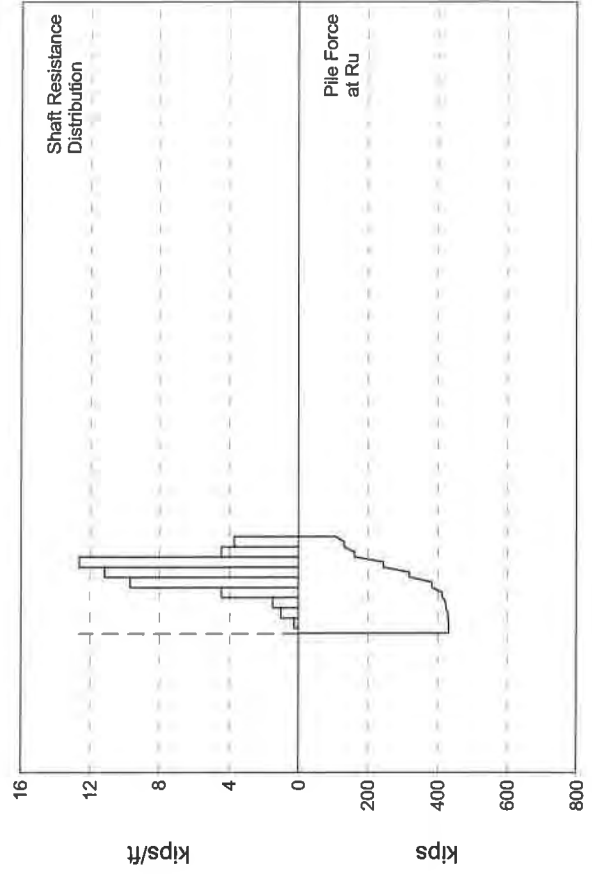
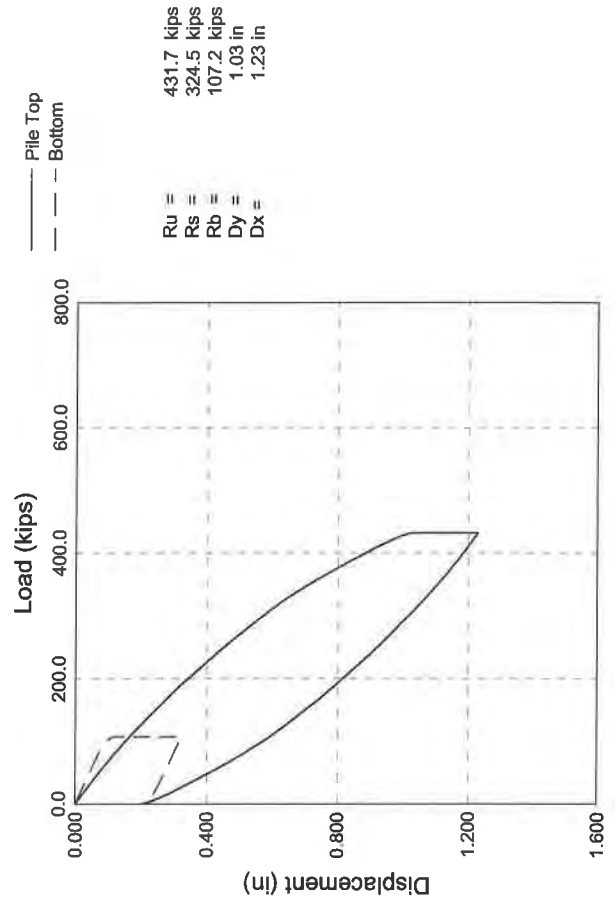
Time Summary

Drive 9 minutes 4 seconds

11:31:29 AM - 11:40:33 AM (6/15/2012) BN 1 - 391



C-50



Bridge 10003; File: Reaction File 4 Restrike  
 12" x 1/4" CIP, D19-42; Blow: 1  
 Braun Intertec Corp.

Test: 18-Jun-2012 08:57:  
 CAPWAP(R) 2006-3  
 OP: KAA

#### CAPWAP SUMMARY RESULTS

Total CAPWAP Capacity:			431.7; along Shaft		324.5; at Toe		107.2 kips		
Soil Sgmnt No.	Dist. Below Gages	Depth Below Grade	Ru kips	Force in Pile kips	Sum of Ru kips	Unit Resist. (Depth) kips/ft	Unit Resist. (Area) ksf	Smith Damping Factor s/ft	Quake in
	ft	ft							
				431.7					
1	9.9	9.1	1.7	430.0	1.7	0.19	0.06	0.402	0.040
2	16.6	15.7	6.8	423.2	8.5	1.03	0.33	0.402	0.040
3	23.2	22.3	9.8	413.4	18.3	1.48	0.47	0.402	0.040
4	29.8	29.0	29.6	383.8	47.9	4.46	1.42	0.402	0.040
5	36.5	35.6	64.2	319.6	112.1	9.68	3.08	0.402	0.040
6	43.1	42.2	74.1	245.5	186.2	11.17	3.56	0.402	0.040
7	49.7	48.9	84.0	161.5	270.2	12.67	4.03	0.402	0.040
8	56.4	55.5	29.6	131.9	299.8	4.46	1.42	0.402	0.040
9	63.0	62.1	24.7	107.2	324.5	3.72	1.19	0.402	0.039
Avg. Shaft			36.1			5.22	1.66	0.402	0.039
Toe			107.2				136.49	0.024	0.094
Soil Model Parameters/Extensions						Shaft	Toe		
Case Damping Factor						7.920	0.156		
Unloading Quake			(% of loading quake)			30	30		
Reloading Level			(% of Ru)			100	100		
Unloading Level			(% of Ru)			21			
Resistance Gap (included in Toe Quake) (in)							0.005		
Soil Plug Weight			(kips)				0.31		
Soil Support Dashpot						5.500	0.000		
Soil Support Weight			(kips)			2.18	0.00		
CAPWAP match quality			=	2.02	(Wave Up Match) ; RSA = 0				
Observed: final set			=	0.200 in;	blow count	=	60 b/ft		
Computed: final set			=	0.165 in;	blow count	=	73 b/ft		
max. Top Comp. Stress			=	48.5 ksi	(T= 31.2 ms, max= 1.015 x Top)				
max. Comp. Stress			=	49.2 ksi	(Z= 9.9 ft, T= 31.6 ms)				
max. Tens. Stress			=	-3.62 ksi	(Z= 16.6 ft, T= 41.8 ms)				
max. Energy (EMX)			=	23.4 kip-ft; max. Measured Top Displ. (DMX)= 0.92 in					

Bridge 10003; File: Reaction Pile 4 Restrike  
 12" x 1/4" CIP, D19-42; Blow: 1  
 Braun Intertec Corp.

Test: 18-Jun-2012 08:57:  
 CAPWAP (R) 2006-3  
 OP: KAA

# EXTREMA TABLE

File Sgmnt No.	Dist. Below Gages ft	max. Force kips	min. Force kips	max. Comp. Stress ksi	max. Tens. Stress ksi	max. Trnsfd. Energy kip-ft	max. Veloc. ft/s	max. Displ. in
1	3.3	447.4	-13.8	48.5	-1.50	23.42	18.1	0.869
2	6.6	450.5	-20.0	48.8	-2.17	22.48	17.8	0.812
3	9.9	453.9	-26.1	49.2	-2.82	21.51	17.0	0.754
4	13.3	452.5	-29.0	49.0	-3.14	20.01	16.5	0.697
5	16.6	453.6	-33.4	49.1	-3.62	19.06	15.4	0.640
6	19.9	440.5	-30.0	47.7	-3.25	16.58	14.7	0.584
7	23.2	441.9	-33.4	47.9	-3.61	15.71	13.1	0.530
8	26.5	422.5	-27.1	45.8	-2.94	13.38	11.2	0.478
9	29.8	425.3	-29.6	46.1	-3.20	12.67	9.5	0.429
10	33.2	375.5	-9.6	40.7	-1.04	9.50	7.6	0.386
11	36.5	379.1	-11.7	41.1	-1.27	9.07	5.7	0.347
12	39.8	301.7	-0.0	32.7	-0.00	5.99	4.8	0.315
13	43.1	304.7	-0.0	33.0	-0.00	5.74	3.5	0.286
14	46.4	233.0	-0.0	25.2	-0.00	3.74	3.0	0.261
15	49.7	235.0	-0.0	25.5	-0.00	3.60	2.6	0.240
16	53.1	180.2	-0.0	19.5	-0.00	2.24	2.4	0.219
17	56.4	181.2	-0.0	19.6	-0.00	2.12	2.0	0.199
18	59.7	148.1	-0.0	16.0	-0.00	1.52	1.9	0.181
19	63.0	148.6	-0.0	16.1	-0.00	1.05	1.5	0.163
Absolute	9.9			49.2			(T =	31.6 ms)
	16.6				-3.62		(T =	41.8 ms)

# CASE METHOD

J =	0.0	0.1	0.2	0.3	0.4	0.5	0.6	0.7	0.8	0.9
RP	535.0	522.2	509.4	496.6	483.7	470.9	458.1	445.3	432.5	419.7
RX	535.0	522.2	509.4	496.6	483.7	470.9	458.1	445.3	432.5	419.7
RU	574.5	565.6	556.7	547.9	539.0	530.1	521.2	512.4	503.5	494.6

RAU = 0.0 (kips); RA2 = 442.6 (kips)

Current CAPWAP Ru = 431.7 (kips); Corresponding J(RP)= 0.81; J(RX) = 0.81

VMX	TVP	VT1*Z	FT1	FMX	DMX	DFN	SET	EMX	QUS
ft/s	ms	kips	kips	kips	in	in	in	kip-ft	kips
19.25	26.04	317.1	346.1	458.4	0.924	0.183	0.200	24.2	517.6

Bridge 10003; Pile: Reaction Pile 4 Restrike  
 12" x 1/4" CIP, D19-42; Blow: 1  
 Braun Intertec Corp.

Test: 18-Jun-2012 08:57:  
 CAPWAP (R) 2006-3  
 OP: KAA

PILE PROFILE AND PILE MODEL

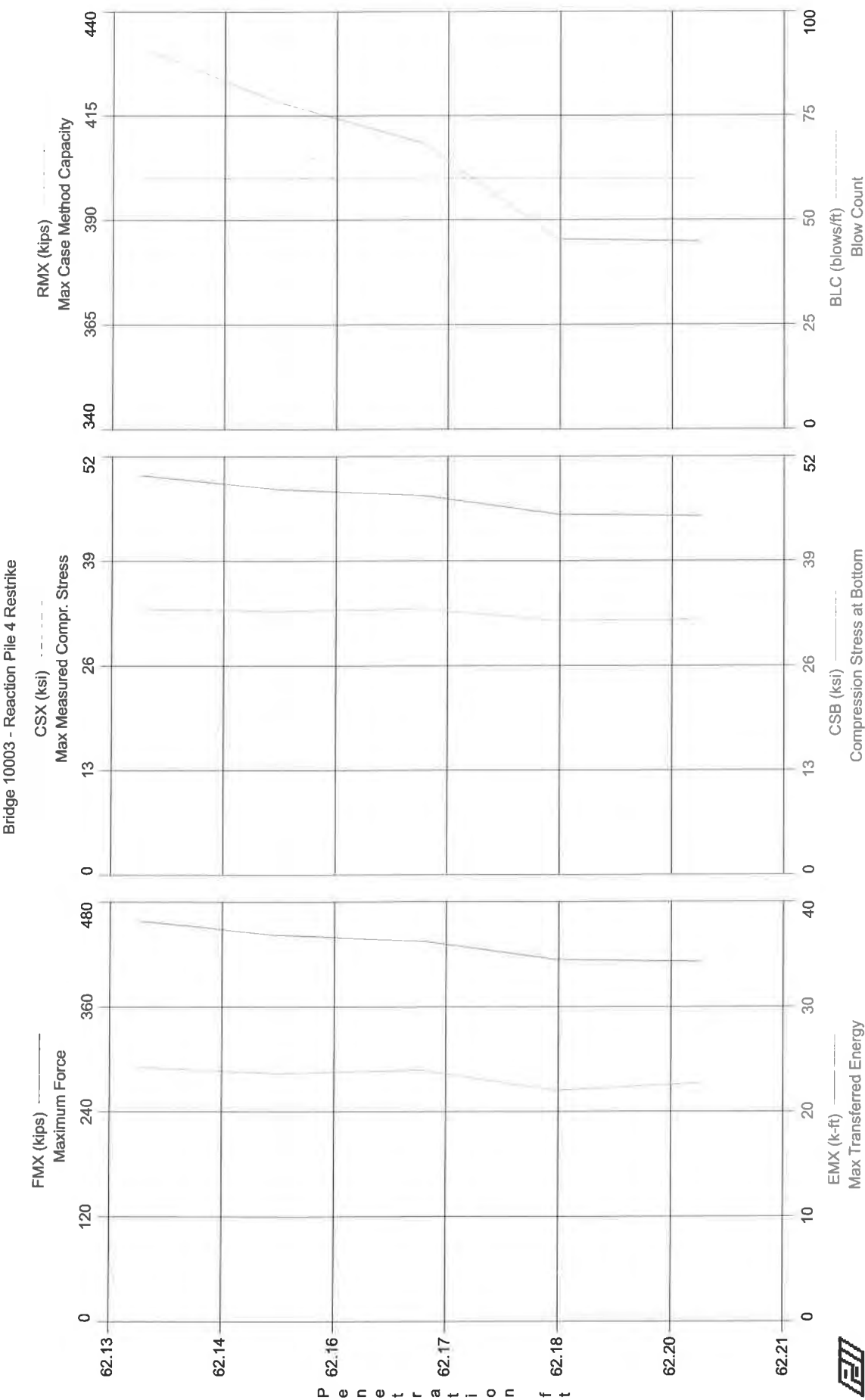
Depth ft	Area in <sup>2</sup>	E-Modulus ksi	Spec. Weight lb/ft <sup>3</sup>	Perim. ft
0.00	9.23	29992.2	492.000	3.142
63.00	9.23	29992.2	492.000	3.142

Toe Area 0.785 ft<sup>2</sup>

Segmnt Number	Dist. B.G. ft	Impedance kips/ft/s	Imped. Change %	Slack in	Tension Eff.	Compression Slack in	Eff.	Perim. ft	Soil Plug kips
1	3.32	16.47	0.00	0.000	0.000	0.000	0.000	3.142	0.00
2	6.63	16.47	0.00	0.000	0.000	0.000	0.000	3.142	0.01
19	63.00	16.47	0.00	0.000	0.000	0.000	0.000	3.142	0.01

Pile Damping 1.0 %, Time Incr 0.197 ms, Wave Speed 16807.9 ft/s, 2L/c 7.5 ms





Braun Intertec Corp.  
Case Method Results

Page 1 of 1  
PDILOT Ver. 2010.2 - Printed: 11-Jul-2012

Bridge 10003 - Reaction Pile 4 Restrike  
OP: KAA

12" x 1/4" CIP, D19-42  
Test date: 18-Jun-2012

AR: 9.23 in^2  
LE: 63.00 ft  
WS: 16,807.9 f/s

SP: 0.492 k/ft3  
EM: 30,000 ksi  
JC: 0.81

FMX: Maximum Force  
EMX: Max Transferred Energy  
CSX: Max Measured Compr. Stress  
CSI: Max F1 or F2 Compr. Stress  
CSB: Compression Stress at Bottom

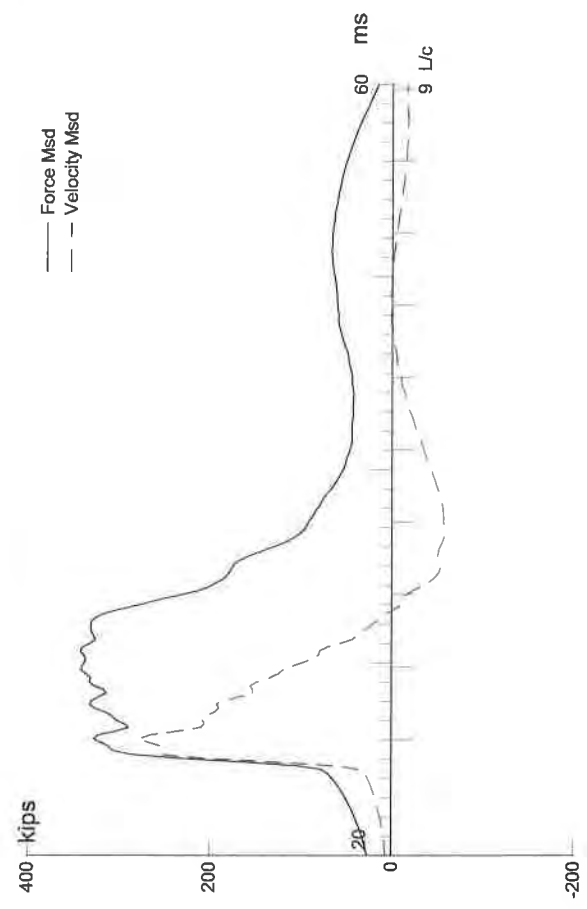
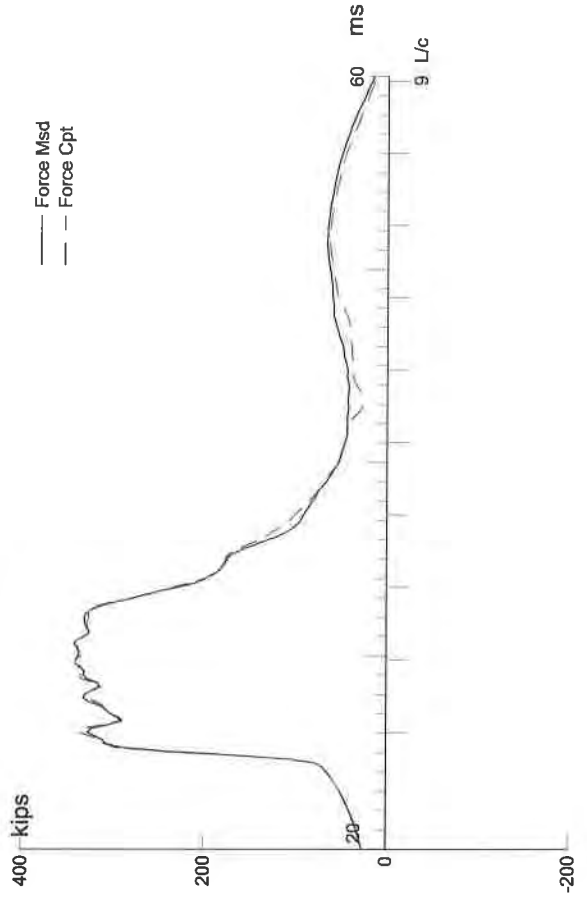
STK: O.E. Diesel Hammer Stroke  
ETH: Energy Transfer Ratio - Stroke  
RX5: Max Case Method Capacity (JC=0.5)  
RMX: Max Case Method Capacity

BL#	depth	BLC	TYPE	FMX	EMX	CSX	CSI	CSB	STK	ETH	RX5	RMX
end	ft	bl/ft		kips	k-ft	ksi	ksi	ksi	ft	(%)	kips	kips
1	62.13	60	AV1	458	24.2	49.7	60.0	33.0	9.3	65.4	471	431
2	62.15	60	AV1	442	23.6	47.9	57.4	32.8	9.1	64.8	459	418
3	62.17	60	AV1	436	24.0	47.2	55.1	33.1	9.2	65.4	450	408
4	62.18	60	AV1	414	22.0	44.9	52.8	31.7	8.7	63.6	427	386
5	62.20	60	AV1	412	22.7	44.6	51.2	31.8	8.8	64.6	427	385

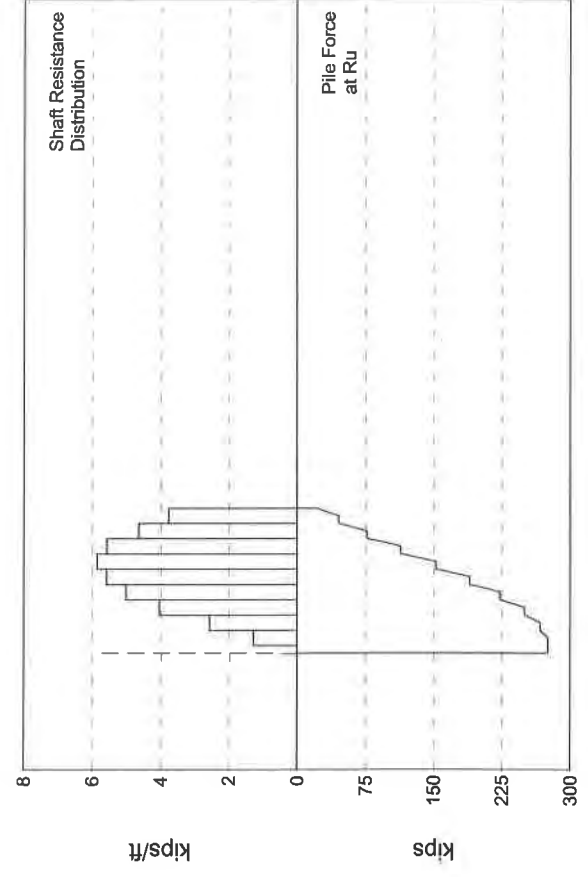
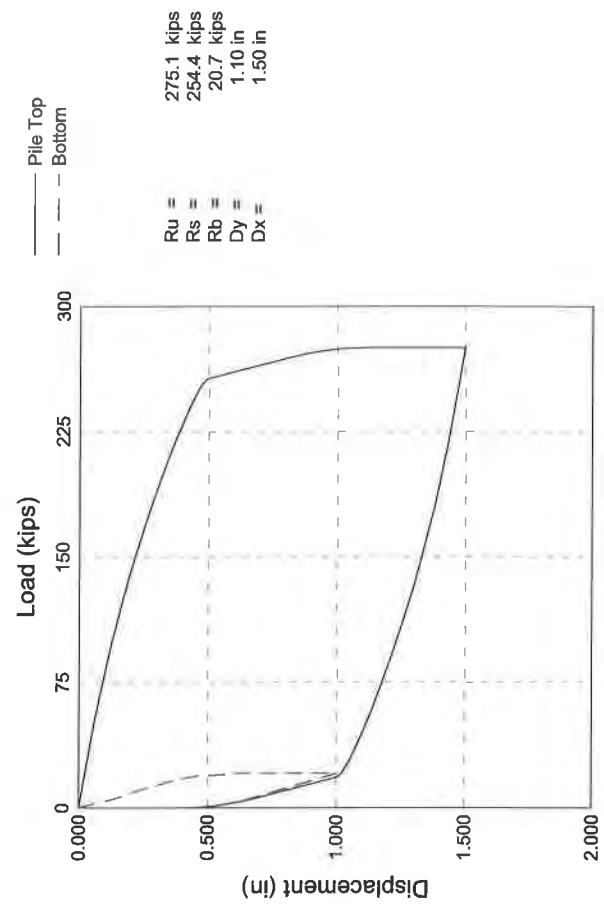
Time Summary

Drive 6 seconds

8:57:10 AM - 8:57:16 AM (6/18/2012) BN 1 - 5



C-56



Bridge 10003; File: Static Test Pile Initial  
 12" x 1/4" CIP, D19-42; Blow: 783  
 Braun Intertec

Test: 15-Jun-2012 11:15:  
 CAPWAP(R) 2006-3  
 OP: KAA

#### CAPWAP SUMMARY RESULTS

Total CAPWAP Capacity: 275.1; along Shaft 254.4; at Toe 20.7 kips

Soil Sgmt No.	Dist. Below Gages ft	Depth Below Grade ft	Ru kips	Force in Pile kips	Sum of Ru kips	Unit Resist. (Depth) kips/ft	Unit Resist. (Area) ksf	Smith Damping Factor s/ft
				275.1				
1	9.9	9.1	8.5	266.6	8.5	0.93	0.30	0.087
2	16.6	15.8	17.0	249.6	25.5	2.56	0.82	0.087
3	23.2	22.4	26.8	222.8	52.3	4.04	1.29	0.087
4	29.8	29.0	33.3	189.5	85.6	5.02	1.60	0.087
5	36.5	35.7	37.1	152.4	122.7	5.59	1.78	0.087
6	43.1	42.3	38.9	113.5	161.6	5.87	1.87	0.087
7	49.7	48.9	37.0	76.5	198.6	5.58	1.78	0.087
8	56.4	55.6	30.8	45.7	229.4	4.64	1.48	0.087
9	63.0	62.2	25.0	20.7	254.4	3.77	1.20	0.087
Avg. Shaft			28.3			4.09	1.30	0.087
Toe			20.7				26.36	0.024

#### Soil Model Parameters/Extensions

		Shaft	Toe
Quake	(in)	0.040	0.465
Case Damping Factor		1.336	0.031
Damping Type			Smith
Unloading Quake	(% of loading quake)	58	100
Reloading Level	(% of Ru)	100	100
Unloading Level	(% of Ru)	0	
Soil Plug Weight	(kips)		0.21

CAPWAP match quality = 2.20 (Wave Up Match) ; RSA = 0  
 Observed: final set = 0.400 in; blow count = 30 b/ft  
 Computed: final set = 0.444 in; blow count = 27 b/ft  
 max. Top Comp. Stress = 37.7 ksi (T= 30.0 ms, max= 1.053 x Top)  
 max. Comp. Stress = 39.8 ksi (Z= 16.6 ft, T= 30.8 ms)  
 max. Tens. Stress = -0.00 ksi (Z= 63.0 ft, T= 3.9 ms)  
 max. Energy (EMX) = 21.0 kip-ft; max. Measured Top Displ. (DMX)= 0.90 in

Bridge 10003; Pile: Static Test Pile Initial  
 12" x 1/4" CIP, D19-42; Blow: 783  
 Braun Intertec

Test: 15-Jun-2012 11:15:  
 CAPWAP(R) 2006-3  
 OP: KAA

# EXTREMA TABLE

Pile Sgmnt No.	Dist. Below Gages ft	max. Force kips	min. Force kips	max. Comp. Stress ksi	max. Tens. Stress ksi	max. Trnsfd. Energy kip-ft	max. Veloc. ft/s	max. Displ. in
1	3.3	348.4	0.0	37.7	0.00	21.04	15.9	0.859
2	6.6	358.0	0.0	38.8	0.00	20.68	15.6	0.824
3	9.9	365.6	-0.0	39.6	-0.00	20.35	15.1	0.791
4	13.3	360.1	-0.0	39.0	-0.00	19.06	14.6	0.758
5	16.6	366.9	-0.0	39.8	-0.00	18.75	13.8	0.725
6	19.9	348.8	-0.0	37.8	-0.00	16.82	13.3	0.696
7	23.2	357.2	-0.0	38.7	-0.00	16.58	12.3	0.668
8	26.5	323.8	-0.0	35.1	-0.00	14.11	11.9	0.643
9	29.8	331.6	-0.0	35.9	-0.00	13.94	10.8	0.619
10	33.2	286.4	-0.0	31.0	-0.00	11.35	10.3	0.600
11	36.5	298.5	-0.0	32.3	-0.00	11.25	9.4	0.581
12	39.8	250.2	-0.0	27.1	-0.00	8.71	8.7	0.566
13	43.1	241.9	-0.0	26.2	-0.00	8.64	7.9	0.552
14	46.4	190.8	-0.0	20.7	-0.00	6.21	7.4	0.542
15	49.7	201.4	-0.0	21.8	-0.00	6.17	8.0	0.532
16	53.1	160.8	-0.0	17.4	-0.00	3.96	8.3	0.525
17	56.4	149.7	-0.0	16.2	-0.00	3.95	8.0	0.519
18	59.7	103.9	-0.0	11.3	-0.00	2.12	8.2	0.516
19	63.0	91.3	-0.0	9.9	-0.00	0.54	8.7	0.513
Absolute	16.6			39.8			(T =	30.8 ms)
	63.0				-0.00		(T =	3.9 ms)

# CASE METHOD

J =	0.0	0.1	0.2	0.3	0.4	0.5	0.6	0.7	0.8	0.9
RP	429.0	415.9	402.9	389.8	376.7	363.6	350.5	337.5	324.4	311.3
RX	427.1	409.1	391.4	374.5	358.3	342.7	327.1	311.4	295.8	280.2
RU	425.9	410.8	395.6	380.5	365.4	350.3	335.1	320.0	304.9	289.7

RAU = 57.6 (kips); RA2 = 346.9 (kips)

Current CAPWAP Ru = 275.1 (kips); Corresponding J(RP)= 1.00; matches RX9 within 5%

VMX	TVP	VT1*Z	FT1	FMX	DMX	DFN	SET	EMX	QUS
ft/s	ms	kips	kips	kips	in	in	in	kip-ft	kips
17.03	26.24	260.3	299.5	343.3	0.899	0.389	0.400	21.6	398.3

Bridge 10003; File: Static Test Pile Initial  
 12" x 1/4" CIP, D19-42; Blow: 783  
 Braun Intertec

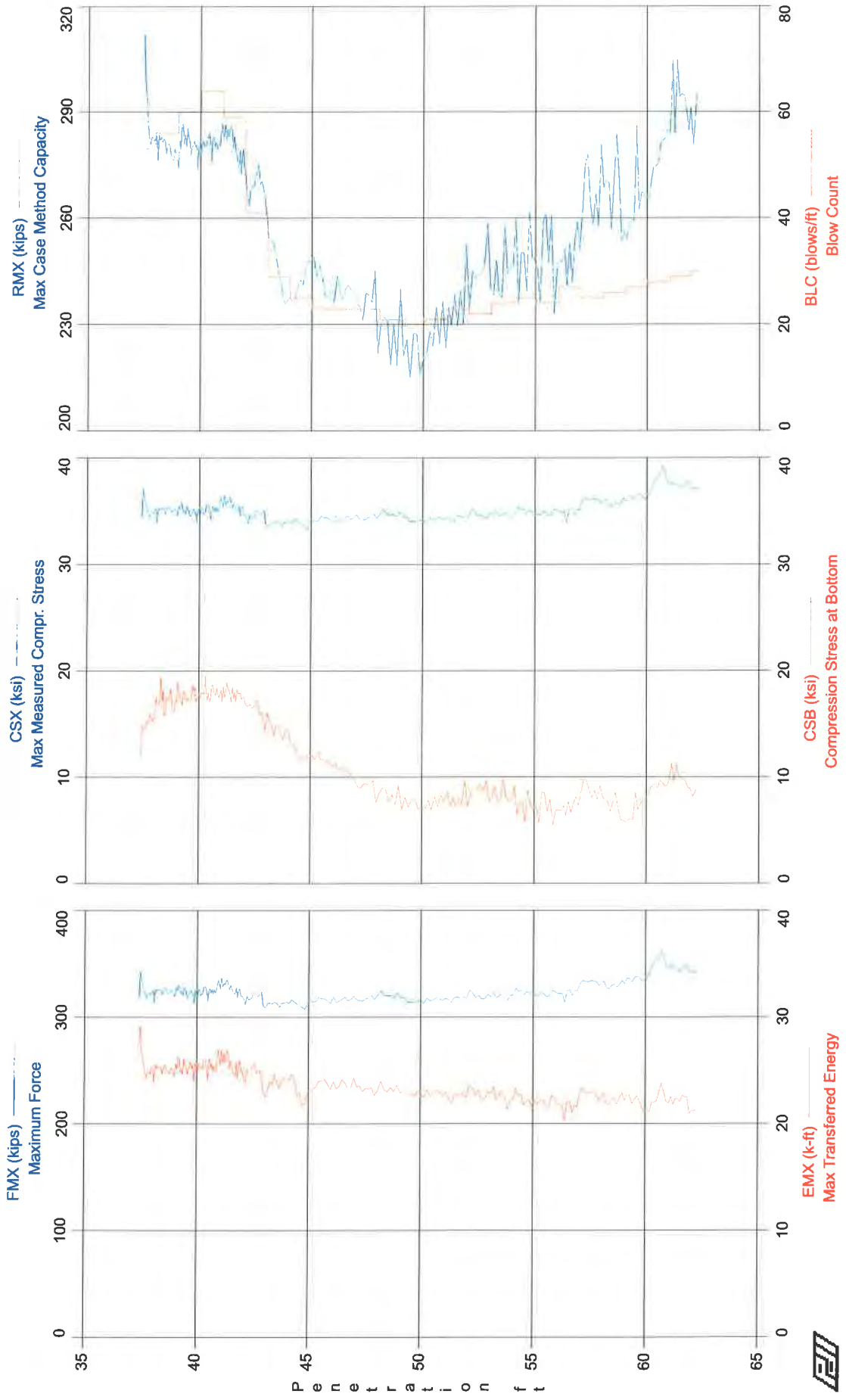
Test: 15-Jun-2012 11:15:  
 CAPWAP(R) 2006-3  
 OP: KAA

PILE PROFILE AND PILE MODEL

Depth ft	Area in <sup>2</sup>	E-Modulus ksi	Spec. Weight lb/ft <sup>3</sup>	Perim. ft
0.00	9.23	29992.2	492.000	3.142
63.00	9.23	29992.2	492.000	3.142
Toe Area	0.785	ft <sup>2</sup>		

Segmnt Number	Dist. B.G. ft	Impedance kips/ft/s	Imped. Change %	Tension Slack in	Eff.	Compression Slack in	Eff.	Perim. ft	Soil Plug kips
1	3.32	16.47	0.00	0.000	0.000	-0.000	0.000	3.142	0.00
2	6.63	16.47	0.00	0.000	0.000	-0.000	0.000	3.142	0.00
19	63.00	16.47	0.00	0.000	0.000	-0.000	0.000	3.142	0.00

Pile Damping 1.0 %, Time Incr 0.197 ms, Wave Speed 16807.9 ft/s, 2L/c 7.5 ms



Bridge 10003 - Static Test Pile Initial  
OP: KAA

12" x 1/4" CIP, D19-42  
Test date: 15-Jun-2012

AR: 9.23 in^2  
LE: 63.00 ft  
WS: 16,807.9 f/s

SP: 0.492 k/ft3  
EM: 30,000 ksi  
JC: 0.90

FMX: Maximum Force  
EMX: Max Transferred Energy  
ETH: Energy Transfer Ratio - Stroke  
CSI: Max F1 or F2 Compr. Stress  
CSX: Max Measured Compr. Stress

CSB: Compression Stress at Bottom  
STK: O.E. Diesel Hammer Stroke  
RX9: Max Case Method Capacity (JC=0.9)  
RMX: Max Case Method Capacity

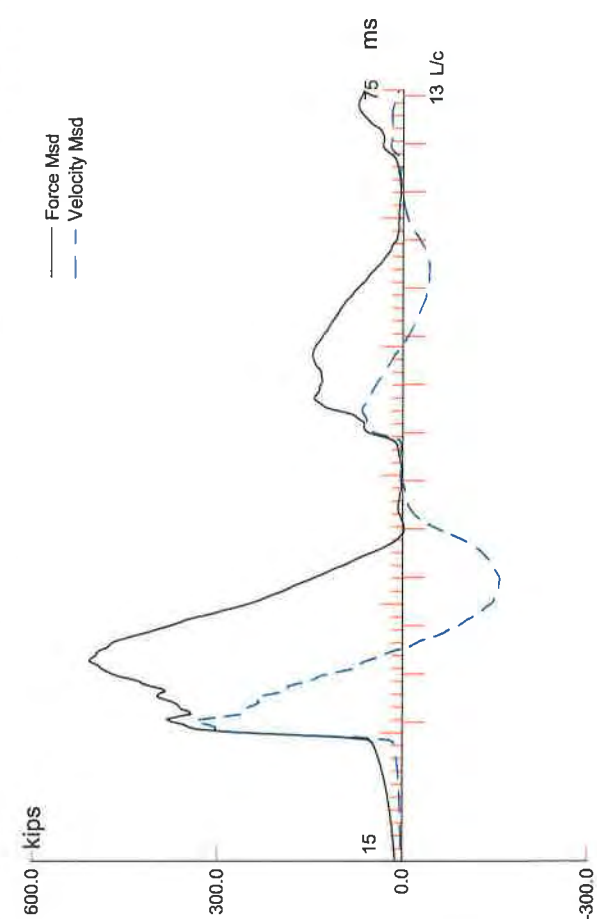
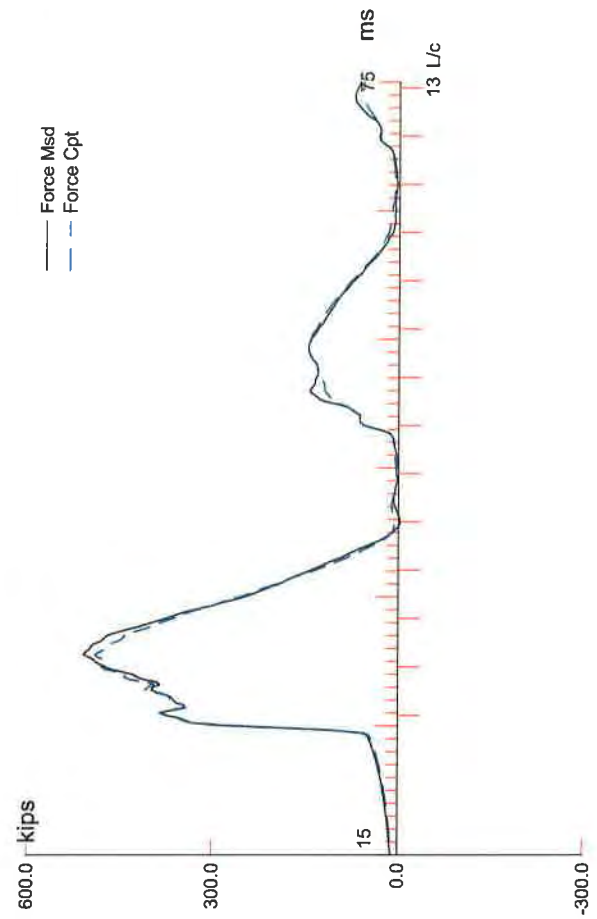
BL#	depth	BLC	TYPE	FMX	EMX	ETH	CSI	CSX	CSB	STK	RX9	RMX
end	ft	bl/ft		kips	k-ft	(%)	ksi	ksi	ksi	ft	kips	kips
32	38.00	53	AV32	326	25.9	81.3	39.8	35.3	14.9	7.9	290	290
88	39.00	56	AV56	324	25.1	79.1	39.6	35.1	17.1	7.9	280	280
148	40.00	60	AV60	324	25.3	79.5	41.8	35.1	17.7	8.0	281	281
212	41.00	64	AV64	326	25.5	79.2	42.1	35.3	18.0	8.1	282	282
271	42.00	59	AV59	328	25.6	78.7	42.1	35.5	17.9	8.1	280	280
312	43.00	41	AV41	319	24.8	77.7	41.9	34.6	16.5	8.0	269	269
341	44.00	29	AV29	313	23.8	77.6	42.7	33.9	14.7	7.7	245	245
366	45.00	25	AV25	312	23.1	77.1	40.8	33.9	12.4	7.5	242	242
389	46.00	23	AV23	316	23.7	78.0	40.1	34.3	11.7	7.6	242	242
412	47.00	23	AV23	317	23.7	77.9	39.1	34.3	10.7	7.6	240	240
435	48.00	23	AV23	317	23.4	76.9	38.7	34.4	9.1	7.6	235	235
456	49.00	21	AV21	321	23.4	76.8	39.1	34.8	8.5	7.6	229	229
476	50.00	20	AV20	316	22.9	75.6	39.4	34.2	7.5	7.6	222	222
497	51.00	21	AV21	316	22.9	75.5	39.3	34.3	7.6	7.6	227	227
520	52.00	23	AV23	318	22.6	74.4	39.3	34.4	8.0	7.6	236	236
542	53.00	22	AV22	320	22.8	74.0	39.0	34.7	8.7	7.7	245	245
566	54.00	24	AV24	320	22.6	72.8	38.8	34.7	8.2	7.8	243	243
591	55.00	25	AV25	323	22.3	72.3	39.2	35.0	7.6	7.7	250	250
615	56.00	24	AV24	322	22.1	71.5	39.3	34.9	7.2	7.7	249	249
642	57.00	27	AV27	323	21.6	70.2	39.9	34.9	7.3	7.7	250	250
667	58.00	25	AV25	333	22.9	71.8	41.4	36.1	8.8	8.0	267	267
693	59.00	26	AV26	330	22.3	70.9	41.2	35.8	7.4	7.9	267	267
720	60.00	27	AV27	335	22.2	69.9	41.9	36.3	7.0	7.9	264	264
748	61.00	28	AV28	350	22.3	69.8	43.3	38.0	9.2	8.0	277	277
775	61.92	29	AV27	346	22.3	70.0	44.2	37.5	10.1	8.0	294	294
785	62.25	30	AV10	342	21.1	68.3	43.8	37.1	8.5	7.7	286	286

Time Summary

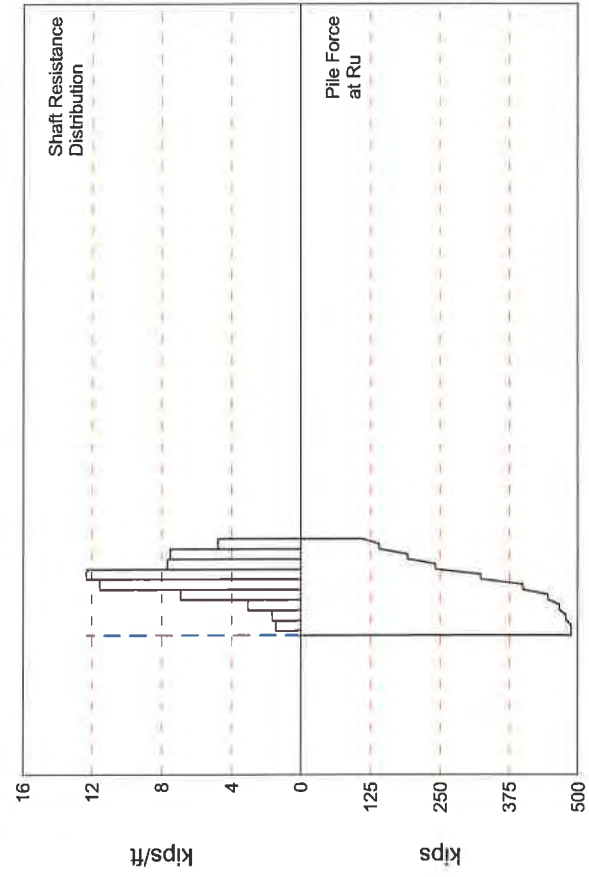
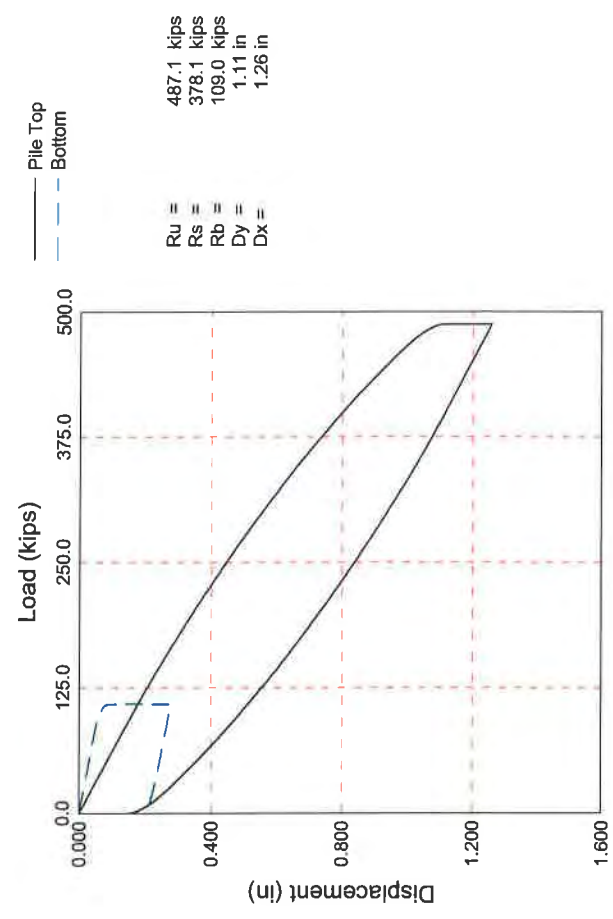
Drive 18 minutes 33 seconds

10:57:11 AM - 11:15:44 AM (6/15/2012) BN 1 - 785





C-62



Bridge 10003; Pile: Static Test Pile Restrike  
 12" x 1/4" CIP, D19-42; Blow: 3  
 Braun Intertec Corp.

Test: 18-Jun-2012 08:34:  
 CAPWAP (R) 2006-3  
 OP: KAA

#### CAPWAP SUMMARY RESULTS

Total CAPWAP Capacity:		487.1; along Shaft	378.1; at Toe	109.0 kips					
Soil Sgmt No.	Dist. Below Gages ft	Depth Below Grade ft	Ru kips	Force in Pile kips	Sum of Ru kips	Unit Resist. (Depth) kips/ft	Unit Resist. (Area) ksf	Smith Damping Factor s/ft	Quake in
				487.1					
1	9.9	9.3	9.7	477.4	9.7	1.04	0.33	0.240	0.133
2	16.6	16.0	11.2	466.2	20.9	1.69	0.54	0.240	0.133
3	23.2	22.6	20.4	445.8	41.3	3.08	0.98	0.240	0.133
4	29.8	29.2	45.9	399.9	87.2	6.92	2.20	0.240	0.133
5	36.5	35.8	76.5	323.4	163.7	11.54	3.67	0.240	0.133
6	43.1	42.5	81.6	241.8	245.3	12.30	3.92	0.240	0.133
7	49.7	49.1	51.0	190.8	296.3	7.69	2.45	0.240	0.133
8	56.4	55.7	50.0	140.8	346.3	7.54	2.40	0.240	0.133
9	63.0	62.4	31.8	109.0	378.1	4.80	1.53	0.240	0.091
Avg. Shaft			42.0			6.06	1.93	0.240	0.129
Toe			109.0				138.78	0.439	0.064

Soil Model Parameters/Extensions			Shaft	Toe
Case Damping Factor			5.509	2.907
Reloading Level (% of Ru)			100	100
Unloading Level (% of Ru)			98	
Soil Plug Weight (kips)				0.31

CAPWAP match quality	=	2.36	(Wave Up Match) ; RSA = 0
Observed: final set	=	0.150 in;	blow count = 80 b/ft
Computed: final set	=	0.155 in;	blow count = 77 b/ft
max. Top Comp. Stress	=	53.3 ksi	(T= 31.0 ms, max= 1.021 x Top)
max. Comp. Stress	=	54.4 ksi	(Z= 9.9 ft, T= 30.2 ms)
max. Tens. Stress	=	-1.81 ksi	(Z= 9.9 ft, T= 41.2 ms)
max. Energy (EMX)	=	28.2 kip-ft;	max. Measured Top Displ. (DMX)= 0.96 in

Bridge 10003; File: Static Test Pile Restrike  
 12" x 1/4" CIP, D19-42; Blow: 3  
 Braun Intertec Corp.

Test: 18-Jun-2012 08:34:  
 CAPWAP (R) 2006-3  
 OP: KAA

# EXTREMA TABLE

File Sgmt No.	Dist. Below Gages ft	max. Force kips	min. Force kips	max. Comp. Stress ksi	max. Tens. Stress ksi	max. Trnsfd. Energy kip-ft	max. Veloc. ft/s	max. Displ. in
1	3.3	492.1	-1.8	53.3	-0.19	28.18	19.3	0.926
2	6.6	499.1	-9.5	54.1	-1.03	26.99	18.7	0.862
3	9.9	502.5	-16.7	54.4	-1.81	25.78	17.7	0.798
4	13.3	488.0	-5.3	52.9	-0.58	22.43	17.0	0.734
5	16.6	492.5	-11.2	53.4	-1.21	21.28	15.5	0.671
6	19.9	474.5	0.0	51.4	0.00	18.32	14.4	0.610
7	23.2	478.1	-3.4	51.8	-0.37	17.26	13.0	0.549
8	26.5	445.1	0.0	48.2	0.00	14.02	11.4	0.492
9	29.8	448.8	0.0	48.6	0.00	13.13	9.6	0.437
10	33.2	387.3	0.0	42.0	0.00	9.38	7.9	0.387
11	36.5	390.7	0.0	42.3	0.00	8.72	6.1	0.340
12	39.8	313.6	0.0	34.0	0.00	5.52	5.2	0.299
13	43.1	316.8	0.0	34.3	0.00	5.05	4.2	0.258
14	46.4	251.7	0.0	27.3	0.00	3.05	3.8	0.224
15	49.7	254.1	0.0	27.5	0.00	2.72	3.1	0.190
16	53.1	211.8	0.0	22.9	0.00	1.78	2.7	0.161
17	56.4	213.1	0.0	23.1	0.00	1.56	2.0	0.133
18	59.7	175.6	0.0	19.0	0.00	1.08	1.7	0.111
19	63.0	176.3	0.0	19.1	0.00	0.82	1.2	0.091
Absolute	9.9			54.4			(T =	30.2 ms)
	9.9				-1.81		(T =	41.2 ms)

# CASE METHOD

J =	0.0	0.1	0.2	0.3	0.4	0.5	0.6	0.7	0.8	0.9
RP	565.6	557.2	548.8	540.4	532.0	523.6	515.2	506.8	498.4	490.0
RX	594.0	581.1	568.3	555.4	542.6	529.7	516.9	504.0	491.5	479.6
RU	641.8	635.5	629.3	623.0	616.8	610.5	604.3	598.0	591.8	585.5

RAU = 3.3 (kips); RA2 = 518.3 (kips)

Current CAPWAP Ru = 487.1 (kips); Corresponding J(RP) = 1.00; J(RX) = 0.84

VMX	TVP	VT1*Z	FT1	FMX	DMX	DFN	SET	EMX	QUS
ft/s	ms	kips	kips	kips	in	in	in	kip-ft	kips
20.72	26.04	306.8	342.9	509.4	0.961	0.143	0.150	28.8	621.6

Bridge 10003; Pile: Static Test Pile Restrike  
 12" x 1/4" CIP, D19-42; Blow: 3  
 Braun Intertec Corp.

Test: 18-Jun-2012 08:34:  
 CAPWAP(R) 2006-3  
 OP: KAA

PILE PROFILE AND PILE MODEL

Depth ft	Area in <sup>2</sup>	E-Modulus ksi	Spec. Weight lb/ft <sup>3</sup>	Perim. ft
0.00	9.23	29992.2	492.000	3.142
63.00	9.23	29992.2	492.000	3.142

Toe Area 0.785 ft<sup>2</sup>

Top Segment Length 3.32 ft, Top Impedance 16.47 kips/ft/s

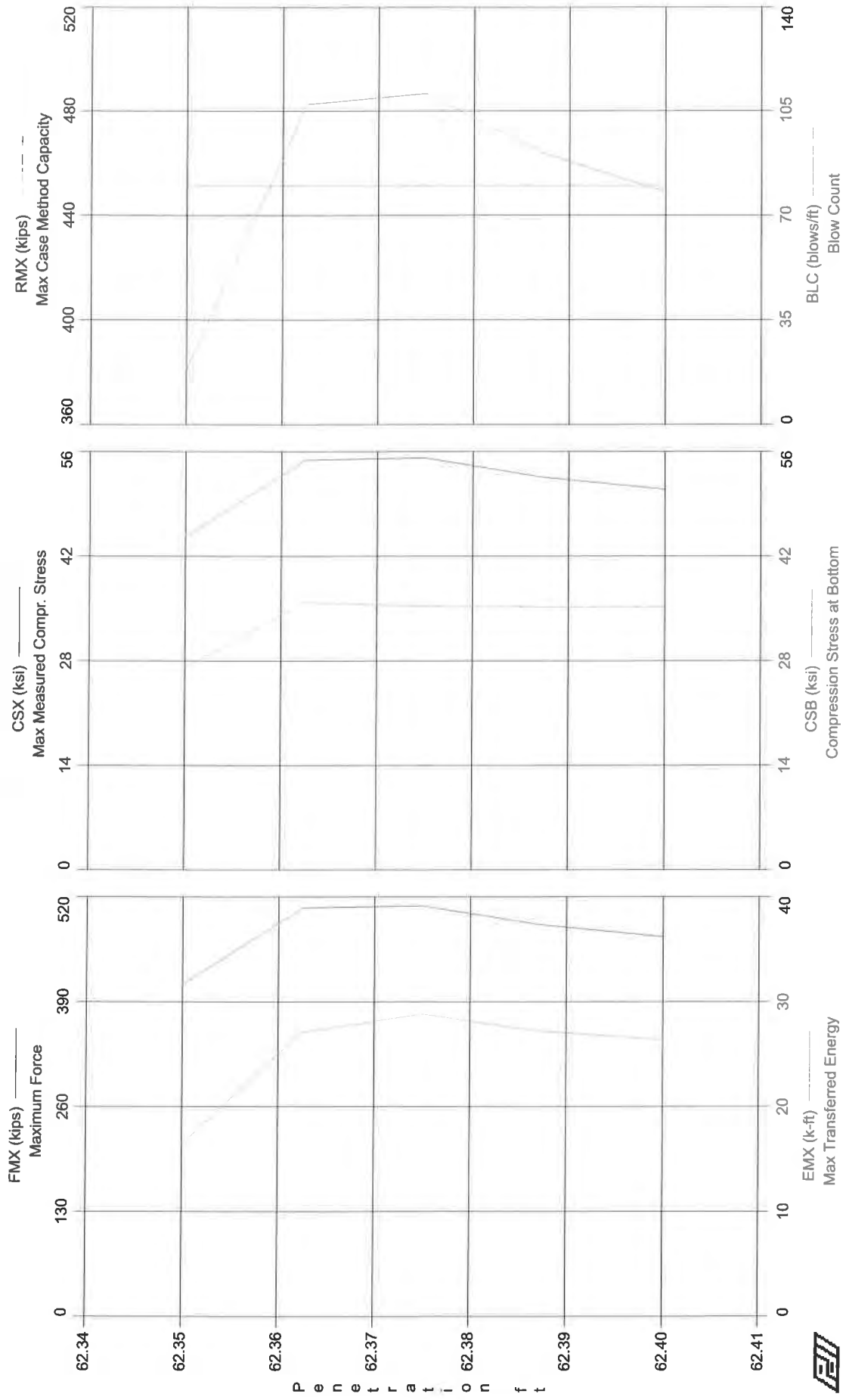
Pile Damping 1.0 %, Time Incr 0.197 ms, Wave Speed 16807.9 ft/s, 2L/c 7.5 ms

Braun Intertec Corp. - Case Method Results

PDILOT Ver. 2010.2 - Printed: 11-Jul-2012

Test date: 18-Jun-2012

Bridge 10003 - Static Test Pile Restrike



Braun Intertec Corp.  
Case Method Results

Page 1 of 1  
PDILOT Ver. 2010.2 - Printed: 11-Jul-2012

Bridge 10003 - Static Test Pile Restrike  
OP: KAA

12" x 1/4" CIP, D19-42  
Test date: 18-Jun-2012

AR: 9.23 in<sup>2</sup>  
LE: 63.00 ft  
WS: 16,807.9 f/s

SP: 0.492 k/ft<sup>3</sup>  
EM: 30,000 ksi  
JC: 0.84

FMX: Maximum Force  
EMX: Max Transferred Energy  
CSX: Max Measured Compr. Stress  
CSI: Max F1 or F2 Compr. Stress  
CSB: Compression Stress at Bottom

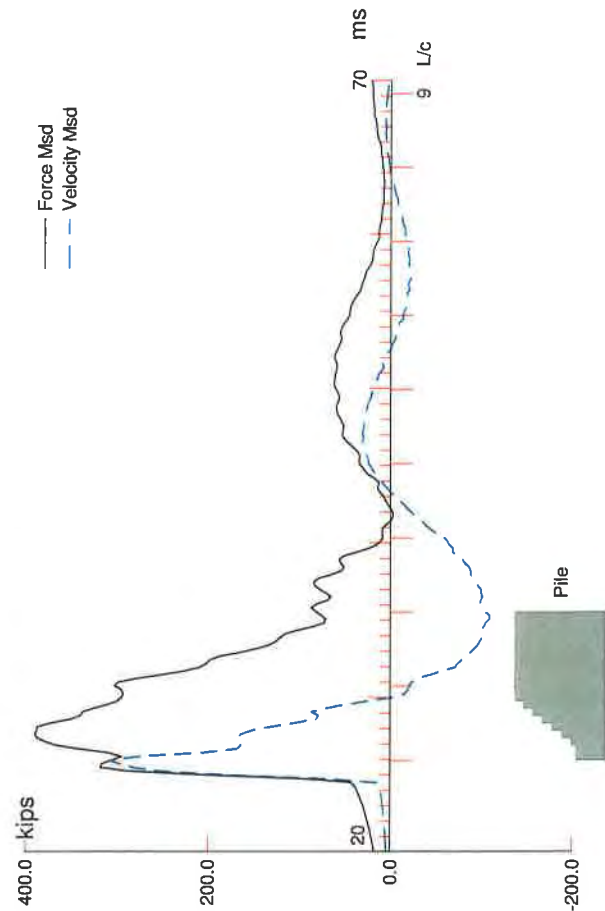
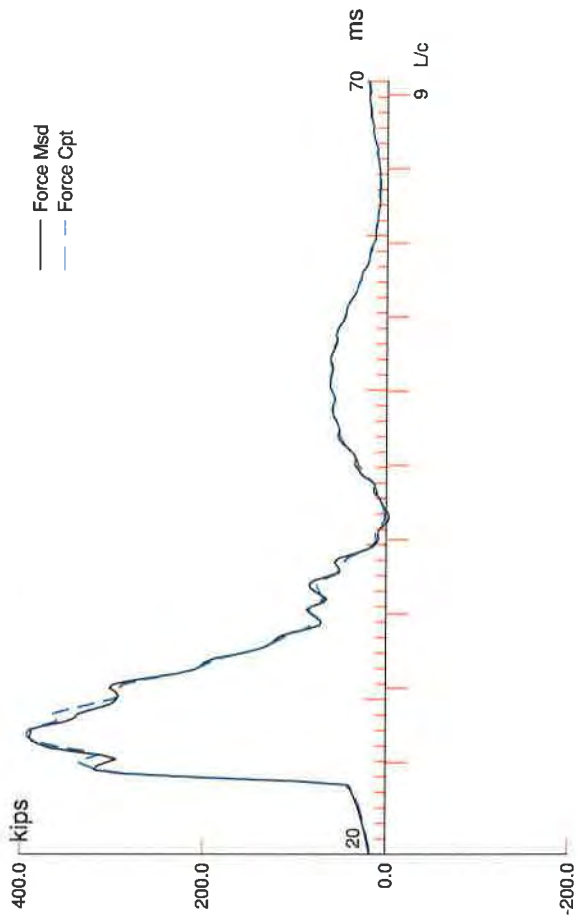
STK: O.E. Diesel Hammer Stroke  
ETH: Energy Transfer Ratio - Stroke  
RX5: Max Case Method Capacity (JC=0.5)  
RMX: Max Case Method Capacity

BL#	depth	BLC	TYPE	FMX	EMX	CSX	CSI	CSB	STK	ETH	RX5	RMX
end	ft	bl/ft		kips	k-ft	ksi	ksi	ksi	ft	(%)	kips	kips
1	62.35	80	AV1	412	16.4	44.6	48.4	27.1	6.8	59.7	407	381
2	62.36	80	AV1	507	27.1	54.9	59.4	35.9	9.4	72.3	523	483
3	62.38	80	AV1	509	28.8	55.2	61.8	35.4	9.6	74.8	530	487
4	62.39	80	AV1	486	27.2	52.7	57.4	35.3	9.3	73.4	507	464
5	62.40	80	AV1	471	26.4	51.0	55.4	35.3	8.9	73.9	491	449

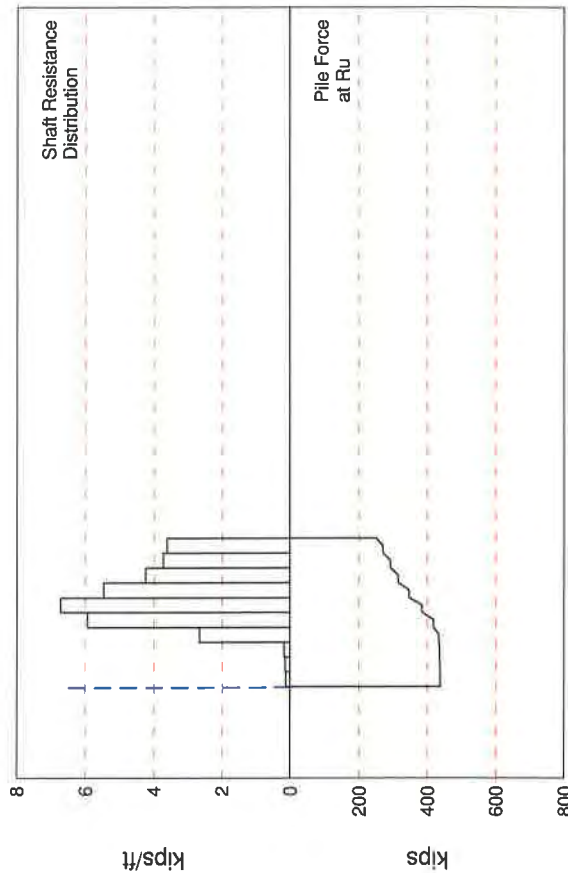
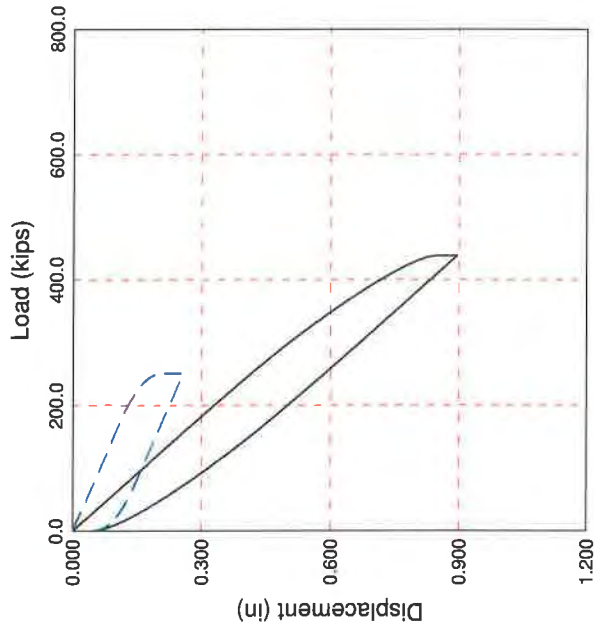
Time Summary

Drive 6 seconds

8:34:09 AM - 8:34:15 AM (6/18/2012) BN 1 - 5



C-68



Bridge 10003 - Static Load Test Pile; Pile: 1-Day After Load Test Test: 26-Jun-2012 13:38:  
 12" x 1/4" CIP - D19-42; Blow: 4 CAPWAP (R) 2006-3  
 Braun Intertec Corp. OP: C. Reese

**CAPWAP SUMMARY RESULTS**

Total CAPWAP Capacity:		437.8; along Shaft		188.6; at Toe		249.2 kips			
Soil Sgmnt No.	Dist. Below Gages ft	Depth Below Grade ft	Ru kips	Force in Pile kips	Sum of Ru kips	Unit Resist. (Depth) kips/ft	Unit Resist. (Area) ksf	Smith Damping Factor s/ft	Quake in
				437.8					
1	8.1	7.5	1.0	436.8	1.0	0.13	0.04	0.167	0.167
2	15.8	15.2	1.1	435.7	2.1	0.14	0.05	0.167	0.167
3	22.7	22.1	1.2	434.5	3.3	0.17	0.06	0.167	0.167
4	28.9	28.3	16.5	418.0	19.8	2.66	0.85	0.167	0.167
5	34.6	34.0	33.8	384.2	53.6	5.94	1.89	0.167	0.167
6	40.3	39.7	38.2	346.0	91.8	6.72	2.14	0.167	0.167
7	46.0	45.4	31.1	314.9	122.9	5.47	1.74	0.167	0.160
8	51.6	51.1	24.1	290.8	147.0	4.24	1.35	0.167	0.144
9	57.3	56.7	21.1	269.7	168.1	3.71	1.18	0.167	0.132
10	63.0	62.4	20.5	249.2	188.6	3.61	1.15	0.167	0.118
Avg. Shaft			18.9			3.02	0.96	0.167	0.154
Toe			249.2				317.29	0.240	0.158

Soil Model Parameters/Extensions			Shaft	Toe
Case Damping Factor			1.917	3.634
Unloading Quake (% of loading quake)			81	139
Reloading Level (% of Ru)			100	100
Unloading Level (% of Ru)			12	
Resistance Gap (included in Toe Quake) (in)				0.045

CAPWAP match quality	=	1.39	(Wave Up Match) ; RSA = 0
Observed: final set	=	0.050 in;	blow count = 240 b/ft
Computed: final set	=	0.011 in;	blow count = 1111 b/ft
max. Top Comp. Stress	=	44.1 ksi	(T= 28.1 ms, max= 1.034 x Top)
max. Comp. Stress	=	45.6 ksi	(Z= 8.1 ft, T= 28.3 ms)
max. Tens. Stress	=	-0.83 ksi	(Z= 8.1 ft, T= 42.5 ms)
max. Energy (EMX)	=	15.3 kip-ft;	max. Measured Top Displ. (DMX)= 0.65 in



Bridge 10003 - Static Load Test File; File: 1-Day After Load TestTest: 26-Jun-2012 13:38:  
 12" x 1/4" CIP - D19-42; Blow: 4 CAPWAP (R) 2006-3  
 Braun Intertec Corp. OP: C. Reese

# EXTREMA TABLE

File Sgmt No.	Dist. Below Gages ft	max. Force kips	min. Force kips	max. Comp. Stress ksi	max. Tens. Stress ksi	max. Trnsfd. Energy kip-ft	max. Veloc. ft/s	max. Displ. in
1	4.0	407.1	-3.4	44.1	-0.37	15.28	16.4	0.578
2	8.1	421.0	-7.7	45.6	-0.83	14.60	14.6	0.525
3	12.0	432.3	-12.1	24.5	-0.69	13.95	12.9	0.480
4	15.8	443.8	-16.9	13.1	-0.50	13.58	11.7	0.448
5	19.3	464.6	-23.1	9.3	-0.46	13.21	10.8	0.422
6	22.7	490.4	-31.0	7.4	-0.47	12.98	10.0	0.401
7	25.9	503.3	-37.4	6.1	-0.45	12.70	9.4	0.382
8	28.9	518.8	-44.4	5.2	-0.45	12.50	9.0	0.364
9	31.8	500.0	-45.1	4.5	-0.40	11.49	8.7	0.349
10	34.6	515.4	-51.5	4.6	-0.46	11.31	8.4	0.333
11	37.4	467.5	-45.1	4.1	-0.40	9.70	8.1	0.319
12	40.3	478.7	-49.8	4.2	-0.44	9.51	7.8	0.303
13	43.1	426.9	-42.8	3.8	-0.38	7.92	7.6	0.287
14	46.0	435.3	-45.8	3.8	-0.40	7.71	7.4	0.270
15	48.8	395.0	-39.9	3.5	-0.35	6.53	7.2	0.254
16	51.6	401.7	-43.5	3.6	-0.38	6.31	7.0	0.237
17	54.5	372.1	-40.1	3.3	-0.35	5.46	6.9	0.220
18	57.3	386.4	-42.0	3.4	-0.37	5.23	6.7	0.202
19	60.2	376.4	-39.9	3.3	-0.35	4.59	6.3	0.186
20	63.0	399.9	-42.1	3.5	-0.37	4.31	5.9	0.170
Absolute	8.1			45.6			(T =	28.3 ms)
	8.1				-0.83		(T =	42.5 ms)

# CASE METHOD

J =	0.0	0.1	0.2	0.3	0.4	0.5	0.6	0.7	0.8	0.9
RP	431.6	412.0	392.3	372.7	353.0	333.3	313.7	294.0	274.4	254.7
RX	431.6	412.0	392.3	372.7	353.0	333.3	313.7	294.0	274.4	254.7
RU	561.6	554.9	548.2	541.6	534.9	528.2	521.6	514.9	508.2	501.6

RAU = 61.8 (kips); RA2 = 356.1 (kips)

Current CAPWAP Ru = 437.8 (kips); Corresponding J(RP)= 0.00; J(RX) = 0.00

VMX	TVP	VT1*Z	FT1	FMX	DMX	DFN	SET	EMX	QUS
ft/s	ms	kips	kips	kips	in	in	in	kip-ft	kips
19.41	26.17	319.7	308.5	394.1	0.652	0.027	0.050	16.6	567.8

Bridge 10003 - Static Load Test Pile; Pile: 1-Day After Load Test Test: 26-Jun-2012 13:38:  
 12" x 1/4" CIP - D19-42; Blow: 4 CAPWAP (R) 2006-3  
 Braun Intertec Corp. OP: C. Reese

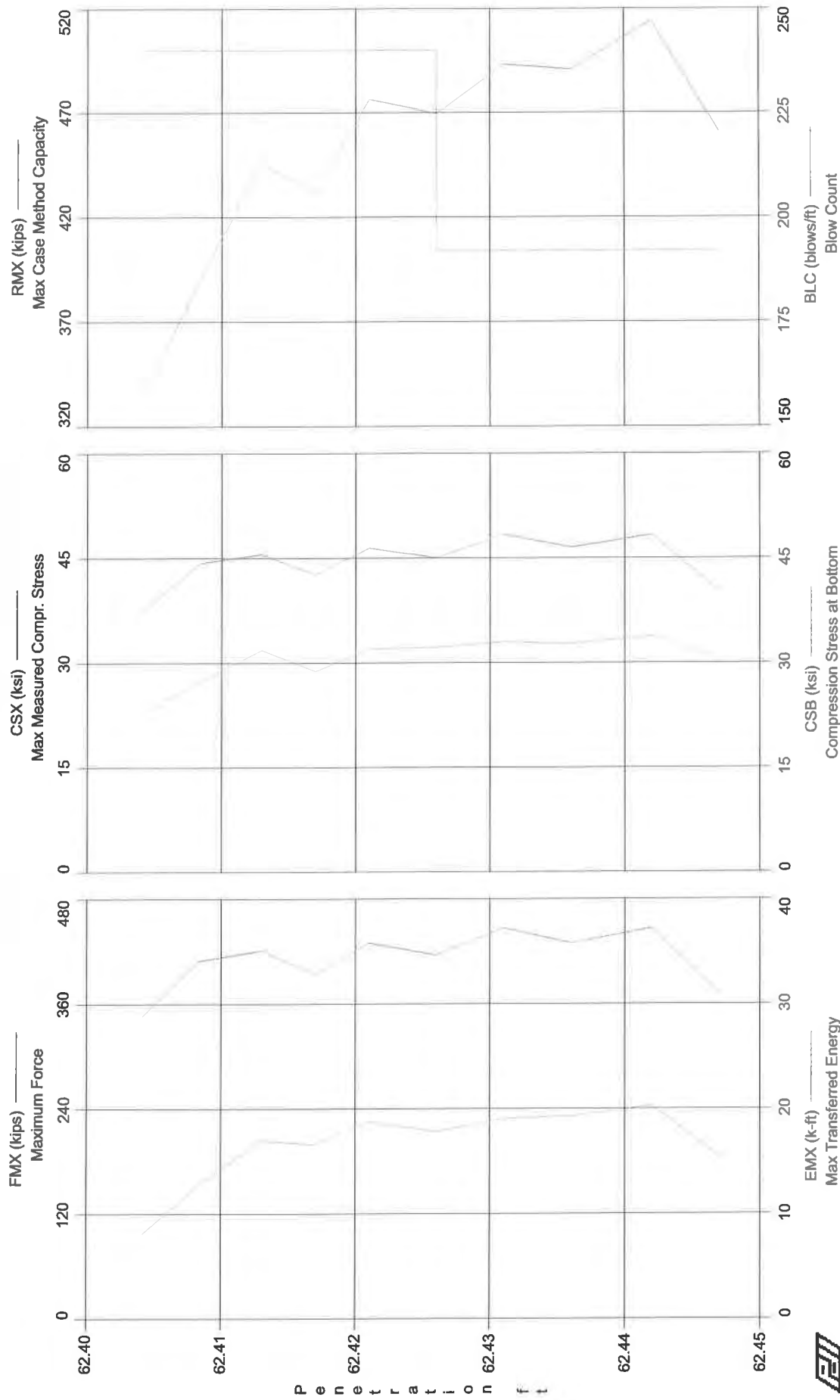
PILE PROFILE AND PILE MODEL

Depth ft	Area in <sup>2</sup>	E-Modulus ksi	Spec. Weight lb/ft <sup>3</sup>	Perim. ft
0.00	9.23	29992.2	492.000	3.142
8.00	9.23	29992.2	492.000	3.142
30.00	113.10	5233.9	173.300	3.142
63.00	113.10	5233.9	173.300	3.142

Toe Area 0.785 ft<sup>2</sup>

Segmnt Number	Dist. B.G. ft	Impedance kips/ft/s	Imped. Change %	Slack in	Tension Eff.	Compression Slack in	Compression Eff.	Perim. ft
1	4.04	16.47	0.00	0.000	0.000	-0.000	0.000	3.142
2	8.07	16.48	0.00	0.000	0.000	-0.000	0.000	3.142
3	12.01	19.19	0.00	0.000	0.000	-0.000	0.000	3.142
4	15.76	24.44	0.00	0.000	0.000	-0.000	0.000	3.142
5	19.33	29.68	0.00	0.000	0.000	-0.000	0.000	3.142
6	22.71	34.93	0.00	0.000	0.000	-0.000	0.000	3.142
7	25.90	40.18	0.00	0.000	0.000	-0.000	0.000	3.142
8	28.90	45.42	0.00	0.000	0.000	-0.000	0.000	3.142
9	31.76	49.67	0.00	0.000	0.000	-0.000	0.000	3.142
10	34.60	50.05	0.00	0.000	0.000	-0.000	0.000	3.142
20	63.00	50.05	0.00	0.000	0.000	-0.000	0.000	3.142

File Damping 1.0 %, Time Incr 0.240 ms, Wave Speed 13120.2 ft/s, 2L/c 9.6 ms



Bridge 10003 - Static Load Test Pile - 1-Day After Load Test Completion  
OP: C. Reese

12" x 1/4" CIP - D19-42  
Test date: 26-Jun-2012

AR: 9.23 in^2  
LE: 63.00 ft  
WS: 16,807.9 f/s

SP: 0.492 k/ft3  
EM: 30,000 ksi  
JC: 0.00

FMX: Maximum Force  
EMX: Max Transferred Energy  
ETH: Energy Transfer Ratio - Stroke  
CSX: Max Measured Compr. Stress  
CSI: Max F1 or F2 Compr. Stress

CSB: Compression Stress at Bottom  
STK: O.E. Diesel Hammer Stroke  
RX8: Max Case Method Capacity (JC=0.8)  
RMX: Max Case Method Capacity

BL#	depth	BLC	TYPE	FMX	EMX	ETH	CSX	CSI	CSB	STK	RX8	RMX
end	ft	bl/ft		kips	k-ft	(%)	ksi	ksi	ksi	ft	kips	kips
1	62.40	240	AV1	346	8.1	0.0	37.5	47.0	22.8	**	231	336
2	62.41	240	AV1	409	12.8	42.4	44.4	53.0	27.3	7.5	289	390
3	62.41	240	AV1	421	16.9	53.8	45.6	50.3	31.9	7.9	286	446
4	62.42	240	AV1	394	16.6	51.5	42.7	47.9	28.9	8.1	274	432
5	62.42	240	AV1	430	18.8	56.4	46.6	58.0	32.0	8.3	308	476
6	62.43	192	AV1	416	17.8	54.4	45.1	57.7	32.3	8.2	314	469
7	62.43	192	AV1	447	19.1	58.2	48.4	66.8	33.1	8.2	348	493
8	62.44	192	AV1	430	19.3	59.2	46.5	68.1	32.7	8.1	359	491
9	62.44	192	AV1	447	20.3	60.9	48.4	76.8	33.9	8.3	396	514
10	62.45	192	AV1	371	15.4	45.8	40.2	65.0	30.5	8.4	343	461

BL#	depth (ft)	Comments
1	62.40	Upper 3-feet is an open pipe, lower portion is filled with concrete
2	62.41	Pile-top buckled during redrive

Time Summary

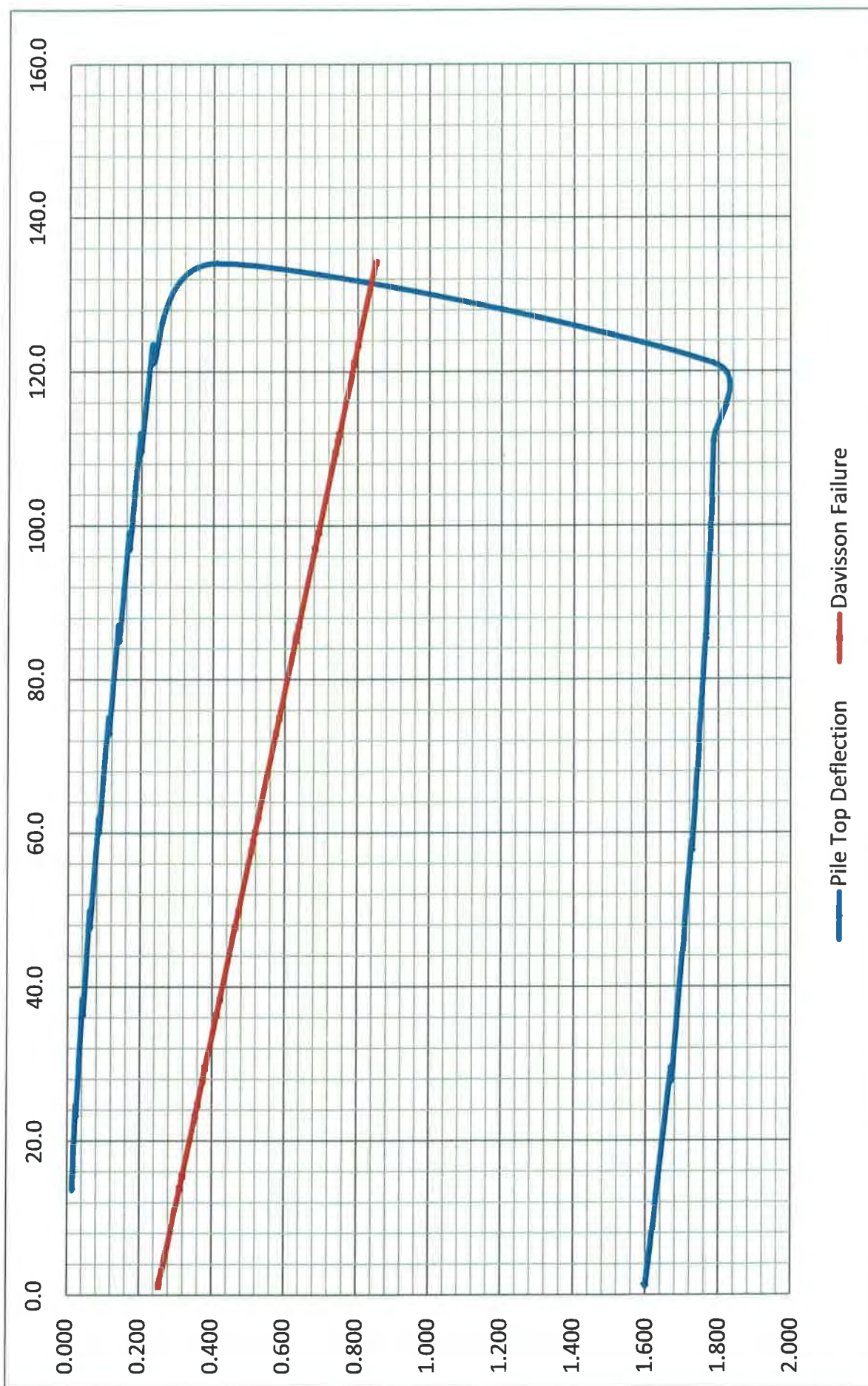
Drive 13 seconds 1:38:10 PM - 1:38:23 PM (6/26/2012) BN 1 - 10

**T.H. 5 Load Test - S.P. 1002-89**  
**Victoria, MN**  
**12 x 1/4" CIP Compression**

Target Load (tons)	Time (minutes)	Clock Time (hr:min)	Target Pressure Gauge Reading (psi)	Actual Pressure Gauge Reading (psi)	Gauge Load (tons)	Target Load Cell Reading (tons)	Actual Load Cell Reading (tons)	Load Cell Load (tons)	Davisson Failure (inches)	Displacement (inches)				Microstrain (µin)			
										Pile Top		Average Movement		SN: 1032597		SN: 1208012	
										NW LVDT	SW LVDT	SE LVDT		Bottom		Bottom	
12.5	0	1:38		50				0.0	0.250	3.582	3.454	3.205	3.414	0.109		0.258	0.081
12.5	10	1:49	180	300	13.9	12.8	15.7	15.4	0.319	3.567	3.446	3.183	0.015	0.717		0.538	1.810
25.0	0	1:50	180	280	12.8	12.8	14.1	13.8	0.312	3.568	3.446	3.184	0.014	0.880		0.813	1.910
25.0	10	1:59	310	440	22.9	25.3	25.0	24.7	0.360	3.558	3.437	3.176	0.023	1.316		1.145	3.360
37.5	0	2:00	310	425	21.9	25.3	23.5	23.2	0.353	3.559	3.435	3.175	0.024	1.404		1.215	3.433
37.5	10	2:09	440	650	36.5	37.9	38.7	36.3	0.421	3.543	3.418	3.155	0.042	1.994		1.980	6.270
37.5	0	2:11	440	610	33.9	37.9	36.7	36.3	0.412	3.542	3.415	3.155	0.043	2.146		2.207	6.469
50.0	0	2:19	571	800	46.1	50.4	50.2	49.8	0.472	3.527	3.396	3.136	0.061	3.138		2.866	9.685
50.0	10	2:20	571	800	48.1	50.4	48.1	47.7	0.463	3.526	3.395	3.135	0.062	3.169		2.801	10.096
62.5	0	2:20	701	1000	59.0	62.9	62.4	62.0	0.526	3.507	3.368	3.111	0.085	4.801		4.333	14.582
62.5	10	2:29	701	970	57.1	62.9	60.5	60.1	0.518	3.506	3.368	3.111	0.085	5.111		4.337	14.992
75.0	0	2:31	831	1160	69.4	75.5	75.4	74.9	0.584	3.484	3.340	3.084	0.111	7.129		6.311	20.478
75.0	10	2:39	831	1150	68.7	75.5	73.4	72.9	0.575	3.483	3.339	3.083	0.112	7.098		6.220	20.787
87.5	0	2:40	961	1350	81.6	88.0	87.4	86.9	0.637	3.460	3.313	3.056	0.137	9.775		8.289	26.107
87.5	10	2:49	961	1320	79.7	88.0	85.5	85.0	0.629	3.457	3.310	3.055	0.140	9.540		7.741	25.634
100.0	0	2:50	1091	1510	91.9	100.5	99.6	99.1	0.682	3.433	3.281	3.028	0.166	13.653		10.441	30.315
100.0	10	2:59	1091	1500	91.3	100.5	97.5	97.0	0.682	3.431	3.281	3.026	0.168	12.608		9.063	29.334
112.5	0	3:00	1221	1700	104.2	113.1	112.4	111.8	0.748	3.403	3.250	2.997	0.197	17.630		13.293	32.127
112.5	10	3:10	1221	1675	102.6	113.1	110.1	109.5	0.738	3.401	3.248	2.996	0.199	15.288		10.176	30.560
125.0	0	3:11	1352	1850	113.9	125.6	124.0	123.4	0.800	3.372	3.216	2.963	0.230	22.658		15.465	33.021
125.0	10	3:20	1352	1825	112.3	125.6	121.7	121.1	0.790	3.369	3.214	2.961	0.232	18.041		10.176	30.826
Plunge Point						138.1	134.7	134.1	0.847	3.184	3.098	2.734	0.408	21.284		9.498	26.197
137.5	0	3:25	1482	1660	101.6	138.1	121.6	121.0	0.788	1.806	1.666	1.410	1.786	23.141		6.691	7.938
137.5	10	3:38	1482	1625	99.4	138.1	111.5	110.9	0.744	1.806	1.666	1.410	1.786	15.350		0.340	4.397
83.2	0	3:41	916	1250	75.2	83.2	85.7	85.2	0.630	1.826	1.689	1.430	1.765	13.436		-1.226	-0.341
83.2	10	3:50	916	1260	75.8	83.2	86.3	85.8	0.632	1.827	1.689	1.430	1.765	11.374		-2.925	-1.485
55.4	0	3:51	627	890	51.9	55.4	58.1	57.7	0.507	1.862	1.729	1.468	1.727	8.143		-4.880	-10.118
55.4	10	4:00	627	925	54.2	55.4	59.3	58.9	0.512	1.863	1.730	1.469	1.726	7.312		-5.495	-10.566
27.7	0	4:01	338	440	22.9	27.7	28.1	27.8	0.374	1.915	1.785	1.526	1.672	2.217		-8.253	-24.824
27.7	10	4:10	338	460	24.2	27.7	29.8	29.5	0.381	1.917	1.786	1.527	1.670	1.923		-8.420	-24.995
0.0	0	4:12	50	60	-1.6	0.0	1.4	1.1	0.255	1.980	1.856	1.603	1.601	0.612		-11.439	-42.524
0.0	10	4:22	50	60	-1.6	0.0	1.6	1.3	0.256	1.983	1.860	1.607	1.597	0.245		-11.615	-42.990
																	0.289

T.H. 5 Static Load Test  
S.P. 1002-89

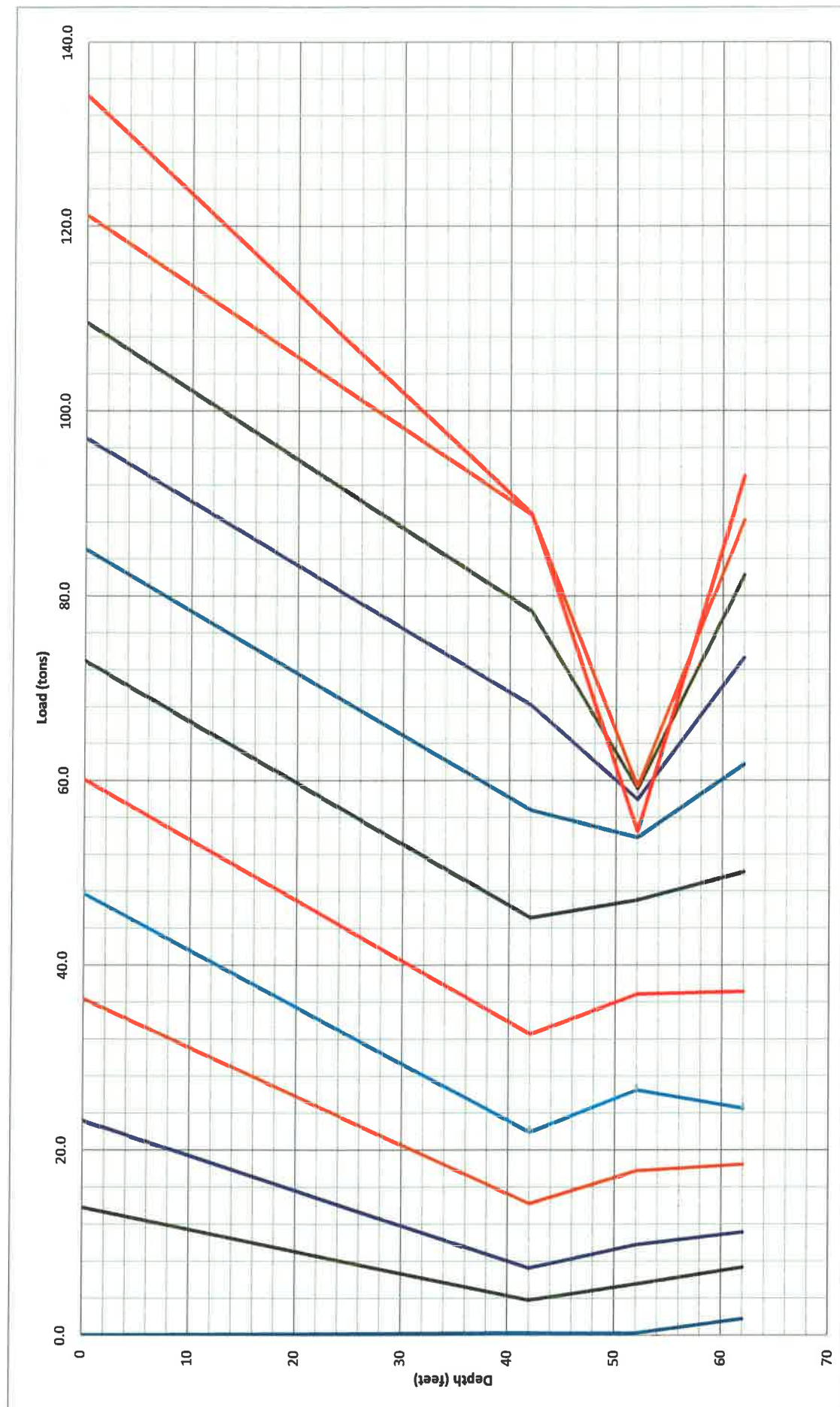
Load (tons) vs. Pile-top Movement (inches)



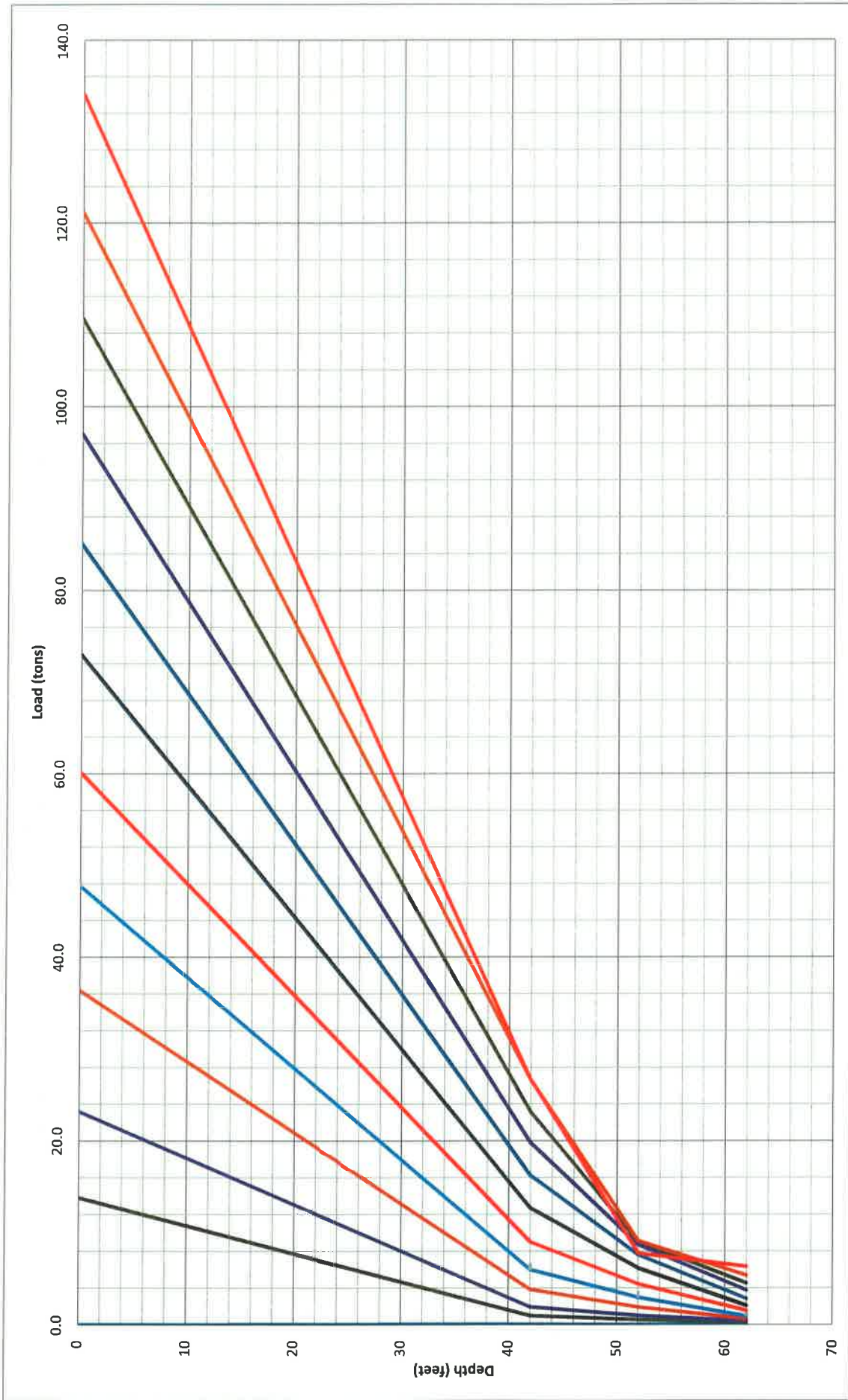
C-75



T.H. 5 Static Load Test  
 S.P. 1002-89  
 Load (tons) vs. Depth (ft)  
 Strain-dependent modulus method (Fellenius, 2001)



T.H. 5 Static Load Test  
 S.P. 1002-89  
 Load (tons) vs. Depth (ft)  
 Constant-strain modulus method





# Calibration Certificate

Date: 6/7/2012

Certificate #: 53892

Calibration Performed By:

**BRAUN**  
**INTERTEC**

For:

BRAUN INTERTEC

11001 HAMPSHIRE AVENUE SOUTH  
BLOOMINGTON, MN 55438

## Equipment Information

I.D.: 13726  
Description: 4 INCH LVDT  
Manufacturer: OMEGA  
Gage Type: LVDT  
Temperature: 70 F  
Rel. Humidity: 25  
Cal Date: 6/7/2012

Serial Number: M930416AD49-02  
Type: LVDT  
Sub-type: 4 INCH  
Model Number: LD620-50  
Performed By: EKNUDSON  
Cal. Due Date: 6/7/2013  
Calibration Result: PASS  
Assigned to:

## Calibration Notes

## Test Points

Seq.	Description	Standard	Tolerance -	Tolerance +	As Found	As Left	Unit
1	1 inch	1.000	0.990	1.010		1.010	in .
2	2 inch	2.000	1.980	2.020		2.010	in .
3	3 inch	3.000	2.970	3.030		3.019	in .
4	4 inch	4.000	3.960	4.040		4.000	in .

## Standards Used To Calibrate Equipment

Company	I.D.	Description	Last Cal.	Cal. Due Date
BRAUN BLOOMINGTON	00791	GAUGE BLOCK SET	11/22/2011	11/22/2016

# Calibration Certificate

Date: 6/7/2012

Certificate #: 53895

Calibration Performed By:

**BRAUN**  
**INTERTEC**

For:

BRAUN INTERTEC

11001 HAMPSHIRE AVENUE SOUTH  
BLOOMINGTON, MN 55438

## Equipment Information

I.D.: 13728  
Description: 4 INCH LVDT  
Manufacturer: OMEGA  
Gage Type: LVDT  
Temperature: 70 F  
Rel. Humidity: 25  
Cal Date: 6/7/2012

Serial Number: M930416AD49-01  
Type: LVDT  
Sub-type: 4 INCH  
Model Number: LD620-50  
Performed By: EKNUDSON  
Cal. Due Date: 6/7/2013  
Calibration Result: PASS  
Assigned to:

## Calibration Notes

## Test Points

Seq.	Description	Standard	Tolerance -	Tolerance +	As Found	As Left	Unit
1	1 inch	1.000	0.990	1.010		1.008	in
2	2 inch	2.000	1.990	2.010		2.009	in
3	3 inch	3.000	2.970	3.030		3.016	in
4	4 inch	4.000	3.960	4.040		4.000	in

## Standards Used To Calibrate Equipment

Company	I.D.	Description	Last Cal.	Cal. Due Date
BRAUN BLOOMINGTON	00791	GAUGE BLOCK SET	11/22/2011	11/22/2016

# Calibration Certificate

Date: 6/7/2012

Certificate #: 53896

Calibration Performed By:

**BRAUN**  
**INTERTEC**

For:

BRAUN INTERTEC

11001 HAMPSHIRE AVENUE SOUTH  
BLOOMINGTON, MN 55438

## Equipment Information

I.D.: 13729  
Description: 4 INCH LVDT  
Manufacturer: OMEGA  
Gage Type: LVDT  
Temperature: 70 F  
Rel. Humidity: 25  
Cal Date: 6/7/2012

Serial Number: M930416AD49-03  
Type: LVDT  
Sub-type: 4 INCH  
Model Number: LD620-50  
Performed By: EKNUDSON  
Cal. Due Date: 6/7/2013  
Calibration Result: PASS

Assigned to:

## Calibration Notes

## Test Points

Seq.	Description	Standard	Tolerance -	Tolerance +	As Found	As Left	Unit
1	1 inch	1.000	0.990	1.010		1.008	in
2	2 inch	2.000	1.980	2.020		2.009	in
3	3 inch	3.000	2.970	3.030		3.016	in
4	4 inch	4.000	3.960	4.040		4.000	in

## Standards Used To Calibrate Equipment

Company	I.D.	Description	Last Cal.	Cal. Due Date
BRAUN BLOOMINGTON	00791	GAUGE BLOCK SET	11/22/2011	11/22/2016



48 Spencer St. Lebanon, NH 03766 USA

## Sister Bar Calibration Report

Model Number: 4911-4

Date of Calibration: August 01, 2011

Serial Number: 1120673

Cable Length: 130 ft.

Prestress: 35,000 psi

Regression Zero: 7003

Calibration Instruction: CI-VW Rebar

Technician: *Elice*

Applied Load (pounds)	Readings				Linearity % Max. Load
	Cycle #1	Cycle #2	Average	Change	
100	7055	7051	7053		
1500	7732	7731	7732	679	-0.01
3000	8463	8462	8463	731	0.06
4500	9186	9187	9187	724	-0.11
6000	9924	9919	9922	735	0.10
100	7052	7051	7052		

*For conversion factor, load to strain, refer to table C-2 of the Installation Manual*

Gage Factor: 0.347 microstrain/ digit (GK-401 Pos. "B")

Calculated Strain = Gage Factor(Current Reading - Zero Reading)

Note: The above calibration uses the linear regression method.

**Users are advised to establish their own zero conditions.**

Linearity: ((Calculated Load - Applied Load)/Max. Applied Load) X 100 percent

The above instrument was found to be in tolerance in all operating ranges.  
The above named instrument has been calibrated by comparison with standards traceable to the NIST, in compliance with ANSI Z540-1.

This report shall not be reproduced except in full without written permission of Geokon Inc.



48 Spencer St. Lebanon, NH 03766 USA

## Sister Bar Calibration Report

Model Number: 4911-4

Date of Calibration: August 01, 2011

Serial Number: 1120674

Cable Length: 130 ft.

Prestress: 35,000 psi

Regression Zero: 7206

Calibration Instruction: CI-VW Rebar

Technician: *Elice*

Applied Load (pounds)	Readings				Linearity % Max. Load
	Cycle #1	Cycle #2	Average	Change	
100	7259	7260	7260		
1500	7928	7931	7930	670	-0.14
3000	8654	8655	8655	725	-0.23
4500	9397	9394	9396	741	0.22
6000	10115	10117	10116	720	-0.02
100	7260	7260	7260		

*For conversion factor, load to strain, refer to table C-2 of the Installation Manual*

Gage Factor: 0.348 microstrain/ digit (GK-401 Pos. "B")

**Calculated Strain = Gage Factor(Current Reading - Zero Reading)**

Note: The above calibration uses the linear regression method.

**Users are advised to establish their own zero conditions.**

Linearity: ((Calculated Load - Applied Load)/Max. Applied Load) X 100 percent

The above instrument was found to be in tolerance in all operating ranges.  
The above named instrument has been calibrated by comparison with standards traceable to the NIST, in compliance with ANSI Z540-1.

This report shall not be reproduced except in full without written permission of Geokon Inc.



48 Spencer St. Lebanon, N.H. 03766 USA

## Sister Bar Calibration Report

Model Number : 4911-4Date of Calibration: November 8, 2010Serial Number: 1032597Cable Length: 62 ft.Prestress: 35,000 psiFactory Zero Reading: 6973Temperature: 21.5 °CRegression Zero: 6971Calibration Instruction: CI-VW RebarTechnician: Ellice

Applied Load: (pounds)	Readings				Linearity % Max.Load
	Cycle #1	Cycle #2	Average	Change	
100	7024	7021	7023		
1,500	7689	7689	7689	667	-0.15
3,000	8420	8417	8419	730	0.10
4,500	9139	9139	9139	721	0.03
6,000	9859	9863	9861	722	0.02
100	7021				

*For conversion factor, load to strain, refer to table C-2 of the Installation Manual.*

**Gage Factor:** 0.349 microstrain/ digit (GK-401 Pos."B")

**Calculated Strain = Gage Factor(Current Reading - Zero Reading)**

Note: The above calibration uses the linear regression method.

**Users are advised to establish their own zero conditions.**

Linearity: ((Calculated Load-Applied Load)/ Max.Applied Load) X 100 percent

The above instrument was found to be In Tolerance in all operating ranges.

The above named instrument has been calibrated by comparison with standards traceable to the NIST, in compliance with ANSI Z540-1.

This report shall not be reproduced except in full without written permission of Geokon Inc.



48 Spencer St. Lebanon, NH 03766 USA

## Sister Bar Calibration Report

Model Number: 4911-4

Date of Calibration: May 04, 2012

Serial Number: 1208012

Cable Length: 95 feet

Prestress: 35,000 psi

Regression Zero: 6977

Temperature: 24.4 °C

Technician: 

Calibration Instruction: CI-VW Rebar

Applied Load (pounds)	Readings				Linearity % Max. Load
	Cycle #1	Cycle #2	Average	Change	
100	7034	7034	7034		
1500	7690	7689	7690	656	-0.33
3000	8415	8416	8416	726	-0.19
4500	9146	9143	9145	729	0.05
6000	9868	9868	9868	723	0.10
100	7034	7034	7034		

*For conversion factor, load to strain, refer to table C-2 of the Installation Manual*

Gage Factor: 0.350 microstrain/ digit (GK-401 Pos. "B")

Calculated Strain = Gage Factor(Current Reading - Zero Reading)

Note: The above calibration uses the linear regression method.

**Users are advised to establish their own zero conditions.**

Linearity: ((Calculated Load - Applied Load)/Max. Applied Load) X 100 percent

The above instrument was found to be in tolerance in all operating ranges  
The above named instrument has been calibrated by comparison with standards traceable to the NIST, in compliance with ANST Z540-1

This report shall not be reproduced except in full without written permission of Geokon Inc

**8002 Calibration Data Sheet***LAGER*Calibration Date: **May 10, 2012**Calibration Recall: **May 10, 2013**Serial Number: **1208938**Calibration Technician: *Heinz A. Schumann*

Calibration Instruction: CI-8002 Initial

Frequency (Hz)	Actual Freq. Counter Reading (Hz)	Computed Reading (Digits) $F^2/1000$	Actual 8002 Reading (Digits)	Error (Digits)*	Allowable Error (Digits) ( $\pm 0.05\%FS$ )
500.0	500.00	250.00	249.9	0.1	$\pm 7.9$
2225.0	2225.00	4950.63	4950.4	0.2	$\pm 7.9$
4000.0	4000.00	16000.00	15997.8	2.2	$\pm 7.9$

\*Error = Computed Reading - Actual Reading

Control Number: **100,488**

This certifies the above named instrument has been calibrated by comparison with standards traceable to the National Institute of Standards and Technology (NIST) in compliance with ANSI/NCSL Z540-1 and is in tolerance as found.

This certificate shall not be reproduced, except in full, without written permission of Geokon, Inc

8002 cal rev: A

Notes: 8002-4-2, LC-2 Brd. USB Software Version 3.0.0, LC-2 4-Channel Mux Brd. V1.2



**Richard Dudgeon, Inc.**  
 1565 Railroad Avenue Bridgeport, CT 06605  
 Tel (203) 336-4459 Fax (203) 333-8417

### JACK CALIBRATION REPORT

Cylinder 1000 Tons Capacity, 12 " Stroke, Serial No. S4123-6  
 Gauge 10,000 PSI Rating, 10 " Dial Dia., Serial No. 2212FHJ

Notice: Calibration reports prepared by Richard Dudgeon, Inc. are submitted on a confidential basis and the data contained therein is our customer's proprietary information. Such reports may or may not be used by others without the express written consent of Richard Dudgeon, Inc. and it's customers.

Dudgeon Order No. L14804 Order Date 3/19/12 Test Date 6/4/12  
 Customer BRAUN INTERTEC CORP Purchase Order No. RAY A HUBER  
 Test Performed By W. Noid In 760 Ton Load Frame, S/N 760TLF-1. Output Measured  
 by 4 x 190 Ton Loadcells S/N 954099WP, 926067RN, BX1272 and DX2045 with Strain  
 Indicator Model P3500, S/N 0140334, Test No. 1.155, Zero Set +/-0000.

Test Method: Cylinder pressure increased in even increments at slow rate by hydraulic pump  
 Output force of cylinder measured by calibrated Loadcells (within a tolerance of one percent)  
 between 50 and 760 tons traceable to the Nat'l Institute of Standards and Technology (formerly  
 the Nat'l Bureau of Standards.

LOAD ON CYLINDER (K <del>IBS</del> /TONS)	GAUGE READING IN PSI AT RAM EXTENSIONS OF			AVERAGE PRESSURE (PSI)
	3 INCHES	5 INCHES	9 INCHES	
50	850	850	850	850
100	1000	1025	1025	1025
150	2400	2400	2425	2400
200	3175	3200	3200	3200
250	3950	3975	3975	3975
300	4725	4750	4750	4750
350	5500	5550	5525	5525
400	6250	6300	6275	6275
450	7050	7050	7050	7050
500	7800	7825	7825	7825

**Richard Dudgeon, Inc.**  
 1565 Railroad Avenue Bridgeport, CT 06605  
 Tel (203) 336-4459 Fax (203) 333-8417  
 Toll Free: 888-383-4366

### LOAD CELL CALIBRATION REPORT

LOAD CELL CAPACITY (TONS) 500 SERIAL NUMBER 07-24954  
 STRAIN INDICATOR MODEL P3 SERIAL NUMBER 199529  
 LOAD CELL TEST NO. (GAUGE FACTOR) 1.329 ZERO SET NO. +000.0

Notice: Calibration reports prepared by Richard Dudgeon, Inc. are submitted on a confidential basis and the data contained therein is our customer's proprietary information. Such reports may or may not be used by others without the express written consent of Richard Dudgeon, Inc. and its customers.

Dudgeon Order No. L16804 Order Date 3/19/12 Test Date 07/4/12  
 Customer BRAUN INTERTEC CORP. Purchase Order No. PAY A HUBER  
 Test Performed By W. Noid In 760 Ton Load Frame, S/N 760TLF-1. Output Measured by  
 4 x 190 Ton Load cells, S/N 926067RN, 954099WP, BX1272, DX2045 with Strain Indicator Model  
P3500, S/N 0140334, Test No. 1.155, Zero Set +/-0000.

Test Method: Load increased in even increments at slow rate by hydraulic jack/pump. Output force of Load Cell measured by calibrated Load Cells (within a tolerance of one percent) between 20 and 190 tons traceable to the Nat'l Institute of Standards and Technology (formerly the Nat'l Bureau of Standards).

STANDARD FORCE KIPS/TONS	LOAD CELL READING			AVERAGE READING
	RUN 1	RUN 2	RUN 3	
0	+000.0	+000.0	+000.0	+000.0
50	051.0	051.4	051.4	051.3
100	099.9	100.1	100.2	100.0
150	149.9	149.6	149.6	149.7
200	199.4	199.4	199.6	199.5
250	249.7	249.5	249.6	249.6
300	299.8	300.1	300.0	300.0
350	350.2	350.5	350.3	350.3
400	400.5	400.8	400.9	400.7
450	451.3	451.4	451.3	451.3
500	502.2	502.1	502.3	502.2

PRESSURE GAUGE CERTIFICATION

CUSTOMER: BRAUN INTERTEC CORPORATION

CUSTOMER'S ORDER NO	DUDGEON ORDER NO.	ORDER DATE
RAY A. HUBER	L16804	03/19/12

GAUGE SERIAL NO.

CAPACITY

2212FHU

10,000 PSI 1/2" φ

WE HEREBY CERTIFY THE ABOVE HYDRAULIC GAUGE HAVE BEEN TESTED AGAINST OUR HEISE DIGITAL PRESSURE INDICATOR, SERIAL NO. S7-9400 AND FOUND TO BE WITHIN A STANDARD ACCURACY (PLUS OR MINUS 1/2%) OF FULL SCALE. OUR TEST EQUIPMENT IS TRACEABLE TO THE NATIONAL BUREAU OF STANDARDS.

REFERENCE PRESSURE  
(PSI)

GAUGE READING  
(PSI)

0  
1000  
2000  
3000  
4000  
5000  
6000  
7000  
8000  
9000  
10000

25  
1025  
2025  
3025  
4025  
5000  
6000  
7000  
8000  
9000  
✓

RICHARD DUDGEON, INC.

W. V. V. V.  
DATE: 03/19/12

## **Appendix D**

**Load Testing Report – TP2 in Arden Hills, MN, January 2013,**

**American Engineering Testing, Inc.**

**Prepared for Lunda Construction Company**



CONSULTANTS  
• ENVIRONMENTAL  
• GEOTECHNICAL  
• MATERIALS  
• FORENSICS

## **REPORT OF STATIC AND DYNAMIC TEST PILE PROGRAM**

Bridge No. 62716

T.H. 694 over CSAH 76

S.P. No. 6285-62716

Arden Hills, Minnesota

---

AET Project No. 22-01025

### **Date:**

January 30, 2013

### **Prepared for:**

Lunda Construction Company  
15601 Clayton Ave. S.  
Rosemount, MN 55068





CONSULTANTS  
• ENVIRONMENTAL  
• GEOTECHNICAL  
• MATERIALS  
• FORENSICS

January 30, 2013

Lunda Construction Company  
15601 Clayton Ave. S.  
Rosemount, MN 55068

Attn: Mr. Bruce Bartelt

RE: Report of Static and Dynamic Test Pile Program  
Bridge No. 62716  
T.H. 694 over CSAH 76  
Arden Hills, Minnesota  
S.P. No. 6285-62716  
AET Report No. 22-01025

Dear Mr. Bartelt:

American Engineering Testing, Inc. (AET) is pleased to present the results of the static and dynamic test pile program at the T.H. 694/CSAH 76 bridge project in Arden Hills, Minnesota. These services were performed according to our proposal to you dated June 23, 2011 and the Subcontract Agreement between Lunda Construction Company and AET dated June 24, 2011.

We are submitting two hard copies of the report to you, along with the electronic data files. Additional electronic copies are being sent to you and MnDOT.

Please contact me if you have any questions about the report.

Sincerely,  
American Engineering Testing, Inc.

A handwritten signature in black ink, appearing to read 'Greg Reuter', written over a horizontal line.

Gregory R. Reuter, PE  
Principal Engineer  
Phone: (651) 789-4660  
Fax: (651) 659-1379  
greuter@amengtest.com

*Page i*



## SIGNATURE PAGE

Prepared for:

Lunda Construction Company  
15601 Clayton Ave. S.  
Rosemount, MN 55068

Attn: Mr. Bruce Bartelt

Prepared by:

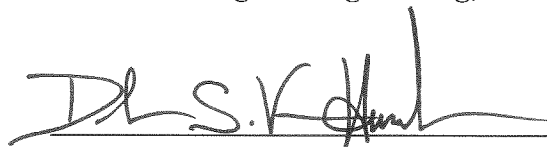
American Engineering Testing, Inc.  
550 Cleveland Avenue North  
St. Paul, Minnesota 55114  
(651) 659-9001/www.amengtest.com

American Engineering Testing, Inc.



Gregory R. Reuter, PE  
Principal Engineer

American Engineering Testing, Inc.



Derek S. Van Heuveln, PE  
Staff Engineer II

I hereby certify that this report was prepared by  
me or under my direct supervision and that I am  
a duly Licensed Professional Engineer under  
Minnesota Statute Section 326.02 to 326.15

Print Name: Gregory R. Reuter

Date: 1/30/13 License #: 19885

Copyright 2013 American Engineering Testing, Inc.  
All Rights Reserved

*Unauthorized use or copying of this document is strictly prohibited by anyone other than the client for the specific project.*

## TABLE OF CONTENTS

Transmittal Letter.....	i
Signature Page .....	ii
TABLE OF CONTENTS.....	iii
1.0 INTRODUCTION .....	1
2.0 SCOPE OF SERVICES .....	1
3.0 PROJECT INFORMATION.....	1
4.0 SUBSURFACE CONDITIONS .....	3
5.0 TEST PILE / REACTION PILE INSTALLATION.....	3
5.1 Description .....	3
5.2 Test Pile Installation .....	4
6.0 HIGH STRAIN DYNAMIC PILE TESTING .....	6
6.1 Methods .....	6
6.2 Summary of Results .....	7
7.0 STATIC LOAD TEST .....	9
7.1 General Information .....	9
7.2 Results .....	10
8.0 DISCUSSION OF RESULTS.....	17
9.0 LIMITATIONS.....	18



**Report of Static and Dynamic Test Pile Program**

TH 694 over CSAH 76, Arden Hills, Minnesota

January 30, 2013

Report No. 22-01025

AMERICAN  
ENGINEERING  
TESTING, INC.

---

APPENDIX A

Figure 1: Test Pile Location Diagram

Figure 2: Instrumentation Locations

MnDOT Pile Driving Record – TP-2

End of Initial Driving, CAPWAP and PDIPILOT – TP-2

Restrike 1, CAPWAP and PDIPILOT – TP-2

Restrike 2, CAPWAP and PDIPILOT – TP-2

MnDOT Pile Driving Record – R-1

Restrike, CAPWAP and PDIPILOT – R-1

MnDOT Pile Driving Record – R-2

End of Initial Driving, CAPWAP and PDIPILOT – R-2

Restrike, CAPWAP and PDIPILOT – R-2

MnDOT Pile Driving Record – R-3

End of Initial Driving, CAPWAP and PDIPILOT – R-3

Restrike, CAPWAP and PDIPILOT – R-3

MnDOT Pile Driving Record – R-4

End of Initial Driving, CAPWAP and PDIPILOT – R-4

Restrike, CAPWAP and PDIPILOT – R-4

Calibration Reports

## **1.0 INTRODUCTION**

American Engineering Testing, Inc. (AET) was retained by Lunda Construction Company (Lunda) to perform a dynamic test pile program, and to observe and document a static pile load test program at the site of the new T.H. 694 bridge project in Arden Hills, Minnesota. This report presents the results.

## **2.0 SCOPE OF SERVICES**

AET's services were performed according to our proposal to you dated June 23, 2011 and Subcontract Agreement between Lunda and AET dated June 24, 2011. The authorized scope consists of the following:

1. Perform high strain dynamic testing on six test piles installed for the construction of bridges 62716 and 62717.
2. Perform high strain dynamic testing on two separate test piles, designated as the static load test piles, along with testing of the associated reaction piles.
3. Observe and document the performance of a static load test on the two test piles referenced in Item 2.

This report addresses Items 2 and 3 above. The test results from Item 1 are presented in separate reports.

## **3.0 PROJECT INFORMATION**

The project consists of the construction of the T.H. 694 bridges over CSAH 76 (Bridge Nos. 62716 and 62717) in Arden Hills. As part of the project, a pile test program was required consisting of high strain dynamic pile testing and static pile load tests. The Minnesota Department of Transportation (MnDOT) project specifications, Section SB-15.8, dated March

**Report of Static and Dynamic Test Pile Program**

TH 694 over CSAH 76, Arden Hills, Minnesota

January 30, 2013

Report No. 22-01025

AMERICAN  
ENGINEERING  
TESTING, INC.

22, 2011, indicated that two static load tests were to be performed at Bridge No. 62717; however, MnDOT modified this scope to require only one test in the east abutment of Bridge No. 62716. The static load test was performed on an east abutment foundation pile, designated as Test Pile No. 2 (TP-2), as shown on the attached Figure 1. High Strain Dynamic Pile Testing (HSDPT) with a Pile Driving Analyzer (PDA) was also performed on this test pile and each of the reaction piles, along with a separate test pile in this abutment designated as Test Pile No. 1 (TP-1). The results of the dynamic testing of TP-1, along with the initial drive and first restrike testing of TP-2, are presented in a separate report (AET Report dated January 21, 2013).

A summary of the test program activities is presented in Table 3-1.

<b>TABLE 3-1. Summary of Test Program Activities</b>					
<b>Test Pile</b>	<b>Final Driven Depth (feet)</b>	<b>Date/Test</b>			
		<b>EOD<sup>2</sup> HSDPT<sup>1</sup></b>	<b>RST<sup>3</sup> 1 HSDPT</b>	<b>SLT<sup>4</sup></b>	<b>RST 2 HSDPT</b>
TP-2 (SLT Pile)	63	12/19/12	12/20/12	1/14/13	1/15/13
R-1 (SE Reaction Pile)	64	12/19/12	12/21/12	None	None
R-2 (SW Reaction Pile)	60	12/19/12	12/21/12	None	None
R-3 (NE Reaction Pile)	60	12/20/12	12/21/12	None	None
R-4 (NW Reaction Pile)	57	12/20/12	12/21/12	None	None

1: HSDPT = High Strain Dynamic Pile Test

2: EOD = End of Initial Drive

3: RST = Restrike

4: SLT = Static Load Test

**Report of Static and Dynamic Test Pile Program**

TH 694 over CSAH 76, Arden Hills, Minnesota

January 30, 2013

Report No. 22-01025

AMERICAN  
ENGINEERING  
TESTING, INC.

As indicated on Plan Sheet No. 4R of 40 "East Abutment Details," dated November 15, 2012, the foundation piles in the east bridge abutment have a computed Factored Design Load of 125.0 tons (250 kips) per pile.

**4.0 SUBSURFACE CONDITIONS**

Based on the results of the closest boring to the east abutment, boring B-3, the subsurface conditions at working grade (approximately elevation 894.5 feet) are generally assumed to consist of about 23 feet of stiff silty clay loam and loam over medium dense sandy loam, and very stiff to loose loam to a depth of approximately 32 feet below working grade (elevation 862.5 feet). Below this depth, the boring encountered medium dense to very dense loam, sandy loam, loamy sand, and sand to a depth of approximately 93 feet below working grade (elevation 801.5 feet). At 93 feet below working grade, the boring encountered 19 feet of loose sandy loam over very dense sand to the boring termination depth at approximately elevation 771 feet. Please refer to the boring log for greater detail.

**5.0 TEST PILE / REACTION PILE INSTALLATION****5.1 Description**

The static load test pile and reaction piles were 12.75-inch diameter, 0.25-inch wall, steel pipe piles. Lunda indicated that the steel had a yield strength of 60 ksi. The piles were driven closed-ended with a flat steel plate welded to the pile toe. The piles were not to be filled with concrete for the static load test. Lunda drove the piles with an APE D25-32 diesel hammer. After a set-up period of one to two days, the piles were restruck with the APE D25-32 hammer. Test Pile No. 2 was also restruck one day after the static load test with the same hammer. A pile inspector from the MnDOT maintained the driving logs; copies of the logs are attached.

The APE D25-32 hammer is a single-acting diesel hammer having a ram weight of 5,512 pounds

and a rated energy range of 29,484 to 58,248 foot-pounds. Typically, however, the actual energy transferred from the hammer to the pile is lower due to friction losses, cushioning material, and other factors.

## **5.2 Test Pile Installation**

### ***5.2.1 Test Pile No. 2 (Static Load Test Pile)***

Test Pile No. 2 (static load test pile) was initially driven on December 19, 2012 to a depth of 63 feet below cutoff elevation. Cutoff elevation is reported to be 895.5 feet; therefore the pile was driven to about elevation 832.5 feet. The reported penetration resistances for the last 3 feet of driving were 62, 56, and 169 bpf, with ½-inch of penetration for the last 10 blows (equivalent to 240 bpf). The observed hammer stroke was 5 to 6 feet, according to the MnDOT driving log.

The pile was restruck on December 20, 2012 and had a restrike penetration resistance of ¾-inch for 10 blows (equivalent to 320 bpf) with an average hammer stroke, as calculated by the PDA, of 8.2 feet. The pile was restruck a second time on January 15, 2013, one day after the static load test. During this second restrike, the pile had a penetration resistance of 1/8-inch for 10 blows (equivalent to 960 bpf) with an average hammer stroke, as calculated by the PDA, of 9.1 feet.

### ***5.2.2 Reaction Pile R-1***

Reaction Pile No. 1 (R-1), located at the southeast corner of the reaction frame, was initially driven on December 19, 2012 to a depth of 64 feet below cutoff elevation for the bridge foundation. Cutoff elevation is 895.5 feet; therefore the pile was driven to elevation 831.5 feet. The reported penetration resistance at the end of driving was ½-inch for 10 blows (equivalent to 240 bpf) with an observed hammer stroke of about 6 feet, according to the driving log. The pile driving ceased when it was observed that the pile top was deforming.

The pile was restruck on December 21, 2012, with an observed penetration of ½-inch for the first 10 hammer blows (equivalent to 240 bpf) with an average hammer stroke, as calculated by the PDA, of about 8.7 feet.

### ***5.2.3 Reaction Pile R-2***

Reaction Pile No. 2 (R-2) was located at the southwest corner of the reaction frame. This pile was initially driven on December 19, 2012 to a depth of 60 feet below cutoff elevation for the bridge foundation. Cutoff elevation is 895.5 feet; therefore the pile was driven to elevation 835.5 feet. The reported penetration resistance at the end of driving was ½-inch for 10 blows (equivalent to 240 bpf) with a hammer stroke, as calculated by the PDA, of about 6 feet.

After a two-day set, the pile was restruck on December 21, 2012. The observed penetration resistance was ¾-inch for the first 10 hammer blows (equivalent to 320 bpf) during restrike, with an average hammer stroke, as calculated by the PDA, of 9.8 feet.

### ***5.2.4 Reaction Pile R-3***

Reaction Pile No. 3 (R-3), located at the northeast corner of the reaction frame, was initially driven on December 20, 2012 to a depth of 60 feet below cutoff elevation for the bridge foundation. Cutoff elevation is 895.5 feet; therefore the pile was driven to elevation 835.5 feet. The reported penetration resistance at the end of driving was ½-inch for 10 blows (equivalent to 240 bpf) with a hammer stroke, as calculated by the PDA, of about 6.7 to 7.0 feet.

The pile was restruck on December 21, 2012, after a one-day waiting period. The observed penetration resistance was ½-inch for the first 10 hammer blows (equivalent to 240 bpf) during restrike, with an average hammer stroke, as calculated by the PDA, of about 8.1 feet.

### ***5.2.5 Reaction Pile R-4***

Reaction Pile No. 4 (R-4) was located at the northwest corner of the reaction frame. This pile was initially driven on December 20, 2012 to a depth of 57 feet below cutoff elevation for the bridge foundation. Cutoff elevation is 895.5 feet; therefore the pile was driven to elevation 838.5 feet. The reported penetration resistance at the end of driving was  $\frac{1}{2}$ -inch for 10 blows (equivalent to 240 bpf) with a hammer stroke, as calculated by the PDA, of about 6.9 to 7.1 feet.

The pile was restruck on December 21, 2012, with an observed penetration of  $\frac{3}{8}$ -inch for the first 10 hammer blows (equivalent to 320 bpf), with an average hammer stroke, as calculated by the PDA, of about 10.1 feet.

## **6.0 HIGH STRAIN DYNAMIC PILE TESTING**

### **6.1 Methods**

We performed HSDPT testing on the test piles with our Model PAK and PAX PDA's. The HSDPT testing was performed in accordance with ASTM: D 4945 procedures, by engineers from AET who have successfully completed certification for high strain dynamic testing of piles by the PDCA/GRL Associates.

The PDA utilizes the Case Method of capacity prediction. To accomplish this, two force transducers and two accelerometers are attached on the pile, generally but not exclusively located near the pile top, and are connected to a field computer by cables. During driving, these gauges generate signals which are proportional to force and velocity. With these signals, the computer provides data outputs which include maximum compressive force at the gauge location, transferred energy from the hammer to the pile, and a prediction of the ultimate mobilized capacity of the pile (at the time of testing).

The Case Pile Wave Analysis Program (CAPWAP) was used to evaluate the test data. CAPWAP is a rigorous numerical analysis procedure, performed on a single hammer blow, which uses the measured force and velocity data collected in the field to solve for soil resistance parameters. The resulting pile top force is computed, and the computed force is compared with the measured force. The agreement between computed and measured pile top force is iteratively improved by modifying the assumed soil model parameters. The final soil parameters then represent the best match dynamic soil model. A predicted pile capacity, along with an estimated load-movement curve, is generated by these analyses.

## **6.2 Summary of Results**

A plot of the PDILOT program results for the static test pile (TP-2) and each reaction pile are attached, along with a data summary for initial driving and restrike. An initial drive PDILOT is not, however, provided for Reaction Pile R-1 as there is no dynamic data from end of drive due to the fact that the gauge location was higher in the leads than the safety line, thus we were unable to attach the sensors, and also due to the fact that the pile head deformed at end of driving. The PDILOT summary shows the pile penetration and blow count for the initial drive and blow number for restrike, maximum force and velocity, computed stress in the pile, predicted mobilized ultimate pile capacity (nominal resistance) at the time of testing, calculated hammer stroke, and transferred hammer energy. Also included are the results of the CAPWAP analyses performed on a blow from near the end of initial driving and a blow from each restrike.

Please note that the predicted capacities shown on the PDILOT are based on one particular damping value. It is likely that the damping value changes with depth. This would affect the plot of predicted capacity with depth for the initial driving, and predicted capacity versus blow number for the restrike. The PDILOT program does not take into account changes in damping, and assumes a constant damping value. Therefore, the predicted capacity plot shown may not reflect the actual capacity with depth. If the predicted capacity is required at a depth (or blow



**Report of Static and Dynamic Test Pile Program**

TH 694 over CSAH 76, Arden Hills, Minnesota

January 30, 2013

Report No. 22-01025

AMERICAN  
ENGINEERING  
TESTING, INC.

number) other than that which the CAPWAP analysis was performed, we recommend performing additional CAPWAP analyses. A summary of the results of the HSDPT CAPWAP analyses are presented in Table 6.2-1.

<b>TABLE 6.2-1. Summary of HSDPT CAPWAP Results</b>					
<b>Test Pile</b>	<b>Test Condition*</b>	<b>Approximate Depth Below Cutoff (ft)</b>	<b>Penetration Resistance (stroke**)</b>	<b>Record ("Blow") Number Analyzed</b>	<b>Predicted Mobilized Nominal Resistance† (kips)</b>
TP-2	EOID	63	½ -inch for 10 blows (7.1 ft)	983	283
TP-2	RST 1	63	⅜ -inch for 10 blows (9.9 ft)	4	398
TP-2	RST 2	63	⅛ -inch for 10 blows (9.1 ft)	10	446
R-1	EOID	64	½ -inch for 10 blows (6-6.5 ft)	††	††
R-1	RST	64	½ -inch for 10 blows (10.9 ft)	6	577
R-2	EOID	60	½ -inch for 10 blows (6.0 ft)	604	223
R-2	RST	60	⅜ -inch for 10 blows (11.4 ft)	5	578
R-3	EOID	60	½ -inch for 10 blows (7.0 ft)	213	287
R-3	RST	60	½ -inch for 10 blows (11.0 ft)	6	464
R-4	EOID	57	½ -inch for 10 blows (7.1 ft)	138	292
R-4	RST	57	⅜ -inch for 10 blows (12.1 ft)	4	510

\*EOID=End of Initial Drive, RST=Restrike, \*\*As calculated by the PDA for the record analyzed.

†At the time of testing ††No CAPWAP analyses performed due to yielding of pile top at end of driving.

In our judgment, the predicted mobilized nominal resistances presented in Table 6.2-1 are likely lower-bound values because the full pile resistance was likely not mobilized due to the small set experienced by each pile at the end of driving and also during restrike.

## **7.0 STATIC LOAD TEST**

### **7.1 General Information**

The static load test was performed by Lunda, with AET providing the displacement sensor instrumentation and data collection. The reaction frame was supplied by MnDOT and had a maximum allowable design capacity of 500 tons (1000 kips). The load to the test piles was applied by a hydraulic jack with a capacity of 800 tons and equipped with a calibrated hydraulic pressure gauge. The actual applied load was measured using a Geokon Model 3000 load cell. Lunda rented the load cell and jack from Richard Dudgeon, Inc.; the calibration reports are appended. We monitored the pile head movement using four electronic LVDT displacement sensors, evenly distributed around the pile head. The displacement sensors were linear potentiometers with a 4-inch travel and an accuracy of 0.0001 inches. Two back-up electronic displacement sensors were also used, each located on opposite sides of the pile. All of these sensors were mounted to two wooden reference beams, located parallel to each other on opposite sides of the pile, with each beam supported 8 feet away from the test pile and reaction piles. The load cell and electronic displacement sensors were logged simultaneously at one second intervals during the test.

Two telltales were also installed in the test pile; however, during initial driving the outer tubing for both telltales detached from the pile shell. As a remedy, the outer tubes were welded to an H-pile section that was placed within the interior of the pipe pile. The H-pile was slightly shorter than the total length of the pipe pile and therefore was not loaded during the pile static load test. The telltales consisted of an oiled, small diameter steel rod encased in the slightly larger outer steel tube. Each telltale was referenced to the pile toe. A separate LVDT displacement sensor was mounted to the top of the pipe pile which then monitored the movement of the telltale relative to the pile head to determine the pile compression during the test. These telltale displacement sensors were logged at one second intervals during the test.

**Report of Static and Dynamic Test Pile Program**

TH 694 over CSAH 76, Arden Hills, Minnesota

January 30, 2013

Report No. 22-01025

AMERICAN  
ENGINEERING  
TESTING, INC.

Additionally, LVDT displacement sensors were placed at each of the four reaction piles in order to monitor the performance of the reaction piles during the test. These were mounted on separate wooden reference beams supported at least 8 feet away from the test pile and the reaction piles. Also, as requested by MnDOT, a strain gauge was attached to two of the reaction piles, one on pile R-1 and the other on pile R-4. These consisted of Geokon Model 4000 arc weldable vibrating wire strain gauges. The strain gauges were monitored every 10 seconds during the test.

The test loading followed the guidance of ASTM D 1143/D 1143M-07, Section 8.1.2, *Procedure A: Quick Test*. The load was applied in targeted intervals of approximately 25 tons (50 kips) each, which is 5% of the maximum test load of 500 tons as specified by the project specifications. Each load interval was held for 4 minutes. The pile was unloaded in four decrements, with each decrement held for 4 minutes each. The last reading was taken 4 minutes after complete removal of the load.

The electronic data files of the LVDT readings will be provided separately from this report.

**7.2 Results**

The static test pile was driven to a depth of 63 feet below grade on December 19, 2012. The pile was near vertical, and the top of the pile was cut off parallel to the bottom of the reaction beam in order to fit the loading stack. The specific pile measurements are presented in Table 7.2-1.

<b>TABLE 7.2-1 Static Test Pile</b>					
<b>Test Pile</b>	<b>Driven Depth (ft.)</b>	<b>Tested Length (ft.)</b>	<b>Batter</b>	<b>Telltale Location (LVDT No.)</b>	
				<b>No. 5</b>	<b>No. 6</b>
TP-2	63	63.0	vertical	Pile Toe	Pile Toe

The movements of the two telltales were referenced to the top of the pile; therefore, the total 63-

foot pile length was measured for compression during the test loading.

The static load test was performed on January 14, 2013 - 26 days after initial driving. The outside air temperature was about 5° F on the day of the test; therefore, Lunda built a shelter surrounding the load frame and heated the enclosure to about 70° to 80° F. A photograph of the load frame enclosure is presented in Figure 7.2-1, and a photograph of the loading stack and pile head instrumentation is presented in Figure 7.2-2.



Figure 7.2-1. Photograph of test site and load frame enclosure.



Figure 7.2-2. Photograph of the loading stack and instrumentation.

The theoretical yield load for the pile, based on the full steel section of the pile and the reported steel yield strength of 60 ksi, is 589 kips. The pile was notched to accommodate the telltales, resulting in some slight loss of steel cross-section; therefore, the actual theoretical yield load would be slightly less than that for the full pile section. It is estimated that there was an approximately  $\frac{1}{2}$  in<sup>2</sup> loss in steel cross-section area due to the notching for the telltales. Assuming this, the theoretical yield load would be about 559 kips.

### ***7.2.1 Pile Head Response***

The test results, in the form of a load versus pile head movement plot for each of the four LVDT's, are shown in Figure 7.2-3. The maximum load applied to the pile during the test was 547 kips, at which point no additional load was applied due to excessive yielding of the pile top steel. The pile yielded toward the direction of LVDT 2 and Telltale 5, and away from LVDT 3 and Telltale 6. This yielding is evident in Figure 7.2-3 by the excessive movement of LVDT 2, which begins to divert away from the movement plot of LVDT 1 after the applied load of about 400 kips, and the reduced movement of LVDT 3, which begins to divert away from the movement plot of LVDT 1 and 2 after the applied load of about 300 kips.

### ***7.2.2 Telltale Results***

The LVDT readings for Telltale No. 6 are plotted in Figure 7.2-4 versus the load applied to the pile head. The data obtained from Telltale No. 5 is, in our judgment, not usable, as it was negatively affected by the yielding of the pile head, and therefore is not plotted in the figure. The movement shown in Figure 7.5-4 is the movement of the top of the telltale rod for No. 6. The base of the LVDT was mounted at the top of the pile to allow direct measurement of pile compression.



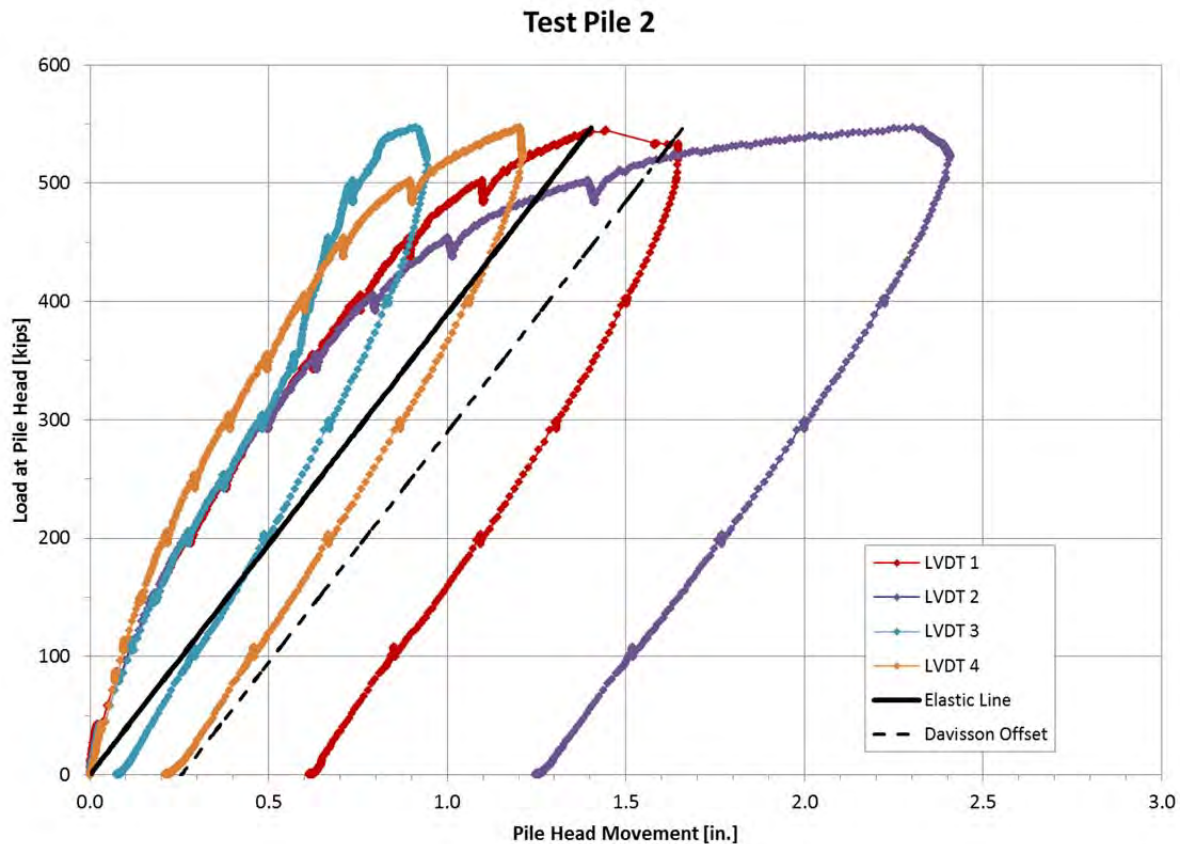


Figure 7.2-3. Load versus pile head movement diagram for each primary LVDT sensor.

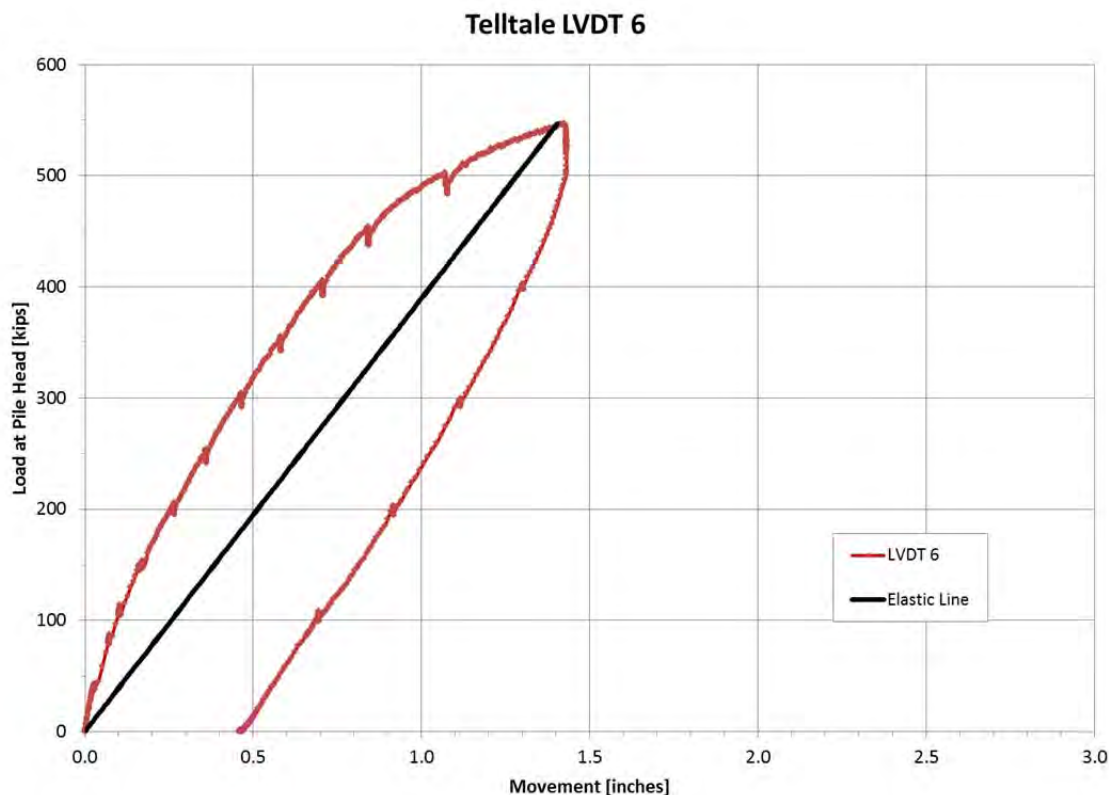


Figure 7.2-4. Pile head load versus measured movement of the top of Telltale 6.

Figure 7.2-5 presents a plot of time for the applied load to the pile head and also for the calculated load at the pile toe based on the results of the Telltale No. 6 measurements. As can be seen in the figure, no load was observed at the pile toe until a load of 200 kips was applied to the pile head, meaning that almost all of the load up to the applied load of 200 kips was resisted mainly by the pile shaft resistance. Please note that the calculated toe load is not valid after the 450 kip applied head load because the results become strongly influenced by the yielding of the steel at the pile head.



## Report of Static and Dynamic Test Pile Program

TH 694 over CSAH 76, Arden Hills, Minnesota

January 30, 2013

Report No. 22-01025

AMERICAN  
ENGINEERING  
TESTING, INC.

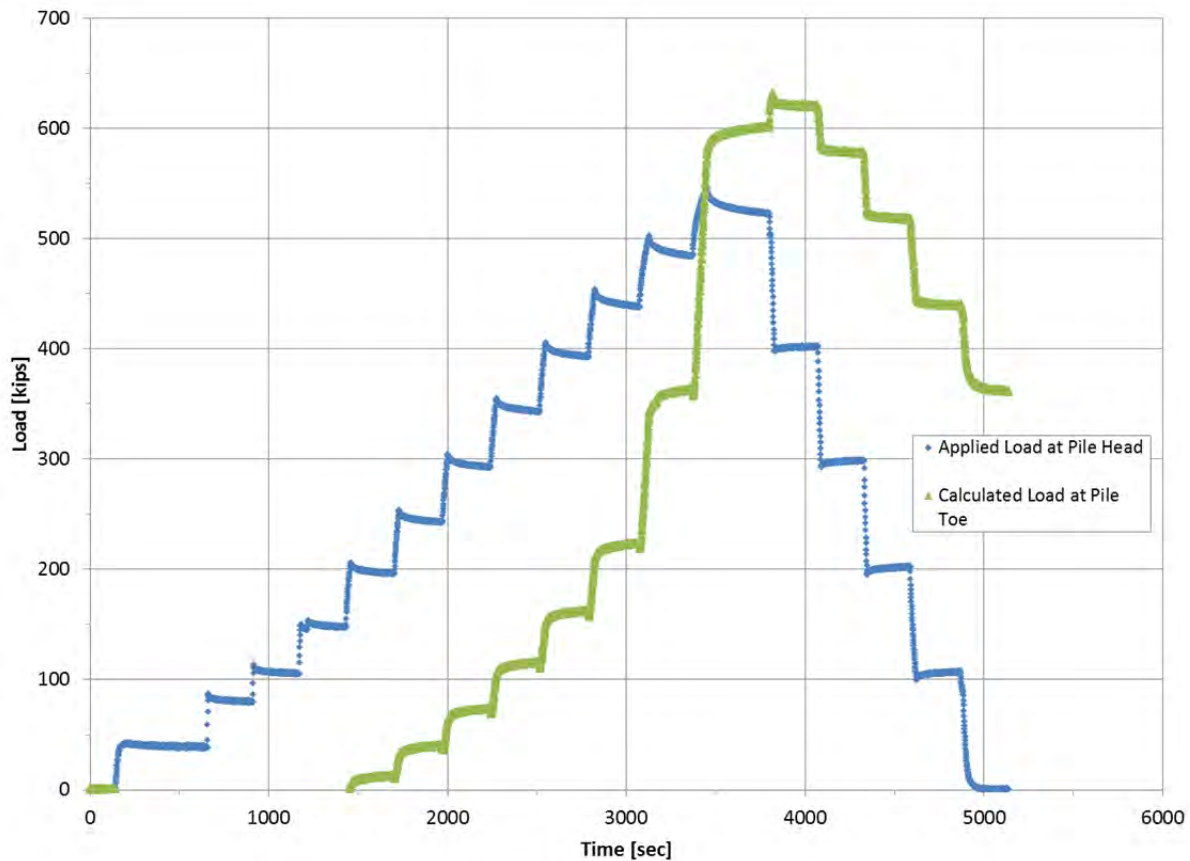


Figure 7.2-5. Applied load at pile head and calculated load at pile toe, based on the results of telltale LVDT 6. Note that the calculated toe loads beyond the 450 kip head load are not valid due to yielding of the pile head steel.

### 7.2.3 Reaction Pile Response

The reaction piles were monitored for movement during the test using LVDT displacement sensors (Nos. 7 through 10), and the results are plotted in Figure 7.2-6. The monitoring found that the reaction piles deflected upward approximately 0.20 to 0.27 inches at the maximum test load of 547 kips. The two strain gauges attached to the reaction piles R-1 and R-4 were also read during the load test.

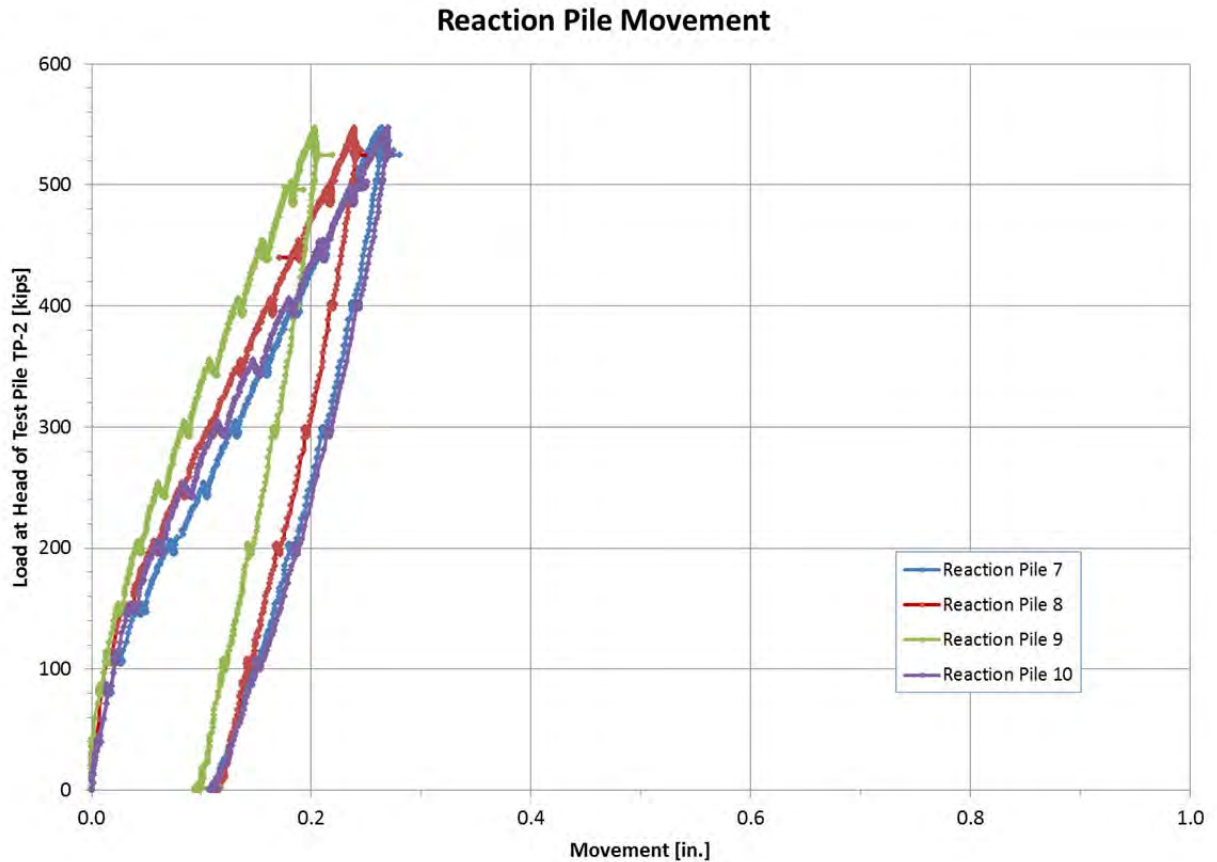


Figure 7.2-6. Reaction pile movement plotted against the load applied to the head of TP-2.

## 8.0 DISCUSSION OF RESULTS

The maximum load applied to the pile during the test was 547 kips, at which point no additional load was applied due to excessive yielding of the pile top steel as the pile failed structurally. The pile yielded in the general direction of LVDT 2. The two LVDT's that appear to be the least affected by the yielding of the pile were LVDT 1 and LVDT 4, although these two LVDT's would also be affected, to a certain degree, by the yielding of the pile head. One method to evaluate the results of a pile load test is to plot the Davisson Offset Limit, which is shown in

Figure 7.2-3. Assuming an averaged load-movement curve of LVDT 1 and 4, an extrapolated Davisson Offset Limit load would be about 575 kips. We also evaluated the results by two other methods; the Chin-Kondner Method, and the Brinch Hansen's (80% Criterion) Method. Using the averaged results from LVDT 1 and 4, these methods have extrapolated ultimate capacities of about 640 kips to 740 kips. It is important to note that we do not recommend using these values for design, as they are only estimates based on extrapolation of the available data. These extrapolated results do, however, suggest that the pile may have been able to carry additional load, if the pile did not fail structurally.

## **9.0 LIMITATIONS**

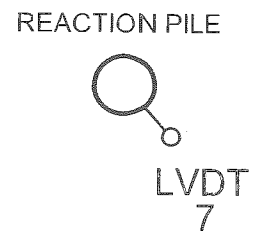
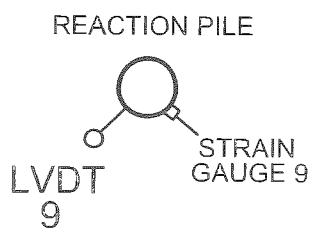
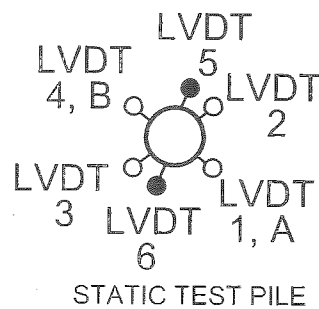
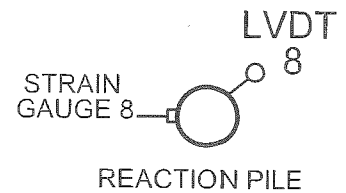
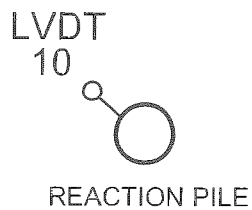
Within the limitations of scope, budget, and schedule, we have endeavored to provide our services according to generally accepted geotechnical engineering practices at this time and location. Other than this, no warranty, either express or implied, is intended.

## Appendix A

---

Figure 1: Test Pile Location Diagram	
Figure 2: Instrumentation Locations	
MnDOT Pile Driving Record – TP-2	
End of Initial Driving, CAPWAP and PDIPILOT – TP-2	
Restrike 1, CAPWAP and PDIPILOT – TP-2	
Restrike 2, CAPWAP and PDIPILOT – TP-2	
MnDOT Pile Driving Record – R-1	
Restrike, CAPWAP and PDIPILOT – R-1	
MnDOT Pile Driving Record – R-2	
End of Initial Driving, CAPWAP and PDIPILOT – R-2	
Restrike, CAPWAP and PDIPILOT – R-2	
MnDOT Pile Driving Record – R-3	
End of Initial Driving, CAPWAP and PDIPILOT – R-3	
Restrike, CAPWAP and PDIPILOT – R-3	
MnDOT Pile Driving Record – R-4	
End of Initial Driving, CAPWAP and PDIPILOT – R-4	
Restrike, CAPWAP and PDIPILOT – R-4	
Calibration Reports	





NOTE:  
 PILE HEAD LVDT = 1-4  
 TELLTALE LVDT = 5, 6  
 REACTION PILE LVDT = 7 - 10  
 BACKUP PILE HEAD LVDT = A, B



AMERICAN  
ENGINEERING  
TESTING, INC.

PROJECT		Bridge 62716 Arden Hills, Minnesota	AET NO. 22-01025
SUBJECT		Instrumentation Locations	DATE January 2013
Scale As shown	Drawn By JM	Checked By GRR	Figure 2

**MnDOT PILE DRIVING RECORD  
TEST PILE NO. 2  
(SLT PILE)**

# TEST PILE REPORT

PILE HAMMER DATA					PILE DATA				JOB DESCRIPTION					
TYPE ("X" ONE)					TEST PILE NO.		STATIC		BRIDGE NUMBER		62716			
X DROP SINGLE ACTING POWER DRIVEN DOUBLE ACTING POWER DRIVEN					TYPE		CIP 12.750" x .250		T.H. NUMBER		694 WB			
					LENGTH in LEADS		75'		S.P. NUMBER		6285-135			
					DIAM. of BUTT & TIP				FED. NUMBER					
MAKE APE					WEIGHT of PILE				COUNTY		Ramsey			
					WEIGHT of CAP		2,050		PIER OR ABUT.		E Abut.			
WT. of RAM 5,512			SIZE or NO. D25-32		CUT-OFF ELEVATION		895.50		CONTRACTOR Lunda					
INSPECTED BY		KC TSW												
1	2	3	4	5	6	1	2	3	4	5	6			
FEET PENET. BELOW CUT-OFF	DROP of HAMMER or RAM (FEET)	ENERGY per BLOW (FT LBS)	BLOWS per MIN per FT	INCHES PENET. per BLOW	BEARING in TONS	FEET PENET. BELOW CUT-OFF	DROP of HAMMER or RAM (FEET)	ENERGY per BLOW (FT LBS)	BLOWS per MIN per FT	INCHES PENET. per BLOW	BEARING in TONS			
30						65								
31						66								
32						67								
33						68								
34						69								
35						70								
36						71								
37						72								
38				13	0.923	73								
39				14	0.857	74								
40				14	0.857	75								
41				14	0.857	76								
42				16	0.750	77								
43				16	0.750	78								
44				16	0.750	79								
45				19	0.632	80								
46				17	0.706	81								
47				20	0.600	82								
48				21	0.571	83								
49				21	0.571	84								
50				21	0.571	85								
51				25	0.480	86								
52				25	0.480	87								
53				38	0.316	88								
54				40	0.300	89								
55				61	0.197	90								
56				42	0.286	91								
57				38	0.316	92								
58				41	0.293	93								
59	5	27560		38	0.316	212.1	94							
60	5	27560		45	0.267	234.4	95							
61	5	27560		62	0.194	278.0	96							
62	5	27560		56	0.214	264.0	97							
63	6	33072		169	0.071	484.4	98							
64							99							

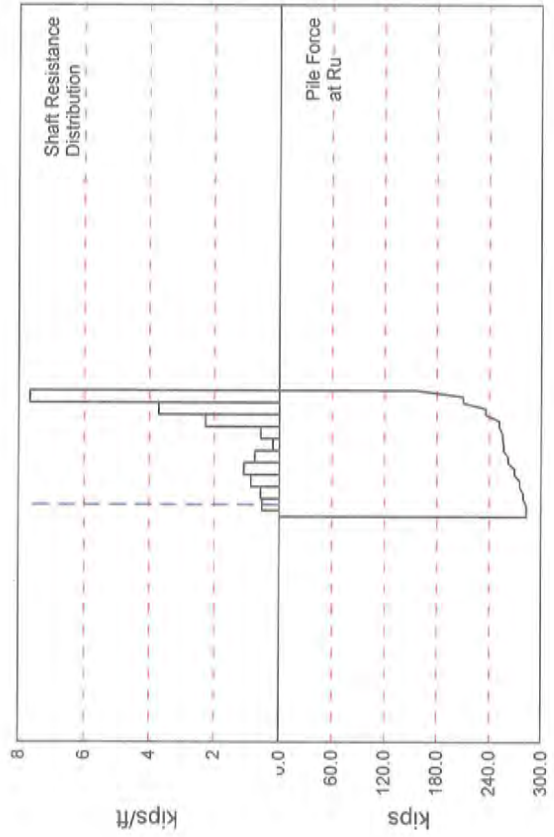
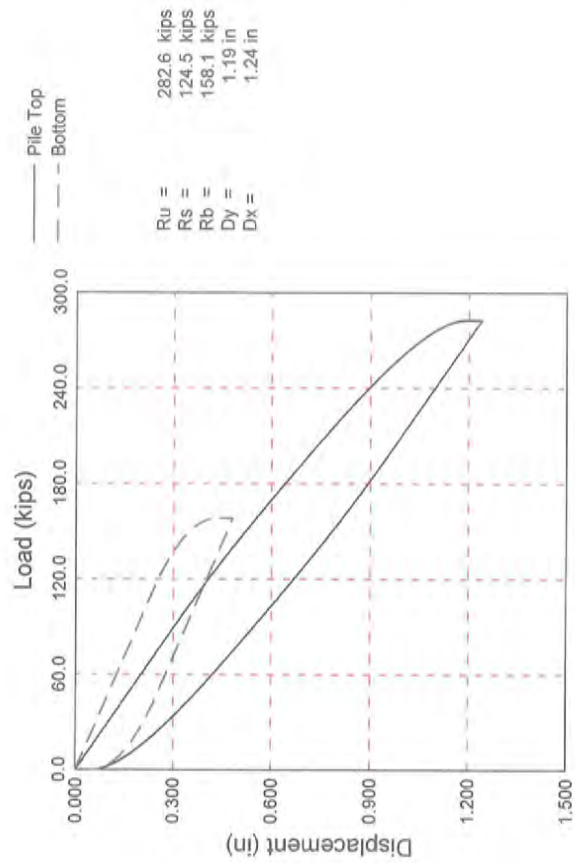
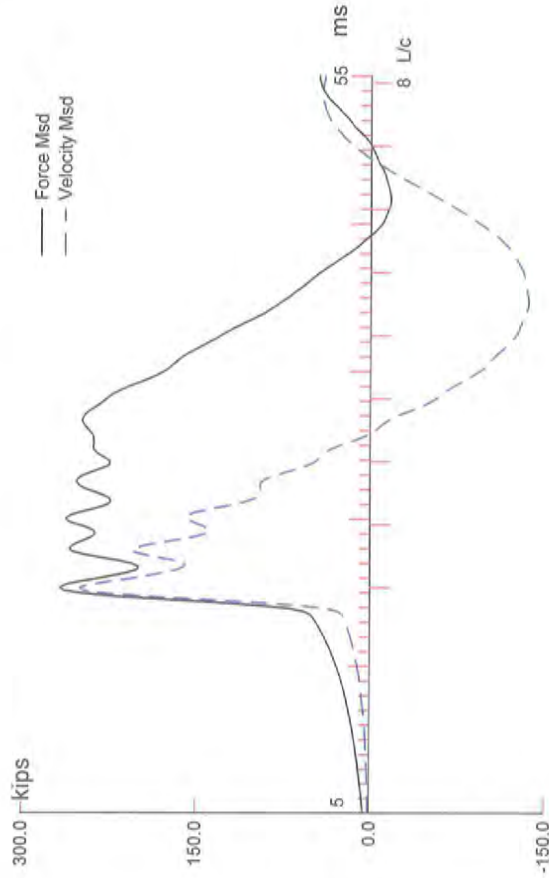
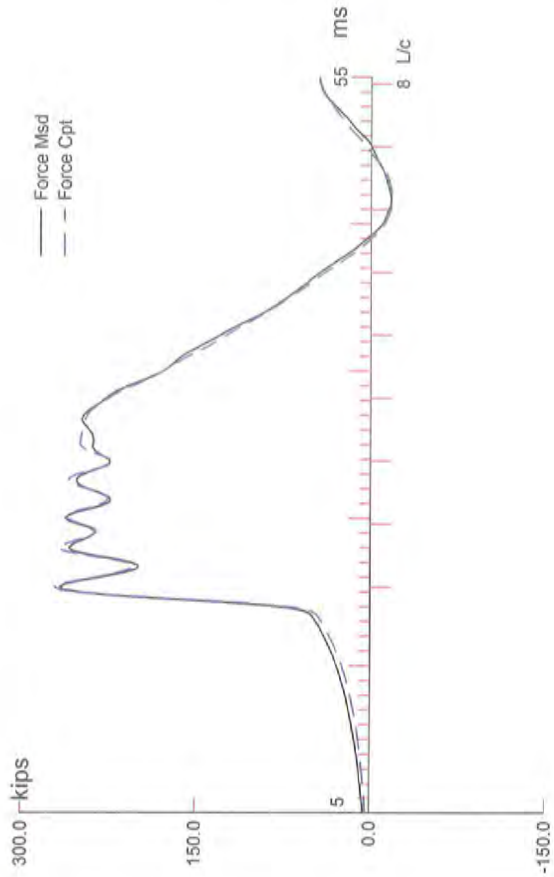
DATE 12/19/2012	START DRIVING TIME 9:15	END DRIVING TIME 10:04	DOWN TIME 15 min	DRIVING TIME 34 min
--------------------	----------------------------	---------------------------	---------------------	------------------------

REMARKS ON DRIVING CONDITIONS, PRE-BORING, ETC. (IDENTIFY BY FEET PENET.)  
Substantial refusal at 63' below cutoff EOID 1/2" in ten blows repeatedly Restrike after 24 hours = 3/8" in ten blows.

FORMULA USED $P = \frac{10.5E}{S + 0.2} \frac{W + 0.1M}{W + M}$	DESIGN BEARING (Tons) 312.5	AUTHORIZED PILE LENGTHS
INSPECTOR SIGNATURE	PROJ. ENGR. SIGNATURE	BRIDGE OFFICE SIGNATURE
		DATE



**TEST PILE NO. 2  
HSDPT RESULTS  
INITIAL DRIVING**



694-Snelling; Pile: TP-2 (SLT)  
 12.75" CIP, APE D25-32, FS=3; Blow: 983  
 American Engineering Testing, Inc.

Test: 05-Dec-2012 12:57:  
 CAPWAP(R) 2006  
 OP: DSV/GRR

# CAPWAP SUMMARY RESULTS

Total CAPWAP Capacity: 282.6; along Shaft 124.5; at Toe 158.1 kips

Soil Sgmnt No.	Dist. Below Gages ft	Depth Below Grade ft	Ru kips	Force in Pile kips	Sum of Ru kips	Unit Resist. (Depth) kips/ft	Unit Resist. (Area) ksf	Smith Damping Factor s/ft
				282.6				
1	10.3	1.5	3.6	279.0	3.6	2.47	0.74	0.205
2	17.1	8.3	3.9	275.1	7.5	0.57	0.17	0.205
3	23.9	15.1	5.9	269.2	13.4	0.86	0.26	0.205
4	30.8	22.0	7.4	261.8	20.8	1.08	0.32	0.205
5	37.6	28.8	5.1	256.7	25.9	0.75	0.22	0.205
6	44.4	35.6	1.4	255.3	27.3	0.20	0.06	0.205
7	51.3	42.5	3.9	251.4	31.2	0.57	0.17	0.205
8	58.1	49.3	15.5	235.9	46.7	2.27	0.68	0.205
9	65.0	56.2	25.4	210.5	72.1	3.71	1.11	0.205
10	71.8	63.0	52.4	158.1	124.5	7.66	2.30	0.205
Avg. Shaft			12.5			1.98	0.59	0.205
Toe			158.1				178.31	0.024

## Soil Model Parameters/Extensions

	Shaft	Toe
Quake	0.295	0.333
Case Damping Factor	1.453	0.220
Damping Type		Smith
Unloading Quake	(% of loading quake)	85
Reloading Level	(% of Ru)	100
Unloading Level	(% of Ru)	0
Soil Plug Weight	(kips)	0.05

CAPWAP match quality = 2.97 (Wave Up Match) ; RSA = 0  
 Observed: final set = 0.050 in; blow count = 240 b/ft  
 Computed: final set = 0.071 in; blow count = 169 b/ft  
 max. Top Comp. Stress = 27.92 ksi (T= 20.7 ms, max= 1.060 x Top)  
 max. Comp. Stress = 29.59 ksi (Z= 58.1 ft, T= 28.9 ms)  
 max. Tens. Stress = -4.5 ksi (Z= 51.3 ft, T= 48.2 ms)  
 max. Energy (EMX) = 19.9 kip-ft; max. Measured Top Displ. (DMX)= 1.11 in

694-Snelling; File: TP-2 (SLT)  
 12.75" CIP, APE D25-32, FS=3; Blow: 983  
 American Engineering Testing, Inc.

Test: 05-Dec-2012 12:57:  
 CAPWAP(R) 2006  
 OP: DSV/GRR

EXTREMA TABLE

File Sgmt No.	Dist. Below Gages ft	max. Force kips	min. Force kips	max. Comp. Stress ksi	max. Tens. Stress ksi	max. Trnsfd. Energy kip-ft	max. Veloc. ft/s	max. Displ. in
1	3.4	274.2	-41.9	27.92	-4.3	19.86	13.9	1.089
2	6.8	277.5	-42.7	28.26	-4.3	19.47	13.7	1.053
3	10.3	281.1	-43.0	28.62	-4.4	19.08	13.5	1.017
4	13.7	272.2	-42.0	27.72	-4.3	17.96	13.3	0.981
5	17.1	281.1	-42.3	28.62	-4.3	17.57	13.0	0.945
6	20.5	280.1	-41.3	28.52	-4.2	16.45	12.7	0.908
7	23.9	287.4	-42.4	29.27	-4.3	16.03	12.4	0.871
8	27.4	282.1	-41.9	28.73	-4.3	14.67	12.1	0.834
9	30.8	283.1	-44.2	28.83	-4.5	14.27	11.9	0.798
10	34.2	273.6	-41.6	27.86	-4.2	12.82	11.7	0.761
11	37.6	279.4	-42.8	28.45	-4.4	12.41	11.5	0.725
12	41.0	279.2	-41.4	28.43	-4.2	11.38	11.4	0.688
13	44.4	287.6	-42.8	29.28	-4.4	11.00	11.2	0.653
14	47.9	288.2	-43.4	29.35	-4.4	10.48	11.0	0.617
15	51.3	288.9	-44.4	29.42	-4.5	10.10	10.6	0.582
16	54.7	284.1	-43.5	28.93	-4.4	9.38	10.1	0.546
17	58.1	290.6	-44.3	29.59	-4.5	9.00	9.5	0.511
18	61.5	273.7	-37.9	27.87	-3.9	7.60	8.9	0.478
19	65.0	278.1	-38.8	28.32	-4.0	7.29	8.7	0.446
20	68.4	244.9	-28.7	24.94	-2.9	5.66	9.0	0.417
21	71.8	245.1	-29.6	24.95	-3.0	3.15	8.8	0.387
Absolute	58.1			29.59			(T =	28.9 ms)
	51.3				-4.5		(T =	48.2 ms)

694-Snelling; File: TP-2 (SLT)  
 12.75" CIP, APE D25-32, FS=3; Blow: 983  
 American Engineering Testing, Inc.

Test: 05-Dec-2012 12:57:  
 CAPWAP(R) 2006  
 OP: DSV/GRR

CASE METHOD										
J =	0.0	0.1	0.2	0.3	0.4	0.5	0.6	0.7	0.8	0.9
RX	365.4	355.1	344.7	334.4	325.7	318.5	311.4	304.2	297.1	290.5
RU	350.7	333.0	315.2	297.5	279.7	262.0	244.2	226.5	208.7	191.0

RAU = 176.5 (kips); RA2 = 341.4 (kips)

Current CAPWAP Ru = 282.6 (kips);

matches RX9 within 5%

VMX	VFN	VT1*Z	FT1	FMX	DMX	DFN	SET	EMX	QUS
ft/s	ft/s	kips	kips	kips	in	in	in	kip-ft	kips
14.72	0.00	257.9	270.4	270.4	1.107	0.030	0.050	20.6	426.5

Peak Velocity Time = 20.55 ms.

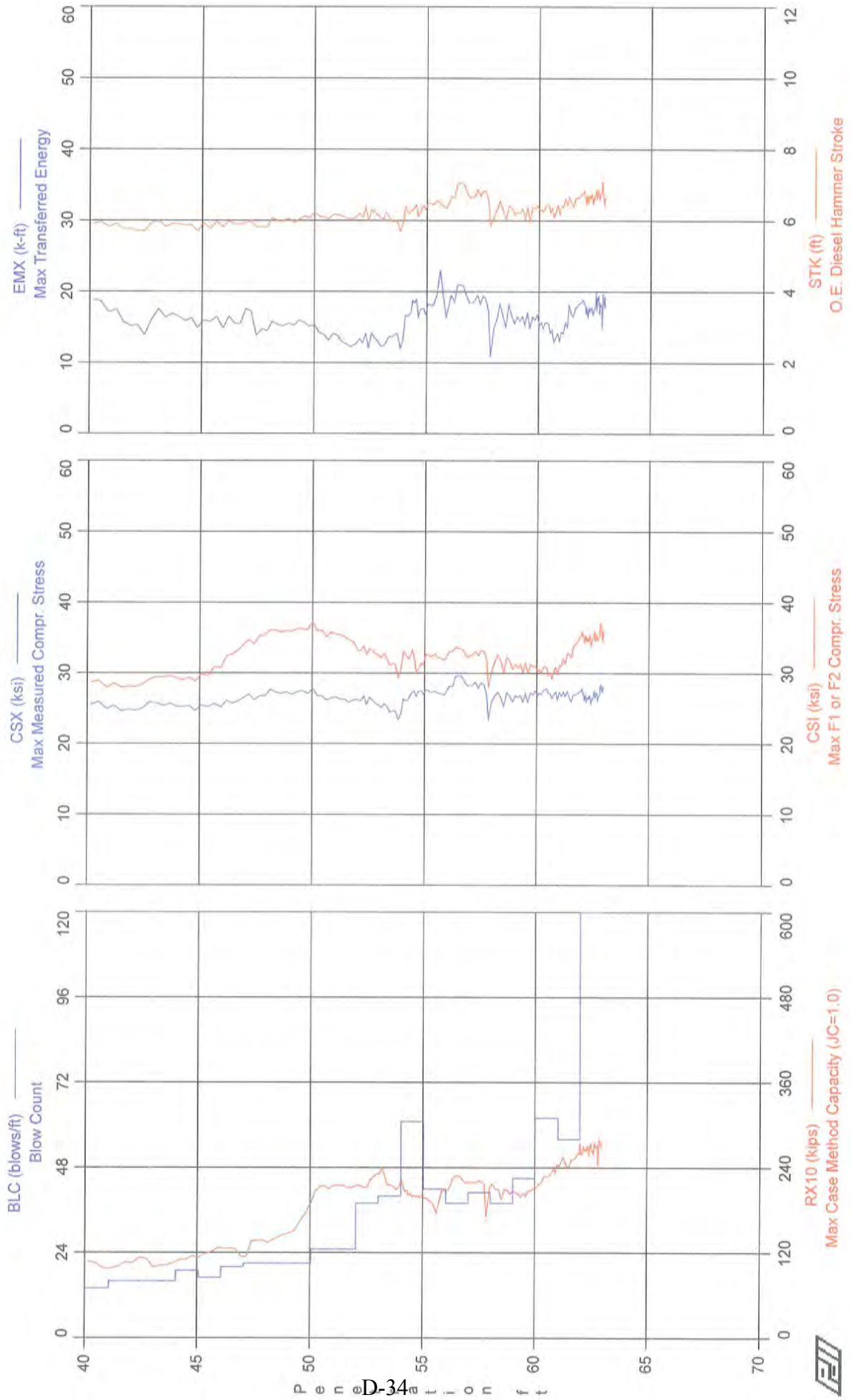
PILE PROFILE AND PILE MODEL				
Depth	Area	E-Modulus	Spec. Weight	Perim.
ft	in <sup>2</sup>	ksi	lb/ft <sup>3</sup>	ft
0.00	9.82	29992.2	492.000	3.338
71.80	9.82	29992.2	492.000	3.338

Toe Area 0.887 ft<sup>2</sup>

Top Segment Length 3.42 ft, Top Impedance 17.52 kips/ft/s

Pile Damping 1.0 %, Time Incr 0.203 ms, Wave Speed 16807.9 ft/s, 2L/c 8.5 ms

694-Snelling - TP-2



694-Snelling - TP-2

12" CIP, APE D25-32, FS=4

OP: DSV/GRR

Test date: 5-Dec-2012

AR: 9.82 in<sup>2</sup>

SP: 0.492 k/ft<sup>3</sup>

LE: 71.80 ft

EM: 30,000 ksi

WS: 16,807.9 f/s

JC: 0.90

FMX: Maximum Force

CSX: Max Measured Compr. Stress

VMX: Maximum Velocity

CSI: Max F1 or F2 Compr. Stress

STK: O.E. Diesel Hammer Stroke

RX10: Max Case Method Capacity (JC=1.0)

EMX: Max Transferred Energy

SFT: Skin friction total

BTA: BETA Integrity Factor

BL#	depth ft	BLC bl/ft	FMX kips	VMX f/s	STK ft	EMX k-ft	BTA (%)	CSX ksi	CSI ksi	RX10 kips	SFT kips
146	40.00	14	241	12.4	5.67	18.6	76.0	24.6	27.6	110	180
157	40.79	14	225	11.3	5.36	14.9	78.0	22.9	26.0	97	167
168	41.50	16	244	12.4	5.85	15.7	79.0	24.9	28.0	98	215
179	42.19	16	255	13.1	6.04	16.2	87.0	26.0	28.9	98	212
190	42.88	16	259	13.0	6.02	16.8	77.0	26.4	29.5	104	204
201	43.56	16	258	13.0	6.03	18.0	78.0	26.3	29.8	101	195
212	44.21	19	250	12.6	5.96	16.9	78.0	25.5	29.4	106	186
223	44.79	19	243	12.2	5.79	15.2	76.0	24.8	29.2	116	182
234	45.41	17	265	13.5	6.29	18.6	76.0	27.0	31.7	113	180
245	46.05	20	234	10.8	5.35	12.9	77.0	23.8	29.2	135	209
256	46.60	20	254	12.4	5.92	15.2	77.0	25.9	32.8	126	219
267	47.14	21	253	12.1	5.77	16.2	78.0	25.8	33.4	114	196
278	47.67	21	262	12.3	5.83	14.8	78.0	26.7	35.5	137	216
289	48.19	21	268	12.1	5.79	15.1	77.0	27.3	36.2	141	205
300	48.71	21	262	11.8	5.70	14.2	76.0	26.7	35.7	148	199
311	49.24	21	275	12.3	5.95	16.9	80.0	28.0	37.0	146	223
322	49.76	21	272	12.8	6.14	15.7	80.0	27.7	36.6	173	214
333	50.24	25	259	12.6	5.94	13.7	100.0	26.3	35.2	209	210
344	50.68	25	257	12.3	6.01	12.9	100.0	26.2	35.9	217	216
355	51.12	25	265	12.8	6.17	14.1	90.0	27.0	35.8	215	205
366	51.56	25	271	12.9	6.37	13.7	100.0	27.6	36.6	219	214
377	52.00	25	255	12.3	5.98	12.6	100.0	26.0	31.8	215	225
388	52.29	38	261	13.0	6.31	14.1	85.0	26.6	33.1	217	221
399	52.58	38	262	13.2	6.43	15.1	80.0	26.7	33.9	211	213
410	52.87	38	255	12.6	6.22	13.2	72.0	26.0	32.9	233	238
421	53.15	40	250	11.8	6.18	11.8	76.0	25.5	33.3	246	230
432	53.43	40	242	11.7	5.96	14.3	77.0	24.7	30.9	213	192
443	53.70	40	248	11.9	6.03	14.4	69.0	25.2	32.2	220	197
454	53.98	40	237	11.9	5.99	14.3	80.0	24.1	30.3	197	185
465	54.16	61	260	13.0	6.33	16.3	75.0	26.5	33.3	215	190
476	54.34	61	259	12.8	6.16	17.1	79.0	26.4	31.9	202	189
487	54.52	61	262	13.0	6.17	17.6	89.0	26.7	31.2	202	186
498	54.70	61	266	13.0	6.18	15.9	88.0	27.1	29.8	208	201
509	54.89	61	272	13.8	6.50	17.6	80.0	27.7	32.0	198	218
520	55.10	42	274	13.9	6.59	19.5	78.0	27.9	33.6	193	227
533	55.40	42	272	13.6	6.61	19.4	78.0	27.7	32.8	193	214
545	55.69	42	271	14.6	6.47	23.4	58.0	27.6	32.5	175	205
563	56.13	38	276	14.1	6.76	18.6	74.0	28.2	32.7	215	204
574	56.42	38	291	15.1	7.12	21.0	70.0	29.6	34.1	228	217
585	56.71	38	289	15.1	7.10	20.7	76.0	29.4	33.7	227	226
596	57.00	38	271	13.4	6.38	17.2	73.0	27.6	31.7	216	216
607	57.27	41	285	14.8	7.00	20.2	60.0	29.0	33.5	220	251
618	57.54	41	285	14.9	7.03	20.2	59.0	29.0	33.8	226	252
629	57.80	41	268	13.5	6.50	17.0	69.0	27.3	32.3	217	216
643	58.16	38	259	13.8	6.21	15.7	83.0	26.4	31.5	214	232
654	58.45	38	267	14.4	6.54	18.2	85.0	27.2	32.8	214	243
665	58.74	38	269	14.3	6.38	17.7	87.0	27.4	32.3	208	233
676	59.02	45	268	14.1	6.42	17.3	89.0	27.3	31.6	208	244
687	59.27	45	265	14.0	6.30	17.2	100.0	27.0	31.4	200	240
698	59.51	45	272	14.8	6.64	18.3	100.0	27.7	32.3	204	247
709	59.76	45	271	14.3	6.39	17.1	100.0	27.6	31.3	208	252
720	60.00	45	265	14.2	6.42	16.2	89.0	27.0	30.7	208	252
731	60.18	62	268	14.4	6.53	16.0	86.0	27.3	30.9	216	261
742	60.35	62	267	13.6	6.23	14.3	83.0	27.2	30.1	228	267
753	60.53	62	261	13.2	6.08	12.9	78.0	26.6	28.7	228	269
764	60.71	62	262	13.1	5.96	13.0	72.0	26.7	29.0	235	266
775	60.89	62	267	14.3	6.53	14.3	78.0	27.2	30.8	236	276
786	61.07	56	250	13.2	6.10	12.6	74.0	25.4	29.5	232	260
797	61.27	56	268	14.6	6.60	14.9	78.0	27.3	32.4	266	265
808	61.46	56	265	14.3	6.58	16.7	82.0	27.0	33.3	245	231

694-Snelling - TP-2

12" CIP, APE D25-32, FS=4

OP: DSV/GRR

Test date: 5-Dec-2012

BL#	depth ft	BLC bl/ft	FMX kips	VMX f/s	STK ft	EMX k-ft	BTA (%)	CSX ksi	CSI ksi	RX10 kips	SFT kips
819	61.66	56	260	14.2	6.48	16.6	88.0	26.5	33.1	251	214
830	61.86	56	258	14.0	6.41	17.0	84.0	26.2	33.7	247	204
841	62.02	166	286	15.9	7.16	20.5	90.0	29.1	37.8	269	211
852	62.08	166	273	15.0	6.85	18.6	90.0	27.8	36.7	268	193
863	62.15	166	264	14.7	6.66	17.9	100.0	26.9	34.8	266	200
874	62.22	166	260	14.2	6.58	17.4	90.0	26.5	35.0	273	198
885	62.28	166	267	15.0	6.89	18.6	88.0	27.2	35.5	275	201
896	62.35	166	264	14.7	6.83	18.1	90.0	26.9	35.7	275	194
907	62.42	166	246	13.7	6.29	16.4	100.0	25.0	33.2	250	184
918	62.48	166	264	13.9	6.84	15.8	88.0	26.9	36.0	290	212
929	62.55	166	261	14.2	6.62	17.4	100.0	26.6	35.3	267	200
940	62.62	166	266	14.5	6.72	23.6	64.0	27.1	34.4	236	162
951	62.68	166	270	14.8	6.87	17.7	88.0	27.5	35.7	280	204
962	62.75	166	267	15.0	6.92	18.7	89.0	27.2	35.3	278	206
973	62.82	166	262	14.6	6.71	16.9	100.0	26.7	35.5	274	215
988	62.91	166	280	14.9	6.75	19.6	90.0	28.5	35.1	271	199
999	62.97	250	275	14.4	6.58	18.1	90.0	28.0	36.6	274	196
Average			262	13.5	6.32	16.4	82.8	26.7	32.7	206	214
Std. Dev.			13	1.1	0.39	2.6	9.5	1.3	2.5	51	25
Maximum			301	20.5	7.28	43.8	100.0	30.7	39.7	290	285
@ Blow#			998	540	582	540	259	998	983	918	755

Total number of blows analyzed: 841

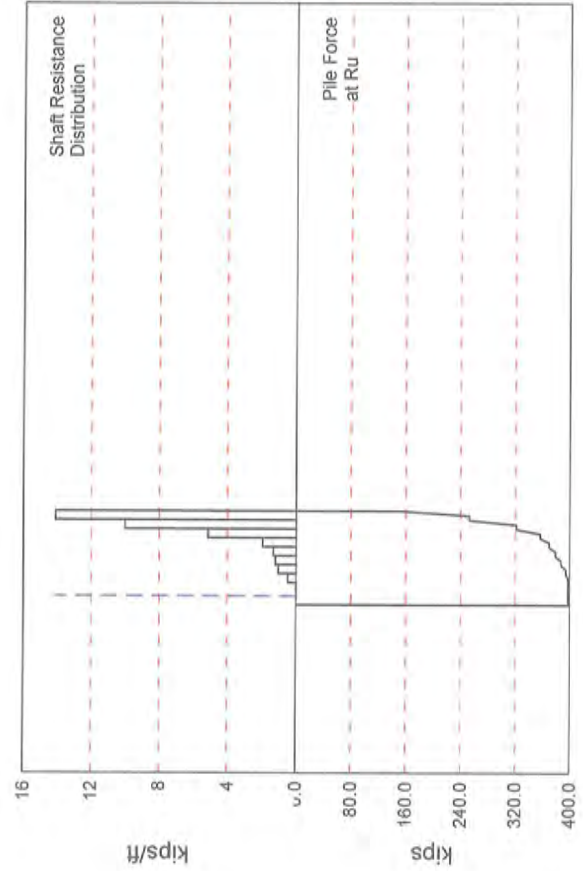
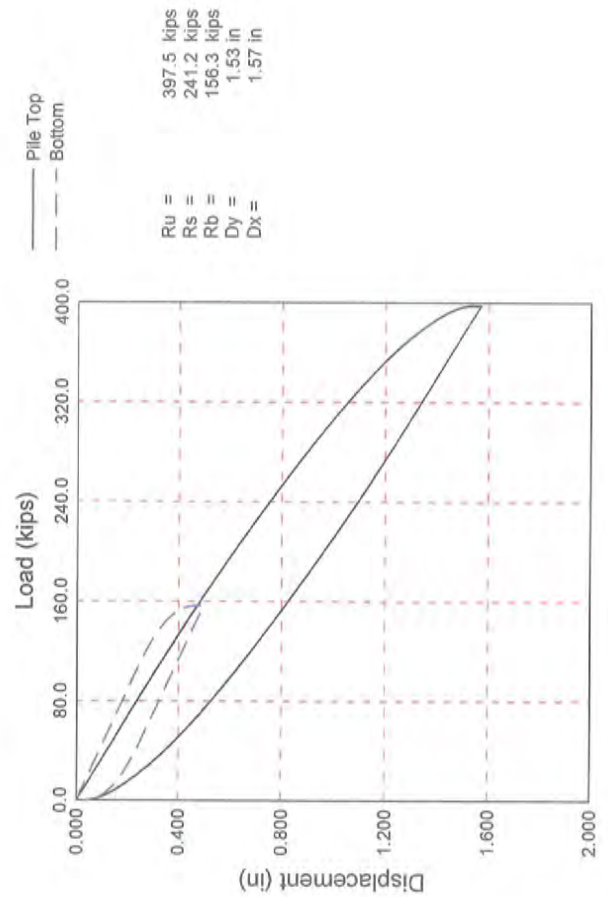
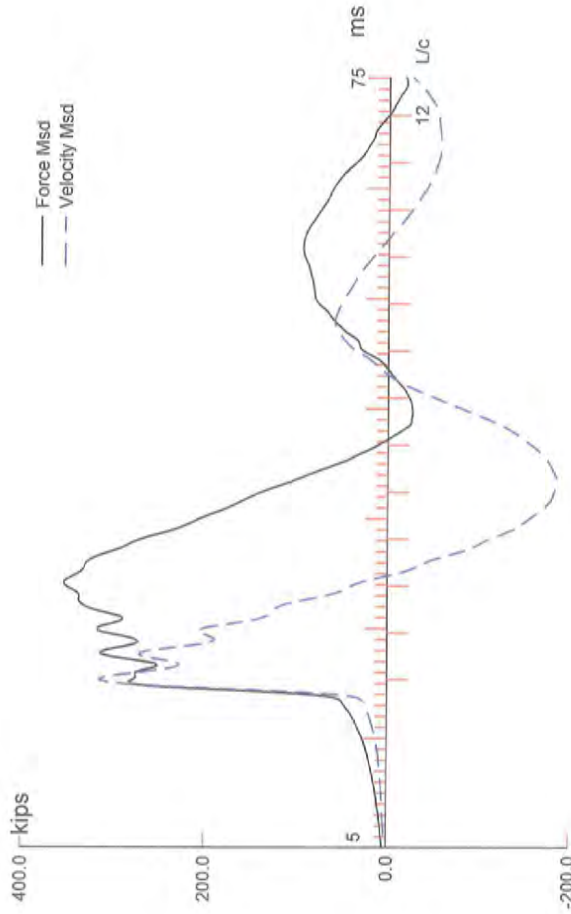
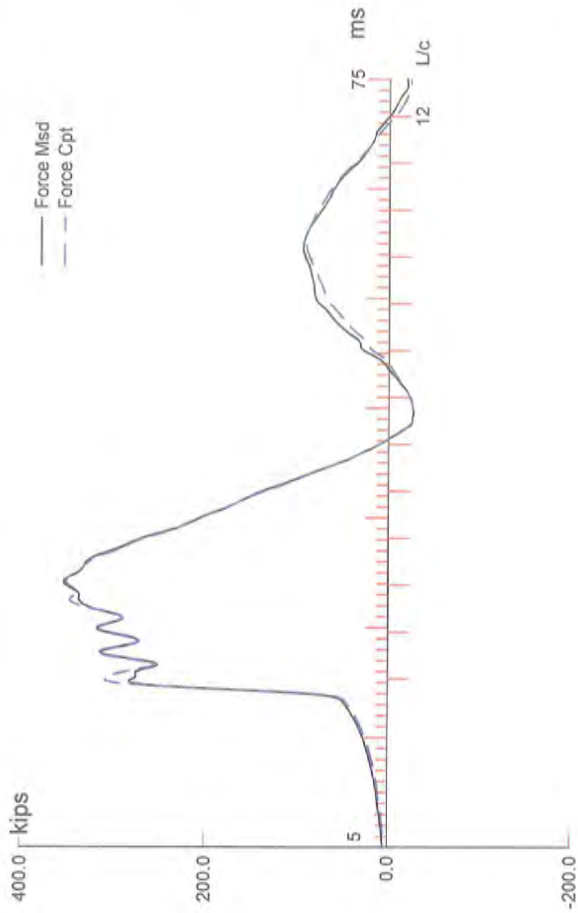
#### Time Summary

Drive 31 minutes 21 seconds 12:26:18 PM - 12:57:39 PM (12/5/2012) BN 1 - 1005  
 Stop 13 days 21 hours 12 minutes 41 seconds 12:57:39 PM - 10:10:20 AM  
 Drive 10:10:20 AM - 10:10:20 AM BN 1006 - 1007

Total time [333:44:02] = (Driving [0:31:21] + Stop [333:12:41])



**TEST PILE 2  
HSDPT RESULTS  
RESTRICK No. 1**



694-Snelling; File: TP-2 (SLT)  
 12.75" CIP, APE D25-32, FS=3; Blow: 4  
 American Engineering Testing, Inc.

Test: 20-Dec-2012 11:45:  
 CAPWAP(R) 2006  
 OP: DSV/JM

CAPWAP SUMMARY RESULTS

Total CAPWAP Capacity: 397.5; along Shaft 241.2; at Toe 156.3 kips								
Soil Sgmt No.	Dist. Below Gages ft	Depth Below Grade ft	Ru kips	Force in File kips	Sum of Ru kips	Unit Resist. (Depth) kips/ft	Unit Resist. (Area) ksf	Smith Damping Factor s/ft
				397.5				
1	10.3	1.5	0.0	397.5	0.0	0.00	0.00	0.000
2	17.1	8.3	0.1	397.4	0.1	0.01	0.00	0.158
3	23.9	15.1	3.3	394.1	3.4	0.48	0.14	0.158
4	30.8	22.0	7.0	387.1	10.4	1.02	0.31	0.158
5	37.6	28.8	8.3	378.8	18.7	1.21	0.36	0.158
6	44.4	35.6	9.1	369.7	27.8	1.33	0.40	0.158
7	51.3	42.5	13.3	356.4	41.1	1.94	0.58	0.158
8	58.1	49.3	35.2	321.2	76.3	5.15	1.54	0.158
9	65.0	56.2	68.5	252.7	144.8	10.02	3.00	0.158
10	71.8	63.0	96.4	156.3	241.2	14.10	4.22	0.158
Avg. Shaft			24.1			3.83	1.15	0.158
Toe			156.3				176.28	0.024

Soil Model Parameters/Extensions		Shaft	Toe
Quake		0.223	0.352
Case Damping Factor		2.172	0.214
Damping Type			Smith
Unloading Quake	(% of loading quake)	73	100
Reloading Level	(% of Ru)	100	100
Unloading Level	(% of Ru)	0	

CAPWAP match quality	=	2.27	(Wave Up Match) ; RSA = 0
Observed: final set	=	0.038 in;	blow count = 320 b/ft
Computed: final set	=	0.004 in;	blow count = 3048 b/ft
max. Top Comp. Stress	=	36.74 ksi	(T= 29.7 ms, max= 1.135 x Top)
max. Comp. Stress	=	41.71 ksi	(Z= 44.4 ft, T= 27.9 ms)
max. Tens. Stress	=	-7.5 ksi	(Z= 44.4 ft, T= 46.4 ms)
max. Energy (EMX)	=	29.9 kip-ft;	max. Measured Top Displ. (DMX)= 1.37 in

694-Snelling; Pile: TP-2 (SLT)  
 12.75" CIP, APE D25-32, FS=3; Blow: 4  
 American Engineering Testing, Inc.

Test: 20-Dec-2012 11:45:  
 CAPWAP(R) 2006  
 OP: DSV/JM

EXTREMA TABLE

Pile Sgmnt No.	Dist. Below Gages ft	max. Force kips	min. Force kips	max. Comp. Stress ksi	max. Tens. Stress ksi	max. Trnsfd. Energy kip-ft	max. Veloc. ft/s	max. Displ. in
1	3.4	360.8	-33.1	36.74	-3.4	29.85	16.1	1.319
2	6.8	368.9	-38.7	37.57	-3.9	29.10	16.1	1.269
3	10.3	374.2	-44.6	38.10	-4.5	28.32	16.0	1.218
4	13.7	377.4	-50.1	38.44	-5.1	27.54	15.9	1.167
5	17.1	385.3	-55.5	39.23	-5.6	26.75	15.8	1.115
6	20.5	393.8	-60.5	40.10	-6.2	25.91	15.5	1.062
7	23.9	400.6	-65.5	40.80	-6.7	25.08	15.3	1.010
8	27.4	400.1	-68.1	40.74	-6.9	23.60	14.9	0.957
9	30.8	401.9	-71.9	40.93	-7.3	22.77	14.6	0.904
10	34.2	398.1	-70.4	40.54	-7.2	20.81	14.2	0.853
11	37.6	408.3	-73.4	41.58	-7.5	20.03	13.8	0.801
12	41.0	403.4	-71.1	41.08	-7.2	18.13	13.4	0.751
13	44.4	409.6	-73.8	41.71	-7.5	17.37	13.0	0.700
14	47.9	397.7	-71.3	40.50	-7.3	15.63	12.4	0.651
15	51.3	399.4	-73.7	40.67	-7.5	14.91	11.7	0.602
16	54.7	383.3	-69.2	39.03	-7.0	13.11	10.7	0.555
17	58.1	387.4	-71.4	39.45	-7.3	12.46	9.6	0.508
18	61.5	344.3	-57.2	35.06	-5.8	9.78	8.5	0.466
19	65.0	347.1	-59.2	35.34	-6.0	9.25	7.9	0.423
20	68.4	270.3	-34.1	27.53	-3.5	6.11	7.6	0.388
21	71.8	273.3	-36.2	27.83	-3.7	2.45	6.9	0.352
Absolute	44.4			41.71			(T =	27.9 ms)
	44.4				-7.5		(T =	46.4 ms)

694-Snelling; Pile: TP-2 (SLT)  
 12.75" CIP, APE D25-32, FS=3; Blow: 4  
 American Engineering Testing, Inc.

Test: 20-Dec-2012 11:45:  
 CAPWAP(R) 2006  
 OP: DSV/JM

	CASE METHOD									
J =	0.0	0.1	0.2	0.3	0.4	0.5	0.6	0.7	0.8	0.9
RX	484.2	473.5	462.8	452.2	441.5	430.9	420.3	409.6	399.9	390.9
RU	457.0	443.0	429.1	415.1	401.1	387.1	373.2	359.2	345.2	331.3

RAU = 194.3 (kips); RA2 = 440.3 (kips)

Current CAPWAP Ru = 397.5 (kips); J(RX) = 0.83

VMX	VFN	VT1*Z	FT1	FMX	DMX	DFN	SET	EMX	QUS
ft/s	ft/s	kips	kips	kips	in	in	in	kip-ft	kips
18.28	0.00	320.3	276.3	355.4	1.370	0.030	0.038	30.8	524.5

Peak Velocity Time = 20.55 ms.

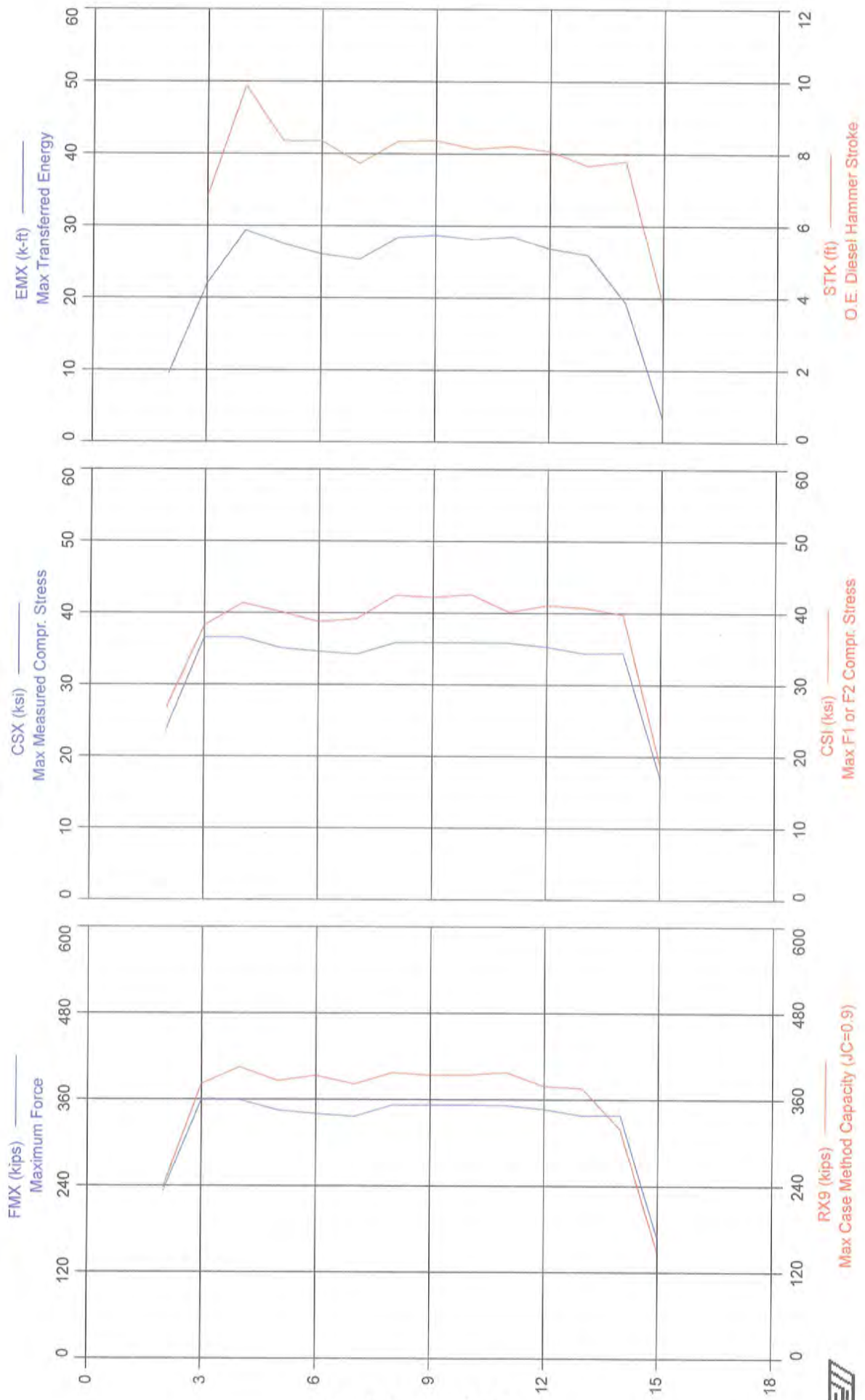
PILE PROFILE AND PILE MODEL				
Depth	Area	E-Modulus	Spec. Weight	Perim.
ft	in <sup>2</sup>	ksi	lb/ft <sup>3</sup>	ft
0.00	9.82	29992.2	492.000	3.338
71.80	9.82	29992.2	492.000	3.338

Toe Area 0.887 ft<sup>2</sup>

Top Segment Length 3.42 ft, Top Impedance 17.52 kips/ft/s

Pile Damping 1.0 %, Time Incr 0.203 ms, Wave Speed 16807.9 ft/s, 2L/c 8.5 ms

694-Snelling - TP-2 (SLT)



694-Snelling - TP-2 (SLT)

12" CIP, APE D25-32, FS=4

OP: DSV/JM

Test date: 20-Dec-2012

AR: 9.82 in^2

SP: 0.492 k/ft3

LE: 71.80 ft

EM: 30,000 ksi

WS: 16,807.9 f/s

JC: 0.70

FMX: Maximum Force

CSX: Max Measured Compr. Stress

VMX: Maximum Velocity

CSI: Max F1 or F2 Compr. Stress

STK: O.E. Diesel Hammer Stroke

RX9: Max Case Method Capacity (JC=0.9)

EMX: Max Transferred Energy

SFT: Skin friction total

BTA: BETA Integrity Factor

BL#	depth ft	FMX kips	VMX f/s	STK ft	EMX k-ft	BTA (%)	CSX ksi	CSI ksi	RX9 kips	SFT kips
2	63.00	233	10.5	0.00	9.6	100.0	23.7	26.7	238	246
3	63.00	360	14.0	6.83	22.1	89.0	36.6	38.3	382	271
4	63.00	359	19.5	9.89	29.4	60.0	36.6	41.4	405	353
5	63.00	345	17.7	8.36	27.5	88.0	35.2	40.2	386	288
6	63.00	340	17.1	8.37	26.1	76.0	34.7	38.8	394	330
7	63.00	336	16.5	7.74	25.4	87.0	34.3	39.2	382	324
8	63.00	352	17.9	8.36	28.4	87.0	35.9	42.5	397	323
9	63.00	353	17.9	8.38	28.7	100.0	35.9	42.3	394	322
10	63.00	352	17.8	8.14	28.1	100.0	35.9	42.6	394	327
11	63.00	352	17.8	8.23	28.5	100.0	35.9	40.2	398	320
12	63.00	347	17.7	8.09	26.9	100.0	35.3	41.1	379	313
13	63.00	338	17.1	7.68	26.0	100.0	34.4	40.8	376	305
14	63.00	339	17.0	7.81	19.4	100.0	34.5	39.8	319	270
15	63.00	167	5.8	3.85	3.4	100.0	17.0	18.8	149	139
Average		327	16.0	7.82	23.5	91.9	33.3	38.1	357	295
Std. Dev.		54	3.5	1.32	7.5	11.5	5.5	6.5	72	51
Maximum		360	19.5	9.89	29.4	100.0	36.6	42.6	405	353
@ Blow#		3	4	4	4	2	3	10	4	4

Total number of blows analyzed: 14

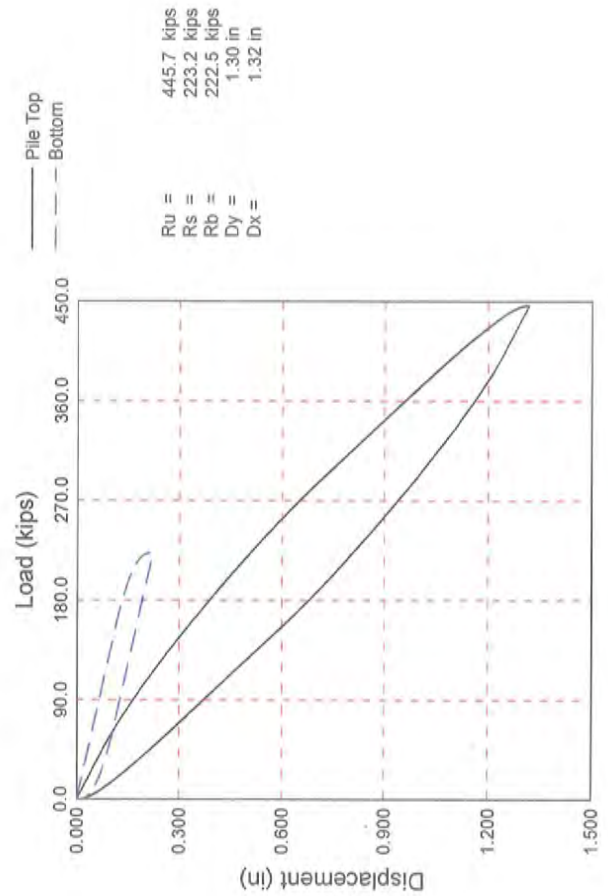
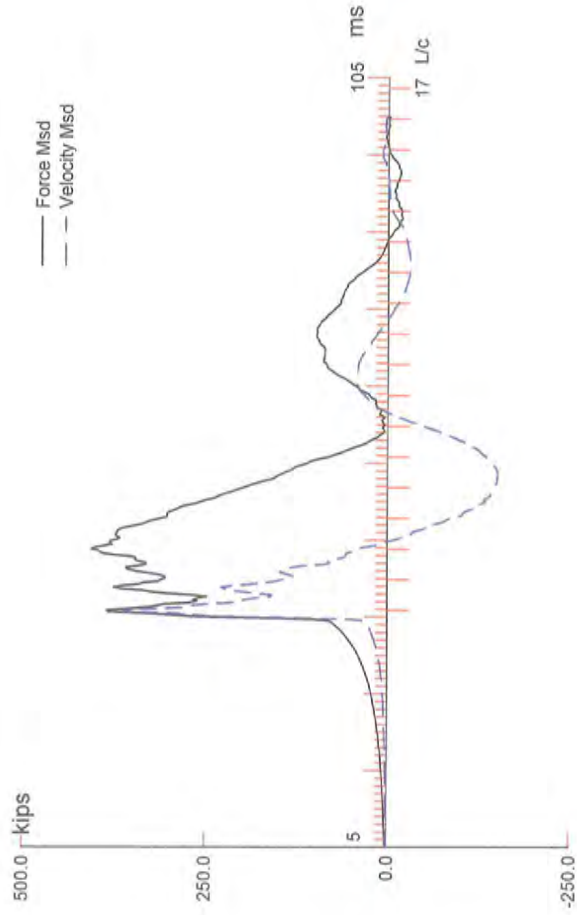
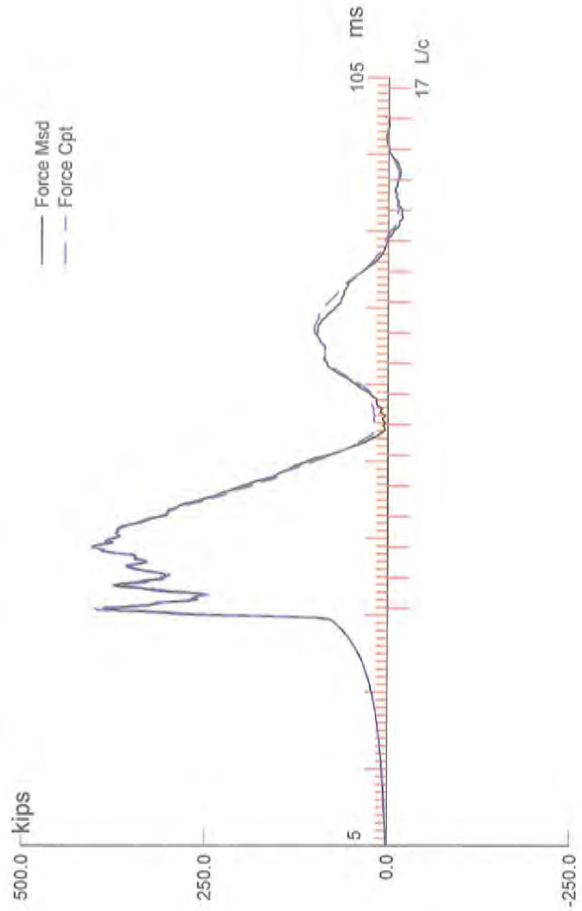
Time Summary

Drive 1 minute

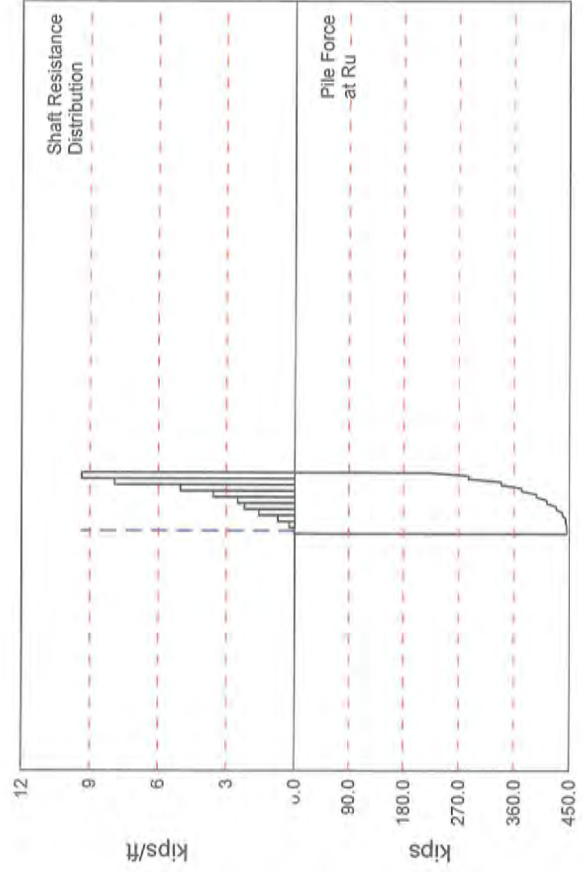
11:45:17 AM - 11:46:17 AM (12/20/2012) BN 1 - 18

**TEST PILE 2  
HSDPT RESULTS  
RESTRICK No. 2**





Ru = 445.7 kips  
Rs = 223.2 kips  
Rb = 222.5 kips  
Dy = 1.30 in  
Dx = 1.32 in



SNELLING; Pile: TP2 RST2  
 APE25-32, 12.75,0.25; Blow: 10  
 American Engineering Testing, Inc.

Test: 15-Jan-2013 13:21:  
 CAPWAP(R) 2006  
 OP: JPB

#### CAPWAP SUMMARY RESULTS

Total CAPWAP Capacity:		445.7; along Shaft	223.2; at Toe	222.5 kips					
Soil Sgmnt No.	Dist. Below Gages ft	Depth Below Grade ft	Ru kips	Force in Pile kips	Sum of Ru kips	Unit Resist. (Depth) kips/ft	Unit Resist. (Area) ksf	Smith Damping Factor s/ft	Quake in
				445.7					
1	6.7	2.7	0.3	445.4	0.3	0.11	0.03	0.128	0.040
2	13.4	9.4	1.6	443.8	1.9	0.24	0.07	0.128	0.040
3	20.1	16.1	5.0	438.8	6.9	0.75	0.22	0.128	0.040
4	26.8	22.8	10.6	428.2	17.5	1.58	0.47	0.128	0.040
5	33.5	29.5	14.9	413.3	32.4	2.22	0.67	0.128	0.040
6	40.2	36.2	16.9	396.4	49.3	2.52	0.76	0.128	0.040
7	46.9	42.9	24.1	372.3	73.4	3.60	1.08	0.128	0.040
8	53.6	49.6	33.8	338.5	107.2	5.04	1.51	0.128	0.040
9	60.3	56.3	53.2	285.3	160.4	7.94	2.38	0.128	0.040
10	67.0	63.0	62.8	222.5	223.2	9.37	2.81	0.128	0.034
Avg. Shaft			22.3			3.54	1.06	0.128	0.038
Toe			222.5				250.95	0.072	0.161

Soil Model Parameters/Extensions				Shaft	Toe
Case Damping Factor				1.632	0.912
Unloading Quake	(% of loading quake)			36	30
Reloading Level	(% of Ru)			100	100
Unloading Level	(% of Ru)			0	
Resistance Gap (included in Toe Quake)					0.009
Soil Plug Weight (kips)					0.00
<hr/>					
CAPWAP match quality		=	2.62	(Wave Up Match) ; RSA = 0	
Observed: final set		=	0.013 in;	blow count	= 960 b/ft
Computed: final set		=	0.066 in;	blow count	= 182 b/ft
max. Top Comp. Stress		=	41.69 ksi	(T= 44.2 ms, max= 1.051 x Top)	
max. Comp. Stress		=	43.81 ksi	(Z= 26.8 ft, T= 43.3 ms)	
max. Tens. Stress		=	-3.8 ksi	(Z= 46.9 ft, T= 61.8 ms)	
max. Energy (EMX)		=	28.5 kip-ft;	max. Measured Top Displ. (DMX)= 1.19 in	

SNELLING; File: TP2 RST2

Test: 15-Jan-2013 13:21:

APE25-32, 12.75,0.25; Blow: 10

CAPWAP (R) 2006

American Engineering Testing, Inc.

OP: JPB

EXTREMA TABLE

File Sgmnt No.	Dist. Below Gages ft	max. Force kips	min. Force kips	max. Comp. Stress ksi	max. Tens. Stress ksi	max. Trnsfd. Energy kip-ft	max. Veloc. ft/s	max. Displ. in
1	3.4	409.4	-14.9	41.69	-1.5	28.45	19.5	1.141
2	6.7	417.8	-16.1	42.54	-1.6	27.59	19.4	1.087
3	10.1	418.1	-17.8	42.58	-1.8	26.62	19.2	1.032
4	13.4	423.8	-19.1	43.16	-1.9	25.70	19.0	0.977
5	16.8	421.8	-19.6	42.95	-2.0	24.47	18.8	0.922
6	20.1	425.7	-20.0	43.35	-2.0	23.51	18.3	0.866
7	23.5	421.3	-20.2	42.91	-2.1	21.78	18.0	0.810
8	26.8	430.2	-24.3	43.81	-2.5	20.80	17.3	0.754
9	30.2	418.1	-25.4	42.57	-2.6	18.46	17.0	0.698
10	33.5	424.2	-29.9	43.20	-3.0	17.51	16.2	0.642
11	36.9	406.9	-30.2	41.44	-3.1	15.03	15.9	0.589
12	40.2	421.6	-34.3	42.93	-3.5	14.14	14.9	0.535
13	43.6	401.4	-35.3	40.88	-3.6	11.90	14.4	0.483
14	46.9	411.6	-37.6	41.91	-3.8	11.08	13.3	0.431
15	50.3	379.7	-35.1	38.66	-3.6	8.84	12.5	0.383
16	53.6	388.1	-35.8	39.52	-3.6	8.12	11.1	0.334
17	57.0	345.2	-31.5	35.15	-3.2	6.04	10.0	0.289
18	60.3	352.2	-31.9	35.86	-3.3	5.42	8.7	0.244
19	63.7	298.3	-24.8	30.38	-2.5	3.54	7.1	0.205
20	67.0	302.6	-25.0	30.81	-2.5	2.15	5.5	0.165
Absolute	26.8			43.81			(T =	43.3 ms)
	46.9				-3.8		(T =	61.8 ms)

SNELLING; File: TP2 RST2  
 APE25-32, 12.75,0.25; Blow: 10  
 American Engineering Testing, Inc.

Test: 15-Jan-2013 13:21:  
 CAPWAP(R) 2006  
 OP: JPB

CASE METHOD										
J =	0.0	0.1	0.2	0.3	0.4	0.5	0.6	0.7	0.8	0.9
RX	558.7	538.7	518.7	498.8	479.3	460.7	450.8	441.2	432.8	426.6
RU	558.7	538.7	518.7	498.8	478.8	458.8	438.8	418.9	398.9	378.9

RAU = 399.7 (kips); RA2 = 436.0 (kips)

Current CAPWAP Ru = 445.7 (kips); J(RX) = 0.65

VMX	VFN	VT1*Z	FT1	FMX	DMX	DFN	SET	EMX	QUS
ft/s	ft/s	kips	kips	kips	in	in	in	kip-ft	kips
20.89	0.00	366.0	392.4	410.8	1.190	0.013	0.013	29.3	584.2

Peak Velocity Time = 36.08 ms.

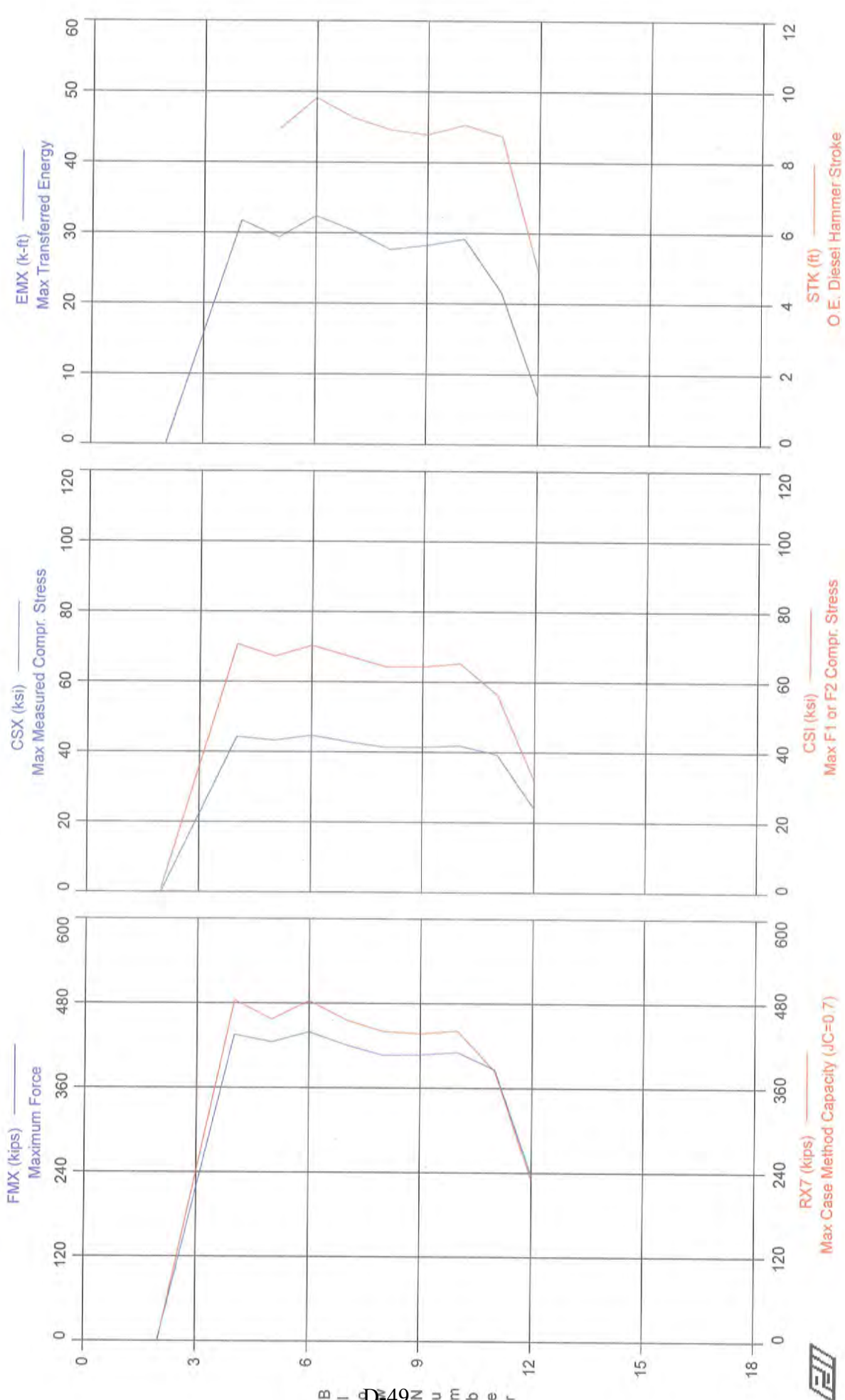
PILE PROFILE AND PILE MODEL				
Depth	Area	E-Modulus	Spec. Weight	Perim.
ft	in <sup>2</sup>	ksi	lb/ft <sup>3</sup>	ft
0.00	9.82	29992.2	492.000	3.338
67.00	9.82	29992.2	492.000	3.338

Toe Area 0.887 ft<sup>2</sup>

Segmnt	Dist.	Impedance	Imped.	Tension	Compression	Perim.	Soil
Number	B.G.		Change	Slack	Slack		Plug
	ft	kips/ft/s	%	in	in	ft	kips
1	3.35	17.52	0.00	0.000	-0.000	3.338	0.00
2	6.70	17.52	0.00	0.000	-0.000	3.338	0.00
20	67.00	17.52	0.00	0.000	-0.000	3.338	0.00

File Damping 1.0 %, Time Incr 0.199 ms, Wave Speed 16807.9 ft/s, 2L/c 8.0 ms

# SNELLING - TP2 RST2



SNELLING - TP2 RST2  
OP: JPB

APE25-32, 12.75, 0.25  
Test date: 15-Jan-2013

AR: 9.82 in<sup>2</sup>  
LE: 67.00 ft  
WS: 16,807.9 f/s

SP: 0.492 k/ft<sup>3</sup>  
EM: 30,000 ksi  
JC: 0.70

FMX: Maximum Force  
VMX: Maximum Velocity  
STK: O.E. Diesel Hammer Stroke  
EMX: Max Transferred Energy  
BTA: BETA Integrity Factor

CSX: Max Measured Compr. Stress  
CSI: Max F1 or F2 Compr. Stress  
RX7: Max Case Method Capacity (JC=0.7)  
SFT: Skin friction total

BL#	depth ft	FMX kips	VMX f/s	STK ft	EMX k-ft	BTA (%)	CSX ksi	CSI ksi	RX7 kips	SFT kips
2	63.00	3	16.3	0.00	0.0	0.0	0.3	1.1	0	0
4	63.00	435	21.8	0.00	31.8	100.0	44.4	70.8	484	393
5	63.00	425	20.2	8.93	29.4	100.0	43.3	67.3	457	373
6	63.00	439	21.7	9.83	32.4	100.0	44.7	70.4	484	386
7	63.00	421	21.0	9.27	30.4	100.0	42.9	67.4	456	364
8	63.00	407	20.5	8.93	27.7	100.0	41.4	64.4	440	316
9	63.00	407	20.5	8.79	28.3	100.0	41.5	64.4	437	322
10	63.00	411	20.9	9.07	29.2	88.0	41.8	65.4	442	319
11	63.00	386	20.1	8.75	21.6	86.0	39.4	56.4	385	295
12	63.00	236	10.0	4.89	6.9	88.0	24.1	32.1	230	207
Average		357	19.3	8.56	23.8	86.2	36.4	56.0	382	298
Std. Dev.		131	3.4	1.42	10.6	29.3	13.3	21.2	145	112
Maximum		439	21.8	9.83	32.4	100.0	44.7	70.8	484	393
@ Blow#		6	4	6	6	4	6	4	4	4
Total number of blows analyzed: 10										

Time Summary

Drive 1 minute 16 seconds

1:19:59 PM - 1:21:15 PM (1/15/2013) BN 1 - 12

**MnDOT PILE DRIVING RECORD  
REACTION PILE NO. 1**

# TEST PILE REPORT

PILE HAMMER DATA					PILE DATA				JOB DESCRIPTION					
TYPE ("X" ONE)					TEST PILE NO.		REACTION 1		BRIDGE NUMBER		62716			
X	DROP				TYPE		CIP 12.750" x .250		T.H. NUMBER		694 WB			
	SINGLE ACTING POWER DRIVEN				LENGTH in LEADS		60+60		S.P. NUMBER		6285-135			
	DOUBLE ACTING POWER DRIVEN				DIAM. of BUTT & TIP				FED. NUMBER					
	MAKE				WEIGHT of PILE		4006		COUNTY		Ramsey			
APE				WEIGHT of CAP		2,050		PIER OR ABUT.		E Abut.				
WT. of RAM		SIZE or NO.			CUT-OFF ELEVATION		895.50		CONTRACTOR					
5,512		D25-32			INSPECTED BY		KC TSW							
1	2	3	4		5	6	1	2	3	4		5	6	
FEET PENET. BELOW CUT-OFF	DROP of HAMMER or RAM (FEET)	ENERGY per BLOW (FT LBS)	BLOWS per MIN FT		INCHES PENET. per BLOW	BEARING in TONS	FEET PENET. BELOW CUT-OFF	DROP of HAMMER or RAM (FEET)	ENERGY per BLOW (FT LBS)	BLOWS per MIN FT		INCHES PENET. per BLOW	BEARING in TONS	
40							75							
41				25	0.480		76							
42				21	0.571		77							
43				23	0.522		78							
44				22	0.545		79							
45				20	0.600		80							
46				20	0.600		81							
47				26	0.462		82							
48				25	0.480		83							
49				29	0.414		84							
50				28	0.429		85							
51				68	0.176		86							
52				64	0.188		87							
53				64	0.188		88							
54				72	0.167		89							
55				58	0.207		90							
56				50	0.240		91							
57	6	33072		112	0.107	299.0	92							
58	6	33072		80	0.150	262.3	93							
59	6	33072		112	0.107	299.0	94							
60	6	33072		88	0.136	273.0	95							
61	6	33072					96							
62	6	33072		108	0.111	295.1	97							
63	6	33072		105	0.114	292.2	98							
64	6	33072		x			99							
65							100							
66							101							
67							102							
68							103							
69							104							
70							105							
71							106							
72							107							
73							108							
74							109							

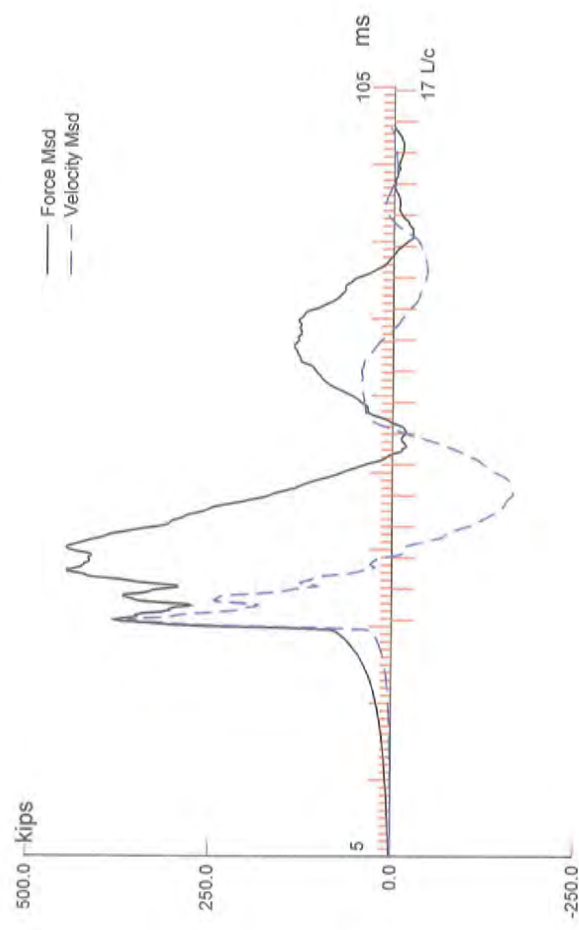
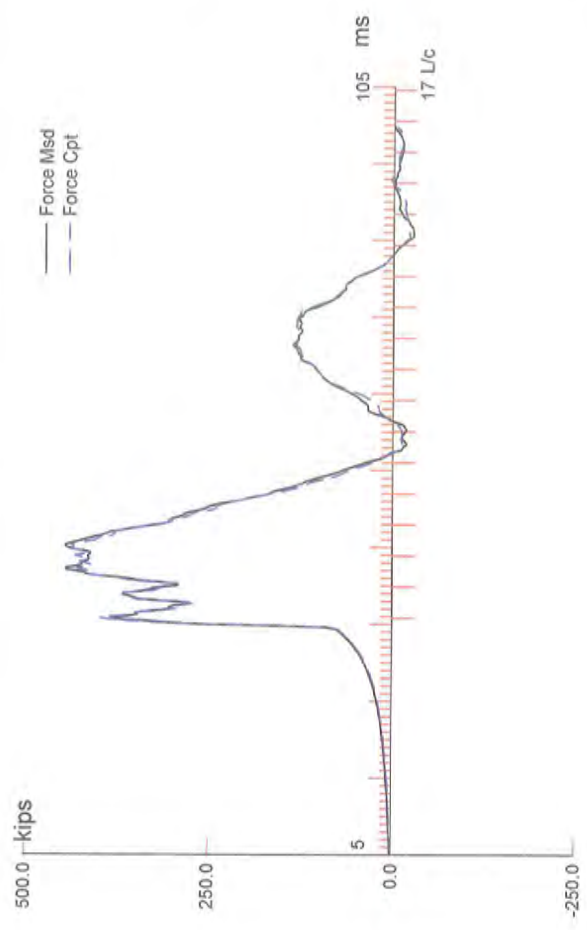
DATE	START DRIVING TIME	END DRIVING TIME	DOWN TIME	DRIVING TIME
12/19/2012	10:52	1:30	1 hr 56 min	42 min

REMARKS ON DRIVING CONDITIONS, PRE-BORING, ETC. (IDENTIFY BY FEET PENET.)  
Substantial refusal at 64' below cutoff 1/2" in ten blows. Restrike 12/21/12 = 1/2" in ten blows with 10' hammer drop.

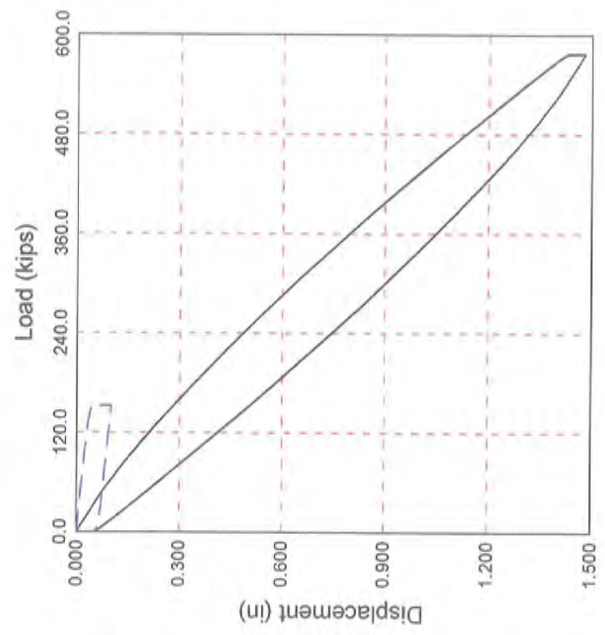
FORMULA USED	DESIGN BEARING (Tons)	AUTHORIZED PILE LENGTHS	
$P = \frac{10.5E}{S + 0.2} \frac{W + 0.1M}{W + M}$	312.5		
INSPECTOR SIGNATURE	PROJ. ENGR. SIGNATURE	BRIDGE OFFICE SIGNATURE	DATE



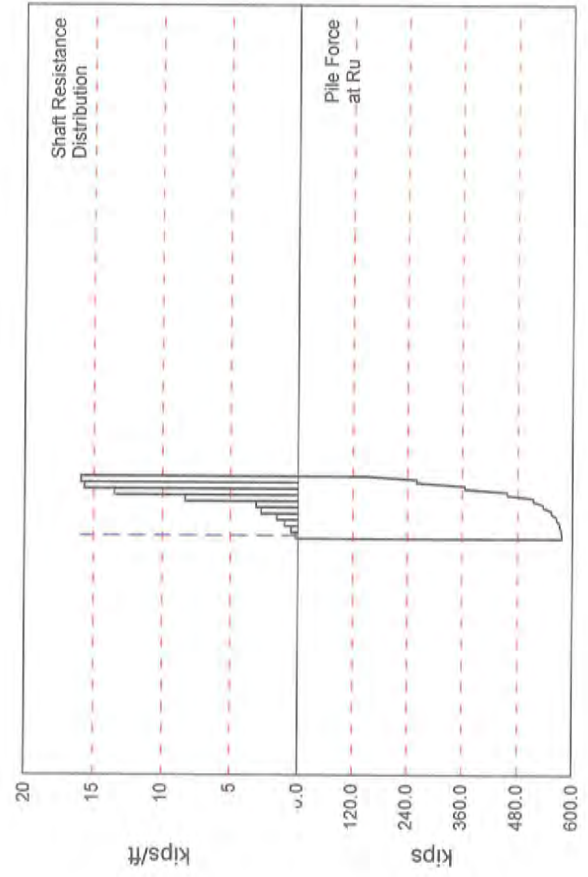
**REACTION PILE 1  
HSDPT RESULTS  
RESTRIKE**



$R_u = 576.8$  kips  
 $R_s = 424.5$  kips  
 $R_b = 152.3$  kips  
 $D_y = 1.43$  in  
 $D_x = 1.48$  in



Pile Top  
 Pile Bottom



BRIDGE 62716; Pile: R1 RST

Test: 21-Dec-2012 11:15:

12.75 OD, 0.25 WALL, APE D25-32, FS=3; Blow: 6

CAPWAP (R) 2006

American Engineering Testing, Inc.

OP: JPB

## CAPWAP SUMMARY RESULTS

Total CAPWAP Capacity:		576.8; along Shaft	424.5; at Toe	152.3 kips					
Soil Sgmnt No.	Dist. Below Gages ft	Depth Below Grade ft	Ru kips	Force in Pile kips	Sum of Ru kips	Unit Resist. (Depth) kips/ft	Unit Resist. (Area) ksf	Smith Damping Factor s/ft	Quake in
				576.8					
1	6.8	1.8	1.3	575.5	1.3	0.72	0.22	0.140	0.040
2	13.6	8.6	3.5	572.0	4.8	0.51	0.15	0.140	0.040
3	20.4	15.4	6.8	565.2	11.6	1.00	0.30	0.140	0.040
4	27.2	22.2	10.7	554.5	22.3	1.57	0.47	0.140	0.040
5	34.0	29.0	18.6	535.9	40.9	2.74	0.82	0.140	0.040
6	40.8	35.8	21.0	514.9	61.9	3.09	0.93	0.140	0.040
7	47.6	42.6	56.4	458.5	118.3	8.29	2.48	0.140	0.040
8	54.4	49.4	91.7	366.8	210.0	13.49	4.04	0.140	0.040
9	61.2	56.2	106.4	260.4	316.4	15.65	4.69	0.140	0.040
10	68.0	63.0	108.1	152.3	424.5	15.90	4.76	0.140	0.038
Avg. Shaft			42.4			6.74	2.02	0.140	0.039
Toe			152.3				171.77	0.077	0.036

## Soil Model Parameters/Extensions

		Shaft	Toe
Case Damping Factor		3.389	0.671
Damping Type			Smith
Unloading Quake	(% of loading quake)	30	100
Reloading Level	(% of Ru)	100	100
Unloading Level	(% of Ru)	64	
Soil Plug Weight	(kips)		0.06

CAPWAP match quality	=	2.47	(Wave Up Match) ; RSA = 0
Observed: final set	=	0.050 in;	blow count = 240 b/ft
Computed: final set	=	0.054 in;	blow count = 223 b/ft
max. Top Comp. Stress	=	45.00 ksi	(T= 45.5 ms, max= 1.065 x Top)
max. Comp. Stress	=	47.94 ksi	(Z= 20.4 ft, T= 42.9 ms)
max. Tens. Stress	=	-4.7 ksi	(Z= 27.2 ft, T= 60.1 ms)
max. Energy (EMX)	=	28.2 kip-ft;	max. Measured Top Displ. (DMX)= 1.11 in

BRIDGE 62716; Pile: R1 RST

Test: 21-Dec-2012 11:15:

12.75 OD, 0.25 WALL, APE D25-32, FS=3; Blow: 6

CAPWAP (R) 2006

American Engineering Testing, Inc.

OP: JPB

## EXTREMA TABLE

Pile Sgmnt No.	Dist. Below Gages ft	max. Force kips	min. Force kips	max. Comp. Stress ksi	max. Tens. Stress ksi	max. Trnsfd. Energy kip-ft	max. Veloc. ft/s	max. Displ. in
1	3.4	441.9	-24.4	45.00	-2.5	28.20	19.4	1.068
2	6.8	446.8	-28.2	45.50	-2.9	27.10	19.2	1.008
3	10.2	443.7	-33.9	45.18	-3.5	25.70	19.0	0.946
4	13.6	459.4	-38.9	46.79	-4.0	24.55	18.6	0.884
5	17.0	457.4	-40.1	46.58	-4.1	22.80	18.3	0.823
6	20.4	470.8	-44.5	47.94	-4.5	21.67	17.8	0.762
7	23.8	458.7	-42.1	46.71	-4.3	19.58	17.4	0.702
8	27.2	469.0	-45.9	47.76	-4.7	18.48	16.6	0.641
9	30.6	450.2	-39.2	45.85	-4.0	16.15	16.1	0.582
10	34.0	461.0	-43.5	46.94	-4.4	15.07	15.2	0.522
11	37.4	432.8	-31.9	44.07	-3.3	12.37	14.5	0.464
12	40.8	455.7	-35.0	46.41	-3.6	11.32	13.2	0.405
13	44.2	429.0	-21.5	43.68	-2.2	9.05	11.5	0.349
14	47.6	440.6	-24.8	44.86	-2.5	8.12	10.0	0.293
15	51.0	376.8	0.0	38.37	0.0	5.33	8.3	0.244
16	54.4	388.9	0.0	39.60	0.0	4.56	6.4	0.193
17	57.8	314.2	0.0	32.00	0.0	2.41	5.4	0.149
18	61.2	316.8	0.0	32.26	0.0	1.86	3.9	0.106
19	64.6	253.9	0.0	25.86	0.0	0.78	3.3	0.072
20	68.0	256.4	0.0	26.11	0.0	0.25	2.7	0.037
Absolute	20.4			47.94			(T =	42.9 ms)
	27.2				-4.7		(T =	60.1 ms)

BRIDGE 62716; Pile: R1 RST

Test: 21-Dec-2012 11:15:

12.75 OD, 0.25 WALL, APE D25-32, FS=3; Blow: 6

CAPWAP(R) 2006

American Engineering Testing, Inc.

OP: JPB

CASE METHOD										
J =	0.0	0.1	0.2	0.3	0.4	0.5	0.6	0.7	0.8	0.9
RX	572.0	555.1	538.1	521.1	504.5	497.9	491.4	485.1	479.1	473.0
RU	0.0	0.0	0.0	0.0	0.0	0.0	0.0	0.0	0.0	0.0

RAU = 458.2 (kips); RA2 = 504.1 (kips)

Current CAPWAP Ru = 576.8 (kips); J(RX) = 0.00

VMX	VFN	VT1*Z	FT1	FMX	DMX	DFN	SET	EMX	QUS
ft/s	ft/s	kips	kips	kips	in	in	in	kip-ft	kips
20.55	0.26	360.0	381.8	446.4	1.109	-0.038	0.050	29.1	601.9

Peak Velocity Time = 36.01 ms.

#### PILE PROFILE AND PILE MODEL

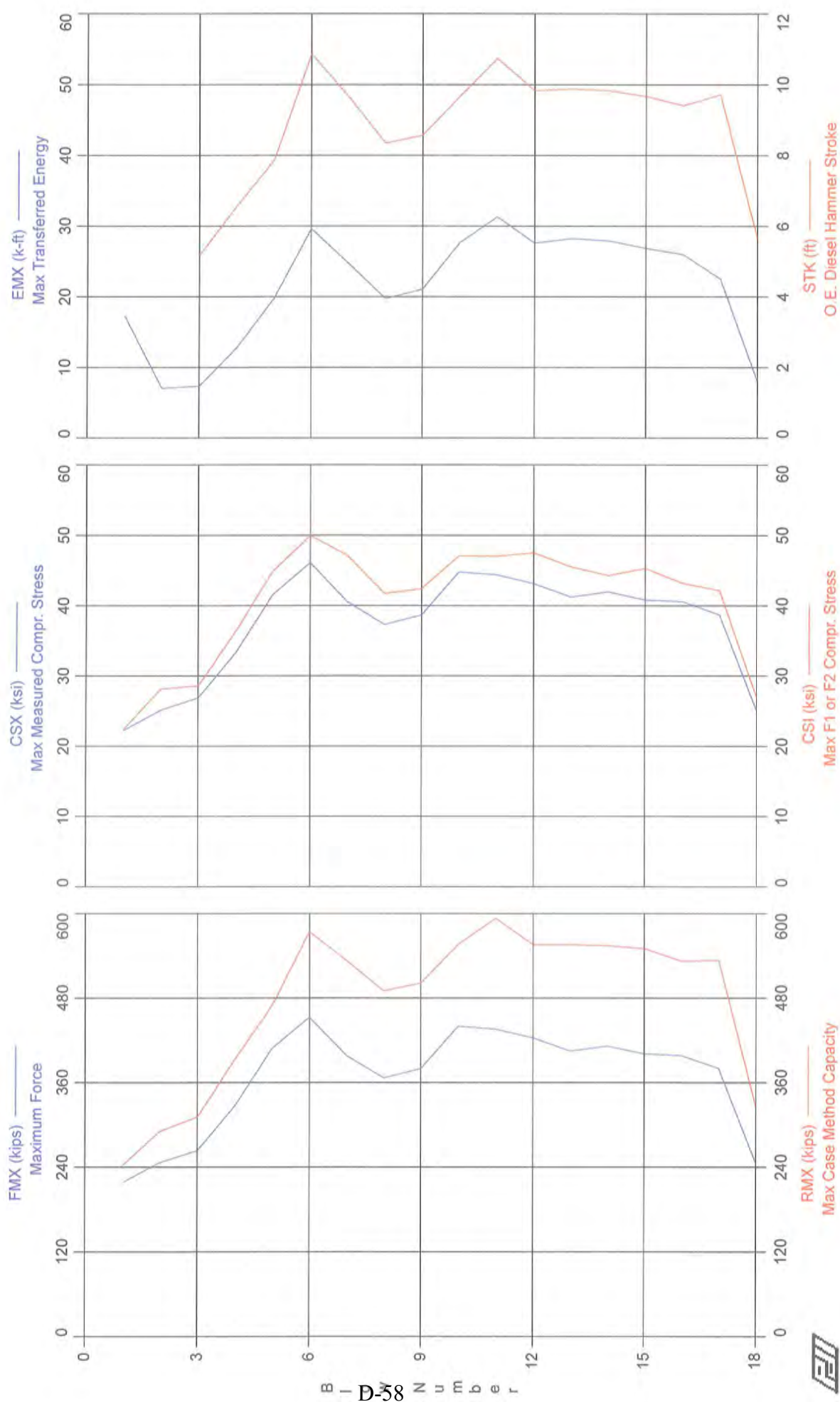
Depth ft	Area in <sup>2</sup>	E-Modulus ksi	Spec. Weight lb/ft <sup>3</sup>	Perim. ft
0.00	9.82	29992.2	492.000	3.338
68.00	9.82	29992.2	492.000	3.338

Toe Area 0.887 ft<sup>2</sup>

Top Segment Length 3.40 ft, Top Impedance 17.52 kips/ft/s

Pile Damping 1.0 %, Time Incr 0.202 ms, Wave Speed 16807.9 ft/s, 2L/c 8.1 ms

## BRIDGE 62716 - R1 RST



BRIDGE 62716 - R1 RST

12.75 OD, 0.25 WALL

OP: JPB

Test date: 21-Dec-2012

AR: 9.82 in<sup>2</sup>

SP: 0.492 k/ft<sup>3</sup>

LE: 68.00 ft

EM: 30,000 ksi

WS: 16,807.9 f/s

JC: 0.00

FMX: Maximum Force

CSX: Max Measured Compr. Stress

VMX: Maximum Velocity

CSI: Max F1 or F2 Compr. Stress

STK: O.E. Diesel Hammer Stroke

RMX: Max Case Method Capacity

EMX: Max Transferred Energy

SFT: Skin friction total

BTA: BETA Integrity Factor

BL#	depth ft	FMX kips	VMX f/s	STK ft	EMX k-ft	BTA (%)	CSX ksi	CSI ksi	RMX kips	SFT kips
1	64.00	218	15.3	0.00	17.3	38.0	22.2	22.4	243	243
2	63.00	247	9.4	0.00	7.1	100.0	25.1	28.1	291	291
3	63.00	264	10.0	5.18	7.4	100.0	26.9	28.6	311	270
4	63.00	327	13.5	6.57	12.8	100.0	33.3	36.4	393	331
5	63.00	409	16.3	7.87	19.8	100.0	41.6	44.9	469	395
6	63.00	453	20.9	10.87	29.7	83.0	46.1	50.0	574	453
7	63.00	398	19.7	9.67	24.8	100.0	40.5	47.2	533	414
8	63.00	366	17.7	8.36	19.8	90.0	37.3	41.8	490	368
9	63.00	380	18.1	8.57	21.1	90.0	38.7	42.4	501	381
10	63.00	440	19.7	9.67	27.7	100.0	44.8	47.1	556	416
11	63.00	436	22.2	10.75	31.3	100.0	44.4	47.1	593	416
12	63.00	423	20.6	9.83	27.6	100.0	43.1	47.5	556	391
13	63.00	405	20.7	9.89	28.3	100.0	41.2	45.5	556	386
14	63.00	412	20.4	9.83	27.9	100.0	42.0	44.3	554	382
15	63.00	401	20.5	9.67	26.9	100.0	40.8	45.3	550	377
16	63.00	398	19.6	9.42	26.0	100.0	40.6	43.2	532	365
17	63.00	380	20.6	9.73	22.5	100.0	38.7	42.2	534	346
18	63.00	246	10.7	5.63	8.0	100.0	25.0	26.9	326	249
Average		367	17.6	8.84	21.4	94.5	37.4	40.6	476	360
Std. Dev.		72	4.0	1.66	7.7	14.5	7.3	8.1	108	59
Maximum		453	22.2	10.87	31.3	100.0	46.1	50.0	593	453
@ Blow#		6	11	6	11	2	6	6	11	6

Total number of blows analyzed: 18

#### Time Summary

Drive 1 minute 37 seconds

11:13:59 AM - 11:15:36 AM (12/21/2012) BN 1 - 18

**MnDOT PILE DRIVING RECORD  
REACTION PILE NO. 2**

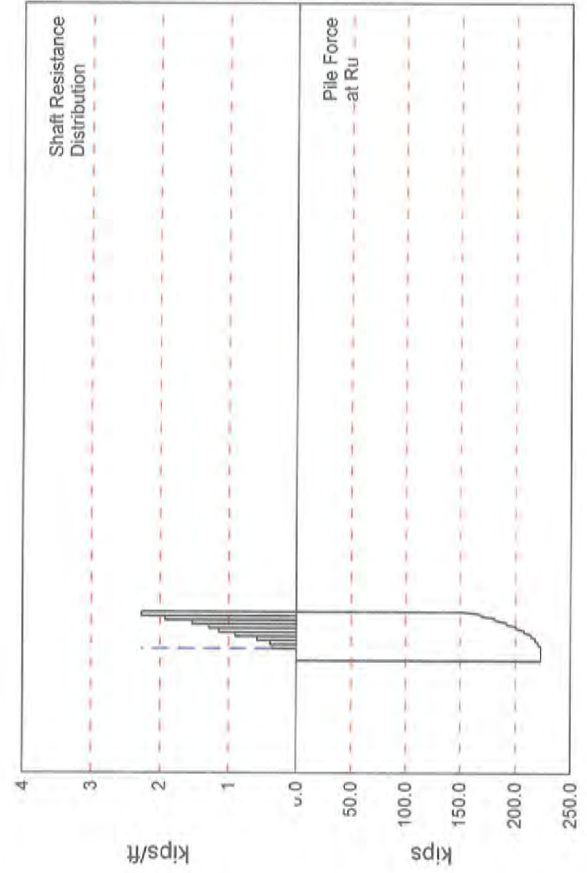
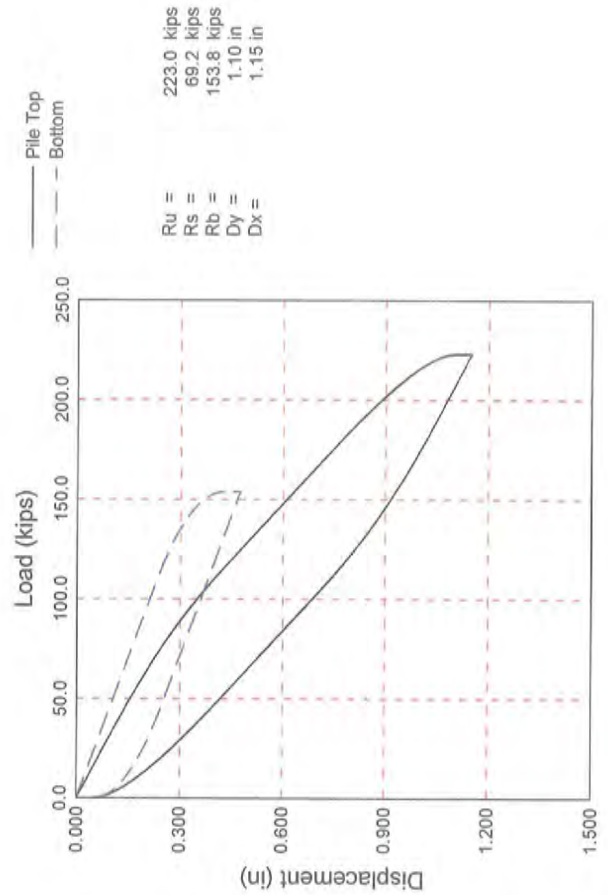
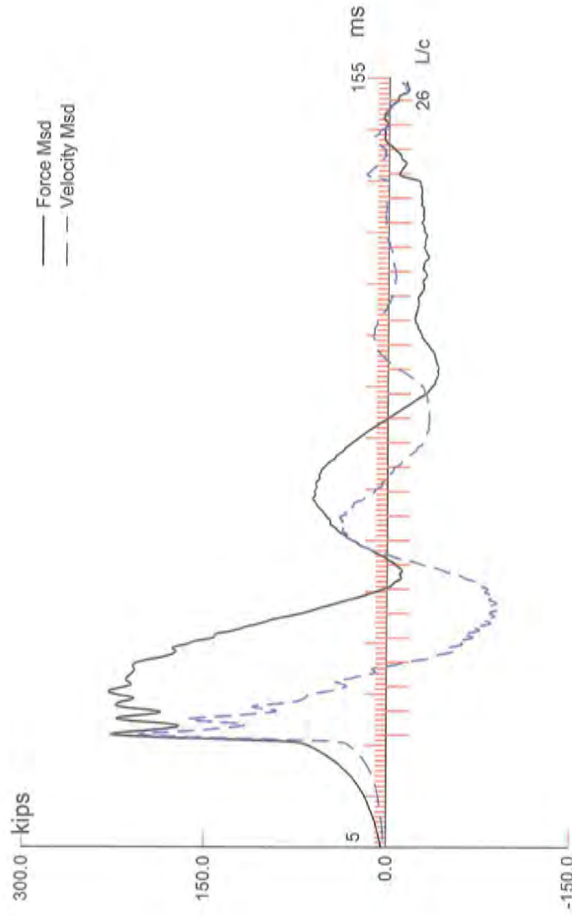
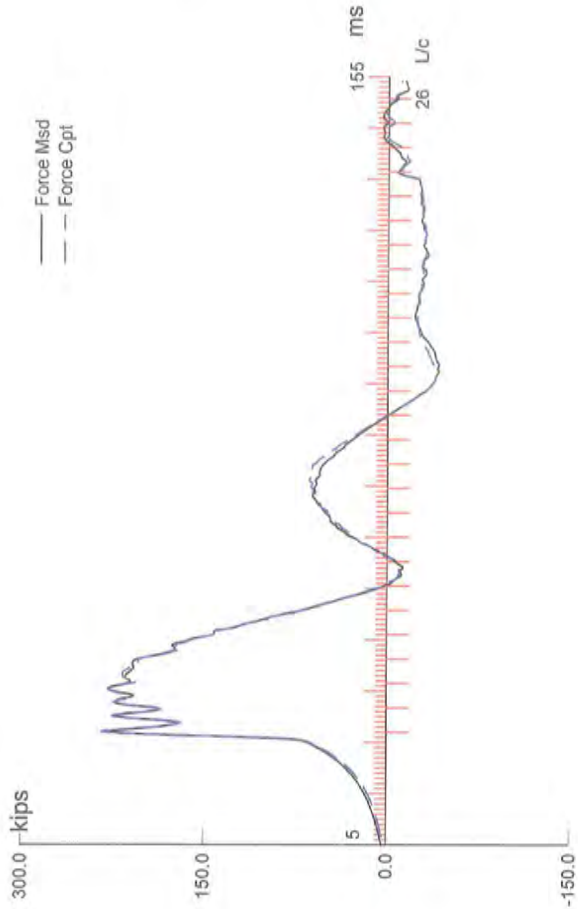


# TEST PILE REPORT

PILE HAMMER DATA					PILE DATA				JOB DESCRIPTION					
TYPE ("X" ONE)					TEST PILE NO.		REACTION 2		BRIDGE NUMBER		62716			
X	DROP				TYPE		CIP 12.750" x .250		T.H. NUMBER		694 WB			
	SINGLE ACTING POWER DRIVEN				LENGTH in LEADS		60+62		S.P. NUMBER		6285-135			
	DOUBLE ACTING POWER DRIVEN				DIAM. of BUTT & TIP				FED. NUMBER					
	MAKE				WEIGHT of PILE		4072		COUNTY		Ramsey			
APE				WEIGHT of CAP		2,050		PIER OR ABUT.		E Abut.				
WT. of RAM		SIZE or NO.			CUT-OFF ELEVATION		895.50		CONTRACTOR Lunda					
5,512		D25-32			INSPECTED BY		KC TSW							
1	2	3	4		5	6	1	2	3	4		5	6	
FEET PENET. BELOW CUT-OFF	DROP of HAMMER or RAM (FEET)	ENERGY per BLOW (FT LBS)	BLOWS per MIN FT		INCHES PENET. per BLOW	BEARING in TONS	FEET PENET. BELOW CUT-OFF	DROP of HAMMER or RAM (FEET)	ENERGY per BLOW (FT LBS)	BLOWS per MIN FT		INCHES PENET. per BLOW	BEARING in TONS	
40				15	0.800		75							
41				15	0.800		76							
42				18	0.667		77							
43				17	0.706		78							
44				18	0.667		79							
45				20	0.600		80							
46				23	0.522		81							
47				27	0.444		82							
48				29	0.414		83							
49				32	0.375		84							
50				47	0.255		85							
51				65	0.185		86							
52				69	0.174		87							
53				54	0.222		88							
54				58	0.207		89							
55				62	0.194		90							
56				86	0.140		91							
57				224	0.054		92							
58				115	0.104		93							
59				92	0.130		94							
60	6	33072		120	0.100	304.7	95							
61							96							
62							97							
63							98							
64							99							
65							100							
66							101							
67							102							
68							103							
69							104							
70							105							
71							106							
72							107							
73							108							
74							109							

DATE 12/19/2012	START DRIVING TIME 2:20	END DRIVING TIME 3:48	DOWN TIME	DRIVING TIME 45min
REMARKS ON DRIVING CONDITIONS, PRE-BORING, ETC. (IDENTIFY BY FEET PENET.) Substantial refusal at 60' below cutoff, 1/2" in ten blows. Restrike 12/21/12 = 3/8" in ten blows with 10.5' hammer drop.				
FORMULA USED P = $\frac{10.5E}{S + 0.2}$ $\frac{W + 0.1M}{W + M}$		DESIGN BEARING (Tons) 312.5	AUTHORIZED PILE LENGTHS	
INSPECTOR SIGNATURE		PROJ. ENGR. SIGNATURE	BRIDGE OFFICE SIGNATURE	DATE

**REACTION PILE NO. 2  
HSDPT RESULTS  
INITIAL DRIVING**



694-Snelling; Pile: R2 (SW Rxn Pile)  
 12.75" CIP, APE D25-32, FS=3; Blow: 604  
 American Engineering Testing, Inc.

Test: 19-Dec-2012 15:47:  
 CAPWAP(R) 2006  
 OP: DSV/GRR

CAPWAP SUMMARY RESULTS

Total CAPWAP Capacity: 223.0; along Shaft 69.2; at Toe 153.8 kips

Soil Sgmnt No.	Dist. Below Gages ft	Depth Below Grade ft	Ru kips	Force in Pile kips	Sum of Ru kips	Unit Resist. (Depth) kips/ft	Unit Resist. (Area) ksf	Smith Damping Factor s/ft
				223.0				
1	26.7	6.7	2.4	220.6	2.4	0.36	0.11	0.403
2	33.3	13.3	2.6	218.0	5.0	0.39	0.12	0.403
3	40.0	20.0	3.9	214.1	8.9	0.59	0.18	0.403
4	46.7	26.7	6.0	208.1	14.9	0.90	0.27	0.403
5	53.3	33.3	7.6	200.5	22.5	1.14	0.34	0.403
6	60.0	40.0	8.6	191.9	31.1	1.29	0.39	0.403
7	66.7	46.7	10.2	181.7	41.3	1.53	0.46	0.403
8	73.3	53.3	12.8	168.9	54.1	1.92	0.58	0.403
9	80.0	60.0	15.1	153.8	69.2	2.27	0.68	0.403
Avg. Shaft			7.7			1.15	0.35	0.403
Toe			153.8				173.46	0.038

Soil Model Parameters/Extensions

	Shaft	Toe
Quake	0.082	0.326
Case Damping Factor	1.591	0.334
Unloading Quake (% of loading quake)	100	101
Reloading Level (% of Ru)	100	100
Unloading Level (% of Ru)	74	
Resistance Gap (included in Toe Quake)		0.003
Soil Plug Weight (kips)		0.17

CAPWAP match quality = 1.98 (Wave Up Match) ; RSA = 0  
 Observed: final set = 0.050 in; blow count = 240 b/ft  
 Computed: final set = 0.072 in; blow count = 167 b/ft  
 max. Top Comp. Stress = 23.94 ksi (T= 27.4 ms, max= 1.098 x Top)  
 max. Comp. Stress = 26.29 ksi (Z= 26.7 ft, T= 31.9 ms)  
 max. Tens. Stress = -4.7 ksi (Z= 26.7 ft, T= 97.8 ms)  
 max. Energy (EMX) = 14.8 kip-ft; max. Measured Top Displ. (DMX)= 1.01 in

694-Snelling; Pile: R2 (SW Rxn Pile)  
 12.75" CIP, APE D25-32, FS=3; Blow: 604  
 American Engineering Testing, Inc.

Test: 19-Dec-2012 15:47:  
 CAPWAP(R) 2006  
 OP: DSV/GRR

EXTREMA TABLE

Pile Sgmnt No.	Dist. Below Gages ft	max. Force kips	min. Force kips	max. Comp. Stress ksi	max. Tens. Stress ksi	max. Trnsfd. Energy kip-ft	max. Veloc. ft/s	max. Displ. in
1	3.3	235.1	-40.3	23.94	-4.1	14.78	11.1	1.001
2	6.7	236.0	-41.2	24.04	-4.2	14.52	11.1	0.972
4	13.3	241.0	-43.1	24.54	-4.4	13.98	10.9	0.913
6	20.0	248.8	-44.6	25.33	-4.5	13.43	10.7	0.853
7	23.3	254.3	-45.3	25.90	-4.6	13.16	10.5	0.823
8	26.7	258.2	-46.1	26.29	-4.7	12.89	10.3	0.793
9	30.0	253.5	-44.1	25.81	-4.5	12.16	10.1	0.763
10	33.3	257.7	-44.7	26.24	-4.6	11.90	9.8	0.734
11	36.7	253.0	-42.2	25.76	-4.3	11.19	9.6	0.705
12	40.0	257.5	-42.7	26.22	-4.3	10.92	9.3	0.675
13	43.3	250.2	-39.1	25.47	-4.0	10.07	8.9	0.645
14	46.7	256.5	-39.6	26.12	-4.0	9.80	8.5	0.616
15	50.0	238.9	-33.8	24.33	-3.4	8.79	8.2	0.588
16	53.3	236.5	-34.4	24.08	-3.5	8.55	7.8	0.560
17	56.7	220.0	-27.4	22.41	-2.8	7.48	7.4	0.533
18	60.0	218.4	-27.8	22.24	-2.8	7.26	7.0	0.505
19	63.3	203.2	-20.1	20.69	-2.0	6.25	6.6	0.480
20	66.7	206.1	-20.7	20.99	-2.1	6.05	6.2	0.454
21	70.0	195.2	-12.3	19.88	-1.3	5.08	5.7	0.430
22	73.3	198.0	-12.8	20.16	-1.3	4.90	5.1	0.406
23	76.7	182.4	-3.4	18.58	-0.3	3.92	5.4	0.383
24	80.0	182.4	-3.9	18.57	-0.4	2.95	5.7	0.359
Absolute	26.7			26.29			(T =	31.9 ms)
	26.7				-4.7		(T =	97.8 ms)

694-Snelling; Pile: R2 (SW Rxn Pile)  
 12.75" CIP, APE D25-32, FS=3; Blow: 604  
 American Engineering Testing, Inc.

Test: 19-Dec-2012 15:47:  
 CAPWAP(R) 2006  
 OP: DSV/GRR

CASE METHOD										
J =	0.0	0.1	0.2	0.3	0.4	0.5	0.6	0.7	0.8	0.9
RX	306.1	293.3	280.5	267.7	256.1	250.6	245.1	239.5	234.8	232.5
RU	306.1	293.3	280.5	267.7	254.9	242.1	229.3	216.5	203.7	190.9

RAU = 130.4 (kips); RA2 = 237.3 (kips)

Current CAPWAP Ru = 223.0 (kips);

matches RX9 within 5%

VMX	VFN	VT1*Z	FT1	FMX	DMX	DFN	SET	EMX	QUS
ft/s	ft/s	kips	kips	kips	in	in	in	kip-ft	kips
11.73	0.00	205.6	228.5	229.2	1.006	0.020	0.050	15.1	343.2

Peak Velocity Time = 27.17 ms.

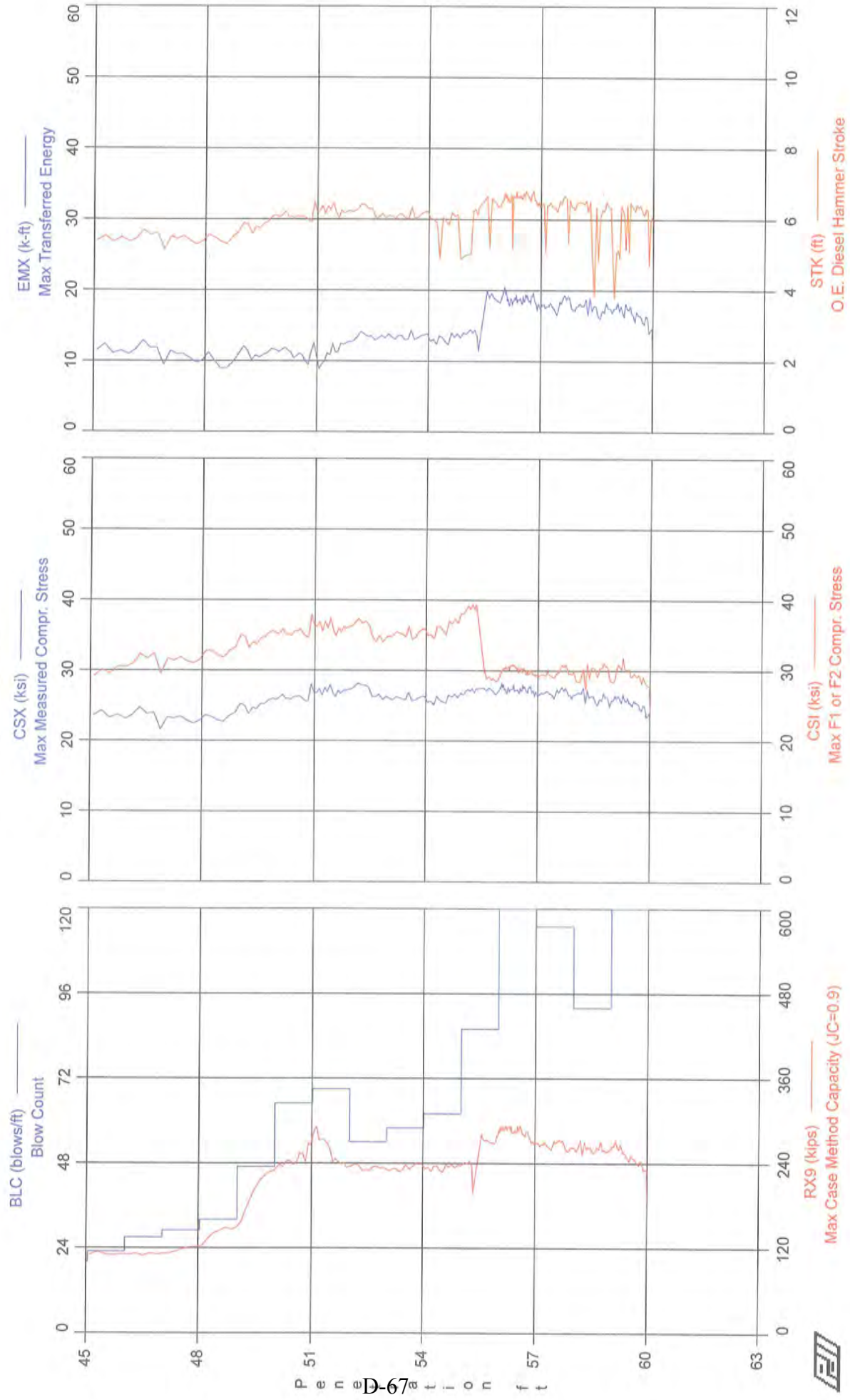
FILE PROFILE AND PILE MODEL				
Depth	Area	E-Modulus	Spec. Weight	Perim.
ft	in <sup>2</sup>	ksi	lb/ft <sup>3</sup>	ft
0.00	9.82	29992.2	492.000	3.338
80.00	9.82	29992.2	492.000	3.338

Toe Area 0.887 ft<sup>2</sup>

Top Segment Length 3.33 ft, Top Impedance 17.52 kips/ft/s

File Damping 1.0 %, Time Incr 0.198 ms, Wave Speed 16807.9 ft/s, 2L/c 9.5 ms

694-Snelling - R-2



694-Snelling - R-2

12" CIP, APE D25-32, FS=4

OP: DSV/GRR

Test date: 19-Dec-2012

AR: 9.82 in^2

SP: 0.492 k/ft3

LE: 57.00 ft

EM: 30,000 ksi

WS: 16,807.9 f/s

JC: 0.70

FMX: Maximum Force

CSX: Max Measured Compr. Stress

VMX: Maximum Velocity

CSI: Max F1 or F2 Compr. Stress

STK: O.E. Diesel Hammer Stroke

RX9: Max Case Method Capacity (JC=0.9)

EMX: Max Transferred Energy

SFT: Skin friction total

BTA: BETA Integrity Factor

BL#	depth ft	BLC bl/ft	FMX kips	VMX f/s	STK ft	EMX k-ft	BTA (%)	CSX ksi	CSI ksi	RX9 kips	SFT kips
49	45.00	20	245	12.2	5.67	12.4	84.0	25.0	30.0	110	152
61	45.52	23	214	10.3	5.09	9.6	85.0	21.8	28.2	113	144
73	46.04	27	238	11.8	5.60	11.6	87.0	24.3	31.5	109	159
85	46.48	27	232	11.6	5.51	11.5	85.0	23.7	31.3	110	159
97	46.93	27	206	10.0	5.01	8.9	80.0	21.0	28.7	112	149
109	47.35	29	235	11.8	5.59	11.2	82.0	23.9	32.4	113	161
121	47.76	29	215	10.6	5.18	9.2	85.0	21.9	30.4	122	145
133	48.16	32	244	12.3	5.82	12.7	74.0	24.8	34.5	121	157
145	48.53	32	238	12.0	5.67	10.4	66.0	24.2	34.0	142	157
157	48.91	32	245	12.6	5.93	12.1	67.0	24.9	34.5	145	171
169	49.19	47	228	11.1	5.44	9.4	76.0	23.2	32.7	170	179
181	49.45	47	255	12.9	6.13	12.2	75.0	26.0	35.7	202	190
193	49.70	47	234	12.0	5.66	10.1	74.0	23.9	32.8	218	188
205	49.96	47	252	12.7	6.02	11.6	73.0	25.7	34.7	227	186
217	50.15	65	264	13.3	6.26	12.2	73.0	26.8	36.3	238	204
229	50.34	65	265	13.8	6.33	11.7	76.0	27.0	36.5	244	194
241	50.52	65	263	12.8	6.20	10.9	76.0	26.8	36.3	236	209
253	50.71	65	266	13.6	6.37	11.0	76.0	27.1	36.8	267	215
265	50.89	65	266	14.0	6.27	11.6	79.0	27.1	36.7	271	215
277	51.07	69	273	13.4	6.41	9.8	72.0	27.8	37.6	287	248
289	51.25	69	270	13.4	6.36	10.4	75.0	27.5	37.2	278	221
301	51.42	69	280	14.3	6.64	11.7	81.0	28.6	38.1	279	195
313	51.59	69	246	12.4	5.73	10.5	77.0	25.1	33.4	227	160
325	51.77	69	264	13.4	6.10	12.0	79.0	26.9	35.8	237	165
337	51.94	69	275	13.8	6.40	13.3	81.0	28.0	37.2	236	171
349	52.15	54	262	13.1	6.08	12.5	100.0	26.7	35.6	229	165
361	52.37	54	268	13.6	6.15	12.8	77.0	27.3	36.0	228	167
373	52.59	54	268	13.9	6.32	14.1	77.0	27.3	35.6	238	186
385	52.82	54	251	13.3	5.99	13.1	74.0	25.5	33.5	231	189
397	53.03	58	260	13.4	6.19	13.4	73.0	26.4	35.3	231	198
409	53.24	58	261	13.6	6.22	14.3	71.0	26.6	35.6	236	202
421	53.45	58	236	11.6	5.60	11.3	77.0	24.1	32.8	219	197
433	53.66	58	254	13.1	6.09	13.3	72.0	25.9	34.7	228	203
445	53.86	58	248	12.7	6.00	12.8	78.0	25.3	34.7	233	197
457	54.07	62	252	12.7	6.01	12.7	64.0	25.6	34.9	231	213
469	54.26	62	253	12.7	6.01	13.2	59.0	25.7	35.4	234	206
481	54.45	62	243	12.2	5.80	11.9	61.0	24.8	34.9	223	178
493	54.65	62	261	13.3	6.28	14.1	68.0	26.6	37.5	239	204
505	54.84	62	248	12.1	5.73	12.0	68.0	25.3	35.4	226	204
517	55.02	86	268	13.5	6.31	14.3	77.0	27.3	38.6	238	213
529	55.16	86	266	13.3	6.27	13.9	78.0	27.1	38.9	240	218
541	55.30	86	257	12.4	5.94	12.8	80.0	26.2	37.5	233	210
570	55.64	86	273	14.9	6.56	20.0	85.0	27.8	28.8	277	218
582	55.78	86	280	15.4	6.85	20.1	83.0	28.5	30.1	281	219
594	55.92	86	258	13.9	6.23	17.8	82.0	26.3	28.5	265	194
606	56.02	224	265	14.3	6.46	18.7	78.0	27.0	29.2	278	187
618	56.08	224	264	14.4	6.37	18.8	80.0	26.9	29.6	286	196
630	56.13	224	270	14.9	6.62	19.0	79.0	27.6	30.9	295	200
642	56.18	224	270	14.8	6.66	18.5	79.0	27.5	30.8	291	196
654	56.24	224	265	14.4	6.57	17.8	76.0	27.0	30.2	287	179
666	56.29	224	270	14.7	6.70	18.3	78.0	27.5	30.8	291	195
678	56.34	224	274	15.2	6.81	19.4	82.0	27.9	31.0	296	200
690	56.40	224	256	14.0	6.34	18.4	86.0	26.1	29.6	284	189
702	56.45	224	276	15.4	6.81	19.9	79.0	28.1	30.3	291	199
714	56.50	224	258	14.2	6.50	17.5	76.0	26.2	30.2	279	191
726	56.56	224	272	15.2	6.88	18.6	75.0	27.7	31.1	288	189
738	56.61	224	268	14.9	6.78	18.3	78.0	27.3	30.4	286	193
750	56.67	224	255	14.0	6.31	18.2	80.0	26.0	28.4	274	178
762	56.72	224	254	13.8	6.30	17.5	78.0	25.9	29.5	274	182
774	56.77	224	267	14.7	6.61	18.6	80.0	27.2	28.9	282	188



694-Snelling - R-2  
OP: DSV/GRR

12" CIP, APE D25-32, FS=4  
Test date: 19-Dec-2012

BL#	depth ft	BLC bl/ft	FMX kips	VMX f/s	STK ft	EMX k-ft	BTA (%)	CSX ksi	CSI ksi	RX9 kips	SFT kips
786	56.83	224	268	14.8	6.56	18.6	75.0	27.3	30.1	278	177
798	56.88	224	271	15.0	6.66	18.6	77.0	27.6	30.1	274	207
810	56.93	224	275	15.3	6.73	18.6	73.0	28.0	29.8	275	205
822	56.99	224	256	13.8	6.28	16.5	70.0	26.1	29.7	263	187
834	57.08	115	260	14.2	6.36	18.2	74.0	26.5	29.4	270	196
846	57.18	115	267	14.5	6.45	18.1	73.0	27.2	29.6	268	196
858	57.29	115	273	15.2	6.66	18.9	71.0	27.8	30.8	274	199
870	57.39	115	255	13.7	6.16	16.3	78.0	26.0	28.7	255	191
882	57.50	115	263	14.2	6.43	17.6	72.0	26.8	29.4	271	198
894	57.60	115	266	14.7	6.54	18.9	72.0	27.1	30.6	272	210
906	57.70	115	255	13.8	6.37	17.3	71.0	26.0	29.7	257	203
918	57.81	115	260	14.1	6.32	17.3	75.0	26.4	29.0	258	212
930	57.91	115	262	14.2	6.41	17.4	75.0	26.7	30.0	259	202
942	58.02	92	252	13.5	6.17	16.6	80.0	25.7	27.9	252	181
954	58.15	92	256	13.8	6.33	17.8	81.0	26.1	30.4	262	214
966	58.28	92	255	13.9	6.35	17.3	78.0	26.0	27.3	258	196
978	58.41	92	261	14.0	0.00	17.9	74.0	26.6	31.1	268	245
990	58.54	92	241	12.6	5.97	15.3	72.0	24.5	29.5	249	232
1002	58.67	92	259	13.9	6.36	17.6	66.0	26.3	30.8	267	224
1014	58.80	92	248	13.2	6.11	16.6	68.0	25.2	29.8	251	217
1026	58.94	92	259	13.9	6.55	18.5	81.0	26.4	29.0	262	210
1038	59.05	120	247	13.3	6.08	17.3	80.0	25.2	27.1	258	192
1050	59.15	120	274	14.9	6.72	19.3	72.0	27.9	32.0	283	217
1062	59.25	120	251	12.5	5.98	16.3	74.0	25.6	31.1	260	231
1074	59.35	120	254	13.7	6.45	17.8	73.0	25.8	30.7	258	227
1086	59.45	120	251	13.4	6.45	17.6	79.0	25.5	30.8	257	214
1098	59.55	120	247	13.1	6.23	15.1	80.0	25.2	28.5	239	202
1110	59.65	120	243	12.9	6.27	15.8	81.0	24.8	29.3	245	202
1122	59.75	120	240	12.7	6.17	15.2	84.0	24.4	28.0	236	204
1134	59.85	120	237	12.2	6.12	16.4	85.0	24.2	28.7	249	216
1146	59.95	120	234	12.2	6.01	14.4	80.0	23.8	27.9	230	198
Average			257	13.6	6.25	15.3	76.9	26.2	32.1	242	196
Std. Dev.			15	1.2	0.39	3.3	5.4	1.5	3.2	48	23
Maximum			295	16.3	7.10	21.7	100.0	30.0	41.7	308	269
@ Blow#			352	603	603	603	349	352	527	278	1064

Total number of blows analyzed: 1087

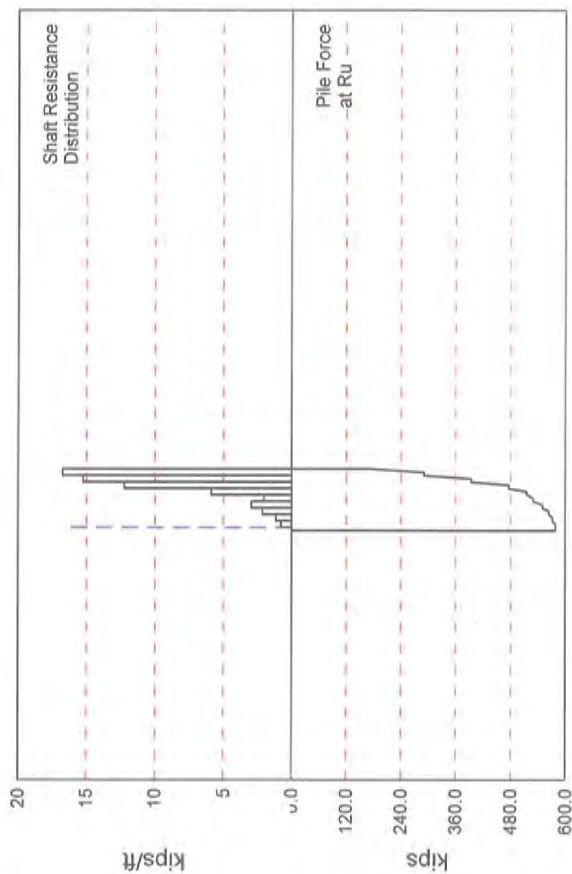
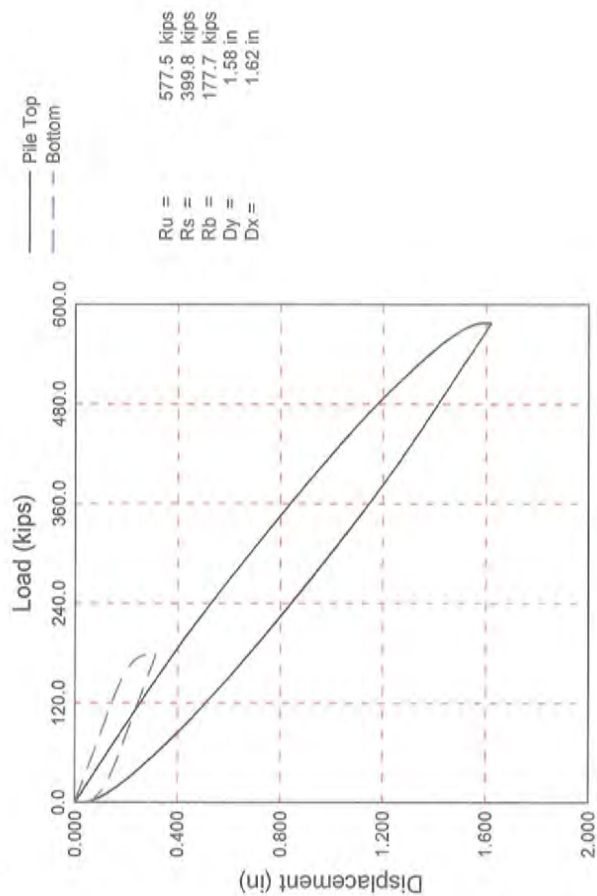
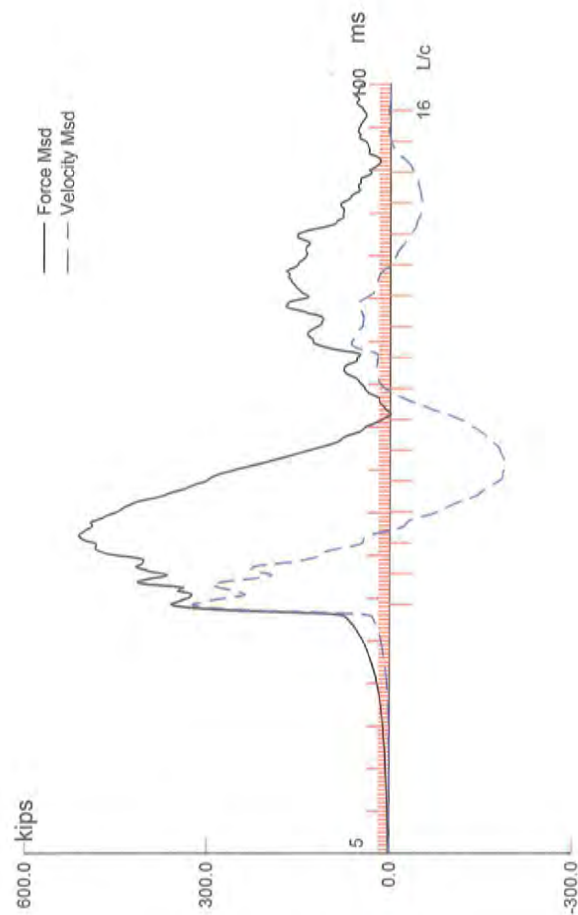
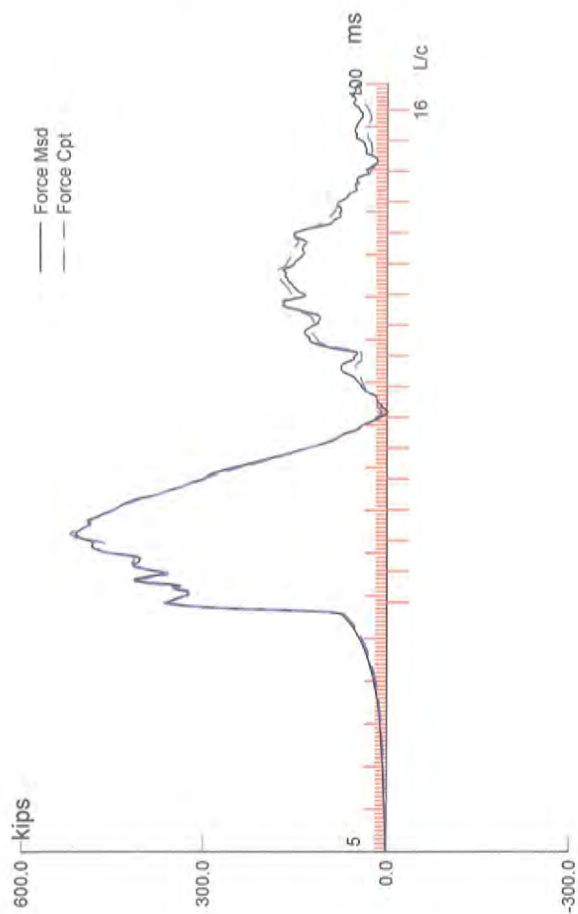
BL#	depth (ft)	Comments
549	55.40	LE = 80; WC = 17021.277

Time Summary

Drive	12 minutes 47 seconds	2:38:01 PM - 2:50:48 PM (12/19/2012) BN 1 - 544
Stop	43 minutes 9 seconds	2:50:48 PM - 3:33:57 PM
Drive	13 minutes 27 seconds	3:33:57 PM - 3:47:24 PM BN 549 - 1152

Total time [1:09:23] = (Driving [0:26:14] + Stop [0:43:09])

**REACTION PILE 2  
HSDPT RESULTS  
RESTRIKE**



BRIDGE 62716; Pile: R2 (SW Rxn Pile)  
 12.75 OD, 0.25 WALL, APE D25-32, FS=3; Blow: 5  
 American Engineering Testing, Inc.

Test: 21-Dec-2012 11:27:  
 CAPWAP(R) 2006  
 OP: JPB

CAPWAP SUMMARY RESULTS

Total CAPWAP Capacity: 577.5; along Shaft 399.8; at Toe 177.7 kips									
Soil Sgmt No.	Dist. Below Gages ft	Depth Below Grade ft	Ru kips	Force in File kips	Sum of Ru kips	Unit Resist. (Depth) kips/ft	Unit Resist. (Area) ksf	Smith Damping Factor s/ft	Quake in
				577.5					
1	10.1	6.1	5.4	572.1	5.4	0.88	0.26	0.080	0.223
2	16.8	12.8	7.9	564.2	13.3	1.17	0.35	0.080	0.223
3	23.6	19.6	14.7	549.5	28.0	2.18	0.65	0.080	0.223
4	30.3	26.3	20.1	529.4	48.1	2.98	0.89	0.080	0.223
5	37.1	33.1	13.9	515.5	62.0	2.06	0.62	0.080	0.223
6	43.8	39.8	39.7	475.8	101.7	5.89	1.77	0.080	0.223
7	50.5	46.5	82.4	393.4	184.1	12.23	3.66	0.080	0.223
8	57.3	53.3	102.8	290.6	286.9	15.26	4.57	0.080	0.219
9	64.0	60.0	112.9	177.7	399.8	16.76	5.02	0.080	0.095
Avg. Shaft			44.4			6.66	2.00	0.080	0.186
Toe			177.7				200.42	0.049	0.213

Soil Model Parameters/Extensions		Shaft	Toe
Case Damping Factor		1.819	0.494
Damping Type			Smith
Unloading Quake	(% of loading quake)	83	100
Reloading Level	(% of Ru)	100	100
Unloading Level	(% of Ru)	0	
Soil Plug Weight	(kips)		0.04

CAPWAP match quality = 2.81 (Wave Up Match) ; RSA = 0  
 Observed: final set = 0.038 in; blow count = 320 b/ft  
 Computed: final set = 0.034 in; blow count = 350 b/ft  
 max. Top Comp. Stress = 53.46 ksi (T= 44.7 ms, max= 1.015 x Top)  
 max. Comp. Stress = 54.24 ksi (Z= 16.8 ft, T= 43.7 ms)  
 max. Tens. Stress = -3.8 ksi (Z= 43.8 ft, T= 61.9 ms)  
 max. Energy (EMX) = 38.8 kip-ft; max. Measured Top Displ. (DMX)= 1.37 in

BRIDGE 62716; Pile: R2 (SW Rxn Pile)  
 12.75 OD, 0.25 WALL, APE D25-32, FS=3; Blow: 5  
 American Engineering Testing, Inc.

Test: 21-Dec-2012 11:27:  
 CAPWAP(R) 2006  
 OP: JPB

EXTREMA TABLE

Pile Sgmnt No.	Dist. Below Gages ft	max. Force kips	min. Force kips	max. Comp. Stress ksi	max. Tens. Stress ksi	max. Trnsfd. Energy kip-ft	max. Veloc. ft/s	max. Displ. in
1	3.4	525.0	0.0	53.46	0.0	38.84	18.0	1.341
2	6.7	528.9	-4.8	53.86	-0.5	37.35	17.7	1.271
3	10.1	529.2	-11.6	53.89	-1.2	35.84	17.4	1.200
4	13.5	526.5	-16.1	53.61	-1.6	33.41	17.2	1.130
5	16.8	532.6	-21.1	54.24	-2.1	31.91	16.7	1.059
6	20.2	526.8	-23.4	53.64	-2.4	29.22	16.3	0.989
7	23.6	530.4	-28.4	54.01	-2.9	27.69	15.8	0.917
8	26.9	514.7	-28.7	52.41	-2.9	24.48	15.3	0.848
9	30.3	523.8	-32.3	53.34	-3.3	23.05	14.8	0.780
10	33.7	506.4	-30.5	51.57	-3.1	19.79	14.5	0.713
11	37.1	510.5	-33.7	51.99	-3.4	18.44	13.9	0.646
12	40.4	496.1	-33.8	50.52	-3.4	16.12	13.1	0.581
13	43.8	498.6	-36.9	50.78	-3.8	14.83	12.1	0.516
14	47.2	454.5	-31.9	46.28	-3.2	11.73	10.9	0.456
15	50.5	458.7	-34.6	46.71	-3.5	10.64	9.7	0.395
16	53.9	382.5	-24.3	38.95	-2.5	7.29	8.5	0.344
17	57.3	388.7	-26.7	39.58	-2.7	6.50	7.9	0.293
18	60.6	296.7	-15.8	30.22	-1.6	4.08	8.2	0.253
19	64.0	296.4	-18.6	30.19	-1.9	1.75	7.3	0.213
Absolute	16.8			54.24			(T =	43.7 ms)
	43.8				-3.8		(T =	61.9 ms)

CASE METHOD

J =	0.0	0.1	0.2	0.3	0.4	0.5	0.6	0.7	0.8	0.9
RX	610.4	601.4	592.4	583.4	574.4	565.4	556.4	547.5	541.5	535.6
RU	563.9	551.4	538.9	526.4	513.9	501.4	488.9	476.4	463.9	451.4

RAU = 178.5 (kips); RA2 = 532.4 (kips)

Current CAPWAP Ru = 577.5 (kips); J(RX) = 0.37

VMX	VFN	VT1*Z	FT1	FMX	DMX	DFN	SET	EMX	QUS
ft/s	ft/s	kips	kips	kips	in	in	in	kip-ft	kips
18.73	0.00	328.3	360.6	512.7	1.369	0.028	0.038	40.2	685.7

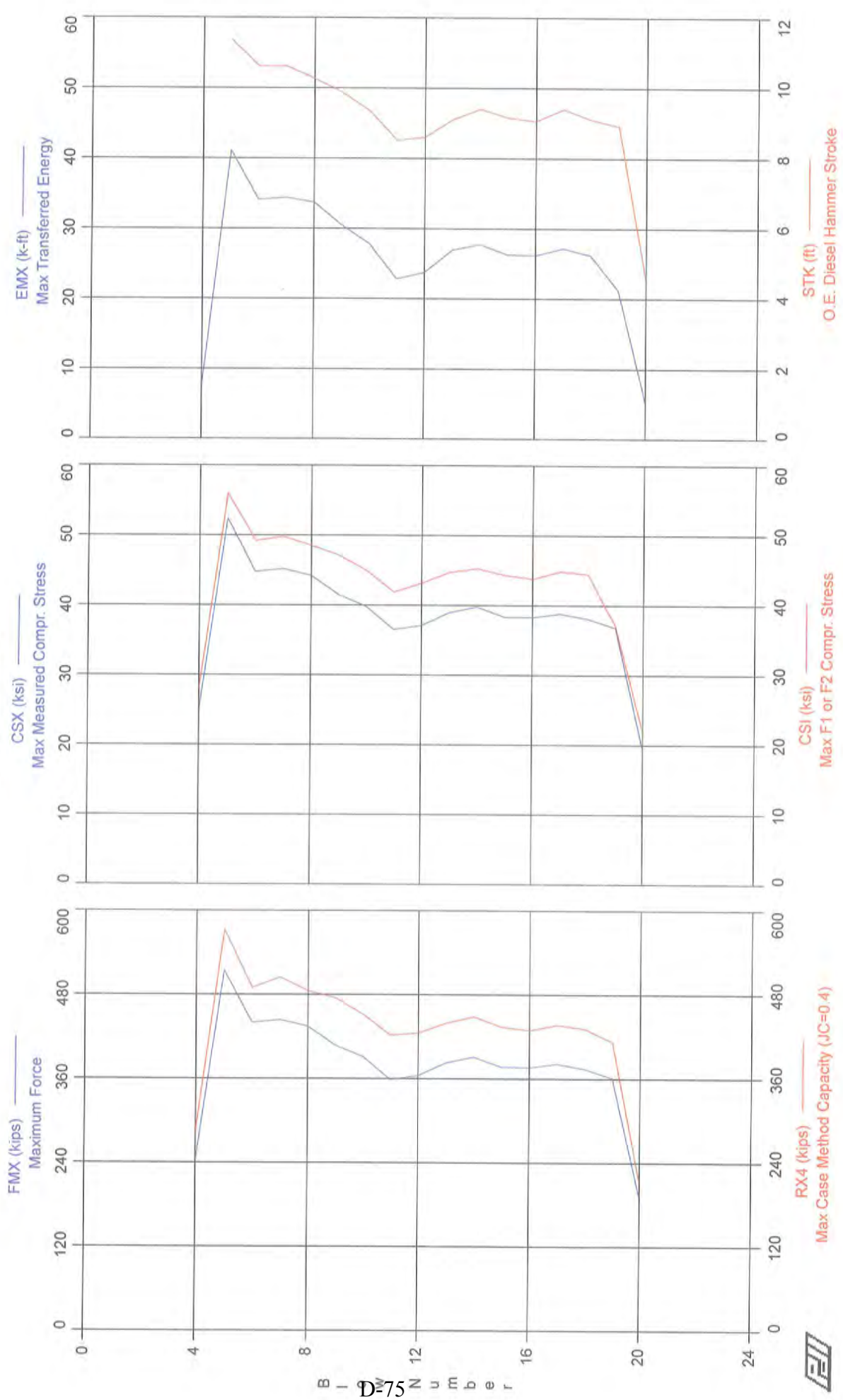
Peak Velocity Time = 36.07 ms.

BRIDGE 62716; Pile: R2 (SW Rxn Pile)  
 12.75 OD, 0.25 WALL, APE D25-32, FS=3; Blow: 5  
 American Engineering Testing, Inc.

Test: 21-Dec-2012 11:27:  
 CAPWAP(R) 2006  
 OP: JPB

PILE PROFILE AND PILE MODEL				
Depth ft	Area in <sup>2</sup>	E-Modulus ksi	Spec. Weight lb/ft <sup>3</sup>	Perim. ft
0.00	9.82	29992.2	492.000	3.338
64.00	9.82	29992.2	492.000	3.338
Toe Area		0.887	ft <sup>2</sup>	
Top Segment Length		3.37 ft, Top Impedance	17.52 kips/ft/s	
Pile Damping 1.0 %, Time Incr 0.200 ms, Wave Speed 16807.9 ft/s, 2L/c 7.6 ms				

BRIDGE 62716 - R2 RST



BRIDGE 62716 - R2 RST  
OP: JPB

12.75 OD, 0.25 WALL  
Test date: 21-Dec-2012

AR: 9.82 in^2  
LE: 64.00 ft  
WS: 16,807.9 f/s

SP: 0.492 k/ft3  
EM: 30,000 ksi  
JC: 0.70

FMX: Maximum Force  
VMX: Maximum Velocity  
STK: O.E. Diesel Hammer Stroke  
EMX: Max Transferred Energy  
BTA: BETA Integrity Factor

CSX: Max Measured Compr. Stress  
CSI: Max F1 or F2 Compr. Stress  
RX4: Max Case Method Capacity (JC=0.4)  
SFT: Skin friction total

BL#	depth ft	FMX kips	VMX f/s	STK ft	EMX k-ft	BTA (%)	CSX ksi	CSI ksi	RX4 kips	SFT kips
4	60.00	243	10.0	0.00	7.7	89.0	24.8	28.0	286	270
5	60.00	515	18.8	11.39	41.2	100.0	52.4	56.1	573	476
6	60.00	440	20.9	10.63	34.1	100.0	44.8	49.2	490	415
7	60.00	444	21.0	10.63	34.4	100.0	45.2	49.8	505	413
8	60.00	434	20.9	10.28	33.7	100.0	44.2	48.6	486	398
9	60.00	407	20.2	9.89	30.5	100.0	41.5	47.2	475	360
10	60.00	391	19.8	9.37	27.9	100.0	39.8	45.0	452	337
11	60.00	359	18.0	8.53	22.9	100.0	36.5	41.9	422	323
12	60.00	364	18.6	8.62	23.8	90.0	37.1	43.2	425	331
13	60.00	383	19.4	9.12	27.0	100.0	39.0	44.8	440	334
14	60.00	391	20.0	9.42	27.8	100.0	39.8	45.3	449	341
15	60.00	377	19.5	9.17	26.3	100.0	38.4	44.4	434	340
16	60.00	376	19.6	9.07	26.2	100.0	38.3	43.8	429	340
17	60.00	381	20.0	9.42	27.2	100.0	38.8	44.9	437	353
18	60.00	374	19.7	9.12	26.2	100.0	38.1	44.5	431	346
19	60.00	361	19.5	8.93	21.3	100.0	36.8	37.1	413	311
20	60.00	190	7.5	4.52	5.2	100.0	19.4	21.8	211	181
Average		378	18.4	9.26	26.1	98.8	38.5	43.3	433	345
Std. Dev.		71	3.6	1.44	8.6	3.4	7.2	7.8	78	61
Maximum		515	21.0	11.39	41.2	100.0	52.4	56.1	573	476
@ Blow#		5	7	5	5	5	5	5	5	5

Total number of blows analyzed: 17

#### Time Summary

Drive 1 minute 40 seconds

11:25:46 AM - 11:27:26 AM (12/21/2012) BN 1 - 20



**MnDOT PILE DRIVING RECORD  
REACTION PILE NO. 3**

# TEST PILE REPORT

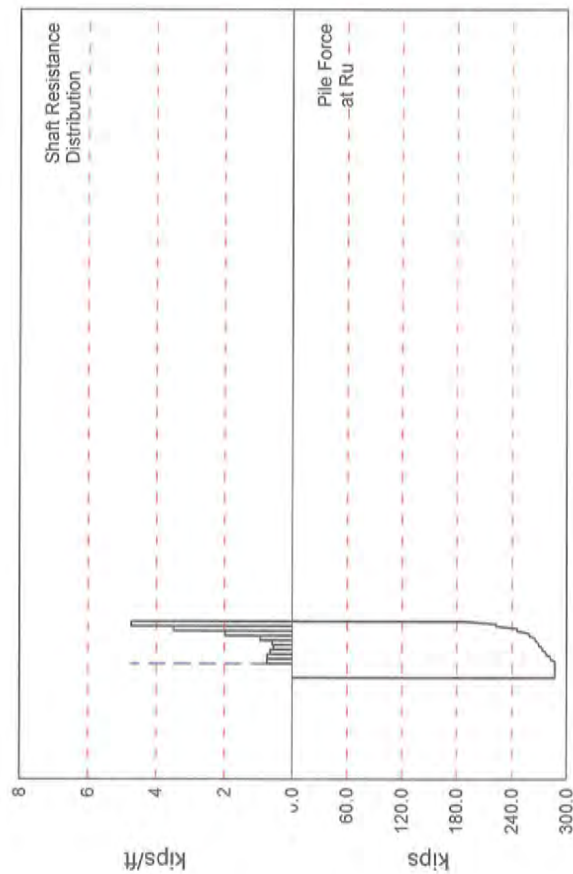
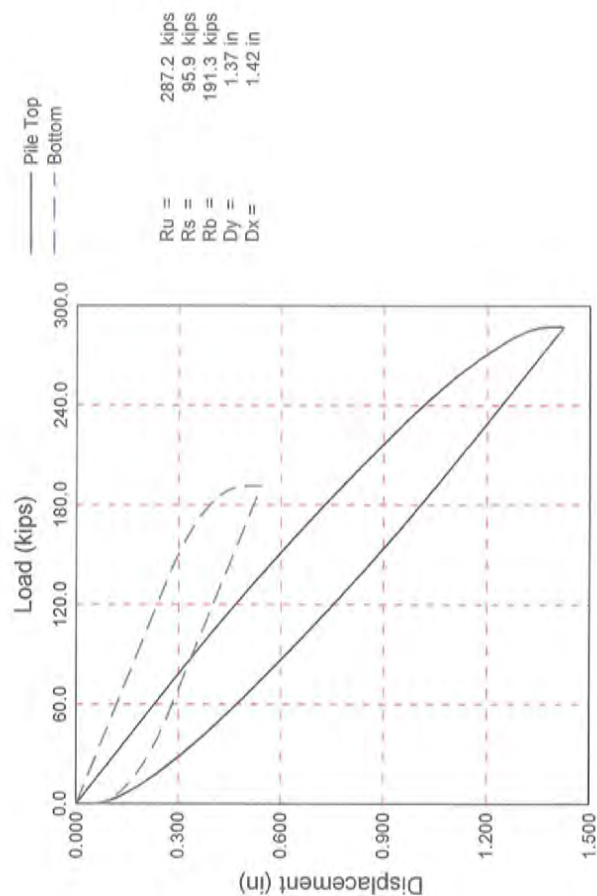
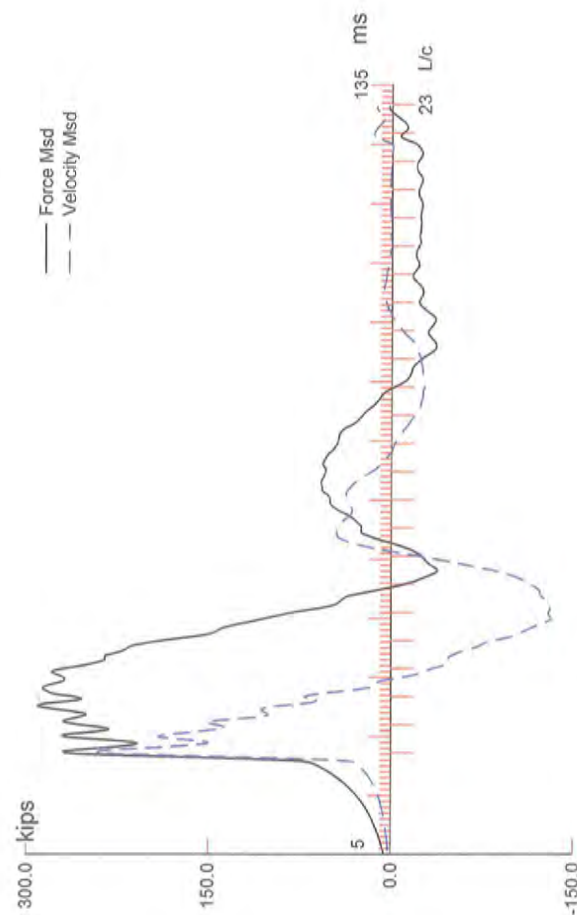
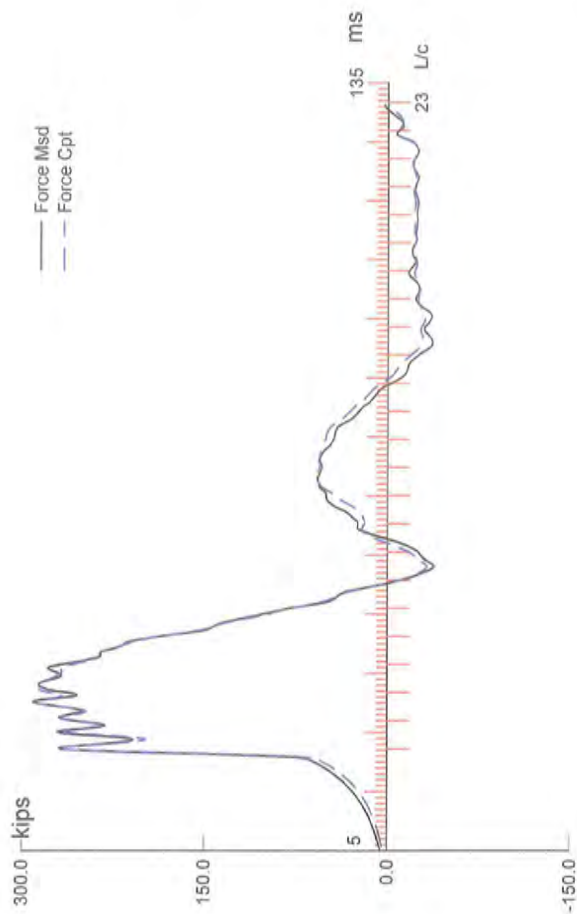
PILE HAMMER DATA					PILE DATA				JOB DESCRIPTION					
TYPE ("X" ONE)					TEST PILE NO.		REACTION 3		BRIDGE NUMBER		62716			
DROP					TYPE		CIP 12.750" x .250		T.H. NUMBER		694 WB			
X SINGLE ACTING POWER DRIVEN					LENGTH in LEADS		60+61		S.P. NUMBER		6285-135			
DOUBLE ACTING POWER DRIVEN					DIAM. of BUTT & TIP				FED. NUMBER					
MAKE					WEIGHT of PILE		4039		COUNTY		Ramsey			
APE					WEIGHT of CAP		2,050		PIER OR ABUT.		E Abut.			
WT. of RAM		SIZE or NO.			CUT-OFF ELEVATION		895.50		CONTRACTOR					
5,512		D25-32			INSPECTED BY		KC TSW		Lunda					
1	2	3	4		5	6	1	2	3	4		5	6	
FEET PENET. BELOW CUT-OFF	DROP of HAMMER or RAM (FEET)	ENERGY per BLOW (FT LBS)	BLOWS per MIN per FT		INCHES PENET. per BLOW	BEARING in TONS	FEET PENET. BELOW CUT-OFF	DROP of HAMMER or RAM (FEET)	ENERGY per BLOW (FT LBS)	BLOWS per MIN per FT		INCHES PENET. per BLOW	BEARING in TONS	
40				12	1.000		75							
41				13	0.923		76							
42				13	0.923		77							
43				13	0.923		78							
44				13	0.923		79							
45				13	0.923		80							
46				14	0.857		81							
47				14	0.857		82							
48				14	0.857		83							
49				15	0.800		84							
50				15	0.800		85							
51				17	0.706		86							
52				17	0.706		87							
53				23	0.522		88							
54				23	0.522		89							
55				25	0.480		90							
56				39	0.308		91							
57				35	0.343		92							
58				45	0.267		93							
59	6	33072		47	0.255	201.2	94							
60				x			95							
61							96							
62							97							
63							98							
64							99							
65							100							
66							101							
67							102							
68							103							
69							104							
70							105							
71							106							
72							107							
73							108							
74							109							

DATE 12/20/2012	START DRIVING TIME 8:12	END DRIVING TIME 9:26	DOWN TIME 1 hr 4 min	DRIVING TIME 10 min
--------------------	----------------------------	--------------------------	-------------------------	------------------------

REMARKS ON DRIVING CONDITIONS, PRE-BORING, ETC. (IDENTIFY BY FEET PENET.)  
Substantial refusal at 60' below cutoff, 1/2" in ten blows. Restrike 12/21/12 = 1/2" in ten blows with 9.5' hammer drop.

FORMULA USED P = $\frac{10.5E}{S + 0.2} \frac{W + 0.1M}{W + M}$	DESIGN BEARING (Tons) 312.5	AUTHORIZED PILE LENGTHS	
INSPECTOR SIGNATURE	PROJ. ENGR. SIGNATURE	BRIDGE OFFICE SIGNATURE	DATE

**REACTION PILE NO. 3  
HSDPT RESULTS  
INITIAL DRIVING**



694-Snelling; Pile: R-3 (NE Rxn Pile)  
 12.75" CIP, APE D25-32, FS=3; Blow: 213  
 American Engineering Testing, Inc.

Test: 20-Dec-2012 09:28:  
 CAPWAP (R) 2006  
 OP: DSV/JM

CAPWAP SUMMARY RESULTS

Total CAPWAP Capacity: 287.2; along Shaft				95.9; at Toe		191.3 kips		
Soil Sgmt No.	Dist. Below Gages ft	Depth Below Grade ft	Ru kips	Force in Pile kips	Sum of Ru kips	Unit Resist. (Depth) kips/ft	Unit Resist. (Area) ksf	Smith Damping Factor s/ft
				287.2				
1	26.7	6.7	5.0	282.2	5.0	0.75	0.22	0.401
2	33.3	13.3	4.9	277.3	9.9	0.74	0.22	0.401
3	40.0	20.0	4.3	273.0	14.2	0.65	0.19	0.401
4	46.7	26.7	3.7	269.3	17.9	0.56	0.17	0.401
5	53.3	33.3	3.9	265.4	21.8	0.59	0.18	0.401
6	60.0	40.0	6.3	259.1	28.1	0.95	0.28	0.401
7	66.7	46.7	13.1	246.0	41.2	1.97	0.59	0.401
8	73.3	53.3	23.2	222.8	64.4	3.48	1.04	0.401
9	80.0	60.0	31.5	191.3	95.9	4.73	1.42	0.401
Avg. Shaft			10.7			1.60	0.48	0.401
Toe			191.3				215.76	0.080
Soil Model Parameters/Extensions					Shaft	Toe		
Quake					0.269	0.378		
Case Damping Factor					2.194	0.874		
Damping Type						Smith		
Reloading Level		(% of Ru)			100	100		
CAPWAP match quality				= 3.19	(Wave Up Match) ; RSA = 0			
Observed: final set				= 0.050 in;	blow count	=	240 b/ft	
Computed: final set				= 0.068 in;	blow count	=	177 b/ft	
max. Top Comp. Stress				= 30.22 ksi	(T= 30.5 ms, max= 1.087 x Top)			
max. Comp. Stress				= 32.85 ksi	(Z= 26.7 ft, T= 31.9 ms)			
max. Tens. Stress				= -6.2 ksi	(Z= 26.7 ft, T= 54.7 ms)			
max. Energy (EMX)				= 22.5 kip-ft;	max. Measured Top Displ. (DMX)= 1.20 in			

694-Snelling; Pile: R-3 (NE Rxn Pile)  
 12.75" CIP, APE D25-32, FS=3; Blow: 213  
 American Engineering Testing, Inc.

Test: 20-Dec-2012 09:28:  
 CAPWAP(R) 2006  
 OP: DSV/JM

EXTREMA TABLE

Pile Sgmnt No.	Dist. Below Gages ft	max. Force kips	min. Force kips	max. Comp. Stress ksi	max. Tens. Stress ksi	max. Trnsfd. Energy kip-ft	max. Veloc. ft/s	max. Displ. in
1	3.3	296.7	-36.2	30.22	-3.7	22.48	13.7	1.225
2	6.7	301.0	-40.2	30.65	-4.1	22.05	13.6	1.187
4	13.3	303.5	-47.7	30.91	-4.9	21.15	13.5	1.110
6	20.0	313.2	-54.7	31.89	-5.6	20.23	13.1	1.032
7	23.3	318.3	-58.1	32.42	-5.9	19.76	12.7	0.993
8	26.7	322.6	-60.9	32.85	-6.2	19.29	12.3	0.954
9	30.0	314.4	-51.8	32.02	-5.3	17.49	12.0	0.915
10	33.3	317.2	-54.5	32.30	-5.6	17.04	11.6	0.877
11	36.7	308.1	-46.2	31.38	-4.7	15.45	11.3	0.839
12	40.0	310.7	-49.0	31.64	-5.0	15.00	11.0	0.800
13	43.3	304.4	-43.0	31.00	-4.4	13.70	10.7	0.763
14	46.7	306.9	-45.9	31.26	-4.7	13.27	10.4	0.725
15	50.0	301.8	-41.5	30.73	-4.2	12.21	10.1	0.688
16	53.3	303.6	-44.2	30.92	-4.5	11.80	9.8	0.651
17	56.7	297.2	-39.6	30.27	-4.0	10.84	9.4	0.614
18	60.0	298.7	-41.9	30.42	-4.3	10.43	8.9	0.578
19	63.3	289.0	-34.2	29.43	-3.5	9.33	8.3	0.542
20	66.7	290.9	-36.1	29.62	-3.7	8.95	7.5	0.507
21	70.0	271.3	-22.3	27.63	-2.3	7.49	6.9	0.473
22	73.3	273.4	-23.9	27.85	-2.4	7.15	6.5	0.440
23	76.7	242.1	-5.5	24.65	-0.6	5.40	6.3	0.409
24	80.0	244.1	-7.0	24.86	-0.7	3.56	5.8	0.379
Absolute	26.7			32.85			(T =	31.9 ms)
	26.7				-6.2		(T =	54.7 ms)

694-Snelling; Pile: R-3 (NE Rxn Pile)  
 12.75" CIP, APE D25-32, FS=3; Blow: 213  
 American Engineering Testing, Inc.

Test: 20-Dec-2012 09:28:  
 CAPWAP(R) 2006  
 OP: DSV/JM

CASE METHOD										
J =	0.0	0.1	0.2	0.3	0.4	0.5	0.6	0.7	0.8	0.9
RX	365.0	355.1	345.7	339.5	333.4	327.3	321.2	317.2	314.0	310.8
RU	356.4	340.6	324.8	309.0	293.2	277.4	261.6	245.8	230.0	214.2

RAU = 99.8 (kips); RA2 = 315.3 (kips)

Current CAPWAP Ru = 287.2 (kips);

Case Method matching requires higher damping factor - please check with PDA-W

VMX	VFN	VT1*Z	FT1	FMX	DMX	DFN	SET	EMX	QUS
ft/s	ft/s	kips	kips	kips	in	in	in	kip-ft	kips
13.90	-0.00	243.6	270.8	291.9	1.203	0.066	0.050	23.0	440.1

Peak Velocity Time = 22.41 ms.

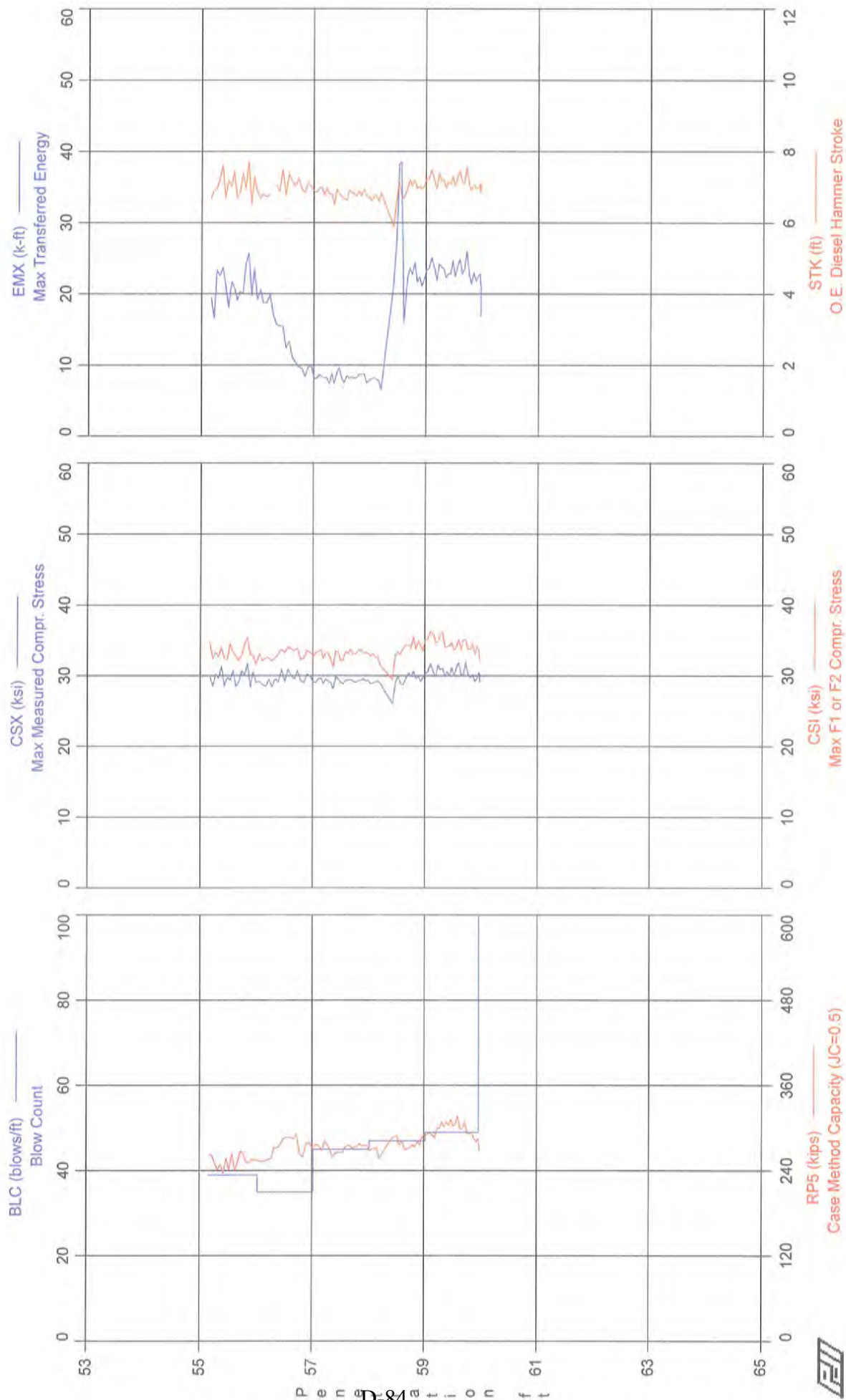
PILE PROFILE AND PILE MODEL				
Depth	Area	E-Modulus	Spec. Weight	Perim.
ft	in <sup>2</sup>	ksi	lb/ft <sup>3</sup>	ft
0.00	9.82	29992.2	492.000	3.338
80.00	9.82	29992.2	492.000	3.338

Toe Area 0.887 ft<sup>2</sup>

Top Segment Length 3.33 ft, Top Impedance 17.52 kips/ft/s

File Damping 1.0 %, Time Incr 0.198 ms, Wave Speed 16807.9 ft/s, 2L/c 9.5 ms

694-Snelling - R-3 (NE)





694-Snelling - R-3 (NE)

12" CIP, APE D25-32, FS=4

OP: DSV/JM

Test date: 20-Dec-2012

AR: 9.82 in^2

SP: 0.492 k/ft^3

LE: 80.00 ft

EM: 30,000 ksi

WS: 16,807.9 f/s

JC: 0.70

FMX: Maximum Force

CSX: Max Measured Compr. Stress

VMX: Maximum Velocity

CSI: Max F1 or F2 Compr. Stress

STK: O.E. Diesel Hammer Stroke

RP5: Case Method Capacity (JC=0.5)

EMX: Max Transferred Energy

SFT: Skin friction total

BTA: BETA Integrity Factor

BL#	depth ft	BLC bl/ft	FMX kips	VMX f/s	STK ft	EMX k-ft	BTA (%)	CSX ksi	CSI ksi	RP5 kips	SFT kips
5	55.15	39	259	10.2	5.15	10.3	90.0	26.4	33.0	253	231
8	55.23	39	257	14.3	6.36	16.0	66.0	26.2	31.6	246	209
11	55.31	39	289	16.0	0.00	21.8	48.0	29.4	32.1	233	285
14	55.38	39	293	15.6	7.14	20.5	26.0	29.8	31.6	238	301
17	55.46	39	304	18.1	7.63	17.8	13.0	31.0	34.0	282	387
20	55.54	39	300	17.7	7.32	24.1	30.0	30.6	35.3	245	223
23	55.62	39	281	16.0	6.76	17.7	21.0	28.6	32.1	242	240
26	55.69	39	278	13.9	6.57	20.0	14.0	28.4	32.4	249	331
29	55.77	39	276	14.3	6.25	19.3	70.0	28.1	33.9	247	232
32	55.85	39	301	17.3	7.37	22.7	62.0	30.6	34.0	251	238
35	55.92	39	304	16.8	7.39	24.5	75.0	31.0	33.7	264	278
38	56.00	39	276	14.4	6.55	17.1	62.0	28.1	30.6	248	226
41	56.09	35	292	14.8	7.17	19.7	59.0	29.8	32.5	257	270
44	56.17	35	286	14.6	6.90	19.6	64.0	29.1	32.4	258	280
47	56.26	35	271	11.8	0.00	16.0	51.0	27.6	31.4	263	210
50	56.34	35	288	10.4	6.93	15.0	54.0	29.3	32.1	275	225
53	56.43	35	300	9.2	7.45	16.5	44.0	30.6	34.2	271	263
56	56.51	35	297	8.1	6.99	13.2	33.0	30.2	34.5	299	258
59	56.60	35	300	7.3	7.28	11.3	19.0	30.5	33.9	288	272
62	56.69	35	287	6.0	7.03	9.1	23.0	29.3	33.7	289	251
65	56.77	35	298	6.1	7.26	10.3	14.0	30.4	33.0	267	264
68	56.86	35	292	5.3	7.04	8.3	15.0	29.8	32.6	264	272
71	56.94	35	296	5.4	6.95	9.8	17.0	30.2	33.9	279	264
74	57.02	45	282	5.2	6.76	7.7	12.0	28.7	32.3	263	273
77	57.09	45	294	5.3	7.13	8.3	10.0	30.0	33.5	287	282
80	57.16	45	291	5.3	6.99	8.2	19.0	29.6	33.8	277	275
83	57.22	45	292	5.3	7.00	8.1	16.0	29.8	33.7	285	266
86	57.29	45	293	5.1	6.87	7.4	17.0	29.9	34.0	277	278
89	57.36	45	281	5.2	6.71	6.9	18.0	28.7	31.2	262	260
92	57.42	45	296	5.4	7.03	9.6	14.0	30.1	33.1	264	279
95	57.49	45	289	5.3	6.93	8.6	15.0	29.5	32.3	266	267
98	57.56	45	282	4.7	6.69	7.5	8.0	28.7	32.0	266	275
101	57.62	45	294	5.1	7.08	9.0	8.0	30.0	33.6	289	260
104	57.69	45	294	5.1	7.10	9.4	15.0	29.9	33.9	278	263
107	57.76	45	286	5.1	6.83	8.6	17.0	29.1	33.0	269	263
110	57.82	45	287	5.0	6.88	9.0	16.0	29.3	33.4	267	261
113	57.89	45	296	5.1	7.16	9.8	13.0	30.2	33.3	280	266
116	57.96	45	289	4.5	6.72	8.3	16.0	29.4	34.0	273	262
119	58.02	47	283	4.6	6.70	8.2	16.0	28.8	32.6	260	259
122	58.09	47	284	4.6	6.71	7.9	14.0	28.9	33.1	265	265
125	58.15	47	285	4.7	6.60	7.7	16.0	29.0	32.4	264	269
128	58.21	47	276	4.6	6.60	5.5	15.0	28.1	30.1	231	212
140	58.47	47	275	19.1	6.28	41.1	100.0	28.0	31.8	264	259
143	58.53	47	298	18.7	7.22	36.3	100.0	30.4	33.8	295	304
146	58.60	47	280	14.1	6.67	11.9	100.0	28.6	34.1	304	309
150	58.68	47	295	15.7	7.08	23.1	100.0	30.0	34.5	269	272
153	58.74	47	290	15.8	7.00	22.2	100.0	29.5	33.8	272	265
156	58.81	47	306	16.7	7.34	24.8	100.0	31.2	35.0	279	278
159	58.87	47	287	15.1	6.79	21.2	100.0	29.2	34.5	276	254
162	58.94	47	282	15.2	6.83	20.1	100.0	28.7	33.6	276	247
165	59.00	47	302	16.6	7.36	24.2	100.0	30.8	35.7	294	269
168	59.06	49	301	16.4	7.27	24.1	100.0	30.7	35.8	290	261
172	59.14	49	302	16.7	7.29	23.6	100.0	30.8	35.8	289	262
175	59.20	49	290	15.3	6.89	22.3	100.0	29.6	36.0	287	244
178	59.27	49	299	15.8	7.12	23.2	100.0	30.4	34.7	293	250
181	59.33	49	305	16.7	7.26	23.9	88.0	31.1	35.2	313	241
184	59.39	49	299	16.3	7.19	22.8	89.0	30.4	34.5	312	264
187	59.45	49	298	16.4	7.22	23.4	100.0	30.4	35.1	311	255
190	59.51	49	294	15.7	7.00	22.2	88.0	30.0	32.6	298	240
193	59.57	49	303	16.3	7.23	23.6	100.0	30.9	33.6	302	246

694-Snelling - R-3 (NE)

12" CIP, APE D25-32, FS=4

OP: DSV/JM

Test date: 20-Dec-2012

BL#	depth ft	BLC bl/ft	FMX kips	VMX f/s	STK ft	EMX k-ft	BTA (%)	CSX ksi	CSI ksi	RP5 kips	SFT kips
196	59.63	49	296	16.1	7.13	22.7	100.0	30.2	33.8	298	249
199	59.69	49	299	15.9	7.19	23.8	89.0	30.4	35.4	296	240
202	59.76	49	289	15.7	7.01	22.3	89.0	29.5	33.6	285	246
205	59.82	49	285	15.0	6.76	21.5	88.0	29.1	34.6	291	249
208	59.88	49	289	15.4	7.00	22.1	87.0	29.4	33.2	292	224
211	59.94	49	289	15.3	6.99	22.5	87.0	29.4	34.3	279	255
214	59.97	250	288	15.3	7.01	21.4	90.0	29.3	32.4	278	269
217	59.98	250	287	14.8	6.71	22.2	100.0	29.2	33.2	281	254
Average			292	11.9	6.99	17.3	55.3	29.7	33.5	276	260
Std. Dev.			12	5.3	0.37	7.7	36.2	1.2	1.3	19	22
Maximum			328	19.4	8.27	41.1	100.0	33.4	37.1	320	387
@ Blow#			6	21	6	140	137	6	180	194	17

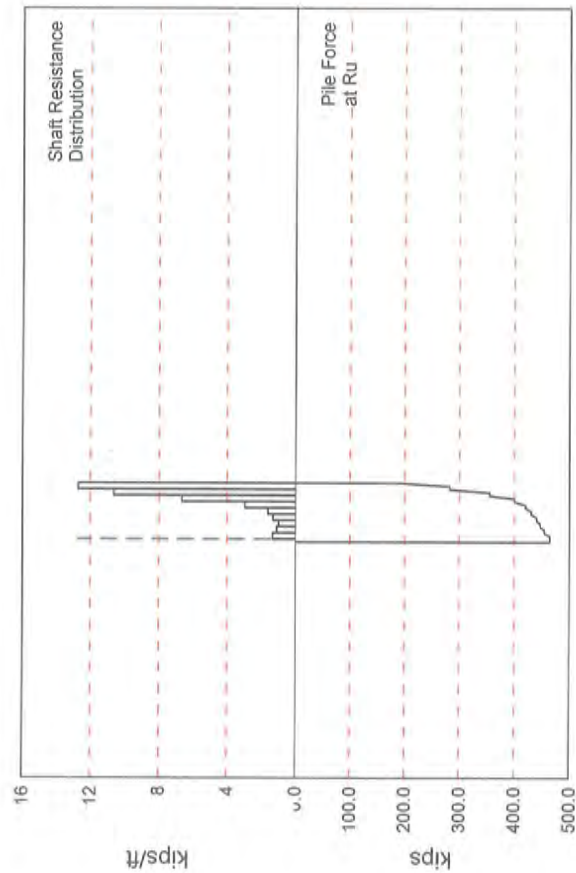
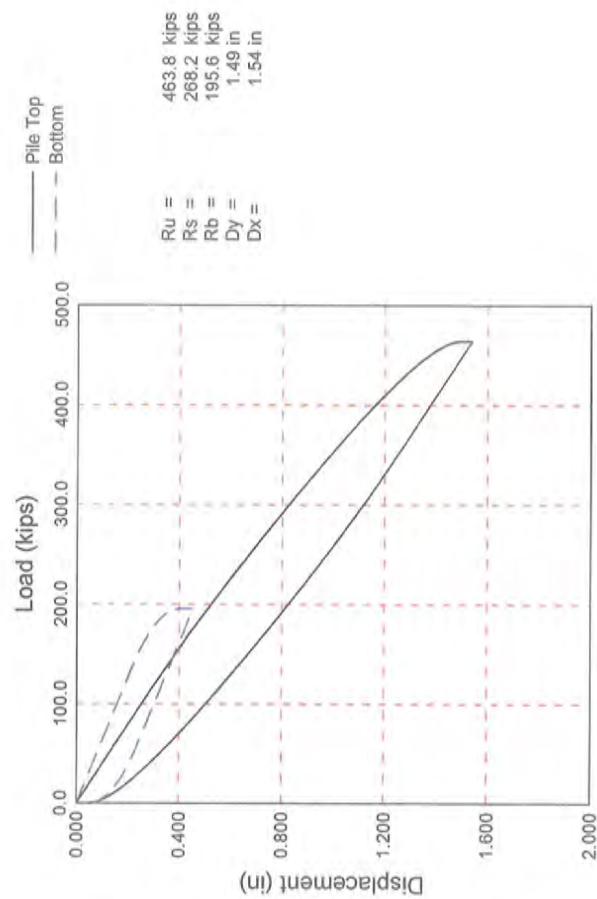
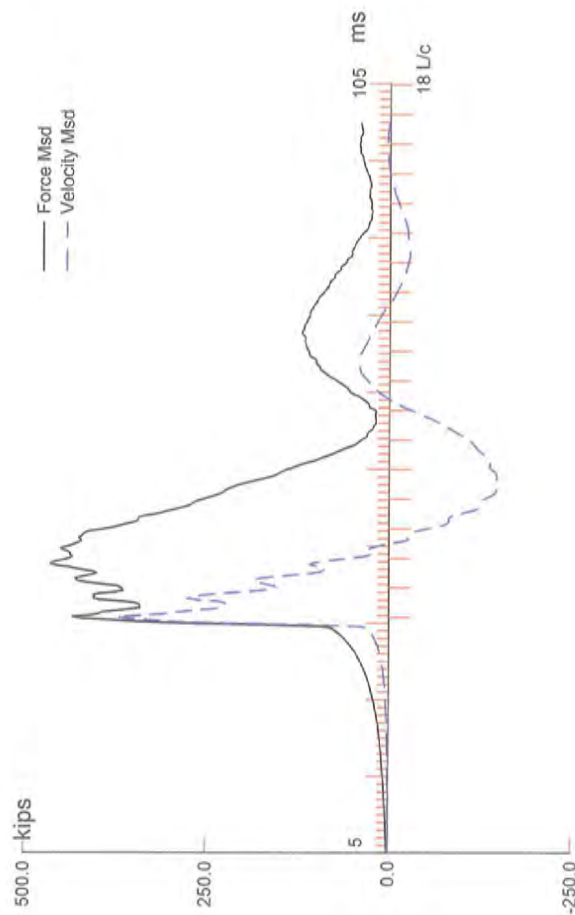
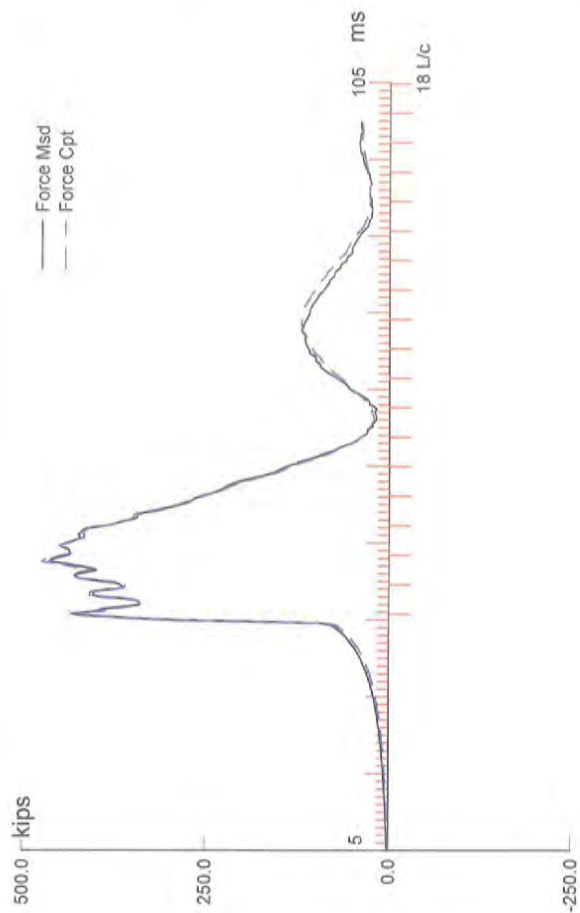
Total number of blows analyzed: 203

Time Summary

Drive 12 minutes 42 seconds

9:16:09 AM - 9:28:51 AM (12/20/2012) BN 1 - 222

**REACTION PILE 3  
HSDPT RESULTS  
RESTRIKE**



BRIDGE 62716; Pile: R3 (NE Rxn Pile)  
 12.75 OD, 0.25 WALL, APE D25-32, FS=3; Blow: 6  
 American Engineering Testing, Inc.

Test: 21-Dec-2012 11:50:  
 CAPWAP(R) 2006  
 OP: JPB

CAPWAP SUMMARY RESULTS

Total CAPWAP Capacity: 463.8; along Shaft 268.2; at Toe 195.6 kips

Soil Sgmt No.	Dist. Below Gages ft	Depth Below Grade ft	Ru kips	Force in Pile kips	Sum of Ru kips	Unit Resist. (Depth) kips/ft	Unit Resist. (Area) ksf	Smith Damping Factor s/ft
				463.8				
1	10.2	5.7	9.3	454.5	9.3	1.64	0.49	0.209
2	17.0	12.5	7.7	446.8	17.0	1.13	0.34	0.209
3	23.8	19.3	6.9	439.9	23.9	1.02	0.30	0.209
4	30.6	26.1	9.0	430.9	32.9	1.33	0.40	0.209
5	37.3	32.8	11.1	419.8	44.0	1.63	0.49	0.209
6	44.1	39.6	20.3	399.5	64.3	2.99	0.90	0.209
7	50.9	46.4	45.2	354.3	109.5	6.66	1.99	0.209
8	57.7	53.2	72.2	282.1	181.7	10.63	3.19	0.209
9	64.5	60.0	86.5	195.6	268.2	12.74	3.82	0.209
Avg. Shaft			29.8			4.47	1.34	0.209
Toe			195.6				220.61	0.109

Soil Model Parameters/Extensions

	Shaft	Toe
Quake	0.295	0.309
Case Damping Factor	3.206	1.221
Damping Type		Smith
Reloading Level (% of Ru)	100	100
Unloading Level (% of Ru)	0	
Resistance Gap (included in Toe Quake)		0.000

CAPWAP match quality = 2.34 (Wave Up Match) ; RSA = 0  
 Observed: final set = 0.050 in; blow count = 240 b/ft  
 Computed: final set = 0.089 in; blow count = 135 b/ft  
 max. Top Comp. Stress = 48.52 ksi (T= 43.2 ms, max= 1.027 x Top)  
 max. Comp. Stress = 49.84 ksi (Z= 10.2 ft, T= 43.6 ms)  
 max. Tens. Stress = 0.0 ksi (Z= 3.4 ft, T= 0.0 ms)  
 max. Energy (EMX) = 38.6 kip-ft; max. Measured Top Displ. (DMX)= 1.32 in

BRIDGE 62716; Pile: R3 (NE Rxn Pile)  
 12.75 OD, 0.25 WALL, APE D25-32, FS=3; Blow: 6  
 American Engineering Testing, Inc.

Test: 21-Dec-2012 11:50:  
 CAPWAP(R) 2006  
 OP: JPB

# EXTREMA TABLE

Pile Sgmnt No.	Dist. Below Gages ft	max. Force kips	min. Force kips	max. Comp. Stress ksi	max. Tens. Stress ksi	max. Trnsfd. Energy kip-ft	max. Veloc. ft/s	max. Displ. in
1	3.4	476.5	0.0	48.52	0.0	38.62	21.0	1.303
2	6.8	483.6	0.0	49.25	0.0	37.51	20.5	1.242
3	10.2	489.4	0.0	49.84	0.0	36.39	19.8	1.181
4	13.6	478.3	0.0	48.70	0.0	32.49	19.4	1.120
5	17.0	482.1	0.0	49.09	0.0	31.38	18.8	1.060
6	20.4	472.4	0.0	48.10	0.0	28.32	18.5	1.000
7	23.8	475.0	0.0	48.37	0.0	27.25	17.8	0.940
8	27.2	466.1	0.0	47.47	0.0	24.72	17.4	0.881
9	30.6	470.0	0.0	47.86	0.0	23.66	16.6	0.821
10	33.9	458.0	0.0	46.64	0.0	21.11	16.1	0.763
11	37.3	460.9	0.0	46.94	0.0	20.10	15.0	0.705
12	40.7	445.3	0.0	45.34	0.0	17.68	14.3	0.649
13	44.1	448.1	0.0	45.63	0.0	16.74	13.0	0.593
14	47.5	421.8	0.0	42.95	0.0	13.97	11.5	0.540
15	50.9	424.8	0.0	43.25	0.0	13.14	10.0	0.487
16	54.3	373.8	0.0	38.06	0.0	9.74	8.5	0.439
17	57.7	377.4	0.0	38.43	0.0	9.08	7.6	0.392
18	61.1	313.1	0.0	31.88	0.0	5.99	6.8	0.352
19	64.5	316.8	0.0	32.26	0.0	3.19	5.7	0.312
Absolute	10.2			49.84			(T =	43.6 ms)
	3.4				0.0		(T =	0.0 ms)

# CASE METHOD

J =	0.0	0.1	0.2	0.3	0.4	0.5	0.6	0.7	0.8	0.9
RX	597.2	575.7	554.2	532.7	520.7	509.5	498.5	487.4	476.3	465.3
RU	596.5	574.6	552.7	530.7	508.8	486.8	464.9	443.0	421.0	399.1

RAU = 201.4 (kips); RA2 = 523.3 (kips)

Current CAPWAP Ru = 463.8 (kips);

matches RX9 within 5%

VMX	VFN	VT1*Z	FT1	FMX	DMX	DFN	SET	EMX	QUS
ft/s	ft/s	kips	kips	kips	in	in	in	kip-ft	kips
21.54	0.00	377.5	438.4	465.2	1.318	0.046	0.050	40.1	703.7

Peak Velocity Time = 35.95 ms.

BRIDGE 62716; Pile: R3 (NE Rxn Pile)

Test: 21-Dec-2012 11:50:

12.75 OD, 0.25 WALL, APE D25-32, FS=3; Blow: 6

CAPWAP(R) 2006

American Engineering Testing, Inc.

OP: JPB

PILE PROFILE AND PILE MODEL

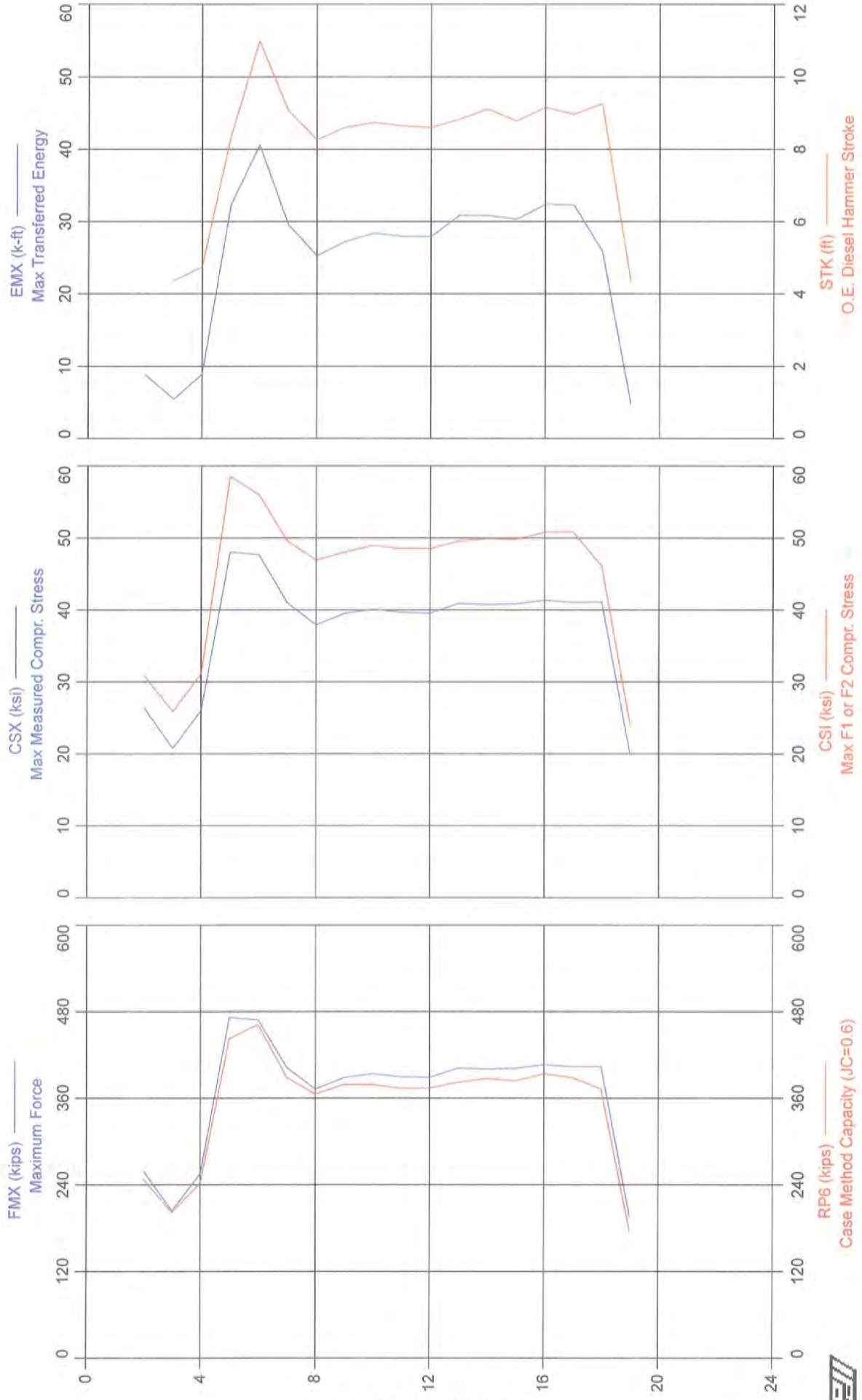
Depth ft	Area in <sup>2</sup>	E-Modulus ksi	Spec. Weight lb/ft <sup>3</sup>	Perim. ft
0.00	9.82	29992.2	492.000	3.338
64.50	9.82	29992.2	492.000	3.338

Toe Area 0.887 ft<sup>2</sup>

Top Segment Length 3.39 ft, Top Impedance 17.52 kips/ft/s

Pile Damping 1.0 %, Time Incr 0.202 ms, Wave Speed 16807.9 ft/s, 2L/c 7.7 ms

BRIDGE 62716 - R3 RST





BRIDGE 62716 - R3 RST  
OP: JPB

12.75 OD, 0.25 WALL  
Test date: 21-Dec-2012

AR: 9.82 in<sup>2</sup> SP: 0.492 k/ft<sup>3</sup>  
LE: 64.50 ft EM: 30,000 ksi  
WS: 16,807.9 f/s JC: 0.70

FMX: Maximum Force CSX: Max Measured Compr. Stress  
VMX: Maximum Velocity CSI: Max F1 or F2 Compr. Stress  
STK: O.E. Diesel Hammer Stroke RP6: Case Method Capacity (JC=0.6)  
EMX: Max Transferred Energy SFT: Skin friction total  
BTA: BETA Integrity Factor

BL#	depth ft	FMX kips	VMX f/s	STK ft	EMX k-ft	BTA (%)	CSX ksi	CSI ksi	RP6 kips	SFT kips
2	60.00	259	10.2	0.00	8.8	86.0	26.4	30.9	248	252
3	60.00	204	7.3	4.38	5.5	83.0	20.8	25.9	202	227
4	60.00	256	9.0	4.76	9.0	100.0	26.1	31.2	243	259
5	60.00	472	16.9	8.36	32.4	100.0	48.1	58.6	443	440
6	60.00	469	21.6	11.00	40.6	100.0	47.7	56.1	463	444
7	60.00	403	18.9	9.07	29.6	100.0	41.0	49.7	389	379
8	60.00	373	17.5	8.27	25.3	90.0	38.0	47.0	366	351
9	60.00	388	18.1	8.62	27.3	100.0	39.6	48.1	379	357
10	60.00	394	18.3	8.75	28.4	100.0	40.1	49.0	379	372
11	60.00	390	18.2	8.66	28.0	100.0	39.7	48.6	374	366
12	60.00	389	18.1	8.62	27.9	100.0	39.6	48.6	374	355
13	60.00	402	18.8	8.84	30.9	100.0	40.9	49.6	382	369
14	60.00	400	19.2	9.12	30.9	100.0	40.8	50.0	387	371
15	60.00	401	18.7	8.79	30.4	100.0	40.9	49.9	384	372
16	60.00	406	19.4	9.17	32.4	100.0	41.4	50.9	394	377
17	60.00	404	19.1	8.98	32.3	90.0	41.1	50.9	389	375
18	60.00	404	19.6	9.27	25.9	100.0	41.2	46.1	373	340
19	60.00	196	6.6	4.37	4.8	100.0	19.9	24.1	177	192
Average		367	16.4	8.18	25.0	97.2	37.4	45.3	353	344
Std. Dev.		79	4.5	1.80	10.2	5.5	8.1	9.8	77	66
Maximum		472	21.6	11.00	40.6	100.0	48.1	58.6	463	444
@ Blow#		5	6	6	6	4	5	5	6	6

Total number of blows analyzed: 18

#### Time Summary

Drive 3 minutes 34 seconds

11:49:38 AM - 11:53:12 AM (12/21/2012) BN 1 - 21

**MnDOT PILE DRIVING RECORD  
REACTION PILE NO. 4**

# TEST PILE REPORT

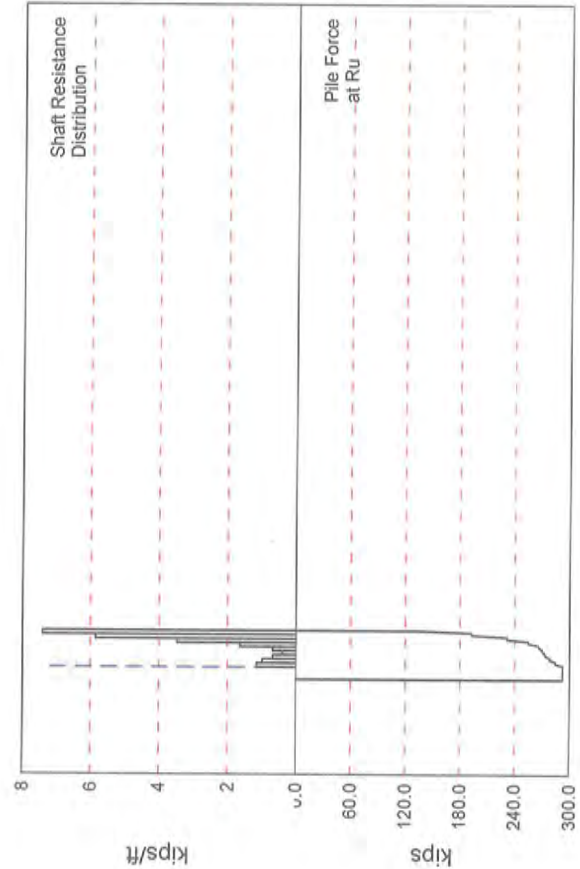
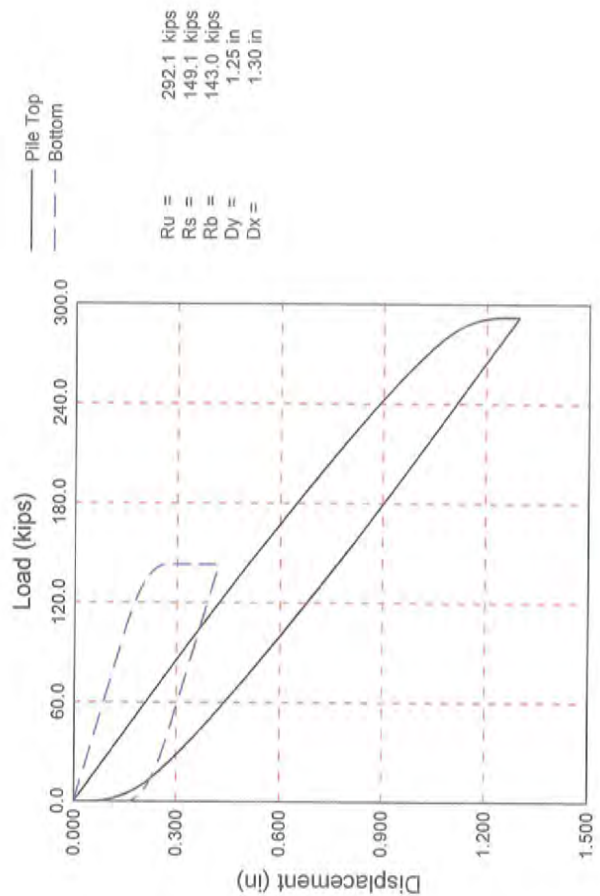
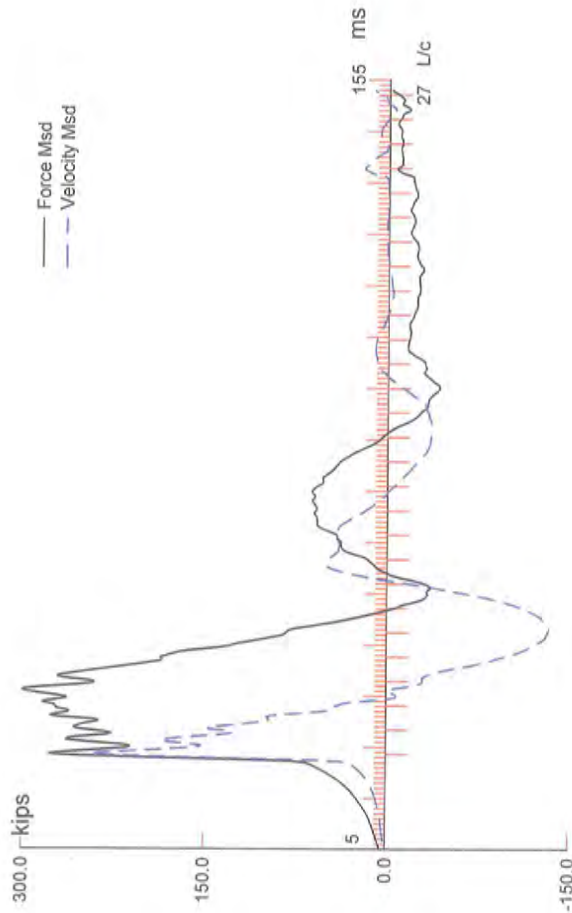
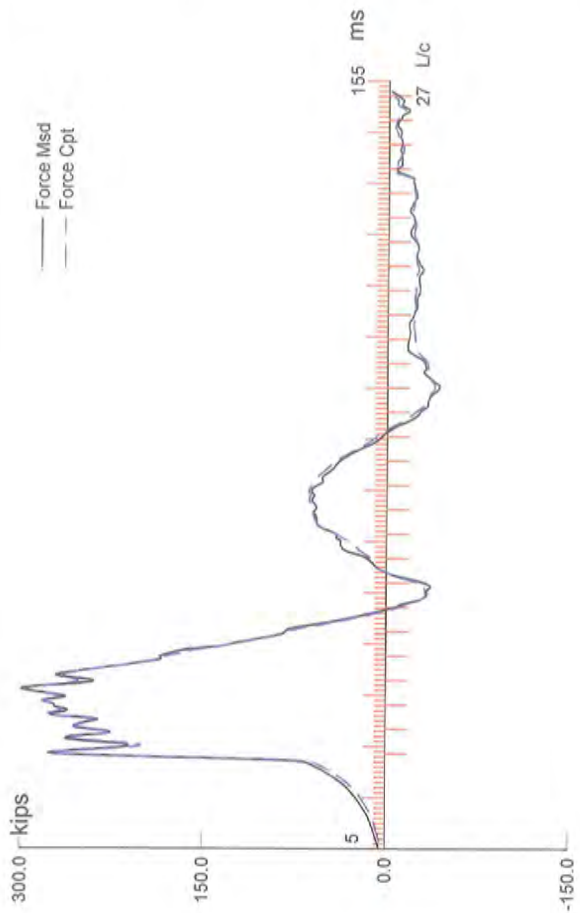
PILE HAMMER DATA					PILE DATA				JOB DESCRIPTION					
TYPE ("X" ONE)					TEST PILE NO.		REACTION 4		BRIDGE NUMBER		62716			
X	DROP				CIP		12.750" x .250		T.H. NUMBER		694 WB			
	SINGLE ACTING POWER DRIVEN				LENGTH in LEADS		60+61		S.P. NUMBER		6285-135			
	DOUBLE ACTING POWER DRIVEN				DIAM. of BUTT & TIP				FED. NUMBER					
	MAKE				WEIGHT of PILE		4039		COUNTY		Ramsey			
APE				WEIGHT of CAP		2,050		PIER OR ABUT.		E Abut.				
WT. of RAM		SIZE or NO.			CUT-OFF ELEVATION		895.50		CONTRACTOR					
5,512		D25-32			INSPECTED BY		KC TSW		Lunda					
1	2	3	4		5	6	1	2	3	4		5	6	
FEET PENET. BELOW CUT-OFF	DROP of HAMMER or RAM (FEET)	ENERGY per BLOW (FT LBS)	BLOWS per MIN	per FT	INCHES PENET. per BLOW	BEARING in TONS	FEET PENET. BELOW CUT-OFF	DROP of HAMMER or RAM (FEET)	ENERGY per BLOW (FT LBS)	BLOWS per MIN	per FT	INCHES PENET. per BLOW	BEARING in TONS	
40				11	1.091		75							
41				12	1.000		76							
42				12	1.000		77							
43				13	0.923		78							
44				13	0.923		79							
45				14	0.857		80							
46				15	0.800		81							
47				15	0.800		82							
48				15	0.800		83							
49				17	0.706		84							
50				17	0.706		85							
51				24	0.500		86							
52				36	0.333		87							
53				32	0.375		88							
54				34	0.353		89							
55				34	0.353		90							
56	6	33072		38	0.316	177.6	91							
57	6	33072		37	0.324	174.7	92							
58				x			93							
59							94							
60							95							
61							96							
62							97							
63							98							
64							99							
65							100							
66							101							
67							102							
68							103							
69							104							
70							105							
71							106							
72							107							
73							108							
74							109							

DATE 12/20/2012	START DRIVING TIME 10:06	END DRIVING TIME 10:15	DOWN TIME	DRIVING TIME 9 min
--------------------	-----------------------------	---------------------------	-----------	-----------------------

REMARKS ON DRIVING CONDITIONS, PRE-BORING, ETC. (IDENTIFY BY FEET PENET.)  
Substantial refusal at 57' below cutoff, 1/2" in ten blows. Restrike 12/21/12 = 3/8" in ten blows with 10' hammer drop.

FORMULA USED $P = \frac{10.5E}{S + 0.2} \frac{W + 0.1M}{W + M}$	DESIGN BEARING (Tons) 312.5	AUTHORIZED PILE LENGTHS	
INSPECTOR SIGNATURE	PROJ. ENGR. SIGNATURE	BRIDGE OFFICE SIGNATURE	DATE

**REACTION PILE NO. 4  
HSDPT RESULTS  
INITIAL DRIVING**



694-Snelling; Pile: R-4 (NW Rxn Pile)  
 12.75" CIP, APE D25-32, FS=3; Blow: 138  
 American Engineering Testing, Inc.

Test: 20-Dec-2012 11:11:  
 CAPWAP(R) 2006  
 OP: DSV/JM

CAPWAP SUMMARY RESULTS

Total CAPWAP Capacity: 292.1; along Shaft 149.1; at Toe 143.0 kips									
Soil Sgmt No.	Dist. Below Gages ft	Depth Below Grade ft	Ru kips	Force in Pile kips	Sum of Ru kips	Unit Resist. (Depth) kips/ft	Unit Resist. (Area) ksf	Smith Damping Factor s/ft	Quake in
				292.1					
1	26.7	6.2	7.8	284.3	7.8	1.26	0.38	0.252	0.295
2	33.3	12.8	6.6	277.7	14.4	0.99	0.30	0.252	0.295
3	40.0	19.5	4.6	273.1	19.0	0.69	0.21	0.252	0.295
4	46.7	26.2	2.8	270.3	21.8	0.42	0.13	0.252	0.295
5	53.3	32.8	4.6	265.7	26.4	0.69	0.21	0.252	0.295
6	60.0	39.5	11.0	254.7	37.4	1.65	0.49	0.252	0.295
7	66.7	46.2	23.2	231.5	60.6	3.48	1.04	0.252	0.295
8	73.3	52.8	39.1	192.4	99.7	5.87	1.76	0.252	0.295
9	80.0	59.5	49.4	143.0	149.1	7.41	2.22	0.252	0.285
Avg. Shaft			16.6			2.51	0.75	0.252	0.292
Toe				143.0			161.28	0.024	0.205

Soil Model Parameters/Extensions		Shaft	Toe
Case Damping Factor		2.141	0.196
Damping Type			Smith
Unloading Quake	(% of loading quake)	100	81
Reloading Level	(% of Ru)	100	100
Unloading Level	(% of Ru)	64	

CAPWAP match quality = 2.27 (Wave Up Match) ; RSA = 0  
 Observed: final set = 0.050 in; blow count = 240 b/ft  
 Computed: final set = 0.041 in; blow count = 293 b/ft  
 max. Top Comp. Stress = 30.17 ksi (T= 36.5 ms, max= 1.089 x Top)  
 max. Comp. Stress = 32.86 ksi (Z= 26.7 ft, T= 32.9 ms)  
 max. Tens. Stress = -6.3 ksi (Z= 26.7 ft, T= 56.1 ms)  
 max. Energy (EMX) = 20.7 kip-ft; max. Measured Top Displ. (DMX)= 1.13 in

694-Snelling; File: R-4 (NW Rxn File)  
 12.75" CIP, APE D25-32, FS=3; Blow: 138  
 American Engineering Testing, Inc.

Test: 20-Dec-2012 11:11:  
 CAPWAP(R) 2006  
 OP: DSV/JM

EXTREMA TABLE

File Sgmnt No.	Dist. Below Gages ft	max. Force kips	min. Force kips	max. Comp. Stress ksi	max. Tens. Stress ksi	max. Trnsfd. Energy kip-ft	max. Veloc. ft/s	max. Displ. in
1	3.3	296.3	-40.1	30.17	-4.1	20.69	13.9	1.156
2	6.7	297.5	-41.3	30.30	-4.2	20.23	13.8	1.118
4	13.3	300.0	-47.5	30.55	-4.8	19.29	13.7	1.039
6	20.0	308.7	-55.0	31.44	-5.6	18.32	13.2	0.959
7	23.3	316.3	-58.5	32.21	-6.0	17.82	12.9	0.919
8	26.7	322.7	-61.9	32.86	-6.3	17.32	12.5	0.878
9	30.0	314.9	-55.2	32.06	-5.6	15.44	12.2	0.838
10	33.3	317.5	-58.3	32.33	-5.9	14.96	11.9	0.799
11	36.7	308.8	-53.8	31.45	-5.5	13.49	11.7	0.760
12	40.0	310.9	-56.4	31.66	-5.7	13.04	11.4	0.722
13	43.3	306.7	-53.1	31.23	-5.4	12.00	11.2	0.684
14	46.7	308.2	-54.7	31.38	-5.6	11.57	11.0	0.647
15	50.0	305.8	-53.0	31.14	-5.4	10.83	10.7	0.609
16	53.3	306.5	-54.4	31.22	-5.5	10.42	10.3	0.573
17	56.7	299.9	-50.7	30.54	-5.2	9.60	9.8	0.537
18	60.0	302.6	-51.8	30.81	-5.3	9.24	9.2	0.502
19	63.3	288.5	-43.3	29.38	-4.4	8.12	8.5	0.469
20	66.7	291.0	-44.3	29.63	-4.5	7.79	7.6	0.435
21	70.0	262.1	-31.2	26.69	-3.2	6.31	6.9	0.405
22	73.3	263.5	-32.0	26.83	-3.3	6.03	6.7	0.374
23	76.7	216.1	-16.8	22.00	-1.7	4.41	6.5	0.348
24	80.0	216.4	-17.5	22.04	-1.8	2.75	5.9	0.322
Absolute	26.7			32.86			(T =	32.9 ms)
	26.7				-6.3		(T =	56.1 ms)

694-Snelling; File: R-4 (NW Rxn File)  
 12.75" CIP, APE D25-32, FS=3; Blow: 138  
 American Engineering Testing, Inc.

Test: 20-Dec-2012 11:11:  
 CAPWAP (R) 2006  
 OP: DSV/JM

CASE METHOD										
J =	0.0	0.1	0.2	0.3	0.4	0.5	0.6	0.7	0.8	0.9
RX	378.5	366.9	359.7	352.5	345.2	338.0	330.8	323.5	316.3	309.3
RU	378.5	364.3	350.1	336.0	321.8	307.6	293.5	279.3	265.2	251.0

RAU = 271.9 (kips); RA2 = 316.4 (kips)

Current CAPWAP Ru = 292.1 (kips);

Case Method matching requires higher damping factor - please check with PDA-W

VMX	VFN	VT1*Z	FT1	FMX	DMX	DFN	SET	EMX	QUS
ft/s	ft/s	kips	kips	kips	in	in	in	kip-ft	kips
13.87	-0.00	243.0	277.1	300.8	1.131	0.032	0.050	21.1	428.8

Peak Velocity Time = 23.80 ms.

PILE PROFILE AND PILE MODEL					
Depth	Area	E-Modulus	Spec. Weight	Perim.	
ft	in <sup>2</sup>	ksi	lb/ft <sup>3</sup>	ft	
0.00	9.82	29992.2	492.000	3.338	
80.00	9.82	29992.2	492.000	3.338	

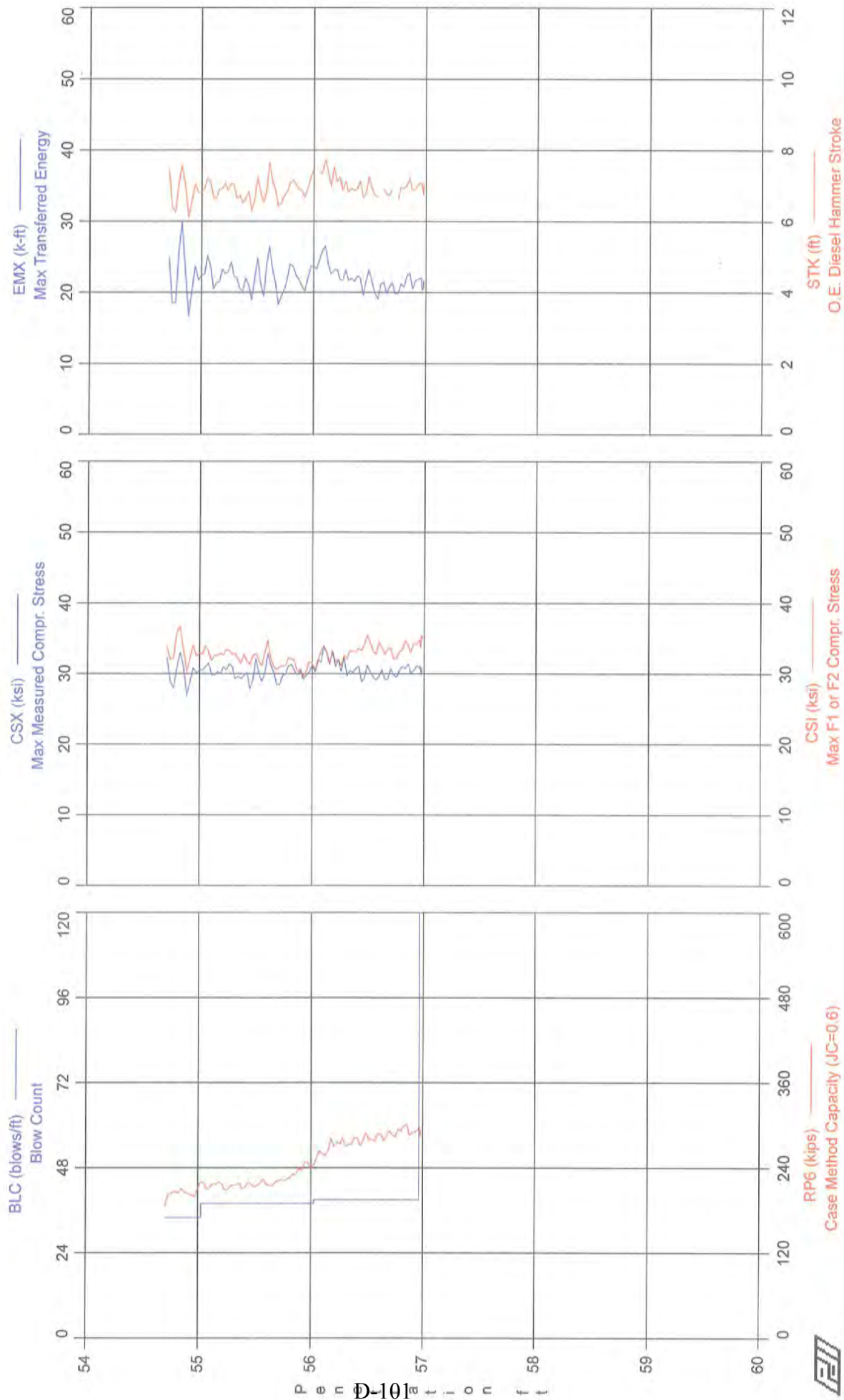
Toe Area 0.887 ft<sup>2</sup>

Top Segment Length 3.33 ft, Top Impedance 17.52 kips/ft/s

File Damping 1.0 %, Time Incr 0.198 ms, Wave Speed 16807.9 ft/s, 2L/c 9.5 ms



694-Snelling - R-4 (NW)



694-Snelling - R-4 (NW)

12" CIP, APE D25-32, FS=4

OP: DSV/JM

Test date: 20-Dec-2012

AR: 9.82 in^2

SP: 0.492 k/ft3

LE: 80.00 ft

EM: 30,000 ksi

WS: 16,807.9 f/s

JC: 0.70

FMX: Maximum Force

CSX: Max Measured Compr. Stress

VMX: Maximum Velocity

CSI: Max F1 or F2 Compr. Stress

STK: O.E. Diesel Hammer Stroke

RP6: Case Method Capacity (JC=0.6)

EMX: Max Transferred Energy

SFT: Skin friction total

BTA: BETA Integrity Factor

BL#	depth ft	BLC bl/ft	FMX kips	VMX f/s	STK ft	EMX k-ft	BTA (%)	CSX ksi	CSI ksi	RP6 kips	SFT kips
54	54.71	34	317	16.4	7.47	25.0	100.0	32.3	33.9	187	279
56	54.76	34	275	13.3	6.27	18.6	100.0	28.0	32.3	205	277
58	54.82	34	325	17.1	7.58	29.9	100.0	33.1	36.7	205	289
60	54.88	34	265	13.1	6.11	16.7	100.0	27.0	30.3	206	272
63	54.97	34	296	15.0	6.81	21.7	100.0	30.1	32.5	200	275
65	55.03	38	300	15.2	6.95	22.7	100.0	30.5	32.8	220	278
67	55.08	38	309	15.9	7.12	23.7	100.0	31.5	33.2	211	283
69	55.13	38	293	14.7	6.64	21.4	100.0	29.8	32.6	218	268
71	55.18	38	295	15.0	6.93	23.3	100.0	30.0	33.0	220	285
73	55.24	38	300	15.4	6.88	22.9	100.0	30.5	33.5	210	263
75	55.29	38	304	15.5	7.02	22.2	100.0	31.0	32.8	215	264
77	55.34	38	291	14.7	6.74	20.5	100.0	29.7	32.2	216	255
79	55.39	38	292	14.6	6.67	22.0	100.0	29.8	32.8	211	274
81	55.45	38	274	13.4	6.31	19.0	100.0	27.9	31.3	220	256
83	55.50	38	315	16.3	7.25	24.8	100.0	32.1	32.9	213	271
85	55.55	38	284	14.4	6.55	19.4	100.0	28.9	31.2	219	249
87	55.61	38	322	16.8	7.67	26.5	100.0	32.8	34.6	217	286
89	55.66	38	296	15.2	6.87	21.3	100.0	30.2	31.1	215	258
91	55.71	38	280	13.9	6.53	19.5	100.0	28.5	31.0	222	280
93	55.76	38	294	15.0	6.84	21.8	100.0	30.0	31.1	222	275
95	55.82	38	308	15.8	7.17	23.7	100.0	31.3	32.1	226	271
97	55.87	38	293	15.0	6.91	21.8	100.0	29.9	30.3	231	261
99	55.92	38	287	14.4	6.69	20.2	100.0	29.2	29.5	236	257
101	55.97	38	297	15.2	7.26	23.7	100.0	30.3	31.7	248	255
103	56.03	39	298	15.3	0.00	23.4	100.0	30.3	30.5	245	245
105	56.08	39	311	16.2	7.37	25.9	100.0	31.6	33.1	264	269
107	56.13	39	324	16.7	7.40	24.0	88.0	33.0	33.1	257	227
109	56.18	39	326	16.9	7.54	23.1	88.0	33.2	33.3	282	249
111	56.23	39	315	16.3	7.25	21.8	87.0	32.1	32.1	277	237
113	56.29	39	316	16.4	7.14	23.2	90.0	32.2	32.6	282	228
115	56.34	39	299	15.2	6.94	22.0	88.0	30.5	33.3	274	253
117	56.39	39	302	15.5	6.91	22.4	89.0	30.8	33.0	282	256
119	56.44	39	283	14.2	6.68	19.7	87.0	28.9	33.3	271	267
121	56.49	39	306	15.8	7.27	23.2	87.0	31.2	35.4	290	252
123	56.54	39	290	14.5	6.74	20.0	90.0	29.5	33.2	280	240
125	56.60	39	291	14.7	0.00	21.2	89.0	29.7	34.5	287	250
127	56.65	39	287	14.2	6.78	19.9	86.0	29.2	32.8	278	237
129	56.70	39	302	15.3	6.93	21.4	100.0	30.8	33.7	293	252
131	56.75	39	290	14.5	6.62	19.9	100.0	29.5	32.1	284	238
133	56.80	39	305	15.6	6.93	20.7	100.0	31.0	33.3	292	245
135	56.86	39	308	15.9	7.24	22.8	90.0	31.4	34.1	301	249
137	56.91	39	299	15.2	6.92	21.7	100.0	30.5	34.4	290	246
139	56.96	39	302	15.5	7.08	22.1	88.0	30.8	34.8	294	246
141	56.97	250	300	15.2	6.97	20.4	100.0	30.6	33.8	298	231
143	56.98	250	294	14.9	6.87	20.5	90.0	29.9	35.5	289	259
145	56.98	250	303	15.0	7.11	21.1	88.0	30.8	35.4	293	246
Average			299	15.2	6.94	22.0	96.8	30.4	32.9	248	259
Std. Dev.			11	0.8	0.30	2.0	5.2	1.2	1.4	34	17
Maximum			332	17.4	7.75	29.9	100.0	33.9	36.7	301	296
@ Blow#			106	106	106	58	54	106	58	135	57

Total number of blows analyzed: 91

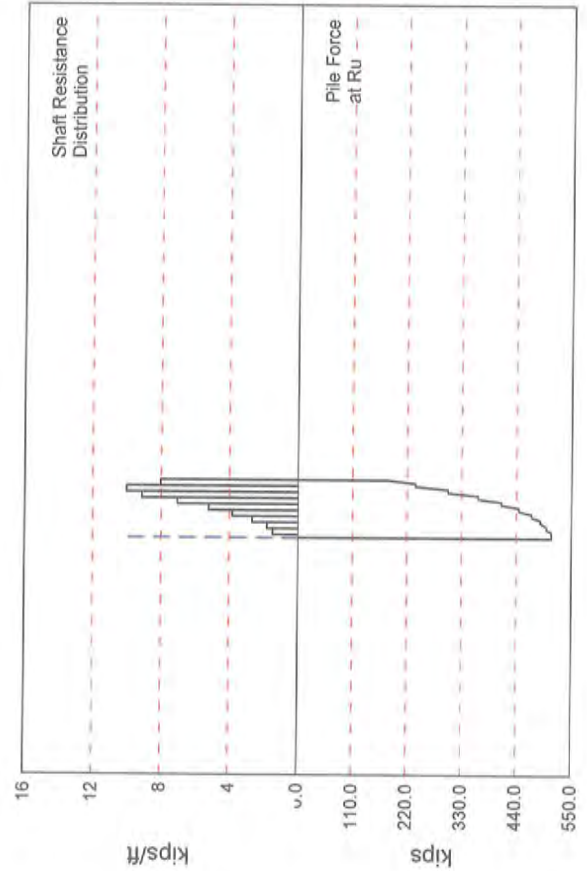
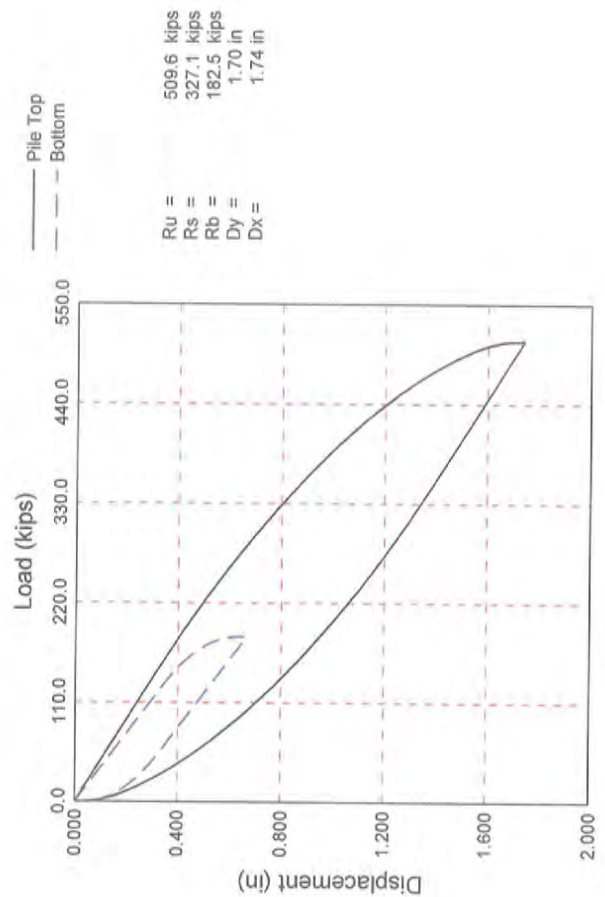
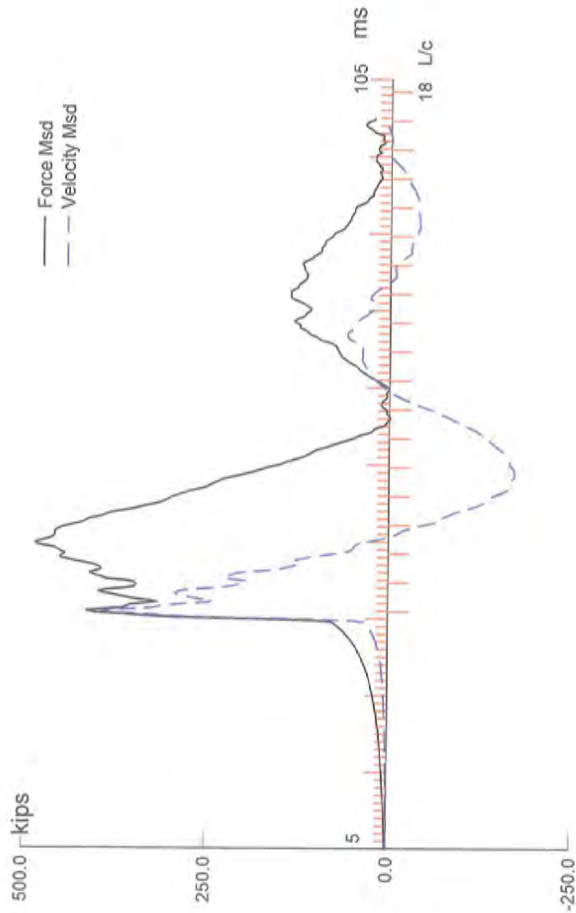
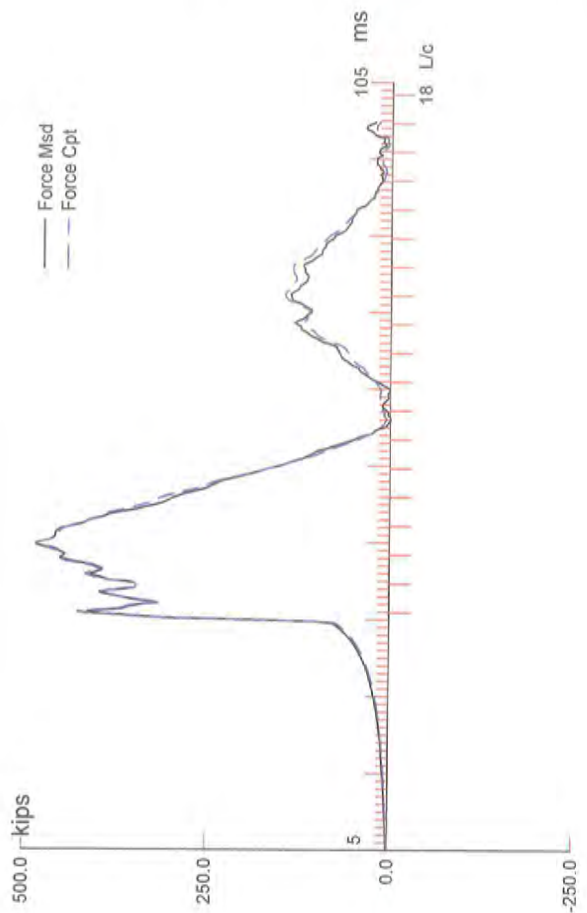
BL#	depth (ft)	Comments
2	53.18	WC = 16807.851

#### Time Summary

Drive		10:02:19 AM - 10:02:19 AM (12/20/2012) BN 1 - 1
Stop	59 minutes 5 seconds	10:02:19 AM - 11:01:24 AM
Drive	10 minutes 5 seconds	11:01:24 AM - 11:11:29 AM BN 2 - 149

Total time [1:09:10] = (Driving [0:10:05] + Stop [0:59:05])

**REACTION PILE 4  
HSDPT RESULTS  
RESTRIKE**



BRIDGE 62716; Pile: R4 (NW Rxn Pile)  
 12.75 OD, 0.25 WALL, APE D25-32, FS=3; Blow: 4  
 American Engineering Testing, Inc.

Test: 21-Dec-2012 11:39:  
 CAPWAP(R) 2006  
 OP: JPB

# CAPWAP SUMMARY RESULTS

Total CAPWAP Capacity: 509.6; along Shaft 327.1; at Toe 182.5 kips

Soil Sgmnt No.	Dist. Below Gages ft	Depth Below Grade ft	Ru kips	Force in Pile kips	Sum of Ru kips	Unit Resist. (Depth) kips/ft	Unit Resist. (Area) ksf	Smith Damping Factor s/ft
				509.6				
1	9.9	6.9	10.0	499.6	10.0	1.44	0.43	0.026
2	16.6	13.6	12.1	487.5	22.1	1.82	0.55	0.026
3	23.2	20.2	17.7	469.8	39.8	2.67	0.80	0.026
4	29.8	26.8	25.5	444.3	65.3	3.85	1.15	0.026
5	36.5	33.5	34.6	409.7	99.9	5.22	1.56	0.026
6	43.1	40.1	46.7	363.0	146.6	7.04	2.11	0.026
7	49.7	46.7	60.6	302.4	207.2	9.14	2.74	0.026
8	56.4	53.4	66.5	235.9	273.7	10.03	3.00	0.026
9	63.0	60.0	53.4	182.5	327.1	8.05	2.41	0.026
Avg. Shaft			36.3			5.45	1.63	0.026
Toe			182.5				205.83	0.084

## Soil Model Parameters/Extensions

	Shaft	Toe
Quake	0.295	0.483
Case Damping Factor	0.481	0.871
Unloading Quake (% of loading quake)	99	72
Reloading Level (% of Ru)	100	100
Unloading Level (% of Ru)	0	
Resistance Gap (included in Toe Quake)		0.013
Soil Plug Weight (kips)		0.01

CAPWAP match quality = 2.70 (Wave Up Match) ; RSA = 0  
 Observed: final set = 0.038 in; blow count = 320 b/ft  
 Computed: final set = 0.077 in; blow count = 156 b/ft  
 max. Top Comp. Stress = 49.72 ksi (T= 45.0 ms, max= 1.016 x Top)  
 max. Comp. Stress = 50.52 ksi (Z= 16.6 ft, T= 44.0 ms)  
 max. Tens. Stress = -3.9 ksi (Z= 56.4 ft, T= 63.9 ms)  
 max. Energy (EMX) = 42.6 kip-ft; max. Measured Top Displ. (DMX)= 1.50 in

BRIDGE 62716; Pile: R4 (NW Rxn Pile)  
 12.75 OD, 0.25 WALL, APE D25-32, FS=3; Blow: 4  
 American Engineering Testing, Inc.

Test: 21-Dec-2012 11:39:  
 CAPWAP(R) 2006  
 OP: JPB

EXTREMA TABLE

Pile Sgmt No.	Dist. Below Gages ft	max. Force kips	min. Force kips	max. Comp. Stress ksi	max. Tens. Stress ksi	max. Trnsfd. Energy kip-ft	max. Veloc. ft/s	max. Displ. in
1	3.3	488.3	0.0	49.72	0.0	42.64	21.5	1.454
2	6.6	490.2	-3.4	49.92	-0.3	41.42	21.3	1.391
3	9.9	492.0	-8.2	50.11	-0.8	40.17	21.0	1.327
4	13.3	489.8	-11.8	49.88	-1.2	37.65	20.8	1.263
5	16.6	496.1	-16.2	50.52	-1.6	36.40	20.5	1.200
6	19.9	485.9	-18.8	49.48	-1.9	33.82	20.2	1.137
7	23.2	487.3	-22.3	49.62	-2.3	32.62	19.7	1.074
8	26.5	473.0	-24.4	48.17	-2.5	29.75	19.4	1.014
9	29.8	482.3	-27.9	49.12	-2.8	28.61	18.8	0.953
10	33.2	461.0	-29.2	46.94	-3.0	25.42	18.4	0.895
11	36.5	463.9	-32.6	47.24	-3.3	24.38	17.6	0.836
12	39.8	428.1	-33.1	43.60	-3.4	21.05	17.2	0.782
13	43.1	431.4	-35.6	43.93	-3.6	20.15	16.3	0.728
14	46.4	385.5	-35.3	39.26	-3.6	16.75	15.8	0.680
15	49.7	391.3	-37.8	39.85	-3.9	16.03	15.0	0.632
16	53.1	331.3	-36.8	33.74	-3.7	12.69	14.5	0.591
17	56.4	334.6	-38.7	34.08	-3.9	12.17	13.8	0.550
18	59.7	272.5	-36.5	27.75	-3.7	9.32	13.8	0.518
19	63.0	289.1	-36.5	29.44	-3.7	7.46	13.0	0.486
Absolute	16.6			50.52			(T =	44.0 ms)
	56.4				-3.9		(T =	63.9 ms)

CASE METHOD

J =	0.0	0.1	0.2	0.3	0.4	0.5	0.6	0.7	0.8	0.9
RX	590.9	569.0	556.2	545.2	534.3	523.5	512.7	503.6	497.0	490.5
RU	590.9	568.7	546.4	524.2	502.0	479.7	457.5	435.2	413.0	390.8

RAU = 264.1 (kips); RA2 = 498.3 (kips)

Current CAPWAP Ru = 509.6 (kips); J(RX) = 0.63

VMX	VFN	VT1*Z	FT1	FMX	DMX	DFN	SET	EMX	QUS
ft/s	ft/s	kips	kips	kips	in	in	in	kip-ft	kips
22.66	0.00	397.1	416.2	486.5	1.504	0.038	0.038	44.1	687.0

Peak Velocity Time = 36.10 ms.

BRIDGE 62716; File: R4 (NW Rxn Pile)

Test: 21-Dec-2012 11:39:

12.75 OD, 0.25 WALL, APE D25-32, FS=3; Blow: 4

CAPWAP(R) 2006

American Engineering Testing, Inc.

OP: JPB

PILE PROFILE AND PILE MODEL

Depth ft	Area in <sup>2</sup>	E-Modulus ksi	Spec. Weight lb/ft <sup>3</sup>	Perim. ft
0.00	9.82	29992.2	492.000	3.338
63.00	9.82	29992.2	492.000	3.338

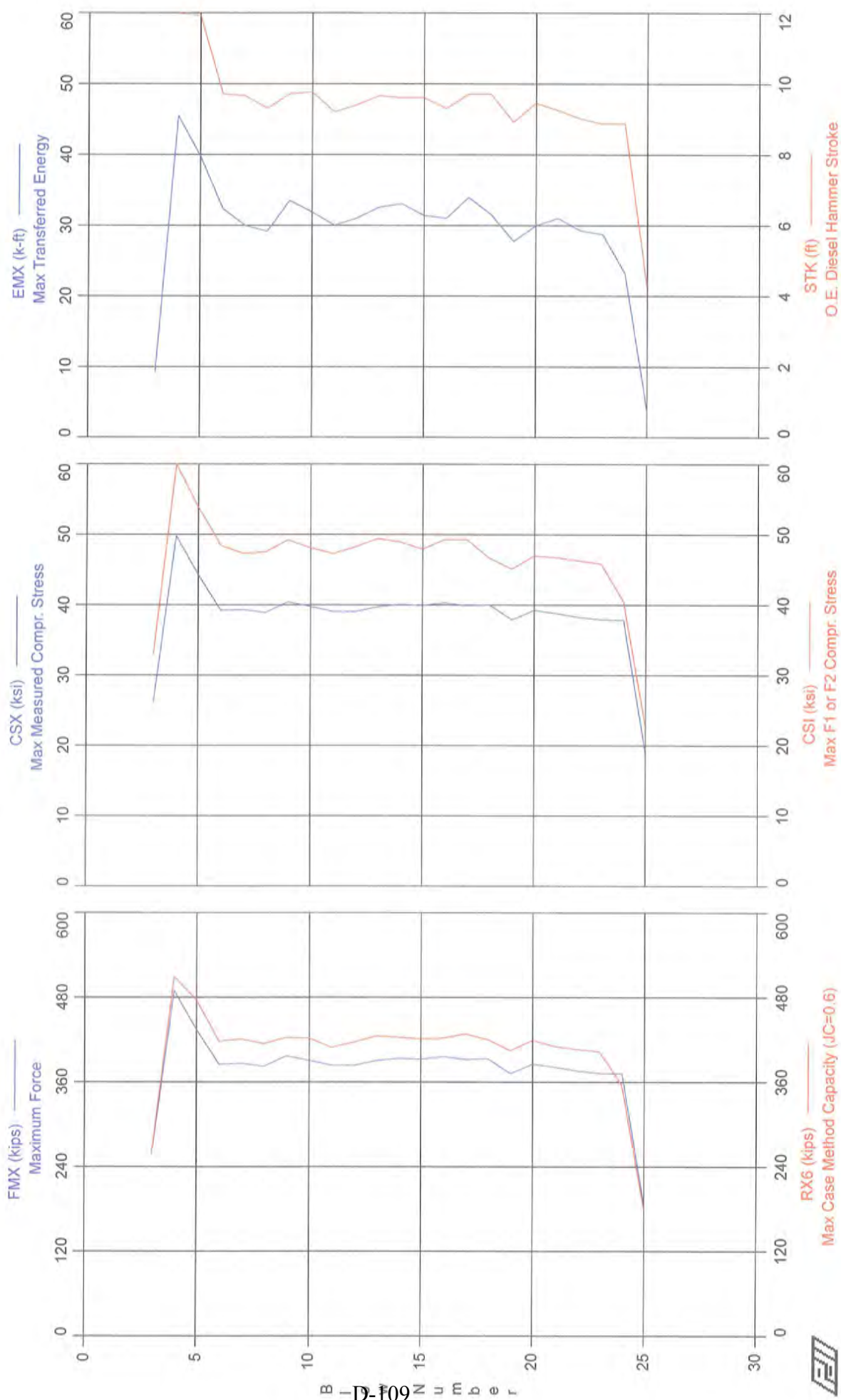
Toe Area 0.887 ft<sup>2</sup>

Top Segment Length 3.32 ft, Top Impedance 17.52 kips/ft/s

Pile Damping 1.0 %, Time Incr 0.197 ms, Wave Speed 16807.9 ft/s, 2L/c 7.5 ms



BRIDGE 62716 - R4 RST



BRIDGE 62716 - R4 RST  
OP: JPB

12.75 OD, 0.25 WALL  
Test date: 21-Dec-2012

AR: 9.82 in^2  
LE: 63.00 ft  
WS: 16,807.9 f/s

SP: 0.492 k/ft3  
EM: 30,000 ksi  
JC: 0.70

FMX: Maximum Force  
VMX: Maximum Velocity  
STK: O.E. Diesel Hammer Stroke  
EMX: Max Transferred Energy  
BTA: BETA Integrity Factor

CSX: Max Measured Compr. Stress  
CSI: Max F1 or F2 Compr. Stress  
RX6: Max Case Method Capacity (JC=0.6)  
SFT: Skin friction total

BL#	depth ft	FMX kips	VMX f/s	STK ft	EMX k-ft	BTA (%)	CSX ksi	CSI ksi	RX6 kips	SFT kips
3	59.50	257	10.4	0.00	9.3	90.0	26.2	33.1	257	231
4	59.50	489	22.8	12.08	45.5	100.0	49.9	60.7	510	382
5	59.50	435	22.7	11.94	39.8	90.0	44.3	53.9	476	366
6	59.50	385	20.6	9.73	32.4	100.0	39.2	48.5	418	304
7	59.50	386	20.3	9.67	30.0	90.0	39.4	47.4	421	332
8	59.50	382	19.7	9.32	29.2	100.0	38.9	47.6	415	319
9	59.50	397	20.8	9.73	33.5	100.0	40.5	49.3	423	328
10	59.50	391	20.7	9.78	31.9	88.0	39.8	48.2	422	328
11	59.50	384	19.7	9.22	30.0	90.0	39.1	47.3	409	316
12	59.50	384	20.2	9.42	31.1	89.0	39.1	48.3	417	321
13	59.50	391	20.6	9.67	32.6	87.0	39.8	49.5	426	328
14	59.50	394	20.7	9.62	33.1	88.0	40.1	49.0	424	327
15	59.50	392	20.3	9.62	31.4	90.0	40.0	48.0	421	334
16	59.50	396	19.8	9.32	31.1	90.0	40.3	49.4	423	328
17	59.50	392	20.9	9.73	34.0	88.0	39.9	49.3	428	334
18	59.50	393	20.8	9.73	31.6	100.0	40.0	46.7	420	326
19	59.50	372	19.3	8.93	27.8	100.0	37.9	45.2	405	308
20	59.50	386	20.1	9.47	30.0	100.0	39.3	47.1	419	334
21	59.50	381	20.2	9.27	31.1	100.0	38.8	46.8	411	319
22	59.50	376	19.5	9.03	29.3	100.0	38.3	46.3	407	316
23	59.50	372	19.3	8.89	28.8	100.0	37.9	45.9	403	317
24	59.50	372	19.4	8.89	23.2	100.0	37.9	40.5	356	280
25	59.50	185	6.4	4.27	3.8	77.0	18.8	22.6	179	161
Average		378	19.4	9.42	29.6	93.8	38.5	46.5	404	315
Std. Dev.		55	3.5	1.38	8.2	6.5	5.6	6.9	64	43
Maximum		489	22.8	12.08	45.5	100.0	49.9	60.7	510	382
@ Blow#		4	4	4	4	4	4	4	4	4

Total number of blows analyzed: 23

#### Time Summary

Drive 1 minute 36 seconds

11:38:55 AM - 11:40:31 AM (12/21/2012) BN 1 - 25

## **CALIBRATION REPORTS**

**Richard Dudgeon, Inc.**  
**100 HICKS STREET, Bridgeport, CT 06605**  
**Tel (203) 336-4459 Fax (203) 333-8417**  
**Toll Free: 888-383-4366**

**LOAD CELL CALIBRATION REPORT**

LOAD CELL CAPACITY (TONS) 500 SERIAL NUMBER 07-24953  
 STRAIN INDICATOR MODEL P3 SERIAL NUMBER 195852  
 LOAD CELL TEST NO. (GAUGE FACTOR) 1.245 ZERO SET NO. +000.0

Notice: Calibration reports prepared by Richard Dudgeon, Inc. are submitted on a confidential basis and the data contained therein is our customer's proprietary information. Such reports may or may not be used by others without the express written consent of Richard Dudgeon, Inc. and its customers.

Dudgeon Order No. L17106 Order Date 11/19/12 Test Date 12/5/12  
 Customer LUNDA CONSTRUCTION Purchase Order No. VERBAL  
 Test Performed By W. Nold In 760 Ton Load Frame, S/N 760TLF-1. Output Measured by  
 4 x 190 Ton Load cells, S/N 926067RN, 954099WP, BX1272, DX2045 with Strain Indicator Model  
P3500, S/N 0140334, Test No. 1.155, Zero Set +/-0000.

Test Method: Load increased in even increments at slow rate by hydraulic jack/pump. Output force of Load Cell measured by calibrated Load Cells (within a tolerance of one percent) between 20 and 190 tons traceable to the Nat'l Institute of Standards and Technology (formerly the Nat'l Bureau of Standards).

STANDARD FORCE KIPS/TONS	LOAD CELL READING			AVERAGE READING
	RUN 1	RUN 2	RUN 3	
0	+000.0	+000.0	+000.0	+000.0
50	052.2	052.2	052.3	052.3
100	102.3	102.4	102.6	102.4
150	152.0	152.4	152.6	152.3
200	201.6	202.1	202.5	202.1
250	251.3	251.9	252.5	251.9
300	301.0	301.7	302.4	301.7
350	350.3	350.7	351.6	350.9
400	399.9	400.4	401.0	400.4
450	449.2	449.6	450.0	449.6
500	498.4	498.9	499.8	499.0

**Richard Dudgeon, Inc.**  
**100 HICKS STREET, Bridgeport, CT 06605**  
**Tel (203) 336-4459 Fax (203) 333-8417**

**JACK CALIBRATION REPORT**

Cylinder 800 Tons Capacity, 12 " Stroke, Serial No. RJ3140  
 Gauge 10,000 PSI Rating, 60 " Dial Dia., Serial No. 220706X

Notice: Calibration reports prepared by Richard Dudgeon, Inc. are submitted on a confidential basis and the data contained therein is our customer's proprietary information. Such reports may or may not be used by others without the express written consent of Richard Dudgeon, Inc. and it's customers.

Dudgeon Order No. L17106 Order Date 11/19/12 Test Date 12/5/12  
 Customer LUNDA CONSTRUCTION Purchase Order No. VERBAL  
 Test Performed By W. Noid In 760 Ton Load Frame, S/N 760TLF-1. Output Measured  
 by 4 x 190 Ton Loadcells S/N 954099WP, 926067RN, BX1272 and DX2045 with Strain  
 Indicator Model P3500, S/N 0140334, Test No. 1.155, Zero Set +/-0000.

Test Method: Cylinder pressure increased in even increments at slow rate by hydraulic pump. Output force of cylinder measured by calibrated Loadcells (within a tolerance of one percent) between 50 and 760 tons traceable to the Nat'l Institute of Standards and Technology (formerly the Nat'l Bureau of Standards).

LOAD ON CYLINDER (KPS/TONS)	GAUGE READING IN PSI AT RAM EXTENSIONS OF			AVERAGE PRESSURE (PSI)
	3 INCHES	5 INCHES	9 INCHES	
50	550	525	550	550
100	1050	1050	1050	1050
150	1550	1550	1550	1550
200	2050	2050	2050	2050
250	2550	2550	2550	2550
300	3050	3050	3050	3050
350	3000	3575	3000	3000
400	4100	4100	4100	4100
450	4000	4000	4000	4000
500	5100	5100	5100	5100

PRESSURE GAUGE CERTIFICATION

CUSTOMER: LUNDA CONSTRUCTION, INC.

CUSTOMER'S ORDER NO	DUDGEON ORDER NO.	ORDER DATE
VERBAL BRUCE	L17106	11/19/12

GAUGE SERIAL NO.

CAPACITY

220706X

10000 PSI 1 1/2"

WE HEREBY CERTIFY THE ABOVE HYDRAULIC GAUGE HAVE BEEN TESTED AGAINST OUR HEISE DIGITAL PRESSURE INDICATOR, SERIAL NO. S7-9400 AND FOUND TO BE WITHIN A STANDARD ACCURACY (PLUS OR MINUS 1/2%) OF FULL SCALE. OUR TEST EQUIPMENT IS TRACEABLE TO THE NATIONAL BUREAU OF STANDARDS.

REFERENCE PRESSURE  
(PSI)

GAUGE READING  
(PSI)

0  
1000  
2000  
3000  
4000  
5000  
6000  
7000  
8000  
9000  
10000

0  
1000  
2000  
3000  
4000  
5000  
6025  
7025  
8025  
9025  
X

RICHARD DUDGEON, INC.

DATE: 12/5/12